DISSERTATION

MODELING SPATIAL AND TEMPORAL VARIABILITY IN A FOLSOM LITHIC SCATTER: VIEWS FROM THE REDDIN SITE, SAN LUIS VALLEY, COLORADO

Submitted by

Kelton A. Meyer

Department of Anthropology and Geography

In partial fulfillment of the requirements

For the Degree of Doctor of Philosophy

Colorado State University

Fort Collins, Colorado

Spring 2025

Doctoral Committee:

Advisor: Jason M. LaBelle

Michael C. Pante
Mary Van Buren
Ben A. Shaby

Copyright by Kelton A. Meyer 2025

All Rights Reserved

ABSTRACT

MODELING SPATIAL AND TEMPORAL VARIABILITY IN A FOLSOM LITHIC SCATTER: VIEWS FROM THE REDDIN SITE, SAN LUIS VALLEY, COLORADO

This dissertation explores Folsom mobility and campsite organization through the analysis of the Reddin site (5SH77), San Luis Valley, southern Colorado. Current models of Folsom mobility in the region focus on sites with buried and spatially discrete components, often representing single occupation events associated with bison hunting, lithic procurement, seasonal aggregation, or a combination of these activities. Reddin is a surface scatter of lithic debris lacking a buried horizon, but it includes a large Folsom assemblage and exhibits evidence of multiple occupations. Lithic analysis suggests Reddin was a place used for residential downtime and retooling broken equipment. I applied spatial statistical methods to detect multiple Folsom camps at the site using artifacts commonly associated with residential areas. Reddin contains at least 14 Folsom camps averaging more than 160 m distant, each with variable artifact densities. I then explored Folsom mobility patterns in each cluster by calculating mean per capita occupation span, based on artifact accumulation over time. I developed a new method of calculating occupation span using the steady accumulation of burned lithic debris, a common attribute of Folsom campsite spaces. The results indicate that each campsite was used for different lengths of time, representing a spectrum of Folsom mobility strategies used in the Valley's center. Multiple Folsom occupations at Reddin suggest the formation of a local cultural geography, which likely evolved in complexity with sequential visits to the site. Unless otherwise noted, all data, tables, maps, and figures in this dissertation were produced by the author.

ACKNOWLEDGEMENTS

This was the most difficult section of my dissertation to write. I am indebted to so many individuals who contributed to this project and my experience as a student at Colorado State University (CSU), and I am unable to fully capture the depth of my gratitude. First and foremost, I am grateful for the guidance, encouragement, camaraderie, publications, employment, and intellectual back-and-forth that I shared with my advisor, Jason LaBelle. Jason was very generous to share resources from the Center for Mountain and Plains Archaeology (CMPA) and the Jim and Audrey Benedict Fund for Mountain Archaeology during my time at CSU. I am especially amazed at Jason's ability to balance the professional growth of his students while also maintaining his own very inspiring career. He has been a wonderful role model. At a critical moment towards the end of my Ph.D. experience, Jason reminded me of my true passions and dreams, and I will be forever in his debt for bringing me back into the fold. I am looking forward to continuing our friendship in the years to come.

I do not think I would have completed this dissertation without the continuous support of my partner, Michelle Dinkel. She handled my demanding adventures in the field, lab, and digital worlds with poise, she accepted my frequent dissociations while thinking about archaeological things, and she never stopped believing in my future. She also helped me work through ideas as I frantically shouted them aloud from my office on a routine basis. She kept us afloat as a stably employed CRM archaeologist while I ebbed and flowed over different jobs and projects over the past five years. I will be repaying her kindness for as long as I possibly can.

I was lucky to have a field project for my dissertation, made successful by the efforts of several field crews. Graduate students who served in the field as leaders, crew members, and

friends include Ray Sumner, Spencer Little, Erika Brooks, Kim Biela, Mary Mitchell, Bob Madden, Aleah Kuhr, and Kayla Rohde. A special thank you goes to William Kane and Spencer Little, who were always the first to reach out with a helping hand. Another special thanks to my "frozen crew" who took the brunt of an anonymously cold couple of days in the Valley, including Michelle Dinkel, Bryn Sullivan, Caden Hooker, Autumn Haas, Aleah Kuhr, Caeli McCusker, and Mink Damrongsang – but we had a hot spring nearby, so it was OK. Lastly, thank you to the two amazing field school crews in 2021 and 2022 who helped us accomplish an incredible survey task – involving 32 undergraduate and graduate participants.

A few individuals provided context and insight to the Smithsonian artifact collection – including Pegi Jodry (Smithsonian Institution) and Marcel Kornfeld (University of Wyoming), whom I thank for sharing their experiences, notes, photos, and support. To me, 1979 and 1983 looked the best time to be in the Valley – and I am forever jealous of the fun they had at Reddin and elsewhere. Jan and Len Carpenter, the family of Gordon Reddin, enriched our field efforts by visiting the team in action during the 2022 field school – and I am thankful for their kindness, speaking to students, and sharing stories about life in the local town of Hooper. From the Bureau of Land Management (BLM), Brian Flynn, Natalie Clark, Rochelle Bennet, and Bridget Weiner helped pave the way for this project – as did Fred Bunch from the Great Sand Dunes (GRSA). Undergraduate students from my ANTH 461: Report Preparation class (Riley Limbaugh, Izzy Dones, William Kane, Alyssa Melkus, and Karlie Dorland) assisted with inventorying the collection. Jeannine Pederson-Guzman, while at AR-CSU, assisted Jason and myself with securing an agreement to curate the collections at CSU for research, and I am thankful for that effort.

There are also several people who simply shared the right words, support, encouragement, and interest at exactly the right time while I was working on this project or near the end of it –

Larry Todd, Marilyn Martorano, Todd Surovell, Spencer Pelton, and Paul Buckner. I would like to include my dissertation committee members in this category as well (Jason LaBelle, Michael Pante, Mary Van Buren, and Ben Shaby), who provided insightful feedback on this dissertation and useful suggestions during the finalization of this document. I would like to extend a final general thank you to Mica Glantz for her care throughout my graduate training and for giving shrewd reviews of my work over the years – and to other CSU Department of Anthropology and Geography faculty and instructors who have been part of my degree(s) from beginning to end and never wavered in the support of my goals.

DEDICATION

This dissertation is dedicated to Myrna C. Meyer (1938-2023) and Dr. William (Tim) Meyer (1940-2024), my grandparents. I owe much of my competitive spirit and resolve to these two individuals who excelled in so many things and travelled far in the world.

TABLE OF CONTENTS

ABSTRACT ii
ACKNOWLEDGEMENTS iii
DEDICATION vi
LIST OF TABLES ix
LIST OF FIGURES xii
CHAPTER 1 - INTRODUCTION 1
Moving with Folsom: Past and Present 5
The Reddin Problem 14
Organization of the Dissertation 16
CHAPTER 2 - BACKGROUND 17
San Luis Valley 17
Closed Basin 22
Climate, Hydrology, and Vegetation 23
Paleoclimate 28
A Legacy of Folsom Research 31
Folsom on the Valley Floor 36
Alamosa Cluster 37
Saguache Cluster 40
Reddin Environment 42
CHAPTER 3 - FIELDWORK 45
Smithsonian Institution 1979-1983 46
Survey Grid 50
Artifact Plotting 54
Block Excavation 58
Backhoe Trenches 60
Supplementary Field Work 63
CSU 2020-2022 64
Retracing the Smithsonian 65
UAV Survey 66
Inventory Surveys 69
Locality A Survey 74
Summary 79
CHAPTER 4 - LITHICS 80
Lithic Raw Materials 81
The Closest Stone – 150 km 84
Far Away Stone – 300 km 89
Exotic Stone – Over 300 km 90
Folsom 93
Projectile Points 93
Preforms and Channel Flakes 107
Other Lithics 116
Cores and Bifaces 118

Flake Tools 122
Debitage 132
Summary 138
CHAPTER 5 - SPACE AND TIME 141
Spatial Data Woes 143
Part 1: Finding Folsom 149
Methods 154
Results 161
Cluster Sensitivity Analysis 164
Part 2: Measuring Folsom 172
Methods 174
Results 181
Part 3: Connecting Folsom 185
Methods 185
Results 191
Stipulations 196
Modeling a Palimpsest 197
Summary 201
CHAPTER 6 - CONCLUSION 203
Final Remarks 208
REFERENCES CITED 210
APPENDICES 231
Appendix A – Lithic Descriptive Coding 232
Appendix B – Lithic Metric Coding 236
Appendix C – Folsom Lithics 239
Appendix D – Post-Folsom Diagnostic Artifacts 276
Appendix E – Other Stone Tools 292
Appendix F – Debitage 309
Appendix G – Faunal Remains 340
Appendix H – Excavated Debitage 342
Appendix I – Folsom Geochemistry 344

LIST OF TABLES

Table 1. List of 40 Folsom sites in the Great Plains, Rocky Mountains, and American Southwest. See figure 3 for site locations..... 5
Table 2. San Luis Valley climate summary for eight weather stations located on the valley floor and foothills of the Closed Basin subarea (Western Regional Climate Center 2024). 24
Table 3. Summary of stream discharge for major water courses in the Closed Basin subarea (average annual acre-feet rounded to the nearest 100 acre-feet). Data compiled from Harmon (2020:table 7.1). Periods of record unreported. Data listed in order of highest contribution to groundwater discharge per mountain range source. 27
Table 4. Published radiocarbon (14C), optically-stimulated luminescence (OSL), and infrared-stimulated luminescence (IRSL) dates from the Mr. Peat site (Schumann and Machette 2007) and the Scott Miller paleowetland (Beeton 2014). Radiocarbon dates recalibrated in this study using IntCal 2020 in OxCal v.4.4.3 (Bronk Ramsey 2009; Reimer et al. 2020). Dates rounded to the nearest 10 years..... 31
Table 5. Summary data for Office of Archaeology and Historic Preservation (OAHP) file search. File search completed in May 2022 for Folsom resources in Alamosa, Conejos, Costilla, Hinsdale, Mineral, Rio Gande, and Saguache County, Colorado. 35
Table 6. Assemblage summary data for Folsom resources in the Alamosa Cluster and Sagauche Cluster, San Luis Valley, Colorado. 38
Table 7. CSU 2021 field school survey data matrix organized by blocks with expected debitage counts vs. other variables of interest (piece-plotted tools, sand cover, and vegetation cover). 72
Table 8. CSU 2022 field school survey data matrix for Locality A, including binned cells with low-to-high debitage counts vs. survey cover variables (plotted tool frequency, survey time, sand cover, dune height, and vegetation cover). 78
Table 9. Lithic raw material sources or general rock types identified in the Reddin lithic assemblage. 84
Table 10. Folsom point lithic sources at Reddin, based on Jodry (1999b:table 6-7) and the combined sample based on CSU fieldwork and reanalysis of the Smithsonian artifact collection. 94
Table 11. Summary data for Folsom point width and thickness measurements (mm) from the Reddin site. Sample based on the combined collections of CSU and the Smithsonian.. 100
Table 12. Folsom point fragment type matrix summarizing Meltzer and Eren (2021:figure 12.3) breakage classes and portions classified in this study. Sample based on the combined collections of CSU and the Smithsonian (n=241 fragments out of 225 total points). 103
Table 13. Summary of observations for impact damage and burning alterations for Folsom point fragments (n=235 fragments out of 225 total points) from the Reddin site. Sample based on the collections of CSU and the Smithsonian..... 104
Table 14. Folsom preform and channel flake lithic sources, based on Jodry's (1999b:table 6-7) published counts of Folsom artifacts and the combined CSU and Smithsonian samples reanalyzed for this study. 110
Table 15. Folsom preform fragment type matrix summarizing Meltzer and Eren's (2021:figure 12.4) breakage classes and portions classified in this study, based on the complete sample

of 110 preforms. Channel flakes included (n=357). Samples based on the combined collections made by CSU and the Smithsonian. 112
Table 16. Summary of basic width and length variables for all Folsom diagnostic artifacts (preforms, channels, and complete points), based on the combined sample from CSU and the Smithsonian collection. 114
Table 17. Core tool summary data from the Reddin site, including specimens collected by the Smithsonian and CSU field crews. 120
Table 18. Biface fragment damage and metric data summary from the Reddin site, based on the combined sample from CSU and the Smithsonian collection. 122
Table 19. Representative lithic sources for cores and bifaces from the Reddin site, based on the combined sample from CSU and the Smithsonian collection. 122
Table 20. Representative lithic sources in retouched and utilized flakes from the Reddin site, based on the combined sample from CSU and the Smithsonian collection..... 125
Table 21. Retouched (n=116) and utilized flake tool (n=45) damage and metric data summary from the Reddin site, based on the combined sample from CSU and the Smithsonian collection. 125
Table 22. Representative lithic sources represented in end scrapers and gravers from the Reddin site, based on the combined samples from CSU and the Smithsonian collection. 129
Table 23. End scraper (n=66) and graver tool (n=34) damage and metric data summary from the Reddin site, based on the combined samples from CSU and Smithsonian collection.... 130
Table 24. Lithic sources represented in debitage from Reddin, based on Smithsonian site inventory and CSU's fine-grained surveys within Locality A (see chapter 3). 134
Table 25. Summary of Smithsonian (1979-1983) debitage attributes recorded in this study, organized by raw material. The majority of debitage, not accounted for here, include non-cortical, incomplete, and unburned flake fragments or angular debris. 135
Table 26. Summary of CSU Locality A (2022) debitage attributes recorded in this study, organized by raw material. The majority of debitage, not accounted for here, include non-cortical, incomplete, and unburned flake fragments or angular debris. 136
Table 27. Supplemental mass analysis of a sample of 505 obsidian flakes from the Reddin site, based on the Smithsonian survey collection. 137
Table 28. Summary of chipped stone tools and different levels of provenience based on field methods. 144
Table 29. Summary of quadrat test null and alternative hypotheses, including expectation, potential results, and outcomes for interpretation. 160
Table 30. Tool summary data for clusters identified using the inhomogeneous goodness-of-fit test in quadrat tiles. 163
Table 31. Debitage summary data for camp clusters identified using the inhomogeneous goodness-of-fit test in quadrat tiles. 164
Table 32. Summary results of the random thinning resampling analysis on cluster detection. .. 168
Table 33. Summary results of kernel bandwidth sensitivity analysis, for 200 simulations of 20 different iterations of varying bandwidths in the null model calculation. 171
Table 34. Summary of concepts related to measuring time based on the accumulation of artifacts, following Surovell (2009) and this study. 173
Table 35. Summary of null and alternative hypothesis for the test of mean per capita occupation span measured across each of the Folsom camp shatter concentrations. 181

Table 36. Ratios of debitage to transported tools and burned artifacts to unburned artifacts from Folsom camp shatter concentrations at the Reddin site. 182
Table 37. Simple linear regression output summary statistics. 182
Table 38. Quantities of unique nodules per lithic raw material type, summarized by Folsom artifact. 189
Table 39. Summary of newly identified conjoining artifact pairs at the Reddin site, including measured distances between connecting artifacts. 192
Table 40. Summary of non-Folsom quadrat test null and alternative hypotheses, including expectation, potential results, and outcomes for interpretation. 197

LIST OF FIGURES

Figure 1. Illustration inspired by the original Folsom discovery in New Mexico. Inset map on the right is based on the 1928 AMNH excavations (Meltzer 2006:figure 7.1). 3
Figure 2. Generalized map of major deposits excavated at the Lindenmeier Folsom site in northern Colorado. Ellipses depict the relative scale of major excavation areas. 3
Figure 3. Map showing the geographic extent of the Folsom tradition (dashed line) and a sample of 40 sites in the core of the Folsom spatial distribution. Numbered sites correspond to table 1. 7
Figure 4. Map of excavations at the Stewart's Cattle Guard site modified and adapted from Jodry (1999a:figure 83, figure 94, figure 95). 11
Figure 5. Map of rocks larger than 40 cm and best-fit ellipse for a Folsom residential structure in Block C at the Mountaineer Folsom site, based on Jayalath 2013 (top row). Folsom structures and surface concentrations at Locality B of the Barger Gulch site, based on Surovell 2022 (bottom row). 12
Figure 6. Site size (measured in square meters) vs. the quantity of diagnostic Folsom lithic artifacts (points, preforms, and channel flakes) for sites listed in table 1. 15
Figure 7. Structural basins map of the Rio Grande Rift Zone, ranging from northern Colorado to Chihuahua, Mexico. Map image adapted and altered from Kirkham and McGee (2020:figure 1.10). 19
Figure 8. Physiographic map of the San Luis Valley, including portions within southern Colorado and northern New Mexico. Map shows major named mountain ranges, the mainstem of the Rio Grande River, and Valley floor subdivisions. 20
Figure 9. Hydrological map of the northern San Luis Valley and Closed Basin subarea. Prominent lakes (blue) and emergent wetland resources (cyan) are depicted. Labeled locations are discussed in the text. 26
Figure 10. Map of Folsom resources (sites and isolated finds) within the Alamosa and Saguache clusters in the Closed Basin. 37
Figure 11. Surficial geology map of the Saguache Folsom Cluster area, depicting Quaternary deposits mapped by Ruleman and Brandt (2021). From oldest to youngest, the deposits include QTla (Alamosa Formation lacustrine clays, mid-Pleistocene), Qao3 (older alluvium, mid-Pleistocene), Qai (intermediate alluvium, mid-to-late Pleistocene), Qeo (older eolian sand sheet/dunes, mid-to-late Pleistocene), Qay (younger alluvium, late Pleistocene), Qey (younger eolian sand sheet, Holocene), Qa (undivided Holocene alluvium). Previously recorded (black) and unrecorded (red) sites depicted. 41
Figure 12. Topographic map of the Reddin site near the La Garita Creek floodplain modeled from open-access LiDAR tiles, showing the outline of CSU's 2021 surface survey grid at the site. Oriented to magnetic north with 10 cm contour intervals. 44
Figure 13. Dennis J. Stanford setting the survey grid at the Reddin site in August 1983. Photo slide courtesy of Margaret A. Jodry (Pegi) and the Smithsonian Institution. 46
Figure 14. University of Wyoming field school instructors Mary Lou Larson (right) and Marcel Kornfeld (left) in 1983. Photo slide courtesy of Pegi Jodry and the Smithsonian Institution. 48

Figure 15. Middle Rio Grande Folsom archaeologist Jerry Dawson (left) and unidentified field school student from the University of Wyoming (right) in 1983. Photo slide courtesy of Pegi Jodry and the Smithsonian Institution. 49
Figure 16. Adapted and colorized map of Folsom tools and debitage at the Reddin site presented by Jodry (1999b:figure 6-11). The map depicts results from the 1979 field season, but not the 1983 field season. Site grid scale in meters. 52
Figure 17. Map of the survey grid at Reddin showing 30 by 30 m grid cells with positive counts of debitage (gray squares), based on Smithsonian 1979-1983 artifact collection. 53
Figure 18. Image depicting an example of a field specimen collection envelope, showing artifact labels and provenience information. 56
Figure 19. Map of all piece-plotted chipped stone tools in the Smithsonian artifact collection (n=359), based on 1979-1983 fieldwork. Blocks selected for fine-grained surveys and 100 percent mapping in 1983 also shown. 57
Figure 20. Map of known excavation areas at the Reddin site. The approximate location of the Cheyenne Trench is depicted (dashed square). 59
Figure 21. University of Wyoming field school students shovel skimming the sand sheet at the Reddin site in 1983. Photo slide courtesy of Pegi Jodry and the Smithsonian Institution. 60
Figure 22. Dennis Stanford (left) and backhoe operator (right) in the Cheyenne Trench in 1983. Photo slide courtesy of Pegi Jodry and the Smithsonian Institution. 62
Figure 23. Dennis Stanford denoting what appears to be thin evaporite strata in the profile wall of the Cheyenne Trench in 1983. There are no profile descriptions of the stratigraphy in this trench or other units at the site. 63
Figure 24. Visualization of the UAV photogrammetric flight process, including the serpentine UAV flightpath design and image sensor overlap. 68
Figure 25. Example of a classified hillshade raster from Reddin, based on UAV orthoimagery collected in 2020. The map shows vegetation (green), sand cover (brown), and hardpan blowouts (tan). The west and east playa pond depressions are depicted here. 69
Figure 26. CSU's 2021 field school crew members resetting the Smithsonian survey grid corners. 71
Figure 27. Map series depicting estimated debitage frequences based on the 2021 CSU field survey (upper left), approximate distribution of sand cover (upper right), approximate distribution of vegetation cover (lower left), and time spent surveying in each block (lower right). Plotted tools from the 2021 field season shown (crosses). 73
Figure 28. Depiction of Locality A surface survey grid and inset location map (upper right). Mapped tools depicted (black crosses). Positive 1 x 1 m survey units displayed in the background. 76
Figure 29. CSU's 2022 field school crew conducting an intensive survey of Locality A. 76
Figure 30. Map series depicting several surface cover variables based on CSU's 2022 field work in Locality A, including debitage frequency in 1 x 1 m units (top left), debitage frequency summarized in 5 x 5 m cells (top right), approximate sand cover (middle left), approximate dune height (middle right), approximate vegetation cover (lower left), and time spent surveying in each cell (lower right). 77
Figure 31. Map showing distance bandwidths from the Reddin site and major lithic raw material sources with known provenience discussed in this study; 1) Trout Creek, 2) Trickle Mountain, 3) Mosca, 4) Cumbres Pass, 5) Taos Plateau volcanic rocks, 6) Jemez

Mountains (Cerro Pedernal, El Rechuelos, Cerro del Medio, Cerro Toledo), 7) Flattop Butte, 8) Narbona Pass, 9) Soccoro, 10) Edwards Plateau. 83
Figure 32. Aerial photo of the Trout Creek Pass area near the location of the 5CF84 jasper quarry. 85
Figure 33. Map of major volcanic domes and shield volcanoes on the northern Taos Plateau. Note the location of Newman Dome and San Antonio Mountain as major sources of archaeological dacite. 88
Figure 34. Selected Folsom lithic materials. Trout Creek (top row), silicified wood (SI-PP-1049), Mosca (SI-PP-1057), Cumbres (CMPA-PP-1038), Trickle Mountain (SI-PP-1076), Morrison (SI-PP-1064), andesite (SI-PP-1133), Pedernal (SI-PP-1021), Jemez obsidian (SI-PP-1134), Narbona (SI-PP-1023), Flattop (SI-PP-1025), and Edwards (SI-PP-1020, CMPA-PP-1017). 95
Figure 35. A sample of classically manufactured Folsom points from the Reddin site, including fluted and ground bases (top row) and lateral splits (bottom row). 96
Figure 36. Sample of non-classic Folsom points from the Reddin site, including pseudo-fluted miniatures (CMPA-PP-1046 and SI-PP-1180), double-fluted point (SI-PP-1035), point fluted on one face only (SI-PP-1019), and point with a reverse flute on one face only (SI-PP-1048) – which is possibly a rebased preform tip. 98
Figure 37. Sample of Midland or unfluted Folsom points from the Reddin site, including examples with collateral flaking and fine lateral edgework. 98
Figure 38. Histogram showing the distribution of the intact (complete) sample of width measurements for Folsom points (n=58 out of 225 points) from the Reddin site. 101
Figure 39. Folsom (and Midland) projectile point fragment codes schematic, adapted and modified from Meltzer and Eren (2021:figure 12.3). 103
Figure 40. Example of impact damaged (burin spall tip) Folsom projectile point from Reddin (top row) and burned (crazed) projectile point (bottom row). 106
Figure 41. Sample of Folsom preform biface fragments and broken channel flakes from the Reddin site. 109
Figure 42. Folsom preform fragment codes schematic, modified and adapted from Meltzer and Eren (2021:figure 12.4). 112
Figure 43. Box plot of all Folsom point fragment lengths (a), point widths (b), preform lengths (c), preform widths (d), channel flake lengths (e), and channel flake widths (f). Note the similarity in fragment size for all artifacts, no matter the measurement axis or artifact type. 115
Figure 44. Example of a recycled double-fluted channel flake with a graver tip from the Reddin site. 115
Figure 45. Generalization of the non-diagnostic lithic artifact classification scheme used in this study. 117
Figure 46. Logged values of maximum tool length vs. the cumulative sum of modified edge length for flake tools at the Reddin site – retouched flake tools (black) and utilized flakes tools (white). 124
Figure 47. Representative sample of retouched flake tools exhibiting evidence of flake blank reduction from bifacial cores. 125
Figure 48. Representative sample of end scraper tools from the Reddin site, showing disto-lateral retouch morphology. 128
Figure 49. Representative sample of gravers from the Reddin site. 128

Figure 50. Histogram summarizing rejuvenation potential in the sample of end scrapers from the Reddin site. The index is a measure of the distance between the point of maximum thickness and the distal end divided by total end scraper length. Values closer to zero represent less rejuvenation potential. 132
Figure 51. Schematic of the simulation routine used to randomly generate precise locations for artifacts with block-level survey provenience: a) potential simulation bandwidth based on a large value of rjitter, b) potential simulation bandwidth based on a lower value of rjitter. Simulated locations shown in blue. 146
Figure 52. Summary plot of rjitter simulation routine for artifacts lacking precise coordinates, depicting objects with real piece-plot provenience used to model the intensity lambda (black, +), survey block corners with unmapped tools (red, +), excavation unit corners with unmapped tools (green, +), and all simulated locations of artifacts lacking original coordinates (blue, +). 148
Figure 53. Summary figure showing the number and proportion of all simulated artifacts in each survey block (left panel) and total plotted artifact counts per survey block (right panel). The sample of simulated artifacts amounts to roughly 23% of the total sample. 149
Figure 54. Generalized depiction of major artifact concentrations and intercluster distances at a sample of single occupation Folsom sites (top row) and multiple occupation Folsom campsites (bottom row)..... 151
Figure 55. Simulated realizations of archaeological debris patterns diffused over sequential timesteps (a-b). The pattern in black represents an intensive residual process as described in text, and the pattern in red represents debris from a second less-intense occupation. Diffusion rates vary randomly at each timestep. 153
Figure 56. Effects of changing perspective on spatial interpretations, including a) fine-grained perspective (p) on a diffused process, and b) broad-perspective (p) on the diffused process..... 153
Figure 57. Kernel density plots of Folsom artifacts using Scott's Rule for adaptive bandwidths, showing projectile points (a), preforms (b), channel flakes (c), and the combined dataset (d). 156
Figure 58. Simulated realizations of a uniform point pattern representing Complete Spatial Randomness (a), and a simulation of an inhomogeneous Poisson process with the same intensity as all Folsom artifacts at Reddin. 159
Figure 59. Hypothetical demonstration of quadrat test goodness-of-fit method, showing observed counts (upper left in cell), expected counts (upper right in cell), and residuals (low center in cell). The image on the left depicts a test of Complete Spatial Randomness with uniform variance in expected counts (a). The image on the right depicts the quadrat expectations under the assumption of an inhomogeneous Poisson process using the variable density of all artifacts. 159
Figure 60. Modeled results of the goodness-of-fit test of the inhomogeneous Poisson process for Folsom camp shatter artifacts. Local quadrat tiles with standard residuals above 1.96 represent camp clusters (outlined in red). 162
Figure 61. Kernel density map showing distribution of camp shatter artifacts (white crosses) and significant quadrat tiles from the goodness-of-fit test. Individual concentrations labeled for reference. Adaptive bandwidth selection based on Scott's Rule. 163
Figure 62. Examples of simulation results for a single run of random thinning in the camp shatter dataset – for intervals at 25% random thinning (0.75), 20% thinning (0.80), 15% thinning

(0.85), 10% thinning (0.90), and 5% thinning (0.95). Note the consistency between original results and the 5% thinning interval. 166
Figure 63. Four-panel box plots summarizing 10 simulations of the random thinning sensitivity analysis across each of six iterations in random thinning – including 75% data retention (thinned by 25%), 80% retention, 85% retention, 90% retention, 95% retention, and no thinning. 167
Figure 64. Examples of simulation results for different iterations of varying KDE bandwidths at fixed intervals for null model calculation (resampled by 5%). The sigma values represent fixed kernel bandwidth distances. 169
Figure 65. Summary results of mean output values for 200 simulations of fixed KDE bandwidth variance used in the sensitivity analysis. Note how cluster detection and p-value variance increase until the "elbow" between 40 and 50 m. The Scott's Rule label represents the maximum value of the adaptive bandwidth used in the original analysis of the study... 170
Figure 66. Graphs of assumed artifact discard relationships between *class a* and *class b* artifacts over time, adapted from Surovell (2009:figures 3.3 and 3.4). Cumulative *class a* and *class b* artifacts discarded over time (a), ratio of *class b*:*class a* artifacts over time (b), ratio of *class a*:*class b* artifacts over time. 176
Figure 67. Distribution of burned artifacts, including plotted tools (a) and simulated locations of burned debitage using the *rjitter* method. Kernel density estimates based on Scott's Rule for adaptive smoothed intensity. 180
Figure 68. Scatterplot and best-fit line of the simple linear regression used to model mean per capita occupation span for eight out of 14 identified Folsom camp shatter concentrations at the Reddin site. 183
Figure 69. Examples of different possible nodule groups for individual lithic raw material types, including Trout Creek jasper (a), Cumbres Pass chert (b), Cerro Pedernal chalcedony (c), Trickle Mountain quartzite (d), and Mosca Creek chert (e). Images based on CMPA lithic raw material comparative collection. 190
Figure 70. Conjoining artifact groups of projectile point fragments from the Reddin site, including previously identified specimens lacking provenience (top row) and newly identified pairs between artifacts found by the Smithsonian (1979, 1983) and CSU (2020-2022) (bottom row). 192
Figure 71. Generalized map of Folsom camp clusters depicting camp shatter (red +) and kill shatter (blue +), with conjoin pair distances. 194
Figure 72. Diagnostic plots of the goodness-of-fit test for the inhomogeneous Poisson process representing post-Folsom artifacts (n=100): smoothed kernel density map of post-Folsom artifacts (a), smoothed kernel density map of Folsom camp shatter (b), modeled quadrat test results, showing significant tiles in green (c). 199

CHAPTER 1 - INTRODUCTION

If you ask someone to picture a significant archaeological site from the Paleoindian period, I guarantee they will not imagine a surface scatter of stone tools. Many expect the oldest sites in North America to be deeply buried with other markers of profound antiquity, such as the remains of extinct animals or plant fossils from ancient ecosystems. The oldest archaeological sites are supposed be neatly situated in stratigraphic layers summarizing cultural and environmental changes over deep time. The truth is that most archaeological sites do not meet this expectation. Many ancient sites rest plainly on the ground surface, lacking distinct stratigraphic separations between materials from different periods. Whether such sites are significant depends entirely on perspective and the questions being asked – a topic this dissertation will address.

Between 1926 and 1928, excavators from the Colorado Museum of Natural History (now, the Denver Museum of Nature & Science) and the American Museum of Natural History (AMNH) made a significant discovery at the Folsom site in northern New Mexico (Meltzer 2006). The team was mining a fossil locality in a deep-set arroyo of the Dry Cimarron River for the remains of *Bison antiquus* (a species of buffalo dated to the late Pleistocene) in the hopes of filling display cases for the museum. In the process, they uncovered several large stone dart points made by human hands, each with an emblematic fluted design that would later define the Folsom culture and technological tradition (figure 1). The Folsom points were found in direct association with ancient bison skeletons, suggesting an unequivocal relationship between a very early population of hunter-gatherers in North America and an extinct species of megafauna. Confirmation of the site's authenticity and age by then-prominent archaeologists (Frank Roberts, AV Kidder) and paleontologists (Barnum Brown) dealt the final blow in a hotly debated argument about the

antiquity of the peopling of the Americas – indigenous people lived in the North American interior at least 10,000 years ago (Meltzer 1983, 1994).

The story at Folsom enamored the archaeological community and paved the way for a new theme in the discipline, Paleoindian archaeology – the study of the first peoples in the New World. In the subsequent decades Paleoindian archaeology grew and grew (Hofman 2002; Meltzer 2006), and the Folsom site served as the archetype. The investigations painted a clear picture; at Folsom, a small band of hunter-gatherers trapped several dozen bison in an arroyo system measuring a few hundred feet in size and butchered them using a small lithic toolkit made primarily of stone sourced hundreds of kilometers away. More recent excavations at Folsom confirmed these details with enhanced resolution and determined that Folsom people occupied the site for a short duration, never to return (Meltzer 2006). Many Folsom localities discovered over the past century exhibit similar evidence as the "type site", suggesting Folsom people were highly mobile as they transported small stone toolkits across great distances and focused their pursuits on bison herds (Amick 1996; Andrews et al. 2008; Bement 2003; Hofman 2002).

Ironically, the second Folsom site ever excavated (1935-1940) did not meet the standards set by the Folsom site in New Mexico (LaBelle and Meyer 2021). The investigations at Lindenmeier, located 25 km north of Fort Collins, Colorado, revealed a complex arrangement of deposits spanning across an ancient valley system (figure 2). The location of the deposits at the site varied, ranging from deeply stratified layers to shallowly buried and wide surface expressions (Haynes Jr. 2003; LaBelle and Meyer 2021; Sellet 2013; Wilmsen and Roberts Jr. 1978).

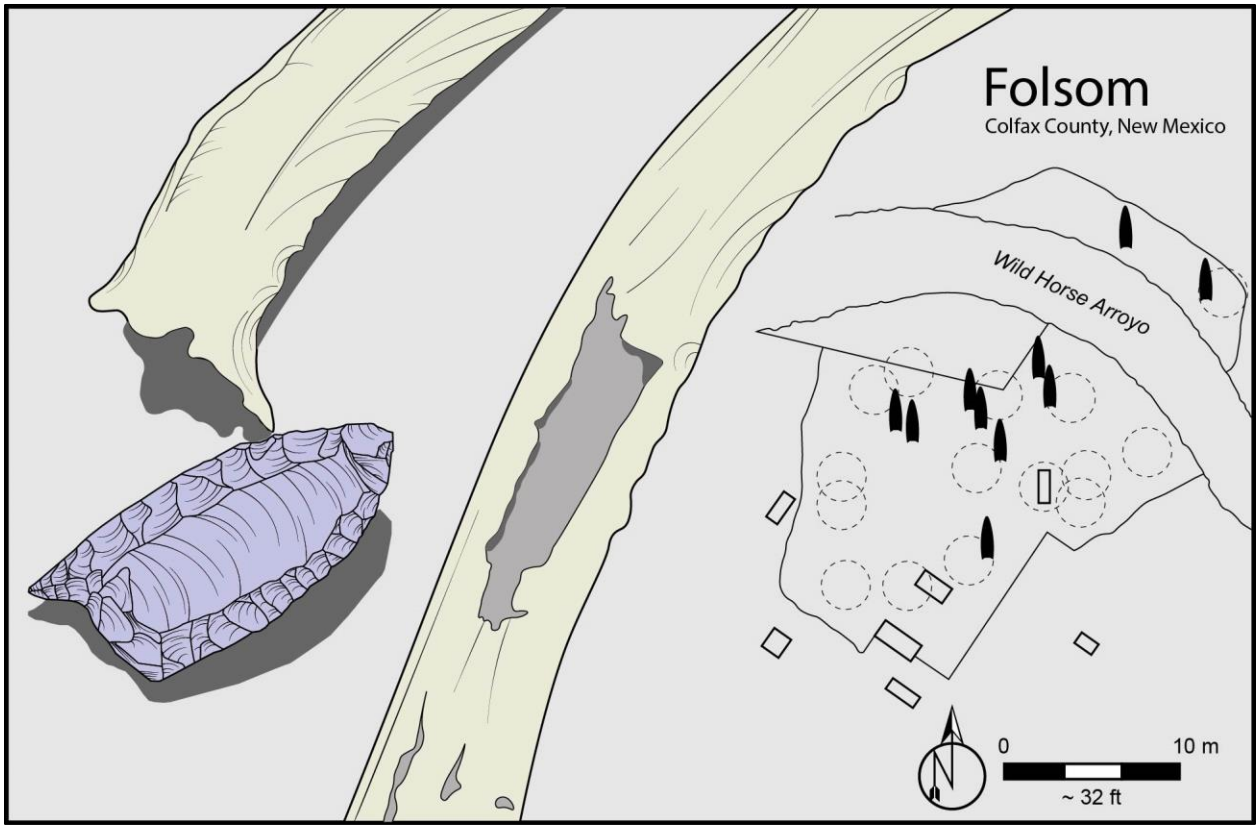


Figure 1. Illustration inspired by the original Folsom discovery in New Mexico. Inset map on the right is based on the 1928 AMNH excavations (Meltzer 2006:figure 7.1).

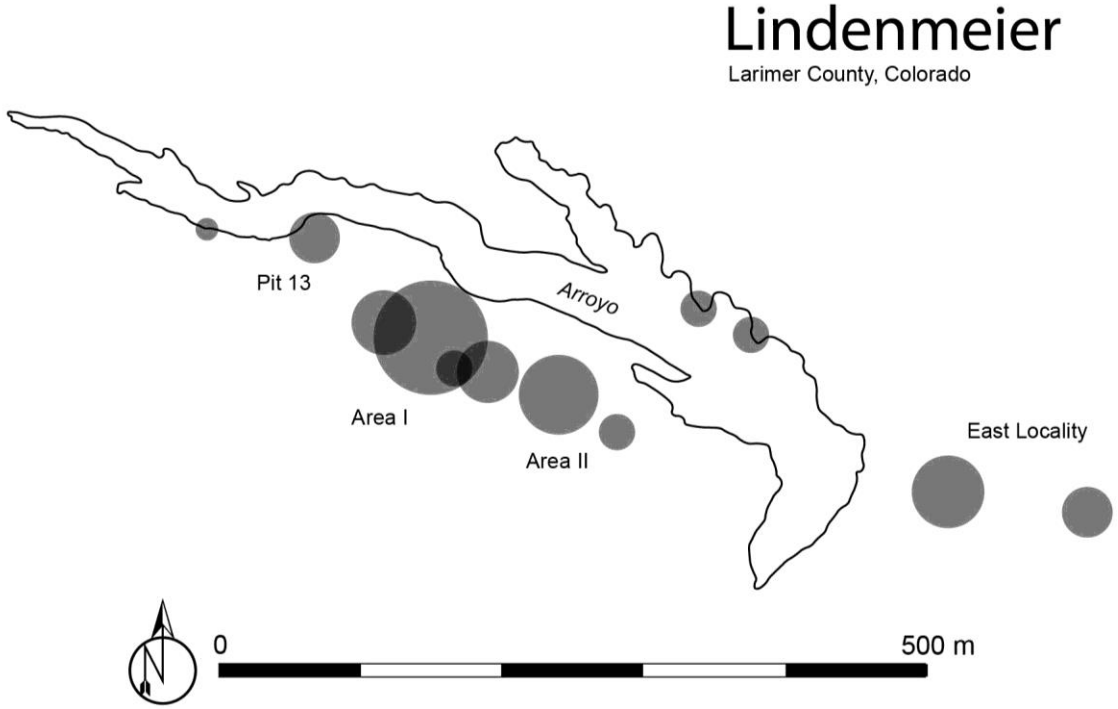


Figure 2. Generalized map of major deposits excavated at the Lindenmeier Folsom site in northern Colorado. Ellipses depict the relative scale of major excavation areas.

Lindenmeier contained artifacts that you would not expect at a bison kill, including mobile artwork like incised bone discs, hematite abraders and beads, bone needles for sewing, and a highly diverse lithic toolkit made for accomplishing tasks other than hunting (LaBelle and Newton 2010; Lyman 2015; Roberts Jr. 1935, 1936). In some places, the site's excavators saw the remains of small hearth features associated with items expected in a residential campsite. In other places, the crew found dense concentrations of articulated bison bone indicating a primary hunting area, though modest in size. Lindenmeier appeared to include other facets of hunter-gatherer settlement behavior that the Folsom site in New Mexico did not express (LaBelle and Meyer 2021), but archaeologists still do not know the complete story of what happened there. It may have been a place that people visited routinely to hunt bison (Roberts Jr. 1936), a place to meet other bands for trading and social connection (Wilmsen 1974), a long-term residence used by one or more large hunter-gatherer groups, or possibly a combination of these scenarios (LaBelle and Meyer 2021; Sellet 2013). Whatever the case, Lindenmeier did not appear to represent the average Folsom settlement system – to archaeologists, it seemed more unique than normal.

How much does site size matter? In the context of Folsom sites, the last several decades of published research show that archaeologists remain interested in this variable on two fronts – 1) assemblage size, and 2) the spatial extent and configuration of deposits. This *Lindenmeier effect* on research topics has much to do with the skewed nature of the Folsom record (Andrews et al. 2008; Hofman 1999, 2002; LaBelle 2012; Surovell 2009). Most sites are spatially small and contain a limited number of artifacts. A much smaller sample of sites, like Lindenmeier, includes unique markers of a different kind of land use system based on unexpectedly high numbers of artifacts spread across wide horizontal areas (table 1). Researchers have made significant strides to contextualize the latter sample of sites in recent years (Andrews et al. 2021; LaBelle and Meyer

2021; Morgan 2015; Sellet 2013), using new theories about mobility systems and advanced spatial modeling techniques, but there are still missing pieces of the Folsom puzzle.

Table 1. List of 40 Folsom sites in the Great Plains, Rocky Mountains, and American Southwest. See figure 3 for site locations.

Site	Size (ha)	Function	Projectile Points	Preforms	Channel Flakes	Total	Reference
Agate Basin[1]	0.19*	Kill-Camp	5	23	122	150	Sellet 2004
Adobe[2]	0.001	Camp	1	0	0	1	Hofman and Ingbar 1988
Barger Gulch[3]	0.02	Camp	24	25	163	212	Surovell 2022
Black Mountain[4]	0.02	Camp	4	6	0	10	Jodry 1999a
Blackwater Draw[5]	10.59*	Kill-Camp	26	16	69	111	Boldurian 1990
Bobtail Wolf[6]	2.13*	Camp	10	3	10	23	Root 2000
Boca Negra Wash[7]	0.13	Kill-Camp	7	5	47	59	Holliday et al. 2006
Carter/Kerr-McGee[8]	0.2*	Kill-Camp	1	2	9	12	Frison 1984
Cattle Guard[9]	0.45*	Kill-Camp	211	76	276	563	Jodry 1999a
Cerro Colorado[10]	NR	Kill-Camp	23	8	56	87	Amick 1994
Chispa Creek[11]	9.45*	Camp	69	55	90	214	Seebach 2004, 2011
Cooper[12]	0.01*	Kill	32	0	0	32	Bement 1999
Folsom[13]	0.13*	Kill	28	0	0	28	Meltzer 2006
Gault[14]	32	Camp	5	9	0	14	Lassen 2013
Hanson[15]	0.39*	Camp	25	47	34	106	Frison and Bradley 1980
Hay Gulch[16]	NR	Camp	17	10	10	37	Kornfeld 2013
Hot Tubb[17]	0.05*	Kill-Camp	13	0	3	16	Meltzer et al. 2005
Indian Creek[18]	1.66*	Camp	2	0	6	8	Davis and Greiser 1992
Johnson[19]	0.01	Camp	11	6	31	48	LaBelle et al. 2021
Krmpotich[20]	0.64	Camp	9	11	54	74	Peterson 2001
La Vega[21]	NR	Kill-Camp	6	5	21	32	Amick 1994
Lake Theo[22]	0.54*	Kill-Camp	14	2	0	16	Harrison and Killen 1978
Lindenmeier[23]	9.32*	Kill-Camp	267	352	952	1571	Sellet 2013
Linger[24]	0.71*	Kill-Camp	23	1	2	26	Jodry 1999b
Lipscomb[25]	0.3*	Kill	30	0	0	30	Hofman 1999
Lone Butte[26]	0.63	Camp	29	43	203	275	Amick and Stanford 2016
L. Twin Mountain[27]	0.5	Camp	6	4	35	45	Kornfeld 2013
Lubbock Lake[28]	2.03*	Kill	6	0	0	6	Johnson 1987
Lunas[29]	NR	Camp?	17	43	67	127	Amick 1994
Martin[30]	4	Camp	14	46	148	208	Reitze et al. 2012
Mockingbird Gap[31]	NR	Camp	289	45	86	420	Amick 1994
Mountaineer[32]	17.03*	Camp	66	50	465	581	Andrews et al. 2021
Ojito Spring[33]	NR	Kill-Camp	6	2	15	23	Amick 1994
Powars[34]	NR	Camp?	25	58	186	269	Jodry 1999a
Rattlesnake Pass[35]	0.02*	Kill-Camp	1	0	0	1	Smith and McNees 1990
Reddin[36]	34	Unknown	225	110	357	692	Jodry 1999a; This study
Rio Rancho[37]	4.62*	Camp	36	51	196	283	Huckell and Kilby 2002
Shifting Sands[38]	4.11*	Kill-Camp	92	20	50	162	Hofman et al. 1990
Waugh[39]	0.89*	Kill	2	0	0	2	Hill and Hofman 1997
Zapata[40]	NR	Kill-Camp	12	2	13	27	Jodry 1999b

*Site sizes reported in Andrews et al. (2008):table 1; NR – Not Reported

Moving with Folsom: Past and Present

The Folsom tradition presently dates between 12,845 and 12,255 calendar years ago (hereafter, cal BP) and spans the Intermountain West, Great Plains, and Southwest, though the number of precisely dated localities remains low (Buchanan et al. 2021). This area covers more

than 4 million kilometers, the better portions of 18 U.S. states, slivers of three Canadian territories, and northern Mexico (figure 3). This range includes known sites and isolated finds with fully fluted Folsom projectile points that are dissimilar from other fluted and roughly contemporaneous projectile point traditions such as Gainey, Debert, Cumberland, and Bull Brook (Gingerich 2013, 2018). The density of sites is not homogenous throughout the Folsom territory (Andrews et al. 2008). The best-known sites rest along the central belt of the Rocky Mountains and adjacent foothills, due partially to the long history of research by academic institutions and museums in these regions, but also legitimate spatial patterning of sites which places the Folsom heartland nearer high elevations in the Intermountain West.

Researchers have been investigating the nomadic settlement patterns of Paleoindians since the discovery of the Folsom type site. However, mobility – or the rate, frequency, and distances of residential and logistical movements made by people on the landscape – is not directly observable in the archaeological record. We make inferences about past mobility systems by investigating indirect evidence of other behaviors, such as subsistence practices or technological choices. For example, the consistent presence of bison bone in most well-preserved Folsom sites – including non-hunting specific sites like lithic quarries and residential bases (Andrews et al. 2021; Surovell 2022) – suggests that Folsom hunter-gatherers moved across the landscape in ways that allowed them to take advantage of roaming bison herds (Bement 1999, 2003; Hofman 2002). While bison likely played a significant role in Folsom mobility, people almost certainly made use of other resources as well, given ecological diversity across the entirety of the Folsom range and the nutritional constraints of a bison-focused diet (e.g. Speth 2020).

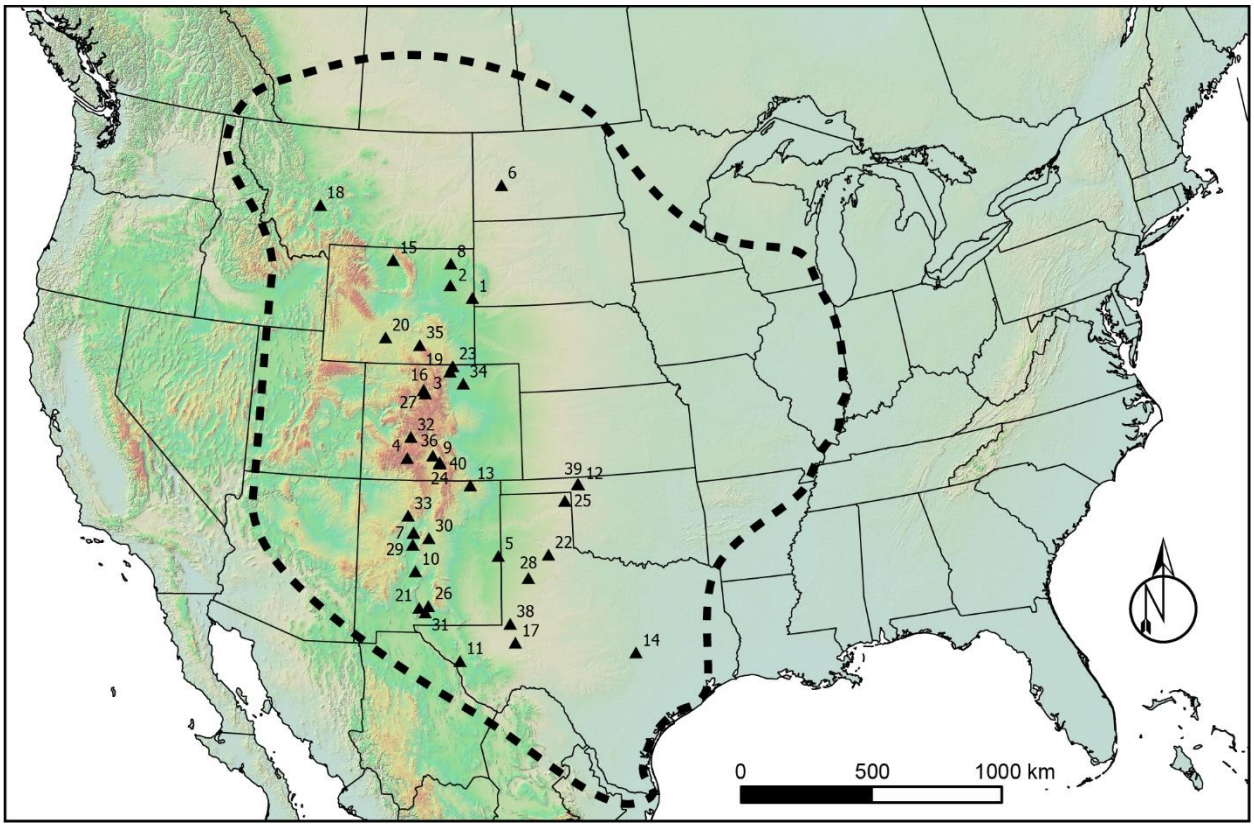


Figure 3. Map showing the geographic extent of the Folsom tradition (dashed line) and a sample of 40 sites in the core of the Folsom spatial distribution. Numbered sites correspond to table 1.

Surovell (2022:4-7) recently compiled a review of Folsom mobility research over the last several decades which focuses on major themes and sites. I condense that context here and provide several additions. Archaeologists started to formalize their models of Folsom mobility in the 1990's. During this era, researchers paid particular attention to lithic raw material sourcing studies combined with a *chaîne opératoire* approach to analysis, focusing on evidence for the manufacture and maintenance of lithic toolkits throughout a settlement area (Amick 1995; Boldurian 1990; Hofman et al. 1990; LeTourneau 2000). Theories about Folsom technological organization drew heavily from the ideas introduced by Kelly and Todd (1988) to describe the Clovis settlement system – an earlier tradition dated between 13,050 and 12,750 cal BP (Buchanan et al. 2022). In the model, hunter-gatherers maximized the utility and longevity of lithic toolkits across wide geographic areas by relying on bifacial cores and flake technologies – a system with extremely

high tool replenishing potential that mitigates the need to restock equipment during foraging rounds. Such a system would be especially attractive to hunter-gatherers that utilized a tethered mobility system linked to a mobile resource base (like Folsom to bison, for example). However, Bamforth (2002) appropriately identified the misapplication of this "high-tech forager" model for Folsom and later Paleoindian culture groups, as did other researchers (e.g. LeTourneau 2000), citing the overall lack of bifacial cores in many sites, the inappropriately singular focus on projectile points as the fulcrum of a technological system, and limited evidence for segmented reduction of raw material stores across samples of sites within a given region – something expected if foragers maximized tool transport efficiency while maintaining toolkits for immediate and anticipated needs.

This era was also the beginning of true site structure analysis at Folsom sites, bolstered by the analogies that ethnoarchaeologists developed in the decades prior as well as emerging quantitative methods (e.g. Kent 1991; Kintigh 1990; O'Connell 1987; O'Connell et al. 1991; Wandsnider 1996). Folsom site structure studies at this time aimed to identify different sorts of activity areas within sites based on spatial analysis of artifacts and features with functional qualities matching what ethnoarchaeologists observed in modern or historical populations. Examples include household debris clusters in residential campsites, gendered work areas such as women's hide working and sewing localities, and primary hunting locales vs. toolkit repair zones (Hofman et al. 1990; Jodry 1999a). The analysis of refit artifacts (artifacts re-connected across reduction stages) and conjoined pieces (broken pieces of artifacts, recombined) played a major role in linking different types of contemporaneous activity areas together within individual campsites, demonstrating the diverse behavioral processes at play during an occupation of a site (Bamforth and Becker 2000; Jodry 1992). In Hofman's (1994) seminal work, he formally

addressed the concept of aggregation in Paleoindian settlement systems and laid out archaeological expectations for identifying evidence that multiple hunter-gatherer bands lived together over an extended amount of time; evidence of aggregation should include "…roughly comparable residential units with associated features (e.g. hearths) and evidence for a wide range of activities. Lithic source studies might provide evidence of distinct raw materials representing sources from different or opposing directions." Hofman (1994:352).

The following era reflects the diverse nature of archaeological theory in the early-mid 2000s and various reactions to previous models of the Folsom settlement system. The high-tech forager model of Early Paleoindian mobility was refined into the ABC model (for Folsom, specifically), after a synthesis of results at two significant sites: **A**gate **B**asin and Stewart's **C**attle Guard (Frison and Stanford 1982; Hofman 2002; Jodry 1999a). Each of the sites contained a large primary bison kill locality, secondary butchering areas, and associated residential campsites with high quantities of exotic (very distant) lithic sources, together indicating an articulated residential system linked to long-range bison hunting – such sites are now referred to as *kill-camps* (figure 4). The results at Stewart's Cattle Guard showed that kill-camps could also serve as places for aggregation as defined by Hofman (1994), introducing the possibility that aspects of the Folsom mobility system revolved around the coordinated schedules of multiple hunter-gatherer bands (Jodry 1999a). Rather than worry about the transport costs of moving food to people, Folsom appeared to move people to food. However, additional sites started to appear in the literature which contradicted the underlying premise of residential mobility in the ABC model. Mountaineer and Barger Gulch, two campsites in the Colorado mountains, yielded evidence of long-term residential behavior without an associated bison hunting locality (Stiger 2006; Surovell 2003). The sites are both found near lithic raw material procurement areas, contain physical or inferred evidence of

residential architecture (winter houses), and lower than typical quantities of non-local raw materials suggesting immense familiarity with local lithic sources (Andrews 2010; Andrews et al. 2021; Morgan 2015; Morgan and Andrews 2016, 2022; Surovell 2022; Surovell et al. 2005; Surovell and Waguespack 2007; Waguespack and Surovell 2014). Figure 5 depicts major architectural characteristics of these Folsom campsites which lack a bison hunting focus near residential spaces.

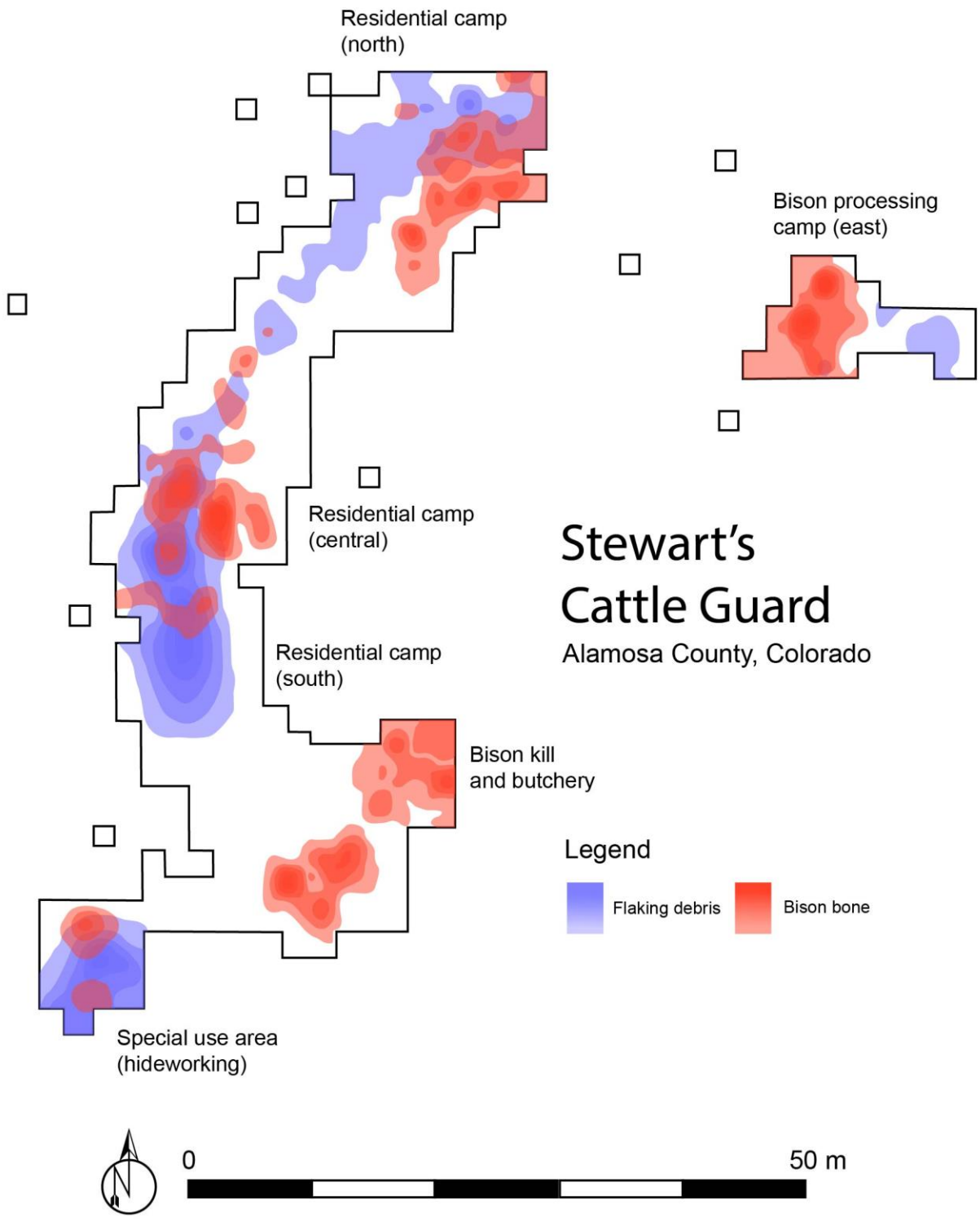


Figure 4. Map of excavations at the Stewart's Cattle Guard site modified and adapted from Jodry (1999a:figure 83, figure 94, figure 95).

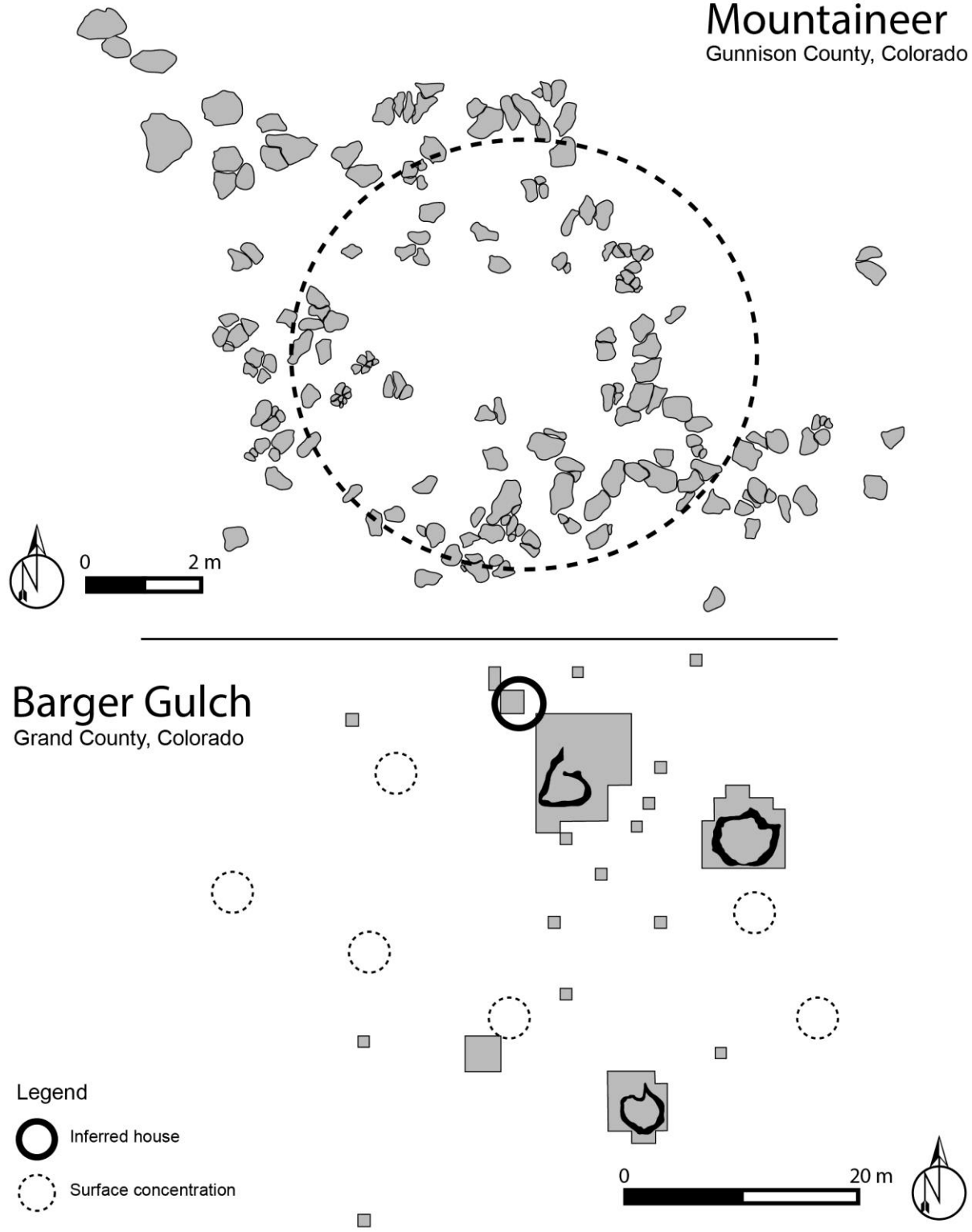


Figure 5. Map of rocks larger than 40 cm and best-fit ellipse for a Folsom residential structure in Block C at the Mountaineer Folsom site, based on Jayalath 2013 (top row). Folsom structures and surface concentrations at Locality B of the Barger Gulch site, based on Surovell 2022 (bottom row).

This era produced a series of papers which provided archaeologists with a multitude of reasons to challenge any one-size-fits-all model of Folsom mobility. Underlying each of these studies rested a firmer appreciation for site formation processes, effects of site sampling on mobility inferences, and site-specific variables like time-averaging of deposits. Sellet (2004, 2013) created models to show how the relative proportions of discarded and manufactured Folsom dart points left clues about the anticipated needs of Folsom groups over the course of a mobility regime. Surovell (2003, 2009) formally established causal relationships between artifact discard patterns, occupation span, and reoccupation effects within sites, allowing for a direct assessment of residential mobility patterns in a settlement system. In a broad comparative analysis, Andrews et al. (2008) identified that the Folsom record holds residuum of short-term occupations, long-term occupations, and reoccupation effects exhibited by the relative size of sites and the distances between activity clusters inside sites.

Presently, researchers are drawing across multi-decadal lines of theory and method to understand Folsom mobility. Recent publications continue to advance Folsom site structure studies (Jayalath et al. 2015; Morgan and Andrews 2016, 2022; Surovell 2022), suggesting this is still a topic of primary interest, and they are paying particular attention to the variables of occupation span and reoccupation as measured within individual localities of sites (Andrews et al. 2021:406-409; Surovell 2022:180-182). Researchers are currently mapping out the degree that Folsom hunter-gatherers devoted time to particular places on the landscape, including sites with evidence of long-term occupation behavior, or reoccupation behavior – suggesting a routine residential investment strategy (LaBelle and Meyer 2021). I link these topics to the Lindenmeier effect that I described earlier, encouraging researchers to spend significant time unravelling complicated site deposits with higher-than-expected quantities of artifacts or broader-than-expected spatial

distributions, or both. Whether such sites are useful for interpreting an average Folsom mobility system is a subject of debate that I will address later. This dissertation falls in line with topics under the Lindenmeier effect, much like these other studies, but revisits some of the primary assumptions of existing mobility models, adds a new perspective to them, and brings additional variables to bear on the broader context of Folsom mobility research.

The Reddin Problem

The Reddin site (5SH77) is a problematic one by all archaeological standards. It is not significantly buried, like most of the well-known sites dating to the late Pleistocene, and the Folsom component there is mixed with cultural deposits spanning the early and later Holocene. It is one of only four sites in North American known to contain at least 500 Folsom artifacts – including projectile points and the production debris from creating them (table 1 and figure 6). Spatially, the site is confoundingly large with approximately 80 acres of contiguous Folsom debris, placing it among a very small sample of sites similar in size to Lindenmeier (figure 6). It is located within a well-known hotbed of Folsom site activity in the San Luis Valley of southern Colorado (Andrews et al. 2008; Hurst 1941; Jodry 1999b, 1999a), but unlike nearby sites there is no obvious evidence of bison hunting – perhaps due to preservation issues.

The archaeological community at large knows very little about Reddin despite the very high number of reported Folsom artifacts there. The results of the Smithsonian Institution's fieldwork (1979 to 1983) were never fully published (Jodry 1999b), but researchers have continuously referred to the Reddin site in articles and books for the last twenty years (Andrews et al. 2008; Buchanan et al. 2019; Sellet 2013). The fact that Reddin is a lithic scatter lacking stratigraphic control or paleosols is probably one of several reasons that the Smithsonian published little about the site. In this sense, Reddin is a problem for Folsom archaeology – an enigma like

Lindenmeier, but even lesser known. However, throughout this dissertation I argue that Reddin is a solution to questions that archaeologists rarely ever ask about such deposits.

The goals of this dissertation are twofold: 1) to formally introduce the Reddin site to the broader community of Folsom researchers, including a summary of previous fieldwork and assemblage contents, and 2) to demonstrate the value of surface scatter sites for Folsom archaeology by developing and testing models of the spatial and temporal arrangements of Folsom artifact concentrations – revealing implications for Folsom behavior and mobility, by proxy. The reader will note that none of the above goals reference the Holocene archaeology of the Reddin site. This is intentional. I cover aspects of post-Folsom archaeology in chapter 5 as well as the appendices – but this is not the focus of my work. This dissertation is about Folsom, and I leave much of the discussion about younger archaeology at Reddin to future research.

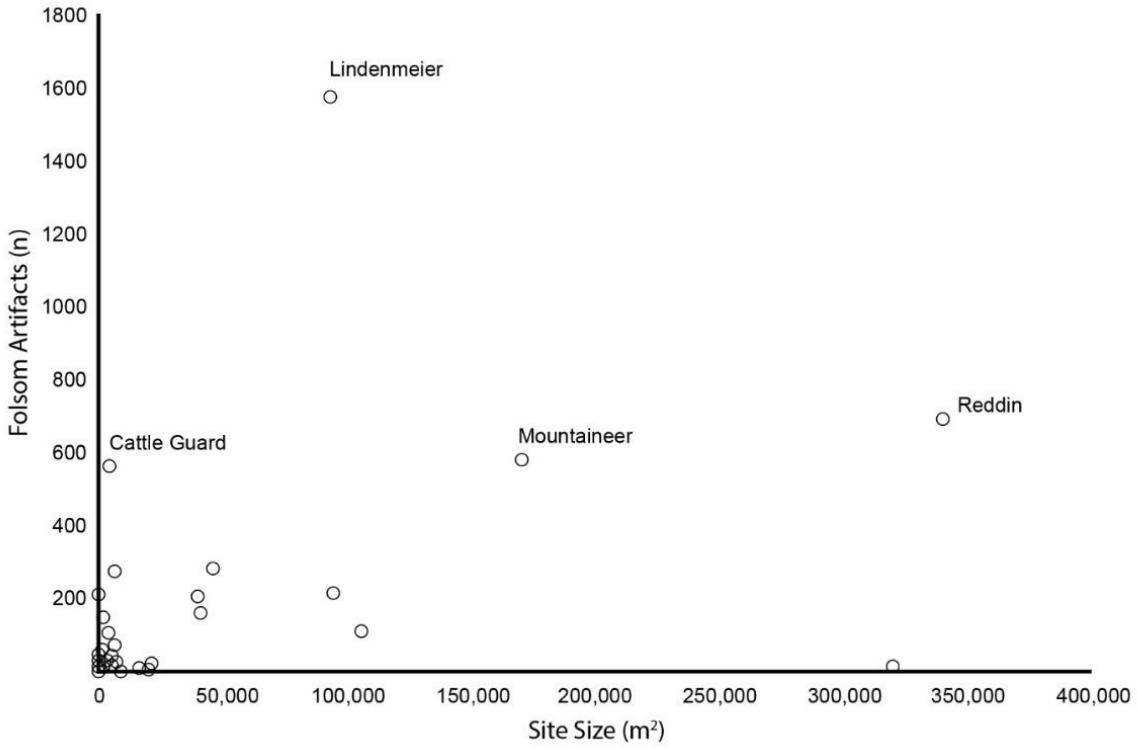


Figure 6. Site size (measured in square meters) vs. the quantity of diagnostic Folsom lithic artifacts (points, preforms, and channel flakes) for sites listed in table 1.

Organization of the Dissertation

I organize this dissertation into six chapters. Chapter 2 introduces the environmental and historical setting of the Reddin site, including a context of Folsom research in the San Luis Valley. In chapter 3, I review the field methods used by the Smithsonian Institution (1979-1983) and Colorado State University (2020-2022) at Reddin. I then describe the lithic artifact assemblage in chapter 4, including a discussion of lithic raw material sources, patterns of breakage, evidence of tool use or repair, and essential summaries of relevant measurements on these items. Chapter 5 is the core of my analysis in this dissertation, which explores spatial attributes of the Folsom assemblage and identifies focal areas of Folsom activity. I build analytical sample units around hotspots of Folsom activity at the site where I test formal hypotheses of site formation, the length of time that people Folsom spent occupying Reddin, and the presence or absence of contemporaneous spaces. In chapter 6, I synthesize the results of the previous five chapters and leave the reader with my interpretation of the site and its context in the broader Folsom archaeological record.

CHAPTER 2 - BACKGROUND

For most readers, a background chapter is not the most thrilling part of a dissertation, but it does lay the necessary groundwork for everything that follows. This chapter is no exception to this unspoken rule. For a site like Reddin and a place like the San Luis Valley, unique environmental circumstances and a long history of Folsom research are legitimately significant. This chapter begins by outlining geography, physiography, and hydrology of the San Luis Valley (hereafter the Valley or SLV). I then introduce more than 80 years of Folsom research in the Valley and draw out the interplaying factors of site visibility, discovery, collaboration, and academic research.

San Luis Valley

The SLV is the largest valley in the Rio Grande Rift zone, measuring about 25,000 km^2 (Kirkham and Magee 2020; Rogers et al. 1992; Upson 1939), and is the byproduct of complex volcanism and tectonics. Throughout the middle Cenozoic and towards the end of the Oligocene (about 25 mya), the Southern Rocky Mountain Volcanic Field erupted with silica-rich stratovolcanoes, calderas, and ignimbrite or ash-flow tuffs – including the world's largest known volcanic explosion from the La Garita caldera, producing more than 5000 km^2 of ash flows (Kirkham and Magee 2020; Lipman and Bachmann 2015). This volcanic field stretched from today's Great Plains, through western Colorado, and from South Park to north-central New Mexico. In the late Cenozoic volcanism slowed and rift expansion followed, producing faults and fractures which fed small shield volcanoes with silica rich basalt, dacite, and rhyolite flows (Kirkham and Magee 2020; Shackley 2011). In south-central Colorado and New Mexico, rifting produced structural basins running in a linear fashion from north to south, distinguishable from

adjacent valleys based on topographic boundaries, rift faults, and internally composed sediments interbedded with volcanics (figure 7). These basins begin just south of Kremmling, Colorado between the Blue River and Williams Fork Valley Grabens and terminate near Chihuahua, Mexico where the Rio Grande Rift meets the loosely defined Basin and Range of the Southwest. The San Luis Basin, geologically synonymous with the SLV, stretches from Pilar, New Mexico to Poncha Pass, Colorado. It is an east-tilted half-graben with a major fault along its east side and a broad hinge on its western flank.

The SLV is an interalpine valley system framed by mountain ranges with elevations that reach into barren alpine tundra (figure 8). Along the Valley's major fault to the east are the serrated peaks of the Sangre de Cristo Range, subdivided into the Northern Sangres, Blanca Massif, and Culebra Range. Further south in New Mexico the Sangres also include the Taos Range. Blanca Peak (*Tsisnaasjini* in Navajo), at the base of the Northern Sangres in the Blanca Massif, measures 14,351 ft above sea level and is one of four Sacred Mountains of the Navajo (Blake 2001; Krall 2016; Mitchell and Krall 2020). The Jicarilla Apache refer to Blanca Peak as Black Belt (*Nishnojini*), and historical Puebloan groups call Blanca Peak *Pintsae'i'i*; the mountain figures prominently in the origin stories of many Native American groups in southern Colorado and northern New Mexico. To the west are the gradually ascending San Juan Mountains above the Valley's half-graben hinge. This range is further subdivided into the Cochetopa Hills (north), La Garita Mountains (central), and East San Juans (south). The Cochetopa Hills meet the southernmost Sawatch Range at the Valley's northwestern border. At the Colorado-New Mexico state line, the Valley's western flank meets the Tusas Mountains – the southeastern component of the San Juans.

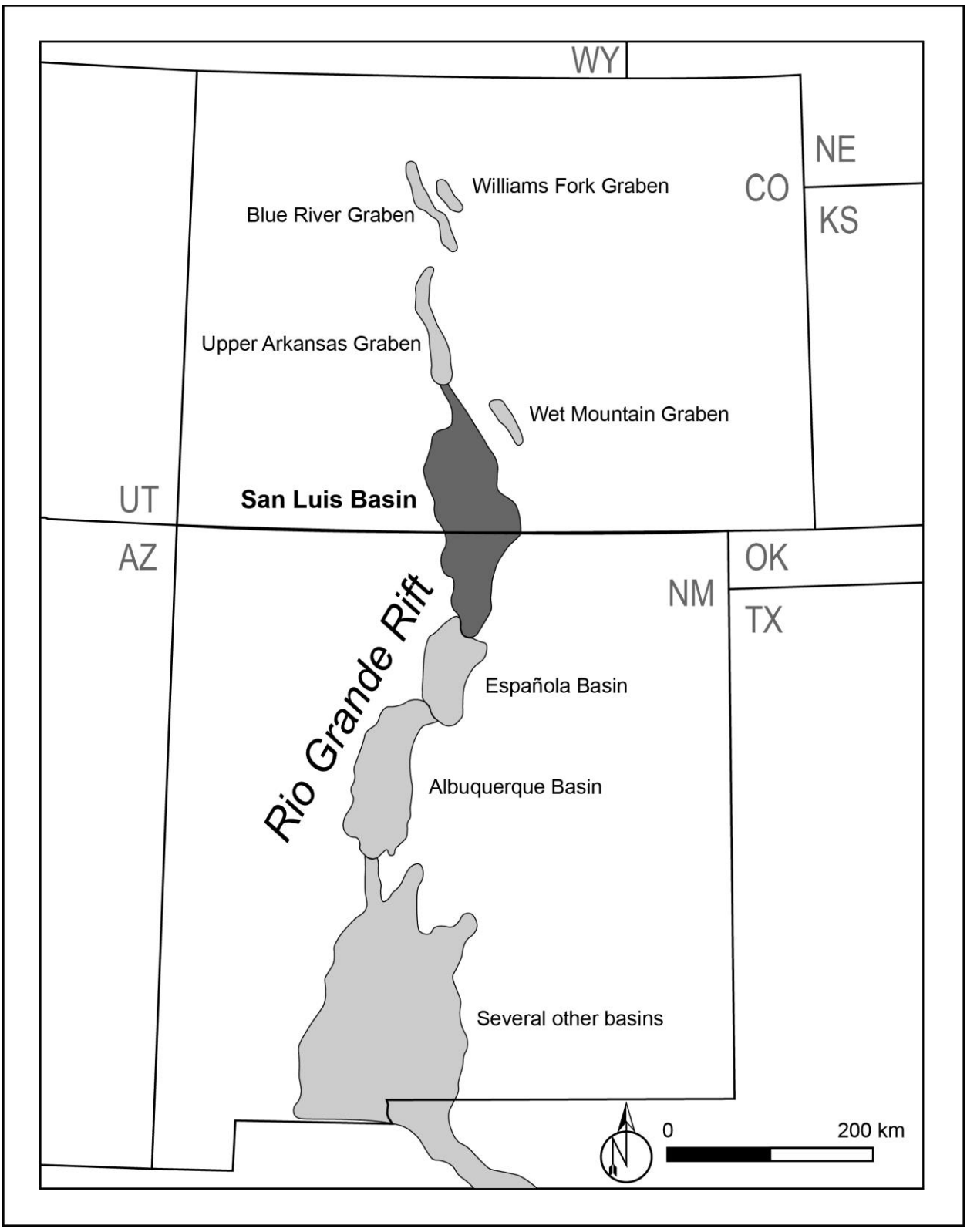


Figure 7. Structural basins map of the Rio Grande Rift Zone, ranging from northern Colorado to Chihuahua, Mexico. Map image adapted and altered from Kirkham and McGee (2020:figure 1.10).



Figure 8. Physiographic map of the San Luis Valley, including portions within southern Colorado and northern New Mexico. Map shows major named mountain ranges, the mainstem of the Rio Grande River, and Valley floor subdivisions.

Broadly speaking, the SLV floor consists of a broad flat plain ranging in elevation from about 7500 ft to 8000 ft above sea level. However, this plain is not fully homogenous. Researchers have partitioned the floor into about five physiographic subareas based on topography and hydrology. The southernmost subarea is the Taos Plateau, a broad volcanic field with diverse petrography consisting of dense clusters of silica rich shield volcanoes including San Antonio Mountain, Ute Mountain, and No Agua Peak, among many others. At the southeastern edge of the Valley near the Colorado-New Mexico border are the Culebra Reentrant, Costilla Plains, and San Luis Hills. The Reentrant is where the Culebra Range is recessed eastward. It is a highly eroded region with complex geology and a prominent mesa landform (San Pedro Mesa). Just west of the Reentrant are the Costilla Plains, a flat subbasin characterized by a mostly uniform mixture of Pleistocene and early Holocene alluvium fed by the Rio Grande River to the west, which overly tertiary basalts (Kirkham and Magee 2020). The San Luis Hills, west of the Costilla Plains, are one of the only obvious elevation changes in the Valley's center; the San Luis Hills are part of an uplifted horst oriented in a northeast to southwest-trending arc averaging 300 ft higher than the surrounding valley floor.

The last and northernmost segment of the Valley floor is the Alamosa Basin, which provides the SLV with its distinctly flat and barren character. The Rio Grande River descends southeast from its headwaters in the Eastern San Juans and forms a broad alluvial fan and hydrological divide bisecting the Valley's center. This distinguishes the Open Basin and Closed Basin portions of the greater Alamosa Basin. The Open Basin encompasses areas south of this divide between the San Luis Hills down to the Taos Plateau, where the Rio Grande's major tributaries meet the mainstem – including the Alamosa, Conejos, and San Antonio Rivers on the west and the Culebra and Trinchera Creeks to the east. The Closed Basin then makes up everything

north of this divide, from the base of Poncha Pass to the southern foothills of the Blanca Massif. The Closed Basin is of particular interest in this dissertation and warrants further discussion; the Closed Basin contains the highest number of Folsom sites in the San Luis Valley, to the near exclusion of the other physiographic subareas.

Closed Basin

From the mid-Pliocene to mid-Pleistocene (roughly 3.5 mya to 440 kya), the Closed Basin formed the bottom of Lake Alamosa. The Servilleta Basalt flowed north along the Taos Plateau to the base of the San Luis Hills and blocked outflow of the Rio Grande River, pooling a massive freshwater lake in the process and creating the topography for an internally drained basin. The lake eventually overtopped its shorelines due to a cumulative process of basin sediment infilling and excessive glacial meltwater. There is some debate over when Lake Alamosa overtopped and drained, but recent estimates place the event sometime between 440 and 360 kya (Davis et al. 2017; Kirkham and Magee 2020; Madole 2020).

Relic lake shoreline features, lagoons, and barrier spits exist at several locations along the Closed Basin's edges, attributable to fluctuating lake levels. Today, the Closed Basin is best known for the Great Sand Dunes National Monument and Preserve (GRSA) which straddles the bajadas along the base of the Northern Sangres. The major dune field associated with the GRSA measures about 440 km^2, though its sand sheet extends much further abroad (Madole 2020). The prominent sand dunes within the GRSA formed over multiple glacial advances in the San Juans that occurred after Lake Alamosa drained, where sand free of clayey particles could travel by wind eastward and unabated over the vast basin floor.

The recent stratigraphy of the Closed Basin is composed primarily of thick Miocene and Pliocene-aged sediments. From oldest to youngest the main units include the pre-rift Conejos

Formation ignimbrite, Sante Fe Group sandstones and claystones, fluviolacustrine (stream and lake) deposits of the Alamosa Formation with interbedded clays and silt with overlying Quaternary sands and gravels. The Alamosa Formation is hundreds of meters thick in some areas at the center of the Closed Basin, and data from the west edge of the GRSA suggest clay beds are laterally discontinuous with interbedded silty and clayey sands as well as loess deposits (Madole 2020). The Quaternary deposits, in contrast, are very thin and composed of alluvium rich with sand and gravel, but evaporites are also common in low-lying sumps. Alluvial fans are found on the edges of the valley where mountain slopes meet the valley base, occasionally forming bajadas (a series of connecting alluvial fans). Alluvial fan stratigraphy is complex depending on age and the character of associated glacial advances in the surrounding high peaks; the oldest fans exhibit microstratigraphy, thin loess, weathered soils, cobbles, and Bt/Bk horizons; the youngest fans have no loess, developed A-C soil horizons, and less weathering (Beeton and Johnson 2020; Madole 2020). On the flattest valley floor, a thin mantle of Pleistocene and early Holocene sand sheets variably covers the youngest alluvium and any surface-exposed sections of Alamosa Formation clays (which are horizontally small exposures, but common in the Valley's center).

Climate, Hydrology, and Vegetation

The Closed Basin encompasses the highest true desert in North America. The mean annual precipitation averages about 8 inches (table 2). The months of July and August average a little more than 1 inch of rain, parallel with the summer monsoon season; the remaining months average between a quarter inch and one-half inch of rain. Cumulative snowfall is especially low. The weather station at the town of Center tracks an average annual snowfall of 25 inches, with snow-bearing months accumulating a low snowpack, between 1 and 2 inches (December through March).

Table 2. San Luis Valley climate summary for eight weather stations located on the valley floor and foothills of the Closed Basin subarea (Western Regional Climate Center 2024).

Weather Station	Location	Elevation	Period of Record	Mean High Temp.	Mean Low Temp.	Mean Precip.	Mean Snowfall
Alamosa (050130)	Central floor	7540 ft.	1948-2016	59.4 °F	23.7 °F	7.1 in.	31.2 in.
Center (051458)	Central floor	7670 ft.	1941-2016	58.4 °F	24.3 °F	7.0 in.	25.0 in.
Monte Vista (055706)	Central floor	7660 ft.	1893-2016	58.7 °F	24.3 °F	7.7 in.	24.3 in.
San Luis Lakes (057433)	Central floor	7540 ft.	1946-1955	60.0 °F	24.4 °F	5.9 in.	NR
Blanca (050776)	Valley edge	7750 ft.	1909-2010	59.0 °F	25.4 °F	8.6 in.	24.3 in.
Crestone (051964)	Valley edge	8120 ft.	1982-2016	59.9 °F	29.5 °F	12.9 in.	61.5 in.
Del Norte (052184)	Valley edge	7880 ft.	1893-2016	58.2 °F	27.4 °F	9.4 in.	39.7 in.
Saguache (057337)	Valley edge	7710 ft.	1894-2009	59.3 °F	26.4 °F	8.3 in.	23.5 in.

NR – Not Reported

The growing season on the floor of the Closed Basin is quite short, at around 120 days (Hoefer 1999). The average annual high temperatures for each of the weather stations in table 2 are under 60°F, and the lows average near 25°F. Peak temperatures occur in July and August, and lows in December and January. Hoefer (1999) documents minor differences in temperature between the Valley floor and the foothills at the edges of the Closed Basin. Average annual precipitation is generally constant on the valley floor, but rainfall and snowfall are higher at the valley edges given the effects of mountainous rain shadows.

Hydrology in the Closed Basin is complex. It is a system comprised of intermittent stream flows, small creeks, seasonal wetlands, and saline ponds. No surface water flows southward to meet the Rio Grande drainage; water is discharged primarily by evapotranspiration (Beeton and Johnson 2020; Harmon 2020; Madole 2020). These scarce surface water resources rest above a shallow water table. An unconfined aquifer contained within Quaternary deposits sits just beneath or at the ground surface, but it is minimally and infrequently recharged by streams and precipitation. Beneath this, the Alamosa Formation contains a blue-clay series which impedes vertical recharge to the deeper confined aquifer that is under constant artesian pressure. Historic

and modern water wells tap into this confined aquifer, which averages 30 m below the surface, but it is as close to 6 m from the surface in some areas (Button 1987; Harmon 2020; Madole 2020).

Streams and creeks feeding the Closed Basin originate in the Northern Sangres and San Juans (figure 9). Table 3 summarizes streamflow discharge into the Closed Basin subarea. The major creeks of the San Juans include those heading in the La Garita Mountains and Cochetopa Hills that flow southeast to the valley center. In order of discharge, these include Saguache Creek, Kerber Creek, La Garita Creek, and Carnero Creek – but of these, only Saguache and La Garita Creek extend seasonally to the valley floor. From the Northern Sangres there are several tributaries of San Luis Creek which drain west, including Sand, Rito Alto, Medano, Zapata, and Deadman Creek, among many others. The streamflow into the Closed Basin amounts to less than 15 percent of the total SLV streamflow, while the remaining 85 percent is encompassed by the Rio Grande and its tributaries, flowing south (Harmon 2020).

The streams of the valley floor confluence in a shallow, nearly invisible lowland called the Trough. It is a massive feature of the Closed Basin measuring roughly 70 km long and about 10 km wide. This lowland arcs along the terminus of the Rio Grande alluvial fan from northwest to southeast where it meets the base of the piedmont slope of the Northern Sangres at the Blanca Massif (Kirkham and Magee 2020; Madole 2020). The gradient of the Trough is barely sloped to the south and drains to the Dry Lakes, also known as the “sump” and the lowest part of the Closed Basin; from end to end the Trough differs in elevation by a mere 30 ft. Wetlands, playa ponds, and small lake beds are common features in the Trough given the flat topography and shallow water table, but the volume and expanse of these impermanent water sources oscillate with subtle changes to precipitation and streamflow regimes; the Trough could be a plentiful marshland in the wettest years, or mostly xeric in years with little precipitation.

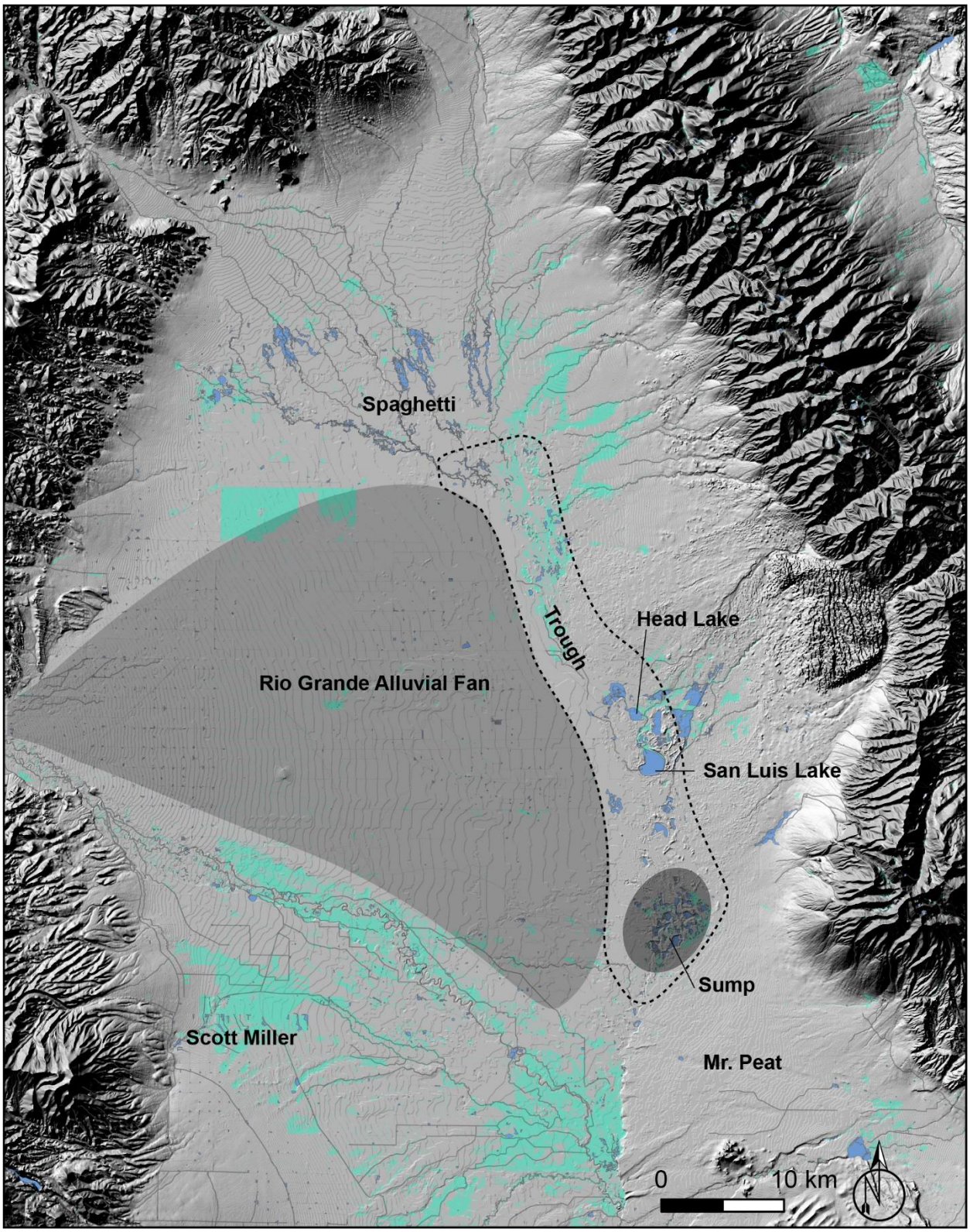


Figure 9. Hydrological map of the northern San Luis Valley and Closed Basin subarea. Prominent lakes (blue) and emergent wetland resources (cyan) are depicted. Labeled locations are discussed in the text.

Table 3. Summary of stream discharge for major water courses in the Closed Basin subarea (average annual acre-feet rounded to the nearest 100 acre-feet). Data compiled from Harmon (2020:table 7.1). Periods of record unreported. Data listed in order of highest contribution to groundwater discharge per mountain range source.

Stream	Mountain Source	Minimum Flow	Maximum Flow	Average Flow
Sagauche Creek	San Juan	16,600	87,300	43,100
Kerber Creek	San Juan	2600	28,900	12,400
La Garita Creek	San Juan	2300	19,000	8200
Carnero Creek	San Juan	200	17,900	3700
San Juan Mountains Total		21,700	153,100	67,400
Sand Creek	Sangre de Cristo	1000	20,100	11,200
Rito Alto Creek	Sangre de Cristo	2100	15,700	8700
Medano Creek	Sangre de Cristo	1200	17,500	8600
North Crestone Creek	Sangre de Cristo	1500	14,500	8500
Cotton Creek	Sangre de Cristo	2900	13,700	8100
Zapata Creek	Sangre de Cristo	600	12,800	6100
San Isabel Creek	Sangre de Cristo	1500	9600	5180
Cottonwood Creek	Sangre de Cristo	1300	8100	4400
Willow Creek	Sangre de Cristo	1200	7500	4100
Deadman Creek	Sangre de Cristo	200	6700	3900
Wild Cherry Creek	Sangre de Cristo	400	3900	2300
South Crestone Creek	Sangre de Cristo	500	4100	2000
Spanish Creek	Sangre de Cristo	500	3400	1900
San Luis Creek	Sangre de Cristo	500	1100	700
Sangre de Cristo Mountains Total		15,400	138,700	76,300
Closed Basin Total		37,100	291,800	143,700

The floor of the Closed Basin is primarily composed of shrubland and wetland ecosystem assemblages that survive outside of the surrounding mountain rain shadows (Button 1987; Duran 2020; Schumann and Machette 2007). Greasewood (*Sarcobatus vermiculatus*) or chico brush is the dominant shrub at elevations between 7500 to 7700 ft above sea level, covering much of the valley floor. Greasewood and related salt-tolerant species thrive in areas enveloped by saline soils (a result of poor drainage), commonly found along the margins of wetlands, playas, and open alkali flats or hardpans. In areas with better drainage, such as the highlines of alluvial fans, rabbitbrush (*Chrysothammus greenei*), Winterfat (*Krasheninnikovia lanata*), and snakeweed (*Gutierrezia sarothrae*) makeup the shrubland communities. Sagebrush (Artemisia tridentata), Four-wing saltbrush (*Atriplex canescens*), and Wax currant (*Ribes cereum*) occupy zones adjacent to the pinon-juniper woodlands that ring the foothills at the edges of the valley floor.

Halophytic grasses grow at the contact of wetlands and alkali flat shrubs in the Closed Basin, including sacton (*Sporobolus* spp.) and heliotropium (*Heliotropium curassavicum*). Cattail

(*Typha latifolia*), saltgrass (*Distichlis spicata*), spikerush (*Eleocharis palustris*), hardstem bulrush (*Schoenoplectus acutus*), mountain rush (*Juncus balictus*), and slimstem reedgrass (*Calamagrostis stricta*) are densely clustered further into wetland areas. Riparian wetlands contain taller overstory vegetation such as narrowleaf or lanceleaf cottonwood (*Populus* spp.) and some willows. Understory non-woody plants in riparian settings include pondweeds (*Potamogeton* spp.), milkweed (*Asclepias* spp.), and American three-square (*Scirpus pungens*) – in addition to many of the wetland plant varieties listed above (Button 1987; Duran 2020; Jodry and Stanford 1996).

Paleoclimate

The Trough and the adjacent riparian zones of the Rio Grande contain wetland resources preserving paleoclimatic data. Today, the wetlands of the Closed Basin are the most biologically diverse habitats in the SLV and the same was likely true of the distant past; semi-aquatic plants and shoreline vegetation, small and large mammals, migratory birds, fish, and insects all congregate around the Valley's wetland resources. Relic or "fossil" wetlands, now inactive, preserve complex fluviolacustrine deposits layered with sand and partially decomposed organic plants and animals that are datable using absolute methods such as radiocarbon dating and luminescence (Beeton 2014; Beeton and Johnson 2020; Jodry and Stanford 1996; Schumann and Machette 2007; Yuan et al. 2013). The organic components of these layers reflect changes to the wildlife regime over time. Sediment cores in the lakes along the Trough provide additional information about the Valley's climate based on datable macrofossils and plant pollen. In recent years, paleoclimatic research in the SLV has focused on geochronological dating of stratigraphic layers in fossil peatbog deposits within paleo-wetlands. Major studies include those conducted at archaeological and paleontological localities at the Mr. Peat site (5AL9709) and the Scott Miller

site in the Monte Vista National Wildlife Refuge (5RN1136) (Beeton 2014; Beeton and Johnson 2020; Johnston 2021; Johnston and Meyer 2024; Schumann and Machette 2007).

At Mr. Peat, studies by multiple research teams have shown that the Valley floor experienced immense paleoclimatic change over generally short time frames (Beeton and Johnson 2020; Schumann and Machette 2007). The site is on an abandoned tributary stream channel just south of the Closed Basin divide and east of Alamosa. As Pinedale glaciation waned in the surrounding mountains (ending 16 to 14 kya), streamflow discharge in the paleo-valley at Mr. Peat accumulated several meters of bedded sands, silt, and overbanking clays (Johnston and Meyer 2024; Schumann and Machette 2007). The valley then transitioned to a slow-moving shallow water setting that lasted between 13.4 and 11 kya, distinguished by an organic and plant fiber-rich mucky peat layer. Fresh-appearing and stratified plant material overlies this mucky peat in a dense reddish-brown "woody" peat layer dating between 12 and 11 kya, characterizing a true bog environment with high biomass and no standing water. After (7 to 4 kya), the paleo-valley changed into a spring-fed environment suggesting a much higher water table; the youngest wetland deposits are characterized by a thick black mat of organic-enriched windblown silt topped by large protruding mounds of calcite-rich tufa. In sum, the paleo-valley at Mr. Peat transformed from a rushing stream channel to near-stagnant surface water as glaciers receded, followed by a dry but saturated bog field and then an artesian spring towards the end of the Pleistocene and beginning of the Holocene.

Head Lake and San Luis Lake are centrally located in the valley within the Trough west of the GRSA. Paleoclimate studies report aquatic plant macrofossils and algae (*Pediastrum*) from sediment cores suggesting water depth and horizontal surface area peaked at the end of the Pleistocene (Beeton 2014; Jodry and Stanford 1996; Yuan et al. 2013). If water level constraints

by the unconfined aquifer were the same in the past, then direct infiltration by precipitate water was the primary cause of higher lake levels. Oak and sagebrush pollen were abundant in lake core sediments at depths presumed to date to the Pleistocene, suggesting cool and wet conditions. In a more recent study of San Luis Lake, Yuan et al. (2013) identified alternating wet and dry conditions over seven major climatic periods between the late Pleistocene and the present. The data are correlated using multiple soil chemistry proxies (e.g. Mg/Ca, inorganic carbon content, δ18O, δ13C). Identified periods include the Big Dry (16.5 to 15.7 kya), the Big Wet (15.7 to 14.9 kya), the Bolling-Allerod warm and dry period (14.9 to 12.7 kya), the Younger Dryas cold and wet period (12.8 to 11.6 kya), an earliest Holocene dry period (10.6 to 6.7 kya), mid-Holocene wet period (6.7 to 2.6 kya), and a late Holocene dry phase extending from about 2.6 kya to present.

The Folsom tradition dates between 12.8 and 12.3 kya based on a recent Bayesian analysis and chronological hygiene study (Buchanan et al. 2021, 2022). This time frame corresponds to the earliest part of the Younger Dryas Chronozone (YDC). The YDC is a climatic interval representing a cold spike, and in some places, a reversal in widespread glacial recession initiated at the end of the Last Glacial Maximum. In the far reaches of the northern hemisphere, glaciers not only halted their retreat but initiated re-advance. YDC data have been observed in a variety of contexts, from Greenland ice cores to deep sea sediment cores, and all signs point to highly seasonal and colder temperatures. However, several studies have shown varied YDC effects on temperature and precipitation in North America (Briles et al. 2012; Lowell and Kelly 2008; Meltzer and Holliday 2010). Some regions were drier than wet, with similar temperatures to the modern climate. In the Southern Rocky Mountains, current research suggests that summer temperatures may have been about 10 °F colder on average, and perhaps 20 degrees colder during the winter. All available information from lake cores and wetland excavations suggests that the SLV was colder and wetter

during the YDC (table 4), the water table was higher than at present, and biomass was concentrated along wetland edges. Researchers have further posited an overall longer growing season during the YDC (Beeton and Johnson 2020; Jodry and Stanford 1996), abundance of nitrogen enriched soils, and thus, expansion of grassland environments leading to greater forage for large migratory herbivores (e.g. *Bison antiquus*).

Table 4. Published radiocarbon (14C), optically-stimulated luminescence (OSL), and infrared-stimulated luminescence (IRSL) dates from the Mr. Peat site (Schumann and Machette 2007) and the Scott Miller paleowetland (Beeton 2014). Radiocarbon dates recalibrated in this study using IntCal 2020 in OxCal v.4.4.3 (Bronk Ramsey 2009; Reimer et al. 2020). Dates rounded to the nearest 10 years.

Location	Lab Number	Age yr B.P.	Lab Error yr	Method	Sample Type	Context	Cal yr B.P. (1σ)	Cal yr B.P. (2σ)
Mr. Peat	MRP-CL1a	34,400	1800	IRSL	Silt	Alluvium	NC	NC
Mr. Peat	MRP-CL1b	29,900	1600	IRSL	Silt	Alluvium	NC	NC
Mr. Peat	MRP-CL2a	20,600	1500	IRSL	Silt	Alluvium	NC	NC
Mr. Peat	MRP-CL1c	20,300	700	OSL	Sand	Alluvium	NC	NC
Mr. Peat	MRP-CL2b	18,000	1100	IRSL	Silt	Alluvium	NC	NC
Mr. Peat	MRP-CL3a	13,800	900	IRSL	Silt	Alluvium	NC	NC
Mr. Peat	MRP-CL3b	13,600	900	IRSL	Silt	Alluvium	NC	NC
Mr. Peat	OS-57740	12,350	50	14C	Plant stems	Alluvium	14,800-14,190	14,840-14,110
Mr. Peat	OS-57714	11,600	50	14C	Organic	Mucky peat	13,580-13,410	13,590-13,330
Mr. Peat	OS-57499	11,350	45	14C	Organic	Mucky peat	13,300-13,170	13,320-13,120
Mr. Peat*	OS-57672	10,550	40	14C	Plant stems	Mucky peat	12,670-12,490	12,690-12,480
Mr. Peat*	OS-56395	10,250	55	14C	Organic	Woody peat	12,050-11,820	12,450-11,750
Mr. Peat*	OS-56641	10,150	55	14C	Organic	Woody peat	11,930-11,650	11,970-11,400
Mr. Peat*	OS-56477	9960	40	14C	Organic	Woody peat	11,600-11,260	11,690-11,250
Mr. Peat*	OS-57712	9930	60	14C	Moss	Mucky peat	11,600-11,240	11,690-11,220
Mr. Peat	MRP-CL2c	9900	500	OSL	Sand	Alluvium	NC	NC
Mr. Peat	MRP-CL3c	6500	300	OSL	Sand	Alluvium	NC	NC
Mr. Peat	OS-53707	5880	50	14C	Organic	Black mat	6780-6640	6850-6550
Mr. Peat	OS-57406	5880	45	14C	Snail shell	Calcite tufa	6750-6650	6840-6560
Mr. Peat	OS-57942	3850	85	14C	Organic	Black mat	4410-4150	4520-3980
Mr. Peat	OS-53176	3580	30	14C	Snail shell	Calcite tufa	3960-3830	3980-3730
Mr. Peat	MRP-DL1	1600	100	OSL	Sand	Sand dune	NC	NC
Scott Miller	NR	11,530	50	14C	Not reported	Evap. silt	13,460-13,340	13,500-13,300
Scott Miller	NR	9120	40	14C	Not reported	Black mat	10,340-10,200	10,410-10,200

*Dates correspond to the Younger Dryas chronozone; NC – Not calibrated

A Legacy of Folsom Research

How did an entire mountain valley in southern Colorado come to be known as a regional Folsom center? The answer to this question has much to do with the high density of sites recorded there. But what are the specific factors underlying this higher-than-average frequency of Folsom

sites? In the SLV, as in Middle Park, Colorado (Kornfeld 2013; Surovell 2022), the abundance of Folsom sites is a byproduct of several things:

1) *a predominantly near-surface (non-buried) archaeological record covering much of the valley floor,*
2) *avocational surface collectors who live there and proactively collaborate with professionals,*
3) *a dedicated Paleoindian research program carried out by an academic institution, but open to collaboration with local collectors.*
4) *a systemic Folsom land use pattern, involving geographically focused movements through the Valley on a frequent basis*

Paleoindian scholars will recognize this basic list of ingredients when comparing the history of Folsom research in other regions outside Colorado, as well (Hofman 2002; LaBelle 2003). But there are also practical variables underlying patterns of Folsom site identification in the Valley. Folsom artifacts are highly visible; Folsom weaponry is fluted and has a technological "calling card" that is easily identified – even from the smallest and most damaged artifacts (Johnston 2021; Merriman 2022). In the Closed Basin, where small open lithic scatters are abundant (Button 1987), lithic raw materials are scarce, and complete (unbroken) tools are rare, it is much easier to identify Folsom projectile points and the byproducts of point manufacture (channel flakes and broken preforms) than it is for other artifacts from different periods. The visibility of Folsom artifacts in the Valley's open desert environments enhances the detection of Folsom resources, reinforcing both the archaeological sampling success and the overall cultural pattern of Folsom land use in the Closed Basin.

The history of Folsom research in the SLV has been reviewed more extensively elsewhere (Jodry 1999a, 1999b; Mitchell and Krall 2020), so I provide an abbreviated discussion here. In the 1930s and 1940s, following the Dust Bowl and comprehensive exposure of Pleistocene-aged sediments across the Great Plains, the Valley witnessed an acute spike in the activities of surface collectors. Etienne (E.B.) Renaud of the University of Denver (DU) and Clarence (C.T) Hurst of Western State College made multiple visits to the San Luis Valley to engage with a growing network of local artifact hunters. Members from the Rio Grande Chapter of the Colorado Archaeological Society (CAS) invited Renaud and Hurst to visit exposed Pleistocene-aged faunal remains and lithic tools on the flanks of the Sangre de Cristo Mountains, near today's GRSA. Hurst conducted preliminary excavations at the Linger bison kill and campsite (5AL91) in 1940 and 1941, providing the first scientific documentation of a Folsom site in the Southern Rocky Mountains (Hurst 1941, 1943). Folsom research then slowed significantly during World War II and the following two decades, but small-scale efforts in the 1950s included test excavations at the Zapata bison kill and camp by Alamosa State College (Jodry 1999b).

Dennis Stanford and the Smithsonian Institution's Paleoindian Research Lab, including partner organizations and individuals, worked to revitalize, expand, and contextualize Folsom research in the SLV beginning in the mid-1970s. They started with re-opening C.T. Hurst's work at the Linger site using new excavations with refined methods (Jodry 1999b; Stanford 1990), which proliferated into excavations and focused surface inventories of all major Folsom localities recognized in the Valley – including Zapata, Stewart's Cattle Guard, Black Mountain, and Reddin (Jodry 1999b). Their team supplemented fine-grained investigations of individual sites with broad scale paleoclimatic studies to understand the subtle fluctuations of the Valley's resource structure and potential impacts on Folsom land use practices (Button 1987; Jodry 1999b; Jodry and Stanford

1996). In the late 1990s and early 2000s, their work expanded into the alpine-subalpine ecotone along the Valley's westernmost margin at the Black Mountain site (Jodry 1999b).

The 1970s also saw development of federal agency cultural resource programs and the parallel growth of cultural resource management (CRM) projects, following the passing of the National Historic Preservation Act (NHPA) in 1966. Broadly speaking, the SLV maintained its rural character throughout this period – and it still does. The overall number of CRM projects conducted there is low, and the spatial footprint of those projects is typically small compared to CRM surveys along the Front Range. However, notable and comprehensive projects have occurred, including the Bureau of Reclamation (BR) Closed Basin Division Project (Button 1987), the Poncha-San Luis Valley 230-kV transmission line (Conner et al. 1980), DU's San Luis Archaeological Project or SLAP surveys (Haas 1981, 1982), and multiple federal land exchange projects (Jodry 1999b). Of these, the Closed Basin Project retains the largest spatial footprint, which covered more than 20,000 acres over a period of 10 years in the center of the Closed Basin (Button 1987). Reclamation archaeologists collaborated with the Smithsonian team on numerous occasions to complete surveys for a comprehensive surface water salvage project involving linear pipeline easements, multiple fields of water wells tapping into the unconfined and confined aquifer, as well as associated construction access roads and borrow pits (Button 1987).

In 1999, the Colorado Council of Professional Archaeologists (CCPA) audited the state files of the Office of Archaeology and Historic Preservation (OAHP) to better understand the quantity and diversity of cultural resources in each of the major river basins. For the Rio Grande River Basin, Jodry (1999b) tallied Folsom sites in each of the counties covering the SLV – including Alamosa, Conejos, Costilla, Hinsdale, Mineral, Rio Gande, and Saguache County. This amounted to 40 documented Folsom components, with 19 of those resources recorded in the field

by professional archaeologists and another 21 assemblages held in private collections. The spatial distribution of Folsom components in each county varied, but noticeable concentrations appeared in Alamosa and Saguache County in the Valley's center, which contained 31 of the total 40 Folsom resources.

The number of professionally recorded Folsom sites and isolates grew over the years since the 1999 CCPA context, from 19 to 27 resources based on an OAHP file search conducted in May 2022 (table 5). However, much of the known sample size is a testament to the extensive Folsom archaeology of the 1970s through the early 2000s. The data show that most sites were recorded within a 5-year period towards the end of the 1970s. The sample consists primarily of open lithic scatters with a few isolated occurrences of Folsom points, occasionally found within mixed assemblages. Partially buried sites are uncommon in the sample, but these sites are the most well-known and thoroughly investigated.

Table 5. Summary data for Office of Archaeology and Historic Preservation (OAHP) file search. File search completed in May 2022 for Folsom resources in Alamosa, Conejos, Costilla, Hinsdale, Mineral, Rio Gande, and Saguache County, Colorado.

Site Number	Site Name	Periods of Record	Indigenous Components Listed
5AL9	None	1948, 1979, 2007	Folsom
5AL29	Kerry	1980, 1983	Folsom (Paleoindian), Middle Archaic, Formative
5AL90	Zapata	1978	Folsom, Archaic (unspecified)
5AL91	Linger	1941, 1978, 1979	Folsom, Archaic (unspecified)
5AL94	Little Clovis	1979	Clovis, Folsom, Archaic (unspecified)
5AL97	Beck Folsom	1979	Folsom, Early Archaic, Formative
5AL101	Stewart's Cattle Guard	1977, 1983-1996	Folsom, Archaic (unspecified)
5AL102	Freeman Stewart	1979	Folsom
5AL113	Rolling Points Blow	1979	Folsom, Archaic (unspecified), Formative
5AL123	One-Two-Three	1979-1980	Folsom, Early and Middle Archaic, Formative
5AL203	None	1979	Folsom?
5AL215	None	1980	Folsom?
5CN22	None	1949, 1987	Folsom, Archaic (unspecified)
5HN55	Black Mountain	1991-1993, 1997	Folsom, post-Folsom (unspecified)
5RN214	None	1980	Folsom
5RN306	None	1982, 2018	Folsom, Archaic (unspecified)
5RN1136	Spring Creek (Scott Miller)	2012	Folsom, Early to Late Archaic, Formative
5SH77	Reddin	1979-1983	Folsom, Early to Late Archaic, Formative
5SH310	None	1978	Folsom
5SH873	Chuck's Folsom	1982	Folsom, Formative
5SH933	Rupright	1983, 1985	Folsom, Middle Archaic, Formative, Protohistoric
5SH964	Little Folsom	1984, 1985	Folsom
5SH1763	None	1997-1998, 2010	Folsom (Paleoindian), Early Archaic
5SH1770	None	1998	Folsom
5SH1875	None	2000	Folsom

Site Number	Site Name	Periods of Record	Indigenous Components Listed
5SH2379	None	2004	Folsom (Paleoindian)
5SH2895	Sleeping Folsom	2005, 2007, 2010	Folsom

Folsom on the Valley Floor

The spatial distribution of Folsom sites in Alamosa and Saguache County is not random or homogenous but instead concentrated into two recognizable clusters – hereafter, the Alamosa Cluster and Saguache Cluster (figure 10). The Alamosa Cluster consists of multiple and thoroughly excavated Folsom sites, including Stewart's Cattle Guard, Linger, and Zapata, but also other smaller Folsom sites straddling the edge of the Zapata Ranch at the base of the GRSA. For the purposes of this dissertation, I define the spatial footprint of the Alamosa Cluster subjectively and it includes eight Folsom resources in about 20 km^2. The Saguache Cluster includes the Reddin site, as well as 12 other Folsom resources spread over 15 km^2 near the confluence of the major streambeds of the Closed Basin, north and west of the GRSA at the northern terminus of the Trough.

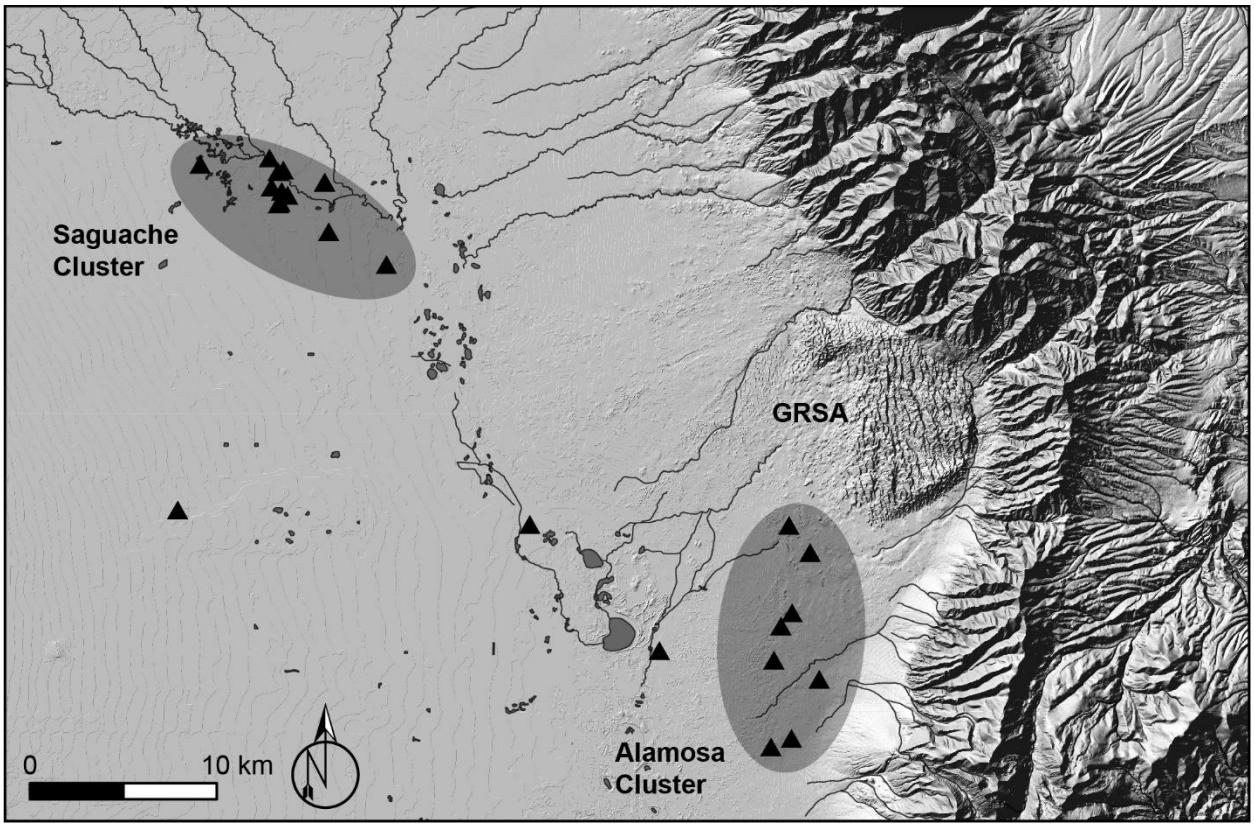


Figure 10. Map of Folsom resources (sites and isolated finds) within the Alamosa and Saguache clusters in the Closed Basin.

Alamosa Cluster

The Alamosa Cluster was the longtime hotbed of the Smithsonian's Paleoindian Research Lab, and as such, defines much of the context of Folsom activity in the SLV – and perhaps even more broadly than that (Hofman 2002; LaBelle and Meyer 2021). Consequently, what we know about Folsom in the region could be biased by these focused research efforts. These studies captured redundant facets of Folsom behavior. The excavations at Linger and Zapata told a similar story; both sites were small bison kills and temporary camps situated near relic interdunal ponds when a large wet meadow corridor presented along the toe slopes of the Sangre de Cristos during the YDC (Jodry 1999b, 1999b; Jodry and Stanford 1996; Mitchell and Krall 2020). These sites contained multiple activity localities, including (at minimum) a primary bison kill area, adjacent processing camps, and lithic tool replenishing zones. The number of individual bison that Folsom

people hunted at these two sites was low, based on published data (table 6), and analysis of the bison dentition suggested a late summer or early fall hunting season at both sites. The lithic toolkits that accompanied Folsom hunters also appeared small, suggesting generally low group sizes and short-term occupations at each site. Lithic raw materials included high proportions of long-distance or exotic rocks sourced from the Southern High Plains, suggesting the SLV may have been a terminal hunting range for plains-based Folsom groups.

Table 6. Assemblage summary data for Folsom resources in the Alamosa Cluster and Sagauche Cluster, San Luis Valley, Colorado.

Site	SLV Cluster	Bison MNI	Points	Preforms	Channel Flakes	Gravers	Scrapers	Reference
Cattle Guard	Alamosa	49	211	76	276	30	69	Jodry 1999a
Linger	Alamosa	5	23	1	2	1	4	Jodry 1999b
Zapata	Alamosa	P	12	2	13	0	0	Jodry 1999b
Little Clovis	Alamosa	NR	1	NR	NR	NR	NR	OAHP File
5AL9	Alamosa	P	1	0	0	0	0	OAHP Site Form
Rolling Points Blow	Alamosa	0	1	0	0	0	0	OAHP Site Form
Beck Folsom	Alamosa	0	2	0	0	0	0	OAHP Site Form
Freeman Stewart	Alamosa	0	P	NR	NR	NR	NR	OAHP Site Form
Reddin	Saguache	NA	225	110	357	34	66	This study
Rupright	Saguache	0	1	1	0	1	NR	OAHP Site Form
Little Folsom	Saguache	0	0	3	1	0	0	OAHP Site Form
Chuck's Folsom	Saguache	0	2	0	0	0	0	OAHP Site Form
CSU-24-01*	Saguache	NA	1	NA	NA	NA	NA	This study
CSU-24-02*	Saguache	NA	1	NA	NA	NA	NA	This study
CSU-24-03*	Saguache	NA	NA	1	NA	NA	NA	This study
CSU-24-04*	Saguache	NA	1	NA	NA	NA	NA	This study
CSU-24-05*	Saguache	NA	1	NA	NA	NA	NA	This study
CSU-24-06*	Saguache	NA	1	NA	NA	NA	NA	This study
CSU-24-07*	Saguache	NA	1	1	NA	NA	NA	This study
CSU-24-08*	Saguache	NA	NA	1	NA	NA	NA	This study

Site Numbers – Cattle Guard (5AL101), Linger (5AL91), Zapata (5AL90), Little Clovis (5AL94), Rolling Points Blow (5AL113), Beck Folsom (5AL97), Freeman Stewart (5AL102), Reddin (5SH77), Rupright (5SH933), Little Folsom (5SH964), Chuck's Folsom (5SH873); * - Denotes temporary site number developed in this study for resources lacking field investigation; NR – Not reported; NA – Not available; P – Present (not reported)

Stewart's Cattle Guard (hereafter, SCG), introduced in chapter 1, remains one of the most clearly understood Folsom sites in North America. The results of excavation there expanded on the behavioral patterns identified at Linger and Zapata, with finer detail. SCG is situated in a former grassland and grazing corridor between interdunal ponds (west) and the foothill-valley ecotone (east). The site was rapidly buried by a moist sand sheet during the Pleistocene and Holocene transition, preserving a higher number of fragmentary bison remains. The lack of

significant overburden at the site permitted extensive horizontal excavation, atypical of many other buried Folsom localities in the Great Plains. Approximately 1400 m^2 of excavation revealed a widely dispersed Folsom residential camp adjacent to a bison kill and processing locality (Jodry 1999a, 1999b; Jodry and Stanford 1992; Jodry et al. 1996).

A Folsom hunting party killed at least 49 bison at SCG during the late summer or early fall (Jodry 1999a). A micro-band consisting of 4-7 family units set up residence adjacent to the bison kill. A combined lithic and spatial analysis identified that individual workspaces contained internally consistent evidence for toolkit replenishment and maintenance, raw material diversity, and artifact damage from use and burning near hearth-centered spaces (Jodry 1999a). Refit and conjoining artifacts, including faunal remains, suggested both widespread contemporaneity between activity areas and mutual reciprocity between household groups (Jodry 1992, 1999a; Jodry and Stanford 1992). Task-specific hide and marrow processing locales further indicated the possibility of gender-specific work areas managed by women (Jodry 1999a). Lithic raw material transported into the site suggested long-distance curation of Folsom toolkits from sources located in New Mexico, in the San Juans, on the Colorado Front Range, at the Valley's edges, and further abroad at the Southern High Plains border; lithic conveyance data suggested the site served as an aggregation for a broad network of mobile Folsom groups operating in the SLV during an opportune hunting season. Altogether, the data from SCG suggested a short-term camp of Folsom hunters, an aggregating micro-band of between 15 to 50 people, focused on the pursuit and processing of bison when the seasonal environment favored congregating animals and social networks of people – these data essentially defined the ABC residential model of Folsom mobility (see chapter 1).

Saguache Cluster

The Saguache Cluster is less known by the archaeological community at large and does not currently contribute greatly to models of Folsom mobility in the region. The Saguache Cluster includes Reddin, a known but underreported Folsom site (the subject of this dissertation), and other peripheral localities identified during the BR's Closed Basin water well survey projects (Button 1987). Multiple Folsom localities presented in figure 10 and table 6 are not yet professionally recorded by archaeologists; some of these presumably small Folsom resources were re-identified during my inventory of the Smithsonian artifact collection from Reddin and geolocated well-outside the site boundary.

Folsom resources in the Saguache Cluster occupy a series of extremely shallow landforms where several of the Valley's intermittent streams confluence at the base of the Trough, bounded to the west by the La Garita Creek mainstem and including Ball Arroyo, Saguache Creek, and a nexus with San Luis Creek on the cluster's eastern flank. The Valley's recently updated surface geology map shows that the Folsom sites and isolated finds occupy surface exposed sections of Alamosa Formation lacustrine clays, Quaternary alluvium dating from the mid-to-late Pleistocene, and Pleistocene-to-Holocene sand sheets overlying the alluvium (Ruleman and Brandt 2021). Topographic relief in the area ranges from 7550 to 7540 ft, or roughly 3 m in an area 11 km wide, but this covers hundreds of thousands of years of deposits that interlace one another over a relatively small area (figure 11).

Geologists in the 1970s nicknamed this landscape the "Spaghetti" given hundreds of braiding Pleistocene and Holocene stream channel scars with fickle trajectories (Button 1987) – a result of the nearly planar surface of the valley floor and impermeable Alamosa Formation clays. The local environment is home to numerous fossil wetlands, shoreline features of oxbow lakes,

and playa depressions. Precise geological and paleoclimatic research in the area is lacking, but the remains of Colombian mammoth and ancient peaty wetland deposits are reported near the Mishak Lakes Preserve near the Saguache Cluster (Beeton, personal communication), which is the largest natural shallow-water wetland in Colorado. There is a lack of absolute dating of geological and archaeological deposits local to the Saguache Cluster, but the area likely exhibited similar YDC climate patterns as identified at Mr. Peat, Scott Miller, San Luis Lake, and Head Lake on the valley floor. A higher water table in this area likely produced seasonally filled lakes and high biomass adjacent to wetlands and riparian zones.

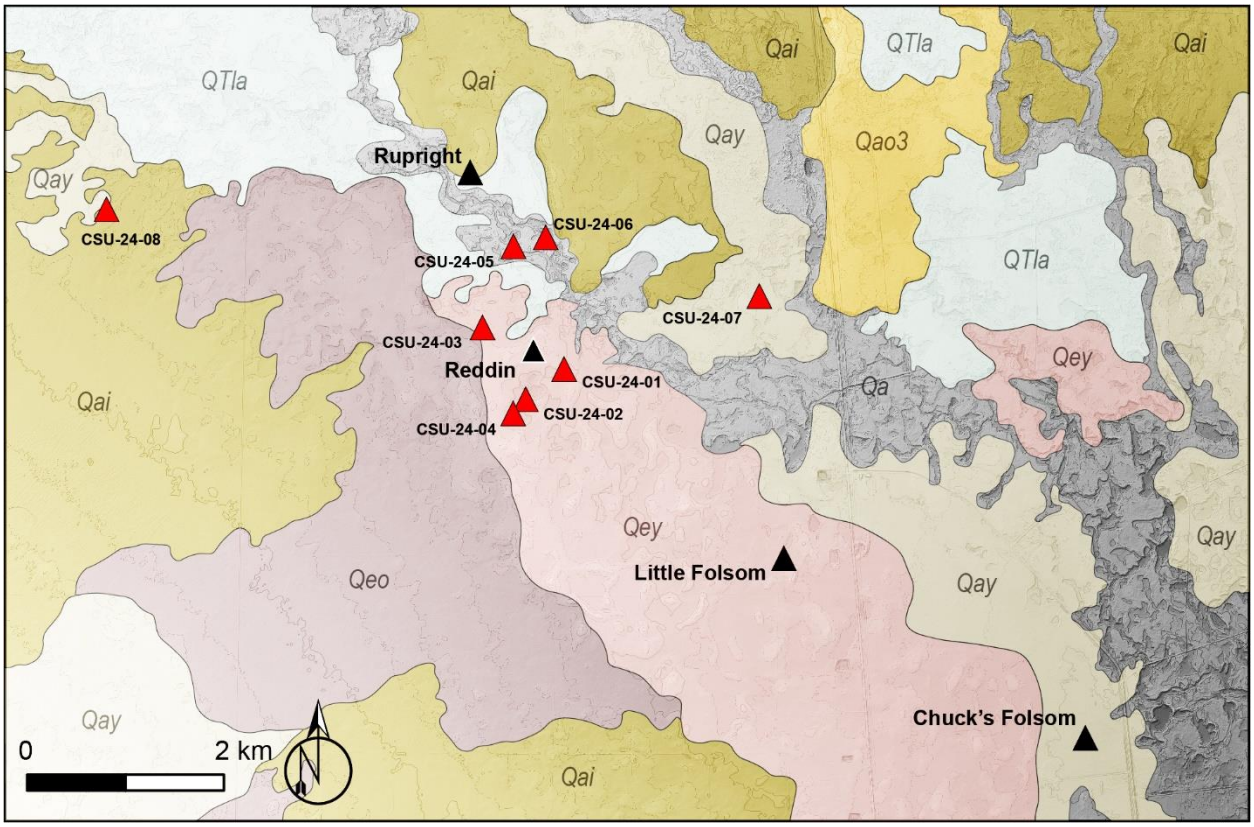


Figure 11. Surficial geology map of the Saguache Folsom Cluster area, depicting Quaternary deposits mapped by Ruleman and Brandt (2021). From oldest to youngest, the deposits include QTla (Alamosa Formation lacustrine clays, mid-Pleistocene), Qao3 (older alluvium, mid-Pleistocene), Qai (intermediate alluvium, mid-to-late Pleistocene), Qeo (older eolian sand sheet/dunes, mid-to-late Pleistocene), Qay (younger alluvium, late Pleistocene), Qey (younger eolian sand sheet, Holocene), Qa (undivided Holocene alluvium). Previously recorded (black) and unrecorded (red) sites depicted.

The Folsom sites in the Saguache Cluster include multiple surface scatters, a stark contrast from the Alamosa Cluster which is defined by several shallowly buried Folsom components. These include named localities identified during the BR Closed Basin surveys: Chuck's Folsom Site (5SH873), Rupright (5SH933), and Little Folsom (5SH964). These few named sites, coupled with additional Folsom locales reported in this dissertation (table 6), contain a small number of time-diagnostic artifacts including one or two Folsom points or preforms each. The OAHP site forms for the previously recorded resources quantify limited debitage and tools, and several sites contain artifacts from much younger Archaic and Formative periods (table 5). Dozens of other sites located nearby lack diagnostic Folsom artifacts but contain other tools commonly associated with Paleoindian-age occupations (e.g. spurred scrapers, gravers). Some of these sites also contain one or multiple Late Paleoindian projectile points (Agate Basin, Cody Complex, and other Plano-like lanceolate points) as well as tools, ceramics, and features from subsequent occupations. Archaeologists have not formally revisited or updated site assessments at any of the resources in the Saguache Cluster since initial recording in the 1980s. It is also uncertain whether the lack of buried components at each surface scatter site is due to formal subsurface testing or simply surface-level observations and assumptions about the integrity of deposits.

Reddin Environment

The Reddin site shares many aspects with nearby Folsom localities in the Saguache Cluster, but differs in significant ways, too. The site measures about 84 acres and occupies a low rise overlooking La Garita Creek, downstream of Ball Arroyo and upstream of a confluence with Saguache Creek – the major drainage of the Spaghetti. The rise is essentially invisible to the naked eye. Onsite elevation averages 7545 ft but the difference across the site is negligible, with a maximum elevation of 7549 and a low point of 7542 ft (a roughly 2 m difference). Surface geology

of the surrounding landscape suggests Reddin sits atop shallow alluvial sediments overlying Alamosa Formation fluviolacustrine clays and intermediate alluvium (figure 11). The alluvium mapped within the area is colloquially referred to as the "Dobe" or Hooper Series hardpan. Interlaced Pleistocene and Holocene sand sheets texturize the surface of the site in low shrub-coppice dunes measuring a few inches tall to more than 3 ft tall above the hardpan surface. The local plant community is predominantly chico brush with lesser quantities of saltgrass distributed linearly along the shorelines of shallow, playa pond-like features found south within the site. The braided structure of abandoned La Garita Creek stream channels, which frame the site on all sides, suggests that most if not all playa-like features in proximity are the remains of relic oxbow lakes and marshlands present during the YDC – like those found just upstream in today's Mishak Lakes Preserve and Russell Lakes State Wildlife Area (figure 12).

The archaeological story at Reddin begins just the same as most other significant Paleoindian discoveries. Gordon Reddin, a local postmaster and grocery shopkeeper from the town of Hooper, found a Folsom projectile point at the site in 1978. At the time, Dennis Stanford, John Albanese, a Smithsonian crew, and the local chapter of CAS were conducting test excavations at the Zapata Folsom site south of the GRSA. Reddin visited Stanford and encouraged a visit to the newfound locality along La Garita Creek, far into the interior of the Closed Basin floor. Confirmation of the site's significance was immediate, and acknowledgement of the site's unique challenges was made clear early on, too. In chapter 3, I review the history of fieldwork at Reddin, including a synthesis of the Smithsonian efforts as well as CSU's more recent surveys of the surface scatter.

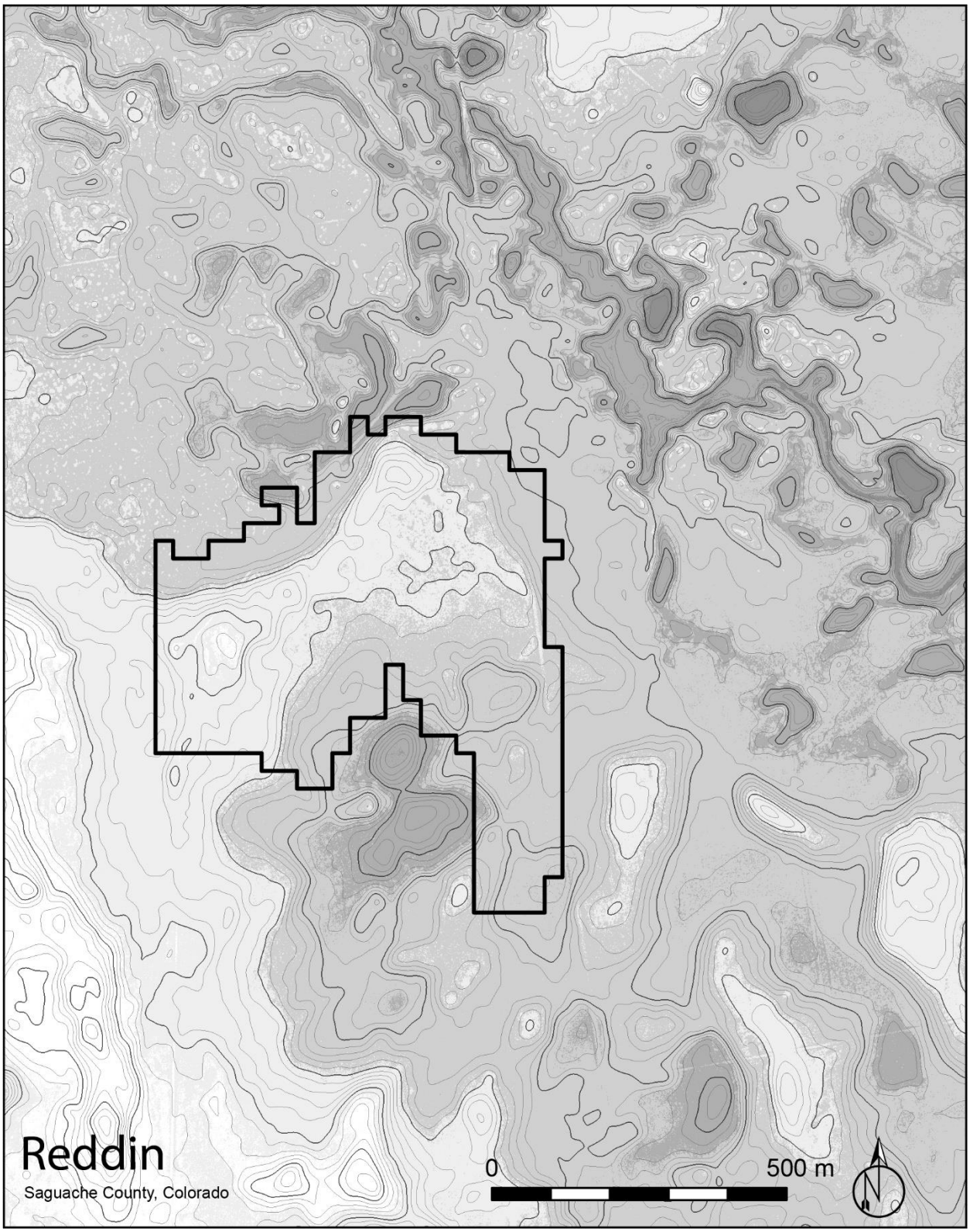


Figure 12. Topographic map of the Reddin site near the La Garita Creek floodplain modeled from open-access LiDAR tiles, showing the outline of CSU's 2021 surface survey grid at the site. Oriented to magnetic north with 10 cm contour intervals.

CHAPTER 3 - FIELDWORK

Open lithic scatters and buried Folsom components require different approaches to fieldwork. In Folsom archaeology, researchers have followed relatively fine-grained excavation protocols for nearly a century. Frank Roberts' excavations at Lindenmeier in the 1930s introduced Folsom archaeologists to precise three-dimensional mapping of artifacts in combination with a block, unit, level excavation system allowing for accurate spatial control (Sellet 2013; Wilmsen and Roberts Jr. 1978), which remains comparable to modern methods. However, no single standard exists for pedestrian surveys of open lithic scatters. Folsom archaeologists have used many different survey methods, rarely overlapping in their approaches (Hofman et al. 1990; Hurst and Johnson 2019; LaBelle and Meyer 2021; Meltzer et al. 2006; Seebach 2004). Specific techniques for survey reflect the archaeologists' specific research goals, which shape the sampling scale, extent, and resolution of each published survey on Folsom lithic scatters.

At Reddin, I worked backwards to understand the Smithsonian Institution's goals and the purpose of field methods used there, more than 40 years ago. Dennis J. Stanford passed away in early 2019, the spring before I started my degree program at CSU. I never spoke with Stanford directly about his past experiences, fieldwork, or any new thoughts and conclusions that he had about Reddin towards the end of his career. Archaeologists cannot re-excavate portions of sites dug by previous research teams, and retracing another's footsteps in a pedestrian survey poses similar challenges. However, one aspect of the original fieldwork seemed immediately clear as my project unfolded; Stanford planned a longitudinal study of the site, one allowing research teams to return periodically, conduct new surveys, and grow an evolving dataset of the Folsom occupation with each visit (figure 13).



Figure 13. Dennis J. Stanford setting the survey grid at the Reddin site in August 1983. Photo slide courtesy of Margaret A. Jodry (Pegi) and the Smithsonian Institution.

This chapter describes the field methods undertaken at Reddin, beginning with a review of the Smithsonian's 1979 and 1983 field seasons. Handwritten notes found in the museum collection artifact bags provide cursory details of the original fieldwork, but no synthetic field notes exist – these critical resources remain missing according to the National Anthropological Archives and Cultural Resources Center in Washington D.C. (personal communication, May 2022). Towards the end of the chapter, I transition to a review of new fieldwork led by CSU. Our work began with high-resolution aerial mapping, followed by resurvey and expansion of the survey area, and ended with new fine-grained surveys targeting one locality with high Folsom artifact densities.

Smithsonian Institution 1979-1983

A previously published summary of the Reddin site in the CCPA's Rio Grande context provides an essential description and visual depiction of the Smithsonian Institution field protocols

carried out in 1979 and 1983 (Martorano et al. 1999; Jodry 1999b). Jodry (1999b:76) wrote that Stanford, Gordon Reddin, and two local volunteers surveyed the site using a systematic artifact collection grid soon after the initial discovery of a Folsom point near the banks of La Garita Creek (see conclusion of chapter 2). I provide details about the survey grid in the following section, including conflicting information about the initial reports of the site's size. Personal conversations with Jan Carpenter (Reddin's daughter) suggest this initial team also included Reddin's close family members, who visited the site and the Smithsonian team frequently during their fieldwork in the Valley. In 1979, the survey team collected all pieces of lithic flaking debris observed on the site surface. They also used a theodolite to precisely map chipped stone tools encountered during the survey.

In 1983, the Smithsonian carried out many more tasks at the site, including new surveys but also subsurface testing. The timing of this six-week field season coincided with the Bureau of Reclamation's Closed Basin survey project, which was conducted in advance of a wide network of water wells and pipelines tapping into the shallow boundary of the Valley's aquifer (see discussion in chapter 2). A proposed well and pipeline corridor (80 ft wide) crossed portions of the northwestern quadrant of the Reddin site, so the Smithsonian and a team of collaborators expanded the survey grid and conducted test excavations to determine potential adverse effects of construction within the pipeline right-of-way and proposed well pad. The team also examined site formation characteristics in 1983, with targeted excavations of Folsom concentrations and playa lake beds. The 1983 crew members included core participants of the Smithsonian Paleoindian Research Lab (Stanford and Jodry), a University of Wyoming field school led by Mary Lou Larson and Marcel Kornfeld, as well as Jerry Dawson – an archaeologist well-versed in Folsom settlement patterns within the Northern and Middle Rio Grande regions (figures 14 and 15).

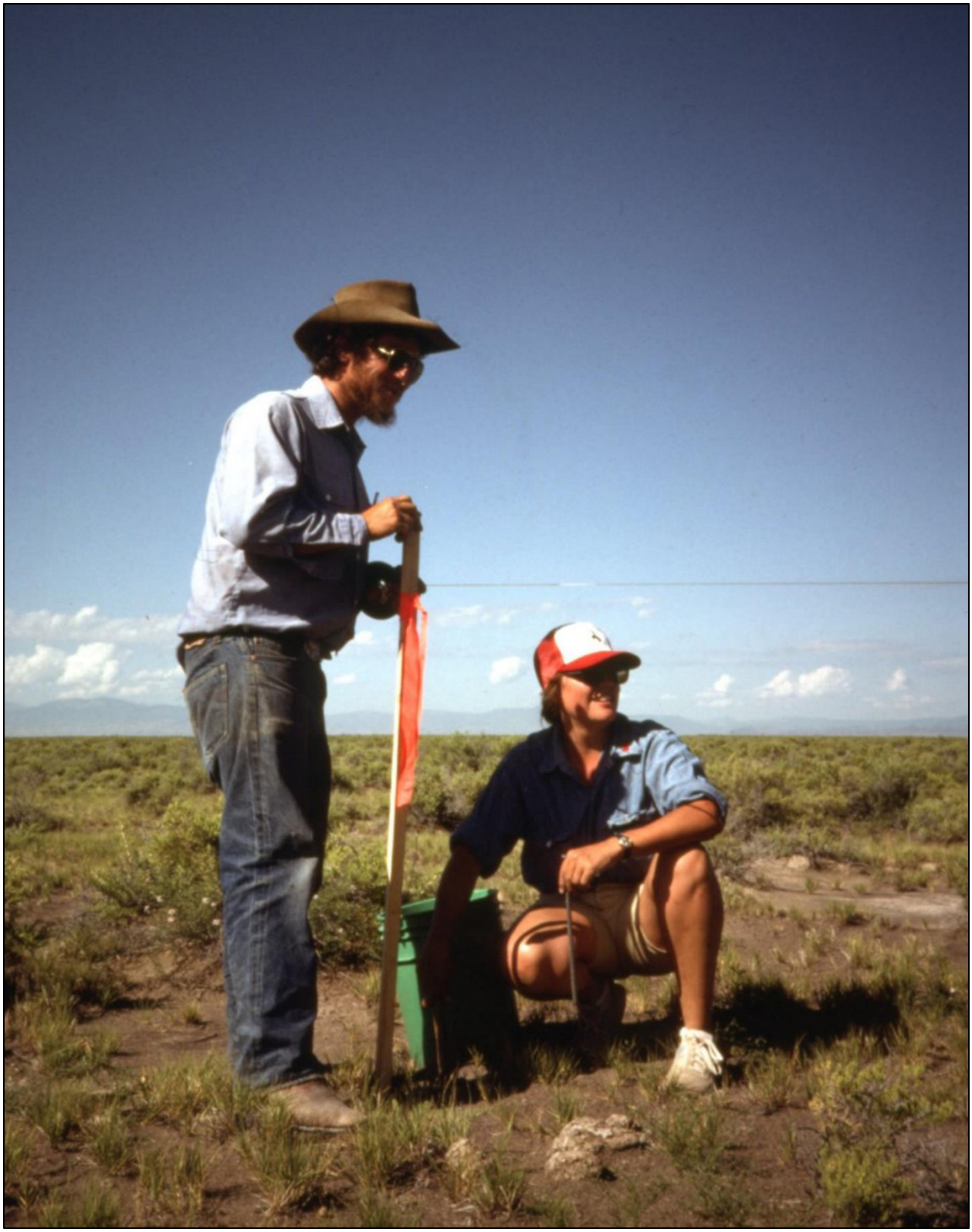


Figure 14. University of Wyoming field school instructors Mary Lou Larson (right) and Marcel Kornfeld (left) in 1983. Photo slide courtesy of Pegi Jodry and the Smithsonian Institution.



Figure 15. Middle Rio Grande Folsom archaeologist Jerry Dawson (left) and unidentified field school student from the University of Wyoming (right) in 1983. Photo slide courtesy of Pegi Jodry and the Smithsonian Institution.

Survey Grid

The Smithsonian survey grid at Reddin provides horizontal spatial control for the distribution of artifacts collected by the field crews in 1979 and 1983. The sampling interval of the survey grid (30 x 30 m) is consistent with some of today's landscape-level cultural resource survey methods (Douglass et al. 2023; Holdaway and Fanning 2008; Leckman and Heilen 2023; Wandsnider and Camilli 1992; Wilshusen et al. 2016). Hereafter, I refer to the spatial scale of the individual units in this broad survey grid as the *block level* – representing the coarsest spatial unit available for analysis at the site. For Folsom archaeologists, the spatial resolution of the individual survey blocks in this grid is significant. Most Folsom sites in the archaeological record would fit comfortably within just one of these large squares (Andrews et al. 2008), so any potential patterning in Folsom artifact discard process measured across a grid with this resolution is unprecedented (see chapter 5 for further theoretical discussion). The application of a grid-based survey at Reddin was also unique among the broader record of surface scatter site investigation during the 1970s (Ammerman 1981; Schiffer et al. 1978). Today, Folsom scholars reference sites like Adair-Steadman and Shifting Sands for the application of accretional mapping projects with persistent survey techniques (Hofman et al. 1990; Hurst and Johnson 2019; LaBelle and Meyer 2021; Ryan 2016), but these other projects focused primarily on piece-plotting Folsom artifacts rather than applying both precise mapping of tools and controlled collections of debitage. In this light, the surface grid at Reddin stands out for its early emphasis on horizontally controlled systematic inventory and the potential for continuous survey observations in the grid system.

Jodry (1999b:76) initially reported that the site measured 6450 m^2 based on the survey grid in 1979, but I believe this was likely an underestimation of the actual surveyed area during the 1979 field project. Figure 6-11 in Jodry's (1999b) site summary illustrates an artifact density map

from the 1979 field season which covers an area spanning roughly 600 m on a north-south axis and about 450 m on an east-west axis (figure 16). This published map alone suggests the 1979 survey grid must have encompassed a more-or-less contiguous area of lithic debris and tools measuring 270,000 m^2, or roughly 67 acres in total. Regardless of these data reporting differences, the published map and Jodry's descriptions give important details about the initial findings – the Smithsonian documented roughly three Folsom artifact concentrations distributed between La Garita Creek and several ancient pond depressions south of the site. Jodry (1999b:76-78) stated that one of these Folsom concentrations overlapped with a cluster of Archaic materials, near La Garita Creek. Contours of debitage density within the map show both diffuse and concentrated patterns of flaking debris in association with Folsom material (figure 16).

The Smithsonian expanded the surface inventory grid in 1983 for additional surface artifact collections. Jodry (1999b:76) reported that the survey inventory grew from 6450 m^2 to 9480 m^2, but this also appears to be an underestimate of the size of the survey in 1983. The Smithsonian collection from the site contains debitage bags with individual provenience labels for survey blocks in the grid, and there is a minimum of 314 spatially unique labels (282,600 m^2 or about 70 acres). This new information, coupled with the published extent of the 1979 survey extent, suggests the total surface inventory spanned a much larger area than previously considered – though there is no definitive source to say exactly how far the grid expanded. Additionally, the artifact collection bags only corroborate positive survey areas containing lithic debris, and any negative survey blocks within or outside of this area remain unaccounted for. I assume that the Smithsonian bounded the extent of the site based on contiguous survey blocks containing artifacts, but this is uncertain. Figure 17 shows the extent of the surface inventory based on collected pieces of debitage.

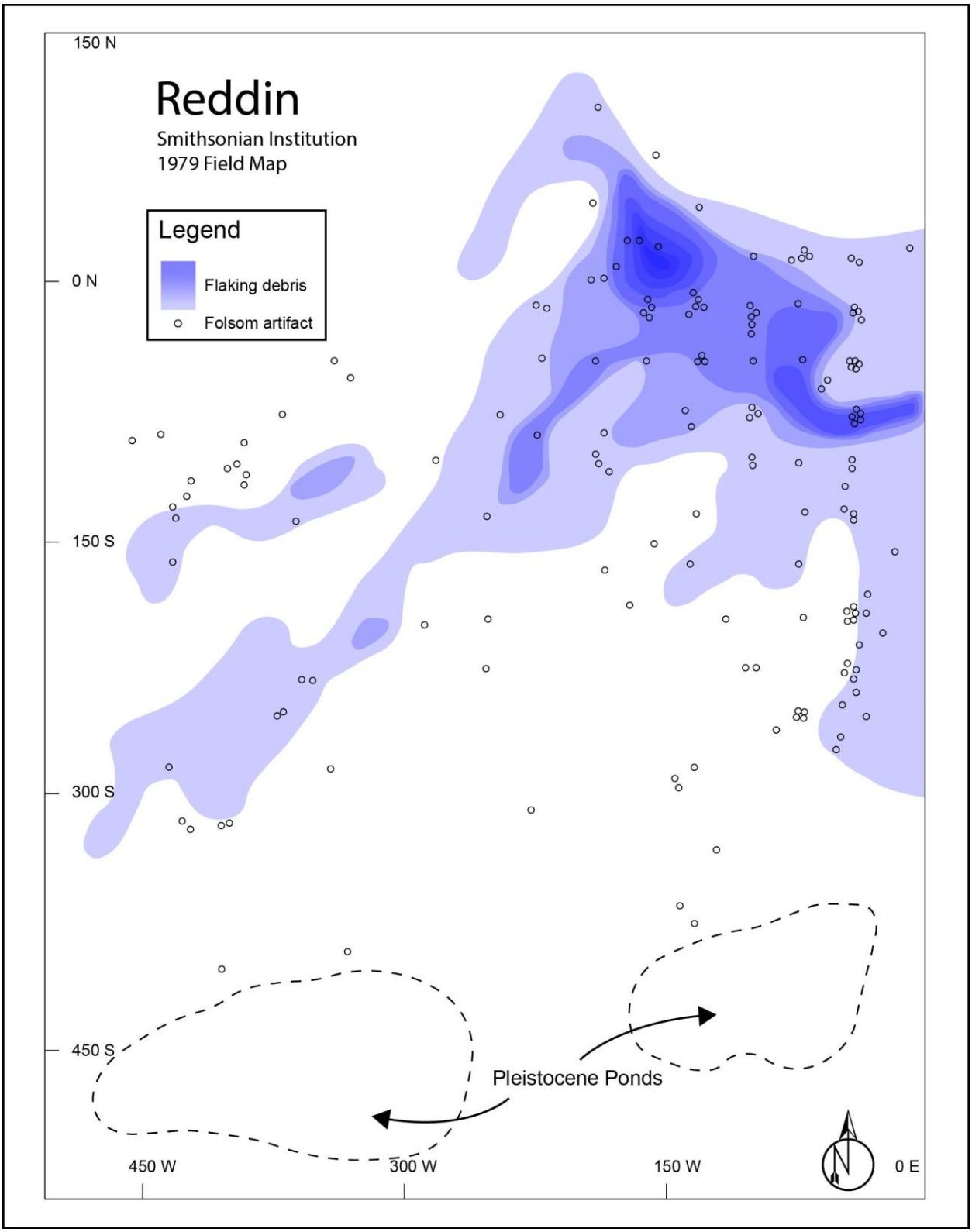


Figure 16. Adapted and colorized map of Folsom tools and debitage at the Reddin site presented by Jodry (1999b:figure 6-11). The map depicts results from the 1979 field season, but not the 1983 field season. Site grid scale in meters.

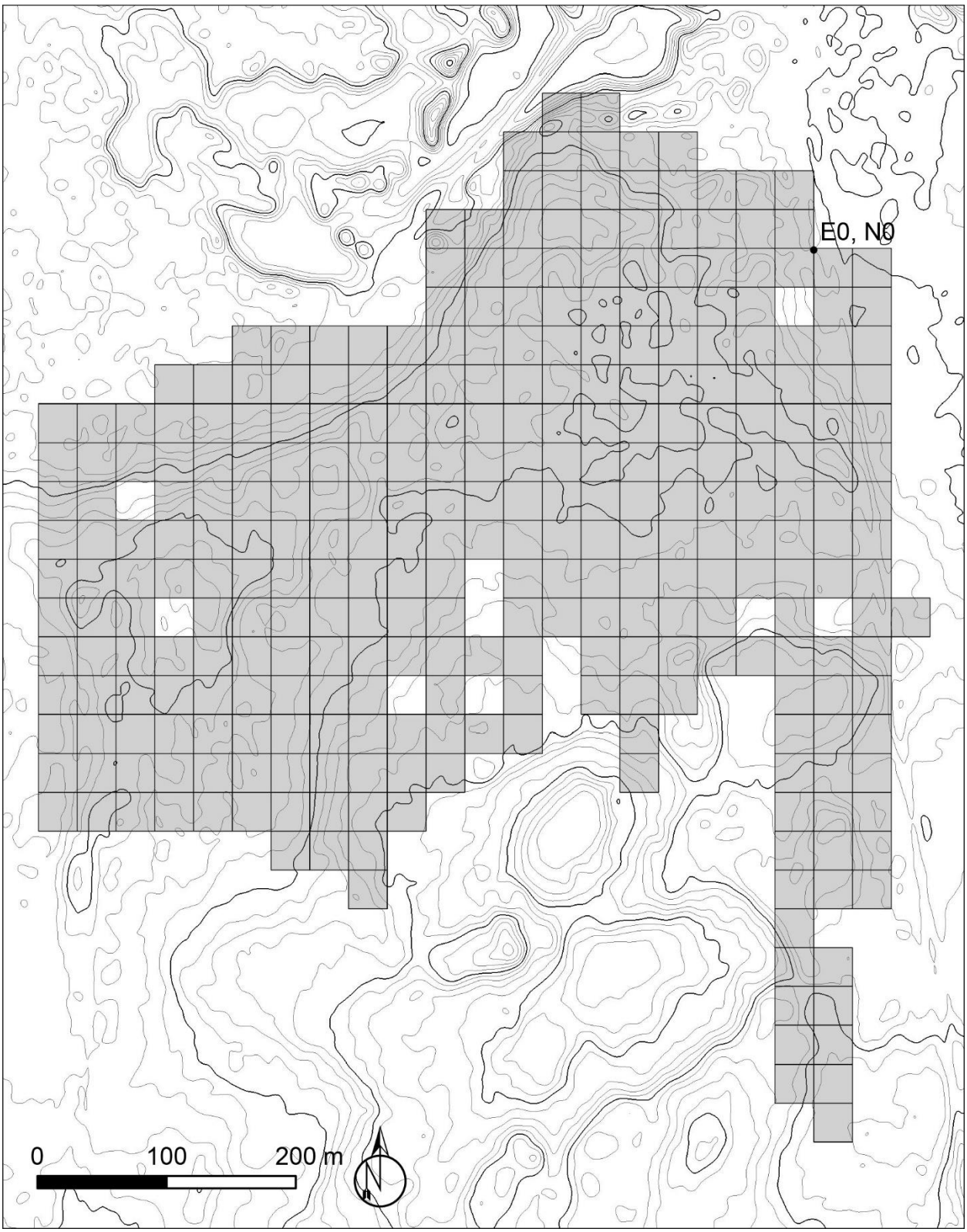


Figure 17. Map of the survey grid at Reddin showing 30 by 30 m grid cells with positive counts of debitage (gray squares), based on Smithsonian 1979-1983 artifact collection.

The shape and orientation of the survey grid is an important factor to consider; it appears controlled by existing infrastructure and natural factors. The grid is set up much like an excavation. The survey block provenience is arbitrary and based on a zero-zero datum, measured in 30 m intervals east, west, north, and south (i.e. a survey block with a southwest corner 30 m east and 120 m north of the datum would read E30, N120). The arbitrary grid is aligned to magnetic north and offset from true north given the orientation of the county road (omitted), which runs north to south and makes up the eastern boundary of the site.

The southern boundary of the surface grid terminates near a series of small lake depressions. As discussed in chapter 2, these depressions most likely represent the shallowly eroded channel beds of the La Garita Creek mainstem, which may have been a connected network of wetlands and oxbow lakes during wet years or more isolated ponds in drier years. The northern and northwestern edges of the survey grid meet the La Garita Creek floodplain, characterized by an eroded shallow stream channel beneath the shallow rise of the eolian sand sheet, covering much of the site surface. The western edge of the survey grid appears arbitrarily divided at the location of a water well access road. To the east, the survey grid extends to the limits of a Bureau of Land Management fence line adjacent to private property. In general, artifact densities appear to have been a driving factor of the surface inventory limits, and thus the overall site boundary reflects its cultural deposits, natural constraints, and mitigated limits of water well and pipeline infrastructure.

Artifact Plotting

The Smithsonian team concentrated most of their efforts on mapping Folsom diagnostic weaponry and associated debris, including projectile points, preforms, and channel flakes – but the team also mapped other artifacts including post-Folsom diagnostics, as well as gravers, bifaces, and flake tools. The Smithsonian plotted the horizontal provenience of each tool they discovered

in place; the team avoided documenting each artifact's vertical position relative to the datum due to the lack of topographic relief and the paucity of a significantly buried component. Surveyors set up a theodolite to map each artifact, measuring distances and angles to piece-plotted items from temporary benchmarks placed at the corners of each survey block in the grid. After the fieldwork, the team labeled each artifact with a unique curation number: SL-17-1, SL-17-2, SL-17-3, and so on. At present, I do not know the specific meaning of the root of the labeling convention (SL-17), but these are likely to represent internal Smithsonian catalog numbers.

Unfortunately, there is no synthesis of artifact provenience to help answer outstanding questions about the chipped stone tool mapping protocol at Reddin, or to help resolve missing provenience information. The Smithsonian collection contains disparately placed paper slips and collection envelopes occasionally listing temporary artifact labels, SL-17 curation numbers, survey blocks, and in the best case – piece-plotted artifact coordinates (figure 18). I was able to join handwritten coordinates to 359 out of 1142 artifacts in the collection, amounting to 31 percent of all labeled items. For 75 of the labeled artifacts, corresponding notes described a specific survey block, but these items presently lack precise piece-plot coordinates. I feel confident that additional provenience information exists for some of the other labeled artifacts in the Smithsonian artifact collection, but I do not know where this information is currently stored (National Anthropological Archives and Cultural Resources Center personal communication, May 2022). Figure 19 shows the distribution of known piece-plotted artifacts, reconstructed by inventorying paper envelopes and other curation materials. A spatial summary and analysis of these artifacts is presented in chapter 5.

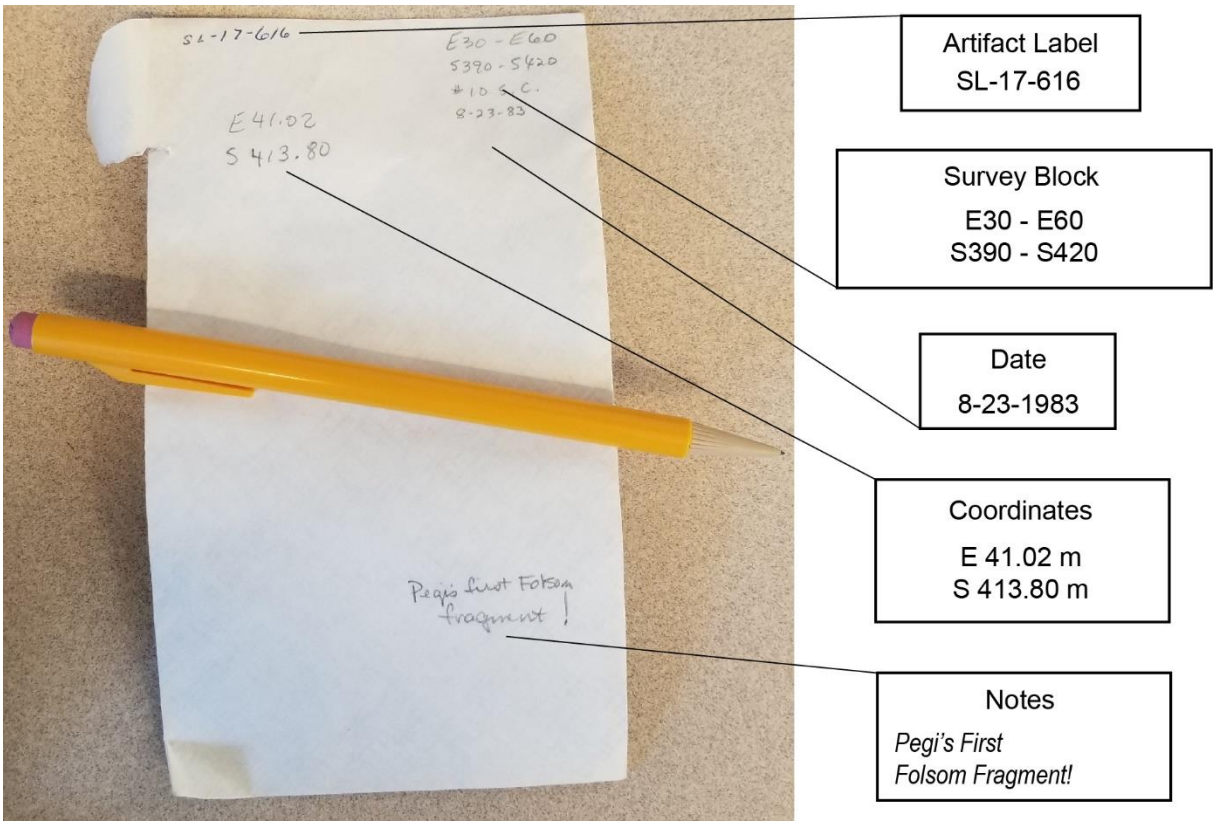


Figure 18. Image depicting an example of a field specimen collection envelope, showing artifact labels and provenience information.

In 1983, the survey team initiated an effort to precisely document the distribution of flake debitage within a few survey blocks of special interest, presumably due to high densities of Folsom chipped stone tools. Jodry (1999b:76) wrote that the team piece-plotted every flake and tool within a 150 m^2 area, but prior to this project, the specific location of this intensive piece-plotting sample area was not known – the size of an individual survey block in the grid system extends well beyond 150 m^2. Field notes provided by Marcel Kornfeld (personal communication, May 2022) shed additional light on this intensive mapping effort, although it is presently not possible to geolocate the coordinates of these precisely mapped debitage pieces. At least five survey blocks were selected for fine-grained inventory and mapping of debitage and tools, covering an area of 4500 m^2. This sampling area included four contiguous survey blocks near the shoreline of the easternmost playa at the site (covering blocks between E0-30, S420-450) and one isolated survey

block further north along the eastern site boundary at E0-30, S270-300 (figure 19). Surveyors walked in transects at opposing orientations (east-west and north-south) during this fieldwork, using intervals spaced between 1 m and 1.5 m. This intensive mapping effort produced 346 piece-plotted artifacts in the "East Playa" locality, and 190 artifacts in the isolated survey block, further north.

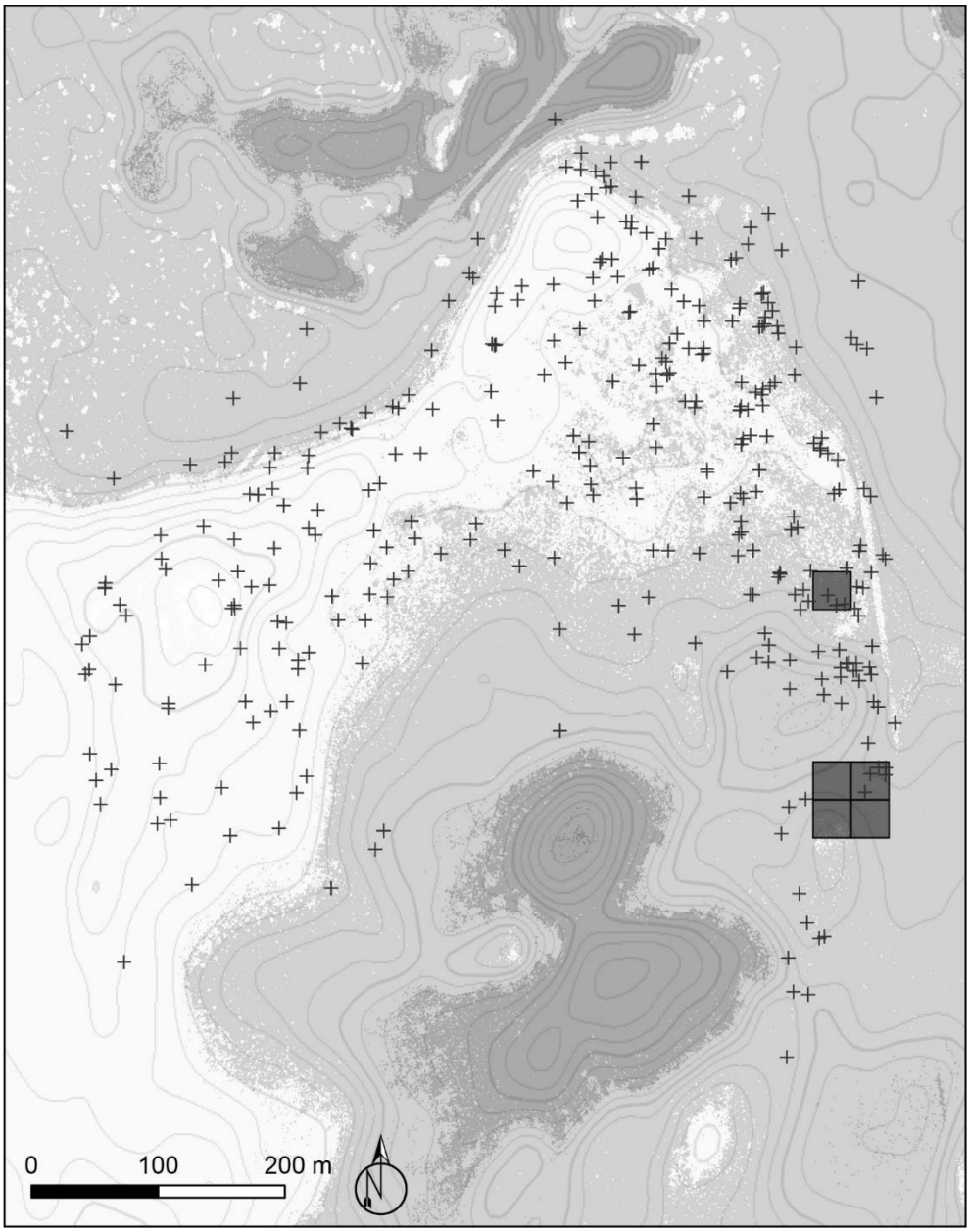


Figure 19. Map of all piece-plotted chipped stone tools in the Smithsonian artifact collection (n=359), based on 1979-1983 fieldwork. Blocks selected for fine-grained surveys and 100 percent mapping in 1983 also shown.

Block Excavation

In Folsom archaeology, sites with more than 100 m^2 of excavation are extremely rare due to multiple factors including generally small Folsom site sizes, deeply stratified and thus costly buried deposits, and a low density of artifacts, on average (Andrews et al. 2008; Hofman 2002; LaBelle and Meyer 2021). Pelton (2018:table 6) tallied 19 Folsom sites with more than 100 m^2 of excavation, and Reddin is near the top of the list with over 750 m^2 reported by Jodry. Jodry (1999b:76) described the purpose and placement of excavations at Reddin; in 1983, the Smithsonian and University of Wyoming field school team excavated 30 units at the site measuring 5 by 5 m each, with 26 units placed in the pipeline project right-of-way and four units positioned in the center of several Folsom artifact concentrations. The pipeline route was ultimately shifted because of their mitigation efforts.

Like piece-plotted tools, much of what I have been able to reconstruct about the excavations at Reddin draws from my review of field notes in the artifact collection as well as photo slides, but there is no specific paperwork describing methods or results for this work. Provenience labels written on some of the artifact bags disclose a total of 27 excavation units in the general area of the pipeline right-of-way and near the present location of a water well on the northwestern edge of the site. The excavation units in this area measured 5 m by 5 m, as described by Jodry (1999b:76), but units of other sizes (1 x 1 m) were apparently placed near the site datum in a Folsom concentration. I estimate the Smithsonian excavated a total of 38 units in four general localities across the site, including 32 units measuring 5 m by 5 m and six units measuring 1 m by 1 m (figure 20). The artifact bag labels and descriptions suggest that at least 806 m^2 were excavated at Reddin.

Jodry's narrative and photographs of the field school team confirm that the excavations did not move far vertically but instead focused on testing the horizontal density of artifacts within the sand sheet overlying the hardpan (figure 21). Field school students used a shovel skimming method in each excavation unit, and the sandy sediment was screened through one-quarter-inch mesh based on handwritten notes. The team found a limited number of artifacts in an unconsolidated sand layer ranging from 1 to 20 cm thick. Only 1116 pieces of debitage and five tools were found across all excavation areas, suggesting much of the Folsom component rested below the sand sheet or in recently deflated deposits. Some cultural material was found within the hardpan underlying the sand sheet, but the Smithsonian team estimated that artifacts were vertically displaced from above and likely not in situ within the ancient alluvium.

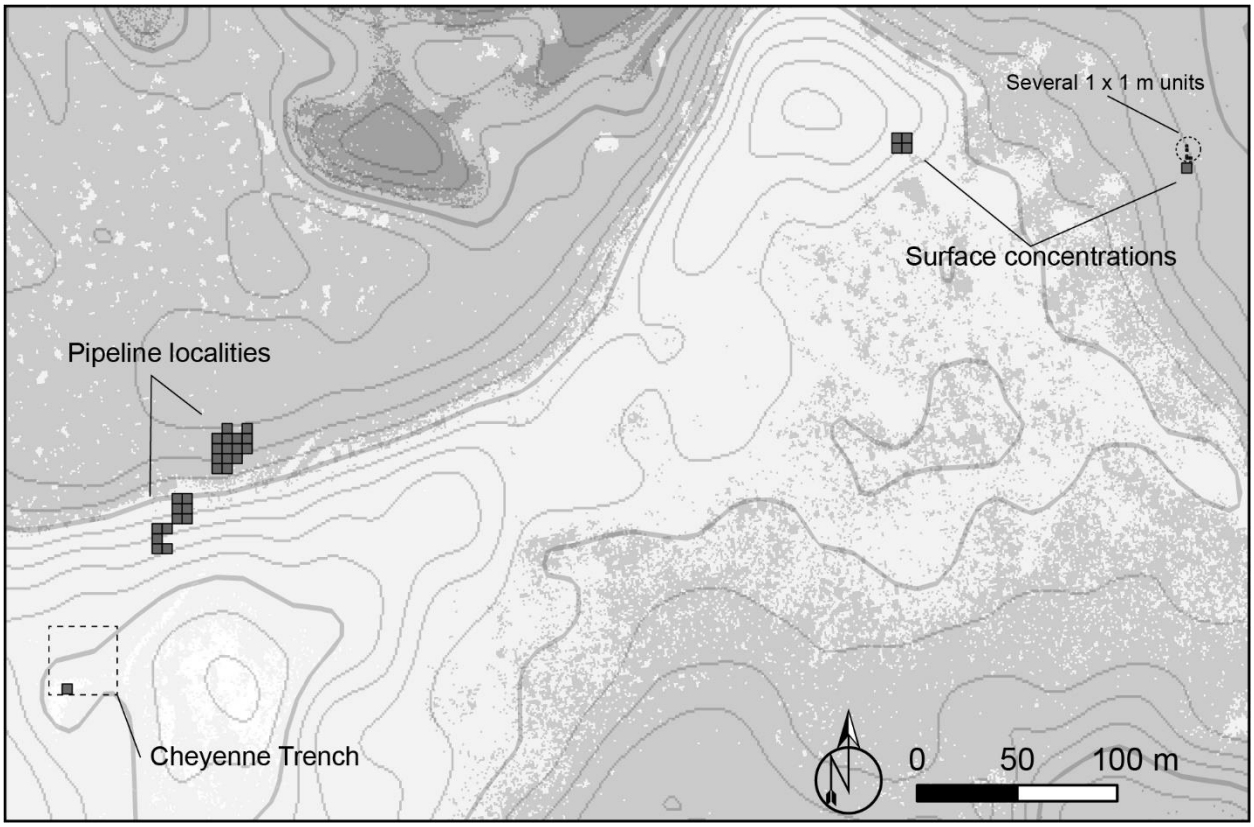


Figure 20. Map of known excavation areas at the Reddin site. The approximate location of the Cheyenne Trench is depicted (dashed square).



Figure 21. University of Wyoming field school students shovel skimming the sand sheet at the Reddin site in 1983. Photo slide courtesy of Pegi Jodry and the Smithsonian Institution.

Backhoe Trenches

Results of geoarchaeological test trenches excavated near the water well and in two of the playa depressions confirmed that the Folsom component post-dated the formation of local hardpan sediments. The Smithsonian established at least three backhoe trenches in each location, but the exact dimensions, precise spatial coordinates of units, and depths of geoarchaeological testing remain unknown. Handwriting on several of the photo slides provided some additional context, however. One backhoe test trench was excavated in the general area known as "West Playa", but the exact location of the trench (shoreline or playa center?) is unknown. The test trench excavated near the water well was known as the "Cheyenne Trench", and labels on the photo slides suggest the trench was excavated somewhere within the W570-600, S270-300 survey block and presumably near one of the 5 m by 5 m units denoted by the artifact bag labels (figure 20). At

present, it is not possible to link photos of the backhoe trench in the "East Playa" locality to a specific location.

The photos of each of the pits show that the depths below surface averaged between chest and head height (perhaps 2 m deep or so) based on the scale of equipment and crew members in the photos (figure 22). The trenches were perhaps 1 m wide, but this is uncertain. Oblique photos of the western profile wall in the Cheyenne Trench appear to show thin evaporite layers (figure 23), a consistent observation at dry lake beds elsewhere in the San Luis Valley – suggesting fluctuations between wet and dry, saline conditions (see environmental descriptions in chapter 2). None of the artifact bags in the Smithsonian artifact collection have provenience labels attributed to any of the geological test pits, further suggesting these were not used to test sediment characteristics near artifact concentrations. Jodry (1999b:76) states that the results of geological tests indicated that Folsom occupations coincided with a slowly aggrading and non-aggrading surface, but much about the surface and subsurface geomorphology of the site remains untested.



Figure 22. Dennis Stanford (left) and backhoe operator (right) in the Cheyenne Trench in 1983. Photo slide courtesy of Pegi Jodry and the Smithsonian Institution.



Figure 23. Dennis Stanford denoting what appears to be thin evaporite strata in the profile wall of the Cheyenne Trench in 1983. There are no profile descriptions of the stratigraphy in this trench or other units at the site.

Supplementary Field Work

The majority of the Smithsonian's fieldwork at Reddin was accomplished during the 1983 field season, considering the volume of labor and range of methods applied during that field season. However, analysis of the artifact collection revealed additional information indicating that members of the Smithsonian team visited the site occasionally to conduct surveys for artifacts. One such effort was conducted in 2005, where Smithsonian and BLM archaeologists piece-plotted at least 36 artifacts across the site surface during a small survey. These efforts were not formally documented, however, but detectable based on the temporary artifact labels and artifact sketches found in the artifact collection.

CSU 2020-2022

In late 2019, the Smithsonian transferred the Reddin artifact collection to the Bureau of Land Management, San Luis Valley Field Office (SLVFO). I visited BLM archaeologist (Brian Flynn) in early 2020 to assess the state of the collection and conduct a preliminary field visit to determine potential for new fieldwork at the site. Reddin was partially covered in snow at the time, but even in patches of bare ground diverse lithic raw materials shone brightly against the background of the hardpan surface – a good sign for survey planning. Dr. Jason LaBelle of CSU, the BLM SLVFO, and CSU's archaeological repository (AR-CSU) coordinated a long-term curation agreement to permanently house the collection at CSU and form the basis of this dissertation. These partnerships and projects emerged to provide needed context to the original findings, but also to address new questions about the site.

Results of the Smithsonian fieldwork, particularly from the broad-scale surface inventory and piece-plot mapping of tools, provide some clues about the presence of Folsom artifact concentrations and the possibility of discrete localities. Their team observed a generally bimodal site distribution with artifacts concentrated along the southern playa depressions and the La Garita Creek channel, to the north (Jodry 1999b). The abundance of Folsom weapon tips near the playas and dehafted weapon bases along the creek edges suggested repetitious hunting and camping activities, reflecting an underlying spatial structure of artifact discard processes related to those activities. However, it was not immediately clear upon review of this previously published data (the 1979 map) how such broad spatial patterns represent intact Folsom activity areas related to one or multiple occupations, or whether certain activities took place in the identified concentrations.

I designed a field protocol to search for Folsom artifact concentrations based on remaining lithic debris on the site surface. I planned to utilize the existing Smithsonian survey grid for most of this effort and to create a longitudinal (cumulative) survey dataset for the site. I also planned to implement new fine-grained surveys within high-density Folsom locales, to detect the presence (or absence) of spatially discrete artifact discard patterns potentially related to specific site activities. I also wanted to ensure that potential cultural patterns, whether large or small in scale, were weighed against other mitigating factors like ground surface visibility, vegetation and sand cover, as well as sampling intensity of the survey method itself. I hoped to learn whether the site told a different story about Folsom hunter-gatherers in the 40 years after initial research, by comparing new field results with a revised analysis of old findings.

Retracing the Smithsonian

My initial fieldwork focused on constructing a baseline map of the site, guided by two main goals. First, I aimed to generate high-resolution aerial imagery of the site surface with enough detail to distinguish between three land cover types: 1) exposed hardpan surfaces or blowouts, 2) areas covered by the Quaternary and Holocene-aged sand sheets, and 3) vegetative communities such as chico brush and cacti. I planned to use aerial image classification in ArcGIS Pro to formally segment the site surface into these land cover types for an artifact visibility assessment. These field data provided a way to test whether Folsom clusters at the site covaried with barren surfaces (see chapter 5). The second goal of this baseline mapping effort was to relocate the Smithsonian survey grid – or fragments of it – to link spatial provenience data from the artifact collection and align a new CSU comparative survey sample with those previously explored areas. Jodry's (1999b:76) description suggested the presence of a site datum with temporary mapping benchmarks distributed across the surface at regular intervals (30 m). Thus, our initial fieldwork focused on

drafting new high-resolution imagery of the surface but also ensuring that we could georectify our survey results with existing data.

In July 2020, we initiated the project described above. Finding the Smithsonian survey grid was not difficult; a line of fixed rebar at regular 30 m intervals ran from east to west (magnetic) from the local county road near the arbitrary datum (E0, N0) out to the water well infrastructure, spanning the complete width of the site. For the remaining corners of the survey blocks, the Smithsonian left in place smaller 6-to-12-inch metal nails and spikes. Some of the nails were partially dislodged or buried by coppice dunes, but the overwhelming majority remained in place – providing an indication of the stability of the local landform. We established a new fixed datum at the southwest corner of the Smithsonian's survey grid at E0-30, N0-30, and changed the arbitrary grid coordinates to E5000, N5000 (see Appendix F). Changing the coordinate system to new grid numbers served one goal: to ensure that spatial analysis of artifacts dealt exclusively in positive coordinates, rather than numbers representing distances north, south, east, and west of the datum (e.g. a square with coordinates W60-90, S120-150 would have a southwest corner of E4910, N4850 in the new grid system).

UAV Survey

I initiated an unmanned aerial vehicle (UAV) photogrammetric survey to draft a high-resolution orthomosaic map (orthoimage) of the site surface. I applied principles of Structure from Motion (SfM) photogrammetry in this data acquisition effort. Sequential overlapping photographs taken throughout the UAV flight path provided raw data to construct a precise 3D and full-color representation of the landscape topography (figure 24). I used the Agisoft Metashape software program to detect matching features between overlapping photographs taken from different angles and locations to align the scene geometry and the 3D position of camera poses (Adamopoulos and

Rinaudo 2020; Campana 2017; Magnani et al. 2020; Waagen 2019). The computer program generated a "sparse" point cloud of the reconstructed scene based on matched feature locations (tie points). After accounting for associated point reprojection errors and user defined tolerances, the program then generated a denser point cloud with fine elevation detail, an overlying "mesh" surface which blankets the spaces between points in the cloud, and a texture atlas that attributed colors to the 3D model from the raw pixel values in the photographs. These products were then geolocated within real space by specifying precise coordinates for physical ground control targets placed in the survey area, prior to the UAV survey.

I used a DJI Phantom 4 Pro for image acquisition, Agisoft Metashape for SfM photogrammetric modeling, and 12 physical control point targets distributed across the site surface to georeference the 3D model and orthoimage. I drafted a serpentine flight path across the known extent of the site and programmed the UAV to follow this path at a specified height above ground level (65 m agl), to allow for 80 percent vertical overlap and 50 percent horizontal overlap between images collected in each flight transect. The flight covered roughly 165 acres, and the UAV took 2181 photos along this flight path. Reprojection errors were strongest along the outside edges of the mapped surface, roughly 12 cm based on the root mean square error (RMSE), but RMSE within the interior of the site (between control points) was between 2-5 cm.

I completed image classification for the modeled UAV orthoimage in ArcGIS Pro using the classification wizard toolset. I chose to develop a supervised classification scheme using trained pixel values and a machine learning algorithm (Support Vector Machine) based on groups of pixels (kernels) selected using a resampling routine and a nonlinear radial basis function (RBF). I digitally sampled 10 representative locations in the orthoimage depicting pixel clusters of 1) barren hardpan surfaces, 2) homogenous sand and coppice dunes, and 3) standing vegetation, including

greasewood and other shrubs. This work produced classified imagery with an estimated 153,670 m^2 of barren hardpan, 338,590 m^2 of sand cover, and 142,110 m^2 of dispersed shrubs (figure 25).

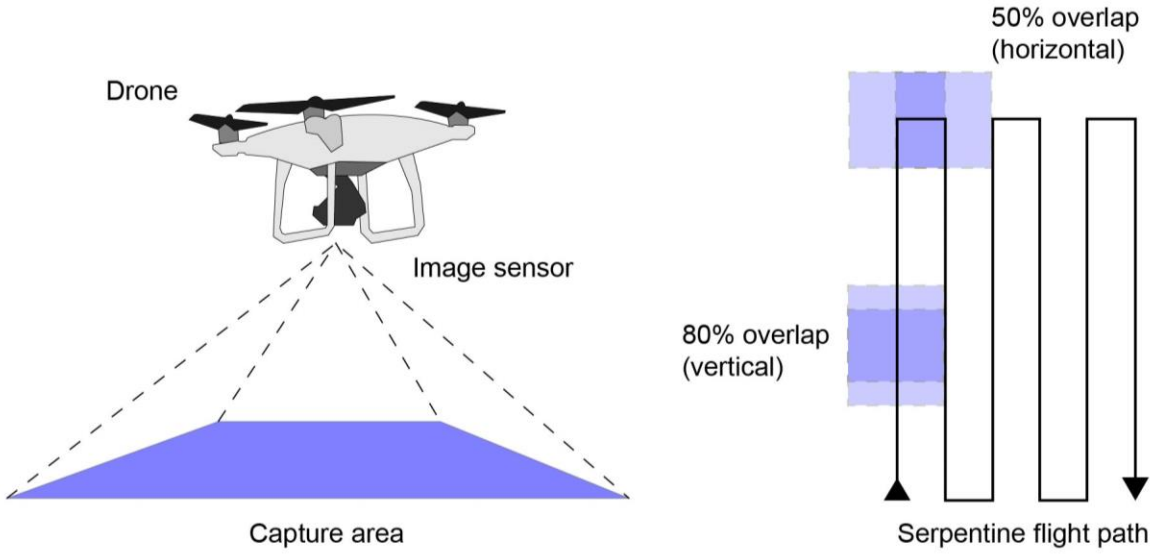


Figure 24. Visualization of the UAV photogrammetric flight process, including the serpentine UAV flightpath design and image sensor overlap.

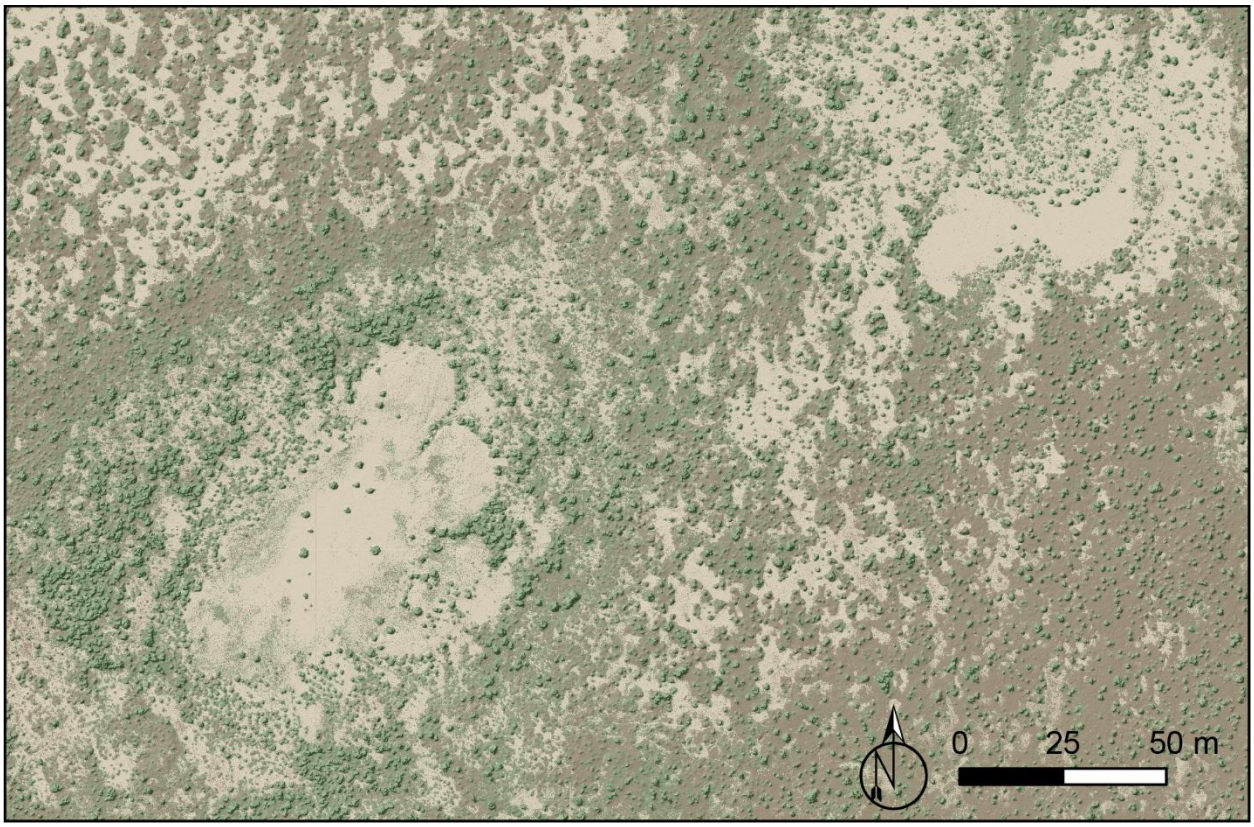


Figure 25. Example of a classified hillshade raster from Reddin, based on UAV orthoimagery collected in 2020. The map shows vegetation (green), sand cover (brown), and hardpan blowouts (tan). The west and east playa pond depressions are depicted here.

Inventory Surveys

The 2020 CSU drone mapping fieldwork at Reddin documented new Folsom artifacts and tools, even though formal pedestrian survey was not a primary goal of the initial project. A total of 17 artifacts were recorded during this early phase of our work, including seven projectile points, three projectile preform fragments, three channel flakes, a biface, and multiple end scrapers (n=3). The sample of mostly Folsom-aged artifacts from this uncontrolled survey while conducting other tasks provided a strong indication that future survey efforts would reveal additional artifact distributions at the site, potentially confirming patterns detected by the Smithsonian team roughly 40 years ago or possibly identifying previously unknown spatial distributions of artifacts.

The 2021 CSU field school conducted the first controlled pedestrian survey of the Reddin site since the Smithsonian team. Our focus for the field season was twofold: 1) to explore any changes to the spatial distribution of the site, including artifact concentrations, and 2) to create a robust dataset of the pedestrian survey method to later test for sampling effects on patterns of artifact discovery. The Smithsonian survey grid served as the backdrop for this survey effort. We prepared the site grid for pedestrian surveys by visually marking the corners of each survey block with alternating color-coded PVC tubes, which rested over existing corner nails left in place by the Smithsonian team (figure 26).

I randomly assigned individual students to survey within one survey block at a time, where they walked in transects at 3 m spacing. Crew members flagged chipped stone tools in each survey block, and then precisely mapped tools with a total station. Artifacts were temporarily labeled with a logical naming convention, using the first letter of the site name and corresponding year of the field season (R21-1, R21-2, and so on). Crew members did not count individual pieces of debitage for the 2021 field survey effort; surveyors estimated the relative quantity of debitage within each square by using logarithmic scale estimates (0 flakes, 1-10 flakes, 11-100 flakes, 101-1000 flakes, > 1000 flakes). This method ensured that our field team would finish surveys across the extent of the site given our 10-day field schedule while balancing efforts to quantify the relative density of flaking debris across the site and note the position of artifact clusters, if present. Table 7 lists an essential summary of these data, and figure 27 provides a map display of plotted tools and flake density from the 2021 field season. Our work expanded the Smithsonian grid somewhat along the edges of the previously laid survey blocks, covering a contiguous area of 84 acres made up of 376 individually surveyed blocks.

Our team generated additional data for the survey process, to help determine sampling effects. Crew members visually assessed the extent of sand cover within each survey block using an ordinal percentage class (0 percent, 25 percent, 50 percent, 75 percent, and 100 percent). These same intervals were used to estimate the relative ubiquity of standing shrubs in each square, as well. Surveyors then recorded additional attributes related to the walking procedure, including start and end times as well as the direction of transects (east to west or north to south). Table 7 summarizes data for several land cover and survey attributes, and figure 27 shows the spatial distribution of multiple survey variables. These data are beyond the immediate scope of this dissertation but will be used in supplementary research on the effectiveness of the field survey.



Figure 26. CSU's 2021 field school crew members resetting the Smithsonian survey grid corners.

Table 7. CSU 2021 field school survey data matrix organized by blocks with expected debitage counts vs. other variables of interest (piece-plotted tools, sand cover, and vegetation cover).

	Survey Bin (estimated debitage count per block)				
	Lowest (n=0)	Low (n=1-10)	Medium (n=11-100)	High (n=101-1000)	Highest (n=1000+)
Plotted Tool Data					
Blocks with Tools	1 of 24 (4%)	21 of 151 (14%)	45 of 175 (26%)	8 of 24 (33%)	1 of 2 (50%)
Total Count of Tools	1 of 111 (<1%)	29 of 111 (26%)	60 of 111 (54%)	17 of 111 (15%)	1 of 111 (<1%)
Range of Tools	0-1	0-2	0-3	0-6	0-1
Mean Tool Count	0.04	0.19	0.34	0.71	0.5
Standard Deviation	0.20	0.51	0.65	1.3	0.7
Sand Data					
Number of Observations	24 of 24	151 of 151	175 of 175	24 of 24	2 of 2
Category 1 – 0%	2 (8%)	5 (3%)	0 (0%)	1 (4%)	0 (0%)
Category 2 – 25%	8 (33%)	44 (29%)	32 (18%)	5 (21%)	1 (50%)
Category 3 – 50%	9 (38%)	47 (31%)	67 (38%)	11 (46%)	0 (0%)
Category 4 – 75%	5 (21%)	44 (29%)	65 (37%)	5 (21%)	1 (50%)
Category 5 – 100%	0 (0%)	11 (7%)	11 (6%)	2 (8%)	0 (0%)
Vegetation Data					
Number of Observations	24 of 24	151 of 151	175 of 175	24 of 24	2 of 2
Category 1 – 0%	0 (0%)	0 (0%)	0 (0%)	0 (0%)	0 (0%)
Category 2 – 25%	15 (63%)	66 (44%)	61 (35%)	13 (54%	0 (0%)
Category 3 – 50%	8 (33%)	68 (45%)	96 (55%)	11 (46%)	2 (100%)
Category 4 – 75%	0 (0%)	14 (9%)	17 (10%)	0 (0%)	0 (0%)
Category 5 – 100%	1 (4%)	3 (2%)	1 (<1%)	0 (0%)	0 (0%)

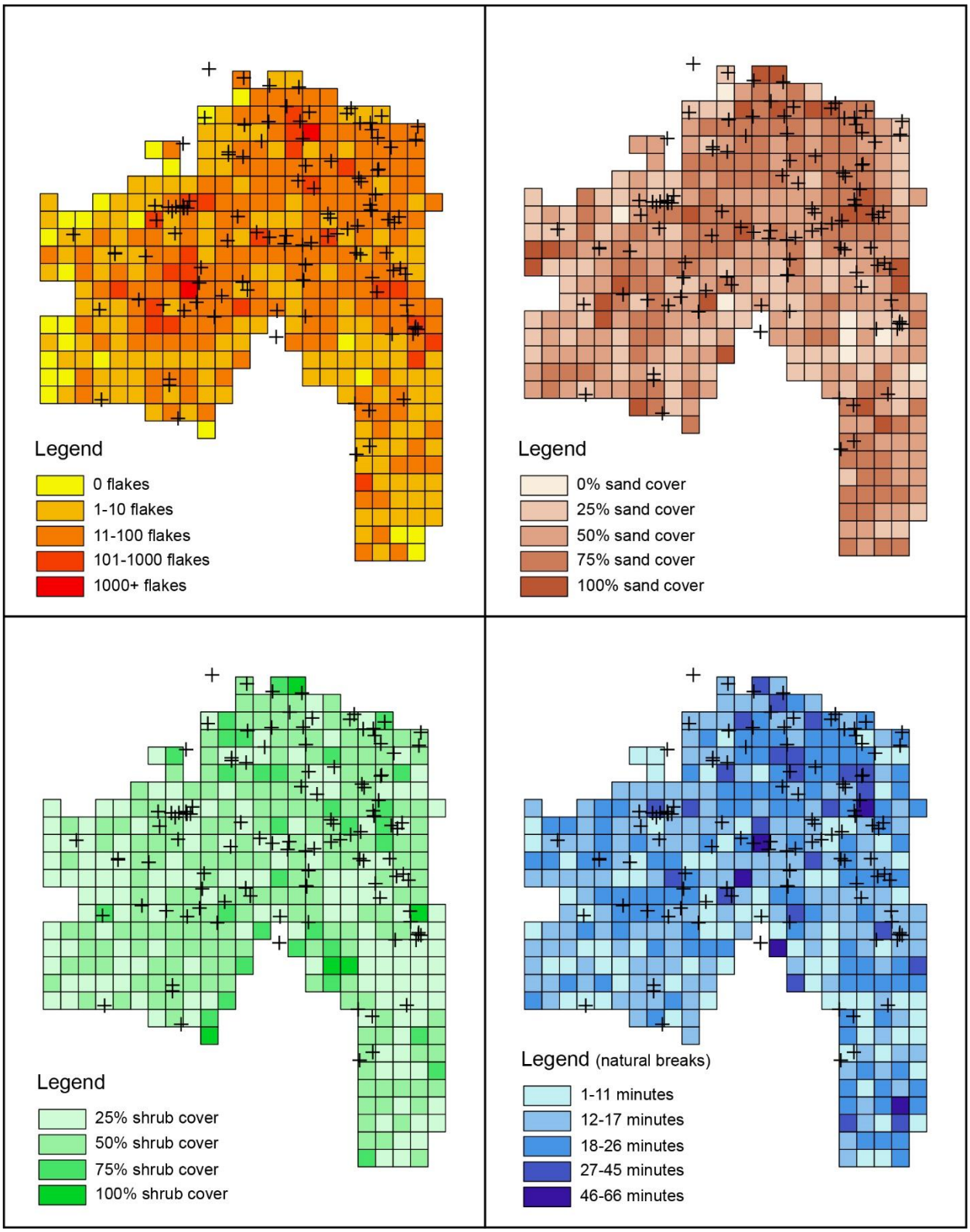


Figure 27. Map series depicting estimated debitage frequences based on the 2021 CSU field survey (upper left), approximate distribution of sand cover (upper right), approximate distribution of vegetation cover (lower left), and time spent surveying in each block (lower right). Plotted tools from the 2021 field season shown (crosses).

Locality A Survey

In 2022, the CSU field school carried out an intensive survey effort within a smaller group of contiguous survey blocks in the grid. I designated Locality A using an exploratory spatial analysis of Folsom projectile preforms and channel flakes, based on artifacts from the Smithsonian collection as well as CSU's 2021 field season. Other researchers have shown that Folsom groups discarded preforms and channel flakes abundantly within residential campsite settings compared to other types of sites or activity areas (Frison 1982; Hofman 1999; Todd 1987; see additional discussion in chapter 5). I wanted to conduct new fine-grained surveys at Reddin within an area comprising mostly residential debris to better understand artifact discard processes related to temporary living spaces (Hofman 1999; Morgan and Andrews 2016; Surovell 2022; Waguespack and Surovell 2014).

Locality A measures 90 m by 90 m, covering 8100 m^2 along the northeastern fringe of the site. The locality includes named survey blocks R53 through R55, S53 through S55, and T53 through T55, with a southwest corner beginning in T53 at the coordinates E4880, N4880 – see Appendix F for a summary of the named grid system. The locality closely aligns with a dense scatter of Folsom artifacts previously detected by the Smithsonian (see Jodry 1999b:figure 6-11 and figure 28, this study). The earlier surveys identified 18 channel flakes, four preforms, and three broken Folsom points in the survey blocks. The Smithsonian recovered only one non-Folsom projectile point, a small Formative arrow base. Non-diagnostic tools recorded in Locality A in 1979 and 1983 include 11 bifaces, one bifacial drill, two gravers, four retouched flake tools, and three utilized flake tools – totaling at least 47 artifacts. CSU plotted additional tools in this area during the 2020 and 2021 field seasons, including one preform, one Folsom point, two end scrapers, one retouched flake, one utilized flake, and two bifaces.

The Locality A surface is a patchwork of clustered coppice dunes, barren hardpan, and shrubs (figure 29). Our team subdivided this 90 by 90 m survey area to facilitate fine-grained survey methods and assessments of ground surface visibility, in the same way as the broad-scale inventory of the site (figure 30). We divided each larger survey *block* in Locality A into 36 equally sized *cells* measuring 5 m by 5 m each, which we named sequentially from southwest to northeast (i.e. R53-1, R53-2, and so on). Each of the corners of the survey cells were mapped in place to approximately 1 cm accuracy using a total station. I assigned students independently and randomly to each cell, where they assessed sand cover, vegetation density, the relative height of coppice dunes, and time spent surveying. The surveyors inventoried (crawled) and collected 100 percent of the observed artifacts in each cell, but at controlled intervals within 1 m squares or *units*. The corners of the smaller unit squares were "roughed in" by drawing across measuring tapes from the previously mapped corners of the larger 5 m by 5 m survey cells. Every 1 m by 1 m *unit* was named based on the overarching 30 m by 30 m *block* (i.e. R53) and 5 m by 5 m *cell* (i.e. R53-1), then arrayed in alphabetical order from southwest to northeast in the grid (i.e. R53-1a, R53-1b, and so on). Like all previous studies, the 2022 CSU field team precisely mapped individual tools using a total station. Figure 30 and table 8 summarize some essential findings from Locality A, but a full analysis of these patterns is beyond the immediate scope of this dissertation. The primary analysis of this dissertation (see chapter 5) covers broad-scale trends in artifact spatial distributions across the entire site, so I omit the fine-grained mapping and surface collection results from Locality A from further discussion to avoid issues with sample intensity variance.

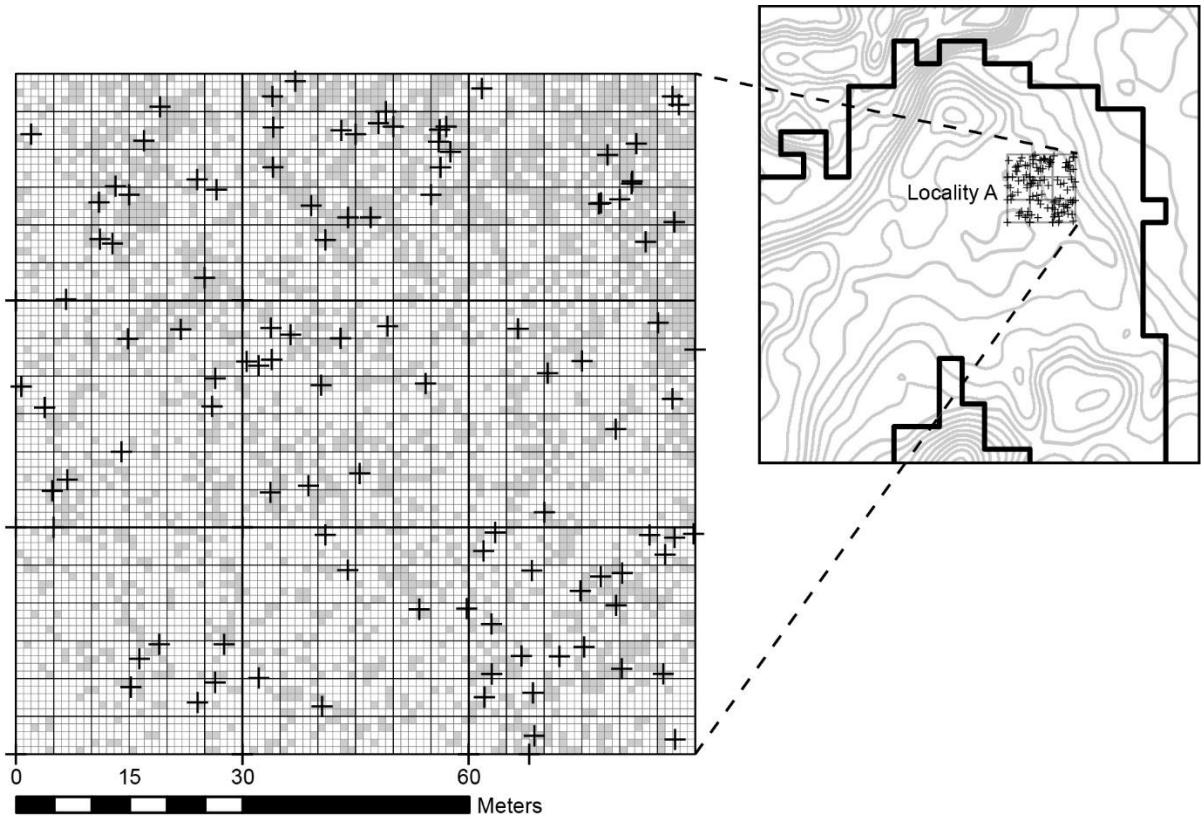


Figure 28. Depiction of Locality A surface survey grid and inset location map (upper right). Mapped tools depicted (black crosses). Positive 1 x 1 m survey units displayed in the background.

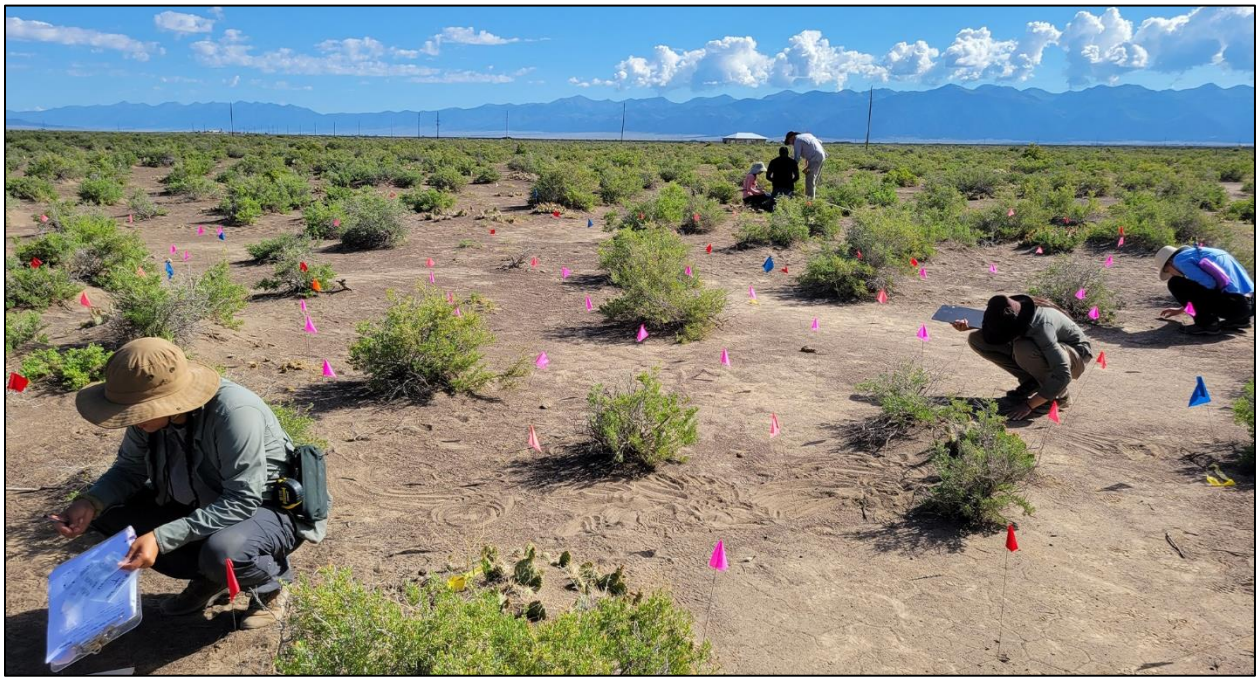


Figure 29. CSU's 2022 field school crew conducting an intensive survey of Locality A.

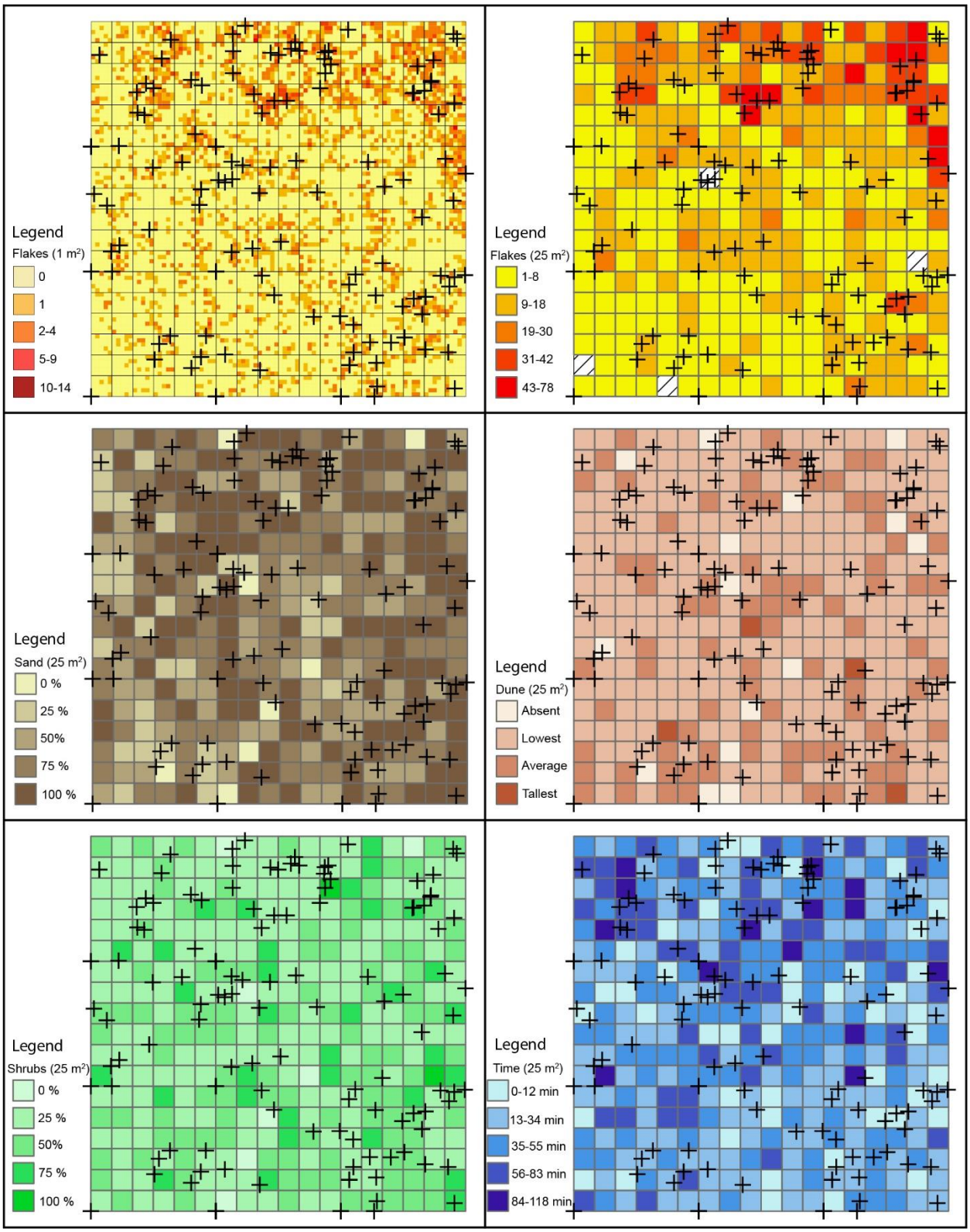


Figure 30. Map series depicting several surface cover variables based on CSU's 2022 field work in Locality A, including debitage frequency in 1 x 1 m units (top left), debitage frequency summarized in 5 x 5 m cells (top right), approximate sand cover (middle left), approximate dune height (middle right), approximate vegetation cover (lower left), and time spent surveying in each cell (lower right).

Table 8. CSU 2022 field school survey data matrix for Locality A, including binned cells with low-to-high debitage counts vs. survey cover variables (plotted tool frequency, survey time, sand cover, dune height, and vegetation cover).

	Survey Bin (observed debitage count per 5 x 5 m cell)				
	Lowest (n=1-8)	Low (n=9-18)	Medium (n=19-30)	High (n=31-42)	Highest (n=43-78)
Debitage Data					
Total Cell Count	153	109	28	20	10
Mean Flake Count	4	12	24	36	55
Standard Deviation	2.2	2.9	3.6	3.4	8.7
Pos. 1 x 1 m Units	571	886	369	290	185
Tool Data					
Cells with Tools	17	14	7	10	5
Total Count of Tools	21	20	13	16	5
Time Data					
Observations (n)	132	68	24	16	8
Range (minutes)	12-101	20-92	25-115	30-94	63-118
Mean Survey Time	29 min	41 min	51 min	47 min	66 min
Standard Deviation	18.6	21.8	33.1	29.8	39.9
Sand Data					
Observations (n)	153	109	28	20	10
Category 1 – 0%	4	2	1	1	0
Category 2 – 25%	24	7	1	0	1
Category 3 – 50%	35	26	2	2	0
Category 4 – 75%	44	32	9	5	3
Category 5 – 100%	46	42	15	12	6
Dune Data					
Observations (n)	153	109	28	20	10
Category 1 – Absent	6	5	3	1	0
Category 2 – Low	109	73	18	15	6
Category 3 – Med.	37	28	7	4	4
Category 4 – Tall	1	3	0	0	0
Vegetation Data					
Observations (n)	153	109	28	20	10
Category 1 – 0%	4	1	1	1	0
Category 2 – 25%	77	59	19	12	6
Category 3 – 50%	55	37	6	4	4
Category 4 – 75%	17	11	2	3	0
Category 5 – 100%	0	1	0	0	0

In mid-October of 2022, a small crew from CSU took part in a preliminary survey of an additional Folsom locality (Locality B) near the easternmost playa pond depression, where previously mapped stone tools suggested the presence of a shoreline Folsom campsite. Over a period of two working days, the CSU crew established a fine-grained collection grid in preparation for detailed surveys – but the crew was forced away from the field early due to a low-pressure weather system and colder-than-average nighttime temperatures. A small sample of chipped stone tools and debitage was collected during this effort, but the artifacts remain to be fully analyzed.

Summary

The Reddin site is a large surface expression of Folsom (and later) materials, covering about 84 acres at the edge of La Garita Creek. Much about the Smithsonian's initial fieldwork at the site remains unknown, but previously published information and handwritten notes shed significant light on the initial team's research goals. Much of their attention was focused on mapping the horizontal extent of Folsom lithic debris, testing aspects of site formation relative to the surface geology of the site, and ensuring the success of repetitive fieldwork efforts given the permanence of the survey grid.

CSU adopted the existing survey methodology created by the Smithsonian to generate a comparative dataset in the same areas, but our team also incorporated new technologies (UAV and image classification) as well as quantitative assessments of natural land cover characteristics. We expanded the known extent of the site based on our surveys. We generated data needed to model the relationships between artifact visibility and survey sampling techniques. Further, our efforts to shrink down surveys into a dense concentration of Folsom material within the site (Locality A) provided the raw data needed to examine artifact discard processes related to residential activities – a topic for future analysis. The results of the Locality A survey are not the primary point of discussion in this dissertation but will be used for future research into multi-scalar patterning of residential material across the Reddin site.

CHAPTER 4 - LITHICS

This chapter establishes basic facts about the Reddin site needed to frame the primary analysis of the dissertation, covered in the following chapter. Facts should be easily agreed upon by peer researchers, and in this case, my efforts begin with a basic description of the lithic assemblage. This part of the dissertation is not intended to reinvent the analytical wheel. However, because Folsom researchers differ subtly in their methods, it is necessary to clarify my approach to lithic analysis.

In this chapter I follow a data collection protocol consistent with other Folsom researchers interested in the same topics as me, which include site formation processes, landscape mobility patterns, and the discard of artifacts from tool manufacture and repair (Andrews et al. 2021; Frison and Bradley 1980; Hofman 1999; Jodry 1992, 1999a; LaBelle and Meyer 2021; Surovell 2022). Multiple interrelated themes of data collection guide my artifact classification scheme as well as the attributes and measurements that I use to characterize assemblage variation. The themes I use generally follow Ahler (1975, 1989, 1994) and focus on systems of 1) raw material procurement, 2) tool manufacture, and 3) damage resulting from artifact use or post-depositional forces. These themes help approximate different outcomes and byproducts of hunter-gatherer decisions given unique technological, social, and environmental constraints – a topic explored with formal analysis in the following chapters. Unfortunately, these themes do not exhaustively cover all aspects of assemblage variation, and I admit to ignoring other important attributes like in-depth morphometric variables, microwear on tool edges, and many others. This chapter simply covers the basics.

I begin with an account of the regional array of lithic raw materials represented in the chipped stone assemblage, followed by detailed descriptions of Folsom fluted weapon technology, the byproducts of its manufacture, and incidences of damage on those items. I analyze the combined sample of Folsom diagnostic tools and debitage based on the Smithsonian's fieldwork at Reddin as well as CSU's, including 225 projectile points, 110 preform bifaces, and 357 channel flakes. I also review data for 479 non-diagnostic tools, including lithic cores (n=4), bifaces (n=214), retouched flake tools (n=116), utilized flake tools (n=45), end scrapers (n=66), and gravers (n=34). Towards the end of the chapter, I layout my approach to analysis of 39,579 pieces of lithic debitage, which I use to inform the spatial and temporal analysis of the site in chapter 5. Appendix F reviews post-Folsom artifacts, including diagnostic projectile points. Appendix G gives a basic description of faunal remains, which are very few.

Lithic Raw Materials

In the archaeology of Folsom mobility, researchers pay attention to the relative abundances of local and non-locally procured stone within sites (Andrews et al. 2021; Buchanan et al. 2019; Hofman 1994, 2003; Jodry 1999a; Kelly and Todd 1988; Surovell 2003, 2009). The logic behind this focus is relatively straightforward. In general, a high proportion of exotic or non-local stone at a site could suggest that Folsom people moved across the landscape far and fast enough to avoid depleting their stock of tools and tool blanks along the way – long distances might reflect a few large residential movements across the landscape, or many short but frequent moves between camps. Conversely, an abundance of local material at a site could suggest a pattern of less frequent movements between raw material sources and sites on the landscape – where groups both expended and replenished tools using stone nearby. A researcher must account for several variables for these circumstances to hold true (see chapter 5). They must make some basic assumptions about

the rate that hunter-gatherers used and discarded artifacts during site occupations, and they must assess the relative distances and transport costs between raw material procurement areas and the sites where artifacts were first made, then used, and finally disposed – which may or may not have occurred in the same place (Bamforth and Becker 2000; Hofman 2003; Surovell 2009). Lastly, archaeologists must justify the absence (or minimal effects) of regional trade and exchange systems involving bands of foragers on the landscape and their mobile lithic supply. Much of the literature covering Paleoindian lithic conveyance suggests that systems of direct acquisition primarily explain the presence of exotic materials in lithic toolkits (e.g. Bamforth 2002; Kelly and Todd 1988; Meltzer 1989; Surovell 2009). In chapter 5, I address this topic further and outline several testable hypotheses concerning the relationships between lithic raw material patterns and Folsom mobility choices. For now, I simply characterize lithic raw material diversity and discuss the distances between raw material sources and the Reddin site.

The bottom floor of the Closed Basin holds no reliable sources of lithic raw material. The trickling streams of the San Juan and Sangre de Cristo Mountains transport only pebble-sized stones into the interior of the Closed Basin, representing the bottom of former Lake Alamosa (see chapter 2). Folsom and later hunter-gatherers at the site nevertheless supplied themselves with a wide array of lithic raw materials before spending time there. I classified individual raw material sources for each artifact by using a macroscopic visual approach, focusing on variations in color, luster, inclusions, and texture. I compared artifact lithic categories with regionally procured samples from quarries available in the Center for Mountain and Plains Archaeology lithic library. For some rock types, a positive source location was not possible using macroscopic methods alone, so I attributed artifacts to a broad geological type based on commonly identified attributes and inclusions in the rock samples. In total, I assigned 14 different lithic source locations or types in

the assemblage. These include varieties of chert, chalcedony, jasper, and agate making up a broader category of fine-grained cryptocrystalline silicates. Other major categories include coarse- and fine-grained quartzites, coarse- and fine-grained igneous rocks, and silicified woods. I organized each of the stone types into three groups representing a distance bandwidth from the Reddin site, including sources within 150 km, 300 km, and exceeding 300 km in a straight line (Euclidean) distance from the site (figure 31). For rock types where a positive source location was not confirmed, I estimated an approximate distance bandwidth by reviewing literature on regional lithology and major geologic units. Table 9 provides an essential summary of each source and type.

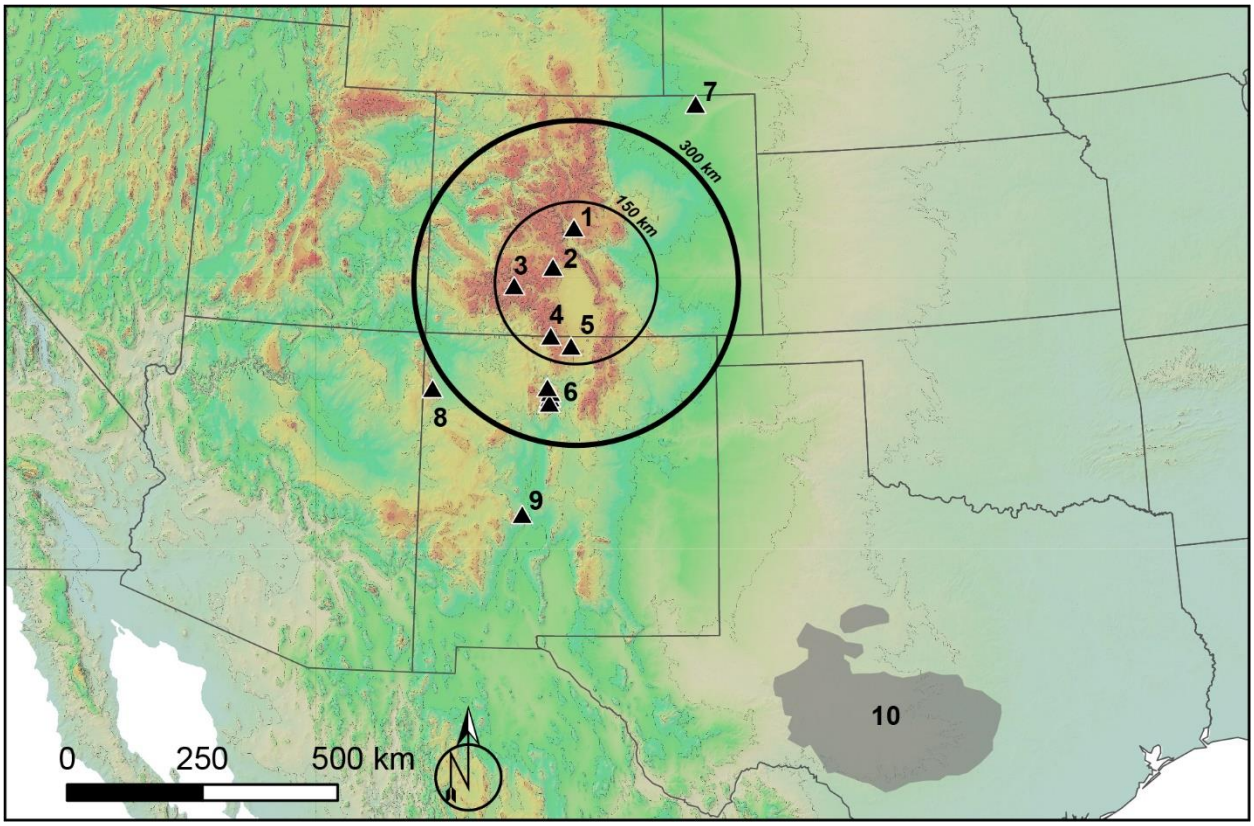


Figure 31. Map showing distance bandwidths from the Reddin site and major lithic raw material sources with known provenience discussed in this study; 1) Trout Creek, 2) Trickle Mountain, 3) Mosca, 4) Cumbres Pass, 5) Taos Plateau volcanic rocks, 6) Jemez Mountains (Cerro Pedernal, El Rechuelos, Cerro del Medio, Cerro Toledo), 7) Flattop Butte, 8) Narbona Pass, 9) Soccoro, 10) Edwards Plateau.

Table 9. Lithic raw material sources or general rock types identified in the Reddin lithic assemblage.

Source Name or Type	Approximate Distance	Short Visual Description	Notable References
150 km Band			
Trout Creek Jasper	110 km	Opaque yellow-brown with black dendrites	Chambellan et al. 1984
Trickle Mtn. Quartzite	55 km	Coarse-grain gray, pink, lavender with inclusions	Jodry 1999a
Mosca Chert	115 km	Opaque and mottled red, white, orange, and gray	Charles 1995
Cumbres Chert	105 km	Opaque and vuggy brown, green, yellow, and gray	Jodry 1999a
Dacite	105-115 km	Fine-grained black rock with phenocrysts	Shackley 2011
Rhyolite	Variable	Coarse-grained gray, brown, lavender with inclusions	Mitchell 2017
Silicified Wood	Variable	Variable grain size with brown, tan, red, black, white	Black 2000
Morrison Quartzite	Variable	Fine-grained and mottled gray, tan, and red	Black 2000
300 km Band			
Pedernal Chert	200 km	Semi-translucent white, gray, blue, black; inclusions	Warren 1974
Jemez Obsidian	210-230 km	Glassy black, opaque to translucent	Shackley 2021
Over 300 km			
Flattop Chalcedony	400 km	Semi-translucent lavender, white, gray, brown, and red	Madden 2024
Narbona Chalcedony	330 km	Mostly translucent pink, orange, gray, and lavender	Banks 1990
Socorro Rhyolite	430 km	Very fine-grained black, gray, and mottled brown	Dello-Russo 2004
Edwards Chert	800 km	Opaque light and dark gray, brown; some inclusions	Banks 1990

The Closest Stone – 150 km

Sources within 150 km of Reddin are geologically diverse. The most widely recognized source is jasper from Trout Creek, an opaque and yellow-brown form of agatized dolomite with dendrites and healed fractures; individual nodules of this stone often look like small pieces glued together by thick pastes of silica. Lithic procurement locales and primary quarrying areas occur in abundance near Trout Creek Pass, about 110 km northeast of Reddin in the Mosquito Range, between South Park and the Arkansas River headwaters (figure 32). However, prior research proves that material visually similar to Trout Creek jasper occurs throughout the Eastern San Juan and Sawatch Ranges, and across much of the western flanks of South Park where dolomite belonging to the Paleozoic Manitou Limestone occurs in discontinuous seams (Black 2000; Black and Theis 2015; Chambellan et al. 1984; Jodry 1999a). Other potential jasper quarries have yet to produce such abundant evidence of lithic procurement intensity, however, and 5CF84 (the best documented site at Trout Creek Pass) contains time-diagnostic material spanning the last 12,000 years (Chambellan et al. 1984). Trout Creek Pass is an intermountain travel corridor, and in a

probabilistic sense, I would argue that the odds of finding this material across many sites in the region are greater than finding potential look-alike materials.



Figure 32. Aerial photo of the Trout Creek Pass area near the location of the 5CF84 jasper quarry.

The Eastern San Juans and lower Sawatch Range contain several raw material sources within 150 km of Reddin. From north to south, these include Trickle Mountain quartzite, Mosca Creek chert, and Cumbres Pass chert (San Juan Volcanic Field). Trickle Mountain quartzite, also known as Alkali Spring quartzite, is well-documented across lithic assemblages in the San Luis Valley and derives from wide exposures of Cretaceous-aged Dakota Formation rocks covered by middle Tertiary volcanics in the Eastern San Juan foothills (Black 2000; Jodry 1999b; Johnston 2021). The material exhibits several color varieties (white, gray, brown, pink, red, and lavender) and commonly shows a patchwork of darker inclusions. This orthoquartzite source bears nodules with medium grain sizes that are variably sorted.

Mosca Creek chert is located far to the west in the San Juans near the headwaters of the Rio Grande River. The material is represented in lithic assemblages throughout Hinsdale County

and extends further east into Folsom and later assemblages on the valley floor (Charles 1995; Jodry 1999b). At present, there is little formal documentation of quarrying activities at the Mosca Creek source. The material occurs in a discontinuous bed of Mississippian-age limestone cobbles, with sourced nodules bearing a waxy luster and patchily banded color combinations of gray, white, red, yellow, and orange. Jodry (1999a:table 46) noted the similarities between Mosca Creek chert and nodules from the Alibates dolomite quarries on the Southern High Plains, though Alibates is typically more banded and Mosca Creek chert is usually mottled. Folsom groups made abundant use of Alibates at sites on the Great Plains, and though Alibates is represented at some Folsom sites in the Valley, in this dissertation I assume (perhaps falsely) that material with these color combinations represents Mosca Creek chert.

Cumbres Pass chert is a poorly documented but well-recognized raw material with a loosely defined procurement locality on a mountain pass dividing the Cumbres Creek and Wolf Creek valleys in the Eastern San Juans. Jodry (1999a:table 46) describes this material as welded tuff likely Cenozoic in age, but little is known of the precise geologic composition and distribution for this source. The material is highly identifiable, however, with characteristic vuggy inclusions (almost fossiliferous in appearance) representing ash-filled silica air pockets in the stone. Color combinations include gray, green, brown, yellow, pink, and lavender with a heavily mottled appearance. Like Trout Creek, potential look-alike cherts occur throughout the San Juan Volcanic field in close relative proximity (Johnston 2021; Mitchell 2012; Wunderlich 2011). Wunderlich (2011) and Mitchell (2012) identified widely distributed secondary (alluvial) deposits of mottled chert and chalcedony originally formed within Oligocene-aged tuff flows in the Eastern San Juans, covering portions of Hinsdale, Saguache, Rio Grande, and Conejos Counties. I do not know if

Folsom and later groups at Reddin procured welded tuff exclusively from Cumbres Pass, but the material is almost certainly sourced within 150 km of the site.

Coarse-grained and fine-grained igneous sources within 150 km of the site include darkly colored toolstones from the Taos Plateau, the southernmost section of the Valley floor. Several sources occur within a cluster of shields and cones in northern New Mexico, and the northernmost edge of this distribution contains two well-documented dacite shield volcanoes producing dark gray and glassy aphyric nodules large enough to produce large bifaces and tool blanks – San Antonio Mountain and Newman Dome (Shackley 2011). Of these, the Newman Dome contains the highest quality material, with a very fine-grained glassy matrix and sparse phenocrysts, but naturally patinated nodules from both sources are visually difficult to distinguish, and San Antonio Mountain is the closer of the two sources to Reddin. Additional lithic materials similar to dacite include glassy andesite, trachy-andesite, trachyte, phonolite, and phono-tephrite, which may be found locally at the edges of these volcanoes and further abroad in the Plateau (figure 33). Selected samples of dacite submitted to Steve Shackley at the Geoarchaeological X-Ray Fluorescence Spectrometry Laboratory identified San Antonio Mountain as the only definitive fine-grained dacite source represented in the Reddin collection (Shackley 2022).

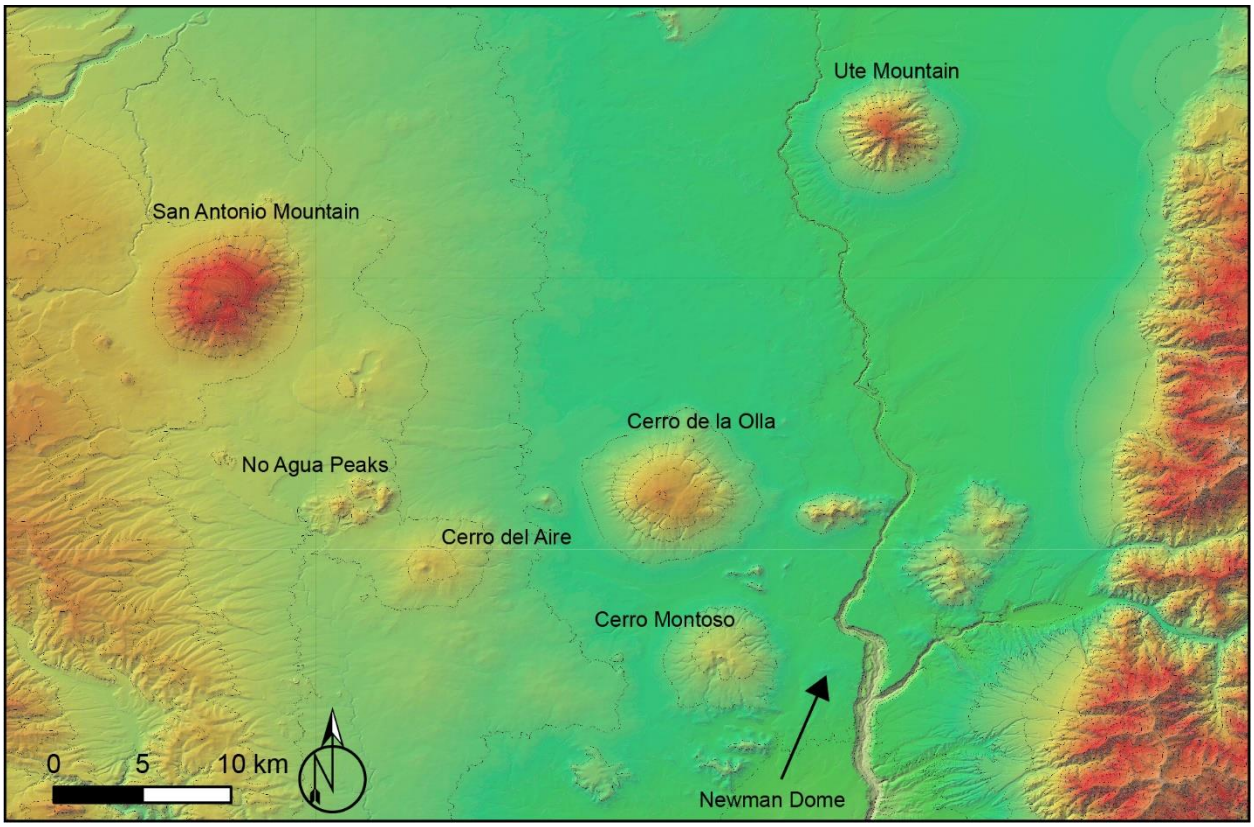


Figure 33. Map of major volcanic domes and shield volcanoes on the northern Taos Plateau. Note the location of Newman Dome and San Antonio Mountain as major sources of archaeological dacite.

I did not precisely source several lithic raw materials likely within 150 km of the Reddin site. These include black, gray, lavender, and brown coarse-grained igneous rocks visually classified as rhyolite, with widely distributed exposures across the Taos Plateau but also along the La Garita Creek and Saguache Creek drainages in the San Juan Mountains. Fine-grained orthoquartzites with gray and banded red-brown colors, dissimilar from the poorly sorted and medium-grain Trickle Mountain nodules, may be derived from Morrison Formation exposures located in the Gunnison Basin northwest of the site (Black 2000; Jodry 1999a; Pitblado et al. 2008), in the Wet Mountain Valley to the northeast (Black 2000), or along numerous Dakota-Morrison Formation exposures found in the hogbacks of the Arkansas River Basin (Black 2000). Researchers in the region commonly source finely made artifacts of silicified palmwood to the Black Forest or Dawson Formations near the Palmer Divide, especially varieties with a

butterscotch color found some 200 km away from Reddin, but dozens of silicified wood sources also occur along the foothills of the San Juans near the valley floor. The English Valley Folsom site is located immediately downstream of a silicified wood procurement area producing large nodules, as well as a locally derived rhyolite material (Mitchell 2017).

Far Away Stone – 300 km

A group of four closely distributed lithic sources demonstrate a raw material connection between the San Luis Valley and northern New Mexico outside of the Taos Plateau region. Chalcedony and chert from Cerro Pedernal and three different obsidian sources from the Valles Caldera establish procurement of high-quality stone from the Chama River Valley and Jemez Mountains, roughly 200 km south of the Reddin site. Pedernal (in Spanish, "flint") is a multi-colored and semi-translucent chalcedony, but common base colors include, white, gray, blue, and black with small red, orange, yellow, and brown inclusions often exhibiting flecks or a peppered appearance. Cerro Pedernal in Rio Arriba County, New Mexico is a well-known mountain vista in the region with a long history of geological and archaeological research (Bryan 1939; Murrell and Murrell 2015; Smith and Huckell 2005; Warren 1974). Like many of the San Juan Volcanic Field chert sources, Pedernal nodules formed in a bed of welded tuff named the Pedernal Chert Member of the Tertiary-aged Abiquiu Tuff. Researchers have also recorded secondary deposits of this material in alluvial beds draining out towards the Albuquerque Basin (Murrell and Murrell 2015).

Shackley (2022) positively identified three obsidian sources from the Valles Caldera located between 10 and 30 km south of Cerro Pedernal, based on a sample of Folsom and later chipped stone tools from Reddin. Representative obsidian rhyolite members include, from north to south, El Rechuelos (also known as Polvadera Peak), Cerro Toledo, and Cerro del Medio. Collectively, these sources represent the most common obsidian throughout the Middle and

Northern Rio Grande regions (Shackley 2021). Cerro Toledo is especially dominant, as the obsidian is widely distributed within secondary deposits of Quaternary alluvium spanning the Rio Grande Rift south and east of the Jemez Mountains. In this dissertation I did not make attempts to visually distinguish between obsidian sources for the majority of artifacts during my lithic analysis. The samples that I submitted to Shackley (2022) for positive source identification, using energy dispersive x-ray fluorescence (EDXRF), document different obsidian sources based on geochemically sourced trace element groups. The close proximity of all three sources in the geochemically sourced sample suggests that most of the obsidian at Reddin derives from the Valles Caldera.

Exotic Stone – Over 300 km

On the Great Plains, many Folsom assemblages contain a disproportionate number of artifacts made from stone procured hundreds of kilometers distant (Bamforth 2002; Hofman 2002, 2003). Even for Folsom sites that lack abundant exotic stone, it is still consistently present (Andrews et al. 2021; Surovell 2003, 2009, 2022). Such patterning alludes to long range Folsom mobility patterns more generally, and perhaps, selective use and discard of favored tool stone based on flintknapping quality, durability, and aesthetics. In this dissertation I define exotic stone as lithic raw material sourced over 300 km from the Reddin site, which roughly doubles the maximum annual range of many ethnographically documented hunter-gatherer bands (Binford 2001; Naze 2013). At Reddin, I identified a minimum of four exotic lithic raw materials ranging between 330 km and roughly 800 km from the site. In order of distance, these include Narbona Pass chalcedony, Flattop Butte chalcedony (White River Group), Socorro rhyolite, and Edwards Plateau chert.

Narbona Pass chalcedony, also called Chuska and colloquially referred to as “paleo pink”, derives from an exploded Tertiary volcanic vent at the divide between the Tunicha and Chuska

Mountains in northern New Mexico (Cameron 2001; Jodry 1999a; Reitze et al. 2012; Ward 2011), about 15 km from the Arizona state line. The material commonly occurs in small translucent nodules with dominant colors of orangish pink, banded gray, and opaque light grays with lavender. The natural lustrous and waxy character of the material is another distinctive visual marker. Reddin is 330 km northeast of this lithic raw material source.

Oligocene-aged chalcedonies of the White River Group occur in abundance in the central Great Plains as primary and secondary deposits of the Chadron Formation, with nodules bearing high-quality flintknapping properties. The best-known source locations include Flattop Butte in northeastern Colorado (Greiser 1983; Hoard et al. 1993; Madden 2024), Table Mountain in eastern Wyoming (Hoard et al. 1993), and the White River Badlands cluster including West Horse chert and Scenic chalcedony (Hoard et al. 1992, 1993). Nodules of this widespread material commonly exhibit opaque to translucent lavender, white, gray, brown, and reddish-purple color varieties, with small circular and banded inclusions found occasionally. However, Flattop Butte remains the best-known source of this material for central High Plains and Colorado foothills archaeological sites; Flattop Butte contains hundreds of deeply excavated quarry pits, and precise lithic sourcing studies have repeatedly shown a close affiliation between Flattop Butte and early paleo lithic networks throughout the Great Plains (Madden 2024). This source is 400 km from the Reddin site.

Socorro rhyolite, colloquially named “Socorro jasper”, derives from the Mogollon-Datil Volcanic Province and is one of several hydrothermally altered Neogene rocks from Socorro County, New Mexico (Dello-Russo 2004; Shackley 2021, 2022). It is a black toolstone not dissimilar in color, hue, and texture from other fine-grained igneous rocks described previously. Shackley (2022) suggests that Folsom hunter-gatherers at Reddin likely procured the material from the Sedillo Hill source (430 km), rather than the Black Canyon source, using hierarchical cluster

analysis of major and trace element chemistry, focusing on proportions of iron (Fe), zircon (Zr), and lead (Pb). This is the first documented use of Socorro rhyolite by Folsom hunter-gatherers, though the material is common in Clovis assemblages in the Middle Rio Grande (Dello-Russo 2004; Merriman 2022).

The presence of Edwards Plateau chert in the Reddin lithic assemblage, despite the extreme distance from source procurement locales, is not totally unexpected. Jodry's (1999a) work at Stewart's Cattle Guard and other Folsom sites in the Alamosa Cluster confirms a wide-ranging Folsom transhumance system stretching from the scarps of the Southern High Plains to the San Luis Valley, based on the presence of both Edwards chert and Alibates flint in those assemblages. However, it remains difficult to link nodules of Edwards chert to specific procurement locales on the Cretaceous-aged Edwards Group limestone that spans roughly one-fifth of central to western Texas (Banks 1990). The closest, well-used exposures of the Edwards Plateau chert occur at the Callahan Divide (Jodry 1999a; Mallouf 1989), about 800 km southeast of Reddin. Examples of this material include opaque (though semi-translucent on thin edges) light and dark gray and tan colored varieties, occasionally with reddish brown fleck-like inclusions.

The color varieties of several exotic stone materials overlap in uncommon nodules. Grayer and more opaque varieties of Narbona and Flattop chalcedony, though rare, visually overlap with thinner sections of classic Edwards Plateau chert. This problem, though not totally unknown to some is largely taken for granted in Folsom literature. However, each of the three visually overlapping lithic sources respond differently when exposed to short- and long-wave ultraviolet (UV) light (Hofman et al. 1991). Shortwave UV fluoresces Edwards chert with a yellow-orange color, while Narbona and Flattop fluoresce bright green. There is little difference between Flattop and Narbona under UV fluorescence, but Flattop commonly presents mottled orange, green, and

gray with longwave UV, whereas Narbona tends to fluoresce a dull green color. Other fine-grained silicates in the collection (e.g. Trout Creek, Mosca Creek) do not fluoresce under UV with exceptional detail.

Folsom

Folsom, like many other Paleoindian traditions, is considered both a cultural and technological manifestation because factors influencing the design and variation of the lithic toolkit included environmental constraints and cultural transmission variables – such as stylistic choices and copy errors, or new inventions undertaken during the manufacture process (Ahler and Geib 2000; Meltzer and Eren 2021). There is abundant evidence of Folsom's emblematic and fully fluted weapon tip design at Reddin, as well as the lithic byproducts of its manufacture, but there are also unusual Folsom artifacts. The Folsom lithics include Folsom or *Folsomoid* (Folsom-like) projectile points, late-stage preform bifaces representing unfinished weaponry stock, and channel flake debitage from the preform fluting process. In this section I summarize the diagnostic Folsom assemblage from Reddin and focus on the themes of analysis for each artifact category (raw material, manufacture, and damage).

Projectile Points

The total Folsom projectile point assemblage exhibits at least 13 distinct lithic raw material sources. The majority of these include rock types available within 150 km, though sources within and beyond 300 km are also present. Lithic raw material diversity is not evenly represented in the sample, however. Trout Creek jasper makes up approximately two-thirds (62%) of the entire sample of Folsom projectile points at the site. The raw materials of the remaining one-third of Folsom points are nearly equally divided among other sources and categories. Figure 34 and table 10 summarize lithic raw material abundance and diversity in the sample of Folsom projectile

points. Jodry (1999b) previously discussed the abundant use of Trout Creek jasper in the projectile point assemblage at Reddin, as well as a similar range and quantity of other rock types, but this study positively identifies other lithic raw materials that were previously unaccounted for – including Trickle Mountain quartzite, Mosca Creek chert, Flattop Butte chalcedony, and geochemically sourced Socorro rhyolite as well as the Cerro del Medio, Cerro Toledo, and El Rechuelos obsidian. This study further stratifies the sample of projectile points made from fine-grained igneous rocks, with Folsom specimens made of unspecified glassy andesite and rhyolite.

Table 10. Folsom point lithic sources at Reddin, based on Jodry (1999b: table 6-7) and the combined sample based on CSU fieldwork and reanalysis of the Smithsonian artifact collection.

Source Name or Type	Published Sample n	Total Sample n (%)	Sample Difference n (% change)
Trout Creek Jasper	99	139 (62%)	+40 (40%)
Morrison Quartzite	16	20 (9%)	+4 (25%)
Silicified Wood	16	11 (5%)	-5 (-31%)
Unknown	26	11 (5%)	-15 (-58%)
Edwards Chert	9	7 (3%)	-2 (-22%)
Narbona Chalcedony	1	8 (4%)	+7 (700%)
Pedernal Chert	0	6 (3%)	+6 (nc)
Jemez Obsidian	11	5 (2%)	-5 (-54%)
Cumbres Chert	6	5 (2%)	-1 (-16%)
Trickle Mountain Quartzite	0	5 (2%)	+5 (nc)
Mosca Chert	0	3 (1%)	+3 (nc)
Dacite or FGV	1	2 (1%)	+1 (100%)
Flattop Chalcedony	0	2 (1%)	+2 (nc)
Socorro Rhyolite	0	1 (<1%)	+1 (nc)
Total	185	225 (100%)	+40 (22%)

FGV – fine-grained volcanic rock; nc – not calculated



Figure 34. Selected Folsom lithic materials. Trout Creek (top row), silicified wood (SI-PP-1049), Mosca (SI-PP-1057), Cumbres (CMPA-PP-1038), Trickle Mountain (SI-PP-1076), Morrison (SI-PP-1064), andesite (SI-PP-1133), Pedernal (SI-PP-1021), Jemez obsidian (SI-PP-1134), Narbona (SI-PP-1023), Flattop (SI-PP-1025), and Edwards (SI-PP-1020, CMPA-PP-1017).

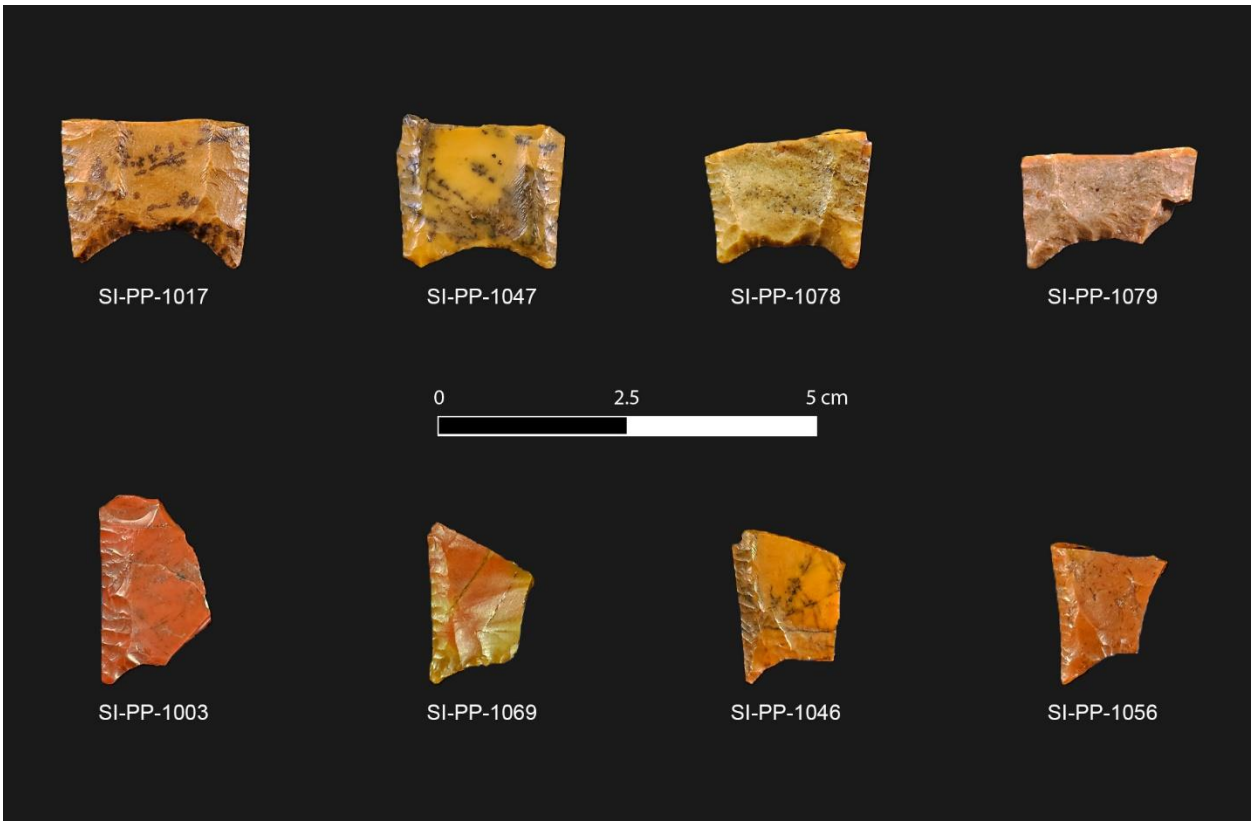


Figure 35. A sample of classically manufactured Folsom points from the Reddin site, including fluted and ground bases (top row) and lateral splits (bottom row).

There is no definitive method for discriminating between abnormal and classically manufactured Folsom projectile points – with every new in-depth analysis of Folsom lithics, variation becomes the norm (Lassen 2013; Meltzer and Eren 2021). Thus far, researchers have generally taken an impressionistic approach to dividing Folsom point assemblages into different possible subgroups and types. Typology is not at the heart of this dissertation, and I take a generalized approach here (but see Lassen 2013 for quantitative methods). I focus on some observable differences in flaking characteristics, general outline shapes, and basic measurements of Folsom points. Of the 225 total Folsom points in the analyzed sample, I consider 135 of those points (or about two-thirds) to accurately represent a classically prepared Folsom point (figure 35). These include small-to-medium sized lanceolate specimens with two fluted faces and very small

perpendicular flake scars running the length of lateral edges from basal to distal ends, with grinding along the base and proximal lateral edges to facilitate hafting to a foreshaft.

At Reddin, there is evidence for other fluting characteristics that differ from the classic Folsom design. Some specimens show faces with multiple parallel flutes running from the base to tip, and some finished points have only one flute on one face (figure 36). In very rare instances, it appears that Folsom flintknappers struck channel flakes from a platform prepared on the distal end of a preform rather than its base. In other cases, Folsom flintknappers at Reddin did not flute points at all, and did not prepare Folsom preforms with a characteristic basal nib (channel flake platform); I consider at least 16 of the Folsom points to be "pseudo-fluted", given the presence of a false channel flake scar running through the interior of each point, often representing the negative scar of an earlier bifacial thinning flake. Folsom flintknappers at Reddin did not always trim away basal nib platforms and instead shaped concave bases around platforms preserving the shape of the nib, intentionally. At the Mountaineer site, Meltzer and Eren (2021:346) speculated that the preservation of the basal nib and careful shaping of the base around this feature suggested a tentative stylistic signature, given there is no obvious functional or technological benefit of making such a decision.

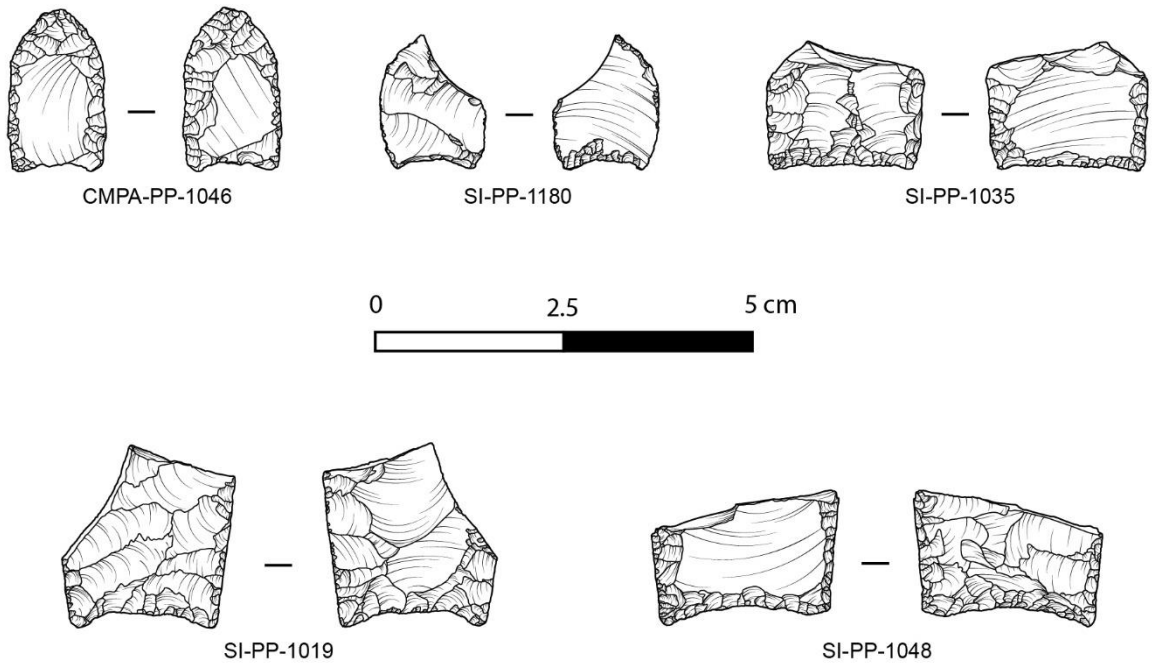


Figure 36. Sample of non-classic Folsom points from the Reddin site, including pseudo-fluted miniatures (CMPA-PP-1046 and SI-PP-1180), double-fluted point (SI-PP-1035), point fluted on one face only (SI-PP-1019), and point with a reverse flute on one face only (SI-PP-1048) – which is possibly a rebased preform tip.



Figure 37. Sample of Midland or unfluted Folsom points from the Reddin site, including examples with collateral flaking and fine lateral edgework.

The Reddin assemblage contains a fair number of classically manufactured Midland or unfluted Folsom points (figure 37). At least 24 Midland or "Midland-oid" projectile points in the collection bear a similar outline shape and morphology to lanceolate Folsom points, except for a few key characteristics. Midland points at Reddin were thinned using a precise and somewhat broad collateral flaking technique as opposed to a process of fluting each face, which produced wide negative flake scars running perpendicular to lateral edges and meeting near the centerline, overlapping minimally. Like Folsom points, most of the Midland point flintknappers retouched the lateral edges after bifacial thinning to produce very small and narrow flake scars along the lateral edges, forming an almost riblike appearance. In this and subsequent chapters, I treat unfluted Midland points as part of the Folsom component rather than a separate cultural-technological tradition given that both types consistently appear in other Folsom site assemblages (Hofman et al. 1990; Jennings 2016; Lassen 2013, 2015; Meltzer et al. 2006). Sites containing only Midland points (without Folsom artifacts) are extremely rare (Blaine et al. 2017).

Miniature points at Reddin represent a final category of alternative, non-classic Folsom point manufacturing choices. Recently, researchers revisited the topic of Folsom miniatures to further expound on their definition and purposes. Some researchers defined miniature Folsom points based on an arbitrary length threshold (e.g. Hofman et al. 1990), others focused on maximum width given the cumulative effects of resharpening on length variables (Lassen 2016), and others considered the standard deviation of width measurements across a large sample of Folsom points from a wide range of sites (Guarino and Sellet 2019). The recent study by Guarino and Sellet (2019) on miniature Folsom points from Lindenmeier defined miniatures as points with width measurements less than two standard deviations below the mean Folsom point width across

a tally of 631 points (Lassen and Williams 2015); they defined miniatures as points with maximum widths less than 13.92 mm using the cumulative sample.

In this dissertation, I define miniature Folsom points as statistical outliers with intact (unbroken) maximum width measurements less than 1.5 times the inter quartile range (IQR) below the first quartile (Q1), but only within the sample available from the Reddin site. I chose to focus on point size at Reddin to define miniatures, exclusive of other sites (see Gaurino and Sellet 2019 for an alternative view), to locally account for confounding factors like regional lithic raw material availability and conservation strategies implemented during the point production process. Table 11 provides an essential data summary for a sample of 58 Folsom projectile points with complete width measurements, which make up only 25 percent of the collection (figure 38). In sum, I consider a total of four projectile points from Reddin to be Folsom miniatures in a statistical sense, each having width measurements less than 13.59 mm. Two of the Folsom miniatures are illustrated in figure 36.

Table 11. Summary data for Folsom point width and thickness measurements (mm) from the Reddin site. Sample based on the combined collections of CSU and the Smithsonian.

Sample Description	Sample Size	Mean Width	Width Range	Standard Deviation	Q1	Q3	IQR
Total Folsom Points	225	14.32	3.04-23.78	4.86	10.16	18.95	8.79
Points w/ Intact Widths	58	19.04	10.09-23.78	2.93	17.97	20.89	2.92
	Sample Size	Mean Thickness	Thickness Range	Standard Deviation	Q1	Q3	IQR
Total Folsom Points	225	3.37	1.64-5.47	0.62	2.99	3.82	0.83
Points w/ Intact Widths	58	2.77	1.95-5.08	0.58	3.37	4.14	0.78

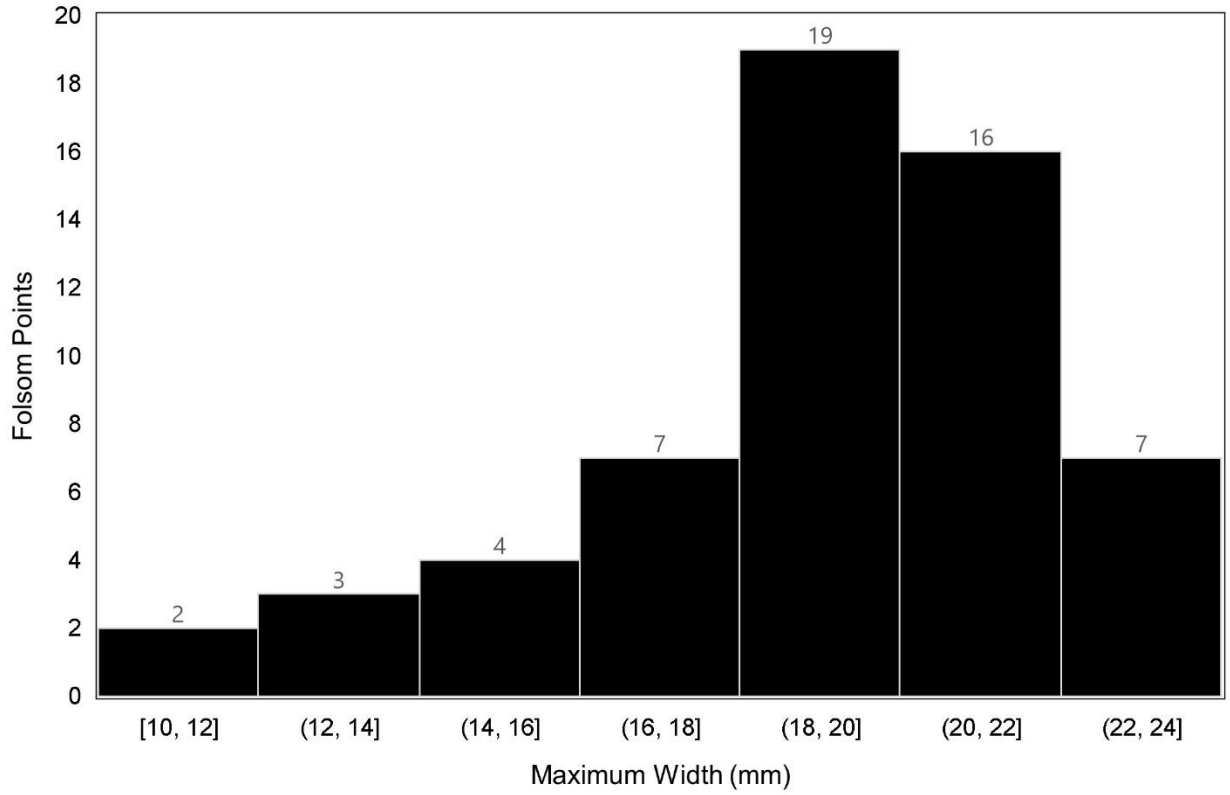


Figure 38. Histogram showing the distribution of the intact (complete) sample of width measurements for Folsom points (n=58 out of 225 points) from the Reddin site.

One of the Folsom miniatures is pseudo-fluted on both sides and is the only fully intact Folsom point recovered from the site (figure 36). It is not surprising that so many of the Folsom points are broken. The lack of local lithic raw material in walkable distance from the site suggests that Folsom hunter-gatherers needed to stock themselves with a large supply of tool blanks in advance of travelling through the center of the Valley. To keep from depleting their stone supply, Folsom flintknappers likely made efforts to rejuvenate weapon tips if they retained sufficient material.

I categorized Folsom point fragment types using the breakage classification scheme published by Meltzer and Eren (2021:figure 12.3), which organizes fragments based on their completeness, anatomical orientation, and the measured lengths of ground edges. These are summarized in figure 39 and table 12. However, I do not formally analyze these fragment types

here for one primary reason. There are 17 possible fragment types in the classification scheme, which overly stratifies the sample for analysis. In this section I simply refer to point fragments as proximal pieces representing portions of the base, medial fragments lacking bases and tips (but with intact widths), lateral portions with blade edges and no base or tip, and distal ends represented by the tip alone (table 12).

The Reddin lithic assemblage contains 27 distal fragments out of 225 analyzed points, but the total sample includes 241 different point fragments (table 12). The low representation of distal ends speaks volumes about the function of the site and, most likely, processes where Folsom flintknappers harvested useable tip fragments for repairing broken weaponry (Hofman 1999). Prior research demonstrates that complete points and distal tip fragments commonly appear in primary hunting and butchering locales (Hofman 1999; Jodry 1999a; LaBelle and Meyer 2021; Todd 1987); Reddin lacks an identifiable bone bed and butchering area, so the paucity of complete points and tips is a line of evidence for the paucity of primary hunting refuse at the site – or a significant emphasis on rebasing broken tips and transporting them offsite. In contrast, there are 104 proximal fragments at Reddin, suggesting an emphasis on dehafting broken bases in a campsite setting. Nineteen out of 39 Folsom point midsections at Reddin bear some evidence of grinding, and 35 out of 70 lateral edges have evidence of grinding. I consider three out of eight conjoining artifact pairs "near-complete" given they include basal-to-distal and medial-to-distal refits, but these are discussed further in chapter 5. The high proportion of bases at Reddin, coupled with near-proximal midsections and lateral edges, suggests that Folsom artifact discard processes emphasized post-hunt dehafting and repair of broken weapons. The lack of complete points and broken tips suggests that most hunting activities may have occurred offsite, or that many usable point fragments were harvested from hunting areas.

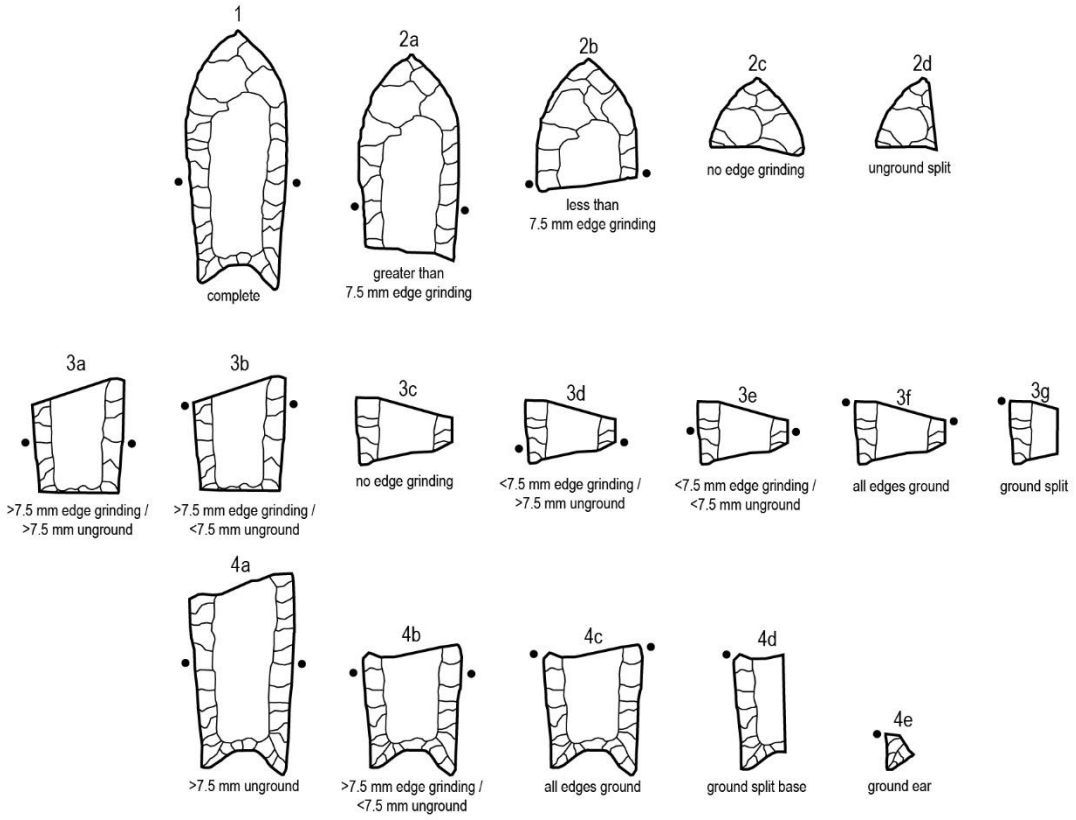


Figure 39. Folsom (and Midland) projectile point fragment codes schematic, adapted and modified from Meltzer and Eren (2021:figure 12.3).

Table 12. Folsom point fragment type matrix summarizing Meltzer and Eren (2021:figure 12.3) breakage classes and portions classified in this study. Sample based on the combined collections of CSU and the Smithsonian (n=241 fragments out of 225 total points).

	Fragment Type				
Meltzer and Eren Code	Complete	Distal	Midsection	Lateral	Proximal
1	1				
2A		2			
2B		1			
2C		20			
2D		4			
3A			1		
3B			2		
3C[1]			21	34	
3D			1		
3E				1	
3F			14		
3G				35	
4A					4
4B					
4C					32
4D					43
4E					25
Total n (%)	1 (<1%)	27 (11%)	39 (16%)	70 (29%)	104 (43%)

Includes several conjoining projectile point fragments; 1 – In Meltzer and Eren's (2021) classification, 3C fragments do not differentiate unground lateral splits from unground midsections with intact widths

One hundred and sixty-nine Folsom point fragments, regardless of their size and orientation, bear evidence of impact from use as a projectile. I quantified the presence and absence of fracture types known to occur in experimental impact studies (Ahler and Geib 2000; Hunzicker 2008), including reverse flute scars, crushed tips with stepped edges, and burin spalls (table 13). I did not consider bent snaps or minor step fractures as definitive evidence of projectile impact. I chose to focus on damaged points with the clearest evidence of impact for this study (figure 40). The high relative incidence of points showing evidence of impact damage suggests they were discarded relatively quickly after being used; attempts to resharpen and conserve projectile points over time would have likely erased impact traces.

Table 13. Summary of observations for impact damage and burning alterations for Folsom point fragments (n=235 fragments out of 225 total points) from the Reddin site. Sample based on the collections of CSU and the Smithsonian.

	Fragment Type					
	Complete	Distal	Midsection	Lateral	Proximal	Total n (%)
Impact Class						
Bend		4	14	2	26	46 (20%)
Burin		3	2	12	16	33 (14%)
Reverse Flute		4	11	18	11	44 (19%)
Stepping	1	6				7 (2%)
Multiple		7	10	13	9	39 (17%)
None		3	2	22	39	66 (28%)
Burning Class						
Crazing			2	1		3 (1%)
Potlids		3	5	19	9	36 (15%)
Potlids and Crazing			4	4	3	11 (5%)
None	1	24	28	43	89	185 (79%)

The last aspect of Folsom projectile point damage that I accounted for is the presence or absence of traces suggesting intense thermal alteration (figure 40). The history of quantifying burned lithic debris at Folsom sites goes back a long way (Hofman et al. 1990; Jodry 1999a), but in the last few decades, Folsom researchers fine-tuned their methods to help identify hearth-centered activity areas using spatial distributions of burned material – even in settings where there is no sedimentological or fuel-based evidence of thermal features (Surovell 2022; Surovell and Waguespack 2007; Waguespack and Surovell 2014).

I coded each Folsom projectile point based on visual categories of different burning traces commonly identified by researchers on fine-grained cryptocrystalline silicate material, including potlid fractures, crazing fractures, or a combination of both types (e.g. Jodry 1999a; LaBelle and Meyer 2021; Surovell 2022). I did not consider color change as a potential indicator of burning, and preferred a conservative approach given that natural raw material color variations could be difficult to distinguish confidently from an intense burning alteration – especially for Trout Creek jasper, which displays naturally reddened varieties. Potlidding refers to cone-like kernels within fine-grained silicates that eject after direct contact with fire, and crazing refers to thin web-like and angular thermal cracks that develop when exposed to heat (figure 40). A total of 50 projectile point fragments (about 20%) at Reddin exhibit one or all of these traces, summarized in table 13.

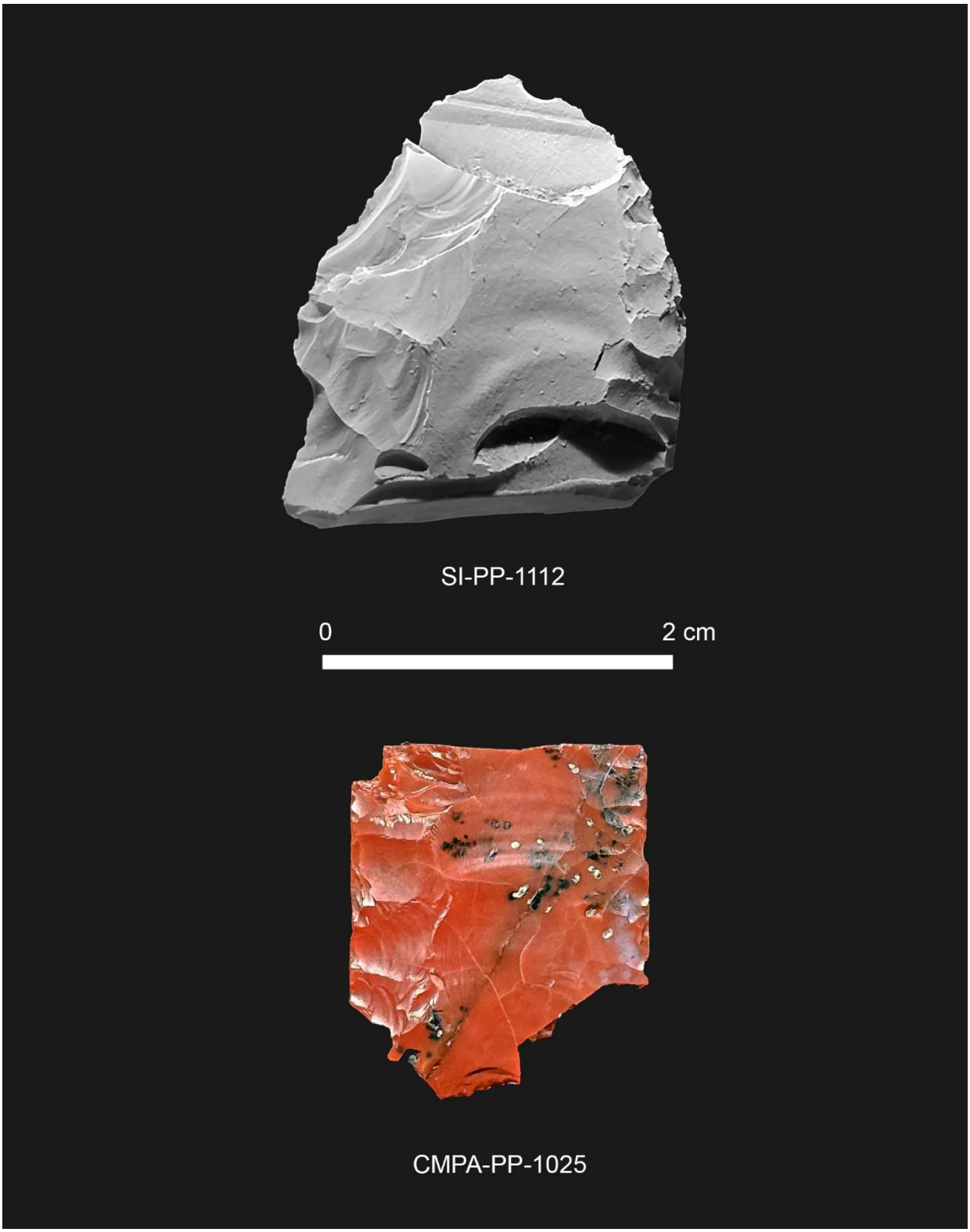


Figure 40. Example of impact damaged (burin spall tip) Folsom projectile point from Reddin (top row) and burned (crazed) projectile point (bottom row).

Preforms and Channel Flakes

The Folsom projectile point manufacture sequence took multiple trajectories, despite a relatively consistent product. Analysis of rejected Folsom preforms at the Lindenmeier site shows a full range of Folsom production techniques (Nami 1999). The process involved everything from tabular nodules to discoidal bifaces and Levallois-like cores at the earliest stages, followed by a consistent path through late-stage biface production including fine bifacial thinning, pressure-flaked edge trimming, channel flake fluting, edge trimming again, and finally basal/lateral edge grinding. At the Reddin site, Folsom flintknappers made use of multiple production trajectories. Initial preform selection included bifacial and discoidal cores as well as large bifacial thinning flake blanks. However, unlike Lindenmeier – and other Folsom sites closely affiliated with lithic procurement areas (Andrews et al. 2021; Root 2000; Surovell 2022) – Reddin does not show any evidence for rejection of early stage preforms. In fact, none of the tools brought to the Reddin site by Folsom (or later) hunter-gatherers appear to be early stage implements. Most artifacts at Reddin were either transported to the site as finished pieces or in the final stages of the manufacturing process. This fact speaks to the paucity of lithic raw material near the site, the provisioning strategies employed by flintknappers, and the planning depth of Folsom decision making.

Preforms at Reddin include those classified as *stage 4 – secondary thinning* as well as early and late *stage 5 – initial shaping* bifaces, based on Nami's (1999) reduction scheme. These stages represent pieces with 1) evidence of soft hammer percussion thinning across both faces, 2) somewhat ovate to regularized biface outlines, 3) final preparations for fluting based on the presence of channel flake nibs, and 4) pressure flaked edges on one or both faces.

Folsom flintknappers used distal beveling to help reinforce preforms against the risky fluting process (Boldurian et al. 1985; LaBelle et al. 2021; Nami 1999). Out of 110 analyzed

preforms, 41 preforms showed evidence of at least one fluting attempt and 25 had two fluted faces, indicating that Folsom flintknappers broke and rejected more than half of the preforms in the final stages of the preform shaping process. All of the preforms lacked a ground basal or lateral edge, and I used this characteristic to distinguish latest-stage preforms from finished points (Meltzer and Eren 2021). Some of the preforms were prepared on a bifacial flake with a smooth negative flake scar running across the midline (pseudo-fluted preforms), and some others were fluted from the distal rather than proximal end (figure 41); the preform assemblage, despite consisting of exclusively late-stage specimens, showed an equally diverse range of preparation techniques as the finished Folsom points discarded at the site. This pattern could reflect copy errors in the preform manufacture process, locally emergent stylistic or technological choices, or raw material stressors on the preform manufacturing decisions – or a combination of these processes.

Channel flakes in the collection represent an attempt (whether successful or not) to flute late-stage preform bifaces (figure 41). I divided channel flake debitage from other bifacial thinning debitage by identifying commonly recognized morphological variables, including dome-shaped dorsal surfaces, generally collateral flaking patterns, and elongated flat ventral surfaces bearing percussion ripples suggesting immense force during the flute percussion process (Boldurian et al. 1987; LaBelle et al. 2021; Reitze et al. 2012).

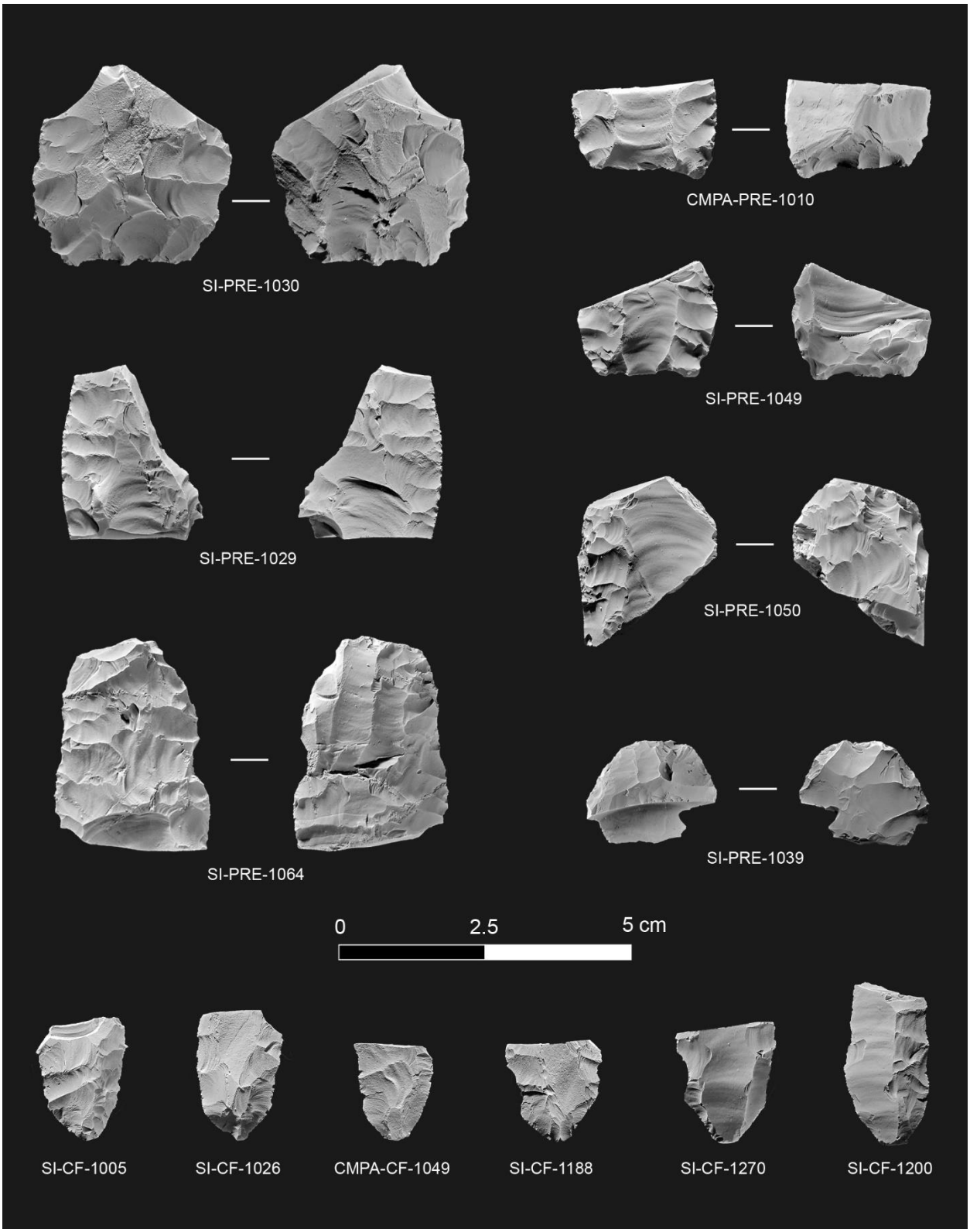


Figure 41. Sample of Folsom preform biface fragments and broken channel flakes from the Reddin site.

Folsom flintknappers at Reddin utilized a similarly diverse range and quantity of lithic raw materials to produce new Folsom points, as compared to finished points discarded on the site (table 14). The preform assemblage, though smaller, exhibited an identical emphasis on Trout Creek jasper (69 out of 110, or 63%). This was also true of channel flakes at the site (221 out of 357 fragments, about 62%). The fact that Trout Creek jasper was equally represented among finished points, preforms, and channel flakes suggests a few things. First, and most obviously, Folsom groups that occupied Reddin on one or multiple occasions used Trout Creek jasper for weapon manufacture preferentially when compared to materials within 150 km of the site. Second, Folsom flintknappers provisioned their stock of "repair equipment" with the same material as their "active use" equipment – Folsom groups geared up their toolkits at the Trout Creek source well in advance of using tools in the middle of the Closed Basin. The high diversity and low quantity of other lithic raw materials in the preform and channel flake assemblages suggest that Folsom groups transported toolkits to Reddin containing recently supplied Trout Creek material, but also residual material from intermittent, long distance, and likely older mobility rounds.

Table 14. Folsom preform and channel flake lithic sources, based on Jodry's (1999b:table 6-7) published counts of Folsom artifacts and the combined CSU and Smithsonian samples reanalyzed for this study.

Source Name or Type	Published Preforms (n)	Total Preforms n (%)	Difference n (% change)	Published Channels (n)	Total Channels n (%)	Difference n (% change)
Trout Creek Jasper	40	69 (63%)	+29 (73%)	178	221 (62%)	+43 (24%)
Morrison Quartzite	7	1 (1%)	-6 (-85%)	1	3 (1%)	+2 (200%)
Silicified Wood	13	8 (7%)	-5 (-38%)	5	30 (8%)	+25 (500%)
Unknown	11	11 (10%)	0 (0%)	12	29[1] (8%)	+17 (142%)
Edwards Chert	2	3 (3%)	+1 (50%)	15	26 (7%)	+11 (73%)
Narbona Chalcedony	0	4 (4%)	+4 (nc)	5	18 (5%)	+13 (260%)
Pedernal Chert	0	4(4%)	+4 (nc)	0	6 (2%)	+6 (nc)
Jemez Obsidian	1	3 (3%)	+2 (200%)	1	1 (<1%)	0 (0%)
Cumbres Chert	2	2 (2%)	0 (0%)	5	12 (3%)	+7 (140%)
Trickle Mtn. Quartzite	0	0 (0%)	0 (0%)	0	3 (1%)	+3 (nc)
Mosca Chert	0	4 (4%)	+4 (nc)	0	3 (1%)	+3 (nc)
Dacite or FGV	0	0 (0%)	0 (0%)	0	3 (1%)	+3 (nc)
Flattop Chalcedony	0	1 (1%)	+1 (nc)	0	2 (1%)	+2 (nc)
Total	76	110 (110%)	+66 (44%)	222	357 (100%)	+135 (61%)

FGV – fine-grained volcanic rock; 1 – includes one specimen made from oolitic or algaelitic chert; nc – not calculated

I expected the preforms and channel flakes from Reddin to be similarly broken as compared to the highly fragmentary Folsom points, for a few reasons. First, apart from a few sites, Folsom researchers have rarely documented fully complete late-stage Folsom preforms – these would have been a missed opportunity for Folsom flintknappers to finish the manufacture process. Most instances of preforms represent failed attempts at making Folsom points; preforms often broke during thinning in earlier reduction stages or (more commonly) during late-stage fluting attempts.

At Reddin, all of the preforms are broken fragments. Meltzer and Eren (2021:figure 12.4) recently devised a set of 14 different fragment codes for Folsom preforms, depicted in figure 42. However, I discuss these more basically as proximal, medial, lateral, and distal fragments. Of these, preform base fragments (proximal ends) are the most common (47 out of 110, or 42%), followed by 29 lateral edges, 27 distal ends, and seven midsections (table 15). The channel flake assemblage includes 81 proximal flake fragments with intact platforms, 162 medial fragments with intact channel flake width measurements, 109 lateral edges, and only five distal ends (table 15). I quantified overshot preform tips from the fluting process as preforms, rather than channel flakes, despite the two artifact types being technically connected in such cases.

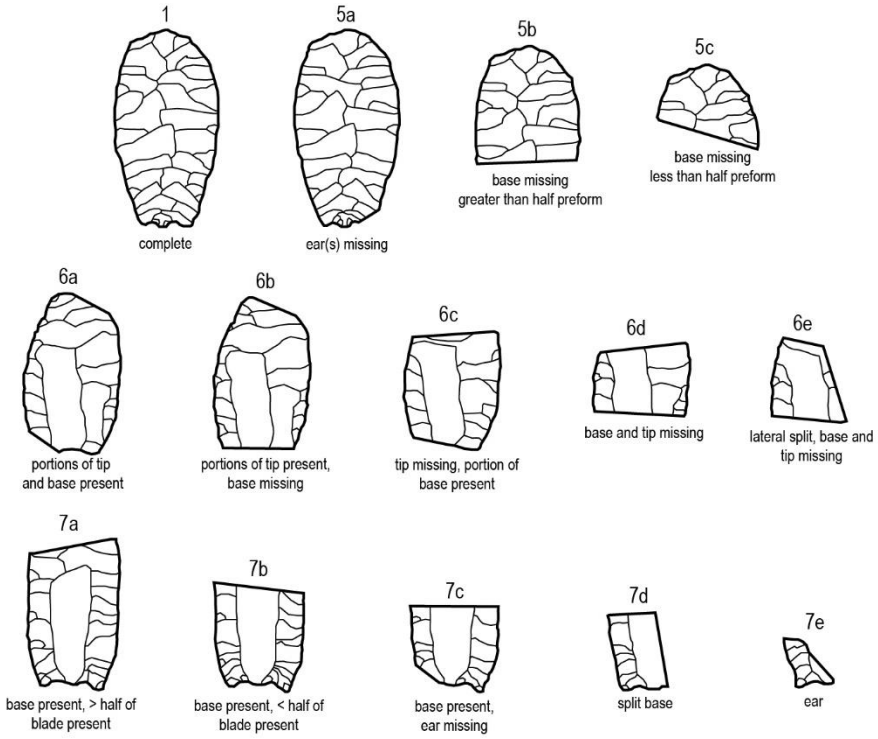


Figure 42. Folsom preform fragment codes schematic, modified and adapted from Meltzer and Eren (2021:figure 12.4).

Table 15. Folsom preform fragment type matrix summarizing Meltzer and Eren's (2021:figure 12.4) breakage classes and portions classified in this study, based on the complete sample of 110 preforms. Channel flakes included (n=357). Samples based on the combined collections made by CSU and the Smithsonian.

	Fragment Type				
Meltzer and Eren Code	Complete	Distal	Midsection	Lateral	Proximal
1					
5A					
5B					
5C		27			
6A					
6B			2		
6C					
6D			5	29	
6E					
7A					
7B					9
7C					4
7D					20
7E					14
Preform Total	0 (0%)	27 (11%)	7 (16%)	29 (29%)	47 (42%)
Channels Total	0 (0%)	5 (1%)	162 (45%)	109 (31%)	81 (23%)

Counting the number of channel flakes allows Folsom researchers to take additional steps towards quantifying the intensity of the point manufacture process, and by proxy, assess the relative degree that Folsom flintknappers manufactured new points and conserved existing stock under conditions of lithic raw material stress (Hurst and Johnson 2016; LaBelle et al. 2021; Sellet 2004, 2013). In a more traditional view, dividing the minimum number of channel flakes by two provides one possible guess of the number of newly manufactured points – most Folsom points are fluted twice, with one flute on both sides. The minimum number of channel flakes includes fragments with an intact flake platform, given that other fragments in combination could originate from few or many channel flakes pending an in-depth study of refitted broken pieces. Using the traditional method, the number of Folsom point manufacture attempts (but not necessarily successes) at Reddin is about 40, and less than half the number of broken preforms at the site.

Some Folsom points are fluted more than twice, and alternatively only once (or never at all). At Reddin, 38 channel flakes have a negative scar on the dorsal surface from a prior flute attempt, proving that multiple fluting did occur. To account for this well-known issue, Sellet (2004) developed the Agate Basin formula which applied knowledge from an intensive refit study of channel flakes, preforms, and points at the Agate Basin site. The study found that multiplying the total number of channel flakes by 0.3 accurately (but not precisely) accounted for the compounding effects of multiple fluting. I used the Agate Basin formula to estimate that Folsom flintknappers at Reddin attempted to make new points about 107 times, a roughly equal number to the total count of broken preforms.

The lack of complete preforms and channel flakes at Reddin is an obvious indicator of artifact damage. The relative sizes of preforms and channel flakes mirror the average size of finished Folsom point fragments in the collection (table 16), with staggering similarity. In fact, one

could reasonably describe the average Folsom artifact at Reddin as a small square with roughly equal width and length dimensions (figure 43). There are no obvious taphonomic effects at the site controlling natural fragmentation patterns to such a high degree across all Folsom artifact classes. Pending other information, the consistent size (rarely longer or wider than 1.5 cm) speaks to the intensive harvesting of usable lithic raw material for repairing broken equipment – likely including larger fragments of debitage, such as channel flakes. At least twenty of the discarded channel flakes from Reddin were recycled into a new tool, including 10 retouched flakes, three gravers (figure 44), and seven edge-utilized flakes; evidence for the discard of previously recycled tools is a good indicator that Folsom flintknappers were mitigating raw material stressors to accomplish onsite tasks. Burning is present but in such low numbers for preforms (15%) and channel flakes (7%) that thermal cracking near campfires is not a likely cause of the severely small tool fragment sizes.

Table 16. Summary of basic width and length variables for all Folsom diagnostic artifacts (preforms, channels, and complete points), based on the combined sample from CSU and the Smithsonian collection.

	Sample Size	Mean Width (mm)	Width Range (mm)	Standard Deviation	Width IQR	Mean Length (mm)	Length Range (mm)	Standard Deviation	Length IQR
Preforms	110	16.1	6.1-29.2	5.7	8.6	16.3	3.7-32.9	5.6	6.2
Channels	357	12.8	5.4-20.6	2.5	3.2	13.0	2.1-25.4	3.3	4.5
Points	225	14.3	3.0-23.8	4.9	8.8	14.4	2.3-43.9	5.6	6.4

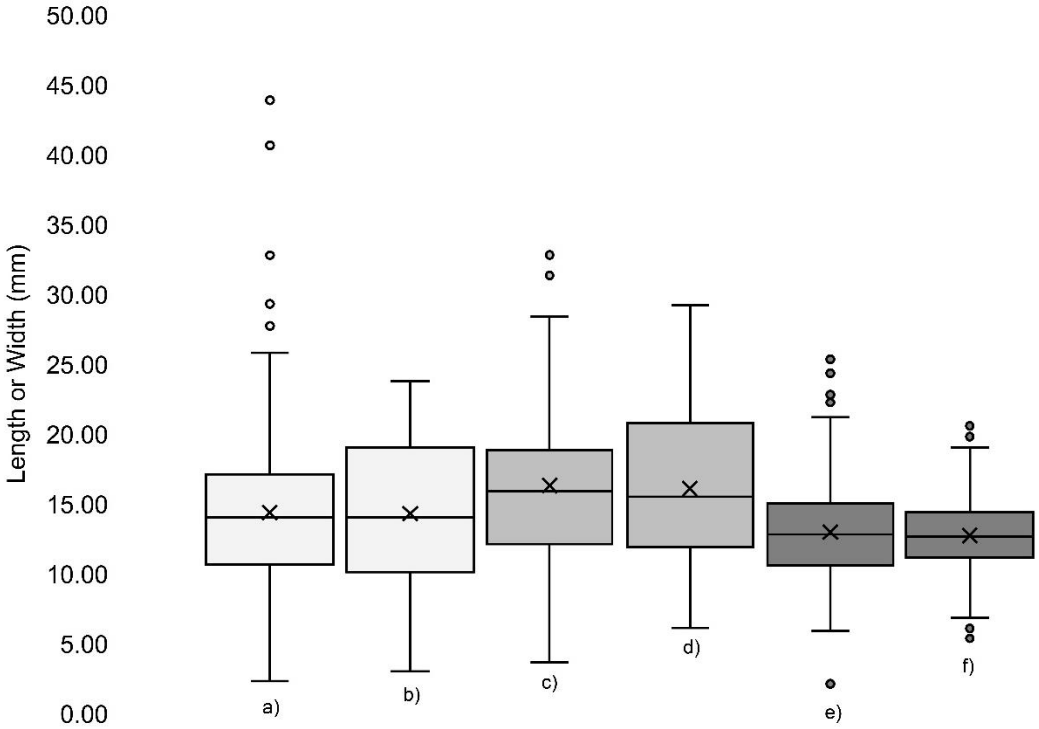


Figure 43. Box plot of all Folsom point fragment lengths (a), point widths (b), preform lengths (c), preform widths (d), channel flake lengths (e), and channel flake widths (f). Note the similarity in fragment size for all artifacts, no matter the measurement axis or artifact type.

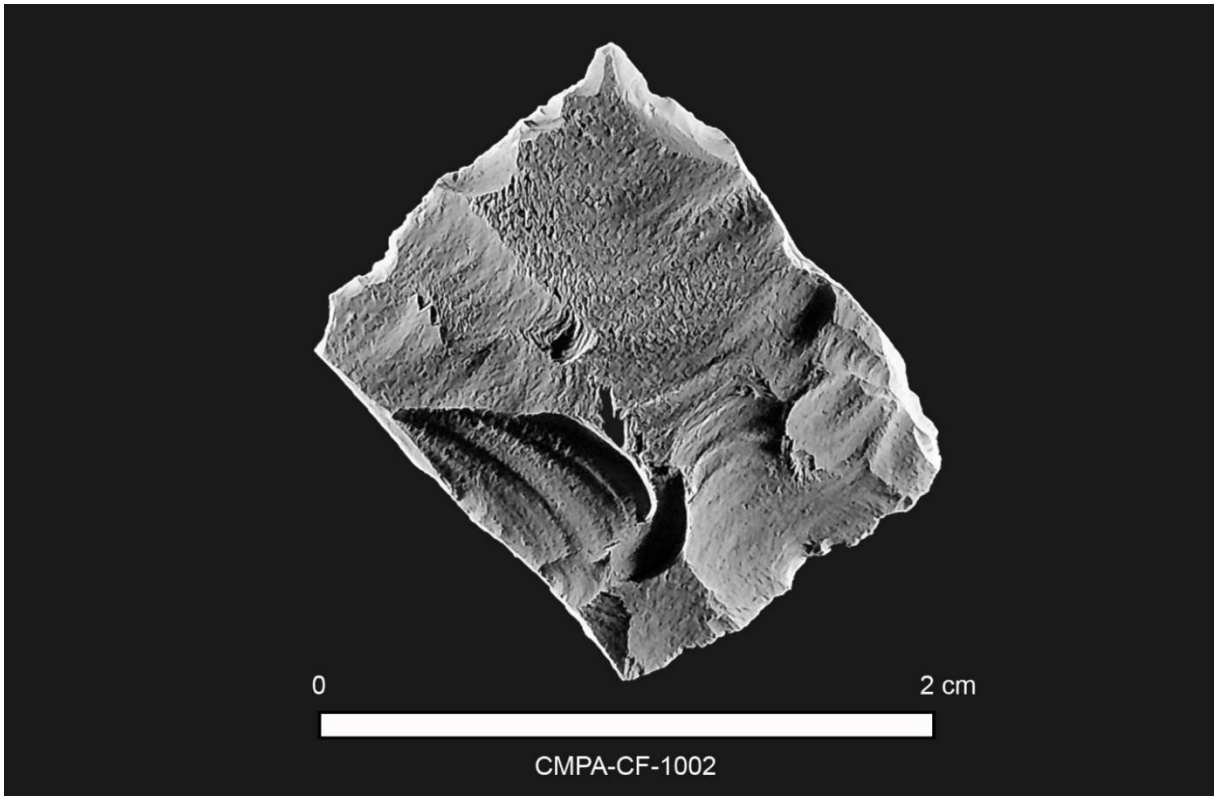


Figure 44. Example of a recycled double-fluted channel flake with a graver tip from the Reddin site.

Other Lithics

The remaining lithics at the site include tools and debitage that I categorized using macroscopic methods (Andrefsky Jr. 2006; Odell 2004), where I focused on variation in the morphological shape of artifacts and manufacture processes. The method that I applied is consistent with other Folsom studies and serves the purpose of communicating broadly accepted terms to describe non-diagnostic chipped stone artifacts in assemblages (i.e. artifacts not definitely associated with the process of making and repairing Folsom weaponry stock). Figure 45 summarizes the general artifact classification scheme for non-diagnostic material and illustrates the hierarchical relationships between morphological types and the strategies used to make them.

In the classification scheme I consider all lithic artifacts as chipped stone tools or debitage. In general, chipped stone tools include objective pieces intentionally manufactured to complete a pre-determined task, whereas debitage includes all other lithic byproducts. Chipped stone tools include different morphological sub-groups or *elements* based on production techniques or functional qualities related to tool morphology. I first divided chipped stone tools into cores, bifaces, and flake tools. I classified cores as objective pieces showing evidence of broad flake preparation and detachment, used in the process of creating flake blanks for producing other types of tools. The biface category consisted of lithic pieces that were flaked and thinned in a manner where the two sides (faces) met to form a sinuous and continuous edge that circumscribed the outline of the artifacts. Speaking generally, cores can be bifaces and bifaces can be cores, but I distinguished the categories by the intensity of edge preparation and thinning, as well as the overall purpose of flake removals – cores were used to make flakes, and bifaces were made to serve a more specialized function such as cutting or piercing. Flake tools included reworked detached pieces from cores that showed evidence of additional modification, usually in the form of

continuous flake scars (retouched edges) from the edge sharpening process, but also irregularly spaced or discontinuous flake scars formed from edge use (utilized edges). All flake tools contained evidence of a dorsal and ventral flake surface, representing the exterior and interior regions of the flake detachment process, respectively. I differentiated cores based on the direction of flake termination, which included multi-directional or blocky cores, bifacial cores, and a sub-category of informally tested cobbles exhibiting a few randomly directed flake detachments. I subdivided biface elements into hafted bifaces and non-hafted bifaces, based on the presence or absence of notches and basal-laterally ground edges. However, I treated specialized projectile point bifaces as an individual category outside of this classification system, given their utility as time-diagnostic artifacts. Flake tools included generalized retouched flake tools and utilized flake tools, but also specialized retouched flake tool categories such as end scrapers and gravers.

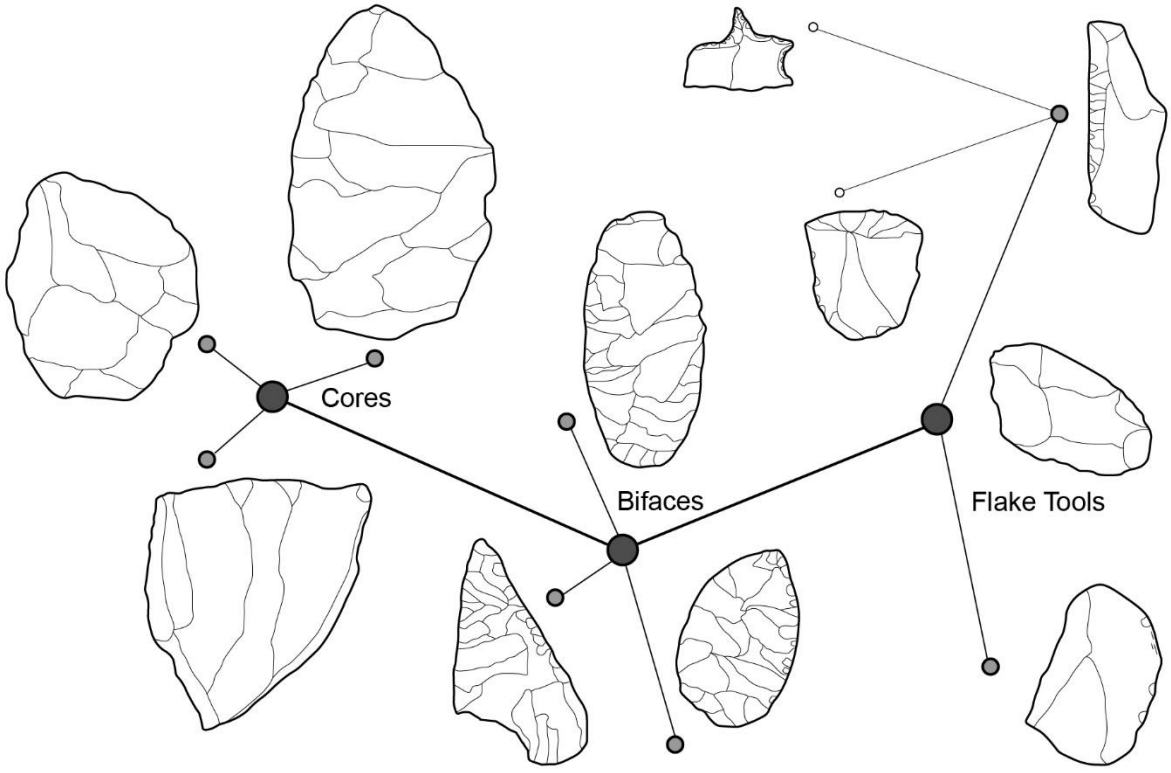


Figure 45. Generalization of the non-diagnostic lithic artifact classification scheme used in this study.

Cores and Bifaces

The relationship between cores, bifacial cores, and non-core bifaces in Folsom assemblages is a topic that researchers routinely investigate, for a few reasons. First, these implements closely reflect lithic provisioning decisions given that cores (whether bifacial or not) serve as lithic raw material supply for mobile groups (Bamforth 2002; Bamforth and Becker 2000; Boldurian 1991; Boldurian et al. 1987; Hofman 2003; Kelly and Todd 1988; Surovell 2009). The way that hunter-gatherers made cores and transported them reflects the flexibility or rigidity of their technological organization. Some cores may be more cost-efficient when considering the amount of material transported from location to location. The potential number and morphology of flakes and tool blanks vary between each type of core, as well. For highly mobile foragers that operated in geographic locations lacking in local raw materials, a useful core technology would likely emphasize raw material conservation over long distances – such a system would maximize flake and tool potential while minimizing raw material costs. Well-prepared bifacial cores and blade cores have long been considered a hallmark of the Paleoindian tradition more broadly (Bamforth 2002; Hofman 2002, 2003; Kelly and Todd 1988), and researchers previously argued that a reliance on such cores suggests provisioning strategies geared explicitly towards transport cost reduction and tool manufacture efficiency over time and space (Hofman 2003; Kelly 1988; Kelly and Todd 1988). However, experimental research over the past several decades has proven negligible differences between specialized and less-specialized core morphologies for the surplus production of tool blank supplies (Eren et al. 2008; Jennings et al. 2010; Prasciunas 2007), generally measured as the total number of manufactured flake edges compared to initial core weight (or some similar ratio). However, individual tool blanks produced from bifacial cores generally retain better edge

to weight ratios than flakes made from blocky, amorphous cores (Jennings et al. 2010; Prasciunas 2004, 2007).

On the Southern High Plains, where most lithic raw material sources are disparately spaced, Folsom hunter-gatherers apparently emphasized a bifacial core technology focusing on the specific shape and size of bifacial flake blank byproducts as well as the reduction of point preforms directly from bifacial cores. However, in the Southern Rocky Mountains, Folsom groups exhibited greater variability in their use of different core forms. Barger Gulch is located adjacent to a lithic procurement area, and the campsite deposits demonstrated an emphasis on blocky core reduction – though bifacial cores and large bifaces are also represented and closely affiliated with the projectile point manufacture process (Surovell 2022). The Mountaineer site in the Gunnison Basin is also located near a lithic procurement source, and the site exhibited a full spectrum of core types including blocky forms, bifacial cores, and unidirectional blade cores (Andrews et al. 2021; Stiger 2006). Variation in the types of cores represented in Colorado's high-altitude environments suggests Folsom people used more localized mobility ranges near areas with abundant lithic sources; Folsom groups may have paid less attention to the long-term costs of core morphology and the long-term preservation of lithic toolkits if materials were local and available. This pattern is the reciprocal of Folsom long-distance travel strategies implemented across the more homogenous table of the Southern High Plains, which lacks many lithic raw materials. However, it should be noted that the most efficient way to transport stone from site to site is simply by carrying a combination of finished tools and a mixture of generalized and ready-made tool blanks instead of cores (Kuhn 1994).

The Reddin site contains only three core fragments and one tested cobble, roughly 0.03 percent of the total tool assemblage, demonstrating that early-stage lithic reduction and tool blank

preparation was not a primary function of the site. The low number of core fragments further confirms that flintknappers preferred to gear up their toolkits offsite, before entering the raw material poor areas of the Valley's center. None of these core tools include evidence of bifacial thinning in preparation for use as a bifacial core. Two of the core fragments are blocky and flaked from multiple directions, and one core and one tested cobble show unidirectional or blade-like flake preparation. The lithic raw materials include obsidian (assumed Valles Caldera, unsourced) as well as Dakota Formation and Morrison Formation quartzites. The cores and tested cobbles are small by standards of some Folsom sites where lithic reduction activities were closely associated with lithic procurement areas. The tool fragments at Reddin average only 30 mm when measured across length, width, and thickness dimensions, with the largest core being roughly 75 mm long, 60 mm wide, and 28 mm thick (table 17). Except for the tested cobble transported to the site, each of the cores likely represents a fully exhausted piece lacking further potential to create useful flakes and tool blanks.

Table 17. Core tool summary data from the Reddin site, including specimens collected by the Smithsonian and CSU field crews.

Lab Number	Element	Form	Material	Flake Scars	Cortex	L	W	T	Mass
SI-COR-1001	Core	Unidirectional	Obsidian	6	75%	20.11	18.79	16.46	6.8
SI-COR-1002	Core	Multidirectional	Obsidian	5	25%	27.13	20.83	9.59	6.7
SI-COR-1003	Cobble	Unidirectional	Dakota Qzt.	2	75%	38.77	35.42	22.62	28.9
CMPA-COR-1001	Core	Multidirectional	Morrison Qzt.	8	75%	74.72	59.70	27.58	170.7

L-length (mm), W-width (mm), T-thickness (mm); Mass (g); Qzt. - quartzite

Bifaces at the Reddin site include *stage 4 – tool preforms* and *stage 5 – finished bifaces* using Andrefsky's (2006:177-200) classification scheme. These are pieces that have been completely thinned using broad and precise flaking to create a flat cross-section, but most completed pieces also show refined outline shaping and edge retouch. This suggests that bifaces were transported to the site as finished or nearly finished tools, and that Reddin did not serve as a place to experiment with creating bifacial cores or reducing early-stage biface nodules into

partially edged pieces. Those activities were performed offsite during toolkit gear-up events, and presumably nearer the locations of lithic raw material sources.

The bifaces at Reddin include primarily broken pieces – suggesting the bifaces were transported as ready-to-go tools and extensively used on the site as cutting tools. Only two of the bifaces are complete and lack significant damage, and there are high proportions of broken end fragments and lateral spalls which represent the functional edges of biface tools (table 18). On average, the biface fragments are between 1 and 2 cm long or wide and lack any remaining utility as repairable and maintainable equipment – the tools were discarded at the end of their utility. The lack of mostly intact biface fragments prohibited in-depth identification of potential ultrathin bifaces in the collection, which are diagnostic Folsom tools commonly associated with bison kill-camp sites in the Plains and Rockies that retain a large width to thickness ratio used for specialized meat filleting techniques (Hofman 2003; Jodry 1999a). Roughly 11 percent of the used biface fragments were burned, given the incidence of potlid scars and crazing fractures.

Lithic raw materials that hunter-gatherers used in the production of bifaces included, predominantly, Trout Creek jasper and lesser quantities of 12 other lithic sources (table 19). However, unlike the diagnostic Folsom assemblage, biface flintknappers utilized greater quantities of obsidian, Pedernal chert and chalcedony, silicified wood, and Dakota Formation quartzites as opposed to more exotic sources like Flattop Butte chalcedony and Narbona Pass chalcedony. My lithic raw material analysis did not identify any Edwards Plateau chert in the biface assemblage, suggesting these distant and high-quality lithic sources were used more exclusively in projectile point manufacture, and that the finished tools from these sources were likely transported across great distances before being discarded.

Table 18. Biface fragment damage and metric data summary from the Reddin site, based on the combined sample from CSU and the Smithsonian collection.

Portion	Burned n	Unburned n	Total Count n (%)	Mean Length (mm)	Mean Width (mm)	Mean Thickness (mm)	Average Mass (g)
Complete		2	2 (<1%)	42.4	18.8	12.3	14.9
End Fragment	6	89	95 (44%)	16.1	18.5	4.8	2.0
Lateral	14	81	95(44%)	16.2	13.7	4.5	1.4
Midsection	3	18	21 (10%)	14.5	19.0	4.6	1.8
Near Complete		1	1 (<1%)	37.4	39.2	10.0	20.7
Total	23 (11%)	191 (89%)	214 (100%)	16.3	16.5	4.7	1.9

Table 19. Representative lithic sources for cores and bifaces from the Reddin site, based on the combined sample from CSU and the Smithsonian collection.

Source Name or Type	Cores n (%)	Bifaces n (%)
Trout Creek Jasper		67 (31%)
Morrison Quartzite	1 (25%)	8 (4%)
Silicified Wood		18 (8%)
Unknown		12 (6%)
Narbona Chalcedony		1 (<1%)
Pedernal Chert		24 (11%)
Jemez Obsidian	2 (50%)	31 (14%)
Cumbres Chert		8 (4%)
Trickle Mtn. Quartzite	1 (25%)	25 (12%)
Mosca Chert		7 (3%)
Dacite or FGV		10 (5%)
Flattop Chalcedony		3 (1%)
Total	4 (100%)	214 (100%)

FGV – fine-grained volcanic rock

Flake Tools

Flintknappers at Reddin designed some flake tools to solve special problems while others were intended to accomplish an array of generalized tasks. I differentiated specialized and generalized categories of flake tools based on the level of effort made in flake tool preparation. In my analysis, all flake tools consisted of modified or utilized parts of flakes detached from a prepared core. I categorized *retouched flakes* as tools made on a flake blank where intentional edge preparation covered most of the length of at least one edge of the tool. In contrast, I categorized *utilized flakes* as tools made on flake blanks exhibiting minimal intentional retouch or instead macroscopic evidence of edge damage covering less than half of one or more flake edges. The location of modification did not factor into my categorizations. Both retouched and utilized pieces included those with unifacial modifications (flake scars or wear on one side of the tools), but

occasionally bifacial modifications were apparent, too (flake scars or wear covering portions of two sides). Similarly, the modifications for both retouched and utilized flakes commonly occurred on one edge margin but sometimes continued onto two or more edge margins depending on the outline shape of the blanks. In sum, I divided retouched flakes from utilized flakes based on the overall proportion of modified or utilized edges, but I did not further group these according to the number of modified faces or edges. Figure 46 shows the differentiation and overlap between these two tool types based on the proportion of modified edges, estimated as the cumulative sum of worked edge length.

I previously mentioned that the lack of bifacial cores at the Reddin site does not necessarily imply the absence of bifacial core technology. Several of the flake tools in the assemblage exhibited characteristics of flake blank detachment from prepared bifacial cores (figure 47), suggested by factors such as very thin and wide cross sections at the distal ends as well as length-to-width ratios exceeding three-to-one for blade-like flakes. Hunter-gatherers in the region may have preferred extremely cost-effective core morphologies or travelling with a near-exclusive mobile toolkit comprised of finished and easily transported pieces. The lack of many core fragments at Reddin could suggest that flintknappers operated under an extreme level of raw material conservation, as the middle of the San Luis Valley would encourage. Table 20 reviews the diverse array of lithic raw materials used in flake tool production, which keeps with similar patterns in the abundance of Trout Creek jasper and lesser quantities of roughly one dozen other material types.

The intense fragmentation of retouched and utilized flake tools hindered my systematic identification of flake blank morphology. I estimated that the average length of retouched and utilized flakes is roughly 1.9 cm and 1.8 cm, respectively, which keeps with the same patterns in

the severity of breakage observed across all tool classes in the assemblage (table 21). I observed high proportions of lateral edges and distal ends in both retouched and utilized flake categories, which represent the functional ends of tools. However, compared to other tool classes, I counted proportionally fewer specimens of retouched and utilized flakes with evidence of intense burning.

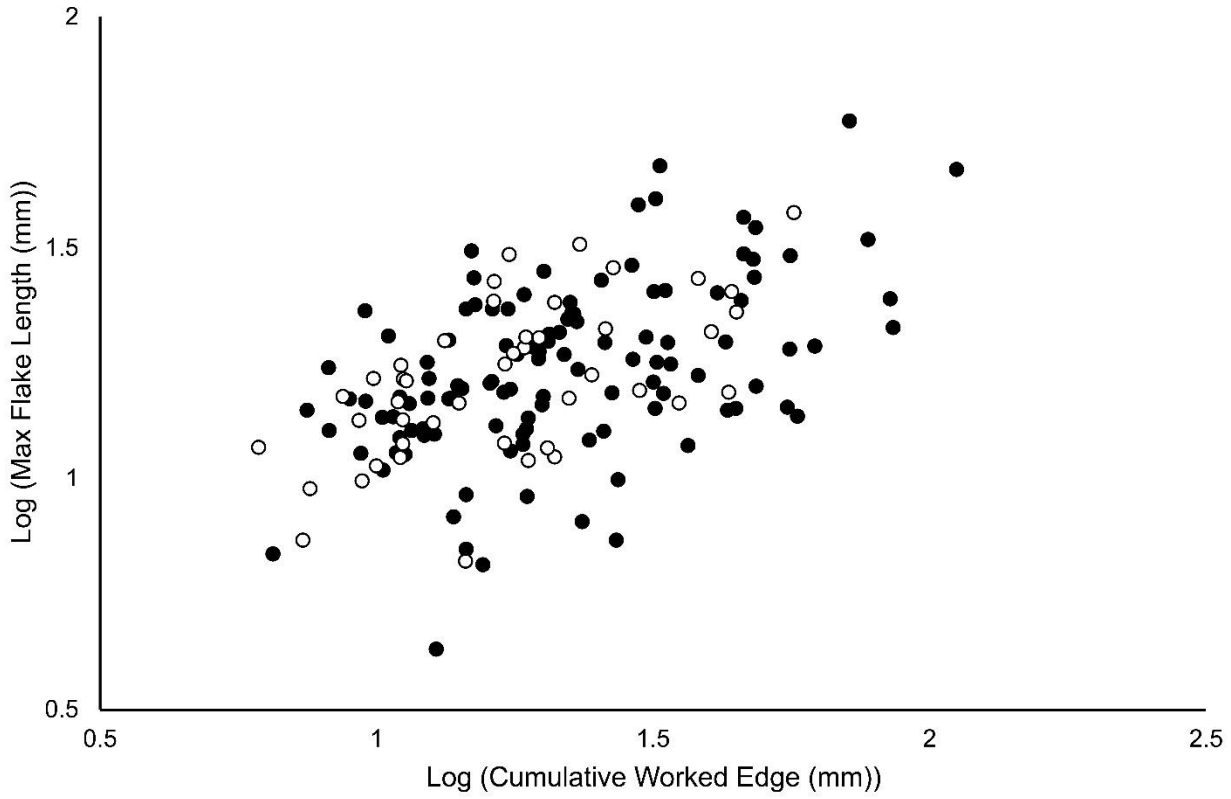


Figure 46. Logged values of maximum tool length vs. the cumulative sum of modified edge length for flake tools at the Reddin site – retouched flake tools (black) and utilized flakes tools (white).

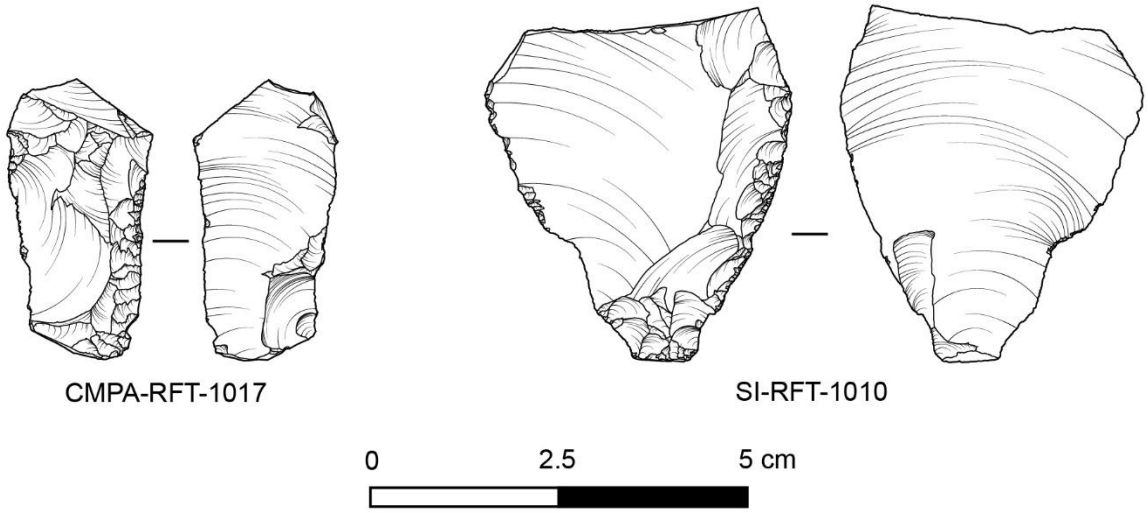


Figure 47. Representative sample of retouched flake tools exhibiting evidence of flake blank reduction from bifacial cores.

Table 20. Representative lithic sources in retouched and utilized flakes from the Reddin site, based on the combined sample from CSU and the Smithsonian collection.

Source Name or Type	Retouched n (%)	Utilized n (%)
Trout Creek Jasper	50 (43%)	20 (44%)
Morrison Quartzite	4 (3%)	2 (4%)
Silicified Wood	15 (13%)	4 (9%)
Unknown	5 (4%)	4 (9%)
Edwards Chert	7 (6%)	0 (0%)
Narbona Chalcedony	2 (2%)	0 (0%)
Pedernal Chert	16 (14%)	3 (7%)
Jemez Obsidian	8 (7%)	5 (11%)
Cumbres Chert	1 (1%)	1 (2%)
Trickle Mtn. Quartzite	4 (3%)	1 (2%)
Mosca Chert	4 (3%)	2 (4%)
Flattop Chalcedony	0 (0%)	3 (7%)
Total	116 (100%)	45 (100%)

Table 21. Retouched (n=116) and utilized flake tool (n=45) damage and metric data summary from the Reddin site, based on the combined sample from CSU and the Smithsonian collection.

Retouched Portion	Burned n	Unburned n	Total Count n (%)	Mean Length (mm)	Mean Width (mm)	Mean Thickness (mm)	Average Mass (g)
Complete		6	6 (5%)	30.2	23.8	7.0	8.3
Distal	1	26	27 (24%)	14.0	17.9	3.5	1.1
Lateral	6	45	51 (44%)	18.1	14.7	4.6	1.4
Midsection	2	9	11 (9%)	20.1	19.7	4.9	2.2
Proximal	1	20	21 (18%)	23.6	19.6	5.7	4.2
Total	10 (9%)	106 (91%)	116 (100%)	19.0	17.3	4.7	2.3

Utilized Portion	Burned n	Unburned n	Total Count n (%)	Mean Length (mm)	Mean Width (mm)	Mean Thickness (mm)	Average Mass (g)
Complete		5	5 (11%)	25.5	19.5	6.7	3.3
Distal	1	8	9 (20%)	19.1	17.9	4.4	1.9
Lateral		15	15 (33%)	13.7	12.9	3.4	0.7
Midsection		8	8 (18%)	19.9	17.9	4.3	1.7
Proximal		8	8 (18%)	15.6	17.5	4.8	1.5
Total	1 (2%)	44 (98%)	45 (100%)	17.5	16.4	4.4	1.6

End Scrapers and Gravers

The retouched flake tool assemblage included additional elements; some retouched flakes exhibited highly consistent shapes, sizes, and flaking patterns similar to well-known tool types recorded at other Folsom sites in the Rockies and Plains. These consisted of end scrapers and gravers, which are tools used in the initial preparation and de-fleshing of hides and in the narrow etching of soft materials like bone, leather, or ochre. I did not identify modified denticulate spalls or notched flake tools in the assemblage, though these are commonly represented flake tool forms at other Folsom campsites (e.g. Hofman et al. 1990; Wilmsen and Roberts Jr. 1978).

I defined end scrapers as disto-lateral retouched flakes taking the outline shape of an isosceles trapezoid (figure 48), and I observed 66 flake tools in the collection matching this description. The end scrapers at Reddin showed extensive evidence of unifacial retouch (resharpening flake scars) along the distal margins of the flake blanks, running continuously across the broad outline shapes of the distal ends; experimental and ethnographic studies have shown that the broad shape of the distal margin helped avoid punctures in the hide de-fleshing process (Blades 2003; Boszhardt and McCarthy 1999; Morrow 1997). At the Lindenmeier site, a high proportion of end scraper tools contained embedded traces of red ochre, and research suggests a potential relationship between red ochre use and anti-bacterial hide treatment (LaBelle and Newton 2010; Wilmsen and Roberts Jr. 1978). Lateral retouch and basal-lateral edge grinding were sometimes used to help facilitate the hafting of stone end scraper pieces to a foreshaft handle, likely made of bone or wood. In the majority of cases, the end scrapers contained only unifacial edge work, though

in some rare instances bifacial edge work towards the proximal end of the flake blanks was apparent – likely associated with precise shaping of the hafting area.

Paleoindian archaeologists commonly identify graver flake tools in campsite localities (Hofman et al. 1990; LaBelle et al. 2021; Pelton et al. 2024; Reitze et al. 2012; Wilmsen and Roberts Jr. 1978), and Reddin contains 34 of these specialized flake tools. I do not treat these as time-diagnostic artifacts per se, but many researchers note the consistent presence of these tools at Folsom sites. One of the gravers at Reddin was manufactured from a discarded channel flake fragment, which is probably the strongest line of evidence for Folsom use of gravers. In general, gravers consist of complete flakes or flake fragments with a chisel-like protrusion or needle-shaped drill bit that is typically narrow, short, and slightly notched towards the base of the graver point (figure 49). The location of the graver chisel is not restricted to the distal or lateral ends of flake blanks, and some graver tools include multiple chisels flaked in sequence along tool edges or along opposing ends of flake blanks. At Reddin, eight of the gravers have multiple chisel points, while the remaining 76 percent contain only one projection. Graver flaking is typically unifacial, although bifacial edge work towards the chisel facet is sometimes present.

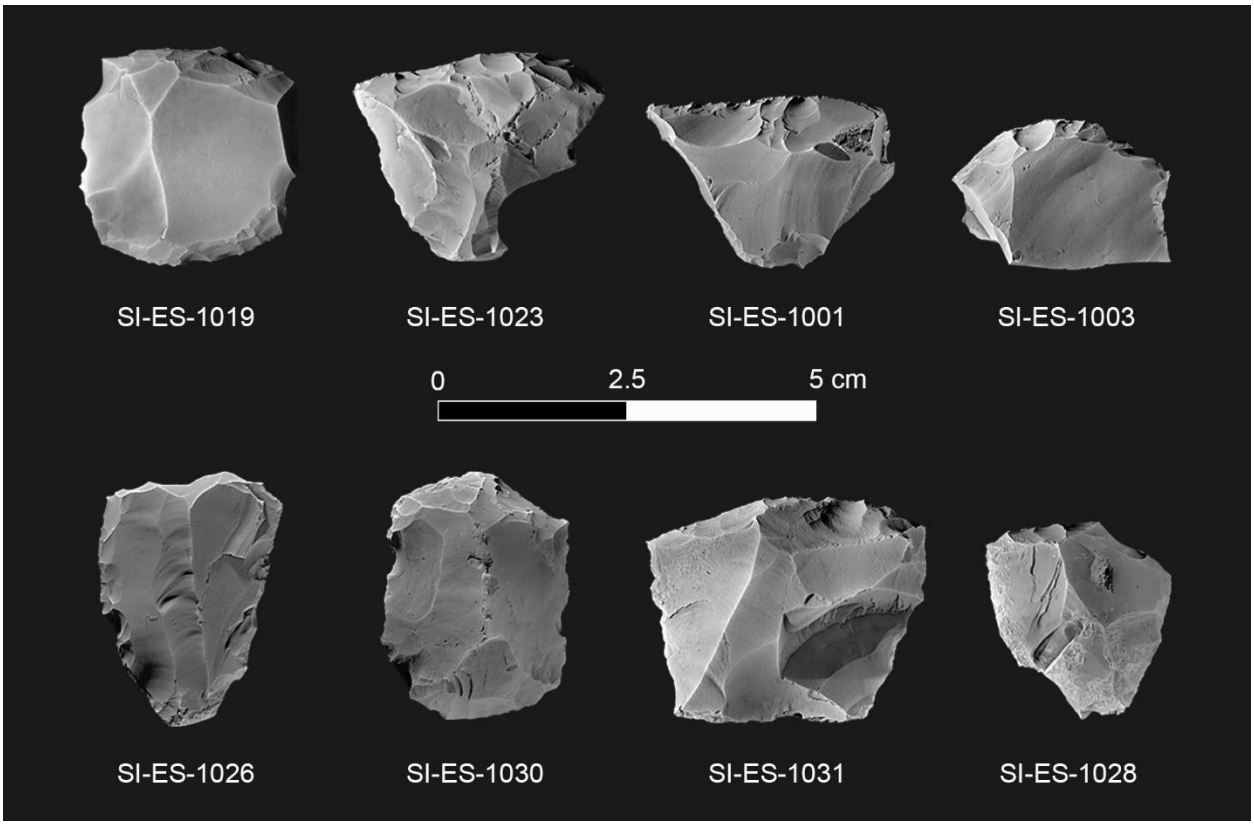


Figure 48. Representative sample of end scraper tools from the Reddin site, showing disto-lateral retouch morphology.

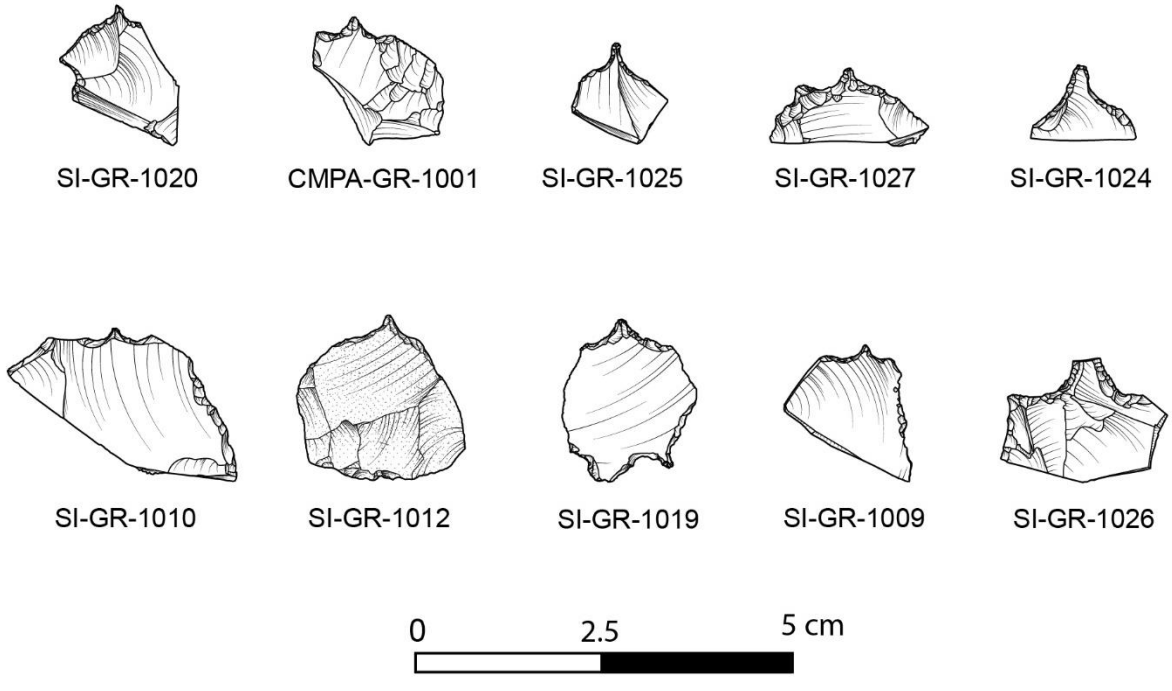


Figure 49. Representative sample of gravers from the Reddin site.

At the Lindenmeier site, the Smithsonian Institution recorded close spatial relationships between gravers and eyed-bone needles (as well as numerous other bone artifacts, like gaming pieces). The colder Younger Dryas climate may have necessitated the manufacture of tailored clothing to improve thermoregulation, and numerous researchers suggest that the abundance of these materials in campsites reflects a Folsom hide-working specialty (Lyman 2015; Osborn 2014; Pelton 2018; Pelton et al. 2024). Gravers may have been used in the production of eyed-bone needles, and they may have been used to puncture hides for sewing.

Flintknappers at Reddin made roughly 70 percent of end scrapers from high quality nodules of Trout Creek jasper and relied minimally on 10 other lithic sources. Flintknappers also utilized Trout Creek jasper more abundantly in the manufacture of gravers, but not significantly (26% of all gravers); graver production was spread much more evenly among 10 lithic raw material types when compared to end scrapers (table 22). In general, flintknappers emphasized the use of fine-grained cryptocrystalline silicate material over coarser igneous rocks and quartzite to make scrapers and gravers, likely owing to the favorable edge sharpness of cherts and chalcedonies for use in the specialized preparation of hides and sewing materials.

Table 22. Representative lithic sources represented in end scrapers and gravers from the Reddin site, based on the combined samples from CSU and the Smithsonian collection.

Source Name or Type	End Scrapers n (%)	Gravers n (%)
Trout Creek Jasper	47 (71%)	9 (26%)
Morrison Quartzite	1 (2%)	1 (3%)
Silicified Wood	3 (5%)	7 (21%)
Unknown	4 (6%)	3 (9%)
Edwards Chert	0 (0%)	2 (6%)
Narbona Chalcedony	1 (2%)	2 (6%)
Pedernal Chert	4 (6%)	4 (12%)
Jemez Obsidian	0 (0%)	2 (6%)
Cumbres Chert	2 (3%)	0 (0%)
Trickle Mtn. Quartzite	1 (2%)	0 (0%)
Mosca Chert	1 (2%)	1 (3%)
Dacite	1 (2%)	1 (3%)
Flattop Chalcedony	1 (2%)	2 (6%)
Total	66 (100%)	34 (100%)

Discarded end scrapers and gravers at Reddin varied little in their overall morphology and damage (table 23). In my analysis, there was a higher representation of complete or unbroken specimens of these tools when compared to all other tool classes; roughly 27 percent of end scrapers and 18 percent of gravers were unbroken. Both end scrapers and gravers showed little evidence of burning, comparable to other flake tools in the assemblage and contrasting with higher percentages of burned projectile points and preforms. Artifact completeness was (at least partially) a prerequisite of successful identification of these specialized flake tool types, however. For example, I only classified retouched flake tools as end scrapers if enough of the tool blank was intact (undamaged) to confirm the direction of flake termination, orientation of flake scars relative to the hafting area, and so on. In the graver assemblage, 18 percent of the flake blanks were complete, but 100 percent of the gravers contained intact chisels lacking significant damage; it would have been impossible to identify gravers if the needle-like tips were broken off.

Table 23. End scraper (n=66) and graver tool (n=34) damage and metric data summary from the Reddin site, based on the combined samples from CSU and Smithsonian collection.

End Scraper Portion	Burned n	Unburned n	Total Count n (%)	Mean Length (mm)	Mean Width (mm)	Mean Thickness (mm)	Average Mass (g)
Complete	1	17	18 (27%)	26.9	25.2	8.3	5.7
Distal	7	23	30 (45%)	14.2	22.0	6.4	2.6
Lateral	5	12	17 (28%)	22.0	19.3	7.8	3.5
Proximal	0	1	1 (2%)	19.6	24.3	7.6	3.7
Total	13 (20%)	53 (80%)	66 (100%)	19.7	22.2	7.3	3.7
Graver Portion	Burned n	Unburned n	Total Count n (%)	Mean Length (mm)	Mean Width (mm)	Mean Thickness (mm)	Average Mass (g)
Complete	0	6	6 (18%)	19.8	15.9	3.2	1.3
Distal	0	14	14 (41%)	13.4	15.5	3.5	0.8
Lateral	0	12	12 (35%)	17.6	13.6	3.4	1.0
Midsection	0	2	2 (6%)	12.5	13.9	3.2	0.5
Total	0 (0%)	34 (100%)	34 (100%)	16.2	14.8	3.4	1.0

Researchers often note the presence or absence of spurred corners on the distal ends of end scrapers (Eren et al. 2013; Morrow 1997; Rogers 1986; Shott 1995; Shott and Weedman 2007). Occasionally, the spurs represent retouched graver tips and a combination of tool forms, but today most researchers agree that the spurs on scrapers are a byproduct of cumulative tool maintenance

and repair – an artifact of the tool rejuvenation process whereby thick flakes are removed on the distal end to make room for a new modified scraping surface (Shott 1995; Shott and Weedman 2007). Only 10 of the end scrapers at Reddin include a distal spur, but none appear to have been recycled into a graver chisel. Previous studies have shown that width and length variables vary according to the scraper rejuvenation process, but thickness is generally held constant and likely controls rejuvenation potential over time (Morrow 1997; Shott 1995); once end scrapers are whittled down to the point of maximum thickness, they are discarded.

I created an index of tool measurements to better understand the relationship between artifact size and rejuvenation potential in end scrapers at Reddin, using the minimum distance between the point of maximum thickness to the distal end divided by the overall length of the tools. End scrapers with ratio values closer to zero represent tools with distal ends resharpened closely to the point of maximum thickness, with little remaining potential for tool repair and recycling of the functioning end. End scrapers with ratio values closer to one represent tools with more potential for extended use and recycling. The data are highly left tailed (values close to zero), demonstrating that most end scrapers were discarded near the end of their use lives (figure 50).

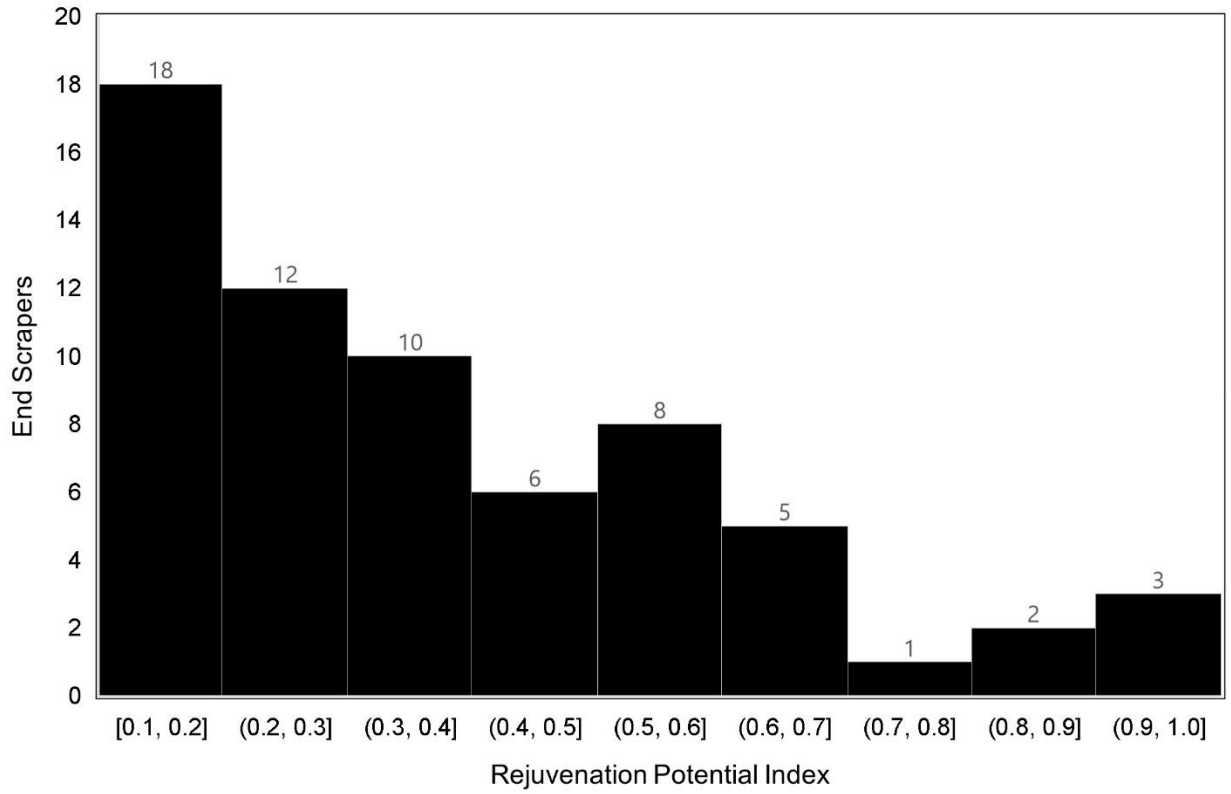


Figure 50. Histogram summarizing rejuvenation potential in the sample of end scrapers from the Reddin site. The index is a measure of the distance between the point of maximum thickness and the distal end divided by total end scraper length. Values closer to zero represent less rejuvenation potential.

Debitage

Reddin is not a lithic quarry, and it comes as no surprise that debitage characteristics at the site reflect the latter stages of the lithic reduction process. Reddin is not a dense lithic scatter when compared to other Folsom sites exhibiting a full range of lithic processing activities. The total amount of lithic waste at the Reddin site is 40,695 pieces – spread over a 70-acre area based on the Smithsonian collection. In contrast, the Barger Gulch and Mountaineer sites are both located near lithic sources and contain 74,285 and 102,297 pieces respectively (Andrews et al. 2021; Surovell 2022). The Stewart's Cattle Guard site, on the eastern side of the Valley floor, holds roughly 17,367 pieces of debitage and is similarly constrained by the lack of local lithic raw material; Cattle Guard and Reddin contain fewer amounts of debitage than other sites given the

paucity of workable stone nearby and the fact that lithic reduction activities focused on late-stage manufacture and repair of transported lithic equipment.

I analyzed 35,556 pieces of debitage from the Smithsonian's pedestrian surveys, which makes up roughly 87 percent of the total debitage. I also recorded debitage from the CSU's fine-grained surveys of Locality A (n=4023, or 10% of the total). I studied these two sample groups independently, however, given the differences in the spatial scale and intensity of survey methods (see chapter 3). In Appendix H, I summarize a limited amount of debitage collected during the Smithsonian excavations along the water well and pipeline route crossing the site (n=1116, or 3% of the total).

My debitage analysis focused on the same themes that I used to analyze chipped stone tools. I considered variation in lithic raw materials, morphological characteristics suggesting different manufacture strategies, as well as artifact damage such as flake completeness and evidence of burning from proximity to thermal features. However, I did not measure these variables for individual flakes or pieces of angular debris; I took more of an aggregate route to debitage analysis (Ahler 1989). I counted and weighed all debitage in each Smithsonian survey block (900 m^2 square) and CSU grid unit (1 m^2 unit). I first organized debitage into groups of lithic raw materials, using the CMPA's comparative lithic raw material library as a guide. I counted and weighed burned and unburned lithics in each raw material group, followed by complete and broken flakes for each group, and then I measured the same variables for cortical and non-cortical debitage in each raw material group. In my analysis, cortex included either parent bedded material attached to flake dorsal surfaces or weathered and occasionally rounded exterior cobble rinds preserved on dorsal surfaces.

In general, I observed nearly identical proportions of lithic raw materials in the debitage as compared to the tool assemblage. The Smithsonian debitage sample included 26,570 pieces of fine-grained cryptocrystalline silicate materials including cherts, chalcedonies, agates, and jaspers. Trout Creek jasper made up roughly 75 percent of the fine-grained silicates sample (table 24). The least abundant rock categories included fine-and-coarse-grained quartzites from the Dakota and Morrison Formations (the nearest raw material source), as well as unsourced silicified woods and igneous rocks like obsidian and dacite. The debitage sample from Locality A exhibited similar proportions of lithic raw materials (table 24), despite the difference in spatial scale for the CSU's sampling methods. The consistency between lithic raw materials observed in the debitage and tool assemblages suggests a close relationship between the discard processes of the two artifact classes.

Table 24. Lithic sources represented in debitage from Reddin, based on Smithsonian site inventory and CSU's fine-grained surveys within Locality A (see chapter 3).

Source Name or Type	Smithsonian (n)	CSU Locality A (n)	Total Sample n (%)
Trout Creek Jasper	20,150	2281	22,431 (57%)
Morrison Quartzite	338	52	390 (1%)
Silicified Wood	861	168	1029 (3%)
Unknown	49[1]	114[2]	1633 (4%)
Edwards Chert	184	143	327 (1%)
Narbona Chalcedony	480	139	619 (2%)
Pedernal Chert	4013	263	4276 (11%)
Jemez Obsidian	1982	344	2326 (6%)
Cumbres Chert	951	132	1083 (3%)
Trickle Mtn. Quartzite	3208	203	3411 (9%)
Mosca Chert	729	59	788 (2%)
Dacite or FGV	2420	76	2496 (6%)
Flattop Chalcedony	14	41	55 (<1%)
Rhyolite	177	8	185 (<1%)
Total	35,556	4023	39,579 (100%)

1 – Includes 20 pieces of quartz crystal and one oolitic or algaelitic flake; 2 – Includes two pieces of quartz crystal

The debitage at Reddin consists nearly exclusively of very small edge finishing or tool resharpening flakes made by pressure flaking; the site shows little evidence of bifacial thinning or earlier core reduction using handheld percussion techniques – with the exception of channel flakes. Two hundred and twenty-seven flakes with cortex on dorsal surfaces include some of the larger bifacial thinning pieces at the site, which weigh 2.1 g on average, but these are poorly represented

and account for just 0.06 percent of debitage in the Smithsonian sample (table 24). Lithic raw material classes exhibiting higher counts of cortical bifacial thinning flakes include dacite with weathered rinds, silicified woods with remnants of exterior wood or bark matrix, as well as Trout Creek jasper and Pedernal chalcedony flakes bearing limestone caprock rinds. In Locality A, cortical pieces make up about one percent of the total sample but are much smaller on average, with individual pieces weighing about 0.4 g.

I recorded 2686 complete (unbroken) flakes in the Smithsonian sample, accounting for roughly 8 percent of the debitage (table 25). The average complete flake and average broken fragment weighed approximately the same, between 0.2 g and 0.3, respectively. I did not observe significant variance in the weight of complete and broken flakes, including those from different lithic raw material classes; flaking debris in the Smithsonian sample included individual pieces of approximately the same size whether broken or not, despite a diverse array of fine-grained and coarse-grained material types. In Locality A, complete flakes and flake fragments were consistently smaller and kept with the same pattern observed for smaller cortical flakes, on average (table 26). The average complete flake in Locality A weighed 0.1 g and the average fragment weighed 0.2 g. These data suggested that CSU identified smaller flakes than the Smithsonian team, perhaps due to the preferential selection of larger debitage during the earliest surveys at the site.

Table 25. Summary of Smithsonian (1979-1983) debitage attributes recorded in this study, organized by raw material. The majority of debitage, not accounted for here, include non-cortical, incomplete, and unburned flake fragments or angular debris.

Source Code	Cortical Fk. (n)	Cortical Fk. Mass (g)	Complete Fk. (n)	Complete Fk. Mass (g)	Burned Fk. (n)	Burned Fk. Mass (g)	Total Count (n)	Total Mass (g)
TRT	38	70.9	1548	270.8	2152	880.3	20,150	4644.1
MOR	0	0.0	23	7.4	0	0.0	338	110.8
SWD	35	35.4	99	38.7	10	7.4	861	365.2
UNK	1	0.5	5	0.9	0	0.0	28	9.3
OOL	0	0.0	0	0.0	0	0.0	1	0.9
QTC	1	8.9	1	0.1	0	0.0	20	15.5
EDW	2	2.5	23	6.0	2	1.8	184	49.3
NARB	6	6.5	70	9.1	51	20.1	480	92.9
PED	49	65.2	386	87.4	296	160.2	4013	1249.3
OBS	7	9.4	195	37.3	0	0.0	1982	473.7
CUMB	3	7.7	57	26.6	110	83.5	951	558.2

Source Code	Cortical Fk. (n)	Cortical Fk. Mass (g)	Complete Fk. (n)	Complete Fk. Mass (g)	Burned Fk. (n)	Burned Fk. Mass (g)	Total Count (n)	Total Mass (g)
DAK	17	99.3	96	49.1	1	0.7	3208	1334.8
MOSC	1	1.8	48	12.6	200	124.2	729	110.8
DAC	59	123.7	125	61.6	0	0.0	2420	1140.0
FLAT	0	0.0	0	0.0	1	1.5	14	15.7
RHY	8	40.6	10	23.7	0	0.0	177	178.8
Total	227	472.4	2686	631.3	2823	1279.7	35,556	10,591.0

Source Code – TRT (Trout Creek), MOR (Morrison Quartzite), SWD (silicified wood), UNK (unknown), OOL (oolitic chert), QTC (quartz crystal), EDW (Edwards Chert), NARB (Narbona Chalcedony), PED (Pedernal Chalcedony), OBS (obsidian), CUMB (Cumbres Chert), DAK (Trickle Mtn. Quartzite), MOSC (Mosca Chert), DAC (dacite or fine-grained volcanic), FLAT (Flattop Chalcedony), RHY (general rhyolite)

Table 26. Summary of CSU Locality A (2022) debitage attributes recorded in this study, organized by raw material. The majority of debitage, not accounted for here, include non-cortical, incomplete, and unburned flake fragments or angular debris.

Source Code	Cortical Fk. (n)	Cortical Fk. Mass (g)	Complete Fk. (n)	Complete Fk. Mass (g)	Burned Fk. (n)	Burned Fk. Mass (g)	Total Count (n)	Total Mass (g)
TRT	18	10.2	425	37.4	331	41.7	2281	307.7
MOR	0	0.0	9	1.6	0	0.0	52	8.7
SWD	7	1.8	51	4.3	12	1.9	168	22.1
UNK	1	0.3	25	3.5	13	2.0	112	13.5
QTC	0	0.0	0	0.0	0	0.0	2	0.2
EDW	1	0.3	46	5.0	7	0.9	143	17.6
NARB	0	0.0	34	1.4	31	2.5	139	9.6
PED	9	3.0	77	8.4	16	2.5	263	30.5
OBS	2	1.4	67	6.6	0	0.0	344	41.7
CUMB	3	0.9	24	4.3	19	5.0	132	34.2
DAK	0	0.0	21	9.4	2	0.7	203	70.0
MOSC	1	0.8	15	1.2	15	3.4	59	8.8
DAC	0	0.0	11	2.7	0	0.0	76	13.3
FLAT	2	0.5	11	0.6	4	0.2	41	6.2
RHY	0	0.0	0	0.0	0	0.0	8	2.5
Total	44	19.2	816	86.4	450	60.7	4023	585.9

Source Code – TRT (Trout Creek), MOR (Morrison Quartzite), SWD (silicified wood), UNK (unknown), OOL (oolitic chert), QTC (quartz crystal), EDW (Edwards Chert), NARB (Narbona Chalcedony), PED (Pedernal Chalcedony), OBS (obsidian), CUMB (Cumbres Chert), DAK (Trickle Mtn. Quartzite), MOSC (Mosca Chert), DAC (dacite or fine-grained volcanic), FLAT (Flattop Chalcedony), RHY (general rhyolite)

I did not record specific length or width variables for individual pieces of flaking debris. In a supplemental study I sieved 505 obsidian flakes from 45 random Smithsonian survey blocks to better understand the relationship between average flake mass and flake size at the site. In the study, about 64 percent of the obsidian flakes were captured in a 5.6 mm wide mesh (G3 size class) and about 35 percent of flakes were captured in a 2.8 mm wide mesh (G4 size class); flakes larger or smaller than these two categories collectively made up only 1 percent of the sample. Obsidian flakes roughly 5.6 mm long weighed 0.3 g on average, and flakes 2.8 mm long weighed 0.08 g on average (table 27). Given these results, I estimated that most flakes at Reddin are roughly half a

centimeter in size or less. These results suggested that flintknappers at the Reddin site did not produce very large flakes; flintknappers focused on the final processes of tool shaping, trimming, and edge repair using pressure flaking methods rather than percussion flaking techniques.

Table 27. Supplemental mass analysis of a sample of 505 obsidian flakes from the Reddin site, based on the Smithsonian survey collection.

Mesh Size	Total Flake Count (n)	Total Mass (g)	Survey Grid Blocks (n)	Mean Flake Count per Block (n)	Range of Flakes per Block (n)	Mean Flake Mass (g)
G1 – 25 mm	0	0	0	0.0	0	0.0
G2 – 12.5 mm	4	5.4	3	1.3	0-2	1.3
G3 – 5.6 mm	324	95.5	36	9.0	0-56	0.3
G4 – 2.8 mm	176	15.6	28	6.3	0-38	0.1
G5 – 2.28 mm	1	< 0.1	1	1.0	0-1	< 0.1
Total	505	116.5	68	7.4	0-56	0.2

Burned lithic waste makes up a low proportion of the debitage in the Smithsonian sample (n=2823, about 8 percent). In Locality A, burned flakes and angular debris comprise 11 percent of the sample; the consistency in the proportion of burned debitage between the Smithsonian and CSU samples suggests that both coarse-grained and fine-grained survey methods adequately monitor this phenomenon across the site. These ratios closely match those of burned Folsom lithics (points, preforms, and channel flakes), suggesting that tools and debitage may have been discarded in similar places at the site and that the rates of accumulation were consistent – see chapter 5 for discussion on artifact accumulation. However, these data do not necessarily indicate that burned flakes (or tools) are distributed uniformly across the site. It is possible that burned debitage correlates with sample size, or even particular raw materials that may be unevenly distributed. Quartzite and fine-grained igneous rocks do not show definitive evidence of heat alteration, but these characteristics are easily visible on fine-grained silicates like chert and chalcedony (table 25 and 26). Some areas within the site may contain lesser quantities of burned lithics based on the overall density of debris or concentrated lithic raw material groups. At Barger Gulch, roughly 75 percent of burned lithics occurred within 0.5 m of a hypothesized hearth feature (Surovell 2022;

Surovell and Waguespack 2007); hearth-centered living spaces at Barger Gulch contained the majority of all recorded debitage and served as the primary areas for late-stage flintknapping activities (Surovell 2022).

Summary

The lithic assemblage at Reddin is diverse. Flintknappers at the site utilized lithic raw materials from sources at the edges of the Valley floor, major intermountain passes throughout the Southern Rockies, as well as exotic rock types from the greater Southwest and Great Plains regions. Hunter-gatherers of the Folsom tradition clearly favored Trout Creek jasper, and apparently geared up with mostly complete tools from this well-known source in south-central Colorado prior to entering the Valley's center. They also carried finished and nearly finished tools made from sources as far as the Soccoro area south of Albuquerque, New Mexico, from across the Llano Estacado near the Edwards Plateau of central Texas, and from the Central High Plains border at Flattop Butte in eastern Colorado. The low quantity of exotic lithic material suggests Folsom groups traveled with toolkits to Reddin containing residual pieces procured directly during a previous mobility round, or from long-distance trade with neighboring groups.

Reddin is one of four sites in North America with over 500 time-diagnostic Folsom artifacts, which include discarded hunting weapons and the byproducts of making new weapons. The Smithsonian and CSU teams collectively document 225 projectile points from Reddin, including classically fluted, pseudo-fluted, and unfluted Folsom or Midland varieties. Tips and complete points are poorly represented in the sample, but bases and ground lateral edges are abundant – suggesting discard processes favored proximal ends of points which are commonly found in Folsom residential campsites in the region; archaeologists expect to find the bottom half of broken Folsom points in places where broken tools were dehafted, emptied from a foreshaft,

and then eventually repaired. A collection of 110 preform bifaces and 357 channel flake fragments confirms new weapon manufacture activities took place at the site. Burned examples of these materials suggest the presence of hearth-centered spaces near campsite localities.

Hunter-gatherers brought more than just hunting weapons with them to the Reddin site. Lithic toolkits also contained late-stage bifaces as well as finely made flake tools including retouched flake knives, scrapers, and gravers. Flintknappers at the site occasionally made expedient use of some flakes for less specialized needs. The lack of cores and core fragments at the site indicates that Reddin was not a place for making early-stage tool blanks. Bifacial cores are absent in the assemblage, a typical hallmark of high-mobility provisioning strategies, yet many of the flake tools show traces of reduction from bifacial cores and blade cores. Basic summaries of the size of tool fragments, including weaponry and non-weapon pieces, suggests that tools measuring more than 1.5 cm long or wide are rare – I believe this is evidence of intensive lithic conservation; flintknappers at Reddin likely made use of any stone large enough to have potential for repair and recycling into different tool forms.

Lithic debitage waste at Reddin includes very small pressure flakes and flake fragments, which differ little in size (generally about 0.5 cm long and about 0.3 g per flake), suggesting a very narrow range of lithic reduction activities. The abundance of these very small pieces of debitage reflects the same signal of lithic conservation indicated by the fragmentary tool assemblage; the lack of local lithic raw materials at the site constrained the types of lithic tool manufacture and processing that occurred there. Flintknappers primarily repaired broken equipment at the site or put the finishing touches on nearly complete tools (like preforms). Tools with rejuvenation potential were likely transported offsite at the conclusion of occupations at Reddin.

This chapter painted a picture of the Reddin site at an aggregate level; the summaries of the tools and debitage presented here concern only the general quantities of different attributes like lithic raw material diversity, artifact manufacture techniques, and damage. The data suggest that Folsom hunter-gatherers did more camping than hunting at the site based on the types of tools and portions of tools discarded there, and that lithic processing activities focused on repairing broken equipment over time. The overall low quantities of debitage and high number of tools suggest that people did not spend too much time at the site. But how much time is represented at Reddin? Do the patterns in the data reflect the average of all site activities over time? How evenly distributed are these artifacts and attributes spread across the site? Do some areas contain more abundant evidence for site activities over others? A spatial analysis is needed, and formal hypotheses must be tested to answer these questions. I will cover these questions in the next chapter.

.

CHAPTER 5 - SPACE AND TIME

Usually, the words *space* and *time* appear in two different chapters of a dissertation. One of those chapters covers a spatial analysis and tries to prove that artifact concentrations on the site represent the living floors of the site's past occupants. The researcher (me) is supposed to find local patterns in artifact types, artifact size, raw materials and manufacture stages, or artifact damage resulting from use, repair, or post-depositional processes. I am supposed to compare those patterns to the ethnographic record of hunter-gatherers to make a case for spatial integrity of the site's deposits. In this perfect hypothetical scenario, my next chapter then tests the integrity and contemporaneity of the site's spatial patterns using absolute chronological methods like radiocarbon dating, or some other. I am supposed to make use of stratigraphic information and argue that artifacts found close together in the same context represent the debris from a single occupation, or at least a series of closely associated events. I am supposed to justify an argument that Folsom hunter-gatherers at the site used certain spaces at the same time, that the patterns you see represent something indicative of one Folsom group's residential, technological, and subsistence system. But in this dissertation, I am talking about the Reddin site – I will achieve almost none of these goals.

The Reddin site is a surface scatter. Most archaeologists think of surface scatters as problems because there is little control over how things spread around and move out of primary context over time. The preservation of desirable organic materials for dating and subsistence studies is also generally quite poor in surface scatters. To top it all off, people will visit sites over time, and surface scatters lack the stratigraphic defenses necessary to separate unassociated materials from comingling together in space. These problems describe the palimpsest effect in

archaeology, a jargon-laden word to describe the very simple fact that traces of individual occupation events can erase or overlap one another over time. This dissertation will not solve these problems by any means, as they are inherent properties of sites lacking deep stratigraphic stories. However, I do hope to show that surface scatters retain great utility for answering questions about the Folsom tradition from a different perspective and a different scale of analysis than is typically explored in a buried component. Surface scatter sites offer a time-averaged view of the totality of people's use of space over time. In this sense, surface scatter sites may be the only appropriate sites to explore questions about the spectrum of people's decisions at timeframes exceeding the day-to-day experience – a solution to a different set of questions, rather than a problem for the same old questions.

This chapter is organized around a few central questions to guide a spatial and temporal analysis of the Folsom component:

1) *Where is the Folsom component located at the Reddin site?*
2) *What kinds of residential mobility strategies did Folsom hunter-gatherers use?*
3) *Does the Folsom component represent a single contemporaneous occupation, or several different occupation events?*

The reader will find out that these questions and the concepts underlying them inevitably intersect; spatial characteristics of the Folsom component will provide lines of evidence supporting a temporal analysis of the site, and vice versa. The chapter is organized into three general sections to guide the analysis of each question. First, I present a set of spatial statistical methods to quantitatively define the location of the Folsom component, which identifies the analytical units necessary to answer the other questions. The reader will note that certain locations within the site,

and within the overall distribution of Folsom material, are better suited to analysis of residential mobility and the contemporaneous use of Folsom spaces. The second section explores the concept of residential mobility with an analysis of artifact accumulation over time in the Folsom component. The analysis is predicated on the fact that time spent occupying a site is time spent not moving (Surovell 2009), and therefore, occupation span is inversely related to a system of residential mobility and may serve as a monitor of that process. I then explore whether Folsom groups occupied certain spaces across the site at approximately the same time in the following section. I use an analysis of conjoining artifact pieces discarded in different places at roughly the same time to demonstrate the overall spatial range of Folsom activities during occupations. The cumulative results of the methods presented here paint a more holistic picture of the Folsom occupation at Reddin, and in the dissertation conclusion (see chapter 6) I discuss how these results contribute to our overall understanding of Folsom mobility in the San Luis Valley.

Spatial Data Woes

Before jumping into each of the major sections I will describe the state of the spatial data from Reddin and discuss how I use those data. In chapter 3, I reviewed the different field protocols undertaken by the Smithsonian and CSU research teams, which involved different ways of surveying, mapping, and collecting artifacts. The spatial data includes varying levels of precision and accuracy because of those different field efforts. Both research teams used either a transit or total station to piece-plot artifacts like chipped stone tools, producing horizontal errors of approximately one centimeter for each artifact. In contrast, the Smithsonian debitage sample includes provenience only at the block level (30 x 30 m sampling square) in the controlled survey grid – those items were not piece-plotted like tools. I also identified new chipped stone tool fragments in the debitage curation bags during my analysis. I can reasonably tie those new tools

to the same survey block as the debitage, but those do not retain a similar level of precision as most of the other tools. I also found a small number of chipped stone tools during analysis of the Smithsonian's excavation units in the pipeline right of way, and in analysis of CSU's small unit samples in Locality A (see chapter 3). In review, the different provenience levels include precise 2D coordinates for many tools, coarser cellular provenience for some tools, as well as variable provenience for debitage found within the survey blocks, excavation units, and intensive sampling units in Locality A.

Table 28. Summary of chipped stone tools and different levels of provenience based on field methods.

Lithic Sample	Piece Plot	Block Survey (30 x 30 m)	Excavated Cell (5 x 5 m)	Intensive Unit (1 x 1 m)	Missing Provenience	Total
Folsom Point	116	14	1	6	88 (39%)	225
Folsom Preform	51	2	0	0	57 (52%)	110
Folsom Channel	107	82	1	13	154 (43%)	357
Other Projectile	89	20	1	0	79 (42%)	189
Other Preform	3	0	1	0	10 (71%)	14
Biface	104	33	0	3	74 (35%)	214
Core	2	0	0	0	1 (33%)	3
Tested Cobble	0	1	0	0	0 (0%)	1
Retouched Flake	48	13	0	1	54 (47%)	116
Utilized Flake	23	1	1	0	20 (44%)	45
End Scraper	31	3	0	0	32 (48%)	66
Graver	10	2	0	1	21 (62%)	34
Drill	3	1	0	0	5 (56%)	9
Total	587	172	5	26	595 (43%)	1383

Includes data from Smithsonian and CSU teams

The total number of tools from the site and the total number of mapped objects with provenience (of any kind) do not add up. Table 28 shows the breakdown of the different provenience types for each tool class represented at Reddin, as well as my estimation of the missing provenience. This is the unfortunate outcome of misplaced field notes and artifact labels from the 1979 and 1983 field seasons. I estimate that roughly 43 percent of chipped stone tools (including conjoining fragments) are missing provenience. Within the Folsom component, this includes more than half of preform fragments (52%), 43 percent of channel flakes, and 39 percent of projectile points. The percentages of artifacts missing provenience scale similarly across all tool classes,

suggesting relatively little inherent sample bias between different tool types. The debitage sample consists exclusively of artifacts with provenience and is considered more representative than tools.

Does it matter that so much of the tool provenience is missing? In short, yes – it does matter. Given that all tool classes are similarly hampered by missing data, I assume that potential spatial patterns at Reddin are representative but not complete, and thus I focus my time looking at gradual trends in the data. In my primary analysis of spatial patterns discussed later, I make use of artifact density (a modeled representation of artifact intensity across the surface) to identify places at the site where certain types of artifacts seem to be significantly represented. I can begin to estimate those differences with gradual trends, but it is important to address the differences in the types of spatial provenience when estimating artifact density. Piece-plotted artifacts must be appropriately modeled alongside those with coarser provenience (e.g. survey blocks). Additionally, it is necessary to take account of sampling effects from the varying levels of survey intensity – so that variance in spatial patterns observed across the site are not simply the byproduct of the sample unit size and time spent surveying (e.g. intensive survey of 1 x 1 m units in Locality A).

As a point of departure in resolving the differences between provenience types, I created a routine in the statistical program R using the spatstat package (Baddeley et al. 2015; Baddeley and Turner 2013). The routine probabilistically simulates a hypothetical location of an artifact with missing piece-plot coordinates. This seemed a better option than reducing the resolution of tools with piece-plot precision down to the underlying cellular space of the survey grid. Why not try to improve the analytical capacity of less valuable data, instead? The routine I created is summarized by the following equation and graphically displayed in figure 51:

$$rjitter(i) = rmax \,/\, (\lambda(i) \cdot s + \epsilon)$$

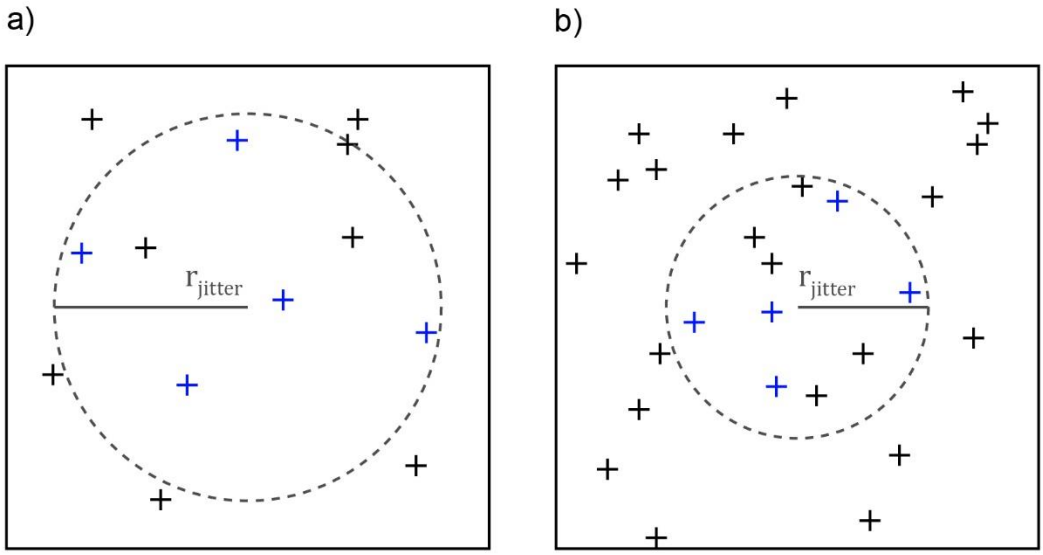


Figure 51. Schematic of the simulation routine used to randomly generate precise locations for artifacts with block-level survey provenience: a) potential simulation bandwidth based on a large value of rjitter, b) potential simulation bandwidth based on a lower value of rjitter. Simulated locations shown in blue.

In the routine, objects lacking precise coordinates (but containing block-level survey provenience) receive a random simulated point location. The potential simulated location is controlled by $rjitter(i)$, which is the radius of an ellipse inversely proportional to the modeled density of plotted artifacts $\lambda(i)$ at the center of the local survey block, cell, or unit. The value of $rjitter(i)$ is controlled by a maximum offset radius $rmax$, and a minimum offset from the center ϵ, adjusted by a scaling factor s, so that the objects always simulate away from the center, but never beyond the local survey block, cell, or unit. I use Scott's rule-of-thumb for kernel density bandwidth selection (Jones et al. 1996; Scott 1992, 2010), which adaptively models artifact density λ across the site. Scott's Rule follows the equation:

$$h_{Scott} = n^{-1/\mathrm{d}+4} \cdot \hat{\sigma} \cdot \sqrt{2\pi}$$

In the equation, the bandwidth of the kernel around each point is h_{Scott}. The size of the bandwidth is constrained by the number of data points in the point pattern followed by an exponent $n^{-1/\mathrm{d}+4}$, which adjusts for the number of dimensions in the data (two, in this case). These values

are multiplied by the standard deviation of the spread of the data $\hat{\sigma}$ based on the x and y coordinates, followed by the shape of the Gaussian kernel constant $\sqrt{2\pi}$. This method of bandwidth selection is applied in all of the following sections of this chapter when developing spatial statistical models relevant to each of the major questions. The method is widely applied in spatial statistics because it balances computing time, sample bias, sample variance, and produces KDE estimates which approximate gradual trends.

In sum, the simulation routine presented here produces new artifact coordinates probabilistically, based on the local density of artifacts with "good" provenience. If the observed local density is high, then the artifacts will simulate randomly but closer to the center of the local square. If the observed density is low, then the artifacts will simulate randomly and potentially further away from the center of the square. The effects of this routine are shown in figure 52, producing a more realistic plot of the total distribution of tools at the site, which is accurate though not precise. To be clear, this method does not falsely boost sample sizes in each location at the site – it simply uses local density as a predictive surface for simulating point locations for artifacts lacking precise coordinates in those same areas. The count of artifacts in each location remains the same even if the simulation routine is not applied. Figure 53 demonstrates that the effects of simulation in each square are minimal, with most survey blocks containing a single simulated artifact. In such cases, the spatial distribution in each square is random rather than clustered. I apply this simulation routine for the following sections of this chapter, but hereafter I do not model tools (or channel flakes) falling outside of the Smithsonian survey grid (n=42), or plotted items from CSU's Locality A intensive survey (n=26) due to the sample intensity bias issues that I previously described (see chapter 3). The total sample of plotted and simulated artifacts in the following sections includes 714 artifacts resting inside the Smithsonian grid.

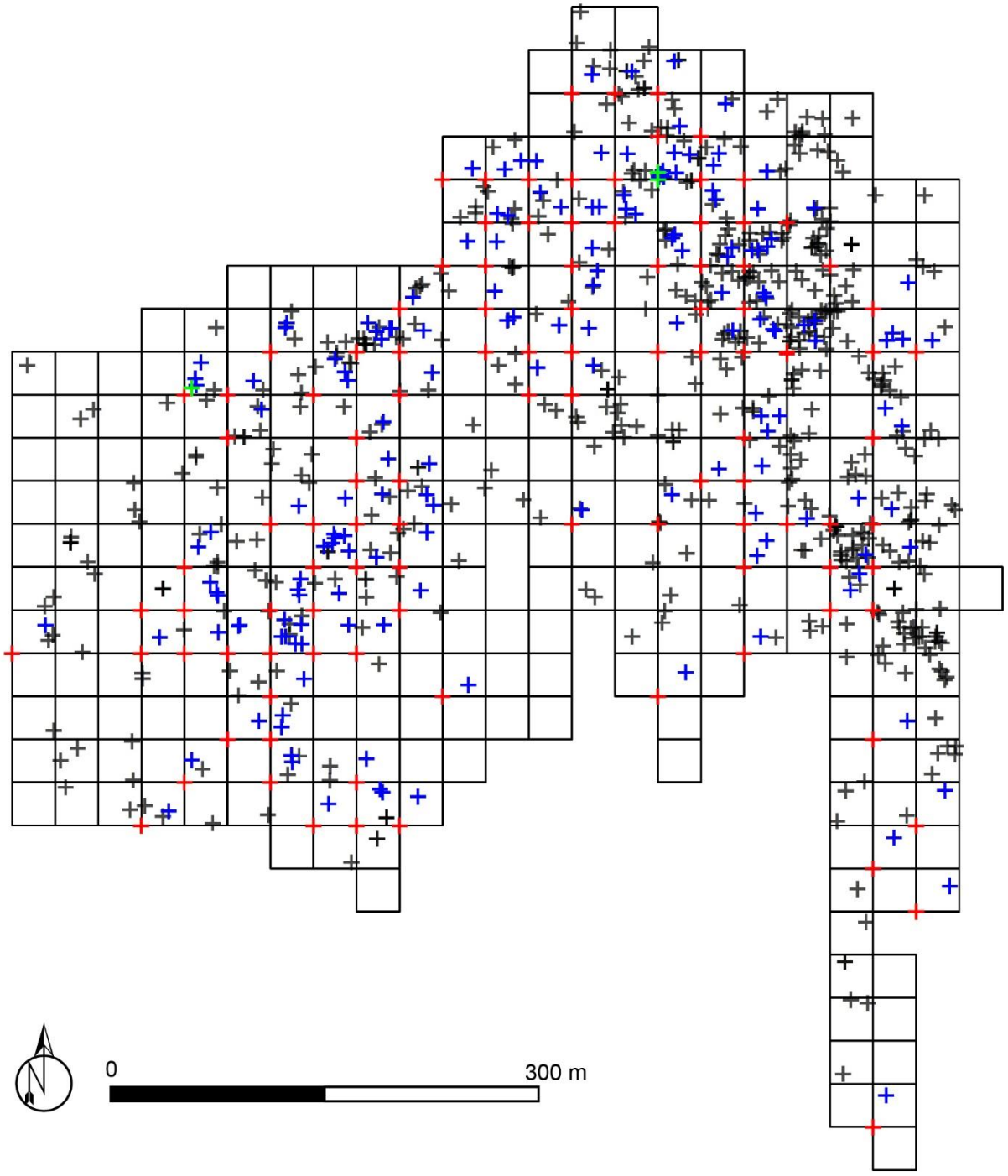


Figure 52. Summary plot of rjitter simulation routine for artifacts lacking precise coordinates, depicting objects with real piece-plot provenience used to model the intensity lambda (black, +), survey block corners with unmapped tools (red, +), excavation unit corners with unmapped tools (green, +), and all simulated locations of artifacts lacking original coordinates (blue, +).

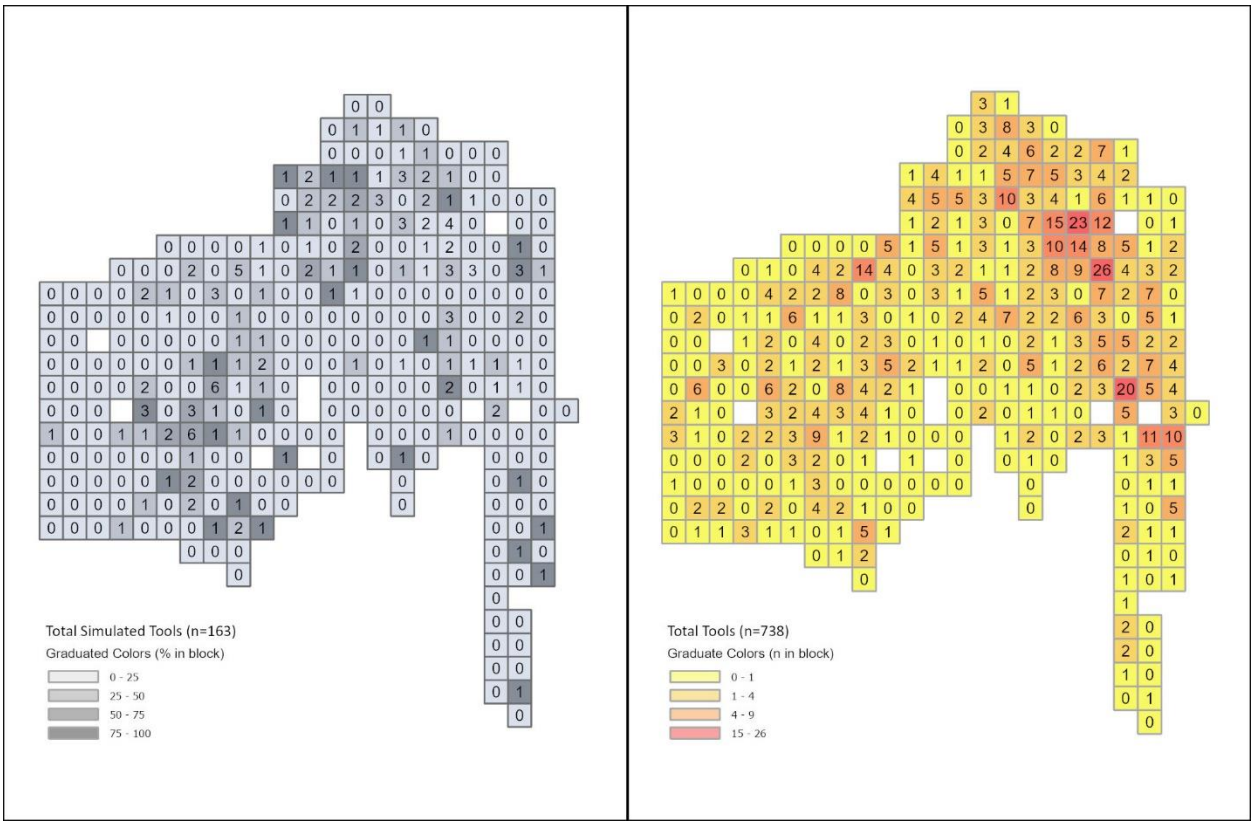


Figure 53. Summary figure showing the number and proportion of all simulated artifacts in each survey block (left panel) and total plotted artifact counts per survey block (right panel). The sample of simulated artifacts amounts to roughly 23% of the total sample.

Part 1: Finding Folsom

It should be clear that the Reddin site is a noisy surface scatter – there are hints of places with different artifact densities, but by and large, most of the site is littered with chipped stone debris. Finding the location of the Folsom component amidst the background noise is my task for this section of the chapter – and it begins with a discussion of how to see and understand spatial patterns across the broad scale of the site. I draw on some comparisons with the Folsom archaeological record to begin this conversation.

If you collapse the excavations from most Folsom campsites into just one contiguous area, most of those will fit comfortably within one of the survey blocks at Reddin (Andrews et al. 2008; Hofman 2002; Sellet 2013). This is especially true for sites representing a single contemporaneous

occupation. The Stewart's Cattle Guard site, likely a one-time aggregation of multiple hunter-gatherer bands – with its complex configurations of residential clusters, specialized hide-scraping areas, and bison processing zones – includes about 796 m^2 of excavation (Jodry 1992, 1999a, 1999b; Pelton 2018). Results from the analysis of the site suggest the occupation may have been relatively long term. Likewise, Locality B at the Barger Gulch site encompasses roughly 163 m^2 of excavation (roughly 50 m by 60 m wide) and contains at least four Folsom residential houses and at least six surface concentrations likely mirroring residences below ground (Surovell 2022; Surovell and Waguespack 2007). There is strong evidence in support of a single long-term occupation at Barger Gulch.

In a study by Andrews et al. (2008), the team observed that the Folsom record at large is composed of articulated multi-cluster sites representing single occupation events, but there is also a range of other possible spatial and temporal configurations. Sites like Lindenmeier and Mountaineer, 20 times and 40 times larger than Cattle Guard, are multi-cluster sites as well – but the distances between major excavation areas are vast; some of the largest Folsom sites have abundant material spread widely and disproportionally when compared to smaller sites. In this latter group, evidence for reoccupation seems to coincide neatly with larger site boundaries as well as long distances between artifact concentrations (Andrews et al. 2008:469-473). The study by Andrews et al. (2008) models the overall breadth of sites as well as the local configuration of activity areas, providing informative prior information for comparing complex spatial patterns at Reddin. Large sites with widely spaced occupation zones generally contain evidence of reoccupation, whereas smaller sites with closely articulated debris patterns often represent single occupations (figure 54). It is thus prudent to try and determine whether there are multiple Folsom artifact concentrations at Reddin, and whether those are spatially contiguous, or not.

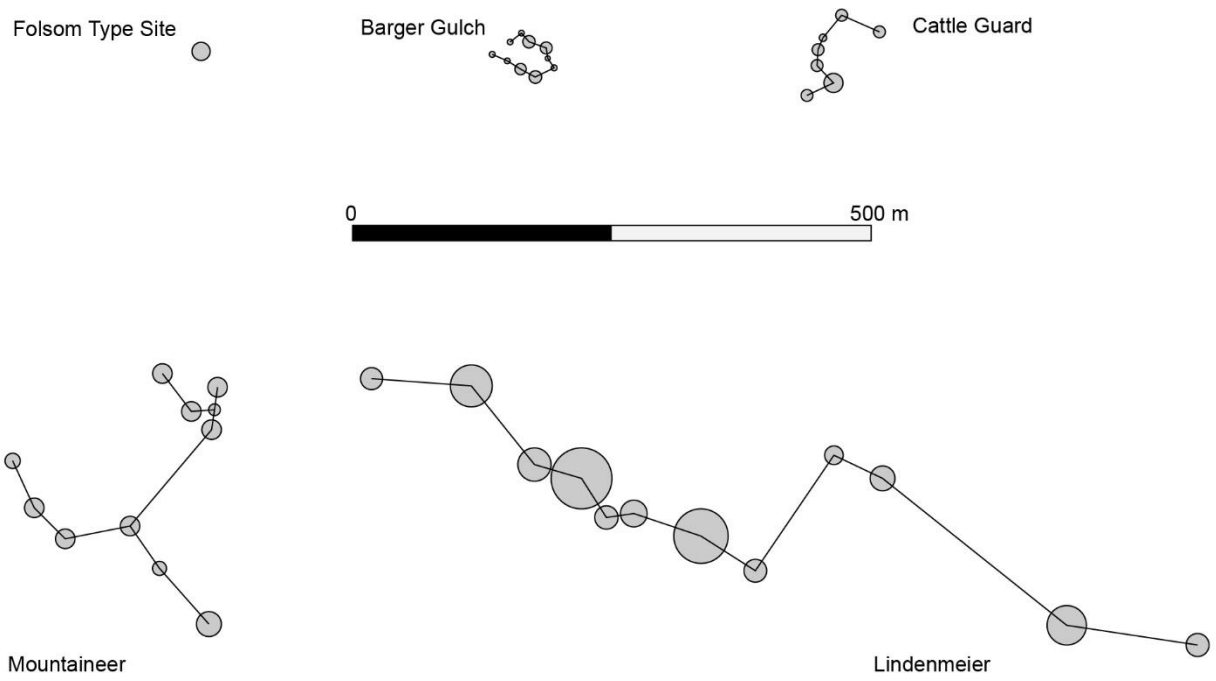


Figure 54. Generalized depiction of major artifact concentrations and intercluster distances at a sample of single occupation Folsom sites (top row) and multiple occupation Folsom campsites (bottom row).

The indirect implication of the multi-scalar study by Andrews et al. (2008) is that there is a relationship between the spatial scale of observation and the emergence of complex temporal patterns. As the spatial scale of observations grows to encompass larger sites, there is an opportunity to detect non-contemporaneous archaeological debris that accumulated over longer time frames. Likewise, shrinking the breadth of your spatial perspective brings local patterns into focus that formed over shorter timescales (Bailey 2007; Holdaway and Wandsnider 2008; Hull 2005). Currently, Folsom archaeologists are better equipped to explain spatial patterns at localized spatial scales because those patterns match the analogies we build from the ethnographic record – think of the hearth-centered spaces, houses, lithic workshops, middens, or other well-known activity areas that we commonly try to identify. In contrast, we have little to no vocabulary to explain the meaning behind a spatial pattern that is several factors bigger than most activity areas,

or even entire sites. How do these issues affect the analysis of the Reddin site? For one, it is difficult to trust that there is meaning behind spatial patterns observed across a site so large. Artifact density at Reddin is not controlled locally within excavation units, concentrations may bleed from one to the next over time, and multiple time frames of accumulation may be present. This is generally the reason that archaeologists ignore surface scatters in favor of spatially controlled excavations. But perspective is key – and Folsom is an archaeologically messy tradition.

Some types of actions conducted over shorter time frames leave a spatial blueprint so dense they are likely to persist through the accumulation of archaeological noise over time, and I refer to these as residual processes. In figure 55a, assume the aftermath of an occupation where the inhabitants focused on the intensive manufacture and maintenance of a lithic toolkit. In one timestep after this initial event (figure 55b), materials from the scatter have diffused somewhat and debris from a new but less intensive occupation has fallen into the same context. The diffusion rates over the next several timesteps change with varying intensity at each step, until at the last timestep both spatial patterns take up much of the observation window and it is difficult to parse the original pattern from the overlying noise. But now imagine that the observation window expands, and your perspective shifts outward – doing so brings the original point pattern back into focus, where much of the artifact density is driven by that initial residual process. Interpoint relationships diffuse overtime in this hypothetical model, but correlation across the point pattern remains intact – albeit at a different spatial scale. For residual processes in surface scatter contexts, expanding the horizon of spatial observation refocuses residual processes and draws out the intensity of the original context (figure 56). Excavated sites may include more precise and intact spatial patterns than surface scatters, but surface scatters afford the opportunity to move between different spatial scales during analysis to refocus on the underlying processes, if needed.

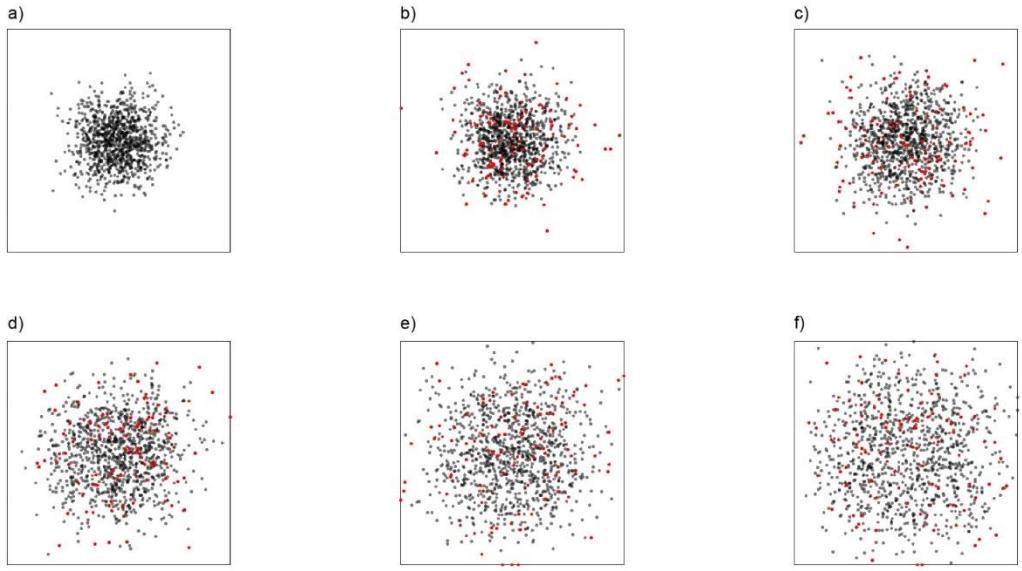


Figure 55. Simulated realizations of archaeological debris patterns diffused over sequential timesteps (a-b). The pattern in black represents an intensive residual process as described in text, and the pattern in red represents debris from a second less-intense occupation. Diffusion rates vary randomly at each timestep.

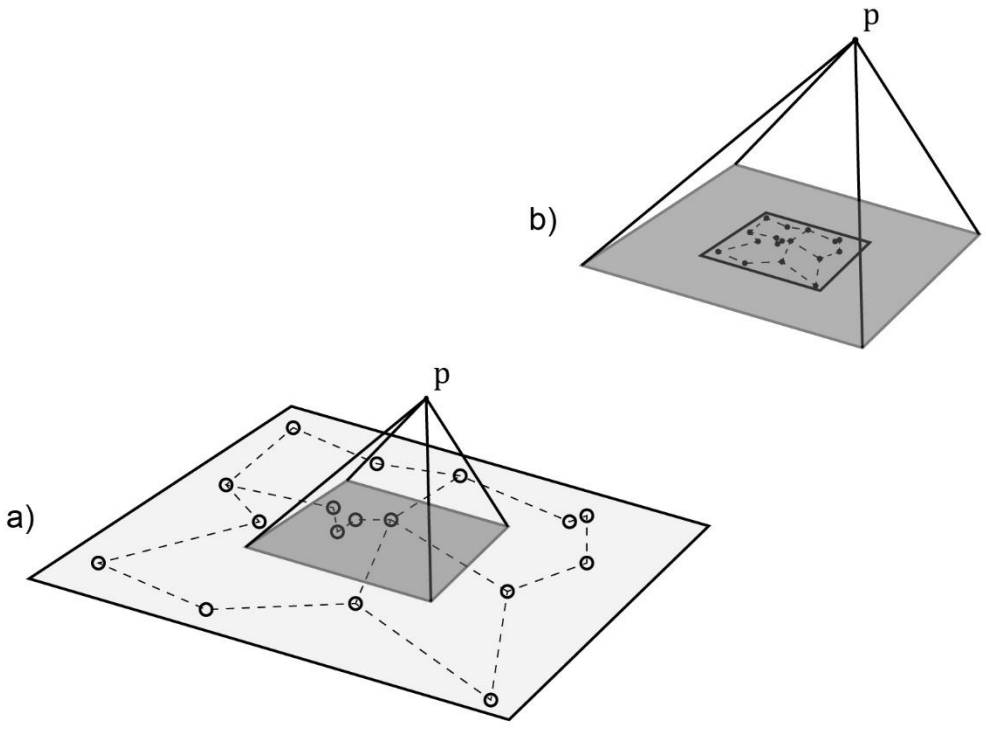


Figure 56. Effects of changing perspective on spatial interpretations, including a) fine-grained perspective (p) on a diffused process, and b) broad-perspective (p) on the diffused process.

Methods

It should be clear that simply plotting the location of all Folsom artifacts will not suffice for detecting the core of the Folsom component at Reddin. Sites may be composed of ephemeral and residual artifact discard patterns that mirror the intensity in the use of space over a given time frame in the past. Focusing on the most residual processes is necessary to answer the main questions of this chapter, which have to do with the amount of time spent at the site (the inverse of residential mobility) as well as the issue of contemporaneity. The best places to detect evidence supporting those main topics include occupation centers or campsites, where people in the past likely spent most of their time and left a more residual footprint of their occupation.

Here I define *camp shatter* as diagnostic Folsom artifacts likely to appear in the primary zones of Folsom habitation. This category includes broken projectile point preforms and channel flake fragments, encompassing the waste byproducts of the new weapon manufacture process, but I also include broken projectile point bases. Other researchers have demonstrated a spatial relationship between preforms and channel flakes within sites (Andrews et al. 2021; Jodry 1999a; Sellet 2004, 2013; Stiger 2006; Surovell 2022), given they are both components of successful and unsuccessful attempts at fluting new points (see chapter 4). Researchers have also shown a relationship between those artifacts and areas within campsites where people spent significant downtime, such as the interior spaces of houses and hearth-centered activity areas (Andrews et al. 2021; Pelton et al. 2016; Stiger 2006; Surovell 2022). The presence of projectile point bases, as opposed to other broken portions of fluted points, represents a related signal of the toolkit maintenance process. Folsom hunters transported broken darts back into campsites after using their weapon tips further afield; the broken bases (fluted or unfluted) were transported while still lodged in the hafts of dart foreshafts and then discarded in camp upon return (Hofman 1999; Hofman et

al. 1990). Thus, the camp shatter category of artifacts represents the manufacture and replacement of fluted or unfluted Folsom dart tips, an activity which may have occurred commonly near living spaces based on comparative research. In this sense, *shatter* refers to the specific pieces of artifacts commonly found in campsite settings – rather than non-flake debitage as commonly used in lithic technology literature (e.g. Andrefsky 2006).

It is tempting to include non-diagnostic artifacts like end scrapers, gravers, and other specialized retouched flake tools into this schema, given that these also commonly appear in single component Folsom campsites and in domestic spaces. However, post-Folsom occupants may have conducted similar tasks in potentially different areas of the site. The inclusion of these other artifact types might dissolve the utility of the camp shatter category for detecting Folsom-specific areas.

There are now many methods for detecting concentrations of artifacts quantitatively, and Folsom researchers maintain a long history of using statistical techniques for doing so (Jayalath et al. 2015; Jodry 1999a; Surovell and Waguespack 2007). An exploration of the data using kernel density estimation (KDE) is a common first step in detecting gradual trends of clustered and dispersed artifacts across a study area, but the interpretation of significant areas is generally subjective (Ruppert and Cline 1994). Figure 57 shows how one might begin to detect those broad trends in the distribution of Folsom artifacts at Reddin – which shows a clear pattern of inhomogeneity (non-uniform intensity) in the data and varying density across the study region. It is a little more difficult to draw fixed lines around artifact concentrations, and the task typically involves a long list of assumptions. In most cases, researchers compare the observed artifact distributions with a null model of some kind. Complete Spatial Randomness, a uniform Poisson process, is perhaps the most common null model that researchers use (Bevan and Conolly 2009; Harvey et al. 1983; Kulldorff 2006; Ricotta 2007). For instance, a uniform Poisson process is the

implied null model in the k-means clustering algorithm used to detect residential areas at Cattle Guard (Jodry 1999a:285), in the Chi-square tests of burned artifacts in the hearth-centered spaces at Barger Gulch (Surovell and Waguespack 2007), as well as the clustering of large rocks making up the outline of houses at the Mountaineer site (Jayalath 2013; Jayalath et al. 2015).

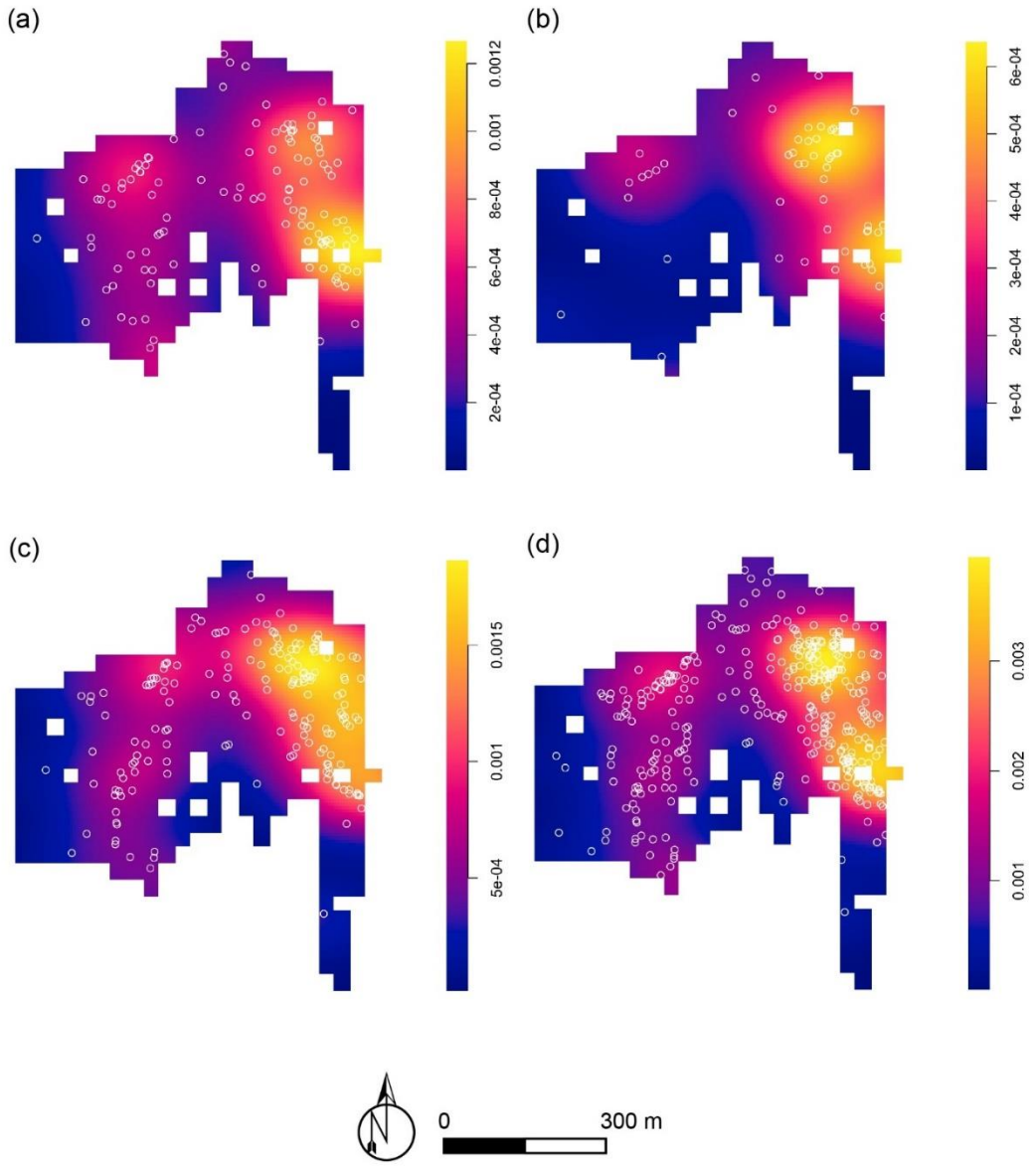


Figure 57. Kernel density plots of Folsom artifacts using Scott's Rule for adaptive bandwidths, showing projectile points (a), preforms (b), channel flakes (c), and the combined dataset (d).

Complete Spatial Randomness assumes that the magnitude of variance is equal in all directions. This type of unbiased null model is appropriate when dealing with excavations, where sampling methods are directly tied to positive artifact counts in units and null values are limited. I argue here that uniform randomness is a poor choice for a null model in the analysis of a surface scatter like Reddin, where the survey and sampling strategies encompass an entire landscape along with underlying environmental covariates that condition site selection choices. People choose to occupy ideal settings in landscapes and avoid less hospitable places – such as the bottom of a playa or the middle of a floodplain. Those ideal environmental settings are likely time-dependent in a place like the Closed Basin, perhaps due to seasonal resource distributions such as fresh water, vegetation, slope, sunlight, visibility, and any other number of factors. It is thus more appropriate to use an inhomogeneous Poisson process (non-uniform intensity) as a null model (Harvey et al. 1983; Kulldorff 2006), one that accounts for first-order effects on all spatial processes at the site. Figure 58 shows the difference between a simulated random spatial pattern with uniform intensity and simulated randomness based on the inhomogeneous distribution of all Folsom artifacts. By using an inhomogeneous Poisson null model, it is possible to measure significantly clustered areas of camp shatter within the overall distribution of Folsom artifacts at the site. This null model assumes that there is patterning of Folsom debris at Reddin because of underlying factors driving overall site selection and occupation intensity.

I use a quadrat goodness-of-fit test of the inhomogeneous Poisson model implemented in R with the spatstat package (Baddeley et al. 2015; Baddeley and Turner 2013; Cressie and Read 1984), which simply counts the number of camp shatter artifacts in equally sized tiles across the study area and compares those counts to the spatially varying expectation of artifact counts based on the null model. Figure 59 shows the premise of the inhomogeneous quadrat test and how it

differs from a typical quadrat test of Complete Spatial Randomness. For my analysis, the quadrat tiles include the survey blocks in the original grid which are known to contain debitage collections (see chapter 3) – a sample of 314 survey block squares. The sample of camp shatter artifacts includes 277 total pieces, comprised of 48 fluted and unfluted point bases, 51 preforms, and 178 channel flakes – these represent the sample of artifacts contained within the 314 tiles, exclusive of artifacts those falling outside of the collection area. The result of the test produces a global Chi-square statistic (X^2) and p-value summarizing the goodness-of-fit between the observed spatial distribution of camp shatter and the null model. I use Monte Carlo simulations (n=1000) of the inhomogeneous Poisson process to account for the low number of expected values, so the p-value is a comparison of the X^2 and the cumulative values of simulation. At a local scale, I calculate standard residuals of the goodness-of-fit test in each of the quadrat tiles. I use an absolute value threshold of 1.96 to distinguish individual tiles in the analysis which deviate significantly from the goodness-of-fit test, indicating significantly higher (or lower) counts of camp shatter artifacts than expected under the null hypothesis. Table 29 summarizes the null and alternative hypotheses of the model and how the potential results of the test relate to questions under consideration in this chapter. If the test fails to reject the null model (NH1), then there is no significant clustering in the data at a global scale – alternatively, camp shatter artifacts are significantly clustered when compared to the overall pattern (AH1). On a local scale, individual tiles may or may not be significantly clustered when viewed independently of the global goodness-of-fit result. If Reddin is a site with one significant concentration of camp shatter artifacts (NH2), then all positively significant tiles with high standard residuals will be contiguous and share all edges, corners, or a combination. Alternatively, if Reddin is a large multi-cluster site then the sample of positively

significant tiles will occur in groups that do not share edges and corners – gaps between significant tiles will be present (AH2).

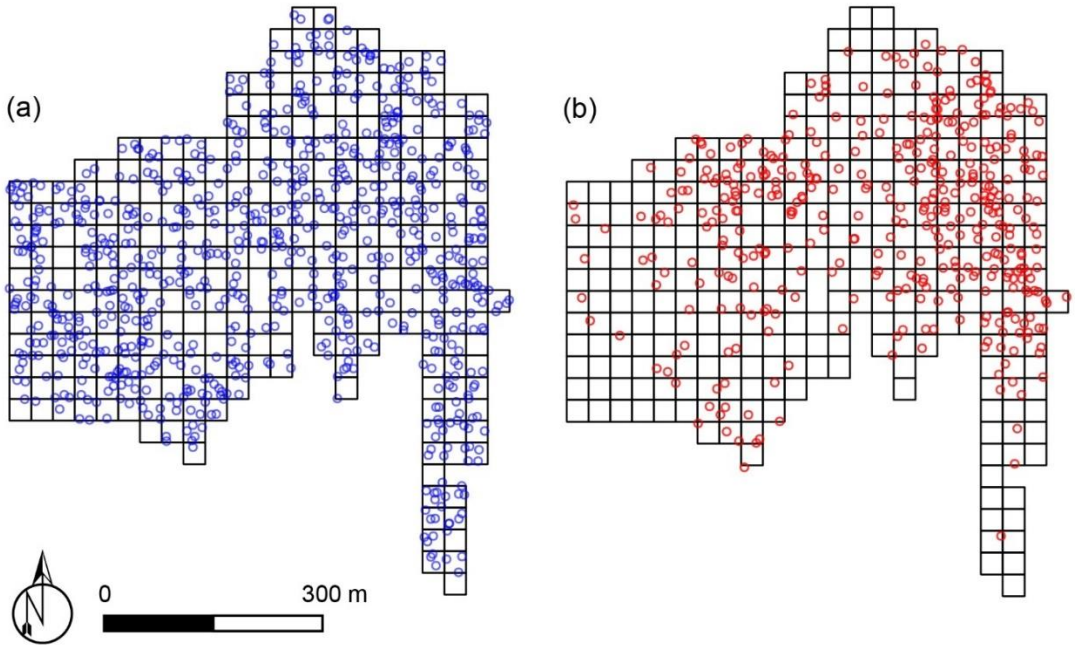


Figure 58. Simulated realizations of a uniform point pattern representing Complete Spatial Randomness (a), and a simulation of an inhomogeneous Poisson process with the same intensity as all Folsom artifacts at Reddin.

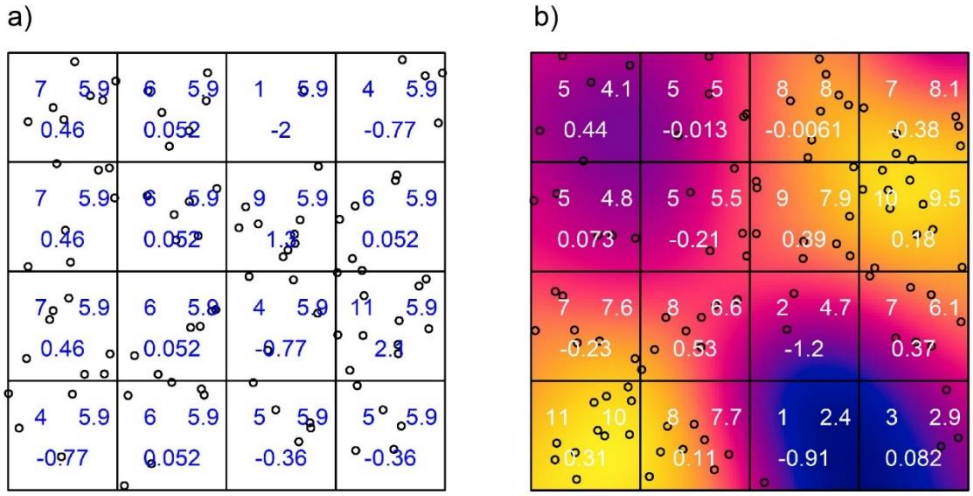


Figure 59. Hypothetical demonstration of quadrat test goodness-of-fit method, showing observed counts (upper left in cell), expected counts (upper right in cell), and residuals (low center in cell). The image on the left depicts a test of Complete Spatial Randomness with uniform variance in expected counts (a). The image on the right depicts the quadrat expectations under the assumption of an inhomogeneous Poisson process using the variable density of all artifacts.

Table 29. Summary of quadrat test null and alternative hypotheses, including expectation, potential results, and outcomes for interpretation.

Global Quadrat Test

Hypothesis Description	Expectation	Result	Conclusion
Null Model (NH1): The spatial distribution of Folsom camp shatter (point bases, preforms, channel flakes) follows the same modeled intensity pattern of all Folsom artifacts at the site.	The observed counts of camp shatter artifacts will not significantly deviate from expected counts under the assumption of the inhomogeneous Poisson process.	Simulated Chi-Square statistic from Monte Carlo simulations (n=1000) of the inhomogeneous Poisson process.	If the p-value > 0.05, fail to reject the null hypothesis: the observed Folsom camp shatter distribution approximates the inhomogeneous Poisson process, and there is no significant clustering.
Alternative Hypothesis (AH1): Folsom camp shatter is significantly clustered and does not follow the same modeled intensity of all Folsom artifacts at the site.	The distribution of Folsom camp shatter is expected to deviate from the inhomogeneous Poisson process, showing significant clustering. The observed counts will significantly exceed the expected counts of camp shatter artifacts.	Simulated Chi-Square statistic from Monte Carlo simulations (n=1000) of the inhomogeneous Poisson process.	If the p-value < 0.05, reject the null hypothesis: the Folsom camp shatter distribution is significantly clustered, indicating that it does not follow the expected inhomogeneous Poisson model.

Local Quadrat Test

Hypothesis Description	Expectation	Result	Conclusion
Null Model (NH2): There is only one significant concentration of Folsom camp shatter at the site – Folsom camp debris is restricted to a single area	Quadrats with higher-than-expected counts of Folsom camp shatter artifacts are located in one contiguous area (sharing all edges and corners of quadrat spaces)	Standard residuals in each quadrat based on the observed and expected counts of Folsom camp shatter, assuming the inhomogeneous Poisson process of Folsom artifact intensity	If the sample of quadrats with standard residuals > 1.96 share sides and corners with no gaps, fail to reject the null hypothesis: the observed distribution of quadrats with higher-than-expected counts of Folsom camp shatter are clustered in a single area.
Alternative Hypothesis (AH2): There are multiple significant concentrations of Folsom camp shatter at the site – Folsom camp debris extends beyond a single occupation center.	Quadrats with higher-than-expected counts of Folsom camp shatter artifacts are found in more than one contiguous area, with multiple quadrats lacking shared edges or corners	Standard residuals in each quadrat based on the observed and expected counts of Folsom camp shatter, assuming the inhomogeneous Poisson process of Folsom artifact intensity	If the sample of quadrats with standard residuals > 1.96 does not share all sides and corners and there are gaps present, reject the null hypothesis: the observed distribution of quadrats with higher-than-expected counts of Folsom camp shatter are clustered in multiple areas.

Results

The calculated X^2 (494.36) and p-value (0.002) of the global goodness-of-fit test reject the null model (NH1) in favor of the alternative hypothesis (AH1). The observed distribution of camp shatter at the Reddin site is significantly clustered when compared to the inhomogeneous Poisson process representing the intensity of all Folsom artifacts. On a more local level, the results of the test reveal 14 independent groups of tiles with significantly higher counts of camp shatter than expected. Therefore, I reject the second null model (NH2) in favor of the alternative hypothesis (AH2). Reddin is a large multi-cluster site with multiple occupation centers or campsites.

Figure 60 illustrates the results of the quadrat test and highlights the distribution of those spatially independent areas containing higher than expected quantities of camp shatter. In figure 61, I label and name these concentrations for reference. I consider adjacent quadrat tiles as part of one cluster unit (Localities A though D), and any discontinuous tiles as their own cluster units (F1-F10, meaning "Folsom" 1 through 10). One of those cluster units includes several of the survey blocks selected for CSU's Locality A surveys – so I keep that original reference name. The artifact concentrations range in size, encompassing a single quadrat tile (900 m^2) to as many as five connecting tiles (4500 m^2) based on shared edges and corners. Likewise, the observed counts of artifacts in each tile varies (tables 30 and 31). How can one survey block with a single preform, channel flake, or point base represent a significant concentration? Well, if there are no Folsom artifacts in the vicinity of those low-density tiles, they will contain more camp shatter pieces than expected under the assumptions of the null model. The presence of campsites within Reddin is not a simple byproduct of the overall size of concentrations or the specific number of artifacts in them, but by their deviation from the overall pattern.

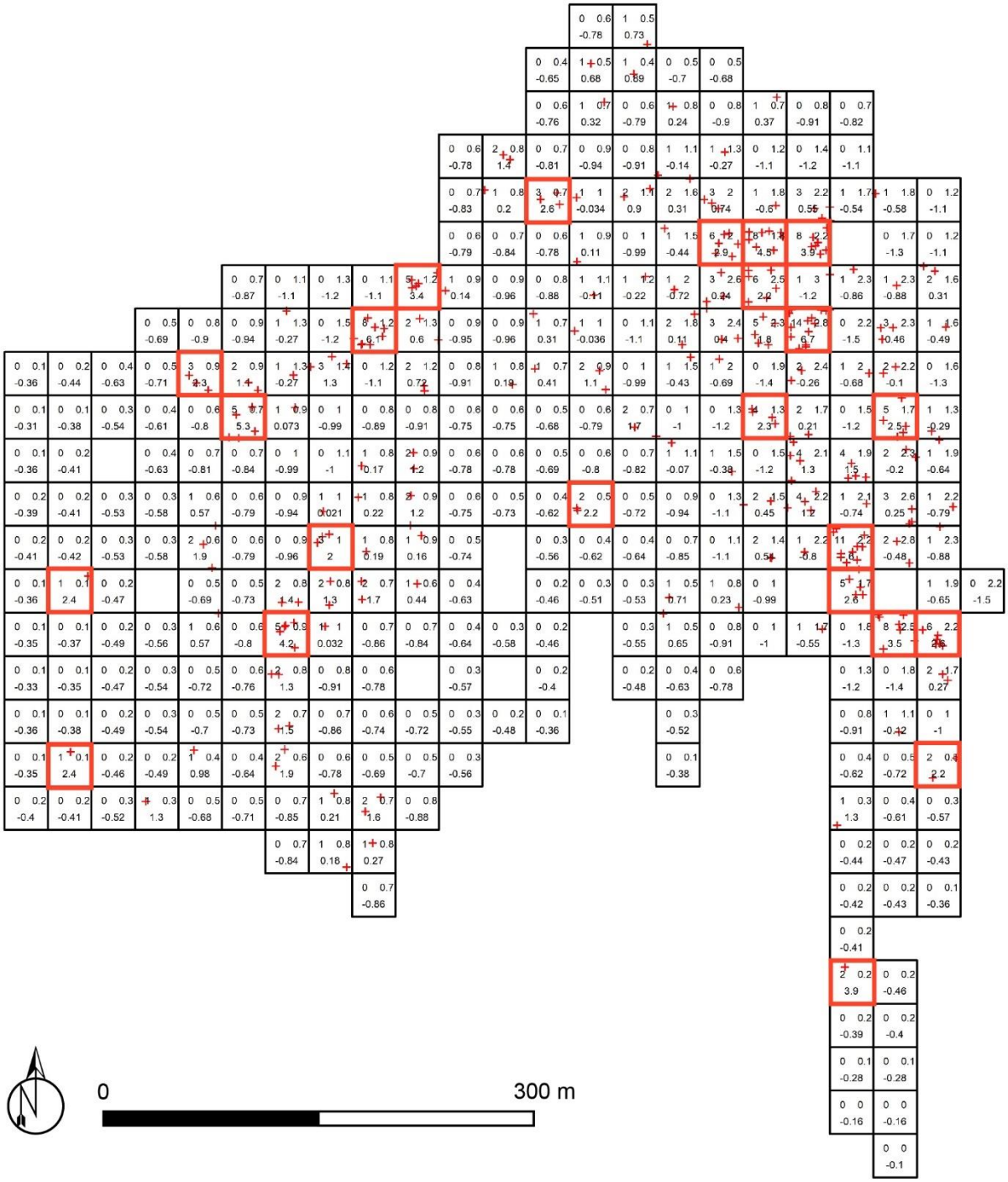


Figure 60. Modeled results of the goodness-of-fit test of the inhomogeneous Poisson process for Folsom camp shatter artifacts. Local quadrat tiles with standard residuals above 1.96 represent camp clusters (outlined in red).

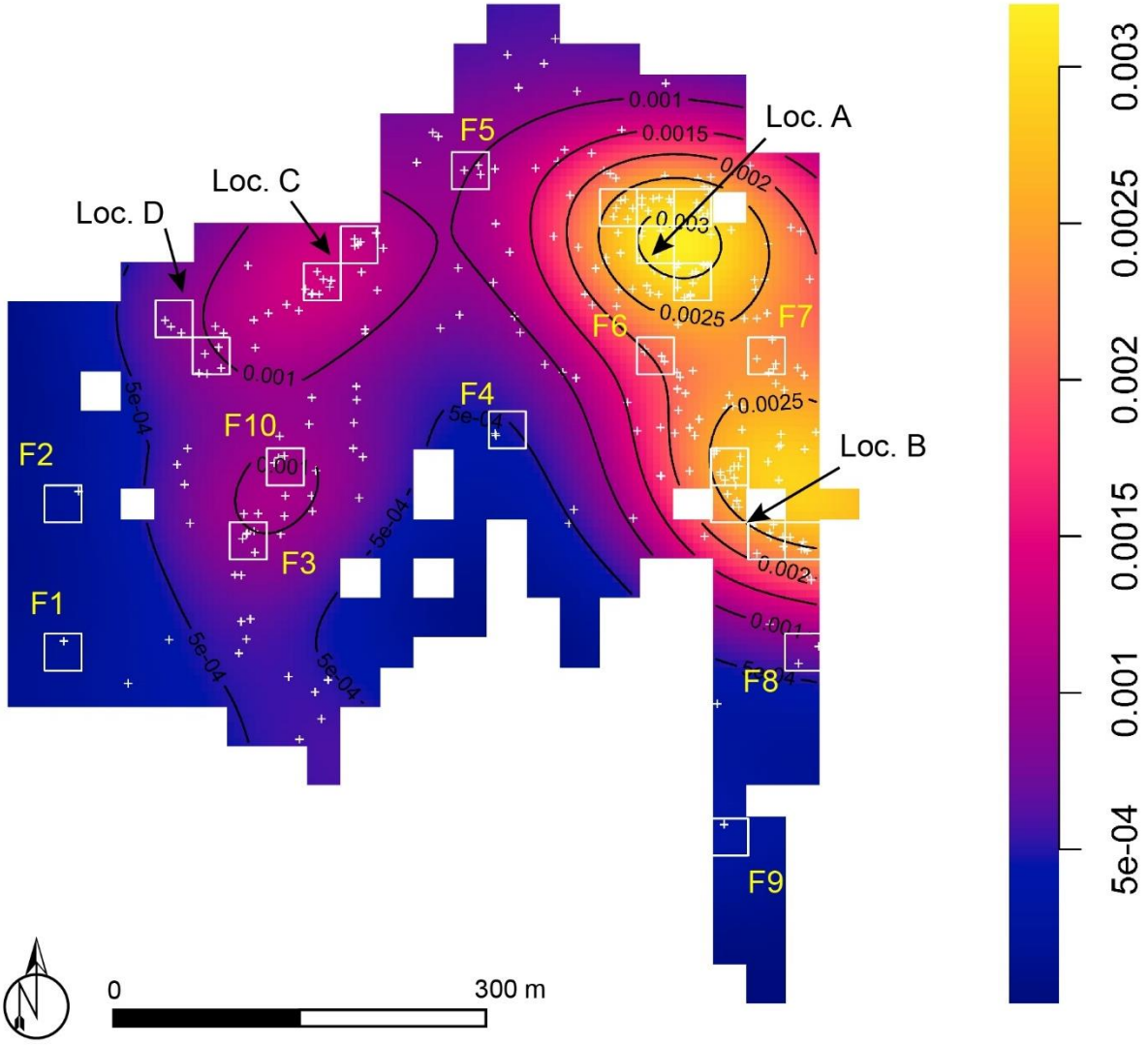


Figure 61. Kernel density map showing distribution of camp shatter artifacts (white crosses) and significant quadrat tiles from the goodness-of-fit test. Individual concentrations labeled for reference. Adaptive bandwidth selection based on Scott's Rule.

Table 30. Tool summary data for clusters identified using the inhomogeneous goodness-of-fit test in quadrat tiles.

Cluster Name	Size (m^2)	Points	Preforms	Channels	Flake Tools	Bifaces	≤150 km Items	≤300 km Items	≥300 km Items
Locality A	4500	15	11	35	12	16	65	6	10
Locality B	3600	13	3	18	4	6	34	3	7
Locality C	1800	4	1	11	2	1	17	0	2
Locality D	1800	4	1	4	1	0	8	0	2
F1	900	0	1	0	0	0	1	0	0

Cluster Name	Size (m^2)	Points	Preforms	Channels	Flake Tools	Bifaces	≤150 km Items	≤300 km Items	≥300 km Items
F2	900	0	0	1	0	0	1	0	0
F3	900	1	0	4	2	1	5	1	2
F4	900	0	0	2	0	0	1	0	1
F5	900	0	1	2	0	0	2	0	0
F6	900	2	0	2	0	1	2	0	2
F7	900	0	0	5	0	0	5	0	0
F8	900	1	1	0	2	0	3	0	0
F9	900	0	0	2	0	0	2	0	0
F10	900	0	0	3	1	2	4	2	1

Items – includes tools and channel flakes, but not general debitage

Table 31. Debitage summary data for camp clusters identified using the inhomogeneous goodness-of-fit test in quadrat tiles.

Cluster Name	Total Debitage	≤150 km Debitage	≤300 km Debitage	≥300 km Debitage	Complete Flakes	Cortical Debitage
Locality A	2176	1846	277	52	258	7
Locality B	418	399	11	8	33	1
Locality C	508	458	37	13	14	3
Locality D	395	365	21	9	20	1
F1	17	17	0	0	0	0
F2	45	29	16	0	3	1
F3	180	97	78	5	10	0
F4	32	19	3	10	2	0
F5	249	201	41	5	7	8
F6	193	176	14	3	20	0
F7	152	136	16	0	15	1
F8	51	51	0	0	9	0
F9	11	6	5	0	3	0
F10	232	182	47	3	14	0

Cluster Sensitivity Analysis

The analysis detected a total of 23 significant quadrat tiles containing higher-than-expected counts of camp shatter artifacts. These tiles are distributed among 14 different clusters which collectively make up 16 percent of all tiles containing Folsom artifacts (23 out of 146 quadrat tiles). Thus, diagnostic Folsom material encompasses about half of the spatial distribution of the entire site (46% of 314 quadrat tiles), and clustered Folsom camp shatter takes up significantly less than that – around 7 percent of the site. From a classical statistics perspective, the low overall quantity of significant tiles in this test introduces some concern about the detection of random spatial clustering in the data – and thus a resampling procedure is warranted. I approached this task in two ways. I first explored the effects of local sample size and density on model outputs by using randomized resampling and thinning of the camp shatter dataset. I then experimented with the

effects of kernel bandwidth selection on model outputs by varying fixed bandwidths in the kernel smoothing of the null model, which influences expected counts in quadrat tiles.

In the first sensitivity test, I resampled and randomly thinned the camp shatter dataset and completed the same quadrat goodness-of-fit test as described in the previous section. I randomly retained a proportion of the original camp shatter data to test whether the original cluster patterns persisted after reducing local density and introducing random noise to the pattern. I completed the test 10 times for six different levels of data retention – including goodness-of-fit tests at 75 percent retention (thinned by 25%), 80 percent retention, 85 percent retention, 90 percent retention, 95 percent retention, and again without any random thinning. I used a set of four metrics to evaluate the effects of random thinning on the cluster model outputs. The metrics included p-values of the global goodness-of-fit test for each simulation run, the number of observed significant cluster tiles, the mean standard residuals observed in cluster tiles, and the mean intercluster distance observed between all cluster tiles (calculated from the centroid of tile squares). Table 32 provides a synthesis of the results which summarize the variance of the resampling procedure, and figures 62 and 63 review the implementation of the simulation runs.

This sensitivity analysis confirmed that the original data are robust to random thinning and that underlying spatial structure in the camp shatter dataset drives deviations from the null model, rather than random chance or the location of specific artifacts in the model. Mean values across each metric varied subtly, except for calculated p-values for the global goodness-of-fit test, which exhibited variance between 75 percent and 90 percent data retention. The number of detected clusters, standard residuals, and mean intercluster distances remained consistent across thinning intervals – with limited variation in the mean and standard deviation for these metrics (table 32).

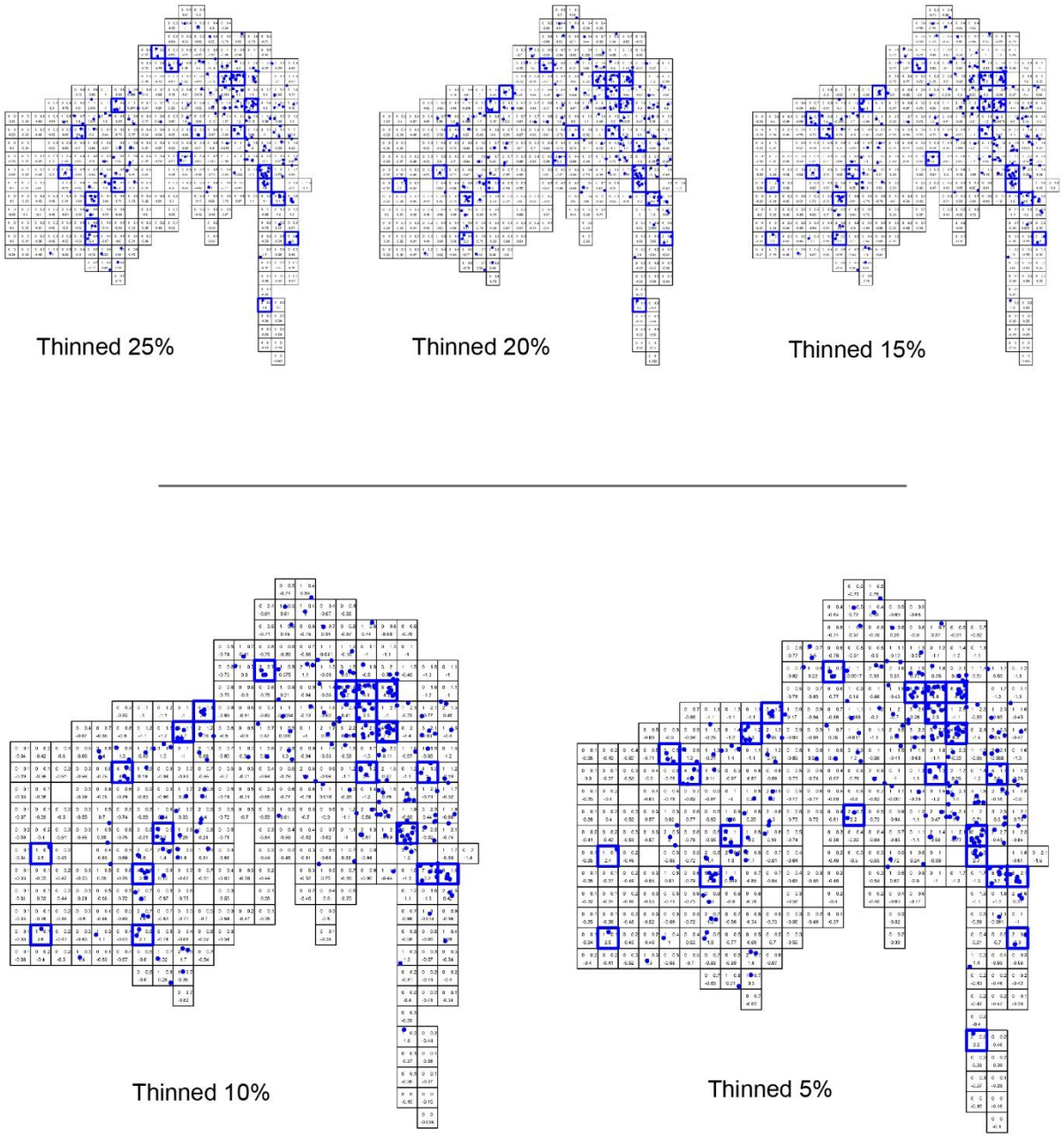


Figure 62. Examples of simulation results for a single run of random thinning in the camp shatter dataset – for intervals at 25% random thinning (0.75), 20% thinning (0.80), 15% thinning (0.85), 10% thinning (0.90), and 5% thinning (0.95). Note the consistency between original results and the 5% thinning interval.

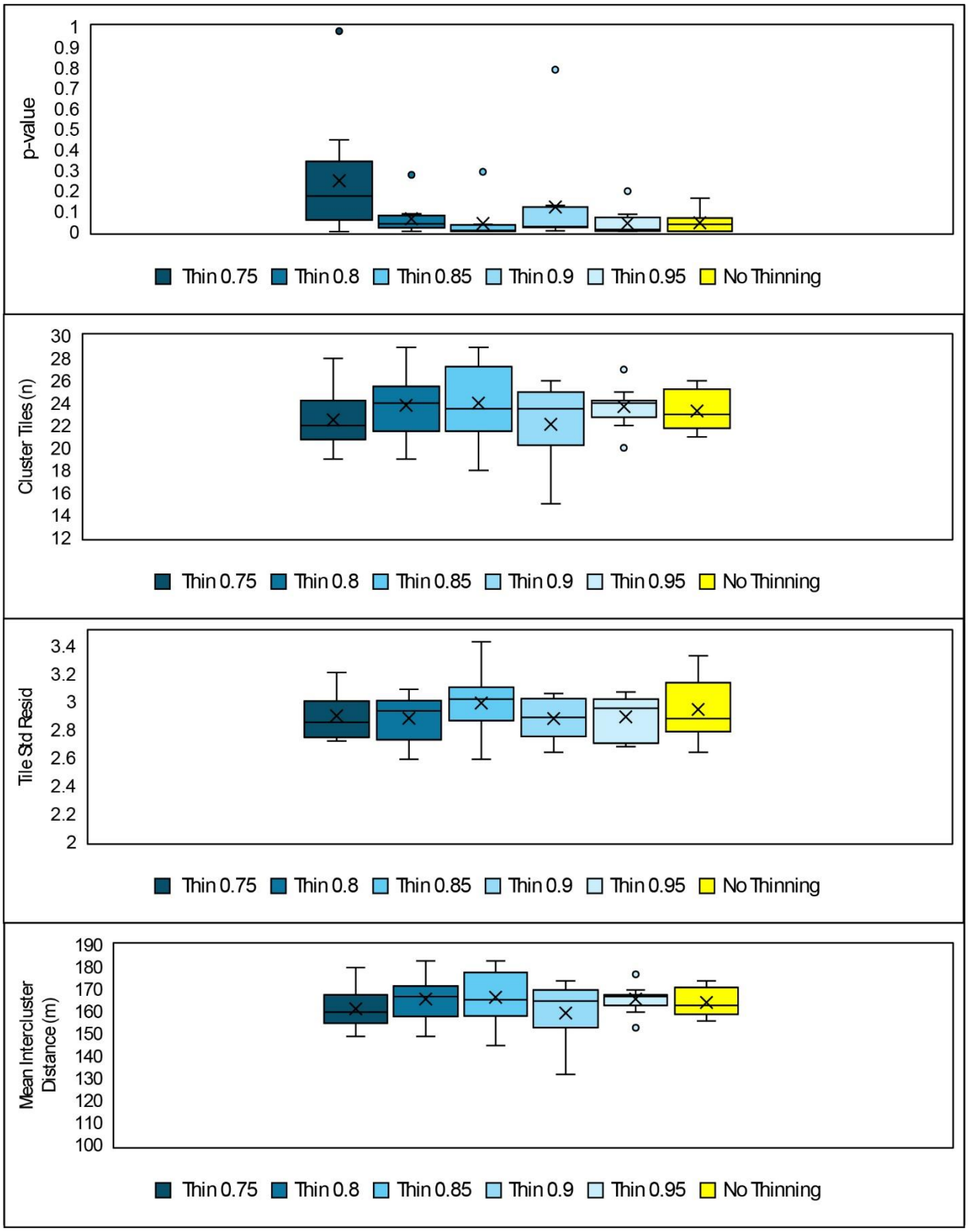


Figure 63. Four-panel box plots summarizing 10 simulations of the random thinning sensitivity analysis across each of six iterations in random thinning – including 75% data retention (thinned by 25%), 80% retention, 85% retention, 90% retention, 95% retention, and no thinning.

Table 32. Summary results of the random thinning resampling analysis on cluster detection.

Thinning Iteration	Number of Simulations	Mean p-value (SD)	Mean Cluster Tiles n (SD)	Mean Cluster Standard Residual (SD)	Average Mean Intercluster Distance m (SD)
0.75 (25% thin)	10	0.161(0.13)	22.5(2.5)	2.9(0.2)	161.7(9.3)
0.80 (20% thin)	10	0.072(0.07)	23.8(3.0)	2.8(0.2)	166.3(10.5)
0.85 (15% thin)	10	0.040(0.08)	24.0(3.5)	2.9(0.2)	166.8(12.4)
0.90 (10% thin)	10	0.121(0.24)	22.1(3.9)	2.8(0.1)	159.2(15.2)
0.95 (5% thin)	10	0.040(0.06)	23.7(1.9)	2.9(0.2)	166.3(6.4)
No thinning	10	0.050(0.05)	23.3(1.9)	2.9(0.2)	164.7(6.6)

Kernel density bandwidth selection is a known issue in spatial statistical analysis (Scott 1992, 2010; Sheather and Jones 1991), as different bandwidths yield different density estimates that may overly smooth local clusters or instead fail to detect broad-scale cluster arrangements. I tested the sensitivity of kernel bandwidth selection on the model outputs by varying the fixed distance of bandwidths in the calculation of the null model – representing the inhomogeneous Poisson process of all Folsom artifacts. In the original model I applied Scott's Rule to the null model which optimizes kernel bandwidths based on site-wide variance. The purpose of this sensitivity analysis was to examine the effects of varying bandwidths on artifact density estimates, which are used in calculation of the inhomogeneous null model and expected values for each quadrat tile. I varied bandwidths at 5 m intervals for 10 simulation runs each, beginning at 5 m and ending at 100 m, for a total of 20 different iterations of kernel bandwidths and 200 simulations. I explored the same model metrics for this test as I did for the previous sensitivity analysis – which included calculated p-values of the global goodness-of-fit test, the number of detected cluster tiles, the standard residuals of the cluster tiles, and the mean intercluster distances between clusters. I also varied the null model by resampling 5 percent of the overall Folsom artifact distribution for each iteration and simulation of the null model. The summary results of the tests are shown in table 33. Figure 64 depicts the premise of the sensitivity analysis for a selected number of the iterations, and key metrics are graphically displayed in figure 65.

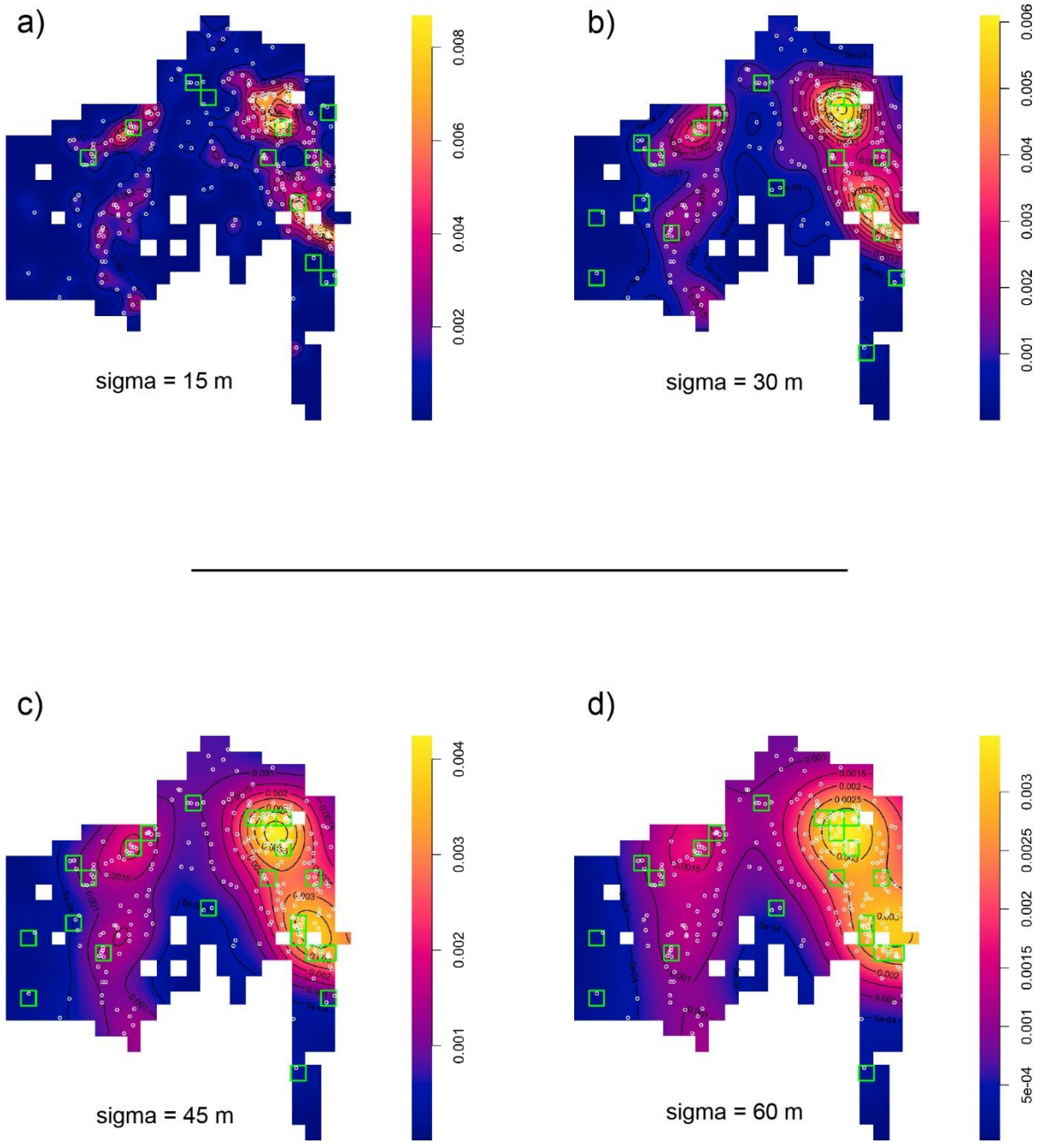


Figure 64. Examples of simulation results for different iterations of varying KDE bandwidths at fixed intervals for null model calculation (resampled by 5%). The sigma values represent fixed kernel bandwidth distances.

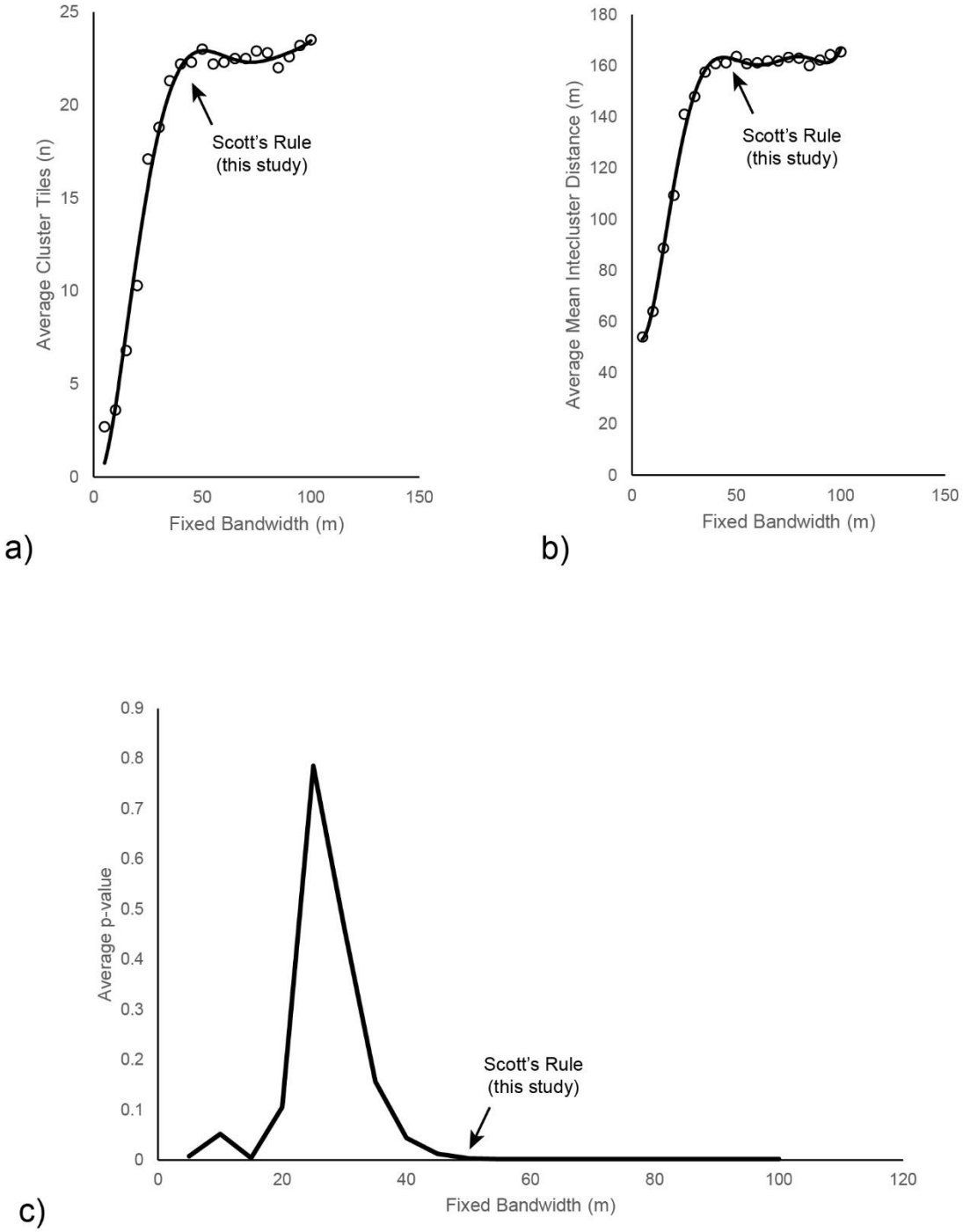


Figure 65. Summary results of mean output values for 200 simulations of fixed KDE bandwidth variance used in the sensitivity analysis. Note how cluster detection and p-value variance increase until the "elbow" between 40 and 50 m. The Scott's Rule label represents the maximum value of the adaptive bandwidth used in the original analysis of the study.

Table 33. Summary results of kernel bandwidth sensitivity analysis, for 200 simulations of 20 different iterations of varying bandwidths in the null model calculation.

Bandwidth Iteration	Number of Simulations	Mean p-value (SD)	Mean Cluster Tiles n (SD)	Mean Cluster Standard Residual (SD)	Average Mean Intercluster Distance m (SD)
5 m	10	0.008(0.01)	2.7(1.4)	23.6(29.2)	54.1(15.6)
10 m	10	0.052(0.15)	3.6(1.1)	2.7(0.9)	64.1(10.1)
15 m	10	0.004(0.00)	6.8(1.1)	2.5(0.1)	88.7(7.5)
20 m	10	0.106(0.05)	10.3(1.2)	2.7(0.1)	109.4(6.7)
25 m	10	0.786(0.12)	17.1(0.9)	2.7(0.1)	141.1(3.6)
30 m	10	0.464(0.08)	18.8(0.4)	2.9(0.0)	148.0(1.7)
35 m	10	0.156(0.02)	21.3(0.6)	3.0(0.0)	157.6(1.8)
40 m	10	0.044(0.01)	22.2(0.5)	3.1(0.1)	160.9(2.3)
45 m	10	0.013(0.01)	22.3(0.7)	3.3(0.0)	161.2(1.7)
50 m	10	0.003(0.01)	23.0(0.9)	3.4(0.0)	163.7(2.4)
55 m	10	0.002(0.00)	22.2(0.7)	3.5(0.1)	160.8(3.3)
60 m	10	0.002(0.00)	22.3(0.9)	3.6(0.1)	161.2(2.4)
65 m	10	0.002(0.00)	22.5(0.5)	3.7(0.1)	161.9(1.9)
70 m	10	0.002(0.00)	22.5(0.9)	3.8(0.1)	161.9(3.0)
75 m	10	0.002(0.00)	22.9(1.0)	3.8(0.1)	163.3(3.5)
80 m	10	0.002(0.00)	22.8(1.1)	3.9(0.1)	163.0(4.1)
85 m	10	0.002(0.00)	22.0(1.0)	4.1(0.1)	160.1(3.8)
90 m	10	0.002(0.00)	22.6(0.5)	4.1(0.1)	162.3(1.9)
95 m	10	0.002(0.00)	23.2(0.4)	4.1(0.1)	164.4(1.5)
100 m	10	0.002(0.00)	23.5(0.5)	4.1(0.1)	165.5(1.9)

The results of the test revealed several key factors about the effects of varying kernel bandwidths on the null model. When applied to the null model in the goodness-of-fit tests, the fine-grained bandwidths (short distances between 5 m and 20 m) produced immense variation in the cluster model outputs, including unstable p-values and large differences in the detected number of clusters and measured distances (table 33 and figure 65). Model metrics stabilized at null model bandwidths ranging between 40 and 50 m, with consistently modeled p-values, counts of cluster tiles detected per simulation, average distances between clusters, and standard residuals representing deviations from the null model. After about 55 m, the null model was apparently overly smoothed to a point where the cluster model results were universally significant and consistent. In my original study, the maximum bandwidth implemented by Scott's Rule (which is adaptive and not fixed) is 53 m and falls within the "elbow" region of the sensitivity results presented here – depicted in figure 65. The elbow in the simulated data represents the point in simulation where local clusters begin merging into broader spatial patterns – hence the purpose of

Scott's Rule, which is to optimize bandwidth selection given the totality of the data structure. Further smoothing of the null model past the elbow region moves the expected counts per tile toward a spatial average. Additional sensitivity tests could be made to determine the cumulative effects and relationships of quadrat tile sizes and kernel bandwidths on model outputs and cluster configurations. In sum of both sensitivity analyses, the pattern of camp shatter artifacts is highly non-random, stable, and resistant to thinning when compared to an appropriately smoothed null model covering the site.

Part 2: Measuring Folsom

The previous results show there is variable density of Folsom artifacts across the surface of Reddin, and there are areas containing higher than expected counts of camp shatter artifacts – which I infer to represent the residual debris patterns of Folsom occupation centers or campsites. The next question that I address in this chapter simply asks: how much time was spent in each of those Folsom occupation centers to create a residual pattern of camp debris? By proxy, this question focuses on the residential mobility patterns of Folsom groups who occupied the site. There is an inverse relationship between the amount of time spent occupying a campsite and time spent moving to new campsites across the broader landscape (Surovell 2009:61). In a small, articulated, and contemporaneous Folsom campsite you might expect to find evidence supporting one type of residential mobility pattern – suggesting relatively frequent or infrequent movements across the landscape – indicated by a short- or long-term occupation, respectively. But for larger multi-cluster sites there is potential to detect either one dominant pattern of residential mobility between the different areas, or possibly a spectrum of residential mobility choices – especially if the site is demonstrated to include multiple occupations. You might even speculate that larger and more dense camp locales reflect longer occupations based on the accumulation of discarded

artifacts over time, and smaller camps might represent shorter amounts of time spent in those areas. But the real point of this chapter is to move out of the realm of speculation and into the process of modeling these relationships formally, given a set of assumptions and expectations. Table 34 provides a set of definitions for some of the major concepts for measuring the duration of site occupations within a site, discussed in the following sections.

Table 34. Summary of concepts related to measuring time based on the accumulation of artifacts, following Surovell (2009) and this study.

Concept or term	Description
Occupation span	The lapsed time from the arrival of the first individual to the departure of the last individual
Occupation intensity	The sum of all time spent at a site by all occupants in units of person time (days, hours)
Mean per capita occupation span	The average length of stay per individual at the site
Residential stability	Length of time spent at a site over the course of one year
Residential mobility	Time spent moving from campsite to campsite on the landscape, inversely related to time spent occupying campsites
Discard rate	The rate that artifacts are discarded on sites, in proportion with the mean use-life of artifacts
class a artifact	An artifact with a discard rate or attribute that decreases over time and becomes less represented in the toolkit or assemblage
class b artifact	An artifact with a discard rate or attribute that increases over time and becomes more represented in the toolkit or assemblage
Local raw material	An artifact made from a lithic raw material source available within 20 km of the site. No local lithic raw material is present at Reddin. This is an example of a *class b* artifact
Nonlocal raw material	An artifact made from lithic raw material sourced beyond 20 km or the maximum daily foraging radius. This is an example of a *class a* artifact
Debitage	Any artifact representing lithic waste byproduct from the toolkit manufacture and repair process (flintknapping). This is an example of a *class b* artifact
Transported tool	Any chipped stone tool manufactured prior to the occupation of a site, comprising a portion of the founding toolkit. This is an example of a *class a* artifact
Unburned artifact	Any lithic debitage or tool lacking traces of high temperature burning damage. This is an example of a *class a* artifact (see discussion)
Burned artifact	Any lithic debitage or tool with potlids and crazing fractures suggesting damage from high temperature burning. This does not include "possibly" burned items based on presumed color changes. This is an example of a *class b* artifact (see discussion)

Methods

Surovell (2009) developed a useful framework for measuring the duration of site occupations based on the accumulation of artifacts by individuals in a campsite, using theoretical principles from behavioral ecology – which I summarize, synthesize, and apply here. Importantly, the framework distinguishes several possible measures of occupation duration, which can be easily confounded in discussion. Occupation span refers to the elapsed amount of time between the arrival of the first individual at a campsite to the departure of the last individual at a campsite, which is differentiated from occupation intensity – the sum of all time spent at a site in units of person time (the sum of time in days, hours, years, etc.). Occupation span and intensity differ from mean per capita occupation span as well, which simply represents the average length of stay per individual. Mean per capita occupation span is a more useful variable to try to model because it is independent of the cumulative effects of reoccupation, as well as the cumulative byproducts of flexible social organization in hunter-gatherer groups. You might expect mean per capita occupation span and general occupation span to correlate positively if you assumed one hunter-gatherer band arrived and departed from a site with all households simultaneously. But these values would differ strongly if the number of individuals per group changed over time during an occupation (Binford 2001; Whitelaw 1991; Yellen 1977), or if sites contained evidence of multiple occupations.

Estimating mean per capita occupation span based on the accumulation of artifacts over time requires several assumptions, which I address here. First, I assume that individuals in a hunter-gatherer group maintained their own lithic toolkits. I also assume that individuals discarded their toolkits into the archaeological record in a probabilistic process. Chipped stone tools had an average use-life, and once expended, they were discarded (Schiffer 1975). I assume their toolkit

maintenance process was similarly probabilistic and conducted at regular intervals over time as the tools broke – to maintain the balance of the toolkit. Thus, I assume that artifacts discarded by hunter-gatherers into a site represent the disposal of regularly used and broken equipment but also regularly manufactured items to maintain the optimal toolkit size. If the toolkit replacement process was gradual over time, then the accumulation of artifacts over time was simply a function of the artifact discard rate.

Different types of artifacts accumulated at different rates over the course of an occupation (Surovell 2009:74-75), in conjunction with the regular process of toolkit discard and replacement. I assume hunter-gatherers traveled to campsites from previous locations with a founding toolkit, and this founding toolkit included a fixed number of artifacts. During the initial stages of occupation, the founding toolkit was highly representative but became increasingly rare in the operational toolkit as the tools gradually wore down and were discarded over time. Equipment from the founding toolkit was discarded at a relatively linear rate until a point in time where hunter-gatherers discarded all original items into the site and the founding toolkit was fully depleted. Artifacts made locally on the site gradually replaced the founding toolkit during the initial stages of occupation, but once the founding toolkit was fully depleted, the new set of artifacts then became increasingly represented simply as a function of time.

These underlying premises form the basis of a model which measures mean per capita occupation span by using the ratios of the two previously described types of artifacts (Surovell 2009:76-77), which include *class a* artifacts (discard rates decreasing over time) and *class b* artifacts (discard rates increasing over time). Figure 66 shows the expected relationships of the model, where the fixed number of discarded *class a* artifacts levels off over time and discarded *class b* artifacts increases over time; the ratio of *class b* to *class a* artifacts is expected to increase

linearly over time, and the reciprocal relationship (*class a* to *class b* artifacts) takes a negative exponential shape. All else being equal, short-term occupations will show generally higher quantities of *class a* artifacts and long-term occupations will show a higher relative quantity of *class b* artifacts.

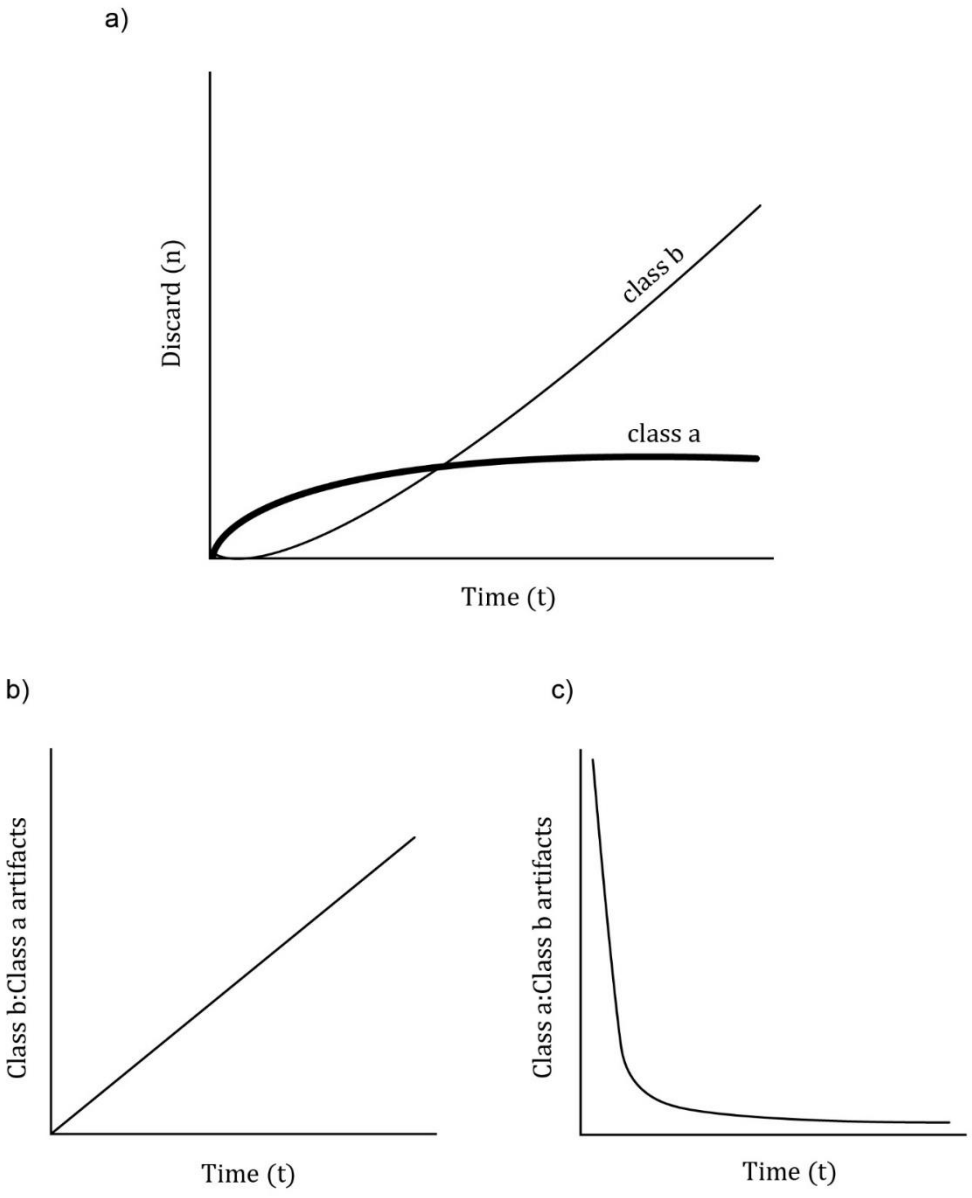


Figure 66. Graphs of assumed artifact discard relationships between *class a* and *class b* artifacts over time, adapted from Surovell (2009:figures 3.3 and 3.4). Cumulative *class a* and *class b* artifacts discarded over time (a), ratio of *class b*:*class a* artifacts over time (b), ratio of *class a*:*class b* artifacts over time.

Surovell (2009:78-90) created two versions of the artifact type ratios to independently test the validity of the model and simultaneously compare differences in mean per capita occupation span across a select sample of Paleoindian sites (including many Folsom sites). The method detected a spectrum of residential mobility strategies across the sample based on the ratios of *class b* to *class a* artifacts. Surovell found a strong positive correlation between the two logged ratios in the model, which included local raw materials (*class b*) to non-local raw materials (*class a*) followed by all debitage (*class b*) to transported tools from the founding toolkit (*class a*). In the first ratio, the model assumed that artifacts made from non-local raw materials (gathered prior to site occupation, beyond the maximum daily foraging radius from a site) became less represented over time, and local raw materials (available within a day's walk) gradually became more represented over time. In the second ratio, the model assumed that debitage (the byproduct of tool maintenance and repair) was made and discarded locally on sites, which gradually became more represented as the initial founding toolkit (transported tools) was depleted. The Pearson r correlation values were quite high when the two logged ratios from each site were submitted to a simple linear regression ($r = 0.90$), although it was difficult to determine statistical significance due to sample size effects and autocorrelation (Surovell 2009:85). However, the results of the study strongly suggested that both artifact type ratios (local to non-local raw materials, and debitage to transported tools) monitored the same phenomenon – mean per capita occupation span.

It is not possible to apply the exact same method devised by Surovell (2009) to the sample of campsites from Reddin, simply because there are no local lithic raw materials within the maximum daily foraging radius (see chapter 4). The nearest raw material source is quartzite from Trickle Mountain, approximately 55 km from Reddin or nearly three days of walking in a straight line. To account for this, I offer another version of the *class b*:*class a* artifact type ratio that I expect

to follow the similar assumptions. The version that I propose monitors the accumulation of an artifact attribute over time, rather than the actual deposition of the artifact types as assumed in the previous ratios. Here, I suggest that burned artifacts containing potlids and crazing fractures, because of intense exposure to high temperature cultural thermal features, become increasingly represented over time in a campsite.

It is now becoming routine for archaeologists to use the spatial distribution of burned artifacts to detect the presence of hearth-centered spaces in camps (Clark et al. 2022; Henry 2012; Kuhn and Stiner 2019; Sobkowiak-Tabaka and Diachenko 2020; Surovell and Waguespack 2007), even in the absence of a preserved thermal feature. The formality of those methods varies between different studies, some more quantitative, some more subjective. In all cases, researchers detect a signal of "phantom" hearth-centered spaces using the radial distributions of burned material. In Paleoindian archaeology more broadly, researchers continue to prove a close relationship between hypothesized fireplaces and lithic workshops that served as areas for downtime to complete tool replacement tasks (Jodry 1999a; Stiger 2006; Surovell 2022; Surovell and Waguespack 2007).

Here, I do not follow the same path of analysis but instead suggest that burned artifact density may be a useful indication of mean per capita occupation span. I assume that hunter-gatherers maintained their lithic toolkits near thermal features when occupying a campsite – whether those spaces existed inside or outside of a residential structure. I assume that the rate of thermal feature use was generally constant over time due to thermoregulatory needs, nighttime lighting for local visibility, social gathering, cooking daily food, smoking meat, and entertainment. I also assume a probabilistic chance that artifacts received damage from proximity to fires when hunter-gatherers discarded lithics as part of the regular use and replacement of the overall lithic toolkit. Regular sweeping and maintenance of hearth-centered spaces may have decreased the

chance that artifacts gained the burning attribute over an occupation, but the chance never decreased to zero, and I expect that the number of burned artifacts only increased with time. Prior research demonstrates that sweeping activities preferentially move larger artifacts away from maintained spaces, but microdebitage stays in place and often gets burned over time – as shown at the Barger Gulch campsite (Surovell 2022; Surovell and Waguespack 2007). If discarded artifacts always maintained a chance to get burned over the course of an occupation, then the pool of potentially burned artifacts only increased with every discard event, as opposed to the sample of unburned artifacts which rose initially at the start of an occupation but then eventually leveled off in comparison to the sample of burned artifacts. In sum, I assume that burned artifacts at Reddin followed the expected accumulation rate of *class b* artifacts, whereas unburned artifacts followed the rate of *class a* artifacts over time. In chapter 4, I discussed the clear presence of these burned artifacts at the site, presented spatially here in figure 67.

I calculate the logged ratios of debitage to transported tools and burned to unburned artifacts for this test. I use a simple linear regression of the values measured across each of the previously identified Folsom camp shatter concentrations. I use a set of hypotheses to guide the interpretation of the results from the simple linear regression, summarized in table 35. I generally assume that the simple linear regression will show highly correlated values of the two ratios. A Folsom concentration with a higher mean per capita occupation span will include abundant debitage as well as burned artifacts relative to transported tools and unburned artifacts – fitting higher on the regression line. Similarly, a shorter occupation span will include a higher representation of transported tools and unburned artifacts relative to all debitage and burned artifacts – presenting lower on the best-fit line. If the vectors along the regression line cluster in a similar range, I will fail to reject a null hypothesis (NH3) that Folsom hunter-gatherers at Reddin

maintained a consistent residential mobility strategy across all areas, emphasizing either short or long-term occupations. If the intercepts span a range along the regression line, then I will reject the null in favor of an alternative hypothesis (AH3) – which simply states that Folsom residential mobility at Reddin varied between each cluster due to different mean per capita occupation spans.

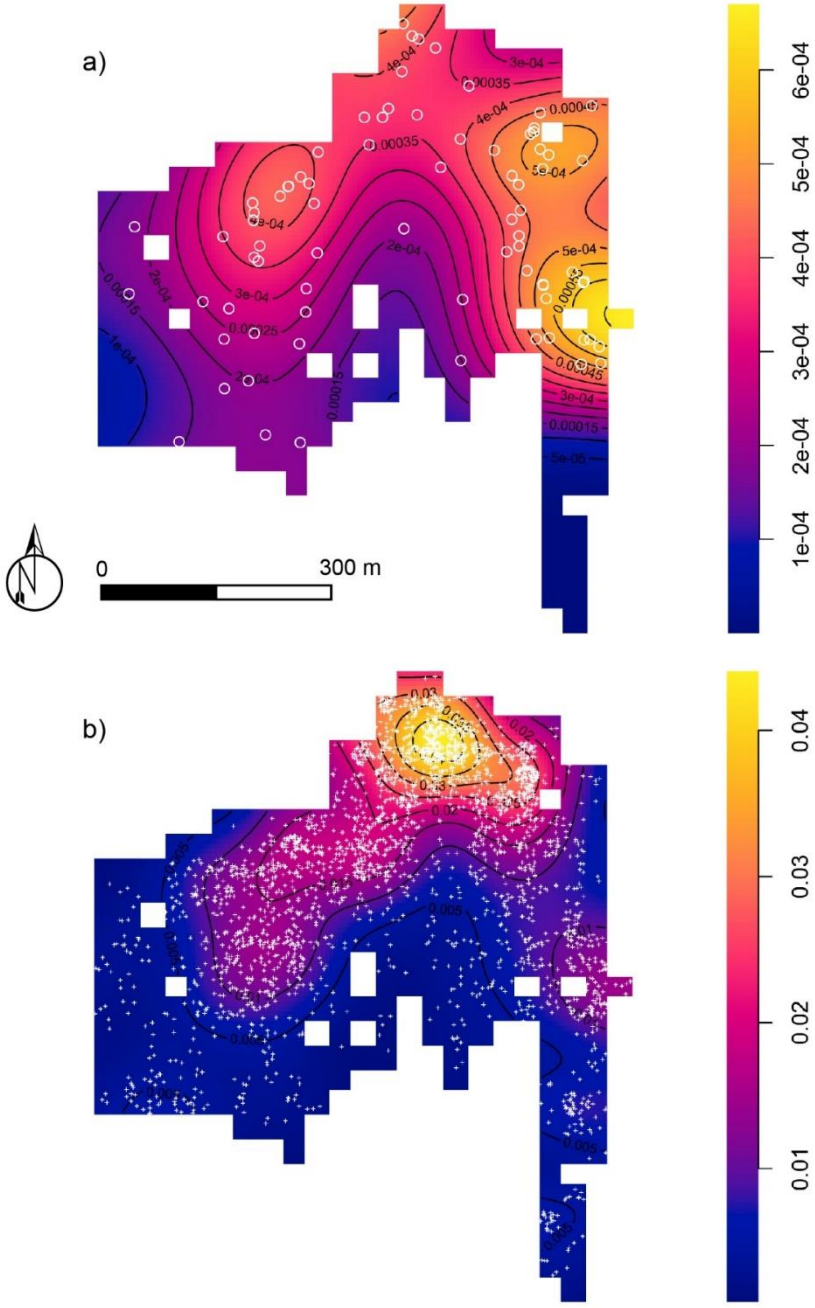


Figure 67. Distribution of burned artifacts, including plotted tools (a) and simulated locations of burned debitage using the *rjitter* method. Kernel density estimates based on Scott's Rule for adaptive smoothed intensity.

Table 35. Summary of null and alternative hypothesis for the test of mean per capita occupation span measured across each of the Folsom camp shatter concentrations.

Hypothesis	Expectation	Results	Conclusion
Null Hypothesis (NH3): Mean per capita occupation span was relatively uniform across the sample of Folsom campsites at Reddin. The uniformity reflects a consistent pattern of residential mobility.	Each campsite will display a similar ratio of tools transported to the site compared to artifacts made onsite. Each campsite will display a similar ratio of burned to unburned artifacts.	Intercepts of a regression line using log-transformed ratios of 1) debitage to transported tools and 2) burned artifacts to unburned artifacts.	If the regression intercept points cluster around a similar value, then fail to reject the null hypothesis: Folsom campsites at Reddin were used for a similar duration and exhibit similar patterns of residential mobility.
Alternative Hypothesis (AH3): Mean per capita occupation span varied across the sample of Folsom campsites at Reddin. The differences in occupation span reflect both long- and short-term residential mobility patterns.	Each campsite will display dissimilar ratios of tools transported to the site compared to artifacts made onsite. Each campsite will display varied ratios of burned to unburned artifacts.	Intercepts of a regression line using log-transformed ratios of 1) debitage to transported tools and 2) burned artifacts to unburned artifacts.	If the regression intercept points vary significantly, then reject the null hypothesis: Folsom campsites at Reddin exhibit variability in occupation duration, reflecting long-term and short-term patterns.

Results

Table 36 summarizes the raw data used to construct the simple linear regression of the logged artifact ratios, and table 37 shows the output of the regression statistics, including an analysis of variance and correlation. Figure 68 depicts a plot of the regression. The logged ratios of debitage:transported tools and burned:unburned artifacts are highly correlated (Pearson's r = 0.98 and $R^2 = 0.96$), suggesting the model performed as predicted overall. Importantly, I was not able to submit all of the Folsom concentrations at Reddin to the simple regression analysis given that the analysis requires at least one transported tool or at least one burned artifact to be present within the cluster assemblage – although the absence of these artifact types and the overall low assemblage sizes within each cluster is probably a good indicator of a short mean per capita occupation span. Multiple of the smallest 900 m^2 clusters did not model given these constraints, including the F1, F2, F4, F5, F7, and F9 camp shatter concentrations. Locality B stands out as an outlier in the regression, with standard residuals of -2.14 for the observed and predicted values. The remaining concentrations closely fit the regression line across a range of vector intercepts,

with Locality C representing the longest occupied camp and the F8 cluster representing the shortest occupied camp in terms of mean per capita occupation span. Locality A and Locality D are joined near the middle of the spectrum by the spatially smaller clusters F6, F3, and F10 – perhaps representing a medium within the overall range of occupation span values at Reddin.

Table 36. Ratios of debitage to transported tools and burned artifacts to unburned artifacts from Folsom camp shatter concentrations at the Reddin site.

Cluster Name	Debitage (D)	Transported Tools (TT)	Log (D:TT)	Burned Artifacts (BA)	Unburned Artifacts (UA)	Log (BA:UA)
Loc. A	2176	29	1.88	146	2119	-1.16
Loc. B	418	16	1.42	59	405	-0.84
Loc. C	508	4	2.10	70	457	-0.81
Loc. D	395	5	1.90	33	372	-1.05
F1	17	0	-	5	14	-0.44
F2	45	0	-	3	43	-1.16
F3	180	3	1.78	11	178	-1.21
F4	32	0	-	0	34	-
F5	249	0	-	42	211	-0.70
F6	193	3	1.81	10	188	-1.27
F7	152	0	-	11	146	-1.12
F8	51	3	1.23	1	54	-1.73
F9	11	0	-	0	13	-
F10	232	4	1.76	12	227	-1.28

Table 37. Simple linear regression output summary statistics.

Analysis of Variance	df	SS	MS	F	Significance F
Regression	1	0.41	0.41	109.47	0.0001
Residual	5	0.01	0.003		
Total	6	0.43			
Regression Statistics					
Pearson's r	0.98				
R Square	0.96				
Adjusted R Square	0.95				
SE of β	0.06				

Observation Standard Residuals – Loc. A (0.78), Loc. B (-2.14), Loc. C (-0.9), Loc. D (-0.67), F3 (-0.16), F6 (1.47), F8 (-1.14), F10 (0.70); Loc. B standard residuals based on outlier-inclusive model

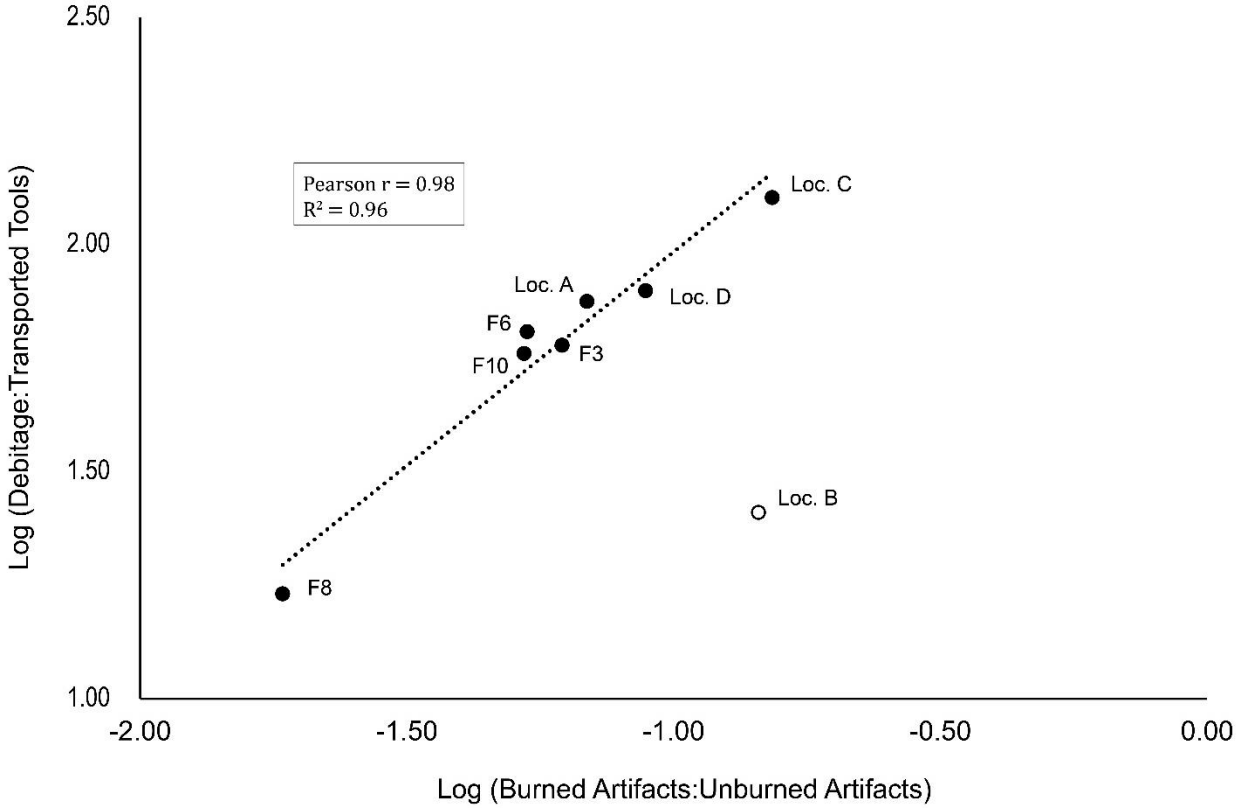


Figure 68. Scatterplot and best-fit line of the simple linear regression used to model mean per capita occupation span for eight out of 14 identified Folsom camp shatter concentrations at the Reddin site.

Given the results of the model, I feel confident that I can reject the null hypothesis that there is a single dominant residential mobility pattern at the site. The results support the alternative hypothesis (AH3), and there appears to be a range of residential mobility patterns reflected in the overall configuration of campsites. Importantly, the measured values of mean per capita occupation span for each area do not simply scale with campsite size (as measured in square meters) or assemblage size (based on the overall quantity of artifacts). The largest camps (except for the Locality B outlier) do trend towards the higher end of mean per capita occupation span on the regression line, but multiple of the smaller camps demonstrate similar values, and there is a wide gap between the intercept of the F8 cluster and the next lowest value (F10). I suspect some of the observed differences have to do with the starting conditions and size of the founding toolkits represented in each of the clusters; if some individuals within Folsom groups arrived to the site

operating under a system of lithic raw material stress, then individuals may have been practicing toolkit conservation strategies and extending artifact use-lives beyond the time expected under a gradual rate of artifact discard (see chapter 4). I also suspect this may be the reason why Locality B presents as an outlier in the regression. Locality B exhibits relatively high counts of burned artifacts but relatively low counts of debitage overall – Folsom flintknappers from Locality B may have maintained toolkits at a lower pace and produced less debitage over time due to conservation strategies, but any discarded artifacts (such as the high count of transported tools) were possibly burned at a constant rate over time – thus skewing the measured value. It is then possible that the Folsom camps which intercept closely to the regression line operated under similar starting conditions or toolkit conservation strategies.

More generally, the results show that burned artifact ratios provide a reasonably strong monitor over the same phenomenon as the ratio of debitage to transported tools, given the positive correlation of the values. I suggest here that both processes monitor mean per capita occupation span. Future researchers may wish to continue to test and refine this method for accumulation research at other Folsom sites. Hofman et al. (1990) speculated that a similar type of process might explain the differences in quantity of burned lithics observed at Shifting Sands and Cattle Guard:

> Significant variation in the frequency of burned artifacts to debitage has been noted at the Folsom camp/processing area at the Cattle Guard site... This pattern may reflect hearth related activities and incidental burning of pieces lost or discarded adjacent to hearth areas. The proportion of burned lithics, might, then, be related to duration of occupation as reflected by the intensity and longevity of hearth use and redundancy of activities around hearths. The low frequency of burned pieces at Shifting Sands as compared to the total assemblage may reflect one of two things. Either hearth use was very limited during occupation, or the length of the occupation was relatively brief. (p. 238)

I could not agree more, and I am encouraged by the fact that other researchers have contemplated similar ways of thinking about the accumulation of burned artifacts over time.

Part 3: Connecting Folsom

The two prior sections of this chapter summarize methods for identifying Folsom camps and determining the relative lengths of time that people spent in those places. Thus far, the results demonstrate two important details: 1) Reddin is a large multi-cluster site with several possible occupation centers, and 2) several of those camps exhibit a range of measured occupation lengths. The two previous sections do not address the issue of contemporaneity between Folsom camps in a direct sense, but it is possible to build a prior expectation that the Reddin site is most likely the byproduct of multiple Folsom occupations. Spatially broad multi-cluster sites generally fit the model of reoccupation as demonstrated by Andrews et al. (2008), and the spectrum of residential mobility patterns measured between each Folsom camp suggests that different Folsom groups may have lived at the site over different time frames. It seems wise to develop an independent method testing these observations – one which focuses on the issue of contemporaneity, directly.

Methods

Even if I had 20 precise radiocarbon dates from one buried A horizon covering the entire Folsom component at Reddin, each with standard lab errors representing a 40-year span or better (+/- 20 yrs), I would still choose to analyze lithic refits and conjoining artifact pieces to model contemporaneity across the site. The question of contemporaneity invokes the archaeology of individual moments over a very short span of time, not likely to be detected by the most precise radiocarbon assays. Fortunately, Folsom researchers are accustomed to testing contemporaneity within sites by using connecting pieces of artifacts that broke away from one another at approximately the same time frame (Jodry 1992; Laughlin 2005; Sellet 2004; Stiger 2006). Lithic refits refer to a group of chipped stone artifacts with surfaces that connect to represent a flintknapping reduction sequence – examples include individual flakes that fit to a core or stone

tool, or in the common case of Folsom diagnostics: channel flakes to preforms or finished points. Conjoining pieces instead represent connected surfaces of a single broken artifact, such as individual portions of one flake or stone tool. Of the two categories, refits are probably better for estimating contemporaneity because of how closely they represent one activity – flintknapping. It is more difficult to prove the temporal relationships of a single broken artifact; in a best-case scenario, conjoining pairs represent the use, damage, and discard of an artifact from an anthropogenic activity, but in the worst case the broken portions of artifacts simply represent a natural fracture event from a taphonomic force like trampling, rock fall, or some other.

Folsom researchers use spatial modeling and Euclidean distances between refit pairs to demonstrate many things about archaeological assemblages. Analysts commonly use the distances of refits to establish the overall space of an individual flintknapping episode, showing the breadth of diffusion among artifacts from one lithic reduction sequence. In this sense, refits provide a line of evidence demonstrating the intactness of a lithic deposit (Laughlin 2005; Surovell et al. 2005); small distances between refit pairs suggest a relatively integrated lithic assemblage. Refits also help establish whether artifact discard processes closely match hypothesized activity areas, such as refits between tool edge resharpening flakes and tool edges found in the same area (Jodry 1992, 1999a). Refits have proven useful for demonstrating deeper temporal properties of Folsom sites, as well. In the Mountaineer lithic assemblage, refits between channel flakes and projectile point bases suggest that Folsom flintknappers manufactured the projectile points in a camp setting but then broke the point while hunting further afield (Meltzer and Eren 2021:335). The hafted basal portion was then brought back to the campsite, demonstrating both long term investment in that space but also the full spectrum of the tool life cycle.

Conjoins may offer deeper temporal characteristics of sites. Famously, Folsom researchers have connected broken portions of tools between hypothesized activity areas and equipment repair zones within residential camps – demonstrating a sequential mobility pattern between different portions of sites. At the Stewart's Cattle Guard site, Jodry (1999a:figure 89) documented conjoining pairs of Folsom projectile points between a primary bison hunting locale (and initial butchery area) and residential camps in proximity – providing the clearest evidence of the ABC residential mobility pattern available (see chapter 1). Jodry (1999a:table 52) documented at least 79 refit and conjoin pairs at Cattle Guard, which connected most areas of the site and proved a strong case for contemporaneity between those areas.

An analysis of refit and conjoining artifact pairs is no simple task, and researchers have found a variety of possible constraints on the success of the method. For one, success is driven by observer experience and characteristics of the artifacts – such as the overall size of artifacts and visual qualities. In most studies, researchers use a threshold on the maximum length of artifacts when compiling a sample for refit attempts, generally between 2 cm and 4 cm long, due to diminishing returns on the refit success rate for artifacts that are smaller (Laughlin and Kelly 2010). This is an obvious problem at Reddin, given that any type of diagnostic Folsom artifact is less than 2 cm long on average (see chapter 4 and figure 43), and most pieces of debitage are essentially microscopic. Nodule-based methods help refine refit and conjoin samples by grouping sets of different stone raw material types that have similar visual properties – such as color-hue, texture, luster, and inclusions (Hurst and Johnson 2016; Larson and Kornfeld 1997; Sellet 2004, 2013). Ideally, the nodule groups monitor an individual supply of stone transported into sites, but the nodules must be sufficiently heterogenous to not visually overlap with other nodules of the same raw material type.

I developed a refit and conjoining artifact analysis at Reddin that focused exclusively on the Folsom diagnostic lithic assemblage, to test for contemporaneity between different significant areas in the surface scatter. I constrained my analysis in several ways. First, I excluded all artifacts lacking spatial provenience – there seemed little value in finding connecting pieces of artifacts from unknown areas for this analysis. Second, I defined analytical groups of nodules within each of the major raw material types present at the site. I used the internal membership of those nodule groups to test refit and conjoin pairs. The nodule groups consisted of stone with roughly identical visual qualities of primary and secondary base colors, inclusions (if present), and overall luster and texture (rough to coarse). I show possible examples of different nodule groups in figure 69, and the artifact appendices provide a summary of nodule group membership for each artifact. Table 38 provides a summary for nodule groups arrayed by Folsom artifact type and overlapping groups between artifact types. For artifacts with provenience, I arrayed potential pairs within each nodule group based on spatial proximity, so that my refit and conjoin attempts focused initially on nearby artifacts within the same nodule category but expanded gradually to include more distant potential pairs in the nodule group.

My analysis was primarily concerned with testing contemporaneity between the major Folsom occupation centers or campsites given the research questions, but I also expected that refits or conjoins could extend into unmodeled portions of the site. To account for this, I performed an additional cluster analysis (quadrat test) for the remaining portions of Folsom projectile points that I did not model previously, which I defined as *kill shatter* – including distal tips, lateral edge spalls, and midsections. At Stewart's Cattle Guard, Jodry (1999a:figure 89) documented a higher frequency of point midsections, lateral edges, and tips within the initial kill and bison butchery area at the site – several of the broken fragments conjoined with point bases in the adjacent

residential areas, proving contemporaneity between the bison kill and campsite. This pattern was also demonstrated between the bison kill and campsite at Mill Iron (Frison 1996). Thus, I expected there could be additional unmodeled concentrations of Folsom artifacts at Reddin, possibly representing hunting locations on the site or secondary processing camps. If Folsom hunter-gatherers were practicing aspects of the ABC kill-to-kill residential mobility model at Reddin (see chapter 1), then those areas should be located close adjacent or directly overlap with the previously identified camp locales. I tested the goodness-of-fit between kill shatter artifacts and the same inhomogeneous Poisson process representing all Folsom artifacts, in the same way as the previous quadrat test. The total sample of kill shatter artifacts for the analysis included 69 pieces.

Table 38. Quantities of unique nodules per lithic raw material type, summarized by Folsom artifact.

Raw Material	Nodules for Points	Nodules for Preforms	Nodules for Channels	Channels to Points (Matching Nodules)	Channels to Preforms (Matching Nodules)
Cumbres Chert	2	2	5	1	1
Dacite	1	0	2	1	0
Trickle Mtn Quartzite	5	0	1	1	0
Edwards Chert	2	1	1	1	1
Flattop Chalcedony	1	1	2	1	1
Morrison Quartzite	3	1	1	1	1
Mosca Chert	3	2	3	0	0
Narbona Chalcedony	2	2	3	2	2
Jemez Obsidian	4	2	1	1	0
Pedernal Chert	4	4	5	3	3
Rhyolite	1	0	0	0	0
Silicified Wood	7	5	5	5	4
Trout Creek Jasper	18	16	18	15	13
Oolitic Chert	0	0	1	0	0
Unknown Chert	7	9	8	5	7
Total	60	45	56	37	33

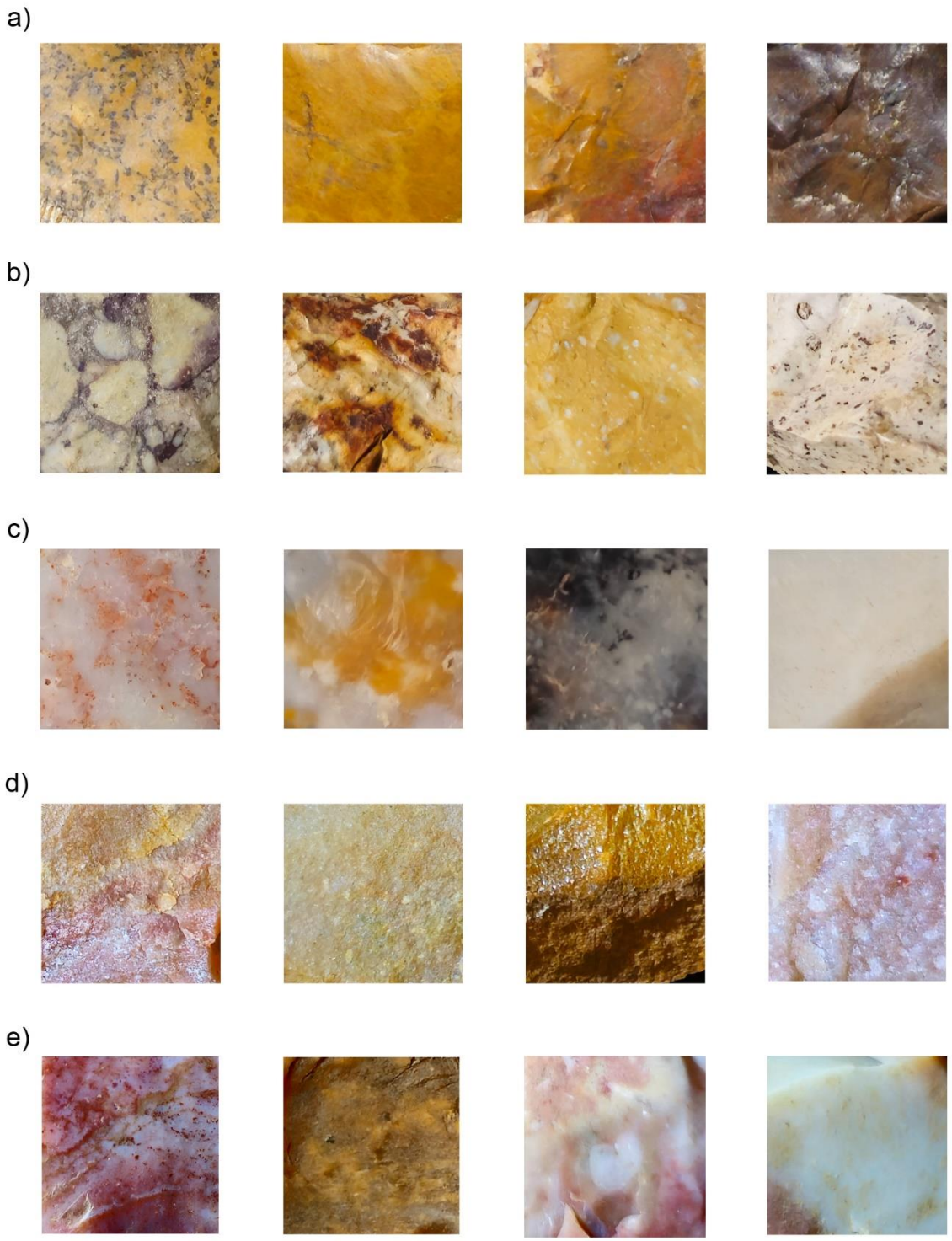


Figure 69. Examples of different possible nodule groups for individual lithic raw material types, including Trout Creek jasper (a), Cumbres Pass chert (b), Cerro Pedernal chalcedony (c), Trickle Mountain quartzite (d), and Mosca Creek chert (e). Images based on CMPA lithic raw material comparative collection.

Results

My refit analysis was unsuccessful. I did not identify any refitting pairs between channel flakes and performs, or between channel flakes and projectile points. I suspect that my lack of success had much to do with the intense damage to the lithic assemblage overall, indicated by the paucity of complete artifacts as well as the small fragment sizes represented in each artifact category. In addition, certain lithic raw material types like Trout Creek exhibited immense heterogeneity within individual specimens, which made it difficult to confidently assign all artifacts to well-defined nodule groups for the analysis. It is also possible that Folsom flintknappers effectively repaired and resharpened many pieces so that previously connecting surfaces were severely altered, making it impossible to confidently refit the artifacts – one might expect such a scenario if Folsom groups practiced methods of toolkit conservation due to lithic raw material stress. In sum, the refit analysis failed to identify any lithic reduction sequences within or between the major Folsom campsites at Reddin.

The conjoin analysis was informative despite an extremely small sample of connecting artifact pairs. I identified four new artifact pairs in the projectile point assemblage using the nodule-based methods described above. Each conjoining artifact pair consisted of one projectile point fragment originally identified by the Smithsonian as well as another fragment identified by the CSU team, roughly 40 years later. The Smithsonian previously identified four projectile point conjoins, which I found labeled together in the curation bags, but unfortunately these lack provenience – so they cannot be used for the test of contemporaneity across the site. Figure 70 shows the full sample of conjoining projectile point fragments from the Reddin site, and table 39 reviews the distances between each pair.



Figure 70. Conjoining artifact groups of projectile point fragments from the Reddin site, including previously identified specimens lacking provenience (top row) and newly identified pairs between artifacts found by the Smithsonian (1979, 1983) and CSU (2020-2022) (bottom row).

Table 39. Summary of newly identified conjoining artifact pairs at the Reddin site, including measured distances between connecting artifacts.

Conjoin Number	Raw Material	Portions and Meltzer Codes	Euclidian Distance (m)	Survey Block(s)	Pair Labels
C1	Edwards	Proximal (4D) and lateral (3G)	15.11	U48	CMPA-PP-1052 / SI-PP-1116
C2	Trout Creek	Proximal (4C) and lateral (3C)	78.47	T46 and T49	CMPA-PP-1011 / SI-PP-1118
C3	Silicified Wood	Proximal ear (4D) and lateral (3G)	168.61*	R52 and M55	CMPA-PP-1042 / SI-PP-1085
C4	Trout Creek	Lateral (3C) and lateral (3C)	294.15	I52 and S50	CMPA-PP-1027 / SI-PP-1124

* SI-PP-108 estimate based on simulated point provenience in survey block

The new sample of conjoining projectile points that I identified demonstrates several things. In Locality B, a split Midland base fragment (C1) made of Edwards chert, found separated by 15.11 m, likely represents a dehafting episode within the campsite. The close distance between these connecting tool fragments suggests the surface scatter in that portion of the site is potentially

intact, perhaps representing one occupation. The remaining conjoins do not connect any significant camp concentrations at the site but demonstrate wide ranging mobility patterns and involve cross-type pairs (camp shatter to kill shatter). The C2 conjoin consists of an intact Trout Creek Folsom point base near Locality B and a sheared lateral spall found near the East Playa, measured more than 78 m apart, which may represent the use and discard of hunting equipment near that area. The C3 conjoin includes two fragments of a silicified wood projectile point: one proximal ear found southeast of Locality A and a lateral edge piece found 169 m further to the west near the edge of the La Garita Creek floodplain – suggesting a different hunting or butchery location across the site. This conjoining piece exceeds the distance of 137 m reported by Roberts (1941:79) and Wilmsen and Roberts (1978:60) for an artifact pair between the Area I and Area II excavations at the Lindenmeier site, which previously represented the longest recorded distance of a Folsom refit or conjoin. However, this distance is overshadowed by the C4 conjoin at Reddin, a pair consisting of two small lateral edge fragments of a Trout Creek jasper projectile point, separated by more than 294 m across the site.

I can only speculate about the vast distance between the C4 artifact pair, which may incorporate the location of a primary hunting area and secondary processing camp; perhaps one of the fragments was left in place near a former hunting area, and then another piece was transported while embedded with disarticulated carcass parts (Hofman 1999:124-135). It is tempting to presume a contemporaneous connection between Locality C (modeled as a long-term occupation) and the F6 camp cluster (modeled as a short-term occupation) based on the proximity of the C4 conjoin to those areas (figure 71). However, the residual patterns of camp activity may overlay those of a previous kill site, or vice versa. The assumption of contemporaneity between Folsom clusters on the west and east ends of the site remains uncertain, yet tantalizingly possible.

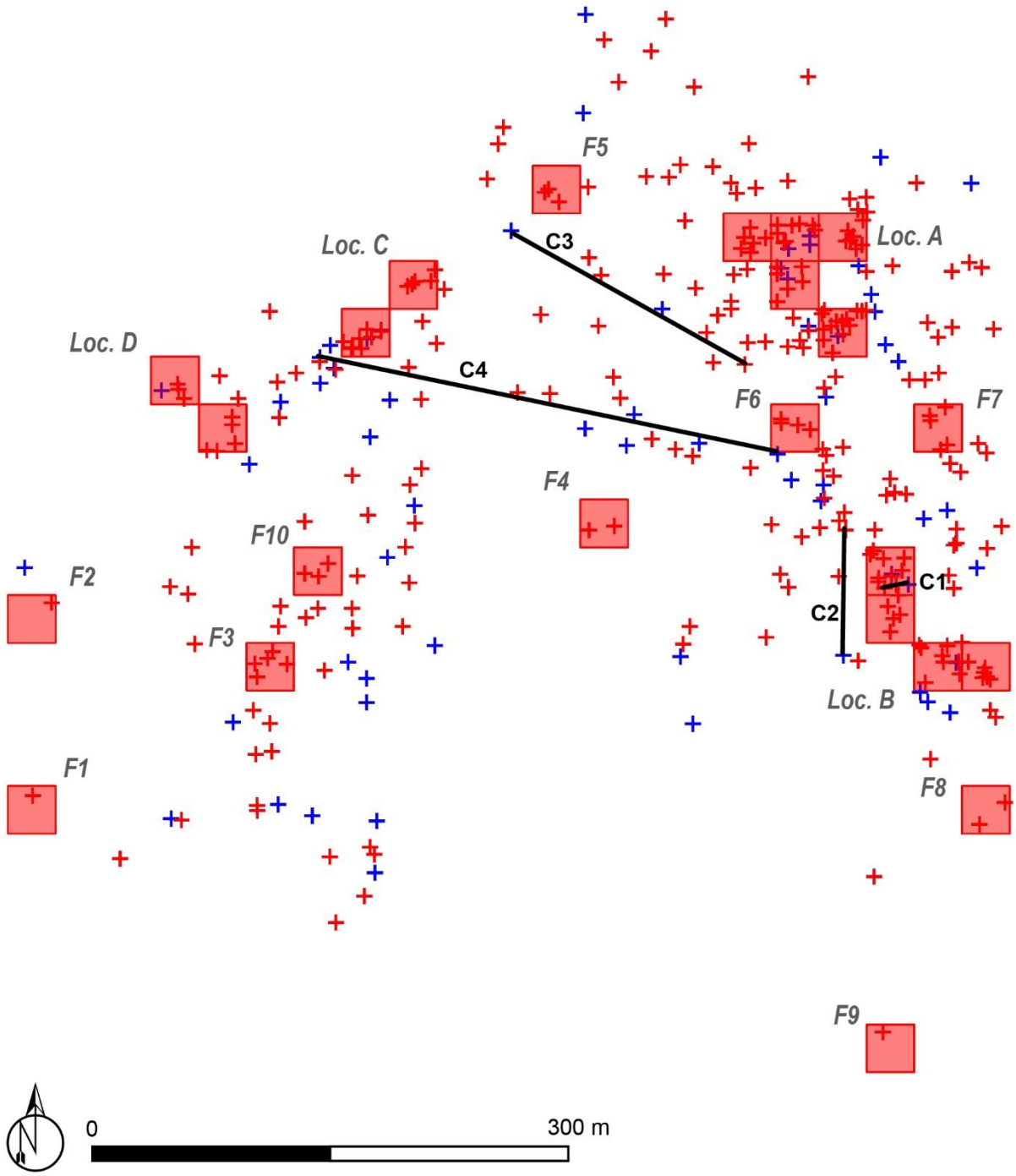


Figure 71. Generalized map of Folsom camp clusters depicting camp shatter (red +) and kill shatter (blue +), with conjoin pair distances.

The calculated X^2 (359.28) and p-value (0.28) of the global goodness-of-fit test for kill shatter artifacts do not reject the null model in favor of the alternative hypothesis (see page 160 and table 29 for a review of the hypothesis test). The observed counts of kill shatter in each quadrat tile do not significantly differ from the expectations of the inhomogeneous Poisson process – representing all Folsom artifacts. As discussed in chapter 4 and shown here in figure 71, the sample of kill shatter artifacts (portions of Folsom points broken above the hafted base) is quite small in comparison to camp shatter artifacts. Does this mean that Reddin was not a hunting site? Not necessarily, but it could suggest that Folsom hunting activities were conducted primarily offsite – or on a very small scale within the site as suggested by the random spatial pattern of kill shatter. Alternatively, different processes might account for the absence of these pieces across the site – such as excessive harvesting of usable tool parts from bonebeds as predicted by Hofman (1999:124) for instances of high processing intensity, high artifact visibility, high carcass accessibility, and dire conservation of lithic material. Folsom people may have transported broken projectile points offsite if individual pieces were large enough to be maintained for an extended tool lifecycle – such as rebasing larger broken tips of points.

In sum of this work, I did not demonstrate contemporaneity between each of the Folsom camps at the site. I did not detect any refitting artifacts representing a sequence of lithic reduction within Folsom camps. The results of the conjoin analysis revealed a broad spectrum of intra-site mobility patterns, however. The observed distances between artifact pairs ranged from about 15 m to over 294 m, and included pieces discarded near residual campsites (camp shatter) and portions left in smaller random spaces across the site (kill shatter). Andrews et al. (2008:481) speculated that large surface scatter sites like Reddin "…provide opportunities to investigate Folsom adaptive behavior at the foraging scale…", and the long-range conjoin distances appear to meet this overall

expectation. The results of the quadrat goodness-of-fit test did not reveal significant clustering of kill shatter artifacts, however. This may indicate that Folsom hunters only conducted small and low intensity hunting efforts across the site, and that more significant hunting events occurred primarily offsite and away from the main camps.

Stipulations

The previous sections of the chapter tell a relatively simple story in a complex way. Reddin appears to be a large site occupied by Folsom people at different times and for different lengths of time during each visit. Artifact discard patterns primarily reflect residual camp debris, but the results of the conjoin analysis show that Folsom people ranged widely across the site to do other tasks during their occupations – producing debris for ephemeral processes while doing so. In this sense, Reddin showcases a spectrum of intra-site mobility patterns that excavations typically do not encounter.

This story is founded on a painfully long set of assumptions. Those assumptions include my theoretical positions for how and why hunter-gatherers make and break chipped stone artifacts over time, but also more practical concerns that I have not addressed. For instance, the prior models assume that Folsom people produced the underlying spatial patterns of the camp debris that I identified – including all of the debitage and non-diagnostic chipped stone tools contained within those specific areas. I do not directly address each of the individual components from the Late Paleoindian, Archaic, and Formative periods in this dissertation – but there were many post-Folsom occupants of the site (see Appendix D). Is it possible that post-Folsom occupants of the site contributed significantly to the artifact discard patterns that I detected? The palimpsest effect is a relevant concern, so here I begin to address this topic probabilistically.

Table 40. Summary of Folsom to post-Folsom artifact quadrat test null and alternative hypotheses, including expectation, potential results, and outcomes for interpretation.

Global Quadrat Test

Hypothesis Description	Expectation	Result	Conclusion
Null Model (NH4): The spatial distribution of all Folsom artifacts follows the same modeled intensity pattern of all other diagnostic artifacts.	The observed counts of Folsom artifacts will not significantly deviate from expected counts under the assumption of the inhomogeneous Poisson process.	Simulated Chi-Square statistic from Monte Carlo simulations (n=1000) of the inhomogeneous Poisson process.	If the p-value > 0.05, fail to reject the null hypothesis: the observed Folsom distribution approximates the same distribution as all other artifacts, and there is no significant clustering.
Alternative Hypothesis (AH4): Folsom camp shatter is significantly clustered and does not follow the same modeled intensity of all other diagnostic artifacts.	The distribution of Folsom artifacts is expected to deviate from the inhomogeneous Poisson process. The observed counts will significantly exceed the expected counts of Folsom artifacts.	Simulated Chi-Square statistic from Monte Carlo simulations (n=1000) of the inhomogeneous Poisson process.	If the p-value < 0.05, reject the null hypothesis: the Folsom distribution is significantly clustered, indicating that it does not follow the expected inhomogeneous Poisson model.

Modeling a Palimpsest

Following my previously established methods, I constructed a new quadrat goodness-of-fit test to examine the spatial covariance of Folsom camp shatter artifacts and post-Folsom artifacts with provenience (n=100). In the previous models, I used the inhomogeneous Poisson process as the null hypothesis which represented the intensity of Folsom artifacts. For this test, I derived the inhomogeneous Poisson process from the density of all post-Folsom artifacts. Thus, the model tested for palimpsest effects of spatially overlapping artifacts from different time periods (not including non-diagnostic tools and debitage). The goodness-of-fit test simply counted the number of Folsom camp shatter artifacts in equally sized tiles (survey blocks) across the study area and compared those counts to the spatially varying expectation of the null model (figure 72). The general criteria of the hypothesis test are presented in table 40. The result of the test produced a global Chi-square statistic (X^2) and p-value summarizing the goodness-of-fit between the observed spatial distribution of camp shatter and the null model. I used Monte Carlo simulations (n=1000)

of the inhomogeneous Poisson process to account for the low number of expected values, so the p-value is a comparison of the X^2 and the cumulative values of simulation. I calculated standard residuals of the goodness-of-fit test in each of the quadrat tiles. I used an absolute value threshold of 1.96 to distinguish individual tiles in the analysis which deviated significantly from the goodness-of-fit test, indicating significantly higher counts of camp shatter artifacts than expected under the null hypothesis.

The calculated X^2 (1149.8) and p-value (0.002) of the global goodness-of-fit test reject the null model in favor of an alternative (AH4). Folsom camp shatter artifacts deviate significantly from the spatial expectations of the inhomogeneous Poisson process, representing the spread of non-Folsom diagnostic material. The observed distribution of Folsom camp shatter at the Reddin site is significantly clustered in different areas when compared to the intensity of all artifacts younger than Folsom (post-Folsom). The results of the test reveal multiple independent groups of survey cells containing significantly high counts of camp shatter artifacts compared to the null model – which closely correspond to the largest and most dense Folsom campsite localities identified in the previous test (figure 72 – and see results of previous cluster tests). The local results also demonstrate that many areas of the site contain relatively even amounts of Folsom and post-Folsom artifacts, suggesting the possibility of more pronounced palimpsest effects in those spaces and thus corroborating the null model in specific areas. Globally, I reject the hypothesis that Folsom and post-Folsom artifacts covary across the same places throughout the entire site, based on the conditional test results. Locally, Folsom camp shatter artifacts deviate significantly from the null expectation in some areas or fall within acceptable limits in other areas. Only 4 percent of the post-Folsom sample falls within detected Folsom concentrations (n=7 projectile points). Thus, the palimpsest effect is variable across the site, yet not strong enough to obscure the residual

processes of artifact discard within Folsom campsites, specifically. I take this to mean that the previously modeled results in the chapter hold weight and continue to demonstrate artifact discard patterns related to Folsom.

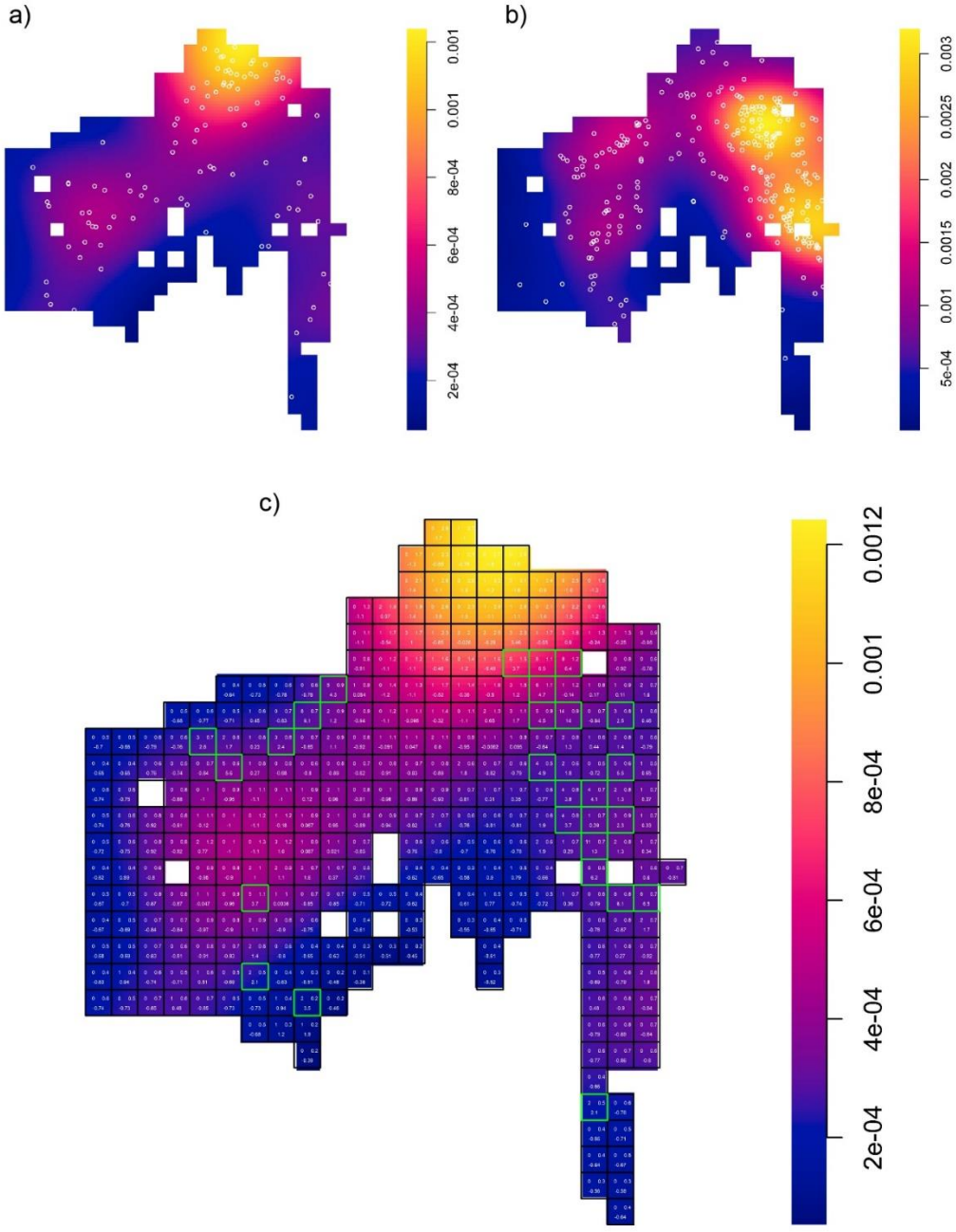


Figure 72. Diagnostic plots of the goodness-of-fit test for the inhomogeneous Poisson process representing post-Folsom artifacts (n=100): smoothed kernel density map of post-Folsom artifacts (a), smoothed kernel density map of Folsom camp shatter (b), modeled quadrat test results, showing significant tiles in green (c).

Are there other potential reasons that Folsom artifacts, and specifically camp-related debris (channel flakes, preforms, and point bases) appear clustered on the site? I think it is possible that other factors have contributed to the precise locations of artifacts more generally, such as natural redeposition by forces such as wind and perhaps water (given proximity to the La Garita Creek). Individual artifact locations might relate to other practical issues such as artifact visibility in the sand sheet and local vegetation, or sampling intensity between the various research teams over the last 40 years. These other factors are presently untested but offer avenues for future research. However, I do not see cause to immediately question the results of the spatial analysis based on these factors. If wind or water significantly transported artifacts and produced the patterns described previously, then a quantitative test of that process should support a hypothesis where natural forces preferentially transported only preforms, channel flakes, and point bases into clustered piles inside the distribution of all other Folsom artifacts at the site – as well as all other artifacts from different time periods. Similarly, sand cover and vegetation would have to be shown to obscure every other type of artifact except for Folsom camp debris. In the face of these other possibilities, I think the simplest answer is easiest to justify – the spatial patterning is primarily a result of cultural artifact discard processes because that is how those artifacts entered the record in the past. This dissertation deals primarily with broad-scale patterning of archaeological phenomena – it omits the vagaries of fine-scale disturbances to spatial structure in the data. Future research may document legitimate relationships between sample intensity variance or artifact visibility regarding fine-grained spatial patterning in artifact locations, but I suspect it will be difficult to scale those processes across the entirety of the site – as they are locally controlled issues.

Summary

This chapter addressed several questions about the Folsom component at Reddin, focusing on the spatial and temporal relationships between fluted weaponry pieces and the byproducts from making them. I developed methods for identifying the focal centers of Folsom occupation within the lithic scatter by using the spatial patterns of camp debris relative to everything else. Reddin is a large site with approximately 14 camp localities that seem to follow a clustered distribution when compared to all Folsom artifacts. A sensitivity analysis of the sample confirmed that the spatial structure of dataset is robust to resampling by random data thinning, and that Scott's Rule for kernel bandwidth selection was appropriately applied to the spatial null hypothesis. I then applied concepts from accumulation theory and human behavioral ecology to model the amount of time Folsom people spent occupying each campsite at Reddin – which varied across localities – suggesting a range of residential mobility strategies. I distinguished the discard rates of artifacts made locally on the site from artifacts transported there, following previously established methods to model mean per capita occupation span. I also justified and applied a new model for measuring mean per capita occupation span based on the steady accumulation of burned artifacts in campsite assemblages over time, which strongly correlates with the previously established model. Finally, I tested for contemporaneity between the different Folsom camp localities at the site with a refit and conjoin analysis. The refit analysis failed, but four new conjoining pairs of projectile points demonstrate the full range of Folsom intra-site mobility strategies at Reddin – representing long-range forays between residual camp centers and ephemeral activity areas. The analysis discovered a conjoining pair separated by 294 m, which represents the longest recorded distance of a successful refit or conjoin in the Folsom archaeological record. However, the analysis did not demonstrate contemporaneity between campsites – the results of this chapter suggest Reddin is a

large, multi-cluster site visited by Folsom people at different times and for different lengths of time. The results of the supplementary test demonstrate a clear distinction between Folsom artifact discard patterns and material left in place by post-Folsom occupants of the site. This is important because of the overarching concerns that most archaeologists have with spatial analysis of surface scatters – at Reddin, it appears that surface concentrations are not severely mixed and maintain consistency regarding the age of materials. Thus, the results of the palimpsest model that I demonstrated here support the overall conclusions drawn from my cluster detection methods and models of residential mobility via mean per capita occupation span.

CHAPTER 6 - CONCLUSION

The results of this dissertation convince me that in-depth analysis of surface archaeological assemblages is a worthwhile endeavor – a question that I posed throughout the previous chapters. However, I accept that sites like Reddin will likely never serve as the archetype of the Folsom tradition, nor will they draw much attention from researchers looking for answers from a single moment in time in the past. Instead, open lithic scatters offer a broader spatial and temporal perspective into the ways that people visited and revisited places – an insight difficult to perceive from the depths of an excavation unit, but perhaps better viewed while on the move across the landscape with eyes to the ground. This chapter continues this discussion while reviewing the major conclusions from my analysis of the Reddin site.

In chapter 2, I demonstrated the complex formation history of the San Luis Valley – with a particular focus on the dynamic wetlands of the northern Closed Basin subarea. The Valley fluctuated between xeric and wet conditions at astonishing rates over time; during the Folsom period, the Valley was likely wetter than today and filled with emergent wetland ecosystems centered on small playas, oxbow lakes, and spring-fed deposits. Folsom nomads concentrated their site distributions in two primary clusters in the Closed Basin, including the Alamosa Cluster (Cattle Guard, Linger, Zapata, and others) and Saguache Cluster (Reddin, and others) – separated by roughly 30 km. Previous research focused intensively on the well-known Folsom bison kills and campsites in the Alamosa Cluster due to the presence of wholly or partially buried components containing faunal material and intact lithic spatial distributions. The research confirmed that aggregating Folsom microbands occasionally settled in a bison grazing corridor situated between

interdunal ponds and the bajada slopes of the Sangre de Cristos (Jodry 1999b, 1999a; Jodry and Stanford 1996).

The results of this dissertation provide additional insight into Folsom residential mobility patterns within the Saguache Cluster, as Reddin contains most of the Folsom material from all sites in the center of the Closed Basin (see chapter 2). Reddin is made up of multiple and seemingly independent Folsom campsite clusters, occupied for different lengths of time, which suggest (to me) that Folsom mobility patterns in this portion of the Valley emphasized *place* irrespective of external constraints on forager mobility choices (Haas et al. 2015; Haas and Kuhn 2019; Kuhn et al. 2016; LaBelle 2010). I argue here that Folsom occupation patterns at Reddin signal the formation of a cultural geography (Binford 1982), one developed locally and actively by people undertaking repetitive mobility patterns over time (Binford 1982; Haas and Kuhn 2019; Kuhn 1995; LaBelle 2010). Folsom people at Reddin may have intentionally provisioned the site over time with technological and social resources, so that a persistent feedback loop formed and improved the residential utility of the Reddin site with each sequential visit – as described by Haas and Kuhn (2019:499-502) for the provisioning of places by mobile foragers. The variable densities of artifacts observed across Reddin, including the relative sizes of campsite spatial footprints, might suggest differences in anticipated mobility (planned length of stay) between Folsom groups who adapted to new methods of site occupation based on previous experiences (Haas and Kuhn 2019; Sellet 2013). The results of this work encourage me, and hopefully others, to look at similarly large Folsom sites such as Lindenmeier for evidence of accretional cultural geographies (LaBelle and Meyer 2021).

In chapter 3, I detailed the original scope and methodology of fieldwork at Reddin which allowed a unique type of spatial analysis and exploration of the topics described above – an

uncommon approach for analysis of most Folsom-aged surface scatter sites. Dennis Stanford and a team of experts carried out one of the most comprehensive controlled surface surveys yet described from the 1970s. The real utility of that work was its framework for supporting new, cumulative field projects at the site. CSU's fieldwork at Reddin further refined previously existing artifact discard patterns within the spatial distribution of Folsom material by using the same survey methodology as the Smithsonian. Our team documented more nuance to the three primary Folsom artifact concentrations that the Smithsonian identified. Our application of UAV-based aerial imaging techniques also proved pivotal for confirming the cultural legitimacy of those patterns, in the face of potential sampling hurdles from surface visibility.

My analysis does not explicitly handle the fine-grained results of CSU's Locality A surveys, given the broad scope of the research questions that I addressed. But for posterity's sake, I anticipate that patterns of residual camp processes observed at broader spatial scales may proceed further into smaller spatial scales at the site. I expect this to occur especially within areas demonstrating strong positive deviations from the overall "brush strokes" of artifact discard processes covering the entire site. I also expect that future research at Reddin will reveal new patterns confirming or contrasting the sitewide data presented here; if the Smithsonian collected 100 percent of everything they detected, and we performed a similar survey and detected abundant new artifacts, then I suspect time-dependent changes to the site will likely disclose new patterns requiring new fieldwork to test and understand. Unlike excavated Folsom sites, surface scatters like Reddin will continue to provide opportunities to explore the relationships between the total spatial scale of archaeological phenomena and our chosen sampling methods.

The descriptive analysis presented in chapter 4 demonstrated the overall fragmentary condition of lithic artifacts at the site, despite their excellent utility for spatial analysis. Only a

single Folsom projectile point was found complete, which also happened to be an unexpected pseudo-fluted miniature version. Most of the 225 Folsom projectile points included classically manufactured pieces – but unfluted Midland points were also present in lower numbers, as were more unique varieties like reverse-fluted points. It was difficult to analyze the Folsom assemblage (points, preforms, and channels) given that most fragments measured less than 2 cm long or wide and exhibited a range of damage traces resulting from impact, burning, and likely intentional recycling of usable tool parts. This problem extended to most other artifact types, including a suite of other bifaces and flake tools. The overall lack of cores and large pieces of debitage within the site assemblage suggested an emphasis on late-stage lithic reduction activities (tool finishing and repair) to the near exclusion of early-stage processes like core detachment and initial preform manufacture. Together, this evidence indicated Folsom groups may have operated under conditions of lithic raw material supply stress – an expected factor given the extreme distances between the site and major lithic procurement areas represented in the sample of tools and debitage.

Chapter 5 covered the bulk of my analysis in this dissertation, where I addressed three primary questions to guide my research:

1) *Where is the Folsom component located at the Reddin site?*
2) *What kinds of residential mobility strategies did Folsom hunter-gatherers use?*
3) *Does the Folsom component represent a single contemporaneous occupation, or several different occupation events?*

It was not easy to answer any of these questions, not even the simplest of the three (component location) – primarily due to the confounding relationships between space and time in surface scatter assemblages. To resolve aspects of the first question I focused on locating places at the site where Folsom people likely spent most of their time – campsites. Fortunately, much of the lithic

assemblage contained artifacts that I expected to find in such a setting, including pieces like preforms and channel flakes which represent the new manufacture of projectile points (a task more likely to occur within a downtime space). Similarly, dehafted point bases, which were likely transported back to campsites in broken dart foreshafts, made up an unexpectedly large proportion of the assemblage. Together, these three artifact types represented a category that I defined as *camp shatter*. By using a quadrat-based goodness-of-fit test, I was able to quantitatively show that these artifacts clustered significantly when compared to the density of all Folsom artifacts at the site – and in multiple areas covering the extent of the site. Those 14 concentrations represent the main occupation centers of the Folsom component.

I addressed the question of Folsom residential mobility (the rate of campsite movement across the landscape) by modeling the inverse phenomenon – occupation duration (the length of time spent in one place). I measured the accumulation of artifacts over time in each of the Folsom concentrations by using methods and theory developed by others (Schiffer 1975; Surovell 2003, 2009, 2022), with some new contributions based on my view of campsite archaeology and site formation processes. Specifically, I assessed the relative differences in mean per capita occupation span for each cluster by arraying two different types of artifact ratios. Both ratios focused on artifact types or attribute frequencies that grow over time (debitage, burned lithics), compared to those which decrease over time in a campsite (founding toolkit, unburned lithics). In a simple linear regression, I demonstrated strong correlation between the logged ratios of these two values (Pearson's $r = 0.98$, $R^2 = 0.96$) as measured across each of the Folsom campsite clusters – the results of the analysis suggested a range of mean per capita occupation spans between the Folsom camps, signifying different residential mobility patterns used by Folsom groups (some more frequent, some less frequent).

Finally, I addressed the issue of contemporaneity between different Folsom camps with attempted refits and conjoins. The refit analysis failed to identify a single connection between a channel flake and a preform, or a channel flake and a projectile point – likely due to the severity of damage to the lithic assemblage and challenging visual characteristics of unique lithic raw material nodules. However, the results of the conjoin analysis were eye-opening for many reasons, few of them having to do with between-camp contemporaneity. I identified a total of four conjoining projectile point fragment pairs, each comprised of one piece identified by the Smithsonian crew (1979 or 1983) and one fragment collected by CSU (2020-2022). Except for one conjoined split base in Locality B (15 m distant), each of the conjoining pieces established a lengthy connection between pieces of *kill shatter* (portions of point tips, lateral edge spalls, midsections) and multiple dehafted basal portions. The longest observed distance for a conjoin connection at the Reddin site is 294 m – which represents the furthest refit or conjoin distance observed in a Folsom site. None of these conjoining artifacts established connections to different Folsom occupation centers at the site (but see chapter 5 results for tentative assignments). However, the results more broadly demonstrated that Reddin is made up of debris related to residual campsite activities in addition to long-distance ephemeral activities carried out across the foraging scale of Folsom mobility (Andrews et al. 2008:481).

Final Remarks

At the outset of the dissertation, I established a few goals for the manuscript: 1) to (re)introduce the Reddin site to the broader community of Folsom researchers, concerning the scope of past fieldwork and details about the Folsom assemblage, and 2) to demonstrate the value of surface scatter sites for Folsom archaeology by developing spatial and temporal models of the artifact concentrations at the site. I hope the chapters that I have provided offer useful facts in

support of these goals. Surface scatter sites will continue to produce as much information as we are willing to glean from them – and I believe this requires sincere effort on the part of archaeologists. Surface scatter sites afford a nuanced view of the totality of foragers' use of space in the deep past, extending into analytical horizons that are difficult to perceive from a narrow spatial and temporal perspective – as is commonly assumed in excavations. If modeled probabilistically, researchers might be able to account for the cumulative blurring of archaeological deposits on surface scatters over time. If tedious, researchers might make connections across vast distances within sites that address aspects of mobility for which we have very little vocabulary. I hope archaeologists rise to a new challenge, to build that vocabulary in ways that might contextualize some of the more unique results presented herein.

REFERENCES CITED

Adamopoulos, Efstathios, and Fulvio Rinaudo.
2020 UAS-Based Archaeological Remote Sensing: Review, Meta-Analysis and State-of-the-Art. *Drones* 4(3):1–28.

Ahler, Stanley A.
1975 Pattern and Variety in Extended Coalescent Lithic Technology. PhD Dissertation, University of Missouri, Columbia.

1989 Mass Analysis of Flaking Debris: Studying the Forest Rather than the Tree. In *Alternative Approaches to Lithic Analysis*, edited by Donald O. Henry and George H. Odell, pp. 85–119. Archaeological Papers No. 1. American Anthropological Association, Washington, D.C.

1994 *A Working Manual for Field and Laboratory Techniques and Methods for the 1992-1996 Lake Ilo Archaeological Project*. Quaternary Studies Program, Northern Arizona University, Flagstaff, Arizona.

Ahler, Stanley A., and Phil R. Geib.
2000 Why Flute? Folsom Point Design and Adaptation. *Journal of Archaeological Science* 27(9):799–820.

Amick, Daniel S.
1995 Patterns of Technological Variation among Folsom and Midland Projectile Points in the American Southwest. *Plains Anthropologist* 40(151):23–38.

1996 Regional Patterns of Folsom Mobility and Land Use in the American Southwest. *World Archaeology* 27(3):411–426.

Ammerman, Albert J.
1981 Surveys and Archaeological Research. *Annual Review of Anthropology*:63–88.

Andrefsky Jr., William.
2006 *Lithics: Macroscopic Approaches to Analysis*. 2nd ed. Cambridge University Press, United Kingdom.

Andrews, Brian N.
2010 Folsom Adaptive Systems in the Upper Gunnison Basin, Colorado: An Analysis of the Mountaineer Site. PhD Dissertation, Southern Methodist University, Dallas, Texas.

Andrews, Brian N., Jason M. LaBelle, and John D. Seebach.
2008 Spatial Variability in the Folsom Archaeological Record: A Multi-Scalar Approach. *American Antiquity* 73(3):464–490.

Andrews, Brian N., David J. Meltzer, and Mark Stiger (editors).
2021 *The Mountaineer Site: A Folsom Winter Camp in the Rockies*. University Press of Colorado, Louisville.

Baddeley, Adrian, E. Rubak, and R. Turner.
2015 *Spatial Point Patterns: Methodology and Applications with R*. Chapman and Hall Press, London.

Baddeley, Adrian, and R. Turner.
2013 Spatstat: An R Package for Analyzing Spatial Point Patterns. *Journal of Statistical Software* 55(11):1–43.

Bailey, Geoff.
2007 Time Perspectives, Palimpsests, and the Archaeology of Time. *Journal of Anthropological Archaeology* 26(2):198–223.

Bamforth, Douglas B.
2002 High-Tech Foragers? Folsom and Later Paleoindian Technology on the Great Plains. *Journal of World Prehistory* 16:55–98.

Bamforth, Douglas B., and Mark S. Becker.
2000 Core/Biface Ratios, Mobility, Refitting, and Artifact Use-Lives: A Paleoindian Example. *Plains Anthropologist* 45(173):273–290.

Banks, L.D.
1990 *From Mountain Peaks to Alligator Stomachs: A Review of Lithic Sources in the Trans-Mississippi South, the Southern Plains, and Adjacent Southwest*. Memoir No. 4. Oklahoma Anthropological Society, Norman.

Beeton, Jared M.
2014 Mammoths and Early North Americans in the San Luis Valley, Colorado. *San Luis Valley Historian* 46(4):9–23.

Beeton, Jared M., and Bradley G. Johnson.
2020 Geomorphology and Climate Change in the San Luis Valley. In *The Geology, Ecology. and Human History of the San Luis Valley*, edited by J.M. Beeton, C.N. Saenz, and B.J. Waddell, pp. 58–80. University Press of Colorado, Louisville.

Bement, Leland C.
1999 *Bison Hunting at Cooper Site*. University of Oklahoma Press, Norman.

2003 Constructing the Cooper Model of Folsom Bison Kills on the Southern Plains. *Great Plains Research* 13:27–41.

Bevan, Anrew, and James Conolly.
2009 Modelling Spatial Heterogeneity and Nonstationarity in Artifact-Rich Landscapes. *Journal of Archaeological Science* 36(4):956–964.

Binford, Lewis R.
1982 The Archaeology of Place. *Journal of Anthropological Archaeology* 1(1):5–31.

2001 *Constructing Fames of Reference: An Analytical Method for Archaeological Theory Building Using Ethnographic and Environmental Data Sets*. University of California Press, Berkeley.

Black, Kevin D.
2000 Lithic Sources in the Rocky Mountains of Colorado. In *Intermountain Archaeology*, edited by David B. Madsen and Michael D. Metcalf, pp. 132–147. University of Utah Press, Salt Lake City.

Black, Kevin D., and Aaron Theis.
2015 Progress and Prospects in Geoarchaeological Research on Chert Sources in Central Colorado. In *Rocky Mountain Archaeology: A Tribute to James Benedict*, edited by Kenneth P. Cannon, Judson B. Finley, and Molly B. Cannon, pp. 337–354. Plains Anthropologist Memoir No. 43.

Blades, Brooke S.
2003 End Scraper Reduction and Hunter-Gatherer Mobility. *American Antiquity* 68:141–156.

Blaine, Jay C., S. Alan Skinner, and Molly A. Hall.
2017 The Saga of Winkler-1: A Midland Site in Southeast New Mexico. *Paleoamerica* 3(1):48-73.

Blake, Kevin S.
2001 Contested Landscapes of the Navajo Sacred Mountains. *North American Geographer* 3(1):29–62.

Boldurian, Anthony T.
1990 Lithic Technology at the Mitchell Locality of Blackwater Draw, a Stratified Folsom Site in Eastern New Mexico. *Plains Anthropologist* 35:iii–103.

1991 Folsom Mobility and Organization of Lithic Technology: A View from Blackwater Draw, New Mexico. *Plains Anthropologist* 36(137):281–296.

Boldurian, Anthony T., George A. Agogino, Phillip H. Shelley, and Mark Slaughter.
1987 Folsom Biface Manufacture, Retooling, and Site Function and the Mitchell Locality of Blackwater Draw. *Plains Anthropologist* 32:281–296.

Boldurian, Anthony T., Phillip T. Fitzgibbons, and Phillip H. Shelley.
1985 Fluting Devices in the Folsom Tradition: Patterning in Debitage Formation and Projectile Point Basal Configuration. *Plains Anthropologist* 30(110):293–303.

Boszhardt, Robert F., and Joelle McCarthy.
1999 Oneota End Scrapers and Experiments in Hide Dressing: An Analysis from the La Crosse Locality. *Midcontinental Journal of Archaeology*:177–199.

Briles, Christy E., Cathy Whitlock, and David J. Meltzer.
2012 Last Glacial-Interglacial Environments in the Southern Rocky Mountains, USA and Implications for Younger Dryas-Age Human Occupation. *Quaternary Research* 77(1):96–103.

Bronk Ramsey, Christopher.
2009 Bayesian Analysis of Radiocarbon Dates. *Radiocarbon* 51(1):337–360.

Bryan, Kirk.
1939 Stone Cultures Near Cerro Pedernal and Their Geological Antiquity. *Bulletin of the Texas Archaeological and Paleontological Society* 87:9–42.

Buchanan, Briggs, Brian N. Andrews, J. David Kilby, and Metin I. Eren.
2019 Settling into the Country: Comparison of Clovis and Folsom Lithic Networks in Western North America Shows Increasing Redundancy of Toolstone Use. *Journal of Anthropological Archaeology* 53:32–42.

Buchanan, Briggs, J. David Kilby, Marcus J. Hamilton, Jason M. LaBelle, Kelton A. Meyer, Jacob Holland-Lulewicz, Brian N. Andrews, et al.
2021 Bayesian Revision of the Folsom Age Range Using IntCal20. *Paleoamerica* 7(2):133–144.

Buchanan, Briggs, J. David Kilby, Jason M. LaBelle, Todd A. Surovell, Jacob Holland-Lulewicz, and Marcus J. Hamilton.
2022 Bayesian Modeling of the Clovis and Folsom Radiocarbon Records Indicates a 200-Year Multigenerational Transition. *American Antiquity* 87(3):567–580.

Button, V. Tries.
1987 *The Closed Basin of Colorado's San Luis Valley: Bureau of Reclamation Archaeological Investigations 1976-1986*. U.S. Department of the Interior, Bureau of Reclamation, Amarillo, Texas.

Cameron, Catherine M.
2001 Pink Chert, Projectile Points, and the Chacoan Regional System. *American Antiquity* 66(1):79–101.

Campana, Stefano.
2017 Drones in Archaeology: State-of-the-Art and Future Perspectives. *Archaeological Prospection* 24(4):275–296.

Chambellan, C., M. Kadziel, T.J. Lennon, and E.K. Wade.
1984 *A Cultural Resource Evaluation of Site 5CF84, Salida Ranger District, Pike and San Isabel National Forests, Colorado*. Western Cultural Resource Management, Boulder, Colorado.

Charles, M.C.
1995 *A Cultural Resources Inventory of the Clauson Timber Sale and the Mosca Road Rehabilitation Projects, Hinsdale County, Colorado.* San Juan National Forest, Columbine District, Durango, Colorado.

Clark, Amy E., Sarah Ranlett, and Mary C. Stiner.
2022 Domestic Spaces as Crucibles of Paleolithic Culture: An Archaeological Perspective. *Journal of Human Evolution* 172:10326.

Conner, C.E., D.L. Langdon, R. Wolf, P.K. Roebuck, and T.F. Rome.
1980 *Poncha-San Luis Valley 230-kV Transmission Line Cultural Resources Inventory*. Grand River Institute, Grand Junction, Colorado. Submitted to Colorado-Ute Electric Association, Inc.

Cressie, Noel, and Timothy R.C. Read.
1984 Multinomial Goodness-of-Fit Tests. *Journal of the Royal Statistical Society Series B: Statistical Methodology* 46(3):440–464.

Davis, Joshua K., Mark R. Hudson, and V.J.S Grauch.
2017 A Paleomagnetic Age Estimate for the Draining of Ancient Lake Alamosa, South-Central Colorado. *Rocky Mountain Geology* 52(2):107–117.

Dello-Russo, R.D.
2004 Geochemical Comparisons of Silicified Rhyolites from Two Prehistoric Quarries and 11 Prehistoric Projectile Points, Socorro County, New Mexico, USA. *Geoarchaeology* 19:237–264.

Douglass, Matthew J., LuAnn Wandsnider, and Simon J. Holdaway.
2023 Surface Artifact Scatters, Data Collection, and Significance: Case Studies from Australia and the United States. *Advances in Archaeological Practice* 11(1):29–41.

Duran, Kristy L.
2020 Plants and Ethnobotany of the San Luis Valley. In *The Geology, Ecology, and Human History of the San Luis Valley*, edited by J.M. Beeton, C.N. Saenz, B.J. Waddell, pp. 241–260. University Press of Colorado, Louisville.

Eren, Metin I., Aaron Greenspan, and C. Garth Sampson.
2008 Are Upper Paleolithic Blade Cores More Productive than Middle Paleolithic Discoidal Cores? A Replication Experiment. *Journal of Human Evolution* 55(6):952–961.

Eren, Metin I., Thomas A. Jennings, and Ashley M. Smallwood.
2013 Paleoindian Unifacial Stone Tool "Spurs": Intended Accessories or Incidental Accidents? *PLoS ONE* 8(11):e78419.

Frison, George C.
1982 The Folsom Components. In *The Agate Basin Site: A Record of Paleoindian Occupation of the Northwestern High Plains*, edited by George C. Frison and Dennis J. Stanford, pp. 37–76. Academic Press, New York.

1996 *The Mill Iron Site*. University of New Mexico Press, Albuquerque.

Frison, George C., and Bruce A. Bradley.
1980 *Folsom Tools and Technology at the Hanson Site, Wyoming*. University of New Mexico Press, Albuquerque.

Frison, George C., and Dennis J. Stanford (editors).
1982 *The Agate Basin Site: A Record of the Paleoindian Occupation of the Northwestern High Plains*. Academic Press, New York.

Gingerich, Joseph A. (editor)
2013 *In the Eastern Fluted Point Tradition*. University of Utah Press, Salt Lake City.

2018 In the Eastern Fluted Point Tradition, Volume II. University of Utah Press, Salt Lake City.

Greiser, Sally T.
1983 A Preliminary Statement About Quarrying Activity at Flattop Mesa. *Southwestern Lore* 49(4):6–14.

Guarino, Michael C., and Frederic Sellet.
2019 An Examination of the Role of Miniature Projectile Points at the Lindenmeier Folsom Site, Colorado. *Paleoamerica* 5(2):132–142.

Haas, J.
1981 *San Luis Archaeological Project – Phase 1*. Unpublished manuscript, Department of Anthropology, University of Denver.

1982 *The San Luis Archaeological Project – Phase II Interim Report*. Unpublished manuscript, Department of Anthropology, University of Denver.

Haas, Randall, Cynthia J. Klink, Greg J. Maggard, and Mark S. Aldenderfer.
2015 Settlement-Size Scaling Among Prehistoric Hunter-Gatherer Settlement Systems. *PLoS ONE* 10(11):e0140127.

Haas, Randall, and Steven L. Kuhn.
2019 Forager Mobility in Constructed Environments. *Current Anthropology* 60(4):499–535.

Harmon, Eric J.
2020 Groundwater Resources of Colorado's San Luis Basin. In *The Geology, Ecology, and Human History of the San Luis Valley*, edited by J.M. Beeton, C.N. Saenz, and B.J. Maxwell, pp. 183–207. University Press of Colorado, Louisville.

Harvey, Paul H., Robert K. Colwell, Jonathan W. Silvertown, and Robert M. May.
1983 Null Models in Ecology. *Annual Review of Ecology and Systematics* 14:189–211.

Haynes Jr., C. Vance.
2003 Dating the Lindenmeier Folsom Site, Colorado, USA, Before the Radiocarbon Revolution. *Geoarchaeology* 18(1):161–174.

Henry, Donald O.
2012 The Palimpsest Problem, Hearth Pattern Analysis, and Middle Paleolithic Site Structure. *Quaternary International* 247:246–266.

Hoard, Robert J., John R. Bozell, Steven R. Holen, Michael D. Glascock, Hector Neff, and J. Michael Elam.
1993 Source Determination of White River Group Silicates from Two Archaeological Sites in the Great Plains. *American Antiquity* 58(4):698–710.

Hoard, Robert J., Steven R. Holen, Michael D. Glascock, Hector Neff, and J. Michael Elam.
1992 Neutron Activation Analysis of Stone from the Chadron Formation and a Clovis Site on the Great Plains. *Journal of Archaeological Science* 19(6):655–665.

Hoefer III, Ted.
1999 Environment. In *Colorado Prehistory: A Context for the Rio Grande Basin*, pp. 6–30. Colorado Council of Professional Archaeologists, Denver.

Hofman, Jack L.
1994 Paleoindian Aggregations on the Great Plains. *Journal of Anthropological Archaeology* 13(4):341–370.

1999 Folsom Fragments, Site Types, and Assemblage Formation. In *Folsom Lithic Technology: Explorations in Structure and Variation*, edited by Daniel S. Amick, pp. 122-143. Archaeological Series No. 12. International Monographs in Prehistory, Ann Arbor, Michigan.

2002 High Points in Folsom Archaeology. In *Folsom Technology and Lifeways*, edited by J.E. Clark, and M.B. Collins, pp. 193–224. Special Publication No. 4. Department of Anthropology, University of Tulsa.

2003 Tethered to Stone or Freedom to Move: Folsom Biface Technology in Regional Perspective. In *Multiple Approaches to the Study of Bifacial Technologies*, edited by Marie Soressi and Harold L. Dibble, pp. 229–250. University of Pennsylvania Museum of Archaeology and Anthropology, Philadelphia.

Hofman, Jack L., Daniel S. Amick, and Richard O. Rose.
1990 Shifting Sands: A Folsom-Midland Assemblage from a Campsite in Western Texas. *Plains Anthropologist* 35:221–253.

Hofman, Jack L., Lawrence C. Todd, and Michael B. Collins.
1991 Identification of Central Texas Edwards Chert at the Folsom and Lindenmeier Sites. *Plains Anthropologist* 36(137):297–308.

Holdaway, Simon, and Patricia Fanning.
2008 Developing a Landscape History as Part of a Survey Strategy: A Critique of Current Settlement System Approaches Based on Case Studies from Western New South Wales, Australia. *Journal of Archaeological Method and Theory* 15:167–189.

Holdaway, Simon, and LuAnn Wandsnider (editors).
2008 *Time in Archaeology: Time Perspectivism Revisited*. University of Utah Press, Salt Lake City.

Hull, Kathleen L.
2005 Process, Perception, and Practice: Time Perspectivism in Yosemite Native Demography. *Journal of Anthropological Archaeology* 24(4):354–377.

Hunzicker, David A.
2008 Folsom Projectile Technology: An Experiment in Design, Effectiveness, and Efficiency. *Plains Anthropologist* 53(207):291–311.

Hurst, Clarence T.
1941 A Folsom Location in the San Luis Valley, Colorado: A Preliminary Report. *Southwestern Lore* 7(2):31–34.

1943 A Folsom Site in a Mountain Valley of Colorado. *American Antiquity* 8(3):250–253.

Hurst, Stance, and Eileen Johnson.
2016 Gearing Up at the Adair-Steadman (41FS2) Folsom Site. *Paleoamerica* 2(3):252–260.

2019 *Adair-Steadman (41FS2) - Survey at a Folsom Site in the Brazos River Drainage on the Southern Plains*. Museum of Texas Tech University, Lubbock.

Jayalath, K.
2013 Spatial Point Process in Pre-Historic House Rocks Structures. PhD Dissertation, Southern Methodist University, Dallas, Texas.

Jayalath, K., Richard F. Gunst, and David J. Meltzer.
2015 Spatial Point Pattern Identification of an Apparent Ice-Age House Structure. *Spatial Statistics* 14:563–580.

Jennings, Thomas A.
2016 The Impact of Stone Supply Stress on the Innovation of a Cultural Variant: The Relationship of Folsom and Midland. *Paleoamerica* 2(2):116–123.

Jennings, Thomas A., Charlotte D. Pevny, and William A. Dickens.
2010 A Biface and Blade Core Efficiency Experiment: Implications for Early Paleoindian Technological Organization. *Journal of Archaeological Science* 37:2155–2164.

Jodry, Margaret A.
1992 Fitting Together Folsom: Refitted Lithics and Site Formation Processes at the Stewart's Cattle Guard Site. In *Piecing Together the Past: Applications of Refitting Studies in Archaeology*, edited by Jack L. Hofman and J.G. Enloe, pp. 179–209. International Series No. 578. British Archaeological Reports, Oxford.

1999a Folsom Technological and Socioeconomic Strategies: Views from Stewart's Cattle Guard and the Upper Rio Grande Basin, Colorado. PhD Dissertation, American University, Washington, D.C.

1999b Paleoindian Stage. In *Colorado Prehistory: A Context for the Rio Grande Basin*, edited by Marilyn A. Martorano, Ted Hoefer III, Margaret A. Jodry, Vince Spero, and Melissa Taylor, pp. 45–115. Colorado Council of Professional Archaeologists, Denver.

Jodry, Margaret A., and Dennis J. Stanford.
1992 Stewart's Cattle Guard Site: An Analysis of Bison Remains in a Folsom Kill-Butchery Campsite. In *Ice Age Hunters of the Rockies,* edited by D. J. Stanford and J. S. Day, pp. 101-168. Denver Museum of Natural History and University Press of Colorado, Niwot, Colorado.

1996 Changing Hydrologic Regimes and Prehistoric Landscape Use in the Northern San Luis Valley, Colorado. In *Geologic Excursions to the Rocky Mountains and Beyond. Fieldtrip Guidebook for the 1996 Annual Meeting of the Geological Society of America, Denver.* Special Publication 44. Colorado Geological Survey.

Jodry, M.A., M.D. Turner, V. Spero, J.C. Turner, and D.J. Stanford.
1996 Folsom in the Colorado High Country. *Current Research in the Pleistocene* 13:25-27.

Johnston, Christopher M.
2021 *Projectile Points from the Scott Miller Site, Rio Grande County, Colorado*. Research Contribution 120. Archaeological Investigations in the San Luis Valley 8. Paleocultural Research Group, Broomfield, Colorado. Submitted to the U.S. Fish and Wildlife Service, Lakewood, Colorado.

Johnston, Christopher M., and Kelton A. Meyer.
2024 *Archaeology of a Relic Wetland, Alamosa County, Colorado*. Research Contribution 130. Archaeological Investigations in the San Luis Valley 11. Paleocultural Research Group, Broomfield, Colorado. Submitted to History Colorado – State Historical Fund, Denver and the Colorado State Land Board, Denver.

Jones, Chris M., James S. Marron, and Simon J. Sheather.
1996 A Brief Survey of Bandwidth Selection for Density Estimation. *Journal of the American Statistical Association* 91(433):401–407.

Kelly, Robert L.
1988 The Three Sides of a Biface. *American Antiquity* 53(4):717–734.

Kelly, Robert L., and Lawrence C. Todd.
1988 Coming into the County: Early Paleoindian Hunting and Mobility. *American Antiquity* 53(2):231–244.

Kent, Susan.
1991 The Relationship Between Mobility Strategies and Site Structure. In *The Interpretation of Archaeological Spatial Patterning*, edited by Ellen M. Kroll and T. Douglas Price, pp. 33–60. Plenum Press, New York.

Kintigh, Keith W.
1990 Intrasite Spatial Analysis: A Commentary on Major Methods. In *Mathematics and Information Science in Archaeology: A Flexible Framework*, edited by Albertus Voorrips, pp. 165–200. Studies in Modern Archaeology No. 3. Holos, Bonn.

Kirkham, Robert M., and A.W. Magee.
2020 Geologic History of the San Luis Valley. In *The Geology, Ecology, and Human History of the San Luis Valley*, pp. 9–57. University Press of Colorado, Louisville.

Kornfeld, Marcel.
2013 *The First Rocky Mountaineers: Coloradans Before Colorado*. University of Utah Press, Salt Lake City.

Krall, Angie.
2016 *Rio Grande National Forest Assessment 12: Areas of Tribal Importance*. Rio Grande National Forest, Monte Vista, CO.

Kuhn, Steven L.
1994 A Formal Approach to the Design Assembly of Mobile Toolkits. *American Antiquity* 59:426–442.

1995 *Mousterian Lithic Technology: An Ecological Perspective*. Princeton University Press, New Jersey.

Kuhn, Steven L., David A. Raichlen, and Amy E. Clark.
2016 What Moves Us? How Mobility and Movement Are at the Center of Human Evolution. *Evolutionary Anthropology* 25(3):86–97.

Kuhn, Steven L., and Mary C. Stiner.
2019 Hearth and Home in the Middle Pleistocene. *Journal of Anthropological Research* 75(3):305–327.

Kulldorff, Martin.
2006 Tests of Spatial Randomness Adjusted for an Inhomogeneity: A General Framework. *Journal of the American Statistical Association* 101(475):1289–1305.

LaBelle, Jason M.
2003 Coffee Cans and Folsom Points: Why We Cannot Continue to Ignore the Artifact Collectors. In *Ethical Issues in Archaeology*, edited by Larry J. Zimmerman, Karen D. Vitelli, and Julie-Hollowell-Zimmer, pp. 115–127. Altamira Press, Walnut Creek, California.

2010 Reoccupation of Place: Late Paleoindian Land Use Strategies in the Central Plains. In *Exploring Variability in Early Holocene Hunter-Gatherer Lifeways*, edited by Stance Hurst and Jack Hofman, pp. 37–72. University of Kansas Publications in Archaeology No. 25. University of Kansas, Lawrence.

2012 Hunter-Gatherer Adaptations of the Central Plains and Rocky Mountains of Western North America. In *Hunter-Gatherer Behavior: Human Response During the Younger Dryas*, edited by Metin I. Eren, pp. 139–164. Left Coast Press, Walnut Creek, California.

LaBelle, Jason M., and Kelton A. Meyer.
2021 Kill, Camp, and Repeat: Return to the Lindenmeier Folsom Site, Colorado. *Great Plains Research* 31:75–96.

LaBelle, Jason M., Kelton A. Meyer, and Raymond V. Sumner.
2021 The Johnson Site in the Foothills of Larimer County, Colorado. *Paleoamerica* 7(2):162–180.

LaBelle, Jason M., and Cody C. Newton.
2010 Red Ochre, End Scrapers, and the Folsom Occupation of the Lindenmeier Site, Larimer County, Colorado. *Current Research in the Pleistocene* 27:112–115.

Larson, Mary Lou, and Marcel Kornfeld.
1997 Chipped Stone Nodules: Theory, Method, and Examples. *Lithic Technology* 22(1):4–18.

Lassen, Robert D.
2013 A Flute Runs Through It, Sometimes...Understanding Folsom-Era Stone Tool Variation. PhD Dissertation, University of Tennessee, Knoxville.

2015 The Folsom-Midland Component of the Gault Site, Central Texas: Context, Technology, and Typology. *Plains Anthropologist* 60(234):150–171.

2016 The Spectrum of Variation in Folsom-Era Projectile Point Technology. *Paleoamerica* 2(2):150–158.

Lassen, Robert D., and Thomas Williams.
2015 Variation in Flintknapping Skill among Folsom-Era Projectile Point Types: A Quantitative Approach. *Journal of Archaeological Science: Reports* 4:164–173.

Laughlin, John.
2005 149 Refits: Assessing Site Integrity and Hearth-Centered Activities at Barger Gulch Locality B. Master's Thesis, University of Wyoming, Laramie.

Laughlin, John, and Robert L. Kelly.
2010 Experimental Analysis of the Practical Limits of Lithic Refitting. *Journal of Archaeological Science* 37(2):427–433.

Leckman, Phillip O., and Michael Heilen.
2023 Our Checkered Past: Sites, Landscapes, Trails, and Transect-Recording Unit Survey. *Advances in Archaeological Practice* 11(1):11–28.

LeTourneau, Philippe D.
2000 Folsom Toolstone Procurement in the Southwest and Southern Plains. PhD Dissertation, University of New Mexico, Albuquerque.

Lipman, P.W., and O. Bachmann.
2015 *Ignimbrites to Batholiths: Integrating Perspectives from Geological, Geophysical, and Geochronological Data*. Geological Society of America, Boulder.

Lowell, Thomas V., and Meredith A. Kelly.
2008 Was the Younger Dryas Global? *Science* 321(5887):348–349.

Lyman, R. Lee.
2015 North American Paleoindian Eyed Bone Needles: Morphometrics, Sewing, and Site Structure. *American Antiquity* 80(1):146–160.

Madden, Robert.
2024 Chronology, Spatial Organization, and Mobility at Flattop Butte (5LO34), a Prehistoric Lithic Quarry in the Central Plains of North America. Master's Thesis, Colorado State University, Fort Collins.

Madole, Rich.
2020 Pleistocene Glaciations and the Evolution of the Great Sand Dunes. In *The Geology, Ecology, and Human History of the San Luis Valley*, edited by J.M. Beeton, C.N. Saenz, B.J. Maxwell, pp. 81–105. University Press of Colorado, Louisville.

Magnani, Matthew, Matthew Douglass, Whittaker Schroder, Jonathan Reeves, and David R. Braun.
2020 The Digital Revolution to Come: Photogrammetry in Archaeological Practice. *American Antiquity* 85(4):737–760.

Mallouf, Robert J.
1989 A Clovis Quarry Workshop in the Callahan Divide. *Plains Anthropologist* 34(124):82–103.

Martorano, Marilyn A., Ted Hoefer III, Margaret A. Jodry, Vince Spero, and Melissa L. Taylor.
1999 *Colorado Prehistory: A Context for the Rio Grande Basin*. Colorado Council of Professional Archaeologists, Denver.

Meltzer, David J.
1983 The Antiquity of Man and the Development of American Archaeology. In *Advances in Archaeological Method and Theory*, edited by Michael B. Schiffer, pp. 1–51. Academic Press, New York.

1989 Was Stone Exchanged Among Eastern North American Paleoindian? In *Eastern Paleoindian Lithic Resource Use*, edited by C.J. Ellis and J.C. Lothrop, pp. 15-36. Westview Press, Boulder, Colorado.

1994 The Discovery of Deep Time: A History of Views on the Peopling of the Americas. In *Method and Theory for Investigating the Peopling of the Americas*, edited by R. Bonnichsen and D.G. Steele, pp. 7–26. Center for the Study of the First Americans, Corvallis, Oregon.

2006 *Folsom: New Archaeological Investigations of a Classic Paleoindian Bison Kill*. University of California Press, Berkeley.

Meltzer, David J., and Metin I. Eren.
2021 The Mountaineer Folsom Projectile Point Assemblage. In *The Mountaineer Site: A Folsom Winter Camp in the Rockies*, edited by Brian N. Andrews, David J. Meltzer, and Mark Stiger, pp. 296–358. University Press of Colorado, Louisville.

Meltzer, David J., and Vance T. Holliday.
2010 Would North American Paleoindians Have Noticed Younger Dryas Age Climate Changes? *Journal of World Prehistory* 23:1–41.

Meltzer, David J., John D. Seebach, and Ryan M. Byerly.
2006 The Hot Tubb Folsom-Midland Site (41CR10), Texas. *Plains Anthropologist* 51(198):157–184.

Merriman, Christopher W.
2022 Paleoindian Response to Climate Change in the Northern Jornada Del Muerto, New Mexico. PhD Dissertation, University of New Mexico, Albuquerque.

Mitchell, Mark D.
2012 *High Altitude Archaeology in the Uncompahgre Wilderness*. Research Contribution 87. Paleocultural Research Group, Broomfield, Colorado. Submitted to History Colorado – State Historical Fund and the U.S. Forest Service, Delta, Colorado.

2017 Introduction. In *Archaeology of the Upper Crossing Stone Enclosures, Saguache County, Colorado*, edited by Mark D. Mitchell and Carl R. Falk, pp. 1–28. Research Contribution 99, Archaeological Investigations in the San Luis Valley 3 No. Paleocultural Research Group, Broomfield, Colorado.

Mitchell, Mark D., and Angie Krall.
2020 Indigenous Lifeways in the San Luis Valley. In *The Geology, Ecology, and Human History of the San Luis Valley*, edited by J.M. Beeton, C.N. Saenz, B.J. Maxwell, pp. 301–332. University Press of Colorado, Louisville.

Morgan, Brooke M.
2015 Folsom Settlement Organization in the Southern Rocky Mountains: An Analysis of Dwelling Space at the Mountaineer Site. PhD Dissertation, Southern Methodist University, Dallas, Texas.

Morgan, Brooke M., and Brian N. Andrews.
2016 Folsom Stone Tools Distribution at the Mountaineer Block C Dwelling: Indoor and Outdoor Spaces as Activity Areas. *Paleoamerica* 2(2):179–187.

2022 Architecture and Human Behavior at a Folsom Period Residential Camp. In *More than Shelter from the Storm: Hunter-Gatherer Houses and the Built Environment*, edited by Brian N. Andrews and Danielle Macdonald, pp. 140–158. University Press of Florida, Gainesville.

Morrow, Juliet E.
1997 End Scraper Morphology and Use-Life: An Approach for Studying Paleoindian Lithic Technology and Mobility. *Lithic Technology* 22(1):70–85.

Murrell, Monica L., and Jesse B. Murrell.
2015 Secondary Raw Material Sources of Pedernal Chert in the Albuquerque Basin, New Mexico. *Kiva* 80(3–4):221–249.

Nami, Hugo G.
1999 The Folsom Biface Reduction Sequence: Evidence from the Lindenmeier Collection. In *Folsom Lithic Technology: Explorations in Structure and Variation*, edited by Daniel S. Amick, pp. 82–97. Archaeological Series No. 12. International Monographs in Prehistory, Ann Arbor, Michigan.

Naze, Brian S.
2013 Evaluating Traditional and Alternative Perspectives on Paleoindian Land Use: The View from the Central Plains and Southern Rocky Mountains. PhD Dissertation, University of Colorado, Boulder.

O'Connell, James F.
1987 Alyawara Site Structure and Its Archaeological Implications. *American Antiquity* 52(1):74–108.

O'Connell, James F., K. Hawkes, and N. Blurton Jones.
1991 Distribution of Refuse-Producing Activities at Hadza Base Camps: Implications for Analyses of Archaeological Site Structure. In T*he Interpretation of Archaeological Spatial Patterning*, edited by Ellen M. Kroll and T. Douglas Price, pp. 61–76. Plenum Press, New York.

Odell, George H.
2004 *Lithic Analysis*. Plenum Press, New York.

Osborn, Alan J.
2014 Eye of the Needle: Cold Stress, Clothing, and Sewing Technology During the Younger Dryas Cold Event in North America. *American Antiquity* 79(1):45–68.

Pelton, Spencer R.
2018 A Thermoregulatory Framework for Hominin Research: Archaeological and Ethnographic Studies with Implications for Global Hominin Dispersal. PhD Dissertation, University of Wyoming, Laramie.

Pelton, Spencer R., Joshua R. Boyd, Heather Rockwell, and Cody C. Newton.
2016 Younger Dryas-Aged Fluting, Cold, and Time Budgeting in the Great Plains and Rocky Mountains. *Paleoamerica* 2(2):169–178.

Pelton, Spencer R., McKenna Litynski, Sarah A. Allaun, Michael Buckley, Jack Govaerts, Todd Schoborg, Matthew O'Brien, et al.
2024 Early Paleoindian Use of Canids, Felids, and Hares for Bone Needle Production at the La Prele Site, Wyoming, USA. *PLoS ONE* 19(11):e0313610.

Pitblado, Bonnie L., Carol Dehler, Hector Neff, and Stephen T. Nelson.
2008 Pilot Study Experiments Sourcing Quartzite, Gunnison Basin, Colorado. *Geoarchaeology* 23(6):742–778.

Prasciunas, Mary M.
2004 Bifacial versus Amorphous Core Technology: Experimental Testing of Differential Flake Tool Production Efficiency. PhD Dissertation, University of Wyoming, Laramie.

2007 Bifacial Cores and Flake Production Efficiency: An Experimental Test of Technological Assumptions. *American Antiquity* 72(2):334–348.

Reimer, Paula J., William E. N. Austin, Edouard Bard, Alex Bayliss, Paul G. Blackwell, Christopher Bronk Ramsey, Martin Butzin, et al.
2020 The IntCal20 Northern Hemisphere Radiocarbon Age Calibration Curve (0–55 Cal kBP). *Radiocarbon* 62:725–757.

Reitze, William T., Christina Sinkovec, and Bruce B. Huckell.
2012 Folsom Technology and Toolstone Use at the Martin Site, North Central New Mexico. *Plains Anthropologist* 57(223):237–259.

Ricotta, Carlo.
2007 Random Sampling Does Not Exclude Spatial Dependence: The Importance of Neutral Models for Ecological Hypothesis Testing. *Folia Geobotanica* 42:153–160.

Roberts Jr., Frank H.H.
1935 *Folsom Complex: Preliminary Report on Investigations at the Lindenmeier Site in Northern Colorado*. Smithsonian Institution, Washington, D.C.

1936 Additional Information on the Folsom Complex: Report on the Second Season's Investigations at the Lindenmeier Site in Northern Colorado. *Smithsonian Miscellaneous Collections* 95(10).

Rogers, Karel L., Edwin E. Larson, Gary Smith, Danny Katzman, Gerald R. Smith, Thure Cerling, Yang Wang, et al.
1992 Pliocene and Pleistocene Geologic and Climatic Evolution in the San Luis Valley of South-Central Colorado. *Paleogeography, Paleoclimatology, Paleoecology* 94:55–86.

Rogers, Richard A.
1986 Spurred End Scrapers as Diagnostic Paleoindian Artifacts: A Distributional Analysis on Stream Terraces. *American Antiquity* 51(2):338–341.

Root, Mathew J. (editor).
2000 *The Archaeology of the Bobtail Wolf Site: Folsom Occupation of the Knife River Flint Quarry Area, North Dakota*. Washington State University Press, Pullman.

Ruleman, C.A., and T.R. Brandt.
2021 *Surficial Geology of the Northern San Luis Valley, Saguache, Fremont, Custer, Alamosa, Rio Grande, Conejos, and Costilla Counties, Colorado*. U.S. Geological Survey, Denver.

Ruppert, David, and Daren B.H. Cline.
1994 Bias Reduction in Kernel Density Estimation by Smoothed Empirical Transformations. *Annals of Statistics* 22(1):185–210.

Ryan, Shannon R.
2016 Recognizing Paleoindian Hideworking Activity Areas on the Great Plains. PhD Dissertation, University of Kansas, Lawrence.

Schiffer, Michael B.
1975 Archaeology as a Behavioral Science. *American Anthropologist* 77:836–848.

Schiffer, Michael B., Alan P. Sullivan, and Timothy C. Klinger.
1978 The Design of Archaeological Surveys. *World Archaeology* 10(1):1–28.

Schumann, R. Randall, and Michael N. Machette.
2007 *Late Pleistocene to Early Holocene Paleoecology of the Mr. Peat Wetland Deposit, Alamosa County, Colorado.* U.S. Geological Survey, Reston, Virginia.

Scott, David W.
1992 *Multivariate Density Estimation: Theory, Practice and Visualization*. Wiley, New York.

2010 Scott's Rule. *Computational Statistics* 2(3):497–502.

Seebach, John D.
2004 Past and Present at the Chispa Creek Folsom Site. *Journal of Big Bend Studies* 16:1–30.

Sellet, Frederic.
2004 Beyond the Point: Projectile Manufacture and Behavioral Inference. *Journal of Archaeological Science* 31(11):1553–1566.

2013 Anticipated Mobility and Its Archaeological Signature: A Case Study of Folsom Retooling Strategies. *Journal of Anthropological Archaeology* 32:383–396.

Shackley, M. Steven.
2011 Sources of Archaeological Dacite in Northern New Mexico. *Journal of Archaeological Science* 38(5):1001–1007.

2021 Distribution and Sources of Secondary Deposit Archaeological Obsidian in Rio Grande Alluvium, New Mexico. *Geoarchaeology* 36:808–825.

2022 *Source Provenance of Obsidian and Volcanic Rock Artifacts from the Reddin Folsom Site (5SH77), Southern Colorado*. Geoarchaeological XRF Laboratory Report, Albuquerque, New Mexico.

Sheather, Simon J. and Michael C. Jones
1991 A Reliable Data-based Bandwidth Selection Method for Kernel Density Estimation. *Journal of the Royal Statistical Society: Series B (Methodological),* 53(3):683-690.

Shott, Michael J.
1995 How Much Is a Scraper? Curation, Use Rates, and the Formation of Scraper Assemblages. *Lithic Technology* 20:53–72.

Shott, Michael J., and Kathryn J. Weedman.
2007 Measuring Reduction in Stone Tools: An Ethnoarchaeological Study of Gamo Hidescrapers from Ethiopia. *Journal of Archaeological Science* 34(7):1016–1035.

Smith, Gary A., and Bruce B. Huckell.
2005 The Geological and Geoarchaeological Significance of Cerro Pedernal, Rio Arriba County, New Mexico. In *Geology of the Chama Basin, 56th Field Conference Guidebook*, edited by Lucas G. Spencer, Kate E. Zeigler, Virgil W. Lueth, and Donald E. Owen, pp. 425–431. New Mexico Geological Society, Albuquerque.

Sobkowiak-Tabaka, Iwona, and Aleksandr Diachenko.
2020 Fire and "Noise" in Late Paleolithic Camps: An Investigation of Issues in Locating Hearths. *Journal of Paleolithic Archaeology* 3(4):509–524.

Speth, John D.
2020 Paleoindian Bison Hunting on the North American Great Plains - Two Critical Nutritional Constraints. *Paleoanthropology*:74–97.

Stanford, Dennis J.
1990 A History of Archaeological Research in the San Luis Valley. *San Luis Valley Historian* 22(3):33–39.

Stiger, Mark.
2006 A Folsom Structure in the Colorado Mountains. *American Antiquity* 71(2):321–351.

Surovell, Todd A.
2003 The Behavioral Ecology of Folsom Lithic Technology. PhD Dissertation, University of Arizona, Tucson.

2009 *Toward A Behavioral Ecology of Lithic Technology: Cases from Paleoindian Archaeology*. University of Arizona Press, Tucson.

2022 *Barger Gulch: A Folsom Campsite in the Rocky Mountains*. University of Arizona Press, Tucson.

Surovell, Todd A., and Nicole M. Waguespack.
2007 Folsom Hearth-Centered Use of Space at Barger Gulch, Locality B. In *Frontiers in Colorado Paleoindian Archaeology: From the Dent Site to the Rocky Mountains*, edited by Robert H. Brunswig and Bonnie L. Pitblado, pp. 219–259. University Press of Colorado, Louisville.

Surovell, Todd A., Nicole M. Waguespack, James H. Mayer, Marcel Kornfeld, and George C. Frison.
2005 Shallow Site Archaeology: Artifact Dispersal, Stratigraphy, and Radiocarbon Dating at the Barger Gulch Locality B Folsom Site, Middle Park, Colorado. *Geoarchaeology* 20(6):627–649.

Todd, Lawrence C.
1987 Analysis of Kill-Butchery Bonebeds and Interpretation of Paleoindian Hunting. In *The Evolution of Human Hunting*, edited by M.H. Nitecki and D.V. Nitecki, pp. 225–266. Plenum Press, New York.

Upson, J.E.
1939 Physiographic Subdivisions of the San Luis Valley, Southern Colorado. *Journal of Geology* 47(7):721–736.

Waagen, Jitte.
2019 New Technology and Archaeological Practice: Improving the Primary Archaeological Recording Process in Excavation by Means of UAS Photogrammetry. *Journal of Archaeological Science* 101:11–20.

Waguespack, Nicole M., and Todd A. Surovell.
2014 A Simple Method for Identifying Households Using Lithic Assemblages: A Case Study from a Folsom Campsite in Middle Park, Colorado. In *Lithics in the West: Using Lithic Analysis to Solve Archaeological Problems in Western North America*, edited by D.H. Macdonald, William Andrefsky Jr., and P.L. Yu, pp. 35–49. University of Montana Press, Missoula.

Wandsnider, LuAnn.
1996 Describing and Comparing Archaeological Spatial Structures. *Journal of Archaeological Method and Theory* 3(4):319–384.

Wandsnider, LuAnn, and Eileen Camilli.
1992 The Character of Surface Archaeological Deposits and Its Influence in Survey Accuracy. *Journal of Field Archaeology* 19:169–188.

Ward, Christine G.
2011 Procurement and Landscape: Lithic Quarries as Places. In *Contemporary Archaeologies of the Southwest*, edited by William H. Walker and Kathryn R. Venzor, pp. 49–66. University Press of Colorado, Boulder.

Warren, A. Helene.
1974 The Ancient Mineral Industries of Cerro Pedernal, Rio Arriba County, New Mexico. In *Guidebook: Ghost Ranch Central-Northern New Mexico, New Mexico Geological Society 25th Annual Fall Field Conference Guidebook*, pp. 87–93. New Mexico Geological Society, Albuquerque.

Western Regional Climate Center
2024 Western U.S. Historical Climate Summaries. Electronic document, https://wrcc.dri.edu/summary/Climsmco.html, accessed June 15, 2024.

Whitelaw, Todd.
1991 Some Dimensions of Variability in the Social Organization of Community Space Among Foragers. In *Ethnoarchaeological Approaches to Mobile Campsites*, edited by Clive S. Gamble and William A. Boismier, pp. 131–188. Archaeological Series No. 12. International Monographs in Prehistory, Ann Arbor, Michigan.

Wilmsen, Edwin M.
1974 *Lindenmeier: A Pleistocene Hunting Society*. Harper and Row, New York.

Wilmsen, Edwin M., and Frank H.H. Roberts Jr.
1978 *Lindenmeier, 1934-1974: Concluding Report on Investigations*. Smithsonian Contributions to Anthropology No. 24. Smithsonian Institution Press, Washington, D.C.

Wilshusen, Richard H., Michael Heilen, Wade Catts, Karyn de Dufour, and Bradford Jones.
2016 Archaeological Survey Data Quality, Durability, and Use in the United States: Findings and Recommendations. *Advances in Archaeological Practice* 4(2):106–117.

Wunderlich, Robert G., Jr.
2011 Flaked Lithics. In *Draft Archaeology of Great Sand Dunes National Park and Preserve, Alamosa and Saguache Counties, Colorado*, edited by Chris M. Bevilacqua, Robert G. Wunderlich Jr., Marilyn A. Martorano, and Eric M. Hendrickson, pp. 63–108. RMC Consultants, Wheatridge, Colorado.

Yellen, John E.
1977 *Archaeological Approaches to the Present: Models for Reconstructing the Past*. Academic Press, New York.

Yuan, Fasong, Max R. Koran, and Andrew Valdez.
2013 Late Glacial and Holocene Record of Climatic Change in the Southern Rocky Mountains from Sediments in San Luis Lake, Colorado, USA. *Paleogeography, Paleoclimatology, Paleoecology* 392:146–160.

APPENDICES

General Codes – All Artifacts

Portion – basic fragment code
- CO (complete)
- NC (near-complete)
- PR (proximal)
- MS (midsection)
- LT (lateral)
- DS (distal)
- END (indeterminate end fragment – distal or proximal)

Burning – burning damage
- POT (potlid fractures present)
- CRZ (crazing fractures present)
- PTCZ (potlid fractures and crazing present)
- NO (not visibly burned)

GENMAT – general lithic raw material type
- CCS (crypto-crystalline silicate including chert, chalcedony, agate, jasper)
- VOL (extrusive igneous rock)
- QZT (quartzite)
- SWD (silicified wood)

SPECMAT – specific lithic raw material type, visually attributed
- TRT (Trout Creek jasper)
- DAC (unsourced dacite, andesite, basalt, or other non-glassy black rock)
- DAK (Dakota Formation quartzite, likely from Trickle Mountain)
- MOR (unsourced Morrison Formation quartzite)
- CUMB (Cumbres Pass chert)
- PED (Cerro Pedernal chalcedony)
- MOSC (Mosca Creek chert)
- FLAT (Flattop Butte or White River Group silicate)
- NARB (Narbona Pass or Chuska Mountains chalcedony)
- RHY (unsourced rhyolite or coarse-grained extrusive igneous rock)
- SWD (unsourced silicified wood)
- OBS (volcanic glass – undifferentiated by geochemical source)
- EDW (Edwards Plateau chert)
- UNK (unknown)

Folsom Codes

Type – time-diagnostic typology
- FOLSOM (Folsom;)
- MIDLAND (Midland;)

- FOLS/MID (either Folsom or Midland;)

Meltzer – Meltzer (2006) or Meltzer and Eren (2021) portion code
- Projectile points
  - 1a – complete
  - 2a – tip with more than 7.5 mm of ground edge length
  - 2b – tip with less than 7.5 mm of ground edge length
  - 2c – tip no edge grinding present
  - 2d – unground lateral split tip edge
  - 3a – midsection with greater than 7.5 mm of ground edge length AND greater than 7.5 mm of unground blade edge
  - 3b – midsection with greater than 7.5 mm of ground edge length AND less than 7.5 mm of unground blade edge
  - 3c – midsection with no edge grinding
  - 3d – midsection with less than 7.5 mm of ground edge length AND greater than 7.5 mm of unground blade edge
  - 3e – midsection with less than 7.5 mm of ground edge length AND less than 7.5 mm of unground blade edge
  - 3f – midsection with all blade edges completely ground
  - 3g – lateral midsection with completely ground blade edge
  - 4a – base with greater than 7.5 mm of unground blade edge
  - 4b – base with less than 7.5 mm of unground blade edge AND greater than 7.5 mm of ground blade edge
  - 4c – base with all blade edges ground
  - 4d – lateral split base with all edges ground
  - 4e – ground basal ear fragment
- Preforms
  - 1a – complete
  - 5a – near-complete with one or more ears missing
  - 5b – distal end with more than half of preform still present
  - 5c – distal end with less than half of preform still present
  - 6a – midsection with portion of distal tip and base present
  - 6b – midsection with portion of tip present, base missing
  - 6c – midsection with tip missing and portion of base present
  - 6d – midsection with tip and base missing
  - 6e – lateral split with base and tip missing
  - 7a – base with greater than half of preform still present
  - 7b – base with less than half of preform still present
  - 7c – base with ear missing
  - 7d – lateral split preform base
  - 7e – unground basal ear fragment

PsFlO; PsFlR – pseudo-fluted obverse face (PsFlO) or reverse face (PsFlR)
- YES (pseudo-fluted)
- NO (not pseudo-fluted)
- NC (fragment too broken for evaluation)

- NF (not fluted)

Nib – fluting platform present
- NC (fragment not complete enough to determine presence of fluting platform)
- NA (not attributable to fragment type)
- NO (fluting platform not present)
- YES (fluting platform present)

Flt – presence of flute for preforms
- YES – at least one channel flake scar present
- NO – no channel flake scar observed

Post-Folsom Projectile Point Codes

Type – time-diagnostic typology
- PLANO (Late Paleo stemmed or lanceolate; est. 10,000 – 7500 BP)
- JAY (Oshara Tradition – Jay type; 10,700 – 7500 BP)
- BAJADA TA (Oshara Tradition – Bajada Type A; 7500 – 4500 BP)
- SAN JOSE (Oshara Tradition – San Jose stemmed; 5000 – 3000 BP)
- MOQUINO (Oshara Tradition – Moquino square-based; 4200 – 2000 BP)
- ARMIJO (Oshara Tradition – Armijo stemmed or side-notched; 4000 – 2500 BP)
- AUGUSTIN (Oshara Tradition – Augustin stemmed; 3500 – 2000 BP)
- EN MEDIO (Oshara Tradition – En Medio corner- and side-notched; 3000 – 1600 BP)
- PELICAN LAKE (Pelican Lake corner-notched; 3250 – 1870 BP)
- UN-ARCHAIC (undetermined Archaic fragment; est. 5000 – 2000 BP)
- FORMATIVE CN (Formative era corner-notched; est. 2000 – 500 BP)
- FORMATIVE SN (Formative era side-notched; est. 1500 – 500 BP)
- FORMATIVE TRI (Formative era tri-notched; est. 500 – 200 BP)
- FORMATIVE STEM (Formative era stemmed; est. 500 – 200 BP)
- FORMATIVE UNN (Formative era unnotched; est. 500 – 200 BP)
- UN-FORMATIVE (undetermined Formative era fragment; est. 2000 – 500 BP)

Shape – hafting element shape
- STEM (stemmed base)
- CN (corner-notched base)
- SN (corner-notched base)
- TRI (tri-notched base)
- LANCE (lanceolate base/blade shape)
- NONE (unnotched triangular base shape)

Serration – blade serration
- NO (blade edges not serrated)
- YES (blade edges serrated)

Flake Tool Codes

SPUR – disto-lateral spur present (end scrapers)
- YES (spur present)
- NO (spur not present)

BfUf – bifacial or unifacial retouch present (retouched and utilized flake tools)
- UF (unifacial retouch only)
- BF (bifacial retouch present)

MULTI – multiple chisel points present (gravers)
- YES (more than one graver tip on flake tool)
- NO (only one graver tip on flake tool)

Appendix B – Lithic Metric Coding

General Codes – All Artifacts

- MxLe – Maximum length in mm (oriented proximal to distal)
- MxWd – Maximum width in mm (oriented proximal to distal)
- MxTx – Maximum thickness in mm
- LGrn – Length of lateral ground edge in mm (left, obverse)
- RGrn – Length of lateral ground edge in mm (right, obverse)
- MxTB – Distance in mm from point of maximum thickness to base
- MxWB – Distance in mm from point of maximum width to base
- BaWd – Base width in mm
- BaCo – Base concavity depth in mm
- <NULL> - measurement not possible

Folsom Codes

- LP – Longest possible axis measurement in mm, not oriented
- WP – Widest possible axis measurement in mm, not oriented
- BaWd – Base width in mm
- BaCo – Base concavity depth in mm
- FlLO – Flute length in mm, obverse face
- FlLR – Flute length in mm, reverse face
- FlTk – Maximum thickness (mm) within the flute scar
- FlWO – Flute width in mm, obverse face
- FlWR – Flute width in mm, reverse face
- NfO – Number of flutes, obverse face

- NfR – Number of flutes, reverse face
- PltWd – Platform width in mm (channel flakes)
- PltTK – Platform thickness in mm (channel flakes)

Post-Folsom Projectile Point Codes

- NckWd – Neck width in mm
- NckLe – Neck length in mm
- ShlWd – Shoulder width in mm
- ShlLe – Shoulder length in mm
- NchDL – Notch depth in mm, left side, obverse face
- NchDR – Notch depth in mm, right side, obverse face
- NchDB – Basal notch depth in mm

Flake Tool Codes

- RetOL – Retouch edge length in mm, left side, dorsal face (retouched flakes and end scrapers)
- RetOR – Retouch edge length in mm, right side, dorsal face (retouched flakes and end scrapers)
- RetODS – Retouch edge length in mm, distal end, dorsal face (retouched flakes and end scrapers)
- RetRL – Retouch edge length in mm, left side, ventral face (retouched flakes and end scrapers)
- RetRR – Retouch edge length in mm, right side, ventral face (retouched flakes and end scrapers)
- RetRDS – Retouch edge length in mm, distal end, ventral face (retouched flakes and end scrapers)
- UtlOL – Utilized edge length in mm (retouch or wear), left side, dorsal face (utilized flakes)

- UtlOR – Utilized edge length in mm (retouch or wear), right side, dorsal face (utilized flakes)
- UtlODS – Utilized edge length in mm (retouch or wear), distal end, dorsal face (utilized flakes)
- UtlRL – Utilized edge length in mm (retouch or wear), left side, ventral face (utilized flakes)
- UtlRR – Utilized edge length in mm (retouch or wear), right side, ventral face (utilized flakes)
- UtlRDS – Utilized edge length in mm (retouch or wear), distal end, ventral face (utilized flakes)
- GrLeL – graver length in mm (primary graver tip or left side for multi-point, dorsal)
- GrWdL – graver width in mm (primary graver tip or left side for multi-point, dorsal)
- GrTkL – graver thickness in mm (primary graver tip or left side for multi-point, dorsal)
- GrLeR – graver length in mm (right side for multi-point, dorsal)
- GrWdR – graver width in mm (right side for multi-point graver, dorsal)
- GrTkR – graver thickness in mm (right side for multi-point graver, dorsal)

C1. Folsom and Midland projectile point descriptive data.

Catalog	Type	Portion	Code	PsFlO	PsFlR	Nib	GENMAT	SPECMAT	Nodule	Burning
CMPA-PP-1001	FOLSOM	LT	3C	NO	NO	NA	CCS	TRT	TRT-05	NO
CMPA-PP-1002	FOLSOM	LT	3G	NO	YES	NA	CCS	TRT	TRT-02	NO
CMPA-PP-1003	FOLSOM	PR	4D	NO	NF	NC	CCS	TRT	TRT-08	NO
CMPA-PP-1004	FOLSOM	PR	4C	NO	YES	YES	QZT	MOR	MOR-01	NO
CMPA-PP-1005	FOLSOM	PR	4D	NO	NO	NC	CCS	TRT	TRT-10	NO
CMPA-PP-1006	FOLSOM	PR	4C	NO	NO	NO	CCS	NARB	NARB-01	NO
CMPA-PP-1007	FOLSOM	PR	4E	NC	NC	NC	CCS	TRT	TRT-07	POT
CMPA-PP-1008	FOLSOM	LT	3C	NO	NC	NA	CCS	UNK	UNK-04	NO
CMPA-PP-1009	FOLSOM	LT	3G	YES	YES	NA	CCS	TRT	TRT-02	NO
CMPA-PP-1010	FOLSOM	LT	3C	NO	NO	NA	CCS	TRT	TRT-07	POT
CMPA-PP-1011	FOLSOM	PR	4C	NO	NO	NO	CCS	TRT	TRT-10	NO
CMPA-PP-1012	FOLSOM	DS	2D	NO	NO	NC	CCS	NARB	NARB-01	POT
CMPA-PP-1013	FOLSOM	PR	4D	NO	NO	NC	CCS	TRT	TRT-02	NO
CMPA-PP-1014	FOLSOM	LT	3G	NO	NF	NA	CCS	TRT	TRT-12	NO
CMPA-PP-1015	FOLSOM	LT	3G	NO	NC	NA	CCS	UNK	UNK-07	POT
CMPA-PP-1016	FOLSOM	LT	3G	NO	NO	NA	CCS	PED	PED-03	NO
CMPA-PP-1017	FOLSOM	PR	4D	NO	NO	NO	CCS	EDW	EDW-01	NO
CMPA-PP-1018	FOLSOM	MS	3C	NO	NC	NA	CCS	TRT	TRT-02	NO
CMPA-PP-1019	FOLSOM	PR	4E	NO	NO	NC	VOL	OBS	OBS-02	NO
CMPA-PP-1020	FOLSOM	LT	3G	NO	NO	NA	CCS	TRT	TRT-02	POT
CMPA-PP-1021	FOLSOM	LT	3G	NO	NO	NA	QZT	MOR	MOR-02	NO
CMPA-PP-1022	FOLSOM	PR	4D	NO	NO	NO	SWD	SWD	SWD-04	NO
CMPA-PP-1023	FOLSOM	LT	3C	NO	NO	NA	QZT	MOR	MOR-02	NO
CMPA-PP-1024	FOLSOM	LT	3G	NO	NO	NA	CCS	TRT	TRT-02	NO
CMPA-PP-1025	FOLSOM	MS	3F	NO	NO	NA	CCS	TRT	TRT-16	PTCZ
CMPA-PP-1026	FOLSOM	PR	4D	NO	NO	NO	CCS	UNK	UNK-01	POT
CMPA-PP-1027	FOLSOM	LT	3C	NO	NO	NA	CCS	TRT	TRT-10	NO
CMPA-PP-1028	FOLSOM	LT	3G	NO	NC	NA	CCS	TRT	TRT-09	PTCZ

Catalog	Type	Portion	Code	PsFlO	PsFlR	Nib	GENMAT	SPECMAT	Nodule	Burning
CMPA-PP-1029	FOLSOM	PR	4A	NO	NO	NO	CCS	TRT	TRT-08	NO
CMPA-PP-1030	FOLSOM	DS	2C	NO	NC	NC	QZT	MOR	MOR-02	NO
CMPA-PP-1031	FOLSOM	LT	3C	NO	NO	NA	CCS	TRT	TRT-02	NO
CMPA-PP-1032	FOLSOM	LT	3G	NO	NO	NA	CCS	UNK	UNK-03	NO
CMPA-PP-1033	FOLSOM	LT	3G	NO	YES	NA	CCS	TRT	TRT-17	POT
CMPA-PP-1034	FOLSOM	PR	4D	NO	NO	NO	CCS	TRT	TRT-10	NO
CMPA-PP-1035	FOLSOM	LT	3G	NO	NO	NA	CCS	TRT	TRT-02	NO
CMPA-PP-1036	FOLSOM	PR	4D	NO	NO	NO	CCS	NARB	NARB-01	POT
CMPA-PP-1037	FOLSOM	MS	3F	NO	NO	NA	CCS	TRT	TRT-02	NO
CMPA-PP-1038	FOLSOM	MS	3C	NO	NO	NA	CCS	CUMB	CUMB-01	NO
CMPA-PP-1039	FOLSOM	LT	3C	YES	YES	NA	CCS	TRT	TRT-08	NO
CMPA-PP-1040	FOLSOM	LT	3C	NO	NO	NA	CCS	TRT	TRT-04	NO
CMPA-PP-1041	FOLSOM	LT	3C	NO	NO	NA	CCS	TRT	TRT-07	PTCZ
CMPA-PP-1042	FOLSOM	PR	4D	NO	NO	NO	SWD	SWD	SWD-03	NO
CMPA-PP-1043	FOLSOM	PR	4D	NO	NO	NO	CCS	TRT	TRT-10	NO
CMPA-PP-1044	FOLSOM	MS	3C	NO	NF	NA	CCS	TRT	TRT-07	PTCZ
CMPA-PP-1045	FOLSOM	LT	3C	NO	NO	NA	CCS	TRT	TRT-17	NO
CMPA-PP-1046	FOLSOM	CO	1A	YES	YES	NO	CCS	TRT	TRT-02	NO
CMPA-PP-1047	FOLSOM	DS	2C	NO	NO	NC	CCS	TRT	TRT-13	NO
CMPA-PP-1048	FOLSOM	MS	3F	NO	NO	NA	CCS	TRT	TRT-08	NO
CMPA-PP-1049	FOLSOM	PR	4E	NO	NO	NC	CCS	TRT	TRT-02	NO
CMPA-PP-1050	FOLSOM	DS	2C	NO	NO	NC	CCS	TRT	TRT-05	NO
CMPA-PP-1051	FOLSOM	DS	2C	NO	NF	NC	CCS	TRT	TRT-09	NO
CMPA-PP-1052	MIDLAND	PR	4D	NF	NF	NC	CCS	EDW	EDW-01	NO
CMPA-PP-1053	FOLS/MID	LT	3G	NF	NF	NA	QZT	MOR	MOR-02	NO
CMPA-PP-1054	MIDLAND	MS	3F	NF	NF	NA	SWD	SWD	SWD-07	NO
CMPA-PP-1055	MIDLAND	PR	4D	NF	NF	NC	CCS	UNK	UNK-05	NO
SI-PP-1001	FOLSOM	MS	3B	NO	NO	NA	CCS	TRT	TRT-01	NO
SI-PP-1002*	FOLSOM	PR	4C	NO	NO	NO	CCS	TRT	TRT-02	NO
SI-PP-1003	FOLSOM	PR	4D	NO	NO	NC	CCS	TRT	TRT-03	NO
SI-PP-1004	FOLSOM	PR	4D	NO	NO	NC	CCS	TRT	TRT-02	NO

Catalog	Type	Portion	Code	PsFlO	PsFlR	Nib	GENMAT	SPECMAT	Nodule	Burning
SI-PP-1005	FOLSOM	MS	3C	NO	NO	NA	CCS	FLAT	FLAT-01	POT
SI-PP-1006	FOLSOM	MS	3F	NO	NO	NA	CCS	TRT	TRT-02	NO
SI-PP-1007	FOLSOM	MS	3C	NO	NO	NA	CCS	TRT	TRT-03	CRZ
SI-PP-1008	FOLSOM	MS	3C	NO	NF	NA	CCS	TRT	TRT-02	POT
SI-PP-1009	FOLSOM	MS	3F	NO	NO	NA	CCS	TRT	TRT-04	POT
SI-PP-1010	FOLSOM	MS	3C	NO	NO	NA	CCS	TRT	TRT-01	NO
SI-PP-1011	FOLSOM	MS	3F	NO	NO	NA	CCS	TRT	TRT-02	CRZ
SI-PP-1012	FOLSOM	PR	4D	NO	NO	NC	CCS	TRT	TRT-02	NO
SI-PP-1013	FOLSOM	MS	3C	NO	NO	NA	CCS	TRT	TRT-02	POT
SI-PP-1014	FOLSOM	MS	3C	NO	NO	NA	CCS	UNK	UNK-01	NO
SI-PP-1015	FOLSOM	MS	3B	NO	NO	NA	CCS	TRT	TRT-01	NO
SI-PP-1016	FOLSOM	PR	4C	NO	NO	NO	CCS	TRT	TRT-01	NO
SI-PP-1017	FOLSOM	PR	4C	NO	NO	YES	CCS	TRT	TRT-02	NO
SI-PP-1018	FOLSOM	PR	4C	NO	NO	NO	CCS	CUMB	CUMB-01	NO
SI-PP-1019	FOLSOM	PR	4C	NO	NF	NO	CCS	TRT	TRT-02	NO
SI-PP-1020	FOLSOM	PR	4C	NO	NO	NO	CCS	EDW	EDW-01	NO
SI-PP-1021	FOLSOM	PR	4C	NO	NO	NO	CCS	PED	PED-01	NO
SI-PP-1022	FOLSOM	PR	4C	NO	NO	NO	CCS	TRT	TRT-05	NO
SI-PP-1023	FOLSOM	MS	3A	NO	NO	NA	CCS	NARB	NARB-01	NO
SI-PP-1024	FOLSOM	PR	4C	NO	NF	NO	CCS	TRT	TRT-01	NO
SI-PP-1025	FOLSOM	MS	3G	NO	NO	NA	CCS	FLAT	FLAT-01	NO
SI-PP-1026	FOLSOM	MS	3G	NO	NO	NA	CCS	TRT	TRT-02	NO
SI-PP-1027	FOLSOM	MS	3C	YES	NO	NA	CCS	TRT	TRT-02	PTCZ
SI-PP-1028	FOLSOM	MS	3F	NO	NO	NA	CCS	TRT	TRT-02	NO
SI-PP-1029	FOLSOM	MS	3C	NC	NC	NA	CCS	TRT	TRT-01	POT
SI-PP-1030	FOLSOM	PR	4E	NO	NO	NA	CCS	TRT	TRT-02	NO
SI-PP-1031	FOLSOM	MS	3G	NO	NO	NA	CCS	CUMB	CUMB-01	NO
SI-PP-1032	FOLSOM	PR	4E	NO	NF	NA	CCS	TRT	TRT-05	NO
SI-PP-1033	FOLSOM	MS	3F	NO	NO	NA	CCS	TRT	TRT-02	NO
SI-PP-1034	FOLSOM	PR	4E	NO	NO	NA	CCS	TRT	TRT-02	POT
SI-PP-1035	FOLSOM	PR	4C	YES	NO	NA	CCS	TRT	TRT-06	NO

Catalog	Type	Portion	Code	PsFlO	PsFlR	Nib	GENMAT	SPECMAT	Nodule	Burning
SI-PP-1036	FOLSOM	PR	4E	NO	NO	NA	CCS	TRT	TRT-05	NO
SI-PP-1037	FOLSOM	PR	4E	NO	NO	NA	CCS	TRT	TRT-03	NO
SI-PP-1038	FOLSOM	LT	3C	YES	YES	NA	CCS	TRT	TRT-03	POT
SI-PP-1039	FOLSOM	PR	4E	NO	NO	NA	CCS	TRT	TRT-02	POT
SI-PP-1040	FOLSOM	PR	4C	NO	NO	NO	CCS	TRT	TRT-07	NO
SI-PP-1041	FOLSOM	DS	2D	NO	YES	NA	CCS	TRT	TRT-03	POT
SI-PP-1042	FOLSOM	PR	4C	NO	NO	NO	SWD	SWD	SWD-01	NO
SI-PP-1043	FOLSOM	MS	3C	YES	NO	NA	CCS	TRT	TRT-01	NO
SI-PP-1044	FOLSOM	PR	4E	NO	NC	NA	CCS	TRT	TRT-02	NO
SI-PP-1045	FOLSOM	DS	2C	NO	NO	NA	CCS	TRT	TRT-05	NO
SI-PP-1046	FOLSOM	PR	4D	NO	NO	NO	CCS	TRT	TRT-02	NO
SI-PP-1047	FOLSOM	PR	4C	NO	NO	NO	CCS	TRT	TRT-02	NO
SI-PP-1048	FOLSOM	PR	4C	YES	NF	NO	CCS	TRT	TRT-08	NO
SI-PP-1049	FOLSOM	PR	4C	NO	NO	NO	SWD	SWD	SWD-02	NO
SI-PP-1050	FOLSOM	LT	3C	YES	NF	NA	CCS	TRT	TRT-02	POT
SI-PP-1051	FOLSOM	PR	4D	NO	NF	YES	CCS	TRT	TRT-02	NO
SI-PP-1052	FOLSOM	PR	4E	NO	NF	NA	CCS	TRT	TRT-05	NO
SI-PP-1053	FOLSOM	LT	3G	NO	NO	NA	CCS	TRT	TRT-07	CRZ
SI-PP-1054	FOLSOM	LT	3C	NO	NO	NA	CCS	TRT	TRT-02	POT
SI-PP-1055	FOLSOM	PR	4E	YES	YES	NA	CCS	TRT	TRT-05	NO
SI-PP-1056	FOLSOM	PR	4D	NO	NO	NC	CCS	TRT	TRT-03	NO
SI-PP-1057*	FOLSOM	PR	4C	NO	NO	NO	CCS	MOSC	MOSC-01	POT
SI-PP-1058	FOLSOM	PR	4D	NO	NO	NC	CCS	EDW	EDW-01	NO
SI-PP-1059	FOLSOM	MS	3C	NO	NO	NA	QZT	MOR	MOR-01	NO
SI-PP-1060	FOLSOM	MS	3C	NO	NF	NA	CCS	TRT	TRT-07	PTCZ
SI-PP-1061	FOLSOM	PR	4D	NO	NO	NC	CCS	TRT	TRT-03	NO
SI-PP-1062	FOLSOM	PR	4D	NO	YES	NC	CCS	TRT	TRT-03	POT
SI-PP-1063	FOLSOM	MS	3C	NO	YES	NA	QZT	MOR	MOR-02	NO
SI-PP-1064	FOLSOM	PR	4A	NO	NO	YES	QZT	MOR	MOR-02	NO
SI-PP-1065	FOLSOM	LT	3G	NO	NO	NA	QZT	MOR	MOR-02	NO
SI-PP-1066	FOLSOM	PR	4D	NO	NO	NO	CCS	TRT	TRT-07	NO

Catalog	Type	Portion	Code	PsFlO	PsFlR	Nib	GENMAT	SPECMAT	Nodule	Burning
SI-PP-1067	FOLSOM	PR	4D	NO	NO	NO	QZT	MOR	MOR-02	NO
SI-PP-1068	FOLSOM	MS	3C	NO	NO	NA	QZT	MOR	MOR-03	NO
SI-PP-1069	FOLSOM	PR	4D	NO	NO	NC	CCS	TRT	TRT-09	NO
SI-PP-1070	FOLSOM	PR	4D	NO	NO	NC	QZT	MOR	MOR-02	NO
SI-PP-1071	FOLSOM	PR	4D	NO	NO	NC	QZT	MOR	MOR-02	NO
SI-PP-1072	FOLSOM	DS	2C	NO	NO	NA	CCS	CUMB	CUMB-01	NO
SI-PP-1073	FOLSOM	MS	3C	NO	NO	NA	CCS	CUMB	CUMB-02	NO
SI-PP-1074	FOLSOM	PR	4D	NO	NO	NC	CCS	TRT	TRT-05	NO
SI-PP-1075	FOLSOM	LT	3C	NO	NO	NA	CCS	TRT	TRT-05	NO
SI-PP-1076	FOLSOM	PR	4C	NO	NO	NO	QZT	DAK	DAK-01	NO
SI-PP-1077	FOLSOM	LT	3G	NO	NO	NA	CCS	TRT	TRT-04	NO
SI-PP-1078	FOLSOM	PR	4C	NO	NO	YES	QZT	DAK	DAK-02	NO
SI-PP-1079	FOLSOM	PR	4C	NO	NO	NO	QZT	MOR	MOR-03	NO
SI-PP-1080	FOLSOM	PR	4E	NO	NC	NA	CCS	EDW	EDW-02	NO
SI-PP-1081	FOLSOM	DS	2C	NO	NC	NA	QZT	MOR	MOR-03	NO
SI-PP-1082	FOLSOM	PR	4E	NO	NC	NA	QZT	DAK	DAK-03	NO
SI-PP-1083*	FOLSOM	MS	3F	NO	NO	NA	QZT	DAK	DAK-04	NO
SI-PP-1084	FOLSOM	PR	4D	NO	NF	NC	CCS	TRT	TRT-03	NO
SI-PP-1085	FOLSOM	LT	3G	NO	NO	NA	SWD	SWD	SWD-03	NO
SI-PP-1086	FOLSOM	PR	4D	NO	NC	NC	CCS	MOSC	MOSC-02	PTCZ
SI-PP-1087	FOLSOM	PR	4C	NO	NO	NO	CCS	UNK	UNK-02	NO
SI-PP-1088	FOLSOM	PR	4E	NO	NC	NA	CCS	TRT	TRT-05	NO
SI-PP-1089	FOLSOM	DS	2C	NO	NC	NA	CCS	PED	PED-02	NO
SI-PP-1090	FOLSOM	PR	4D	NO	NF	NC	CCS	TRT	TRT-10	NO
SI-PP-1091*	FOLSOM	LT	3C	NO	NO	NA	CCS	TRT	TRT-10	NO
SI-PP-1092	FOLSOM	LT	3G	NO	NO	NA	CCS	TRT	TRT-09	NO
SI-PP-1093	FOLSOM	LT	3C	NO	NC	NA	QZT	MOR	MOR-02	NO
SI-PP-1094	FOLSOM	LT	3C	NO	NO	NA	CCS	TRT	TRT-02	NO
SI-PP-1095	FOLSOM	LT	3C	NO	NO	NA	CCS	TRT	TRT-11	POT
SI-PP-1096	FOLSOM	PR	4E	NC	NC	NA	CCS	TRT	TRT-11	POT
SI-PP-1097	FOLSOM	LT	3G	NO	NO	NA	CCS	TRT	TRT-04	NO

Catalog	Type	Portion	Code	PsFlO	PsFlR	Nib	GENMAT	SPECMAT	Nodule	Burning
SI-PP-1098	FOLSOM	LT	3G	NO	NO	NA	CCS	NARB	NARB-02	NO
SI-PP-1099	FOLSOM	PR	4E	NO	NF	NA	CCS	PED	PED-01	NO
SI-PP-1100	FOLSOM	LT	3G	NO	NC	NA	CCS	MOSC	MOSC-02	POT
SI-PP-1101	FOLSOM	DS/PR	2B/4A	NO	NO	NO	CCS	UNK	UNK-03	NO
SI-PP-1102	FOLSOM	DS/MS/PR	2C/3C/4D	NO	NO	NO	CCS	TRT	TRT-03	POT
SI-PP-1103	FOLSOM	DS/LT	2C/3D	NO	NO	NA	CCS	TRT	TRT-05	NO
SI-PP-1104	FOLSOM	PR	4D/4D	NO	NO	NO	CCS	TRT	TRT-06	NO
SI-PP-1105	FOLSOM	LT	3C	NO	NC	NA	CCS	TRT	TRT-05	NO
SI-PP-1106	FOLSOM	LT	3C	NO	NO	NA	CCS	TRT	TRT-12	POT
SI-PP-1107	FOLSOM	LT	3G	NC	NC	NA	CCS	TRT	TRT-02	POT
SI-PP-1108*	FOLSOM	LT	3G	NO	NO	NA	CCS	CUMB	CUMB-01	POT
SI-PP-1109	FOLSOM	MS	3C	NO	NO	NA	CCS	TRT	TRT-10	NO
SI-PP-1110	FOLSOM	DS	2D	NO	NO	NA	CCS	UNK	UNK-07	NO
SI-PP-1111	FOLSOM	LT	3C	NO	NO	NA	SWD	SWD	SWD-04	NO
SI-PP-1112	FOLSOM	DS	2A	NO	NF	NA	SWD	SWD	SWD-05	NO
SI-PP-1113	FOLSOM	LT	3C	NO	NO	NA	CCS	PED	PED-03	NO
SI-PP-1114	FOLSOM	LT	3C	NO	NO	NA	CCS	TRT	TRT-02	NO
SI-PP-1115	FOLSOM	DS	2C	NO	NO	NA	CCS	TRT	TRT-05	NO
SI-PP-1116	MIDLAND	LT	3G	NO	NF	NC	CCS	EDW	EDW-01	NO
SI-PP-1117	FOLSOM	DS	2A	NO	NO	NA	SWD	SWD	SWD-06	NO
SI-PP-1118	FOLSOM	LT	3C	NO	NC	NA	CCS	TRT	TRT-10	NO
SI-PP-1119	FOLSOM	PR	4D	NO	NO	NO	CCS	UNK	UNK-10	POT
SI-PP-1120	FOLSOM	PR	4E	NO	NO	NA	CCS	TRT	TRT-14	NO
SI-PP-1121	FOLSOM	PR	4E	NO	NO	NA	SWD	SWD	SWD-07	NO
SI-PP-1122	FOLSOM	DS	2C	NO	NO	NA	CCS	TRT	TRT-02	NO
SI-PP-1123	FOLSOM	LT	3C	NO	NO	NA	CCS	TRT	TRT-07	PTCZ
SI-PP-1124	FOLSOM	LT	3C	NO	NO	NA	CCS	TRT	TRT-10	NO
SI-PP-1125	FOLSOM	PR	4E	NO	NF	NA	CCS	TRT	TRT-13	NO
SI-PP-1126	FOLSOM	LT	3G	NO	NF	NA	CCS	NARB	NARB-01	POT
SI-PP-1127	FOLSOM	LT	3G	NO	NO	NA	CCS	TRT	TRT-02	NO
SI-PP-1128	FOLSOM	LT	3C	NO	YES	NA	CCS	TRT	TRT-02	NO

Catalog	Type	Portion	Code	PsFlO	PsFlR	Nib	GENMAT	SPECMAT	Nodule	Burning
SI-PP-1129	FOLSOM	PR	4D	NO	NF	NO	CCS	TRT	TRT-06	NO
SI-PP-1130	FOLSOM	DS	2C	YES	NC	NA	CCS	TRT	TRT-02	NO
SI-PP-1131	FOLSOM	LT	3G	NO	YES	NA	CCS	TRT	TRT-02	POT
SI-PP-1132	FOLSOM	LT	3G	NO	NO	NA	CCS	TRT	TRT-02	NO
SI-PP-1133	FOLSOM	PR	4D	NO	NO	NO	VOL	DAC	DAC-02	NO
SI-PP-1134	FOLSOM	PR	4D	NO	NO	NC	VOL	OBS	OBS-02	NO
SI-PP-1135	FOLSOM	PR	4D	NO	NO	NO	VOL	DAC	DAC-02	NO
SI-PP-1136	FOLSOM	PR	4E	NO	NC	NA	VOL	OBS	OBS-03	NO
SI-PP-1137	FOLSOM	PR	4D	NO	NO	NC	VOL	OBS	OBS-01	NO
SI-PP-1138	FOLSOM	PR	4E	YES	NO	NA	VOL	OBS	OBS-04	NO
SI-PP-1139	FOLSOM	LT	3C	NO	NO	NA	CCS	TRT	TRT-05	NO
SI-PP-1140	FOLSOM	LT	3G	NO	NF	NA	CCS	TRT	TRT-02	POT
SI-PP-1141	FOLSOM	PR	4E	NO	NO	NA	CCS	TRT	TRT-10	NO
SI-PP-1142	FOLSOM	PR	4E	NO	NO	NA	CCS	TRT	TRT-12	NO
SI-PP-1143	FOLSOM	MS	3F	NO	NF	NA	QZT	MOR	MOR-02	NO
SI-PP-1144	FOLSOM	PR	4E	NO	NO	NA	CCS	TRT	TRT-20	NO
SI-PP-1145	FOLSOM	PR	4D	NO	NO	NC	VOL	RHY	RHY-01	NO
SI-PP-1146	FOLSOM	LT	3C	YES	NO	NA	CCS	TRT	TRT-05	POT
SI-PP-1147	FOLSOM	PR	4D	NO	NF	NC	QZT	DAK	DAK-09	NO
SI-PP-1148	FOLSOM	DS	2C	NO	NO	NA	QZT	MOR	MOR-02	NO
SI-PP-1149	FOLSOM	LT	3C	NO	NO	NA	CCS	TRT	TRT-10	NO
SI-PP-1150	FOLSOM	DS	2C	YES	NC	NA	CCS	TRT	TRT-05	NO
SI-PP-1151	FOLSOM	DS	2C	NO	NC	NA	CCS	TRT	TRT-08	NO
SI-PP-1152	FOLSOM	MS	3C	NO	NO	NA	CCS	PED	PED-02	NO
SI-PP-1153	FOLSOM	PR	4D	NO	NO	NC	CCS	TRT	TRT-03	PTCZ
SI-PP-1154	FOLSOM	LT	3C	NC	NC	NA	SWD	SWD	SWD-07	NO
SI-PP-1155	FOLSOM	DS	2C	YES	NF	NA	QZT	MOR	MOR-02	NO
SI-PP-1156	FOLSOM	LT	3C	NO	NO	NA	CCS	UNK	UNK-07	POT
SI-PP-1157	FOLSOM	LT	3C	NO	NC	NA	CCS	TRT	TRT-05	NO
SI-PP-1158	FOLSOM	LT	3G	NO	NC	NA	CCS	NARB	NARB-02	PTCZ
SI-PP-1159	FOLSOM	LT	3G	NO	NO	NA	CCS	TRT	TRT-08	POT

Catalog	Type	Portion	Code	PsFlO	PsFlR	Nib	GENMAT	SPECMAT	Nodule	Burning
SI-PP-1160	FOLSOM	LT	3E	NO	NC	NA	CCS	TRT	TRT-02	POT
SI-PP-1161	FOLS/MID	DS	2D	NF	NF	NA	CCS	TRT	TRT-02	NO
SI-PP-1162	FOLS/MID	DS	2C	NF	NF	NA	SWD	SWD	SWD-06	NO
SI-PP-1163	FOLS/MID	LT	3C	NF	NF	NA	CCS	MOSC	MOSC-04	NO
SI-PP-1164	FOLS/MID	DS	2C	NF	NF	NA	CCS	TRT	TRT-02	NO
SI-PP-1165	FOLS/MID	MS	3F	NF	YES?	NA	CCS	TRT	TRT-02	NO
SI-PP-1166	MIDLAND	PR	4C	NF	NF	NO	CCS	TRT	TRT-13	NO
SI-PP-1167	MIDLAND	PR	4C	NF	NF	NO	CCS	TRT	TRT-06	NO
SI-PP-1168	MIDLAND	PR	4D	NF	NF	NO	CCS	TRT	TRT-08	NO
SI-PP-1169	MIDLAND	PR	4C	NF	NF	NO	CCS	TRT	TRT-07	PTCZ
SI-PP-1170	MIDLAND	PR	4C	NF	NF	NO	CCS	TRT	TRT-02	NO
SI-PP-1171	MIDLAND	PR	4C	NF	NF	NC	CCS	EDW	EDW-01	NO
SI-PP-1172	MIDLAND	PR	4C	NF	NF	NO	QZT	DAK	DAK-03	NO
SI-PP-1173	FOLS/MID	MS	3F	NF	NF	NA	CCS	EDW	EDW-01	NO
SI-PP-1174	MIDLAND	PR	4C	NF	NF	NO	CCS	TRT	TRT-02	NO
SI-PP-1175*	MIDLAND	PR	4C	NF	NF	NO	CCS	PED	PED-05	NO
SI-PP-1176	MIDLAND	MS	3F	NF	NF	NA	QZT	MOR	MOR-01	NO
SI-PP-1177	MIDLAND	PR	4C	NF	NF	NO	CCS	TRT	TRT-15	NO
SI-PP-1178	FOLS/MID	DS	2C	NF	NF	NA	CCS	NARB	NARB-01	NO
SI-PP-1179	MIDLAND	LT	3G	NF	NF	NA	CCS	TRT	TRT-08	NO
SI-PP-1180	FOLS/MID	PR	4A	YES?	NF	NO	CCS	TRT	TRT-09	NO

* Potentially offsite specimen – see chapter 2 (table 6, figure 11)

C2. Folsom and Midland projectile point metric data.

Catalog	LP	WP	MxLe	MxWd	BaWd	BsCo	FlLO	FlLR	FlTk	MxTk	FlWO	FlWR	LGrn	RGrn	MxTB	MxWB	NfO	NfR	Mass (g)
CMPA-PP-1001	9.83	6.13	9.37	6.39	<Null>	<Null>	<Null>	<Null>	2.26	2.28	<Null>	<Null>	<Null>	<Null>	2.56	2.56	1	1	0.1
CMPA-PP-1002	9.49	7.46	9.49	7.46	<Null>	<Null>	<Null>	<Null>	3.18	3.26	<Null>	<Null>	<Null>	9.06	6.70	3.70	1	1	0.3
CMPA-PP-1003	16.03	7.82	15.21	8.14	<Null>	<Null>	<Null>	<Null>	3.38	3.66	<Null>	<Null>	14.05	<Null>	10.20	1.58	1	0	0.4
CMPA-PP-1004	21.14	9.36	9.55	20.86	<Null>	<Null>	<Null>	<Null>	4.03	4.32	6.34	<Null>	4.49	10.07	6.90	6.90	1	1	1.0
CMPA-PP-1005	22.98	9.78	22.98	9.78	<Null>	<Null>	<Null>	<Null>	3.39	3.86	<Null>	<Null>	22.70	<Null>	19.39	3.78	1	1	0.8

Catalog	LP	WP	MxLe	MxWd	BaWd	BsCo	FlLO	FlLR	FlTk	MxTk	FlWO	FlWR	LGrn	RGrn	MxTB	MxWB	NfO	NfR	Mass (g)
CMPA-PP-1006	18.25	10.13	8.84	15.90	14.21	1.95	<Null>	<Null>	1.91	2.68	11.50	8.07	7.85	0.66	7.74	0.67	1	1	0.3
CMPA-PP-1007	11.63	7.48	10.88	5.75	<Null>	<Null>	<Null>	<Null>	<Null>	2.96	<Null>	<Null>	9.84	<Null>	5.14	1.91	<Null>	<Null>	0.2
CMPA-PP-1008	12.23	7.79	7.98	11.69	<Null>	<Null>	<Null>	<Null>	3.23	3.86	<Null>	<Null>	<Null>	<Null>	2.86	2.86	1	1	0.4
CMPA-PP-1009	12.68	11.51	9.33	8.22	<Null>	<Null>	<Null>	<Null>	2.83	2.97	<Null>	<Null>	9.33	<Null>	7.73	1.14	1	1	0.4
CMPA-PP-1010	11.60	9.83	9.83	11.60	<Null>	<Null>	<Null>	<Null>	2.89	3.16	<Null>	<Null>	<Null>	<Null>	7.24	7.24	1	1	0.3
CMPA-PP-1011	24.72	23.79	16.67	20.18	16.20	2.57	<Null>	<Null>	2.97	3.44	16.63	12.57	15.43	16.42	13.97	13.97	1	1	1.5
CMPA-PP-1012	11.44	6.32	11.44	6.32	<Null>	<Null>	<Null>	<Null>	2.13	2.51	<Null>	<Null>	<Null>	<Null>	6.88	6.88	1	1	0.2
CMPA-PP-1013	15.77	4.83	6.45	15.23	<Null>	<Null>	<Null>	<Null>	2.35	2.86	<Null>	<Null>	3.33	<Null>	3.33	6.45	1	1	0.2
CMPA-PP-1014	17.08	14.19	15.38	11.98	<Null>	<Null>	<Null>	<Null>	3.81	3.81	<Null>	<Null>	<Null>	13.03	9.94	12.34	1	0	0.8
CMPA-PP-1015	11.33	6.48	11.33	6.48	<Null>	<Null>	<Null>	<Null>	1.95	2.22	<Null>	<Null>	<Null>	8.85	8.85	8.85	1	<Null>	0.3
CMPA-PP-1016	12.45	6.79	12.45	6.79	<Null>	<Null>	<Null>	<Null>	2.17	2.33	<Null>	<Null>	7.76	<Null>	7.67	7.67	1	1	0.2
CMPA-PP-1017	20.77	16.53	15.81	17.15	<Null>	<Null>	<Null>	<Null>	3.14	3.21	<Null>	<Null>	<Null>	13.23	4.73	10.47	1	1	1.3
CMPA-PP-1018	15.64	10.56	10.46	14.86	<Null>	<Null>	<Null>	<Null>	<Null>	2.72	11.48	<Null>	<Null>	<Null>	3.76	5.83	1	<Null>	0.4
CMPA-PP-1019	12.74	7.21	7.21	12.74	<Null>	<Null>	<Null>	<Null>	2.86	3.36	<Null>	<Null>	5.91	<Null>	6.26	6.26	1	1	0.3
CMPA-PP-1020	11.77	8.61	7.83	11.24	<Null>	<Null>	<Null>	<Null>	3.36	3.42	<Null>	<Null>	7.09	<Null>	7.83	7.83	1	1	0.3
CMPA-PP-1021	13.75	4.61	4.61	13.75	<Null>	<Null>	<Null>	<Null>	2.91	3.29	<Null>	<Null>	<Null>	4.20	2.16	2.16	1	1	0.2
CMPA-PP-1022	11.61	10.16	11.61	10.16	<Null>	1.75	<Null>	<Null>	2.86	3.28	<Null>	<Null>	11.61	<Null>	7.92	7.92	1	1	0.5
CMPA-PP-1023	16.64	10.33	10.33	16.64	<Null>	<Null>	<Null>	<Null>	2.42	2.82	<Null>	<Null>	<Null>	<Null>	5.28	5.28	1	1	0.4
CMPA-PP-1024	8.57	3.49	3.49	8.57	<Null>	<Null>	<Null>	<Null>	2.73	3.01	<Null>	<Null>	3.49	<Null>	2.18	2.18	1	1	0.2
CMPA-PP-1025	17.82	14.90	17.82	14.90	<Null>	<Null>	<Null>	<Null>	3.06	3.42	9.64	7.10	12.15	11.49	13.30	4.01	1	1	1.3
CMPA-PP-1026	13.26	12.16	12.16	13.26	<Null>	1.90	<Null>	<Null>	3.80	4.27	<Null>	<Null>	11.12	<Null>	12.16	7.40	1	1	0.8
CMPA-PP-1027	10.81	9.06	9.06	10.81	<Null>	<Null>	<Null>	<Null>	2.02	2.31	<Null>	<Null>	<Null>	<Null>	5.32	5.32	1	1	0.4
CMPA-PP-1028	11.82	10.16	11.82	10.16	<Null>	<Null>	<Null>	<Null>	<Null>	2.91	<Null>	<Null>	9.57	<Null>	0.00	6.69	1	<Null>	0.3
CMPA-PP-1029	40.69	23.78	40.69	23.78	16.85	2.58	<Null>	<Null>	3.48	4.14	13.32	13.02	17.72	18.45	26.05	26.05	1	1	4.5
CMPA-PP-1030	25.15	22.23	25.15	22.23	<Null>	<Null>	<Null>	<Null>	3.45	3.82	11.43	<Null>	<Null>	<Null>	0.00	0.00	1	<Null>	2.3
CMPA-PP-1031	13.54	9.70	9.70	13.54	<Null>	<Null>	<Null>	<Null>	2.91	3.27	<Null>	<Null>	<Null>	<Null>	0.00	0.00	1	1	0.4

Catalog	LP	WP	MxLe	MxWd	BaWd	BsCo	FlLO	FlLR	FlTk	MxTk	FlWO	FlWR	LGrn	RGrn	MxTB	MxWB	NfO	NfR	Mass (g)
CMPA-PP-1032	14.74	12.54	14.74	12.54	<Null>	<Null>	<Null>	<Null>	3.05	3.31	<Null>	<Null>	14.74	<Null>	14.74	7.44	1	1	0.6
CMPA-PP-1033	13.15	12.12	13.15	12.12	<Null>	<Null>	<Null>	<Null>	2.12	2.31	<Null>	<Null>	5.32	<Null>	10.95	10.95	1	1	0.4
CMPA-PP-1034	14.53	11.87	14.53	11.87	<Null>	3.33	<Null>	<Null>	2.81	3.88	<Null>	<Null>	13.43	<Null>	7.65	7.65	1	1	0.6
CMPA-PP-1035	22.10	11.67	22.10	11.67	<Null>	<Null>	<Null>	<Null>	3.60	3.93	<Null>	<Null>	8.55	<Null>	6.72	0.00	1	1	1.1
CMPA-PP-1036	16.06	10.21	16.06	10.21	<Null>	<Null>	<Null>	<Null>	3.15	3.38	<Null>	<Null>	10.27	<Null>	5.71	5.71	1	1	0.7
CMPA-PP-1037	21.66	11.59	11.59	21.66	<Null>	<Null>	<Null>	<Null>	3.12	3.42	14.35	<Null>	2.73	10.01	0.00	2.73	1	1	1.0
CMPA-PP-1038	20.19	13.36	13.36	20.19	<Null>	<Null>	<Null>	<Null>	3.34	4.19	9.93	10.01	<Null>	<Null>	0.00	0.00	1	1	1.4
CMPA-PP-1039	14.58	11.95	11.95	14.58	<Null>	<Null>	<Null>	<Null>	2.35	2.40	<Null>	<Null>	<Null>	<Null>	11.95	11.95	1	1	0.5
CMPA-PP-1040	10.67	8.83	10.67	8.83	<Null>	<Null>	<Null>	<Null>	2.87	2.95	<Null>	<Null>	<Null>	<Null>	8.17	8.17	1	1	0.4
CMPA-PP-1041	12.91	12.79	12.79	12.91	<Null>	<Null>	<Null>	<Null>	3.32	3.71	<Null>	<Null>	<Null>	<Null>	12.79	12.79	1	1	0.6
CMPA-PP-1042	12.56	7.63	12.56	7.63	<Null>	1.24	<Null>	<Null>	2.50	3.28	<Null>	<Null>	12.56	<Null>	12.56	0.00	1	1	0.4
CMPA-PP-1043	12.08	9.11	9.11	12.08	<Null>	2.48	<Null>	<Null>	3.18	3.66	<Null>	<Null>	6.67	<Null>	9.11	9.11	1	1	0.4
CMPA-PP-1044	22.32	8.92	8.92	22.32	<Null>	<Null>	<Null>	<Null>	4.10	4.31	13.22	<Null>	<Null>	<Null>	0.00	0.00	1	0	0.9
CMPA-PP-1045	17.76	11.11	17.76	11.11	<Null>	<Null>	<Null>	<Null>	3.48	3.93	<Null>	<Null>	<Null>	<Null>	0.00	0.00	1	1	0.8
CMPA-PP-1046	19.76	11.93	19.76	11.93	9.82	1.54	11.24	13.57	2.71	3.05	8.35	9.18	8.43	<Null>	14.42	3.90	1	1	0.8
CMPA-PP-1047	15.09	14.67	15.09	14.67	<Null>	<Null>	<Null>	<Null>	2.40	2.65	<Null>	<Null>	<Null>	<Null>	0.00	4.65	1	1	0.6
CMPA-PP-1048	20.88	15.67	15.67	20.88	<Null>	<Null>	<Null>	<Null>	2.60	3.40	13.55	11.70	10.24	6.57	15.67	3.58	1	1	1.3
CMPA-PP-1049	9.49	8.74	8.74	9.49	<Null>	<Null>	<Null>	<Null>	2.32	2.77	<Null>	<Null>	7.51	<Null>	0.00	0.00	1	1	0.2
CMPA-PP-1050	16.57	16.20	16.57	16.20	<Null>	<Null>	<Null>	<Null>	2.80	3.72	<Null>	<Null>	7.89	<Null>	0.00	3.80	1	1	1.2
CMPA-PP-1051	15.36	14.36	14.36	15.36	<Null>	<Null>	<Null>	<Null>	<Null>	3.81	10.82	<Null>	<Null>	<Null>	0.00	3.26	1	0	1.0
CMPA-PP-1052	21.91	9.95	21.91	9.95	<Null>	<Null>	<Null>	<Null>	<Null>	3.58	<Null>	<Null>	9.49	<Null>	11.51	21.91	0	0	0.9
CMPA-PP-1053	6.93	4.73	4.73	6.93	<Null>	<Null>	<Null>	<Null>	<Null>	2.66	<Null>	<Null>	4.17	<Null>	1.74	1.74	0	0	0.1
CMPA-PP-1054	18.59	11.45	11.45	18.59	<Null>	<Null>	<Null>	<Null>	<Null>	2.96	<Null>	<Null>	5.80	5.16	0.00	0.00	0	0	0.9
CMPA-PP-1055	18.36	10.96	18.36	10.96	<Null>	<Null>	<Null>	<Null>	<Null>	5.47	<Null>	<Null>	14.57	<Null>	16.85	18.36	0	0	1.0
SI-PP-1001	25.93	19.74	15.82	19.19	<Null>	<Null>	<Null>	<Null>	2.78	4.07	14.24	12.08	10.50	15.33	15.82	13.55	1	1	1.6
SI-PP-1002	28.64	24.77	20.87	21.50	20.44	2.27	<Null>	<Null>	3.38	3.87	15.19	10.33	13.09	17.05	17.76	13.39	1	1	1.9
SI-PP-1003	22.10	13.72	21.34	12.94	<Null>	<Null>	<Null>	<Null>	2.95	3.69	<Null>	<Null>	18.80	<Null>	18.80	9.36	1	1	1.2

Catalog	LP	WP	MxLe	MxWd	BaWd	BsCo	FlLO	FlLR	FlTk	MxTk	FlWO	FlWR	LGrn	RGrn	MxTB	MxWB	NfO	NfR	Mass (g)
SI-PP-1004	24.20	14.78	15.45	19.08	<Null>	<Null>	<Null>	<Null>	2.49	3.06	13.31	11.05	14.79	<Null>	15.45	14.79	1	1	0.9
SI-PP-1005	18.35	19.02	17.95	18.37	<Null>	<Null>	<Null>	<Null>	2.66	3.34	<Null>	<Null>	<Null>	<Null>	13.36	13.36	1	1	1.0
SI-PP-1006	21.24	18.59	15.08	17.38	<Null>	<Null>	<Null>	<Null>	3.25	3.76	9.41	12.23	9.59	8.45	15.04	15.04	1	1	1.4
SI-PP-1007	15.73	10.54	10.08	13.95	<Null>	<Null>	<Null>	<Null>	2.71	2.91	<Null>	<Null>	<Null>	<Null>	7.49	8.29	1	1	0.4
SI-PP-1008	23.32	15.25	11.85	20.23	<Null>	<Null>	<Null>	<Null>	3.35	3.49	14.98	<Null>	<Null>	<Null>	8.28	5.80	1	0	1.3
SI-PP-1009	23.70	11.75	14.83	21.06	<Null>	<Null>	<Null>	<Null>	3.34	3.98	15.67	16.75	14.19	5.66	8.16	8.16	1	1	1.2
SI-PP-1010	16.22	12.35	12.35	16.22	<Null>	<Null>	<Null>	<Null>	3.41	3.57	<Null>	<Null>	<Null>	<Null>	8.83	8.83	1	1	0.8
SI-PP-1011	22.28	10.42	10.42	22.28	<Null>	<Null>	<Null>	<Null>	2.80	3.27	18.11	15.19	7.62	7.25	8.64	8.64	1	1	1.2
SI-PP-1012	23.01	15.48	21.41	14.72	<Null>	<Null>	<Null>	<Null>	2.55	3.23	<Null>	<Null>	<Null>	<Null>	10.83	5.70	1	1	0.8
SI-PP-1013	23.27	21.23	15.63	18.82	<Null>	<Null>	<Null>	<Null>	3.51	3.87	15.19	<Null>	<Null>	<Null>	13.77	13.77	1	1	1.4
SI-PP-1014	21.45	19.12	16.53	18.48	<Null>	<Null>	<Null>	<Null>	3.21	3.47	11.73	14.59	<Null>	<Null>	11.30	5.39	1	1	1.4
SI-PP-1015	24.72	20.67	16.19	20.07	<Null>	<Null>	<Null>	<Null>	3.68	3.97	12.27	10.89	12.11	12.75	14.33	16.19	1	1	1.5
SI-PP-1016	25.47	24.48	18.94	21.32	20.29	2.53	<Null>	<Null>	3.08	3.81	15.23	16.53	14.86	10.18	12.92	10.29	1	1	1.9
SI-PP-1017	27.03	21.13	17.96	22.26	18.83	4.11	<Null>	<Null>	3.27	3.78	12.57	11.01	16.84	17.19	16.16	16.16	1	1	1.8
SI-PP-1018	23.97	20.46	16.11	20.02	18.32	2.24	<Null>	<Null>	2.99	3.63	13.05	14.36	14.87	13.74	13.58	13.58	1	1	1.4
SI-PP-1019	25.51	22.64	20.28	19.15	16.62	2.31	<Null>	<Null>	3.08	3.54	7.79	<Null>	17.82	8.13	20.28	5.03	1	0	1.6
SI-PP-1020	24.01	15.02	14.81	18.30	17.39	2.38	<Null>	<Null>	2.96	3.13	14.21	12.25	14.81	9.77	9.77	9.77	1	1	1.1
SI-PP-1021	24.94	23.09	21.31	21.16	<Null>	<Null>	<Null>	<Null>	2.95	3.78	13.62	10.04	11.16	16.50	15.12	15.12	1	1	1.9
SI-PP-1022	26.30	25.48	18.27	21.61	17.78	5.47	<Null>	<Null>	3.21	3.58	15.39	8.62	14.71	16.95	13.34	17.41	1	1	1.3
SI-PP-1023	29.43	16.13	29.43	16.13	<Null>	<Null>	<Null>	<Null>	3.31	3.91	10.01	12.04	16.01	10.14	12.53	12.53	1	1	2.6
SI-PP-1024	23.17	22.32	15.96	19.54	16.39	2.06	<Null>	<Null>	2.95	3.44	11.35	<Null>	13.41	14.36	7.47	15.96	1	0	1.3
SI-PP-1025	19.43	10.29	10.29	19.65	<Null>	<Null>	<Null>	<Null>	2.81	2.79	<Null>	<Null>	6.20	<Null>	8.02	10.29	1	1	0.6
SI-PP-1026	17.40	11.92	12.29	13.51	<Null>	<Null>	<Null>	<Null>	2.75	2.89	<Null>	<Null>	8.56	<Null>	3.89	8.05	1	1	0.7
SI-PP-1027	13.67	10.09	13.67	10.09	<Null>	<Null>	<Null>	<Null>	2.66	2.77	<Null>	<Null>	<Null>	<Null>	7.36	7.36	1	1	0.5
SI-PP-1028	23.00	22.66	11.53	20.83	<Null>	<Null>	<Null>	<Null>	3.80	3.93	15.91	14.84	9.91	10.87	10.33	10.33	1	1	1.6
SI-PP-1029	22.29	21.53	9.78	21.10	<Null>	<Null>	<Null>	<Null>	3.15	3.61	<Null>	<Null>	<Null>	<Null>	8.21	8.21	1	1	0.8
SI-PP-1030	14.84	10.10	12.51	9.18	<Null>	<Null>	<Null>	<Null>	2.96	3.14	<Null>	<Null>	6.19	<Null>	9.98	7.54	1	1	0.4
SI-PP-1031	16.58	9.86	16.58	9.86	<Null>	<Null>	<Null>	<Null>	2.86	3.04	<Null>	<Null>	16.58	<Null>	9.68	16.58	1	1	0.7
SI-PP-1032	17.14	11.75	17.16	11.04	<Null>	<Null>	<Null>	<Null>	2.42	3.21	<Null>	<Null>	12.83	<Null>	17.16	13.55	1	0	0.6

Catalog	LP	WP	MxLe	MxWd	BaWd	BsCo	FlLO	FlLR	FlTk	MxTk	FlWO	FlWR	LGrn	RGrn	MxTB	MxWB	NfO	NfR	Mass (g)
SI-PP-1033	19.85	10.51	10.89	19.57	<Null>	<Null>	<Null>	<Null>	3.84	4.31	12.65	10.64	9.52	1.69	6.04	6.04	1	1	1.0
SI-PP-1034	20.91	16.46	11.74	19.58	<Null>	<Null>	<Null>	<Null>	2.69	3.46	16.16	<Null>	10.76	<Null>	6.99	8.82	1	1	0.6
SI-PP-1035	22.77	20.50	16.31	20.11	17.16	1.03	<Null>	<Null>	3.08	3.91	15.73	12.67	12.46	11.24	11.55	11.55	1	2	1.4
SI-PP-1036	17.76	11.76	16.39	11.96	<Null>	<Null>	<Null>	<Null>	3.81	4.06	<Null>	<Null>	13.44	<Null>	10.95	13.22	1	1	0.8
SI-PP-1037	21.92	11.59	19.39	11.22	<Null>	<Null>	<Null>	<Null>	2.55	3.47	<Null>	<Null>	18.77	<Null>	12.71	19.39	1	1	0.7
SI-PP-1038	21.31	16.37	18.43	16.10	<Null>	<Null>	<Null>	<Null>	2.71	2.86	<Null>	<Null>	<Null>	<Null>	11.39	11.39	1	1	1.0
SI-PP-1039	26.53	13.33	19.23	20.55	<Null>	<Null>	<Null>	<Null>	2.96	3.25	<Null>	<Null>	17.72	<Null>	10.13	15.43	1	1	0.9
SI-PP-1040	18.68	10.98	7.41	17.94	16.41	0.72	<Null>	<Null>	2.39	2.57	8.92	10.21	6.69	7.74	6.54	6.72	1	2	0.4
SI-PP-1041	17.25	11.86	16.30	15.33	<Null>	<Null>	<Null>	<Null>	2.71	2.78	<Null>	<Null>	<Null>	<Null>	12.50	13.15	1	1	0.6
SI-PP-1042	18.67	18.11	13.19	15.67	14.72	1.89	<Null>	<Null>	2.56	3.23	9.84	9.95	10.27	8.79	9.49	9.49	1	1	0.7
SI-PP-1043	20.66	9.12	9.19	20.25	<Null>	<Null>	<Null>	<Null>	3.36	3.47	<Null>	<Null>	<Null>	<Null>	5.96	5.96	1	1	0.6
SI-PP-1044	16.28	7.12	15.44	9.41	<Null>	<Null>	<Null>	<Null>	2.11	3.34	<Null>	<Null>	12.98	<Null>	10.05	2.14	1	<Null>	0.3
SI-PP-1045	22.80	16.94	21.19	19.85	<Null>	<Null>	<Null>	<Null>	4.51	4.66	11.20	13.12	<Null>	<Null>	2.91	2.91	1	1	1.3
SI-PP-1046	18.69	13.06	18.69	13.66	<Null>	<Null>	<Null>	<Null>	2.73	3.28	<Null>	<Null>	<Null>	<Null>	16.83	16.83	1	1	0.9
SI-PP-1047	25.13	23.18	18.16	20.04	16.14	2.24	<Null>	<Null>	3.65	4.28	10.90	11.66	15.12	12.92	11.17	11.17	1	1	1.9
SI-PP-1048	27.41	17.83	15.10	23.07	19.60	2.06	<Null>	<Null>	2.45	3.11	17.31	<Null>	11.10	13.74	12.20	12.20	1	0	1.4
SI-PP-1049	29.85	28.50	20.21	22.87	20.38	4.33	<Null>	<Null>	4.42	4.53	18.05	13.65	20.46	19.92	14.24	18.80	1	1	2.6
SI-PP-1050	14.94	11.32	9.37	13.51	<Null>	<Null>	<Null>	<Null>	2.04	2.24	<Null>	<Null>	<Null>	<Null>	4.93	4.93	1	0	0.4
SI-PP-1051	14.02	13.39	11.91	10.17	<Null>	<Null>	<Null>	<Null>	3.09	3.25	<Null>	<Null>	10.50	<Null>	9.29	1.20	1	0	0.4
SI-PP-1052	11.87	7.90	11.79	7.93	<Null>	<Null>	<Null>	<Null>	3.04	3.05	<Null>	<Null>	11.87	<Null>	8.93	8.93	1	0	0.2
SI-PP-1053	15.01	13.82	13.88	11.55	<Null>	<Null>	<Null>	<Null>	2.87	3.21	<Null>	<Null>	10.30	<Null>	6.43	11.63	1	1	0.6
SI-PP-1054	15.86	14.78	11.45	12.47	<Null>	<Null>	<Null>	<Null>	2.98	3.28	<Null>	<Null>	<Null>	<Null>	5.76	9.67	1	1	0.7
SI-PP-1055	15.57	12.15	2.33	13.04	<Null>	<Null>	<Null>	<Null>	11.26	2.59	<Null>	<Null>	8.14	<Null>	6.40	8.41	1	1	0.4
SI-PP-1056	18.31	15.85	16.77	13.25	<Null>	<Null>	<Null>	<Null>	3.51	3.69	<Null>	<Null>	16.28	<Null>	15.20	15.20	1	1	0.7
SI-PP-1057	20.73	15.16	13.41	17.24	17.24	2.29	<Null>	<Null>	2.65	3.31	13.08	<Null>	10.81	1.69	8.82	1.28	1	1	0.7
SI-PP-1058	17.23	16.79	16.09	10.13	<Null>	<Null>	<Null>	<Null>	3.11	3.19	<Null>	<Null>	14.89	<Null>	11.81	5.76	1	1	0.5
SI-PP-1059	25.84	25.73	17.60	23.43	<Null>	<Null>	<Null>	<Null>	4.87	5.08	16.44	14.89	<Null>	<Null>	5.42	5.42	1	1	2.7
SI-PP-1060	13.97	12.61	11.27	13.37	<Null>	<Null>	<Null>	<Null>	3.17	3.20	<Null>	<Null>	<Null>	<Null>	7.33	7.33	1	0	0.4
SI-PP-1061	12.81	12.07	10.86	9.41	<Null>	<Null>	<Null>	<Null>	2.19	2.58	<Null>	<Null>	10.67	<Null>	8.51	9.96	1	1	0.3

Catalog	LP	WP	MxLe	MxWd	BaWd	BsCo	FlLO	FlLR	FlTk	MxTk	FlWO	FlWR	LGrn	RGrn	MxTB	MxWB	NfO	NfR	Mass (g)
SI-PP-1062	15.43	15.21	14.21	12.70	<Null>	<Null>	<Null>	<Null>	3.25	3.25	<Null>	<Null>	12.21	<Null>	8.96	1.53	1	1	0.6
SI-PP-1063	30.42	24.02	28.14	18.04	<Null>	<Null>	<Null>	<Null>	4.20	4.26	14.07	14.98	<Null>	<Null>	6.65	6.65	1	1	3.2
SI-PP-1064	29.99	27.20	27.75	19.66	17.55	1.12	<Null>	<Null>	3.35	3.58	13.54	12.45	14.70	15.21	10.31	10.31	1	1	2.5
SI-PP-1065	20.62	17.68	19.10	17.64	<Null>	<Null>	<Null>	<Null>	2.63	3.12	<Null>	<Null>	15.39	<Null>	14.13	14.13	1	1	1.3
SI-PP-1066	19.37	14.66	14.69	14.08	<Null>	1.26	<Null>	<Null>	3.14	3.15	<Null>	6.67	10.70	<Null>	7.68	1.06	1	1	0.6
SI-PP-1067	21.94	20.15	20.87	17.06	<Null>	<Null>	<Null>	<Null>	3.99	4.41	<Null>	<Null>	16.83	<Null>	16.83	16.83	1	1	1.7
SI-PP-1068	24.78	16.58	16.11	20.89	<Null>	<Null>	<Null>	<Null>	3.38	3.46	13.90	13.41	<Null>	<Null>	9.58	9.58	1	1	1.4
SI-PP-1069	18.55	12.21	18.55	12.21	<Null>	<Null>	<Null>	<Null>	2.78	3.22	<Null>	<Null>	18.55	<Null>	9.87	12.17	1	1	0.8
SI-PP-1070	16.55	9.31	15.88	9.06	<Null>	<Null>	<Null>	<Null>	3.07	3.52	<Null>	<Null>	15.88	<Null>	13.59	2.33	1	1	0.5
SI-PP-1071	16.80	15.52	13.62	10.68	<Null>	<Null>	<Null>	<Null>	3.41	3.63	<Null>	<Null>	13.74	<Null>	11.01	8.95	1	1	0.7
SI-PP-1072	22.40	19.96	19.62	20.55	<Null>	<Null>	<Null>	<Null>	2.94	3.17	11.92	10.03	<Null>	<Null>	10.38	10.21	1	1	1.6
SI-PP-1073	21.98	20.64	13.55	19.12	<Null>	<Null>	<Null>	<Null>	3.32	4.14	10.59	9.95	<Null>	<Null>	6.84	6.84	1	1	1.6
SI-PP-1074	21.95	14.41	17.19	14.86	<Null>	<Null>	<Null>	<Null>	3.16	3.90	<Null>	<Null>	16.30	<Null>	8.23	17.19	1	1	1.0
SI-PP-1075	16.98	16.09	14.31	14.32	<Null>	<Null>	<Null>	<Null>	3.10	3.42	<Null>	<Null>	<Null>	<Null>	6.62	6.62	1	1	0.9
SI-PP-1076	26.33	25.55	19.47	21.74	19.04	3.63	<Null>	<Null>	4.19	4.31	14.58	16.95	17.20	15.78	8.74	13.09	1	1	2.4
SI-PP-1077	14.64	9.64	14.64	9.64	<Null>	<Null>	<Null>	<Null>	3.26	3.41	<Null>	<Null>	10.87	<Null>	8.31	0.95	1	1	0.5
SI-PP-1078	22.04	21.76	15.41	19.96	15.60	2.60	<Null>	<Null>	3.78	4.35	10.97	14.21	14.71	13.12	9.11	14.71	1	1	1.5
SI-PP-1079	24.80	18.46	14.06	21.83	<Null>	<Null>	<Null>	<Null>	3.75	4.26	11.47	13.40	14.03	<Null>	8.37	14.03	1	1	1.4
SI-PP-1080	14.42	8.39	14.42	8.39	<Null>	<Null>	<Null>	<Null>	3.23	3.24	<Null>	<Null>	14.42	<Null>	6.62	6.62	1	<Null>	0.2
SI-PP-1081	14.34	10.96	12.48	11.21	<Null>	<Null>	<Null>	<Null>	2.28	2.65	<Null>	<Null>	<Null>	<Null>	3.12	3.12	1	<Null>	0.4
SI-PP-1082	12.86	10.80	9.74	9.86	<Null>	<Null>	<Null>	<Null>	2.87	3.36	<Null>	<Null>	9.72	<Null>	7.29	9.74	1	<Null>	0.3
SI-PP-1083	24.74	12.43	17.74	21.55	<Null>	<Null>	<Null>	<Null>	4.08	4.22	11.31	12.78	12.73	4.13	11.26	17.74	1	1	1.7
SI-PP-1084	15.63	13.93	11.76	14.28	<Null>	<Null>	<Null>	<Null>	2.96	3.07	<Null>	<Null>	11.25	<Null>	7.08	11.42	1	0	0.5
SI-PP-1085	19.23	14.16	19.23	14.16	<Null>	<Null>	<Null>	<Null>	3.72	4.14	<Null>	<Null>	16.25	<Null>	12.43	5.75	1	1	1.4
SI-PP-1086	19.14	12.21	16.61	10.35	<Null>	<Null>	<Null>	<Null>	2.30	3.01	<Null>	<Null>	10.69	<Null>	5.44	12.94	1	<Null>	0.5
SI-PP-1087	19.95	19.26	9.93	18.14	16.68	3.52	<Null>	<Null>	3.29	3.46	11.10	9.16	7.98	9.06	7.16	8.88	1	1	0.6
SI-PP-1088	8.73	6.61	8.73	6.61	<Null>	<Null>	<Null>	<Null>	2.47	2.33	<Null>	<Null>	8.42	<Null>	5.60	5.60	1	<Null>	0.1
SI-PP-1089	17.07	12.66	13.63	16.73	<Null>	<Null>	<Null>	<Null>	2.62	2.97	10.49	<Null>	<Null>	<Null>	4.12	1.86	1	<Null>	0.6
SI-PP-1090	13.99	13.22	11.40	9.71	<Null>	<Null>	<Null>	<Null>	2.79	3.32	<Null>	<Null>	11.56	<Null>	4.53	3.68	1	0	0.4

Catalog	LP	WP	MxLe	MxWd	BaWd	BsCo	FlLO	FlLR	FlTk	MxTk	FlWO	FlWR	LGrn	RGrn	MxTB	MxWB	NfO	NfR	Mass (g)
SI-PP-1091	22.97	12.84	19.22	15.42	<Null>	<Null>	<Null>	<Null>	3.38	3.99	12.28	<Null>	<Null>	<Null>	7.59	17.69	1	1	1.1
SI-PP-1092	10.95	9.76	9.72	7.12	<Null>	<Null>	<Null>	<Null>	1.88	2.01	<Null>	<Null>	9.48	<Null>	9.20	1.74	1	1	0.2
SI-PP-1093	9.29	4.97	9.29	4.97	<Null>	<Null>	<Null>	<Null>	2.07	2.09	<Null>	<Null>	<Null>	<Null>	0.63	0.63	1	<Null>	0.1
SI-PP-1094	12.24	3.75	4.35	11.78	<Null>	<Null>	<Null>	<Null>	3.05	3.51	<Null>	<Null>	<Null>	<Null>	1.40	1.40	1	1	0.1
SI-PP-1095	16.88	11.88	12.03	15.07	<Null>	<Null>	<Null>	<Null>	2.30	3.01	<Null>	<Null>	<Null>	<Null>	1.93	6.08	1	1	0.6
SI-PP-1096	13.65	7.83	13.65	7.83	<Null>	<Null>	<Null>	<Null>	<Null>	2.82	<Null>	<Null>	6.92	<Null>	7.50	7.74	<Null>	<Null>	0.3
SI-PP-1097	13.27	9.06	8.45	9.21	<Null>	<Null>	<Null>	<Null>	2.18	3.31	<Null>	<Null>	4.73	<Null>	3.93	1.30	1	1	0.2
SI-PP-1098	16.21	5.95	5.95	16.21	<Null>	<Null>	<Null>	<Null>	3.68	4.12	<Null>	<Null>	5.34	<Null>	4.80	4.80	1	1	0.3
SI-PP-1099	13.27	5.85	5.95	13.38	<Null>	<Null>	<Null>	<Null>	2.30	2.73	<Null>	<Null>	5.78	<Null>	5.67	3.71	1	0	0.2
SI-PP-1100	13.21	8.58	11.90	8.68	<Null>	<Null>	<Null>	<Null>	2.12	2.26	<Null>	<Null>	11.69	<Null>	5.30	9.22	1	1	0.2
SI-PP-1101	32.82	19.42	32.82	19.42	17.03	1.12	23.07	<Null>	3.50	3.84	9.97	11.96	10.04	19.21	16.08	11.93	1	1	2.1
SI-PP-1102	43.92	23.15	43.92	23.15	<Null>	<Null>	32.50	31.39	3.06	3.26	13.33	11.16	15.30	<Null>	20.11	20.11	1	1	3.2
SI-PP-1103	29.33	17.65	29.33	17.65	<Null>	<Null>	<Null>	<Null>	2.61	2.99	12.21	10.89	5.22	<Null>	12.51	16.41	1	1	1.9
SI-PP-1104	24.85	21.22	17.96	21.24	18.47	2.51	<Null>	<Null>	2.69	3.52	14.16	10.46	14.66	12.05	13.34	9.51	1	1	1.4
SI-PP-1105	14.37	7.71	14.37	7.71	<Null>	<Null>	<Null>	<Null>	2.56	2.73	<Null>	<Null>	<Null>	<Null>	8.08	8.08	1	<Null>	0.2
SI-PP-1106	16.92	15.78	10.56	15.35	<Null>	<Null>	<Null>	<Null>	3.28	3.69	<Null>	<Null>	<Null>	<Null>	4.68	1.47	1	1	0.8
SI-PP-1107	18.25	3.04	18.25	3.04	<Null>	<Null>	<Null>	<Null>	<Null>	3.39	<Null>	<Null>	18.18	<Null>	9.72	18.25	<Null>	<Null>	0.5
SI-PP-1108	20.06	14.93	14.06	15.04	<Null>	<Null>	<Null>	<Null>	3.28	3.53	<Null>	<Null>	13.44	<Null>	7.14	7.14	1	1	1.0
SI-PP-1109	23.02	11.88	11.88	23.02	<Null>	<Null>	<Null>	<Null>	3.28	3.31	15.13	<Null>	<Null>	<Null>	8.14	8.14	1	1	1.2
SI-PP-1110	25.59	14.42	25.59	14.42	<Null>	<Null>	<Null>	<Null>	2.86	3.24	<Null>	<Null>	<Null>	<Null>	10.55	3.45	1	1	1.2
SI-PP-1111	15.35	11.75	15.35	11.75	<Null>	<Null>	<Null>	<Null>	3.35	3.29	<Null>	<Null>	<Null>	<Null>	10.95	10.95	1	1	0.9
SI-PP-1112	25.25	20.49	22.68	19.84	<Null>	<Null>	<Null>	<Null>	3.75	4.53	9.29	<Null>	8.16	<Null>	11.32	9.27	1	0	2.3
SI-PP-1113	15.62	13.94	16.27	14.62	<Null>	<Null>	<Null>	<Null>	3.31	3.42	<Null>	<Null>	<Null>	<Null>	9.71	8.11	1	1	0.8
SI-PP-1114	17.47	11.55	12.29	15.78	<Null>	<Null>	<Null>	<Null>	3.75	4.03	<Null>	<Null>	<Null>	<Null>	3.81	9.83	1	1	0.8
SI-PP-1115	12.96	12.29	12.29	12.96	<Null>	<Null>	<Null>	<Null>	2.38	2.66	<Null>	<Null>	<Null>	<Null>	9.61	2.28	1	1	0.5
SI-PP-1116	19.94	9.98	11.76	17.07	<Null>	<Null>	<Null>	<Null>	3.28	3.44	<Null>	<Null>	5.37	<Null>	7.39	2.37	0	0	0.7
SI-PP-1117	25.59	18.89	23.80	19.47	<Null>	<Null>	<Null>	<Null>	3.54	3.96	11.90	12.24	14.92	6.76	11.61	11.61	1	1	2.1
SI-PP-1118	10.70	10.58	10.70	10.58	<Null>	<Null>	<Null>	<Null>	2.67	2.67	<Null>	<Null>	<Null>	<Null>	5.19	10.70	1	1	0.4
SI-PP-1119	10.49	10.48	10.49	10.48	<Null>	<Null>	<Null>	<Null>	2.40	3.07	<Null>	<Null>	3.52	<Null>	5.75	5.75	1	1	0.4

Catalog	LP	WP	MxLe	MxWd	BaWd	BsCo	FlLO	FlLR	FlTk	MxTk	FlWO	FlWR	LGrn	RGrn	MxTB	MxWB	NfO	NfR	Mass (g)
SI-PP-1120	10.26	7.20	10.26	7.20	<Null>	<Null>	<Null>	<Null>	2.19	2.27	<Null>	<Null>	10.26	<Null>	8.22	4.67	1	1	0.2
SI-PP-1121	9.77	9.11	9.11	9.77	<Null>	<Null>	<Null>	<Null>	2.41	3.22	<Null>	<Null>	9.11	<Null>	3.59	2.66	1	1	0.2
SI-PP-1122	19.91	18.02	19.91	18.02	<Null>	<Null>	<Null>	<Null>	2.67	3.05	12.20	7.91	<Null>	<Null>	7.38	2.64	1	1	1.1
SI-PP-1123	16.76	12.79	15.92	14.33	<Null>	<Null>	<Null>	<Null>	3.75	3.92	<Null>	<Null>	<Null>	<Null>	9.48	3.50	1	1	0.8
SI-PP-1124	11.12	7.16	7.12	10.11	<Null>	<Null>	<Null>	<Null>	2.38	2.67	<Null>	<Null>	<Null>	<Null>	7.12	7.12	1	1	0.2
SI-PP-1125	12.81	7.67	12.81	7.67	<Null>	<Null>	<Null>	<Null>	3.38	3.85	<Null>	<Null>	12.81	<Null>	4.77	4.77	1	0	0.3
SI-PP-1126	9.58	7.59	9.58	7.59	<Null>	<Null>	<Null>	<Null>	2.30	2.33	<Null>	<Null>	9.58	<Null>	4.05	9.58	1	0	0.2
SI-PP-1127	9.71	4.38	4.38	9.71	<Null>	<Null>	<Null>	<Null>	3.51	4.03	<Null>	<Null>	4.38	<Null>	4.38	4.38	1	1	0.2
SI-PP-1128	16.20	7.76	8.38	14.91	<Null>	<Null>	<Null>	<Null>	2.97	2.98	<Null>	<Null>	<Null>	<Null>	1.63	1.63	1	1	0.4
SI-PP-1129	15.79	11.73	14.07	12.54	12.52	2.75	<Null>	<Null>	2.89	3.39	<Null>	<Null>	13.66	<Null>	3.66	2.26	1	0	0.5
SI-PP-1130	18.29	14.85	17.47	15.30	<Null>	<Null>	<Null>	<Null>	4.10	4.26	9.07	<Null>	<Null>	<Null>	8.33	8.33	1	<Null>	1.2
SI-PP-1131	14.52	9.93	10.57	10.54	<Null>	<Null>	<Null>	<Null>	3.75	3.89	<Null>	<Null>	7.48	<Null>	7.41	7.41	1	1	0.5
SI-PP-1132	14.58	12.30	14.58	12.30	<Null>	<Null>	<Null>	<Null>	2.88	3.43	<Null>	<Null>	13.21	<Null>	13.15	13.15	1	1	0.8
SI-PP-1133	25.84	21.74	25.84	21.74	<Null>	4.26	<Null>	<Null>	3.36	3.70	11.82	17.35	17.32	<Null>	11.58	17.58	1	1	2.5
SI-PP-1134	15.25	10.40	15.25	10.40	<Null>	<Null>	<Null>	<Null>	2.73	3.23	<Null>	<Null>	14.35	<Null>	15.25	10.01	1	1	0.6
SI-PP-1135	10.03	9.92	10.03	9.92	<Null>	1.35	<Null>	<Null>	2.44	3.02	<Null>	<Null>	6.55	<Null>	10.03	5.88	1	1	0.3
SI-PP-1136	9.22	9.12	9.22	9.12	<Null>	<Null>	<Null>	<Null>	2.19	3.82	<Null>	<Null>	8.05	<Null>	9.22	9.22	1	<Null>	0.4
SI-PP-1137	11.69	5.97	11.69	5.97	<Null>	3.54	<Null>	<Null>	2.42	2.99	<Null>	<Null>	9.03	<Null>	11.69	5.18	1	1	0.2
SI-PP-1138	17.53	10.53	17.53	10.53	<Null>	7.63	<Null>	<Null>	3.74	3.96	<Null>	<Null>	<Null>	<Null>	12.08	12.08	1	1	0.5
SI-PP-1139	17.92	8.30	17.92	8.30	<Null>	<Null>	<Null>	<Null>	4.30	4.74	<Null>	<Null>	<Null>	<Null>	17.92	17.92	1	1	0.8
SI-PP-1140	15.14	10.52	15.14	10.52	<Null>	<Null>	<Null>	<Null>	2.94	3.02	<Null>	<Null>	15.14	<Null>	3.03	3.03	1	0	0.6
SI-PP-1141	9.42	8.84	8.84	9.42	<Null>	<Null>	<Null>	<Null>	2.42	2.87	<Null>	<Null>	4.16	<Null>	0.00	8.84	1	1	0.3
SI-PP-1142	14.81	9.01	14.81	9.01	<Null>	<Null>	<Null>	<Null>	2.51	2.78	<Null>	<Null>	13.65	<Null>	5.82	5.82	1	1	0.3
SI-PP-1143	17.07	10.72	10.72	17.07	<Null>	<Null>	<Null>	<Null>	2.73	3.18	11.25	<Null>	10.72	2.26	2.85	10.72	1	0	0.7
SI-PP-1144	10.14	9.88	10.14	9.88	<Null>	3.12	<Null>	<Null>	2.64	3.43	<Null>	<Null>	3.03	<Null>	10.14	10.14	1	1	0.4
SI-PP-1145	14.38	9.91	14.38	9.91	<Null>	2.84	<Null>	<Null>	2.92	3.41	<Null>	<Null>	13.33	<Null>	8.85	14.38	1	1	0.7
SI-PP-1146	11.73	6.90	6.90	11.73	<Null>	<Null>	<Null>	<Null>	2.52	2.57	<Null>	<Null>	<Null>	<Null>	0.00	0.00	1	1	0.3
SI-PP-1147	13.66	10.74	13.66	10.74	<Null>	2.19	<Null>	<Null>	2.98	3.30	<Null>	<Null>	10.15	<Null>	13.66	13.66	1	0	0.6
SI-PP-1148	25.16	20.76	25.16	20.76	<Null>	<Null>	<Null>	<Null>	3.39	3.37	12.17	11.48	<Null>	<Null>	0.00	4.37	1	1	2.3

Catalog	LP	WP	MxLe	MxWd	BaWd	BsCo	FlLO	FlLR	FlTk	MxTk	FlWO	FlWR	LGrn	RGrn	MxTB	MxWB	NfO	NfR	Mass (g)
SI-PP-1149	19.43	9.17	19.43	9.17	<Null>	<Null>	<Null>	<Null>	2.44	3.31	<Null>	<Null>	<Null>	<Null>	14.75	14.75	1	1	0.5
SI-PP-1150	9.61	6.08	6.08	9.61	<Null>	<Null>	<Null>	<Null>	1.55	1.64	<Null>	<Null>	<Null>	<Null>	0.00	0.00	1	<Null>	0.1
SI-PP-1151	10.92	10.06	10.92	10.06	<Null>	<Null>	<Null>	<Null>	1.75	1.90	<Null>	<Null>	<Null>	<Null>	0.00	0.00	1	<Null>	0.2
SI-PP-1152	20.39	16.57	16.57	20.39	<Null>	<Null>	<Null>	<Null>	3.47	4.15	13.16	14.32	<Null>	<Null>	16.57	16.57	1	1	1.6
SI-PP-1153	19.58	12.32	15.39	12.65	<Null>	<Null>	<Null>	<Null>	2.94	3.54	<Null>	<Null>	11.09	<Null>	7.85	0.00	1	1	0.6
SI-PP-1154	9.11	3.62	9.11	3.62	<Null>	<Null>	<Null>	<Null>	<Null>	1.96	<Null>	<Null>	<Null>	<Null>	0.00	0.00	<Null>	<Null>	0.1
SI-PP-1155	15.37	11.81	11.81	15.37	<Null>	<Null>	<Null>	<Null>	2.21	2.42	13.54	<Null>	<Null>	<Null>	0.00	0.00	1	0	0.6
SI-PP-1156	13.23	12.88	12.88	13.23	<Null>	<Null>	<Null>	<Null>	2.09	3.01	<Null>	<Null>	<Null>	<Null>	0.00	0.00	1	1	0.6
SI-PP-1157	12.64	6.88	12.64	6.88	<Null>	<Null>	<Null>	<Null>	2.22	2.42	<Null>	<Null>	<Null>	<Null>	7.60	7.60	1	<Null>	0.3
SI-PP-1158	8.88	5.61	5.61	8.88	<Null>	<Null>	<Null>	<Null>	2.04	2.12	<Null>	<Null>	8.88	<Null>	0.00	0.00	1	<Null>	0.1
SI-PP-1159	18.06	15.20	18.06	15.20	<Null>	<Null>	<Null>	<Null>	3.29	3.97	<Null>	<Null>	5.35	<Null>	4.49	4.49	1	1	1.0
SI-PP-1160	12.05	9.08	12.05	9.08	<Null>	<Null>	<Null>	<Null>	2.19	3.18	<Null>	<Null>	8.38	<Null>	8.38	8.38	1	<Null>	0.3
SI-PP-1161	20.65	13.68	20.65	13.68	<Null>	<Null>	<Null>	<Null>	<Null>	4.34	<Null>	<Null>	<Null>	<Null>	4.17	4.17	0	0	1.2
SI-PP-1162	13.48	9.26	13.48	9.26	<Null>	<Null>	<Null>	<Null>	<Null>	2.80	<Null>	<Null>	<Null>	<Null>	1.29	1.29	0	0	0.4
SI-PP-1163	14.51	7.54	14.51	7.54	<Null>	<Null>	<Null>	<Null>	<Null>	4.40	<Null>	<Null>	<Null>	<Null>	2.91	2.91	0	0	0.6
SI-PP-1164	22.84	17.58	17.58	22.84	<Null>	<Null>	<Null>	<Null>	<Null>	3.75	<Null>	<Null>	<Null>	<Null>	2.73	2.73	0	0	1.3
SI-PP-1165	20.95	17.14	15.72	19.32	<Null>	<Null>	<Null>	<Null>	3.40	3.60	<Null>	13.45	11.28	4.57	0.00	3.93	0	1	1.2
SI-PP-1166	26.60	26.10	18.73	21.18	18.76	2.61	<Null>	<Null>	<Null>	3.94	<Null>	<Null>	17.38	16.58	18.73	11.27	0	0	2.0
SI-PP-1167	20.53	20.21	16.02	16.85	13.48	2.21	<Null>	<Null>	<Null>	3.62	<Null>	<Null>	12.65	16.02	14.71	16.02	0	0	1.2
SI-PP-1168	17.61	14.44	11.80	16.56	<Null>	<Null>	<Null>	<Null>	<Null>	4.12	<Null>	<Null>	11.80	<Null>	11.80	7.86	0	0	0.9
SI-PP-1169	22.27	20.12	14.23	20.06	17.28	3.99	<Null>	<Null>	<Null>	3.83	<Null>	<Null>	13.54	4.47	14.23	6.44	0	0	1.2
SI-PP-1170	17.57	16.80	9.64	16.82	13.73	3.18	<Null>	<Null>	<Null>	2.73	<Null>	<Null>	6.65	7.67	9.64	7.67	0	0	0.5
SI-PP-1171	18.16	13.68	13.78	14.81	<Null>	<Null>	<Null>	<Null>	<Null>	3.61	<Null>	<Null>	12.89	<Null>	7.65	10.93	0	0	0.8
SI-PP-1172	25.71	21.26	17.01	20.81	18.63	3.39	<Null>	<Null>	<Null>	4.26	<Null>	<Null>	13.33	13.17	17.01	15.40	0	0	1.9
SI-PP-1173	22.24	16.84	17.59	15.39	<Null>	<Null>	<Null>	<Null>	<Null>	3.38	<Null>	<Null>	8.73	14.56	17.59	7.34	0	0	1.1
SI-PP-1174	22.41	21.24	15.12	19.16	17.18	2.75	<Null>	<Null>	<Null>	3.34	<Null>	<Null>	14.45	11.68	14.04	14.04	0	0	1.2
SI-PP-1175	16.11	14.46	8.86	15.09	13.70	1.51	<Null>	<Null>	<Null>	3.89	<Null>	<Null>	<Null>	<Null>	8.86	1.51	0	0	0.6
SI-PP-1176	22.33	21.85	12.53	19.81	<Null>	<Null>	<Null>	<Null>	<Null>	3.85	<Null>	<Null>	11.07	10.98	5.96	5.96	0	0	1.4
SI-PP-1177	19.25	18.77	12.82	17.41	15.05	2.61	<Null>	<Null>	<Null>	4.58	<Null>	<Null>	11.80	6.73	12.82	12.82	0	0	1.2

Catalog	LP	WP	MxLe	MxWd	BaWd	BsCo	FlLO	FlLR	FlTk	MxTk	FlWO	FlWR	LGrn	RGrn	MxTB	MxWB	NfO	NfR	Mass (g)
SI-PP-1178	12.66	11.54	10.69	12.43	<Null>	<Null>	<Null>	<Null>	<Null>	2.29	<Null>	<Null>	<Null>	<Null>	3.38	3.83	0	0	0.3
SI-PP-1179	14.61	6.85	6.85	14.61	<Null>	<Null>	<Null>	<Null>	<Null>	2.93	<Null>	<Null>	6.06	<Null>	6.85	0.00	0	0	0.2
SI-PP-1180	16.15	12.95	16.15	12.95	9.57	1.53	<Null>	<Null>	1.52	1.95	11.60	<Null>	7.10	6.69	1.53	9.95	1?	0	0.4

C3. Folsom preform descriptive data.

Catalog	Portion	Code	Flt	PsFlO	PsFlR	Nib	GENMAT	SPECMAT	Nodule	Burning
CMPA-PRE-1001	LT	6E	YES	NO	NF	NA	CCS	UNK	UNK-01	NO
CMPA-PRE-1002	DS	5C	NO	NF	NF	NA	CCS	CUMB	CUMB-02	NO
CMPA-PRE-1003	PR	7D	YES	NO	NO	NC	CCS	TRT	TRT-02	NO
CMPA-PRE-1004	DS	5C	NO	NF	NF	NA	CCS	TRT	TRT-02	NO
CMPA-PRE-1005	PR	7D	NO	NF	NF	NC	CCS	TRT	TRT-08	NO
CMPA-PRE-1006	PR	7E	NO	NF	NF	NC	CCS	TRT	TRT-12	NO
CMPA-PRE-1007	LT	6E	YES	NO	NF	NA	CCS	TRT	TRT-07	POT
CMPA-PRE-1008	PR	7E	NO	NC	NC	NC	CCS	TRT	TRT-07	NO
CMPA-PRE-1009	PR	7D	YES	YES	YES	NC	CCS	TRT	TRT-05	NO
CMPA-PRE-1010	PR	7B	YES	NO	NF	NO	CCS	FLAT	FLAT-02	NO
CMPA-PRE-1011	LT	6E	YES	NO	NF	NA	CCS	TRT	TRT-16	POT
CMPA-PRE-1012	LT	6E	YES	NO	NC	NA	CCS	TRT	TRT-07	POT
CMPA-PRE-1013	LT	6E	YES	NO	NC	NA	SWD	SWD	SWD-07	NO
CMPA-PRE-1014	PR	7E	YES	NO	NC	NC	CCS	PED	PED-03	NO
CMPA-PRE-1015	PR	7D	YES	NO	NO	NO	CCS	UNK	UNK-05	NO
CMPA-PRE-1016	DS	5C	NO	NF	NF	NA	CCS	MOSC	MOSC-04	NO
CMPA-PRE-1017	DS	5C	NO	NF	NF	NA	CCS	TRT	TRT-15	NO
CMPA-PRE-1018	PR	7E	YES	NO	NO	NC	CCS	TRT	TRT-08	NO
CMPA-PRE-1019	DS	5C	NO	NF	NF	NA	CCS	TRT	TRT-16	POT
CMPA-PRE-1020	PR	7E	NO	NC	NC	NC	CCS	NARB	NARB-01	NO
CMPA-PRE-1021	PR	7E	NO	NF	NF	NC	CCS	TRT	TRT-02	NO
CMPA-PRE-1022	PR	7E	NO	NF	NF	NC	CCS	TRT	TRT-10	NO
CMPA-PRE-1023	DS	5C	NO	NF	NF	NA	CCS	TRT	TRT-07	NO
CMPA-PRE-1024	LT	6E	NO	NF	NF	NA	CCS	TRT	TRT-10	NO

Catalog	Portion	Code	Flt	PsFlO	PsFlR	Nib	GENMAT	SPECMAT	Nodule	Burning
SI-PRE-1001	PR	7D	YES	NO	NO	NO	CCS	TRT	TRT-10	NO
SI-PRE-1002	LT	6E	YES	NO	NF	NA	CCS	TRT	TRT-08	NO
SI-PRE-1003	PR	7B	NO	NF	NF	NO	CCS	TRT	TRT-08	NO
SI-PRE-1004	LT	6E	YES	NO	NO	NA	CCS	TRT	TRT-12	NO
SI-PRE-1005	PR	7D	YES	NO	NO	YES	CCS	TRT	TRT-06	NO
SI-PRE-1006	PR	7E	YES	NO	NC	NC	CCS	NARB	NARB-01	NO
SI-PRE-1007	LT	6E	NO	NF	NF	NA	SWD	SWD	SWD-02	NO
SI-PRE-1008	PR	7D	YES	NO	NO	NC	CCS	TRT	TRT-11	NO
SI-PRE-1009	LT	6E	YES	NO	NF	NA	SWD	SWD	SWD-02	NO
SI-PRE-1010	MS	6D	YES	NO	NF	NA	CCS	TRT	TRT-08	POT
SI-PRE-1011	PR	7B	YES	NO	NF	YES	CCS	MOSC	MOSC-02	PTCZ
SI-PRE-1012	PR	7D	NO	NF	NF	YES	SWD	SWD	SWD-01	NO
SI-PRE-1013	PR	7D	YES	NO	NF	YES	SWD	SWD	SWD-01	NO
SI-PRE-1014	PR	7E	YES	NO	NC	YES	CCS	TRT	TRT-09	POT
SI-PRE-1015	PR	7E	YES	NO	NC	YES	CCS	UNK	UNK-03	NO
SI-PRE-1016	PR	7E	YES	NO	NC	NC	CCS	NARB	NARB-02	NO
SI-PRE-1017	LT	6E	YES	NO	NO	NA	CCS	TRT	TRT-18	NO
SI-PRE-1018	LT	6E	YES	NO	NO	NA	CCS	UNK	UNK-08	NO
SI-PRE-1019	LT	6E	YES	NO	NO	NA	CCS	TRT	TRT-15	NO
SI-PRE-1020	DS	5C	NO	NF	NF	NA	CCS	TRT	TRT-05	NO
SI-PRE-1021	PR	7D	YES	NO	NO	NC	CCS	TRT	TRT-08	NO
SI-PRE-1022	LT	6E	YES	NO	NO	NA	CCS	TRT	TRT-17	POT
SI-PRE-1023	PR	7C	YES	NO	NO	YES	CCS	TRT	TRT-08	NO
SI-PRE-1024	MS	6B	YES	NO	NO	NA	CCS	TRT	TRT-17	NO
SI-PRE-1025	PR	7D	YES	NO	NF	YES	CCS	TRT	TRT-10	NO
SI-PRE-1026	MS	6B	NO	NF	NF	NA	CCS	TRT	TRT-19	NO
SI-PRE-1027	DS	5C	NO	NF	NF	NA	CCS	TRT	TRT-19	NO
SI-PRE-1028	PR	7E	NO	NC	NC	NC	CCS	TRT	TRT-06	NO
SI-PRE-1029	LT	6E	YES	NO	NO	NA	CCS	TRT	TRT-10	NO
SI-PRE-1030	PR	7B	NO	NF	NF	YES	CCS	TRT	TRT-02	NO
SI-PRE-1031	LT	6E	YES	NO	NF	NA	CCS	TRT	TRT-12	NO

Catalog	Portion	Code	Flt	PsFlO	PsFlR	Nib	GENMAT	SPECMAT	Nodule	Burning
SI-PRE-1032*	PR	7D	YES	NO	NO	NC	CCS	PED	PED-04	CRZ
SI-PRE-1033*	PR	7D	YES	NO	NF	NC	CCS	TRT	TRT-20	NO
SI-PRE-1034	LT	6E	YES	NO	NF	NA	CCS	UNK	UNK-07	POT
SI-PRE-1035*	DS	5C	YES	NO	NO	NA	CCS	TRT	TRT-05	NO
SI-PRE-1036	LT	6E	YES	NO	NF	NA	CCS	UNK	UNK-07	NO
SI-PRE-1037	MS	6D	YES	NO	NF	NA	CCS	PED	PED-02	NO
SI-PRE-1038	LT	6E	YES	NO	YES	NA	CCS	EDW	EDW-01	NO
SI-PRE-1039	DS	5C	NO	NC	NC	NA	CCS	UNK	UNK-07	POT
SI-PRE-1040	PR	7D	YES	NO	NO	YES	CCS	UNK	UNK-07	NO
SI-PRE-1041	DS	5C	NO	NC	NC	NA	CCS	EDW	EDW-01	NO
SI-PRE-1042	DS	5C	NO	NC	NC	NA	CCS	TRT	TRT-17	NO
SI-PRE-1043	PR	7B	NO	NF	NF	YES	CCS	TRT	TRT-02	POT
SI-PRE-1044	PR	7D	YES	NO	NF	NO	CCS	TRT	TRT-02	POT
SI-PRE-1045	PR	7D	YES	NO	NF	NC	CCS	TRT	TRT-19	NO
SI-PRE-1046	PR	7C	YES	NO	NO	NC	CCS	UNK	UNK-04	NO
SI-PRE-1047	LT	6E	YES	NO	NO	NA	CCS	TRT	TRT-10	NO
SI-PRE-1048	PR	7D	YES	NO	NF	YES	CCS	TRT	TRT-05	NO
SI-PRE-1049	PR	7B	YES	NO	NO	YES	CCS	TRT	TRT-10	NO
SI-PRE-1050	LT	6E	YES	NO	NF	NA	CCS	TRT	TRT-11	POT
SI-PRE-1051	DS	5C	NO	NF	NF	NA	SWD	SWD	SWD-05	NO
SI-PRE-1052	DS	5C	YES	NO	YES	NA	CCS	TRT	TRT-12	NO
SI-PRE-1053	DS	5C	NO	NF	NF	NA	CCS	TRT	TRT-02	NO
SI-PRE-1054	MS	6D	YES	NO	NF	NA	CCS	TRT	TRT-12	NO
SI-PRE-1055	DS	5C	NO	NF	NF	NA	CCS	TRT	TRT-08	NO
SI-PRE-1056	DS	5C	NO	NF	NF	NA	CCS	UNK	UNK-09	NO
SI-PRE-1057	LT	6E	YES	NO	NF	NA	CCS	NARB	NARB-02	NO
SI-PRE-1058	PR	7D	YES	NO	NO	NC	CCS	TRT	TRT-02	POT
SI-PRE-1059	PR	7E	YES	NO	NC	NC	CCS	TRT	TRT-10	NO
SI-PRE-1060	DS	5C	NO	NF	NF	NA	CCS	TRT	TRT-05	NO
SI-PRE-1061	PR	7E	YES	NO	NC	YES	CCS	TRT	TRT-05	NO
SI-PRE-1062	DS	5C	YES	NO	NF	NA	CCS	TRT	TRT-05	NO

Catalog	Portion	Code	Flt	PsFlO	PsFlR	Nib	GENMAT	SPECMAT	Nodule	Burning
SI-PRE-1063	DS	5C	NO	NF	NF	NA	CCS	TRT	TRT-07	POT
SI-PRE-1064	DS	5C	YES	NO	NF	NA	CCS	TRT	TRT-08	NO
SI-PRE-1065	DS	5C	YES	NO	NF	NA	CCS	TRT	TRT-08	NO
SI-PRE-1066	DS	5C	YES	NO	NF	NA	CCS	TRT	TRT-02	NO
SI-PRE-1067	DS	5C	NO	NF	NF	NA	CCS	TRT	TRT-05	NO
SI-PRE-1068	DS	5C	YES	NO	NF	NA	CCS	TRT	TRT-12	POT
SI-PRE-1069	LT	6E	YES	NO	NO	NA	SWD	SWD	SWD-04	NO
SI-PRE-1070	PR	7D	YES	NO	NF	NC	CCS	PED	PED-07	NO
SI-PRE-1071	MS	6D	NO	NF	NF	NA	QZT	MOR	MOR-02	NO
SI-PRE-1072	PR	7B	NO	NF	NF	YES	CCS	UNK	UNK-02	NO
SI-PRE-1073	PR	7C	NO	NF	NF	YES	CCS	TRT	TRT-08	NO
SI-PRE-1074	PR	7C	YES	NO	YES	NO	CCS	PED	PED-02	NO
SI-PRE-1075	DS	5C	NO	NF	NF	NA	CCS	TRT	TRT-12	NO
SI-PRE-1076	LT	6E	NO	NF	NF	NA	CCS	TRT	TRT-02	NO
SI-PRE-1077	DS	5C	NO	NF	NF	NA	SWD	SWD	SWD-07	NO
SI-PRE-1078	MS	6D	YES	NO	NF	NA	CCS	TRT	TRT-08	NO
SI-PRE-1079	LT	6E	NO	NF	NF	NA	CCS	TRT	TRT-02	NO
SI-PRE-1080	LT	6E	YES	NO	NF	NA	VOL	OBS	OBS-02	NO
SI-PRE-1081	PR	7D	YES	NO	NF	NO	VOL	OBS	OBS-01	NO
SI-PRE-1082	PR	7B	NO	NF	NF	YES	VOL	OBS	OBS-02	NO
SI-PRE-1083	PR	7B	NO	NF	NF	YES	CCS	UNK	UNK-12	NO
SI-PRE-1084	LT	6E	NO	NF	NF	NA	CCS	TRT	TRT-03	NO
SI-PRE-1085	LT	6E	NO	NF	NF	NA	CCS	TRT	TRT-02	NO
SI-PRE-1086	LT	6E	YES	NO	NF	NA	CCS	EDW	EDW-01	NO
SI-PRE-1087	DS	5C	NO	NF	NF	NA	CCS	MOSC	MOSC-04	NO
SI-PRE-1088	PR	7D	YES	NO	NF	YES	CCS	TRT	TRT-10	NO
SI-PRE-1089	PR	7D	YES	NO	NF	YES	CCS	CUMB	CUMB-01	NO

* Potentially offsite specimen – see chapter 2 (table 6, figure 11)

C4. Folsom preform metric data.

Catalog	LP	WP	MxLe	MxWd	BaWd	BsCo	FlLO	FlLR	FlTk	MxTk	FlWO	FlWR	MxTB	MxWB	Mass (g)
CMPA-PRE-1001	18.60	9.23	17.83	8.13	<Null>	<Null>	<Null>	<Null>	2.66	3.48	<Null>	<Null>	3.76	8.37	0.5
CMPA-PRE-1002	17.87	12.34	11.16	17.26	<Null>	<Null>	<Null>	<Null>	<Null>	5.59	<Null>	<Null>	2.34	2.34	1.2
CMPA-PRE-1003	24.78	10.80	24.20	9.65	<Null>	<Null>	<Null>	<Null>	3.79	3.92	<Null>	<Null>	19.01	5.32	1.3
CMPA-PRE-1004	20.79	12.20	13.38	20.56	<Null>	<Null>	<Null>	<Null>	<Null>	4.57	<Null>	<Null>	6.49	1.81	1.4
CMPA-PRE-1005	14.55	8.63	13.02	8.37	<Null>	<Null>	<Null>	<Null>	<Null>	2.02	<Null>	<Null>	2.93	10.05	0.3
CMPA-PRE-1006	13.62	6.20	13.38	6.13	<Null>	<Null>	<Null>	<Null>	<Null>	3.86	<Null>	<Null>	4.95	4.95	0.3
CMPA-PRE-1007	13.56	6.73	13.56	6.73	<Null>	<Null>	<Null>	<Null>	3.51	3.68	<Null>	<Null>	7.35	7.35	0.3
CMPA-PRE-1008	16.60	9.23	8.59	14.56	<Null>	<Null>	<Null>	<Null>	<Null>	5.14	<Null>	<Null>	5.73	1.98	0.6
CMPA-PRE-1009	13.86	10.68	8.92	12.17	<Null>	<Null>	<Null>	<Null>	2.63	2.69	<Null>	<Null>	2.58	8.92	0.5
CMPA-PRE-1010	24.45	20.27	14.40	22.98	15.88	1.80	<Null>	<Null>	5.11	5.27	9.60	<Null>	12.41	14.01	2.1
CMPA-PRE-1011	19.80	12.23	13.06	15.65	<Null>	<Null>	<Null>	<Null>	3.36	3.57	<Null>	<Null>	4.13	6.07	0.8
CMPA-PRE-1012	14.16	9.27	9.27	14.16	<Null>	<Null>	<Null>	<Null>	2.93	3.19	<Null>	<Null>	5.14	5.14	0.4
CMPA-PRE-1013	12.24	9.03	12.24	9.03	<Null>	<Null>	<Null>	<Null>	3.13	3.27	<Null>	<Null>	6.05	1.97	0.5
CMPA-PRE-1014	11.25	8.96	9.89	8.92	<Null>	2.16	<Null>	<Null>	2.41	2.69	<Null>	<Null>	5.57	5.57	0.3
CMPA-PRE-1015	12.98	11.67	11.67	12.98	<Null>	<Null>	<Null>	<Null>	2.61	3.25	<Null>	<Null>	0.00	11.67	0.7
CMPA-PRE-1016	25.07	12.81	12.81	25.07	<Null>	<Null>	<Null>	<Null>	<Null>	5.60	<Null>	<Null>	0.00	0.00	2.0
CMPA-PRE-1017	15.96	11.44	11.44	15.96	<Null>	<Null>	<Null>	<Null>	<Null>	3.18	<Null>	<Null>	0.00	0.00	0.5
CMPA-PRE-1018	14.32	9.51	14.32	9.51	<Null>	<Null>	<Null>	<Null>	3.02	3.78	<Null>	<Null>	10.85	4.81	0.4
CMPA-PRE-1019	20.89	20.01	20.89	20.01	<Null>	<Null>	<Null>	<Null>	<Null>	3.90	<Null>	<Null>	20.89	8.15	1.9
CMPA-PRE-1020	18.52	8.61	18.52	8.61	<Null>	<Null>	<Null>	<Null>	<Null>	4.98	<Null>	<Null>	8.42	8.42	0.7
CMPA-PRE-1021	15.68	7.05	15.68	7.05	<Null>	<Null>	<Null>	<Null>	<Null>	3.49	<Null>	<Null>	0.00	0.00	0.4
CMPA-PRE-1022	13.69	9.17	3.69	9.17	<Null>	<Null>	<Null>	<Null>	<Null>	3.11	<Null>	<Null>	7.18	0.00	0.4
CMPA-PRE-1023	18.71	10.57	10.57	18.71	<Null>	<Null>	<Null>	<Null>	<Null>	5.43	<Null>	<Null>	10.57	0.00	0.7
CMPA-PRE-1024	22.63	14.67	22.63	14.67	<Null>	<Null>	<Null>	<Null>	<Null>	6.12	<Null>	<Null>	11.38	11.38	2.5
SI-PRE-1001	15.36	11.38	12.05	14.80	<Null>	<Null>	<Null>	<Null>	1.63	2.09	<Null>	<Null>	8.66	9.62	0.4
SI-PRE-1002	18.31	7.89	18.31	7.89	<Null>	<Null>	<Null>	<Null>	2.91	2.98	<Null>	<Null>	11.09	13.13	0.6
SI-PRE-1003	24.41	22.20	17.67	20.19	18.30	2.17	<Null>	<Null>	<Null>	6.84	<Null>	<Null>	15.09	15.33	2.5
SI-PRE-1004	25.21	22.86	18.30	21.67	<Null>	<Null>	<Null>	<Null>	3.02	3.88	13.33	<Null>	5.41	5.41	1.5
SI-PRE-1005	13.50	12.38	13.50	12.38	<Null>	<Null>	<Null>	<Null>	4.21	4.52	<Null>	<Null>	13.23	7.29	0.9

Catalog	LP	WP	MxLe	MxWd	BaWd	BsCo	FlLO	FlLR	FlTk	MxTk	FlWO	FlWR	MxTB	MxWB	Mass (g)
SI-PRE-1006	14.14	8.64	11.65	10.04	<Null>	<Null>	<Null>	<Null>	2.47	2.61	<Null>	<Null>	5.44	2.66	0.2
SI-PRE-1007	21.29	15.95	15.40	21.00	<Null>	<Null>	<Null>	<Null>	<Null>	3.97	<Null>	<Null>	10.77	2.38	1.4
SI-PRE-1008	18.59	13.69	15.79	11.95	<Null>	<Null>	<Null>	<Null>	3.55	4.11	<Null>	<Null>	8.73	13.97	0.8
SI-PRE-1009	17.23	10.69	9.76	13.34	<Null>	<Null>	<Null>	<Null>	2.92	3.27	<Null>	<Null>	4.23	0.94	0.6
SI-PRE-1010	22.01	21.67	9.87	21.00	<Null>	<Null>	<Null>	<Null>	3.59	3.68	14.67	<Null>	3.78	3.78	1.3
SI-PRE-1011	21.04	18.83	12.88	18.79	<Null>	<Null>	<Null>	<Null>	3.25	3.21	13.63	<Null>	11.88	11.88	1.2
SI-PRE-1012	15.38	9.96	11.52	8.83	<Null>	<Null>	<Null>	<Null>	<Null>	3.04	<Null>	<Null>	3.05	3.05	0.3
SI-PRE-1013	14.02	8.17	12.33	9.72	<Null>	<Null>	<Null>	<Null>	3.02	3.66	<Null>	<Null>	3.38	3.38	0.3
SI-PRE-1014	11.24	8.25	11.24	8.25	<Null>	<Null>	<Null>	<Null>	2.92	3.28	<Null>	<Null>	5.51	3.05	0.3
SI-PRE-1015	14.58	8.60	11.59	11.97	<Null>	<Null>	<Null>	<Null>	3.29	3.33	<Null>	<Null>	4.68	2.73	0.3
SI-PRE-1016	17.55	8.26	17.55	8.26	<Null>	<Null>	<Null>	<Null>	2.55	2.75	<Null>	<Null>	5.45	1.91	0.3
SI-PRE-1017	28.41	11.74	28.41	11.74	<Null>	<Null>	<Null>	<Null>	3.88	3.95	<Null>	<Null>	4.08	24.54	1.9
SI-PRE-1018	17.01	11.80	11.80	17.01	<Null>	<Null>	<Null>	<Null>	5.11	5.29	<Null>	<Null>	5.20	5.20	1.0
SI-PRE-1019	21.04	17.16	17.16	16.12	<Null>	<Null>	<Null>	<Null>	3.14	3.29	<Null>	<Null>	7.03	1.67	0.8
SI-PRE-1020	25.22	13.17	25.22	13.17	<Null>	<Null>	<Null>	<Null>	<Null>	5.41	<Null>	<Null>	6.64	1.62	1.9
SI-PRE-1021	21.07	14.49	21.07	14.49	<Null>	<Null>	<Null>	<Null>	3.16	2.99	<Null>	<Null>	5.82	15.24	1.0
SI-PRE-1022	19.88	13.83	17.59	16.27	<Null>	<Null>	<Null>	<Null>	3.30	3.85	<Null>	<Null>	3.54	8.27	0.8
SI-PRE-1023	21.03	12.60	10.19	20.58	<Null>	<Null>	<Null>	<Null>	3.93	4.20	16.22	10.56	4.19	10.19	1.0
SI-PRE-1024	18.51	9.88	18.51	9.88	<Null>	<Null>	<Null>	<Null>	2.28	2.34	<Null>	<Null>	5.54	10.22	0.5
SI-PRE-1025	19.51	11.88	17.65	13.43	<Null>	<Null>	<Null>	<Null>	2.78	2.86	<Null>	<Null>	3.53	3.53	0.4
SI-PRE-1026	22.68	19.38	22.68	19.38	<Null>	<Null>	<Null>	<Null>	<Null>	4.26	<Null>	<Null>	5.57	9.38	1.3
SI-PRE-1027	18.35	17.79	17.79	18.35	<Null>	<Null>	<Null>	<Null>	<Null>	4.22	<Null>	<Null>	14.14	9.49	1.6
SI-PRE-1028	25.94	13.06	25.94	13.06	<Null>	<Null>	<Null>	<Null>	<Null>	3.77	<Null>	<Null>	12.07	5.86	0.8
SI-PRE-1029	29.26	21.11	27.26	21.47	<Null>	<Null>	<Null>	<Null>	3.04	3.87	<Null>	11.90	4.80	4.80	2.7
SI-PRE-1030	31.38	29.96	31.38	29.26	16.77	1.68	<Null>	<Null>	<Null>	5.82	<Null>	<Null>	28.21	28.21	5.8
SI-PRE-1031	19.44	8.55	19.44	8.55	<Null>	<Null>	<Null>	<Null>	3.62	3.66	<Null>	<Null>	7.85	4.53	1.0
SI-PRE-1032	23.03	15.82	17.89	16.31	<Null>	<Null>	<Null>	<Null>	4.47	5.23	<Null>	<Null>	16.39	17.89	1.6
SI-PRE-1033	20.54	12.10	20.54	12.10	<Null>	<Null>	17.51	<Null>	3.45	3.71	<Null>	<Null>	7.34	7.34	1.1
SI-PRE-1034	22.10	18.79	18.32	18.85	<Null>	<Null>	<Null>	<Null>	4.19	4.80	<Null>	<Null>	12.04	4.48	1.9
SI-PRE-1035	25.99	15.53	25.99	15.53	<Null>	<Null>	<Null>	<Null>	3.87	4.02	<Null>	<Null>	5.96	3.24	1.9

Catalog	LP	WP	MxLe	MxWd	BaWd	BsCo	FlLO	FlLR	FlTk	MxTk	FlWO	FlWR	MxTB	MxWB	Mass (g)
SI-PRE-1036	23.75	12.72	23.75	12.72	<Null>	<Null>	<Null>	<Null>	4.53	4.73	<Null>	<Null>	18.11	10.29	1.5
SI-PRE-1037	17.75	12.94	12.92	14.48	<Null>	<Null>	<Null>	<Null>	1.77	3.14	<Null>	<Null>	8.88	11.03	0.6
SI-PRE-1038	16.33	12.45	16.33	12.45	<Null>	<Null>	<Null>	<Null>	3.04	3.25	<Null>	<Null>	3.90	14.64	0.6
SI-PRE-1039	21.67	17.29	16.98	21.64	<Null>	<Null>	<Null>	<Null>	<Null>	5.20	<Null>	<Null>	11.79	9.08	1.6
SI-PRE-1040	24.57	13.30	24.57	13.30	<Null>	<Null>	17.80	<Null>	4.34	4.61	<Null>	<Null>	10.13	21.61	2.2
SI-PRE-1041	16.99	15.33	16.99	15.33	<Null>	<Null>	<Null>	<Null>	<Null>	3.75	<Null>	<Null>	4.34	4.34	0.9
SI-PRE-1042	17.92	16.66	16.66	17.92	<Null>	<Null>	<Null>	<Null>	<Null>	4.03	<Null>	<Null>	11.21	2.81	1.6
SI-PRE-1043	25.76	13.50	13.50	25.76	15.39	1.39	<Null>	<Null>	<Null>	6.21	<Null>	<Null>	12.50	13.50	2.2
SI-PRE-1044	21.84	12.54	12.54	21.84	<Null>	<Null>	<Null>	<Null>	3.74	3.90	<Null>	<Null>	11.49	11.49	1.3
SI-PRE-1045	19.29	11.88	19.29	11.88	<Null>	<Null>	<Null>	<Null>	4.08	4.42	<Null>	<Null>	14.75	1.05	1.0
SI-PRE-1046	24.93	17.58	17.80	24.75	<Null>	<Null>	<Null>	<Null>	3.30	4.12	15.50	14.28	10.03	10.03	2.0
SI-PRE-1047	16.46	12.31	16.46	12.31	<Null>	<Null>	<Null>	<Null>	3.35	3.52	<Null>	<Null>	10.32	10.32	0.9
SI-PRE-1048	25.65	12.39	25.65	12.39	<Null>	<Null>	<Null>	<Null>	2.72	3.07	<Null>	<Null>	8.02	1.88	1.0
SI-PRE-1049	23.66	20.09	17.17	21.79	14.29	1.37	<Null>	<Null>	2.52	2.73	8.23	17.17	9.89	9.89	1.4
SI-PRE-1050	29.50	21.56	25.26	25.31	<Null>	<Null>	<Null>	<Null>	4.40	4.94	<Null>	<Null>	13.41	13.41	3.4
SI-PRE-1051	25.50	21.40	16.81	24.49	<Null>	<Null>	<Null>	<Null>	<Null>	6.52	<Null>	<Null>	15.48	2.19	2.8
SI-PRE-1052	24.05	12.57	24.05	12.57	<Null>	<Null>	<Null>	<Null>	2.91	2.95	<Null>	<Null>	16.11	16.11	1.1
SI-PRE-1053	23.02	15.76	13.72	17.67	<Null>	<Null>	<Null>	<Null>	<Null>	3.60	<Null>	<Null>	8.92	8.92	1.0
SI-PRE-1054	21.52	18.96	10.74	21.16	<Null>	<Null>	<Null>	<Null>	2.25	2.75	14.58	<Null>	6.66	6.66	0.9
SI-PRE-1055	22.96	13.95	13.95	22.96	<Null>	<Null>	<Null>	<Null>	<Null>	5.06	<Null>	<Null>	8.58	2.22	1.7
SI-PRE-1056	23.27	22.45	22.45	23.27	<Null>	<Null>	<Null>	<Null>	<Null>	7.52	<Null>	<Null>	2.43	8.97	3.7
SI-PRE-1057	16.46	10.50	16.46	10.50	<Null>	<Null>	<Null>	<Null>	4.17	4.95	<Null>	<Null>	9.81	16.46	0.9
SI-PRE-1058	15.23	12.31	15.23	12.31	<Null>	<Null>	<Null>	<Null>	2.67	3.01	<Null>	<Null>	10.27	7.07	0.6
SI-PRE-1059	11.31	9.20	7.89	8.98	<Null>	<Null>	<Null>	<Null>	2.84	3.10	<Null>	<Null>	3.70	5.68	0.2
SI-PRE-1060	16.87	7.09	7.09	16.87	<Null>	<Null>	<Null>	<Null>	<Null>	3.05	<Null>	<Null>	2.19	2.19	0.4
SI-PRE-1061	14.94	8.52	12.37	9.53	<Null>	<Null>	<Null>	<Null>	3.22	3.51	<Null>	<Null>	5.10	5.10	0.4
SI-PRE-1062	9.19	7.58	9.19	7.58	<Null>	<Null>	<Null>	<Null>	3.32	3.53	<Null>	<Null>	4.71	4.71	0.4
SI-PRE-1063	19.62	17.03	17.03	19.62	<Null>	<Null>	<Null>	<Null>	<Null>	4.29	<Null>	<Null>	7.65	7.65	1.9
SI-PRE-1064	35.86	32.06	32.85	24.15	<Null>	<Null>	<Null>	<Null>	3.38	4.03	12.50	<Null>	20.54	6.01	4.4
SI-PRE-1065	23.46	13.02	16.82	19.50	<Null>	<Null>	<Null>	<Null>	1.88	3.27	14.01	<Null>	12.70	12.70	0.9

Catalog	LP	WP	MxLe	MxWd	BaWd	BsCo	FlLO	FlLR	FlTk	MxTk	FlWO	FlWR	MxTB	MxWB	Mass (g)
SI-PRE-1066	22.27	12.43	11.97	20.51	<Null>	<Null>	<Null>	<Null>	2.36	2.43	12.97	<Null>	8.87	5.50	0.7
SI-PRE-1067	20.49	9.81	9.81	20.49	<Null>	<Null>	<Null>	<Null>	<Null>	4.73	<Null>	<Null>	8.25	3.92	1.0
SI-PRE-1068	26.24	24.87	26.24	24.87	<Null>	<Null>	<Null>	<Null>	4.81	5.10	8.67	<Null>	6.80	6.80	3.8
SI-PRE-1069	17.03	12.22	17.03	12.22	<Null>	<Null>	<Null>	<Null>	3.47	4.36	<Null>	<Null>	7.04	5.63	1.1
SI-PRE-1070	15.20	11.98	15.20	11.98	<Null>	<Null>	<Null>	<Null>	5.52	5.92	<Null>	<Null>	7.89	4.27	1.3
SI-PRE-1071	32.84	25.64	26.17	25.36	<Null>	<Null>	<Null>	<Null>	<Null>	5.79	<Null>	<Null>	10.58	26.17	4.1
SI-PRE-1072	25.74	12.39	12.39	25.74	25.74	<Null>	<Null>	<Null>	<Null>	6.56	<Null>	<Null>	7.48	4.32	2.1
SI-PRE-1073	25.44	10.26	20.26	25.44	<Null>	<Null>	<Null>	<Null>	<Null>	4.13	<Null>	<Null>	4.44	4.44	1.2
SI-PRE-1074	17.95	9.87	13.02	13.54	<Null>	<Null>	<Null>	<Null>	3.11	3.23	7.82	10.61	3.85	3.85	0.6
SI-PRE-1075	18.27	9.72	9.72	18.27	<Null>	<Null>	<Null>	<Null>	<Null>	5.08	<Null>	<Null>	2.65	2.65	0.8
SI-PRE-1076	24.14	10.94	10.94	24.14	<Null>	<Null>	<Null>	<Null>	<Null>	4.80	<Null>	<Null>	5.53	5.53	1.3
SI-PRE-1077	20.76	20.08	20.76	20.08	<Null>	<Null>	<Null>	<Null>	<Null>	4.93	<Null>	<Null>	7.18	7.18	2.2
SI-PRE-1078	25.16	9.97	9.97	25.16	<Null>	<Null>	<Null>	<Null>	3.21	3.41	18.85	<Null>	5.41	5.41	1.1
SI-PRE-1079	21.33	16.63	16.89	19.79	<Null>	<Null>	<Null>	<Null>	<Null>	4.09	<Null>	<Null>	7.57	1.76	1.4
SI-PRE-1080	21.75	19.26	19.26	21.75	<Null>	<Null>	<Null>	<Null>	6.33	6.70	11.03	<Null>	7.33	7.33	2.9
SI-PRE-1081	16.09	15.90	15.90	16.09	<Null>	2.27	<Null>	<Null>	5.13	5.39	10.76	<Null>	11.59	0.00	1.1
SI-PRE-1082	23.66	20.02	20.02	23.66	15.09	1.03	<Null>	<Null>	<Null>	7.41	<Null>	<Null>	15.72	15.72	3.2
SI-PRE-1083	22.81	13.10	13.10	22.81	13.94	1.96	<Null>	<Null>	<Null>	3.71	<Null>	<Null>	13.10	13.10	1.2
SI-PRE-1084	31.74	27.65	31.74	27.65	<Null>	<Null>	<Null>	<Null>	<Null>	5.48	<Null>	<Null>	23.32	0.00	4.5
SI-PRE-1085	15.71	11.20	15.71	11.20	<Null>	<Null>	<Null>	<Null>	<Null>	3.34	<Null>	<Null>	0.00	0.00	0.8
SI-PRE-1086	16.47	12.77	16.47	12.77	<Null>	<Null>	<Null>	<Null>	2.30	3.50	<Null>	<Null>	16.47	16.47	0.8
SI-PRE-1087	17.57	10.47	10.47	17.57	<Null>	<Null>	<Null>	<Null>	<Null>	4.83	<Null>	<Null>	10.47	0.00	0.8
SI-PRE-1088	17.11	13.88	17.11	13.88	<Null>	2.43	<Null>	<Null>	3.20	3.60	<Null>	<Null>	0.00	0.00	0.8
SI-PRE-1089	14.87	7.48	14.87	7.48	<Null>	1.73	<Null>	<Null>	2.08	3.01	<Null>	<Null>	7.19	1.73	0.3

C5. Channel flake descriptive and metric data.

Catalog	Portion	GENMAT	SPECMAT	Nodule	Burning	Double	MxLe	MxWd	MxTk	PltWd	PltTk	NegWd	Mass (g)
CMPA-CF-1001	DS	CCS	TRT	TRT-04	NO	YES	14.61	8.74	1.41	<Null>	<Null>	4.60	0.2
CMPA-CF-1002	MS	CCS	PED	PED-02	NO	NO	12.79	15.52	2.45	<Null>	<Null>	<Null>	0.7
CMPA-CF-1003	PR	CCS	TRT	TRT-05	NO	YES	10.42	13.95	2.03	5.62	1.94	7.01	0.4

Catalog	Portion	GENMAT	SPECMAT	Nodule	Burning	Double	MxLe	MxWd	MxTk	PltWd	PltTk	NegWd	Mass (g)
CMPA-CF-1004	PR	CCS	UNK	UNK-04	NO	NO	14.99	12.26	2.33	4.51	1.85	<Null>	0.4
CMPA-CF-1005	MS	CCS	TRT	TRT-13	NO	NO	14.81	12.46	1.24	<Null>	<Null>	<Null>	0.4
CMPA-CF-1006	PR	CCS	EDW	EDW-01	NO	NO	13.91	11.33	2.35	7.02	2.35	<Null>	0.3
CMPA-CF-1007	PR	CCS	TRT	TRT-01	NO	NO	13.73	12.56	1.98	4.12	1.10	<Null>	0.4
CMPA-CF-1008	MS	CCS	TRT	TRT-13	NO	NO	13.97	13.24	1.84	<Null>	<Null>	<Null>	0.4
CMPA-CF-1009	MS	CCS	TRT	TRT-10	NO	NO	15.17	9.93	1.81	<Null>	<Null>	<Null>	0.3
CMPA-CF-1010	MS	SWD	SWD	SWD-04	NO	NO	13.05	16.35	1.83	<Null>	<Null>	<Null>	0.5
CMPA-CF-1011	MS	CCS	TRT	TRT-10	NO	NO	10.63	10.71	1.79	<Null>	<Null>	<Null>	0.3
CMPA-CF-1012	PR	CCS	TRT	TRT-14	NO	YES	13.15	13.76	1.81	5.75	1.81	7.51	0.3
CMPA-CF-1013	MS	CCS	TRT	TRT-03	POT	NO	12.56	16.54	2.26	<Null>	<Null>	<Null>	0.4
CMPA-CF-1014	MS	CCS	UNK	UNK-05	NO	NO	12.64	16.80	2.47	<Null>	<Null>	<Null>	0.6
CMPA-CF-1015	PR	CCS	UNK	UNK-06	NO	NO	15.74	15.09	2.31	5.15	2.08	<Null>	0.6
CMPA-CF-1016	MS	CCS	TRT	TRT-10	NO	NO	7.04	18.67	2.18	<Null>	<Null>	<Null>	0.4
CMPA-CF-1017	MS	QZT	DAK	DAK-01	NO	NO	9.28	11.76	1.61	<Null>	<Null>	<Null>	0.2
CMPA-CF-1018	MS	CCS	TRT	TRT-02	NO	NO	10.35	14.34	2.01	<Null>	<Null>	<Null>	0.4
CMPA-CF-1019	MS	CCS	UNK	UNK-08	NO	NO	12.61	15.29	2.23	<Null>	<Null>	<Null>	0.5
CMPA-CF-1020	PR	CCS	TRT	TRT-15	NO	NO	11.55	13.72	2.44	4.61	1.88	<Null>	0.4
CMPA-CF-1021	MS	CCS	TRT	TRT-13	NO	NO	9.64	12.72	2.06	<Null>	<Null>	<Null>	0.3
CMPA-CF-1022	PR	CCS	TRT	TRT-02	NO	NO	15.73	12.68	2.26	4.82	1.89	<Null>	0.4
CMPA-CF-1023	MS	CCS	TRT	TRT-03	NO	NO	7.24	15.99	1.87	<Null>	<Null>	<Null>	0.3
CMPA-CF-1024	MS	CCS	TRT	TRT-12	NO	YES	12.25	12.70	1.89	<Null>	<Null>	<Null>	0.4
CMPA-CF-1025	MS	CCS	TRT	TRT-06	NO	NO	10.20	11.57	1.72	<Null>	<Null>	<Null>	0.3
CMPA-CF-1026	MS	CCS	TRT	TRT-16	NO	NO	7.43	13.75	1.74	<Null>	<Null>	<Null>	0.2
CMPA-CF-1027	MS	CCS	TRT	TRT-10	NO	NO	13.93	7.22	2.27	<Null>	<Null>	<Null>	0.4
CMPA-CF-1028	PR	CCS	TRT	TRT-12	NO	NO	16.97	11.57	1.98	3.88	1.23	<Null>	0.4
CMPA-CF-1029	PR	CCS	TRT	TRT-02	NO	NO	12.51	8.13	1.62	3.86	1.39	<Null>	0.2
CMPA-CF-1030	MS	CCS	TRT	TRT-13	NO	NO	16.31	10.68	1.57	<Null>	<Null>	<Null>	0.3
CMPA-CF-1031	MS	CCS	TRT	TRT-12	NO	NO	11.11	11.32	1.67	<Null>	<Null>	<Null>	0.2
CMPA-CF-1032	PR	CCS	EDW	EDW-01	NO	NO	10.76	12.40	1.78	4.95	1.71	<Null>	0.2

Catalog	Portion	GENMAT	SPECMAT	Nodule	Burning	Double	MxLe	MxWd	MxTk	PltWd	PltTk	NegWd	Mass (g)
CMPA-CF-1033	MS	CCS	TRT	TRT-17	NO	NO	13.93	14.88	2.08	<Null>	<Null>	<Null>	0.4
CMPA-CF-1034	LT	CCS	EDW	EDW-01	NO	NO	9.66	10.35	1.27	<Null>	<Null>	<Null>	0.2
CMPA-CF-1035	LT	CCS	TRT	TRT-08	NO	NO	11.47	9.14	1.46	<Null>	<Null>	<Null>	0.2
CMPA-CF-1036	PR	CCS	TRT	TRT-02	NO	YES	15.52	14.94	2.01	4.34	1.69	<Null>	0.6
CMPA-CF-1037	LT	CCS	TRT	TRT-05	NO	NO	13.14	5.39	1.22	<Null>	<Null>	<Null>	0.1
CMPA-CF-1038	LT	QZT	MOR	MOR-02	NO	YES	12.18	8.84	1.42	<Null>	<Null>	<Null>	0.3
CMPA-CF-1039	MS	CCS	TRT	TRT-10	POT	NO	10.22	15.36	2.05	<Null>	<Null>	<Null>	0.3
CMPA-CF-1040	LT	CCS	TRT	TRT-08	NO	NO	7.90	12.80	1.73	<Null>	<Null>	<Null>	0.3
CMPA-CF-1041	PR	CCS	FLAT	FLAT-02	NO	NO	12.18	9.01	1.65	3.82	1.65	<Null>	0.2
CMPA-CF-1042	MS	CCS	EDW	EDW-01	NO	NO	8.83	14.39	1.44	<Null>	<Null>	<Null>	0.3
CMPA-CF-1043	PR	CCS	CUMB	CUMB-03	NO	NO	12.07	9.69	1.58	3.86	1.58	<Null>	0.2
CMPA-CF-1044	LT	CCS	NARB	NARB-01	POT	YES	10.25	8.07	1.59	<Null>	<Null>	<Null>	0.1
CMPA-CF-1045	PR	VOL	DAC	DAC-01	NO	NO	8.98	9.58	1.70	4.29	1.65	<Null>	0.2
CMPA-CF-1046	LT	CCS	TRT	TRT-13	NO	NO	7.18	9.87	1.40	<Null>	<Null>	<Null>	0.1
CMPA-CF-1047	LT	CCS	TRT	TRT-08	NO	YES	19.73	8.11	1.63	<Null>	<Null>	4.18	0.3
CMPA-CF-1048	MS	CCS	TRT	TRT-15	NO	NO	17.61	11.47	1.92	<Null>	<Null>	<Null>	0.5
CMPA-CF-1049	PR	CCS	TRT	TRT-17	POT	NO	15.41	12.43	2.33	4.56	1.44	<Null>	0.5
CMPA-CF-1050	PR	CCS	TRT	TRT-10	NO	NO	17.54	11.37	2.46	3.74	1.47	<Null>	0.5
CMPA-CF-1051	MS	CCS	TRT	TRT-08	NO	NO	15.09	19.05	2.77	<Null>	<Null>	<Null>	0.9
CMPA-CF-1052	LT	CCS	PED	PED-03	NO	NO	16.48	13.96	2.58	<Null>	<Null>	<Null>	0.5
CMPA-CF-1053	LT	CCS	TRT	TRT-01	NO	YES	9.89	13.88	1.24	<Null>	<Null>	<Null>	0.2
CMPA-CF-1054	LT	CCS	TRT	TRT-02	NO	YES	11.89	10.03	1.11	<Null>	<Null>	<Null>	0.2
CMPA-CF-1055	LT	CCS	TRT	TRT-17	POT	YES	12.17	10.06	2.35	<Null>	<Null>	<Null>	0.4
CMPA-CF-1056	MS	CCS	TRT	TRT-08	NO	YES	15.63	12.63	2.25	<Null>	<Null>	5.66	0.6
CMPA-CF-1057	PR	CCS	TRT	TRT-02	NO	NO	19.84	12.40	1.94	4.91	1.94	<Null>	0.4
CMPA-CF-1058	LT	CCS	TRT	TRT-02	NO	YES	13.74	9.65	1.84	<Null>	<Null>	<Null>	0.2
CMPA-CF-1059	PR	CCS	TRT	TRT-02	NO	NO	14.65	18.24	2.61	5.51	1.94	<Null>	0.6
CMPA-CF-1060	DS	SWD	SWD	SWD-04	NO	NO	10.73	13.88	3.21	<Null>	<Null>	<Null>	0.3
CMPA-CF-1061	PR	CCS	EDW	EDW-01	NO	NO	15.08	10.98	1.73	<Null>	1.73	<Null>	0.3

Catalog	Portion	GENMAT	SPECMAT	Nodule	Burning	Double	MxLe	MxWd	MxTk	PltWd	PltTk	NegWd	Mass (g)
CMPA-CF-1062	MS	SWD	SWD	SWD-04	NO	NO	14.30	15.28	1.92	<Null>	<Null>	<Null>	0.5
SI-CF-1001	MS	SWD	SWD	SWD-07	NO	NO	14.15	12.11	2.92	<Null>	<Null>	<Null>	0.7
SI-CF-1002	PR	CCS	TRT	TRT-04	NO	NO	12.59	12.13	2.35	4.09	2.19	<Null>	0.4
SI-CF-1003	PR	CCS	TRT	TRT-02	NO	NO	13.09	14.32	1.80	3.26	1.36	<Null>	0.3
SI-CF-1004	PR	CCS	TRT	TRT-02	NO	NO	16.45	13.88	2.50	4.01	1.81	<Null>	0.6
SI-CF-1005	PR	CCS	UNK	UNK-07	NO	NO	18.08	13.68	2.27	3.56	1.48	<Null>	0.6
SI-CF-1006	MS	SWD	SWD	SWD-05	NO	NO	14.50	13.62	2.66	<Null>	<Null>	<Null>	0.6
SI-CF-1007	PR	CCS	TRT	TRT-08	NO	NO	14.62	15.01	2.38	5.83	1.18	<Null>	0.5
SI-CF-1008	PR	SWD	SWD	SWD-05	NO	NO	12.22	11.52	1.88	3.34	1.51	<Null>	0.3
SI-CF-1009	PR	CCS	TRT	TRT-08	NO	NO	13.51	13.90	2.69	4.44	1.80	<Null>	0.5
SI-CF-1010	PR	CCS	TRT	TRT-02	NO	NO	14.30	12.08	2.08	2.89	1.98	<Null>	0.4
SI-CF-1011	PR	CCS	TRT	TRT-02	NO	NO	14.15	19.04	2.17	4.30	1.39	<Null>	0.7
SI-CF-1012	PR	CCS	TRT	TRT-10	NO	NO	13.52	15.18	2.94	4.96	1.83	<Null>	0.6
SI-CF-1013	PR	CCS	TRT	TRT-08	NO	NO	8.96	10.38	2.23	4.47	2.23	<Null>	0.2
SI-CF-1014	PR	CCS	TRT	TRT-10	NO	NO	12.42	12.82	2.06	3.63	1.33	<Null>	0.4
SI-CF-1015	PR	CCS	TRT	TRT-08	NO	NO	14.11	10.14	2.60	5.49	2.37	<Null>	0.4
SI-CF-1016	PR	CCS	TRT	TRT-13	POT	YES	13.46	16.14	2.21	3.04	1.46	7.22	0.5
SI-CF-1017	PR	CCS	TRT	TRT-10	NO	NO	14.32	11.93	1.85	4.33	1.19	<Null>	0.3
SI-CF-1018	PR	CCS	TRT	TRT-02	NO	NO	10.22	8.83	2.06	4.64	1.84	<Null>	0.2
SI-CF-1019	MS	SWD	SWD	SWD-04	NO	NO	13.15	11.86	1.95	<Null>	<Null>	<Null>	0.5
SI-CF-1020	LT	CCS	TRT	TRT-13	NO	NO	9.15	5.66	0.88	<Null>	<Null>	<Null>	0.1
SI-CF-1021	LT	CCS	TRT	TRT-15	NO	NO	8.93	6.86	1.49	<Null>	<Null>	<Null>	0.1
SI-CF-1022	LT	CCS	EDW	EDW-01	NO	NO	8.23	8.77	1.75	<Null>	<Null>	<Null>	0.2
SI-CF-1023	LT	CCS	UNK	UNK-07	NO	NO	8.23	10.95	2.09	<Null>	<Null>	<Null>	0.3
SI-CF-1024	LT	CCS	TRT	TRT-19	POT	YES	19.86	10.34	1.73	<Null>	<Null>	7.43	0.5
SI-CF-1025	MS	CCS	TRT	TRT-12	NO	NO	20.97	11.75	1.89	<Null>	<Null>	<Null>	0.6
SI-CF-1026	PR	CCS	TRT	TRT-02	NO	NO	18.72	12.13	1.91	2.63	1.44	<Null>	0.5
SI-CF-1027	LT	CCS	TRT	TRT-02	NO	NO	14.19	13.70	2.54	<Null>	<Null>	<Null>	0.6
SI-CF-1028	LT	CCS	TRT	TRT-06	NO	NO	18.53	20.61	2.83	<Null>	<Null>	<Null>	1.1

Catalog	Portion	GENMAT	SPECMAT	Nodule	Burning	Double	MxLe	MxWd	MxTk	PltWd	PltTk	NegWd	Mass (g)
SI-CF-1029	LT	CCS	TRT	TRT-02	NO	NO	12.85	14.40	2.52	<Null>	<Null>	<Null>	0.6
SI-CF-1030	MS	CCS	TRT	TRT-12	NO	NO	16.43	14.81	2.10	<Null>	<Null>	<Null>	0.5
SI-CF-1031	LT	CCS	TRT	TRT-02	NO	NO	14.76	14.65	2.57	<Null>	<Null>	<Null>	0.7
SI-CF-1032	MS	CCS	TRT	TRT-06	NO	NO	8.50	13.01	1.79	<Null>	<Null>	<Null>	0.3
SI-CF-1033	MS	CCS	TRT	TRT-02	NO	NO	14.94	14.65	2.41	<Null>	<Null>	<Null>	0.6
SI-CF-1034	MS	CCS	TRT	TRT-01	NO	NO	12.12	15.84	2.26	<Null>	<Null>	<Null>	0.5
SI-CF-1035	MS	CCS	TRT	TRT-10	NO	YES	12.30	13.52	1.56	<Null>	<Null>	5.18	0.3
SI-CF-1036	MS	CCS	TRT	TRT-04	NO	NO	13.58	14.89	1.88	<Null>	<Null>	<Null>	0.4
SI-CF-1037	MS	CCS	TRT	TRT-06	NO	NO	13.64	14.50	2.15	<Null>	<Null>	<Null>	0.5
SI-CF-1038	MS	CCS	TRT	TRT-02	NO	NO	8.82	15.42	1.85	<Null>	<Null>	<Null>	0.4
SI-CF-1039	MS	CCS	UNK	UNK-01	NO	NO	15.37	16.72	2.35	<Null>	<Null>	<Null>	0.6
SI-CF-1040	MS	CCS	TRT	TRT-07	POT	NO	13.58	11.54	1.64	<Null>	<Null>	<Null>	0.4
SI-CF-1041	MS	CCS	TRT	TRT-13	NO	NO	2.13	15.36	1.98	<Null>	<Null>	<Null>	0.6
SI-CF-1042	MS	CCS	NARB	NARB-01	NO	NO	7.64	12.90	1.29	<Null>	<Null>	<Null>	0.2
SI-CF-1043	LT	CCS	NARB	NARB-01	NO	NO	11.39	16.02	1.56	<Null>	<Null>	<Null>	0.4
SI-CF-1044	LT	CCS	TRT	TRT-06	NO	NO	10.98	12.71	2.16	<Null>	<Null>	<Null>	0.3
SI-CF-1045	MS	CCS	TRT	TRT-08	NO	NO	11.34	12.88	1.64	<Null>	<Null>	<Null>	0.3
SI-CF-1046	MS	CCS	NARB	NARB-01	PTCZ	NO	9.17	12.74	1.86	<Null>	<Null>	<Null>	0.3
SI-CF-1047	MS	CCS	TRT	TRT-02	NO	NO	10.51	12.80	1.88	<Null>	<Null>	<Null>	0.3
SI-CF-1048	MS	CCS	TRT	TRT-07	NO	NO	9.94	13.58	1.90	<Null>	<Null>	<Null>	0.3
SI-CF-1049	LT	CCS	TRT	TRT-10	NO	NO	7.90	14.52	1.55	<Null>	<Null>	<Null>	0.2
SI-CF-1050	MS	CCS	UNK	UNK-05	NO	NO	16.21	12.12	2.64	<Null>	<Null>	<Null>	0.5
SI-CF-1051	MS	CCS	UNK	UNK-06	NO	NO	14.66	11.43	1.64	<Null>	<Null>	<Null>	0.3
SI-CF-1052	LT	CCS	TRT	TRT-06	NO	NO	15.72	11.87	1.75	<Null>	<Null>	<Null>	0.5
SI-CF-1053	MS	CCS	TRT	TRT-02	NO	NO	10.78	14.38	2.31	<Null>	<Null>	<Null>	0.5
SI-CF-1054	MS	CCS	UNK	UNK-05	NO	NO	14.36	11.76	1.90	<Null>	<Null>	<Null>	0.4
SI-CF-1055	MS	CCS	TRT	TRT-06	NO	NO	12.43	14.61	2.31	<Null>	<Null>	<Null>	0.6
SI-CF-1056	MS	CCS	TRT	TRT-08	NO	NO	9.83	14.59	1.71	<Null>	<Null>	<Null>	0.4
SI-CF-1057	MS	CCS	TRT	TRT-05	NO	NO	14.48	15.82	2.26	<Null>	<Null>	<Null>	0.6

Catalog	Portion	GENMAT	SPECMAT	Nodule	Burning	Double	MxLe	MxWd	MxTk	PltWd	PltTk	NegWd	Mass (g)
SI-CF-1058	LT	CCS	TRT	TRT-05	NO	NO	14.21	14.65	2.24	<Null>	<Null>	<Null>	0.6
SI-CF-1059	MS	CCS	TRT	TRT-02	NO	NO	12.48	11.89	2.17	<Null>	<Null>	<Null>	0.5
SI-CF-1060	MS	CCS	UNK	UNK-06	NO	NO	11.59	14.76	1.98	<Null>	<Null>	<Null>	0.4
SI-CF-1061	MS	CCS	TRT	TRT-12	NO	NO	10.71	11.21	1.38	<Null>	<Null>	<Null>	0.2
SI-CF-1062	MS	CCS	TRT	TRT-08	NO	NO	13.80	10.33	1.81	<Null>	<Null>	<Null>	0.4
SI-CF-1063	MS	SWD	SWD	SWD-04	NO	YES	13.09	13.87	1.97	<Null>	<Null>	6.17	0.4
SI-CF-1064	MS	CCS	TRT	TRT-10	NO	NO	9.91	14.50	1.26	<Null>	<Null>	<Null>	0.3
SI-CF-1065	LT	CCS	NARB	NARB-01	POT	NO	14.07	9.15	1.79	<Null>	<Null>	<Null>	0.3
SI-CF-1066	MS	CCS	NARB	NARB-01	NO	NO	11.34	14.54	1.71	<Null>	<Null>	<Null>	0.3
SI-CF-1067	LT	CCS	TRT	TRT-10	NO	NO	16.01	11.43	2.27	<Null>	<Null>	<Null>	0.6
SI-CF-1068	MS	CCS	TRT	TRT-02	NO	NO	13.04	18.65	2.27	<Null>	<Null>	<Null>	0.7
SI-CF-1069	MS	CCS	TRT	TRT-07	NO	NO	12.18	14.07	1.68	<Null>	<Null>	<Null>	0.4
SI-CF-1070	LT	CCS	TRT	TRT-18	NO	NO	10.41	13.97	1.88	<Null>	<Null>	<Null>	0.2
SI-CF-1071	MS	CCS	TRT	TRT-10	PTCZ	NO	8.76	16.49	1.79	<Null>	<Null>	<Null>	0.4
SI-CF-1072	MS	CCS	TRT	TRT-06	NO	NO	10.82	11.45	1.81	<Null>	<Null>	<Null>	0.3
SI-CF-1073	LT	CCS	TRT	TRT-05	NO	NO	14.39	10.80	1.45	<Null>	<Null>	<Null>	0.2
SI-CF-1074	LT	CCS	TRT	TRT-06	NO	NO	12.15	13.34	1.98	<Null>	<Null>	<Null>	0.4
SI-CF-1075	MS	CCS	TRT	TRT-02	NO	NO	12.60	14.73	2.23	<Null>	<Null>	<Null>	0.5
SI-CF-1076	MS	CCS	TRT	TRT-02	NO	NO	12.75	10.57	1.31	<Null>	<Null>	<Null>	0.2
SI-CF-1077	MS	CCS	TRT	TRT-08	NO	NO	10.05	13.36	1.82	<Null>	<Null>	<Null>	0.3
SI-CF-1078	MS	CCS	TRT	TRT-10	NO	NO	9.11	11.75	1.27	<Null>	<Null>	<Null>	0.2
SI-CF-1079	LT	CCS	CUMB	CUMB-01	NO	NO	12.24	12.95	1.87	<Null>	<Null>	<Null>	0.3
SI-CF-1080	MS	CCS	UNK	UNK-01	NO	NO	11.12	11.01	1.51	<Null>	<Null>	<Null>	0.2
SI-CF-1081	MS	CCS	TRT	TRT-05	NO	NO	17.47	11.10	1.59	<Null>	<Null>	<Null>	0.4
SI-CF-1082	PR	CCS	NARB	NARB-02	NO	NO	18.39	12.03	1.66	1.63	0.94	<Null>	0.4
SI-CF-1083	MS	CCS	TRT	TRT-01	NO	NO	9.91	12.38	1.65	<Null>	<Null>	<Null>	0.3
SI-CF-1084	MS	CCS	TRT	TRT-12	NO	NO	14.65	9.63	1.68	<Null>	<Null>	<Null>	0.3
SI-CF-1085	MS	CCS	CUMB	CUMB-01	NO	NO	11.25	15.48	1.95	<Null>	<Null>	<Null>	0.4
SI-CF-1086	LT	SWD	SWD	SWD-04	NO	NO	15.26	7.58	1.40	<Null>	<Null>	<Null>	0.2

Catalog	Portion	GENMAT	SPECMAT	Nodule	Burning	Double	MxLe	MxWd	MxTk	PltWd	PltTk	NegWd	Mass (g)
SI-CF-1087	MS	CCS	CUMB	CUMB-01	NO	NO	9.13	9.78	1.36	<Null>	<Null>	<Null>	0.1
SI-CF-1088	LT	CCS	TRT	TRT-02	NO	NO	12.96	9.08	1.78	<Null>	<Null>	<Null>	0.3
SI-CF-1089	MS	CCS	TRT	TRT-04	NO	NO	9.11	13.04	2.22	<Null>	<Null>	<Null>	0.3
SI-CF-1090	MS	CCS	TRT	TRT-13	NO	NO	12.99	12.47	1.12	<Null>	<Null>	<Null>	0.2
SI-CF-1091	MS	CCS	TRT	TRT-02	NO	NO	9.53	15.28	1.98	<Null>	<Null>	<Null>	0.4
SI-CF-1092	LT	CCS	TRT	TRT-12	NO	NO	13.68	12.91	1.55	<Null>	<Null>	<Null>	0.3
SI-CF-1093	MS	SWD	SWD	SWD-01	NO	NO	14.30	15.20	2.35	<Null>	<Null>	<Null>	0.5
SI-CF-1094	MS	CCS	TRT	TRT-08	NO	NO	10.91	14.73	1.92	<Null>	<Null>	<Null>	0.4
SI-CF-1095	PR	CCS	UNK	UNK-05	NO	NO	14.16	8.57	1.58	2.63	1.58	<Null>	0.2
SI-CF-1096	MS	CCS	TRT	TRT-05	NO	NO	11.40	14.71	1.51	<Null>	<Null>	<Null>	0.3
SI-CF-1097	LT	CCS	TRT	TRT-12	NO	YES	13.74	12.23	1.53	<Null>	<Null>	<Null>	0.4
SI-CF-1098	MS	CCS	TRT	TRT-12	NO	NO	10.43	12.87	2.07	<Null>	<Null>	<Null>	0.4
SI-CF-1099	LT	CCS	UNK	UNK-06	NO	NO	12.27	7.63	1.53	<Null>	<Null>	<Null>	0.2
SI-CF-1100	LT	CCS	TRT	TRT-10	NO	NO	11.94	9.45	1.72	<Null>	<Null>	<Null>	0.3
SI-CF-1101	LT	CCS	TRT	TRT-08	NO	NO	9.41	11.39	1.53	<Null>	<Null>	<Null>	0.2
SI-CF-1102	LT	CCS	TRT	TRT-17	NO	YES	9.73	13.08	1.49	<Null>	<Null>	<Null>	0.2
SI-CF-1103	MS	CCS	TRT	TRT-08	NO	NO	6.96	11.82	1.79	<Null>	<Null>	<Null>	0.2
SI-CF-1104	LT	SWD	SWD	SWD-06	NO	NO	9.51	9.99	1.71	<Null>	<Null>	<Null>	0.2
SI-CF-1105	LT	CCS	TRT	TRT-10	NO	NO	8.45	14.60	1.67	<Null>	<Null>	<Null>	0.3
SI-CF-1106	MS	CCS	MOSC	MOSC-07	NO	NO	12.48	12.73	2.37	<Null>	<Null>	<Null>	0.5
SI-CF-1107	PR	CCS	TRT	TRT-02	NO	NO	12.61	10.05	2.09	2.45	1.75	<Null>	0.3
SI-CF-1108	PR	CCS	TRT	TRT-01	NO	YES	13.75	9.07	1.90	2.85	1.74	<Null>	0.3
SI-CF-1109	MS	CCS	PED	PED-01	NO	NO	7.50	11.81	1.79	<Null>	<Null>	<Null>	0.2
SI-CF-1110	MS	SWD	SWD	SWD-04	NO	NO	8.87	13.31	1.90	<Null>	<Null>	<Null>	0.3
SI-CF-1111	LT	CCS	NARB	NARB-01	NO	YES	14.62	11.43	1.86	<Null>	<Null>	<Null>	0.3
SI-CF-1112	MS	CCS	PED	PED-01	NO	NO	5.90	11.14	1.24	<Null>	<Null>	<Null>	0.1
SI-CF-1113	MS	CCS	TRT	TRT-08	NO	NO	22.28	18.58	2.41	<Null>	<Null>	<Null>	1.2
SI-CF-1114	MS	CCS	TRT	TRT-10	NO	NO	20.07	16.41	2.32	<Null>	<Null>	<Null>	0.8
SI-CF-1115	LT	CCS	TRT	TRT-13	NO	NO	15.86	15.49	1.50	<Null>	<Null>	<Null>	0.4

Catalog	Portion	GENMAT	SPECMAT	Nodule	Burning	Double	MxLe	MxWd	MxTk	PltWd	PltTk	NegWd	Mass (g)
SI-CF-1116	MS	CCS	TRT	TRT-13	NO	NO	18.73	17.60	2.15	<Null>	<Null>	<Null>	1.0
SI-CF-1117	LT	CCS	MOSC	MOSC-08	NO	NO	12.19	8.38	1.43	<Null>	<Null>	<Null>	0.2
SI-CF-1118	LT	CCS	TRT	TRT-10	POT	NO	9.81	9.59	1.48	<Null>	<Null>	<Null>	0.1
SI-CF-1119	LT	CCS	TRT	TRT-13	NO	NO	10.52	10.27	1.55	<Null>	<Null>	<Null>	0.2
SI-CF-1120	MS	SWD	SWD	SWD-04	NO	NO	6.59	14.03	2.40	<Null>	<Null>	<Null>	0.3
SI-CF-1121	MS	CCS	CUMB	CUMB-04	NO	NO	14.36	20.19	2.26	<Null>	<Null>	<Null>	1.0
SI-CF-1122	LT	SWD	SWD	SWD-06	NO	NO	11.35	10.72	1.33	<Null>	<Null>	<Null>	0.2
SI-CF-1123	MS	CCS	TRT	TRT-17	NO	NO	6.60	14.22	2.23	<Null>	<Null>	<Null>	0.2
SI-CF-1124	MS	CCS	NARB	NARB-01	NO	NO	11.98	14.17	1.36	<Null>	<Null>	<Null>	0.3
SI-CF-1125	LT	SWD	SWD	SWD-04	NO	NO	10.73	11.92	2.13	<Null>	<Null>	<Null>	0.3
SI-CF-1126	MS	CCS	NARB	NARB-01	NO	NO	10.01	15.45	2.58	<Null>	<Null>	<Null>	0.5
SI-CF-1127	MS	CCS	TRT	TRT-07	NO	NO	10.49	12.04	1.59	<Null>	<Null>	<Null>	0.3
SI-CF-1128	MS	SWD	SWD	SWD-04	NO	NO	10.54	14.34	1.93	<Null>	<Null>	<Null>	0.4
SI-CF-1129	MS	CCS	TRT	TRT-10	NO	NO	9.19	12.34	2.20	<Null>	<Null>	<Null>	0.3
SI-CF-1130	MS	CCS	TRT	TRT-02	NO	NO	15.61	15.19	2.22	<Null>	<Null>	<Null>	0.5
SI-CF-1131	MS	CCS	TRT	TRT-06	NO	NO	10.61	13.04	1.90	<Null>	<Null>	<Null>	0.3
SI-CF-1132	MS	CCS	TRT	TRT-10	NO	NO	16.29	15.55	1.63	<Null>	<Null>	<Null>	0.5
SI-CF-1133	MS	CCS	TRT	TRT-02	NO	NO	16.06	12.94	2.86	<Null>	<Null>	<Null>	0.7
SI-CF-1134	LT	SWD	SWD	SWD-04	NO	NO	14.23	14.08	1.86	<Null>	<Null>	<Null>	0.5
SI-CF-1135	LT	CCS	TRT	TRT-12	CRZ	NO	11.82	12.08	2.01	<Null>	<Null>	<Null>	0.3
SI-CF-1136	PR	CCS	TRT	TRT-01	NO	NO	18.09	14.08	2.68	3.16	1.56	<Null>	0.7
SI-CF-1137	LT	CCS	TRT	TRT-02	NO	NO	13.61	14.19	2.30	<Null>	<Null>	<Null>	0.5
SI-CF-1138	MS	CCS	TRT	TRT-01	NO	NO	15.23	19.83	2.23	<Null>	<Null>	<Null>	0.9
SI-CF-1139	LT	CCS	TRT	TRT-10	NO	NO	14.32	12.52	2.31	<Null>	<Null>	<Null>	0.5
SI-CF-1140	LT	CCS	TRT	TRT-12	NO	NO	11.05	16.48	1.97	<Null>	<Null>	<Null>	0.5
SI-CF-1141	MS	CCS	UNK	UNK-03	NO	NO	19.19	12.85	2.47	<Null>	<Null>	<Null>	0.7
SI-CF-1142	LT	CCS	TRT	TRT-02	NO	NO	16.29	11.34	1.83	<Null>	<Null>	<Null>	0.5
SI-CF-1143	MS	CCS	UNK	UNK-03	NO	YES	17.68	16.43	2.82	<Null>	<Null>	10.13	1.0
SI-CF-1144	MS	CCS	TRT	TRT-08	NO	NO	14.25	17.57	2.79	<Null>	<Null>	<Null>	0.9

Catalog	Portion	GENMAT	SPECMAT	Nodule	Burning	Double	MxLe	MxWd	MxTk	PltWd	PltTk	NegWd	Mass (g)
SI-CF-1145	PR	CCS	TRT	TRT-12	NO	NO	15.26	12.15	2.80	4.37	2.03	<Null>	0.5
SI-CF-1146	MS	CCS	CUMB	CUMB-04	NO	NO	9.69	12.09	1.76	<Null>	<Null>	<Null>	0.3
SI-CF-1147	MS	SWD	SWD	SWD-04	NO	NO	13.23	15.77	2.40	<Null>	<Null>	<Null>	0.7
SI-CF-1148	MS	CCS	TRT	TRT-10	NO	NO	21.23	14.23	2.37	<Null>	<Null>	<Null>	0.9
SI-CF-1149	MS	CCS	TRT	TRT-06	NO	NO	16.27	14.07	2.25	<Null>	<Null>	<Null>	0.7
SI-CF-1150	MS	CCS	TRT	TRT-01	NO	NO	22.85	16.72	2.16	<Null>	<Null>	<Null>	1.1
SI-CF-1151	MS	CCS	TRT	TRT-13	NO	NO	15.90	17.56	1.72	<Null>	<Null>	<Null>	0.6
SI-CF-1152	MS	CCS	TRT	TRT-10	NO	NO	14.13	11.34	1.81	<Null>	<Null>	<Null>	0.4
SI-CF-1153	MS	CCS	TRT	TRT-02	NO	NO	20.78	15.84	2.54	<Null>	<Null>	<Null>	1.1
SI-CF-1154	LT	CCS	PED	PED-06	NO	NO	13.36	11.86	1.99	<Null>	<Null>	<Null>	0.4
SI-CF-1155	MS	CCS	TRT	TRT-05	NO	NO	14.39	14.71	2.12	<Null>	<Null>	<Null>	0.6
SI-CF-1156	DS	CCS	UNK	UNK-07	NO	NO	15.85	14.42	2.02	<Null>	<Null>	<Null>	0.5
SI-CF-1157	LT	CCS	UNK	UNK-07	NO	NO	13.13	12.52	2.04	<Null>	<Null>	<Null>	0.4
SI-CF-1158	DS	CCS	UNK	UNK-07	NO	NO	13.89	12.02	2.12	<Null>	<Null>	<Null>	0.5
SI-CF-1159	LT	CCS	TRT	TRT-06	NO	NO	17.29	12.65	1.65	<Null>	<Null>	<Null>	0.4
SI-CF-1160	LT	CCS	TRT	TRT-02	NO	NO	17.40	10.34	1.48	<Null>	<Null>	<Null>	0.4
SI-CF-1161	MS	SWD	SWD	SWD-07	NO	NO	15.08	16.75	2.01	<Null>	<Null>	<Null>	0.5
SI-CF-1162	MS	SWD	SWD	SWD-04	NO	NO	11.08	12.19	1.39	<Null>	<Null>	<Null>	0.3
SI-CF-1163	MS	CCS	TRT	TRT-08	NO	NO	15.55	15.92	2.24	<Null>	<Null>	<Null>	0.6
SI-CF-1164	LT	CCS	NARB	NARB-01	NO	NO	11.83	12.97	1.54	<Null>	<Null>	<Null>	0.3
SI-CF-1165	LT	CCS	UNK	UNK-05	NO	NO	14.53	11.87	2.14	<Null>	<Null>	<Null>	0.5
SI-CF-1166	MS	CCS	TRT	TRT-02	NO	NO	16.57	11.19	2.01	<Null>	<Null>	<Null>	0.5
SI-CF-1167	MS	CCS	TRT	TRT-10	NO	NO	12.12	15.42	2.51	<Null>	<Null>	<Null>	0.6
SI-CF-1168	MS	CCS	TRT	TRT-10	NO	NO	11.67	14.98	1.49	<Null>	<Null>	<Null>	0.4
SI-CF-1169	MS	CCS	TRT	TRT-16	NO	NO	14.26	14.08	2.12	<Null>	<Null>	<Null>	0.6
SI-CF-1170	LT	CCS	NARB	NARB-01	NO	NO	10.27	11.72	1.90	<Null>	<Null>	<Null>	0.3
SI-CF-1171	MS	CCS	TRT	TRT-12	PTCZ	NO	10.96	16.21	2.24	<Null>	<Null>	<Null>	0.5
SI-CF-1172	PR	CCS	TRT	TRT-13	NO	NO	15.12	14.91	2.44	4.70	1.65	<Null>	0.5
SI-CF-1173	PR	CCS	TRT	TRT-02	NO	NO	14.27	12.99	1.86	4.53	1.70	<Null>	0.4

Catalog	Portion	GENMAT	SPECMAT	Nodule	Burning	Double	MxLe	MxWd	MxTk	PltWd	PltTk	NegWd	Mass (g)
SI-CF-1174	LT	CCS	TRT	TRT-02	NO	NO	10.84	12.31	1.86	<Null>	<Null>	<Null>	0.3
SI-CF-1175	LT	CCS	TRT	TRT-02	NO	NO	11.61	14.02	1.93	<Null>	<Null>	<Null>	0.4
SI-CF-1176	MS	CCS	TRT	TRT-10	POT	NO	13.30	12.59	1.53	<Null>	<Null>	<Null>	0.3
SI-CF-1177	MS	CCS	CUMB	CUMB-01	NO	NO	10.59	13.61	1.65	<Null>	<Null>	<Null>	0.3
SI-CF-1178	PR	CCS	UNK	UNK-03	NO	NO	11.92	12.24	1.58	3.25	1.39	<Null>	0.3
SI-CF-1179	LT	CCS	TRT	TRT-02	NO	NO	14.68	12.20	2.72	<Null>	<Null>	<Null>	0.6
SI-CF-1180	LT	CCS	CUMB	CUMB-01	NO	NO	7.81	12.62	1.20	<Null>	<Null>	<Null>	0.1
SI-CF-1181	PR	CCS	CUMB	CUMB-01	NO	NO	8.39	12.12	2.53	7.91	2.53	<Null>	0.2
SI-CF-1182	MS	CCS	TRT	TRT-03	POT	NO	14.55	12.20	2.18	<Null>	<Null>	<Null>	0.5
SI-CF-1183	MS	CCS	TRT	TRT-10	NO	NO	7.58	14.31	1.75	<Null>	<Null>	<Null>	0.3
SI-CF-1184	LT	CCS	TRT	TRT-02	NO	NO	11.13	10.26	1.71	<Null>	<Null>	<Null>	0.3
SI-CF-1185	MS	CCS	TRT	TRT-17	NO	NO	8.93	14.80	1.77	<Null>	<Null>	<Null>	0.3
SI-CF-1186	MS	CCS	TRT	TRT-17	NO	NO	10.96	16.01	1.51	<Null>	<Null>	<Null>	0.4
SI-CF-1187	MS	CCS	OOL	OOL-01	NO	NO	21.13	18.24	2.76	<Null>	<Null>	<Null>	1.4
SI-CF-1188	PR	CCS	UNK	UNK-05	NO	NO	16.20	15.21	2.09	3.41	1.05	<Null>	0.5
SI-CF-1189	PR	CCS	TRT	TRT-05	NO	NO	11.28	11.45	1.74	3.62	1.54	<Null>	0.3
SI-CF-1190	PR	CCS	TRT	TRT-12	NO	NO	15.75	11.42	1.57	3.36	1.48	<Null>	0.3
SI-CF-1191	PR	CCS	EDW	EDW-01	NO	NO	12.01	10.40	1.96	3.88	1.96	<Null>	0.2
SI-CF-1192	PR	CCS	CUMB	CUMB-05	NO	NO	17.69	10.45	1.75	3.75	1.33	<Null>	0.3
SI-CF-1193	LT	CCS	NARB	NARB-02	NO	YES	13.84	10.85	2.35	<Null>	<Null>	<Null>	0.5
SI-CF-1194	PR	CCS	FLAT	FLAT-01	NO	NO	13.80	10.75	2.24	2.69	1.60	<Null>	0.3
SI-CF-1195	PR	CCS	TRT	TRT-12	NO	NO	20.14	13.39	2.62	5.27	2.40	<Null>	0.7
SI-CF-1196	LT	CCS	EDW	EDW-01	NO	NO	13.20	9.07	2.21	<Null>	<Null>	<Null>	0.3
SI-CF-1197	PR	CCS	TRT	TRT-12	NO	NO	17.52	12.90	3.08	4.29	2.21	<Null>	0.6
SI-CF-1198	PR	CCS	TRT	TRT-08	NO	NO	15.76	16.87	2.87	4.01	1.83	<Null>	0.7
SI-CF-1199	PR	CCS	TRT	TRT-01	POT	NO	15.43	11.91	2.42	4.24	1.37	<Null>	0.5
SI-CF-1200	PR	CCS	UNK	UNK-03	POT	YES	24.37	12.90	2.18	4.53	1.25	7.12	0.7
SI-CF-1201	PR	CCS	TRT	TRT-10	NO	NO	10.89	13.49	2.11	3.24	1.47	<Null>	0.3
SI-CF-1202	LT	CCS	UNK	UNK-06	NO	YES	11.85	10.79	1.23	<Null>	<Null>	<Null>	0.2

Catalog	Portion	GENMAT	SPECMAT	Nodule	Burning	Double	MxLe	MxWd	MxTk	PltWd	PltTk	NegWd	Mass (g)
SI-CF-1203	LT	CCS	TRT	TRT-02	NO	YES	12.51	11.18	2.09	<Null>	<Null>	<Null>	0.3
SI-CF-1204	PR	CCS	TRT	TRT-10	NO	NO	13.32	12.23	1.89	4.49	1.86	<Null>	0.3
SI-CF-1205	MS	CCS	TRT	TRT-02	POT	NO	16.49	16.53	2.40	<Null>	<Null>	<Null>	0.8
SI-CF-1206	MS	CCS	TRT	TRT-08	NO	NO	15.31	17.08	2.37	<Null>	<Null>	<Null>	0.6
SI-CF-1207	MS	CCS	NARB	NARB-02	NO	NO	11.72	12.36	2.06	<Null>	<Null>	<Null>	0.3
SI-CF-1208	LT	CCS	TRT	TRT-12	NO	NO	25.37	10.77	2.46	<Null>	<Null>	<Null>	0.9
SI-CF-1209	MS	CCS	TRT	TRT-10	NO	NO	17.21	15.36	2.42	<Null>	<Null>	<Null>	0.7
SI-CF-1210	PR	CCS	TRT	TRT-10	POT	NO	17.57	15.03	2.64	3.62	1.58	<Null>	0.7
SI-CF-1211	PR	CCS	TRT	TRT-02	NO	NO	16.31	12.46	2.51	4.35	1.63	<Null>	0.5
SI-CF-1212	PR	CCS	TRT	TRT-18	NO	NO	15.82	14.18	2.24	2.17	1.08	<Null>	0.4
SI-CF-1213	PR	CCS	TRT	TRT-05	NO	NO	12.16	13.83	1.96	3.12	1.28	<Null>	0.3
SI-CF-1214	LT	QZT	DAK	DAK-01	NO	NO	11.63	15.91	3.06	<Null>	<Null>	<Null>	0.7
SI-CF-1215	PR	CCS	TRT	TRT-10	NO	NO	11.45	10.41	1.76	4.35	1.44	<Null>	0.2
SI-CF-1216	MS	CCS	TRT	TRT-10	NO	NO	13.09	15.51	1.72	<Null>	<Null>	<Null>	0.4
SI-CF-1217	PR	CCS	TRT	TRT-10	NO	NO	15.06	13.91	1.81	3.21	1.12	<Null>	0.4
SI-CF-1218	LT	CCS	TRT	TRT-08	NO	NO	8.46	11.75	1.67	<Null>	<Null>	<Null>	0.2
SI-CF-1219	MS	CCS	TRT	TRT-08	NO	NO	11.38	15.81	2.46	<Null>	<Null>	<Null>	0.5
SI-CF-1220	LT	CCS	TRT	TRT-10	NO	NO	18.46	10.19	2.09	<Null>	<Null>	<Null>	0.3
SI-CF-1221	PR	CCS	TRT	TRT-05	NO	NO	17.43	13.55	2.41	3.96	1.59	<Null>	0.6
SI-CF-1222	MS	CCS	TRT	TRT-02	NO	NO	10.65	13.56	1.81	<Null>	<Null>	<Null>	0.3
SI-CF-1223	LT	CCS	TRT	TRT-02	NO	NO	11.66	9.12	1.83	<Null>	<Null>	<Null>	0.3
SI-CF-1224	PR	CCS	TRT	TRT-01	NO	NO	11.54	11.86	1.77	4.39	1.51	<Null>	0.2
SI-CF-1225	LT	CCS	TRT	TRT-08	NO	YES	9.99	9.05	1.90	<Null>	<Null>	<Null>	0.3
SI-CF-1226	LT	CCS	TRT	TRT-10	NO	NO	13.39	8.99	1.98	<Null>	<Null>	<Null>	0.3
SI-CF-1227	DS	CCS	TRT	TRT-10	PTCZ	NO	9.58	11.34	1.73	<Null>	<Null>	<Null>	0.2
SI-CF-1228	MS	CCS	TRT	TRT-02	NO	NO	9.30	13.76	2.35	<Null>	<Null>	<Null>	0.4
SI-CF-1229	LT	CCS	TRT	TRT-03	POT	NO	13.70	10.32	2.31	<Null>	<Null>	<Null>	0.4
SI-CF-1230	MS	VOL	DAC	DAC-02	NO	NO	15.34	10.89	1.89	<Null>	<Null>	<Null>	0.4
SI-CF-1231	PR	VOL	DAC	DAC-02	NO	NO	10.63	9.46	1.84	3.45	1.24	<Null>	0.2

Catalog	Portion	GENMAT	SPECMAT	Nodule	Burning	Double	MxLe	MxWd	MxTk	PltWd	PltTk	NegWd	Mass (g)
SI-CF-1232	MS	CCS	UNK	UNK-13	NO	NO	7.89	12.30	1.47	<Null>	<Null>	<Null>	0.2
SI-CF-1233	PR	CCS	TRT	TRT-08	NO	YES	11.93	14.24	1.55	2.73	1.06	9.23	0.3
SI-CF-1234	LT	SWD	SWD	SWD-04	NO	NO	9.76	11.79	1.67	<Null>	<Null>	<Null>	0.3
SI-CF-1235	MS	CCS	EDW	EDW-01	NO	NO	11.18	15.41	1.99	<Null>	<Null>	<Null>	0.5
SI-CF-1236	MS	CCS	EDW	EDW-01	NO	NO	19.07	11.94	2.56	<Null>	<Null>	<Null>	0.6
SI-CF-1237	MS	CCS	EDW	EDW-01	NO	NO	16.28	14.21	2.13	<Null>	<Null>	<Null>	0.6
SI-CF-1238	LT	CCS	EDW	EDW-01	NO	NO	15.16	9.72	1.76	<Null>	<Null>	<Null>	0.4
SI-CF-1239	LT	CCS	EDW	EDW-01	NO	NO	12.20	12.92	2.14	<Null>	<Null>	<Null>	0.4
SI-CF-1240	LT	CCS	EDW	EDW-01	NO	NO	9.47	14.17	2.28	<Null>	<Null>	<Null>	0.4
SI-CF-1241	LT	CCS	EDW	EDW-01	NO	NO	9.14	14.63	2.03	<Null>	<Null>	<Null>	0.4
SI-CF-1242	LT	CCS	EDW	EDW-01	NO	NO	14.88	8.50	1.49	<Null>	<Null>	<Null>	0.2
SI-CF-1243	LT	CCS	EDW	EDW-01	NO	NO	10.44	13.06	2.07	<Null>	<Null>	<Null>	0.3
SI-CF-1244	MS	CCS	EDW	EDW-01	NO	NO	8.63	12.68	2.18	<Null>	<Null>	<Null>	0.3
SI-CF-1245	LT	CCS	EDW	EDW-01	NO	NO	10.91	8.83	1.18	<Null>	<Null>	<Null>	0.2
SI-CF-1246	LT	CCS	EDW	EDW-01	NO	NO	6.95	13.19	1.81	<Null>	<Null>	<Null>	0.3
SI-CF-1247	LT	CCS	EDW	EDW-01	NO	NO	10.41	12.36	1.68	<Null>	<Null>	<Null>	0.2
SI-CF-1248	LT	CCS	EDW	EDW-01	NO	NO	12.37	10.12	1.05	<Null>	<Null>	<Null>	0.2
SI-CF-1249	PR	CCS	UNK	UNK-07	NO	NO	10.95	11.19	1.68	3.84	1.68	<Null>	0.2
SI-CF-1250	LT	SWD	SWD	SWD-07	NO	NO	8.79	7.52	1.87	<Null>	<Null>	<Null>	0.2
SI-CF-1251	LT	CCS	NARB	NARB-03	POT	NO	18.26	14.34	2.18	<Null>	<Null>	<Null>	0.7
SI-CF-1252	LT	SWD	SWD	SWD-07	NO	YES	8.69	11.07	1.30	<Null>	<Null>	<Null>	0.2
SI-CF-1253	LT	CCS	CUMB	CUMB-01	NO	NO	10.00	6.95	1.44	<Null>	<Null>	<Null>	0.2
SI-CF-1254	LT	QZT	MOR	MOR-02	NO	NO	18.27	9.71	2.01	<Null>	1.94	<Null>	0.5
SI-CF-1255	PR	SWD	SWD	SWD-04	NO	NO	17.62	13.01	2.08	4.70	1.79	<Null>	0.5
SI-CF-1256	MS	CCS	TRT	TRT-08	NO	NO	9.97	12.45	1.50	<Null>	<Null>	<Null>	0.3
SI-CF-1257	LT	CCS	TRT	TRT-05	NO	YES	11.63	10.34	2.06	<Null>	<Null>	<Null>	0.2
SI-CF-1258	LT	CCS	EDW	EDW-01	NO	NO	16.83	12.29	1.58	<Null>	<Null>	<Null>	0.6
SI-CF-1259	LT	CCS	NARB	NARB-02	NO	NO	13.84	9.88	1.22	<Null>	<Null>	<Null>	0.2
SI-CF-1260	PR	CCS	EDW	EDW-01	NO	NO	15.02	11.77	1.47	4.69	1.19	<Null>	0.3

Catalog	Portion	GENMAT	SPECMAT	Nodule	Burning	Double	MxLe	MxWd	MxTk	PltWd	PltTk	NegWd	Mass (g)
SI-CF-1261	MS	SWD	SWD	SWD-07	NO	NO	15.50	11.13	1.97	<Null>	<Null>	<Null>	0.4
SI-CF-1262	PR	CCS	UNK	UNK-05	NO	NO	15.75	10.03	2.27	6.09	2.18	<Null>	0.4
SI-CF-1263	LT	VOL	OBS	OBS-04	NO	NO	12.52	12.48	2.27	<Null>	<Null>	<Null>	0.4
SI-CF-1264	PR	SWD	SWD	SWD-04	NO	NO	19.85	10.08	1.43	3.68	1.29	<Null>	0.4
SI-CF-1265	MS	SWD	SWD	SWD-07	NO	NO	11.75	14.24	1.69	<Null>	<Null>	<Null>	0.3
SI-CF-1266	LT	CCS	NARB	NARB-02	NO	YES	16.45	8.55	1.23	<Null>	<Null>	<Null>	0.2
SI-CF-1267	LT	CCS	UNK	UNK-07	NO	YES	15.19	14.96	1.95	<Null>	<Null>	<Null>	0.3
SI-CF-1268	LT	CCS	TRT	TRT-02	NO	NO	12.30	12.58	1.64	<Null>	<Null>	<Null>	0.3
SI-CF-1269	MS	CCS	TRT	TRT-08	NO	NO	11.26	14.76	1.73	<Null>	<Null>	<Null>	0.4
SI-CF-1270	PR	SWD	SWD	SWD-01	NO	YES	16.79	13.96	1.03	3.17	0.95	7.48	0.4
SI-CF-1271	LT	CCS	TRT	TRT-08	NO	NO	7.69	11.23	1.55	<Null>	<Null>	<Null>	0.2
SI-CF-1272	MS	CCS	TRT	TRT-03	NO	NO	9.85	10.68	1.32	<Null>	<Null>	<Null>	0.2
SI-CF-1273	MS	CCS	TRT	TRT-07	POT	NO	13.69	13.51	1.98	<Null>	<Null>	<Null>	0.4
SI-CF-1274	MS	CCS	TRT	TRT-02	NO	NO	14.23	11.31	2.12	<Null>	<Null>	<Null>	0.3
SI-CF-1275	MS	CCS	TRT	TRT-13	NO	NO	7.22	12.20	1.34	<Null>	<Null>	<Null>	0.2
SI-CF-1276	PR	SWD	SWD	SWD-04	NO	YES	18.01	13.60	1.96	3.79	1.13	6.23	0.6
SI-CF-1277	MS	CCS	TRT	TRT-05	NO	NO	10.22	11.94	1.23	<Null>	<Null>	<Null>	0.1
SI-CF-1278	PR	CCS	TRT	TRT-13	NO	NO	14.70	14.01	1.85	3.18	1.41	<Null>	0.4
SI-CF-1279	MS	CCS	TRT	TRT-03	NO	NO	13.53	16.54	2.91	<Null>	<Null>	<Null>	0.7
SI-CF-1280	PR	CCS	TRT	TRT-08	NO	NO	10.37	11.00	1.63	1.48	1.09	<Null>	0.2
SI-CF-1281	LT	CCS	NARB	NARB-01	NO	YES	10.89	10.13	1.04	<Null>	<Null>	<Null>	0.1
SI-CF-1282	LT	CCS	TRT	TRT-05	NO	YES	13.66	6.09	1.24	<Null>	<Null>	<Null>	0.1
SI-CF-1283	MS	CCS	MOSC	MOSC-06	NO	NO	12.88	13.49	1.91	<Null>	<Null>	<Null>	0.4
SI-CF-1284	LT	CCS	TRT	TRT-10	NO	YES	13.27	12.73	1.27	<Null>	<Null>	<Null>	0.2
SI-CF-1285	MS	CCS	TRT	TRT-13	NO	NO	15.17	13.40	1.76	<Null>	<Null>	<Null>	0.5
SI-CF-1286	MS	CCS	TRT	TRT-13	NO	NO	15.73	14.48	2.49	<Null>	<Null>	<Null>	0.6
SI-CF-1287	LT	CCS	EDW	EDW-01	NO	NO	13.08	9.14	1.16	<Null>	<Null>	<Null>	0.2
SI-CF-1288	MS	QZT	DAK	DAK-01	NO	NO	9.93	12.15	1.98	<Null>	<Null>	<Null>	0.3
SI-CF-1289	MS	CCS	EDW	EDW-01	NO	NO	10.22	14.15	1.92	<Null>	<Null>	<Null>	0.3

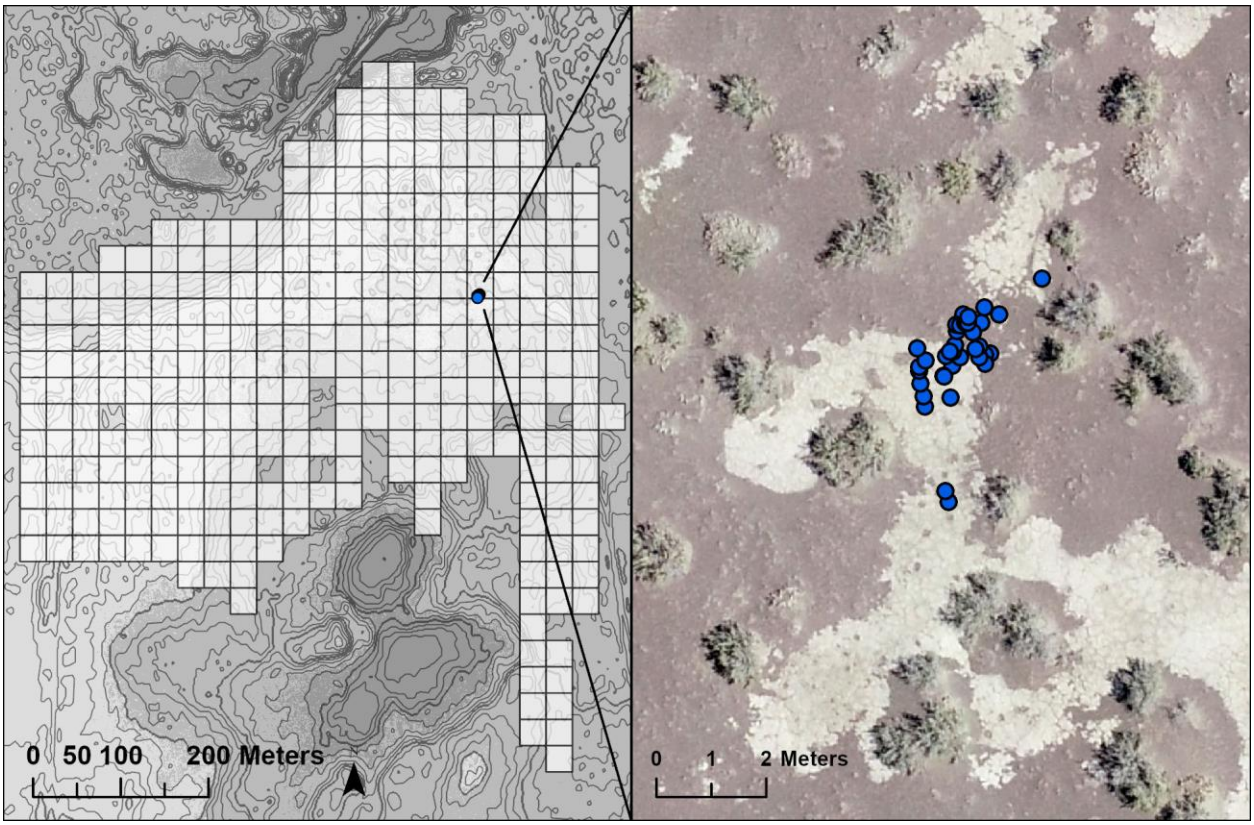
Catalog	Portion	GENMAT	SPECMAT	Nodule	Burning	Double	MxLe	MxWd	MxTk	PltWd	PltTk	NegWd	Mass (g)
SI-CF-1290	PR	QZT	MOR	MOR-02	NO	NO	12.07	11.91	1.68	4.25	1.36	<Null>	0.3
SI-CF-1291	MS	CCS	PED	PED-07	NO	NO	14.49	10.24	0.93	<Null>	<Null>	<Null>	0.2
SI-CF-1292	PR	CCS	TRT	TRT-07	NO	NO	12.43	7.79	1.94	3.77	1.55	<Null>	0.2
SI-CF-1293	MS	SWD	SWD	SWD-04	NO	YES	18.54	11.63	1.81	<Null>	<Null>	6.40	0.4
SI-CF-1294	LT	CCS	TRT	TRT-05	NO	NO	9.38	13.54	1.92	<Null>	<Null>	<Null>	0.3
SI-CF-1295	MS	CCS	CUMB	CUMB-06	NO	NO	14.33	14.40	2.54	<Null>	<Null>	<Null>	0.7



D1. Sample image of post-Folsom time-diagnostic projectile points.



D2. Plain grayware ceramic sherds recovered in a “pot drop” ceramic scatter spanning about 2 m^2 in survey block S52 (see Appendix F for survey block location in site grid).



D3. Location of plainware ceramic scatter at the Reddin site. Aerial image based on UAV flight.



D4. Jason LaBelle surveying location of plainware ceramic scatter at Reddin, July 2021.

D5. Post-Folsom projectile point descriptive data.

Catalog	Type	Portion	GENMAT	SPECMAT	Burning	Serration	Shape
CMPA-OTPP-1001	SAN JOSE	PR	CCS	PED	POT	NO	STEM
CMPA-OTPP-1002	UN-FORMATIVE	PR	VOL	OBS	NO	NO	UNK
CMPA-OTPP-1003	UN-FORMATIVE	MS	QZT	DAK	NO	YES	UNK
CMPA-OTPP-1004	SAN JOSE	PR	VOL	OBS	NO	NO	STEM
CMPA-OTPP-1005	EN MEDIO	NC	VOL	DAC	NO	NO	CN
CMPA-OTPP-1006	FORMATIVE STEM	NC	VOL	DAC	NO	YES	STEM
CMPA-OTPP-1007	UN-ARCHAIC	MS	VOL	OBS	NO	NO	UNK
CMPA-OTPP-1008	UN-FORMATIVE	PR	VOL	OBS	NO	NO	UNK
CMPA-OTPP-1009	UN-ARCHAIC	PR	VOL	OBS	NO	NO	SN
CMPA-OTPP-1010	MOQUINO	PR	VOL	DAC	NO	NO	SN
CMPA-OTPP-1011	FORMATIVE SN	NC	CCS	PED	NO	NO	SN
CMPA-OTPP-1012	UN-ARCHAIC	MS	CCS	CUMB	NO	NO	CN
CMPA-OTPP-1013	UN-ARCHAIC	CO	QZT	MOR	NO	NO	SN
CMPA-OTPP-1014	EN MEDIO	CO	QZT	MOR	NO	NO	SN
CMPA-OTPP-1015	SAN JOSE	PR	QZT	DAK	NO	YES	STEM
CMPA-OTPP-1016	FORMATIVE STEM	CO	CCS	TRT	NO	YES	STEM
CMPA-OTPP-1017	UN-ARCHAIC	PR	CCS	CUMB	NO	NO	UNK
CMPA-OTPP-1018	UN-ARCHAIC	DS	CCS	TRT	NO	YES	UNK
CMPA-OTPP-1019	FORMATIVE SN	PR	CCS	MOSC	PTCZ	NO	SN
CMPA-OTPP-1020	UN-ARCHAIC	MS	QZT	DAK	NO	YES	CN
CMPA-OTPP-1021	UN-FORMATIVE	NC	CCS	PED	NO	NO	UNK
CMPA-OTPP-1022	UN-ARCHAIC	LT	QZT	DAK	NO	NO	CN
CMPA-OTPP-1023	FORMATIVE SN	NC	CCS	PED	NO	NO	SN
CMPA-OTPP-1024	AUGUSTIN	NC	QZT	MOR	NO	YES	STEM
CMPA-OTPP-1025	UN-ARCHAIC	PR	CCS	MOSC	NO	NO	CN
CMPA-OTPP-1026	UN-ARCHAIC	DS	QZT	DAK	NO	NO	UNK
CMPA-OTPP-1027	UN-ARCHAIC	MS	CCS	TRT	NO	NO	UNK
CMPA-OTPP-1028	UN-ARCHAIC	DS	SWD	SWD	NO	NO	UNK
CMPA-OTPP-1029	EN MEDIO	CO	CCS	CUMB	NO	NO	CN
SI-OTPP-1001	UN-ARCHAIC	DS	CCS	EDW	NO	YES	UNK

Catalog	Type	Portion	GENMAT	SPECMAT	Burning	Serration	Shape
SI-OTPP-1002	FORMATIVE SN	CO[2]	CCS	PED	NO	NO	SN
SI-OTPP-1003	FORMATIVE CN	PR	CCS	TRT	POT	NO	CN
SI-OTPP-1004	UN-FORMATIVE	PR	CCS	TRT	NO	NO	UNK
SI-OTPP-1005	FORMATIVE CN	PR	SWD	SWD	NO	NO	CN
SI-OTPP-1006	AUGUSTIN	PR	CCS	PED	NO	NO	STEM
SI-OTPP-1007	AUGUSTIN	PR	CCS	TRT	NO	NO	STEM
SI-OTPP-1008	UN-ARCHAIC	MS	CCS	PED	POT	NO	UNK
SI-OTPP-1009	AUGUSTIN	PR	CCS	UNK	POT	NO	STEM
SI-OTPP-1010	UN-ARCHAIC	PR	CCS	PED	NO	NO	UNK
SI-OTPP-1011	UN-ARCHAIC	DS	CCS	MOSC	NO	NO	UNK
SI-OTPP-1012	UN-ARCHAIC	PR	CCS	UNK	NO	NO	STEM
SI-OTPP-1013	UN-ARCHAIC	MS	CCS	PED	NO	NO	UNK
SI-OTPP-1014	UN-FORMATIVE	PR	QZT	DAK	NO	NO	UNK
SI-OTPP-1015	FORMATIVE SN	MS	QZT	DAK	NO	NO	SN
SI-OTPP-1016	FORMATIVE SN	CO	QZT	DAK	NO	NO	SN
SI-OTPP-1017	UN-ARCHAIC	DS	CCS	TRT	NO	NO	UNK
SI-OTPP-1018	UN-ARCHAIC	MS	CCS	TRT	NO	NO	UNK
SI-OTPP-1019	FORMATIVE CN	PR	QZT	DAK	NO	NO	CN
SI-OTPP-1020	UN-ARCHAIC	MS	CCS	UNK	NO	YES	UNK
SI-OTPP-1021	UN-FORMATIVE	DS	CCS	CUMB	NO	NO	UNK
SI-OTPP-1022	FORMATIVE SN	CO	CCS	TRT	NO	YES	SN
SI-OTPP-1023	FORMATIVE TRI	MS	QZT	DAK	NO	NO	TRI
SI-OTPP-1024	FORMATIVE STEM	CO	SWD	SWD	NO	YES	STEM
SI-OTPP-1025	FORMATIVE SN	CO	CCS	TRT	NO	NO	SN
SI-OTPP-1026	ARMIJO	CO	QZT	MOR	NO	YES	STEM
SI-OTPP-1027	EN MEDIO	CO	SWD	SWD	NO	NO	CN
SI-OTPP-1028	SAN JOSE	PR	QZT	DAK	NO	NO	STEM
SI-OTPP-1029	PELICAN LAKE	PR	CCS	FLAT	NO	NO	CN
SI-OTPP-1030	FORMATIVE SN	CO	QZT	DAK	NO	NO	SN
SI-OTPP-1031	UN-ARCHAIC	LT	CCS	TRT	NO	NO	UNK
SI-OTPP-1032	UN-FORMATIVE	MS	QZT	TRT	NO	NO	UNK

Catalog	Type	Portion	GENMAT	SPECMAT	Burning	Serration	Shape
SI-OTPP-1033	EN MEDIO	PR	QZT	DAK	NO	NO	SN
SI-OTPP-1034	EN MEDIO	PR	QZT	DAK	NO	NO	CN
SI-OTPP-1035	UN-ARCHAIC	PR	CCS	TRT	NO	NO	UNK
SI-OTPP-1036	FORMATIVE CN	CO	CCS	PED	NO	NO	CN
SI-OTPP-1037	FORMATIVE STEM	PR	SWD	SWD	NO	NO	STEM
SI-OTPP-1038	FORMATIVE SN	PR	CCS	NARB	NO	NO	SN
SI-OTPP-1039	FORMATIVE SN	LT	CCS	PED	NO	NO	SN
SI-OTPP-1040	UN-FORMATIVE	MS	CCS	TRT	NO	YES	UNK
SI-OTPP-1041	UN-FORMATIVE	MS	CCS	TRT	NO	YES	UNK
SI-OTPP-1042	UN-FORMATIVE	DS	CCS	TRT	NO	NO	UNK
SI-OTPP-1043	EN MEDIO	LT	CCS	TRT	NO	NO	CN
SI-OTPP-1044	BAJADA TA	PR	QZT	DAK	NO	NO	STEM
SI-OTPP-1045	EN MEDIO	PR	QZT	MOR	NO	NO	CN
SI-OTPP-1046	EN MEDIO	CO	QZT	DAK	NO	NO	CN
SI-OTPP-1047	UN-ARCHAIC	PR	CCS	UNK	NO	NO	CN
SI-OTPP-1048	SAN JOSE	PR	CCS	PED	NO	NO	STEM
SI-OTPP-1049	FORMATIVE STEM	CO	QZT	DAK	NO	YES	STEM
SI-OTPP-1050	UN-ARCHAIC	DS	CCS	TRT	NO	NO	UNK
SI-OTPP-1051	PLANO	PR	QZT	DAK	NO	NO	LANCE
SI-OTPP-1052	SAN JOSE	PR	CCS	UNK	PTCZ	NO	STEM
SI-OTPP-1053	FORMATIVE SN	PR	CCS	UNK	NO	NO	SN
SI-OTPP-1054	FORMATIVE STEM	CO	CCS	UNK	NO	NO	STEM
SI-OTPP-1055	UN-FORMATIVE	DS	SWD	SWD	NO	NO	UNK
SI-OTPP-1056	UN-FORMATIVE	DS	CCS	TRT	NO	NO	UNK
SI-OTPP-1057	UN-FORMATIVE	MS	CCS	PED	NO	NO	UNK
SI-OTPP-1058	UN-FORMATIVE	PR	CCS	PED	NO	NO	UNK
SI-OTPP-1059	UN-FORMATIVE	MS	CCS	TRT	NO	NO	STEM
SI-OTPP-1060	UN-ARCHAIC	MS	VOL	OBS	NO	YES	UNK
SI-OTPP-1061	FORMATIVE CN	PR	QZT	DAK	NO	NO	CN
SI-OTPP-1062	UN-FORMATIVE	DS	CCS	PED	NO	NO	UNK
SI-OTPP-1063	UN-FORMATIVE	MS	CCS	PED	NO	NO	UNK

Catalog	Type	Portion	GENMAT	SPECMAT	Burning	Serration	Shape
SI-OTPP-1064	FORMATIVE CN	LT	SWD	SWD	POT	NO	CN
SI-OTPP-1065	UN-ARCHAIC	DS	CCS	MOSC	NO	NO	UNK
SI-OTPP-1066	EN MEDIO	MS	VOL	RHY	NO	NO	SN
SI-OTPP-1067	UN-ARCHAIC	PR	SWD	SWD	NO	NO	CN
SI-OTPP-1068	UN-FORMATIVE	PR	QZT	DAK	NO	NO	CN
SI-OTPP-1069	UN-ARCHAIC	PR	CCS	PED	NO	NO	UNK
SI-OTPP-1070	UN-ARCHAIC	DS	VOL	DAC	NO	YES	UNK
SI-OTPP-1071	UN-FORMATIVE	PR	VOL	OBS	NO	NO	SN
SI-OTPP-1072	UN-FORMATIVE	DS	QZT	MOR	NO	NO	UNK
SI-OTPP-1073	FORMATIVE SN	PR	VOL	RHY	NO	NO	SN
SI-OTPP-1074	UN-ARCHAIC	LT	CCS	TRT	PTCZ	YES	STEM
SI-OTPP-1075	UN-FORMATIVE	DS	QZT	DAK	NO	NO	UNK
SI-OTPP-1076	UN-FORMATIVE	MS	CCS	PED	NO	YES	UNK
SI-OTPP-1077	FORMATIVE STEM	MS	CCS	TRT	NO	YES	STEM
SI-OTPP-1078	FORMATIVE STEM	CO	CCS	PED	NO	YES	STEM
SI-OTPP-1079	FORMATIVE STEM	PR	CCS	TRT	NO	NO	STEM
SI-OTPP-1080	SAN JOSE	PR	QZT	MOR	NO	NO	STEM
SI-OTPP-1081	UN-FORMATIVE	MS	CCS	MOSC	NO	NO	UNK
SI-OTPP-1082	UN-FORMATIVE	PR	CCS	PED	NO	NO	CN
SI-OTPP-1083	UN-FORMATIVE	PR	CCS	MOSC	NO	NO	CN
SI-OTPP-1084	UN-FORMATIVE	MS	CCS	CUMB	NO	YES	UNK
SI-OTPP-1085	FORMATIVE STEM	CO	CCS	PED	NO	NO	STEM
SI-OTPP-1086	UN-FORMATIVE	MS	QZT	DAK	NO	NO	UNK
SI-OTPP-1087	UN-ARCHAIC	DS	CCS	PED	NO	NO	UNK
SI-OTPP-1088	FORMATIVE SN	LT	CCS	MOSC	NO	NO	SN
SI-OTPP-1089	UN-FORMATIVE	MS	CCS	TRT	NO	NO	UNK
SI-OTPP-1090	ARMIJO	LT	VOL	OBS	NO	NO	SN
SI-OTPP-1091	FORMATIVE UNN	PR	QZT	DAK	NO	NO	NONE
SI-OTPP-1092	UN-ARCHAIC	MS	VOL	DAC	NO	NO	UNK
SI-OTPP-1093	UN-ARCHAIC	MS	VOL	OBS	NO	NO	UNK
SI-OTPP-1094	UN-ARCHAIC	MS	VOL	DAC	NO	NO	UNK

Catalog	Type	Portion	GENMAT	SPECMAT	Burning	Serration	Shape
SI-OTPP-1095	UN-ARCHAIC	PR	VOL	DAC	NO	NO	STEM
SI-OTPP-1096	UN-ARCHAIC	MS	VOL	OBS	NO	YES	UNK
SI-OTPP-1097	UN-ARCHAIC	LT	VOL	OBS	NO	NO	UNK
SI-OTPP-1098	UN-FORMATIVE	LT	CCS	TRT	NO	NO	UNK
SI-OTPP-1099	UN-ARCHAIC	MS	VOL	DAC	NO	YES	UNK
SI-OTPP-1100	FORMATIVE UNN	CO	SWD	SWD	NO	NO	NONE
SI-OTPP-1101	SAN JOSE	NC	VOL	DAC	NO	NO	STEM
SI-OTPP-1102	FORMATIVE UNN	NC	CCS	TRT	NO	NO	NONE
SI-OTPP-1103	SAN JOSE	PR	VOL	DAC	NO	NO	STEM
SI-OTPP-1104	FORMATIVE STEM	PR	CCS	TRT	NO	NO	STEM
SI-OTPP-1105	ARMIJO	NC	VOL	DAC	NO	YES	STEM
SI-OTPP-1106	UN-ARCHAIC	MS	CCS	TRT	NO	NO	UNK
SI-OTPP-1107	ARMIJO	CO	VOL	OBS	NO	YES	STEM
SI-OTPP-1108	ARMIJO	CO	VOL	DAC	NO	YES	STEM
SI-OTPP-1109	PLANO	PR	CCS	UNK	PTCZ	NO	LANCE
SI-OTPP-1110	PLANO	NC	VOL	DAC	NO	NO	LANCE
SI-OTPP-1111	JAY	PR	VOL	DAC	NO	NO	STEM
SI-OTPP-1112	PLANO	LT	VOL	DAC	NO	NO	LANCE
SI-OTPP-1113	UN-FORMATIVE	PR	VOL	OBS	NO	NO	UNK
SI-OTPP-1114	FORMATIVE STEM	NC	VOL	OBS	NO	YES	STEM
SI-OTPP-1115	PLANO	PR	VOL	DAC	NO	NO	UNK
SI-OTPP-1116	UN-FORMATIVE	PR	VOL	OBS	NO	NO	STEM
SI-OTPP-1117	UN-FORMATIVE	DS	VOL	OBS	NO	NO	UNK
SI-OTPP-1118	UN-ARCHAIC	PR	VOL	OBS	NO	NO	STEM
SI-OTPP-1119	UN-FORMATIVE	PR	VOL	OBS	NO	NO	UNK
SI-OTPP-1120	EN MEDIO	PR	VOL	DAC	NO	NO	CN
SI-OTPP-1121	UN-ARCHAIC	PR	VOL	OBS	NO	NO	UNK
SI-OTPP-1122	UN-FORMATIVE	PR	VOL	OBS	NO	NO	SN
SI-OTPP-1123	UN-ARCHAIC	PR	VOL	OBS	NO	NO	UNK
SI-OTPP-1124	UN-FORMATIVE	DS	CCS	PED	NO	NO	UNK
SI-OTPP-1125	UN-FORMATIVE	PR	QZT	DAK	NO	NO	UNK

Catalog	Type	Portion	GENMAT	SPECMAT	Burning	Serration	Shape
SI-OTPP-1126	UN-FORMATIVE	LT	CCS	PED	NO	NO	SN
SI-OTPP-1127	UN-FORMATIVE	DS	VOL	OBS	NO	YES	UNK
SI-OTPP-1128	FORMATIVE STEM	NC	CCS	NARB	PTCZ	NO	STEM
SI-OTPP-1129	FORMATIVE CN	CO	CCS	PED	NO	NO	CN
SI-OTPP-1130	UN-ARCHAIC	DS	CCS	PED	NO	NO	UNK
SI-OTPP-1131	UN-FORMATIVE	MS	CCS	TRT	NO	NO	UNK
SI-OTPP-1132	UN-FORMATIVE	MS	VOL	OBS	NO	NO	UNK
SI-OTPP-1133	UN-FORMATIVE	PR	VOL	OBS	NO	NO	UNK
SI-OTPP-1134	UN-FORMATIVE	MS	QZT	DAK	NO	NO	UNK
SI-OTPP-1135	UN-FORMATIVE	MS	VOL	OBS	NO	YES	UNK
SI-OTPP-1136	UN-FORMATIVE	PR	CCS	MOSC	NO	NO	UNK
SI-OTPP-1137	UN-FORMATIVE	PR	CCS	TRT	NO	NO	UNK
SI-OTPP-1138	UN-FORMATIVE	PR	CCS	CUMB	NO	NO	STEM
SI-OTPP-1139	AUGUSTIN	PR	VOL	OBS	NO	NO	STEM
SI-OTPP-1140	UN-FORMATIVE	PR	VOL	OBS	NO	NO	UNK
SI-OTPP-1141	FORMATIVE SN	PR	CCS	TRT	NO	NO	SN
SI-OTPP-1142	UN-ARCHAIC	PR	QZT	DAK	NO	NO	STEM
SI-OTPP-1143	UN-FORMATIVE	DS	VOL	OBS	NO	NO	UNK
SI-OTPP-1144	UN-ARCHAIC	PR	QZT	DAK	NO	NO	UNK
SI-OTPP-1145	UN-FORMATIVE	MS	CCS	PED	NO	NO	UNK
SI-OTPP-1146	UN-FORMATIVE	PR	VOL	OBS	NO	NO	UNK
SI-OTPP-1147	UN-FORMATIVE	PR	QZT	DAK	NO	NO	UNK
SI-OTPP-1148	UN-ARCHAIC	PR	CCS	PED	PTCZ	NO	CN
SI-OTPP-1149	UN-FORMATIVE	PR	SWD	SWD	NO	NO	UNK
SI-OTPP-1150	UN-ARCHAIC	PR	QZT	DAK	NO	NO	UNK
SI-OTPP-1151	UN-ARCHAIC	PR	VOL	OBS	NO	NO	UNK
SI-OTPP-1152	FORMATIVE SN	PR	VOL	DAC	NO	NO	SN
SI-OTPP-1153	UN-ARCHAIC	DS	QZT	DAK	NO	NO	UNK
SI-OTPP-1154	FORMATIVE SN	PR	CCS	PED	NO	NO	SN
SI-OTPP-1155	UN-FORMATIVE	PR	QZT	DAK	NO	NO	UNK
SI-OTPP-1156	UN-FORMATIVE	PR	QZT	DAK	NO	NO	UNK

Catalog	Type	Portion	GENMAT	SPECMAT	Burning	Serration	Shape
SI-OTPP-1157	UN-ARCHAIC	PR	CCS	UNK	NO	NO	UNK
SI-OTPP-1158	UN-FORMATIVE	PR	QZT	DAK	NO	NO	UNK
SI-OTPP-1159	UN-FORMATIVE	PR	CCS	TRT	NO	NO	UNK
SI-OTPP-1160	UN-FORMATIVE	PR	QZT	DAK	NO	NO	UNK

Typological References:

Birkmann, Joseph M., Bruce B. Huckell, M. Steven Shackley, and C. Vance Haynes Jr.
2023 The Paleoindian and Archaic Occupation of Grants, New Mexico: A Review and Reanalysis of the Grants San Jose Sites and Projectile Point Collections. *Kiva* 89(4): 429-462.

Chapin, Nicholas D.
2005 Hunter-gatherer Technological Organization: The Archaic Period in the Northern New Mexico. PhD Dissertation, University of New Mexico, Albuquerque.
2017 *Oshara Revisited: The Archaic Period in Northern New Mexico*. Anthropological Papers 10. Maxwell Museum of Anthropology, University of New Mexico, Albuquerque.

Irwin Williams, Cynthia
1973 *The Oshara Tradition: Origins of Anasazi Culture*. Contributions in Anthropology 5(1). Paleoindian Institute, Eastern New Mexico University, Portales.

Johnston, Christopher M.
2021 *Projectile Points from the Scott Miller Site, Rio Grande County, Colorado.* Research Contribution 120. Archaeological Investigations in the San Luis Valley 8. Paleocultural Research Group, Broomfield, Colorado. Submitted to the U.S. Fish and Wildlife Service, Lakewood, Colorado.

D6. Post-Folsom projectile point metric data.

Catalog	MxLe	MxWd	BaWd	BaCo	NckWd	NckLe	ShlWd	ShlLe	NchDL	NchDR	NchDBs	MxTk	LGrn	RGrn	MxTB	MxWB	Mass (g)
CMPA-OTPP-1001	14.40	16.43	14.75	2.43	12.95	9.74	16.56	9.74	<Null>	<Null>	<Null>	3.49	<Null>	<Null>	14.40	11.48	1.0
CMPA-OTPP-1002	6.10	13.56	13.56	1.06	<Null>	<Null>	<Null>	<Null>	<Null>	<Null>	<Null>	3.25	<Null>	<Null>	6.10	1.06	0.3
CMPA-OTPP-1003	11.66	9.46	<Null>	<Null>	<Null>	<Null>	<Null>	<Null>	<Null>	<Null>	<Null>	4.96	<Null>	<Null>	2.06	2.06	0.7
CMPA-OTPP-1004	12.53	18.48	<Null>	<Null>	16.91	12.56	<Null>	12.56	<Null>	<Null>	<Null>	6.76	6.86	<Null>	12.53	12.53	1.5
CMPA-OTPP-1005	31.77	20.22	<Null>	<Null>	11.33	8.50	20.22	9.40	3.63	<Null>	<Null>	5.65	<Null>	<Null>	17.72	9.40	3.3
CMPA-OTPP-1006	21.12	13.75	11.43	1.35	10.39	6.33	13.75	6.33	<Null>	<Null>	<Null>	4.26	<Null>	<Null>	6.22	6.33	1.3
CMPA-OTPP-1007	12.45	17.37	<Null>	<Null>	9.49	<Null>	19.54	<Null>	<Null>	<Null>	<Null>	2.85	<Null>	<Null>	7.12	7.12	0.7
CMPA-OTPP-1008	6.96	12.79	12.79	<Null>	8.70	6.92	<Null>	<Null>	<Null>	<Null>	<Null>	3.39	<Null>	<Null>	6.96	0.00	0.3
CMPA-OTPP-1009	5.71	17.57	17.57	<Null>	14.87	5.71	<Null>	<Null>	<Null>	<Null>	<Null>	3.68	<Null>	<Null>	5.71	0.00	0.4
CMPA-OTPP-1010	12.53	19.90	19.90	<Null>	12.58	12.41	<Null>	<Null>	<Null>	<Null>	<Null>	4.52	<Null>	<Null>	12.53	0.00	1.4
CMPA-OTPP-1011	16.14	12.12	11.64	<Null>	7.15	5.26	11.97	7.41	2.34	2.93	<Null>	2.79	<Null>	<Null>	11.41	5.26	0.6
CMPA-OTPP-1012	22.31	21.24	<Null>	<Null>	11.35	8.31	19.65	11.01	4.96	3.06	<Null>	4.74	<Null>	<Null>	17.93	11.01	2.2

Catalog	MxLe	MxWd	BaWd	BaCo	NckWd	NckLe	ShlWd	ShlLe	NchDL	NchDR	NchDBs	MxTk	LGrn	RGrn	MxTB	MxWB	Mass (g)
CMPA-OTPP-1013	22.63	24.21	24.21	<Null>	18.71	8.03	21.11	10.93	1.66	2.21	<Null>	3.58	<Null>	<Null>	12.09	0.00	1.9
CMPA-OTPP-1014	18.63	16.32	13.13	1.37	12.64	6.99	16.63	6.99	2.03	1.83	<Null>	4.20	<Null>	<Null>	13.51	6.99	1.3
CMPA-OTPP-1015	25.01	17.43	9.21	2.47	11.63	9.45	17.43	9.45	<Null>	<Null>	<Null>	5.91	<Null>	<Null>	15.01	9.45	2.9
CMPA-OTPP-1016	18.16	13.54	5.83	<Null>	5.19	5.15	13.22	5.15	<Null>	<Null>	<Null>	2.85	<Null>	<Null>	10.12	5.15	0.5
CMPA-OTPP-1017	11.18	16.81	14.21	<Null>	15.09	6.56	<Null>	<Null>	<Null>	<Null>	<Null>	3.21	<Null>	<Null>	11.18	11.18	0.8
CMPA-OTPP-1018	19.50	12.41	<Null>	<Null>	<Null>	<Null>	<Null>	<Null>	<Null>	<Null>	<Null>	4.25	<Null>	<Null>	0.00	0.00	0.9
CMPA-OTPP-1019	16.19	14.57	8.08	1.38	8.13	4.83	<Null>	<Null>	4.34	<Null>	<Null>	3.80	<Null>	<Null>	6.95	6.95	0.8
CMPA-OTPP-1020	29.25	32.81	<Null>	<Null>	15.57	<Null>	<Null>	<Null>	<Null>	<Null>	<Null>	3.98	<Null>	<Null>	0.00	4.57	4.5
CMPA-OTPP-1021	13.47	9.35	<Null>	<Null>	6.11	<Null>	9.67	<Null>	<Null>	<Null>	<Null>	2.28	<Null>	<Null>	0.00	0.00	0.3
CMPA-OTPP-1022	16.19	14.61	<Null>	<Null>	<Null>	8.06	<Null>	10.10	4.97	<Null>	<Null>	5.17	<Null>	<Null>	16.19	16.19	1.5
CMPA-OTPP-1023	19.03	14.54	14.54	1.40	8.10	6.36	<Null>	9.28	3.24	3.31	<Null>	2.94	<Null>	<Null>	9.23	0.00	0.8
CMPA-OTPP-1024	26.54	21.33	<Null>	<Null>	13.07	<Null>	21.33	<Null>	<Null>	<Null>	<Null>	3.75	<Null>	<Null>	9.45	9.45	2.2
CMPA-OTPP-1025	9.07	18.95	18.95	<Null>	13.25	9.07	<Null>	<Null>	<Null>	<Null>	<Null>	4.74	<Null>	<Null>	8.59	0.00	0.7
CMPA-OTPP-1026	21.04	12.90	<Null>	<Null>	<Null>	<Null>	<Null>	<Null>	<Null>	<Null>	<Null>	6.71	<Null>	<Null>	0.00	0.00	1.7
CMPA-OTPP-1027	15.26	12.71	<Null>	<Null>	<Null>	<Null>	<Null>	<Null>	<Null>	<Null>	<Null>	3.69	<Null>	<Null>	0.00	0.00	0.9
CMPA-OTPP-1028	15.33	13.64	<Null>	<Null>	<Null>	<Null>	<Null>	<Null>	<Null>	<Null>	<Null>	3.09	<Null>	<Null>	0.00	0.00	0.5
CMPA-OTPP-1029	70.97	29.83	23.17	<Null>	18.25	11.52	29.83	11.34	4.41	6.61	<Null>	6.71	<Null>	<Null>	36.83	11.34	12.4
SI-OTPP-1001	24.95	17.27	<Null>	<Null>	<Null>	<Null>	<Null>	<Null>	<Null>	<Null>	<Null>	5.67	<Null>	<Null>	6.61	6.61	1.9
SI-OTPP-1002	30.44	13.67	11.71	1.15	10.50	4.58	13.20	7.58	1.69	1.43	<Null>	3.14	<Null>	<Null>	9.11	6.54	1.2
SI-OTPP-1003	7.47	8.79	7.80	<Null>	6.22	3.69	<Null>	4.85	<Null>	1.93	<Null>	2.75	<Null>	<Null>	6.37	6.37	0.2
SI-OTPP-1004	7.15	14.66	14.66	1.52	11.34	7.15	<Null>	<Null>	<Null>	<Null>	<Null>	3.54	<Null>	<Null>	3.54	1.52	0.4
SI-OTPP-1005	8.69	11.07	9.71	<Null>	8.82	4.45	<Null>	6.55	2.20	2.26	<Null>	3.86	<Null>	<Null>	8.69	0.00	0.4
SI-OTPP-1006	15.59	17.49	9.58	<Null>	10.70	6.70	17.49	6.70	<Null>	<Null>	<Null>	4.68	5.84	<Null>	15.59	6.70	1.4
SI-OTPP-1007	12.95	13.58	11.02	<Null>	13.35	12.95	<Null>	12.95	<Null>	<Null>	<Null>	4.71	<Null>	<Null>	12.95	12.95	1.0
SI-OTPP-1008	10.33	13.86	<Null>	<Null>	<Null>	<Null>	<Null>	<Null>	<Null>	<Null>	<Null>	4.54	<Null>	<Null>	3.61	3.61	0.7
SI-OTPP-1009	11.86	13.70	10.04	1.81	<Null>	9.51	<Null>	9.51	<Null>	<Null>	<Null>	4.16	<Null>	<Null>	11.86	11.86	0.8
SI-OTPP-1010	7.82	18.61	18.61	<Null>	<Null>	<Null>	<Null>	<Null>	<Null>	<Null>	<Null>	4.23	<Null>	<Null>	7.82	3.31	0.7
SI-OTPP-1011	11.87	8.42	<Null>	<Null>	<Null>	<Null>	<Null>	<Null>	<Null>	<Null>	<Null>	4.70	<Null>	<Null>	2.26	2.26	0.5
SI-OTPP-1012	11.48	12.35	11.78	<Null>	11.46	11.48	<Null>	<Null>	<Null>	<Null>	<Null>	4.21	<Null>	<Null>	11.48	1.66	0.7
SI-OTPP-1013	15.52	10.58	<Null>	<Null>	<Null>	<Null>	<Null>	<Null>	<Null>	<Null>	<Null>	3.17	<Null>	<Null>	3.14	3.14	0.5

Catalog	MxLe	MxWd	BaWd	BaCo	NckWd	NckLe	ShlWd	ShlLe	NchDL	NchDR	NchDBs	MxTk	LGrn	RGrn	MxTB	MxWB	Mass (g)
SI-OTPP-1014	5.08	12.29	12.29	<Null>	<Null>	<Null>	<Null>	<Null>	<Null>	<Null>	<Null>	1.72	<Null>	<Null>	5.08	0.00	0.1
SI-OTPP-1015	13.60	12.55	<Null>	<Null>	6.66	5.29	12.33	7.26	3.06	<Null>	<Null>	3.12	<Null>	<Null>	9.76	7.26	0.6
SI-OTPP-1016	17.60	11.95	10.88	<Null>	6.60	3.63	9.80	5.81	1.94	2.21	<Null>	3.02	<Null>	<Null>	8.75	1.91	0.5
SI-OTPP-1017	27.95	18.11	<Null>	<Null>	<Null>	<Null>	18.11	<Null>	<Null>	<Null>	<Null>	3.53	<Null>	<Null>	11.36	0.00	1.7
SI-OTPP-1018	16.52	23.21	<Null>	<Null>	13.86	<Null>	23.21	<Null>	<Null>	<Null>	<Null>	5.40	<Null>	<Null>	2.19	1.15	2.1
SI-OTPP-1019	17.62	15.75	12.77	1.42	10.32	4.21	15.75	6.78	2.37	3.11	<Null>	4.27	<Null>	<Null>	8.74	6.78	1.3
SI-OTPP-1020	17.65	11.88	<Null>	<Null>	<Null>	<Null>	<Null>	<Null>	<Null>	<Null>	<Null>	5.22	<Null>	<Null>	4.72	4.72	1.2
SI-OTPP-1021	15.68	12.38	<Null>	<Null>	7.14	<Null>	12.38	<Null>	2.27	3.43	<Null>	2.07	<Null>	<Null>	5.42	5.42	0.3
SI-OTPP-1022	21.83	14.99	14.80	2.08	7.21	6.29	10.35	7.91	2.51	2.43	<Null>	2.80	<Null>	<Null>	9.98	6.29	0.6
SI-OTPP-1023	18.93	13.98	<Null>	2.75	8.25	7.07	13.98	8.06	3.53	<Null>	2.70	2.77	<Null>	<Null>	8.06	8.06	0.7
SI-OTPP-1024	17.96	11.07	5.68	<Null>	5.68	3.99	10.38	3.99	<Null>	<Null>	<Null>	1.95	<Null>	<Null>	14.13	5.75	0.4
SI-OTPP-1025	14.92	9.58	9.05	<Null>	6.99	5.01	9.10	7.24	1.60	1.30	<Null>	1.76	<Null>	<Null>	8.31	8.31	0.3
SI-OTPP-1026	23.53	15.48	10.14	<Null>	9.79	6.44	15.48	6.44	<Null>	<Null>	<Null>	5.41	<Null>	<Null>	9.71	9.71	1.7
SI-OTPP-1027	25.39	22.59	10.91	<Null>	10.29	4.58	22.59	6.63	3.77	4.56	<Null>	5.32	<Null>	<Null>	13.78	6.63	2.4
SI-OTPP-1028	34.29	19.63	16.58	1.21	14.14	10.22	19.63	10.22	<Null>	<Null>	<Null>	6.40	8.42	9.14	17.79	10.22	5.0
SI-OTPP-1029	26.97	22.24	<Null>	<Null>	8.59	7.04	22.24	5.28	5.88	7.94	<Null>	4.39	<Null>	<Null>	18.79	5.28	2.3
SI-OTPP-1030	21.69	12.74	12.74	<Null>	7.23	3.82	11.47	5.91	2.01	2.89	<Null>	2.70	<Null>	<Null>	7.25	0.00	0.7
SI-OTPP-1031	19.08	14.93	<Null>	<Null>	<Null>	<Null>	<Null>	<Null>	<Null>	<Null>	<Null>	3.64	<Null>	<Null>	7.24	7.24	1.1
SI-OTPP-1032	16.25	9.07	<Null>	<Null>	<Null>	<Null>	<Null>	<Null>	<Null>	<Null>	<Null>	4.23	<Null>	<Null>	0.00	0.00	0.8
SI-OTPP-1033	19.41	17.11	12.65	<Null>	9.72	4.80	<Null>	7.86	3.98	<Null>	<Null>	4.78	<Null>	<Null>	10.57	10.57	1.8
SI-OTPP-1034	19.77	25.35	17.91	<Null>	14.54	7.70	<Null>	10.84	6.25	<Null>	<Null>	7.07	6.55	5.87	11.06	11.06	3.4
SI-OTPP-1035	10.73	17.25	17.25	<Null>	13.88	10.73	<Null>	<Null>	<Null>	<Null>	<Null>	3.39	<Null>	<Null>	10.73	0.00	0.8
SI-OTPP-1036	23.86	14.22	12.50	<Null>	9.10	4.92	14.22	7.28	2.23	2.89	<Null>	4.84	<Null>	<Null>	10.21	7.28	1.4
SI-OTPP-1037	9.39	11.41	8.65	<Null>	9.37	6.22	<Null>	6.22	<Null>	<Null>	<Null>	2.91	<Null>	<Null>	9.39	9.39	0.4
SI-OTPP-1038	9.67	7.41	6.33	1.51	5.02	3.73	7.09	4.61	1.38	1.65	<Null>	3.19	<Null>	<Null>	7.61	7.09	0.3
SI-OTPP-1039	8.21	9.88	<Null>	<Null>	<Null>	2.31	<Null>	3.21	2.21	<Null>	<Null>	2.61	<Null>	<Null>	8.21	8.21	0.2
SI-OTPP-1040	10.11	13.22	<Null>	<Null>	<Null>	<Null>	<Null>	<Null>	<Null>	<Null>	<Null>	3.33	<Null>	<Null>	3.92	0.00	0.3
SI-OTPP-1041	11.77	14.61	<Null>	<Null>	<Null>	<Null>	<Null>	<Null>	<Null>	<Null>	<Null>	2.65	<Null>	<Null>	2.26	2.26	0.6
SI-OTPP-1042	14.91	14.13	<Null>	<Null>	<Null>	<Null>	<Null>	<Null>	<Null>	<Null>	<Null>	1.96	<Null>	<Null>	12.96	4.24	0.4
SI-OTPP-1043	24.87	16.43	<Null>	<Null>	11.06	4.59	<Null>	9.16	4.06	<Null>	<Null>	5.19	<Null>	<Null>	10.59	10.59	1.5

Catalog	MxLe	MxWd	BaWd	BaCo	NckWd	NckLe	ShlWd	ShlLe	NchDL	NchDR	NchDBs	MxTk	LGrn	RGrn	MxTB	MxWB	Mass (g)
SI-OTPP-1044	16.71	18.03	14.40	3.25	15.23	16.71	<Null>	16.71	<Null>	<Null>	<Null>	6.08	12.78	9.92	16.71	3.25	1.9
SI-OTPP-1045	14.82	18.83	15.86	<Null>	13.06	7.26	18.83	9.35	3.72	2.12	<Null>	3.91	<Null>	<Null>	13.78	9.35	1.3
SI-OTPP-1046	25.14	21.38	16.91	<Null>	14.97	4.34	21.38	7.36	2.54	3.42	<Null>	5.46	<Null>	<Null>	20.45	7.36	2.9
SI-OTPP-1047	15.12	20.20	11.47	<Null>	10.88	5.83	19.04	7.10	1.98	2.31	<Null>	6.29	<Null>	<Null>	13.54	13.54	1.7
SI-OTPP-1048	26.64	22.94	13.61	1.84	14.39	9.79	22.07	9.79	<Null>	<Null>	<Null>	5.99	<Null>	<Null>	26.64	26.64	4.1
SI-OTPP-1049	16.66	13.58	13.58	0.67	10.88	4.87	11.68	4.87	<Null>	<Null>	<Null>	3.71	<Null>	<Null>	9.01	0.00	0.8
SI-OTPP-1050	33.13	15.78	<Null>	<Null>	<Null>	<Null>	<Null>	<Null>	<Null>	<Null>	<Null>	6.88	<Null>	<Null>	0.00	0.00	4.6
SI-OTPP-1051	25.79	18.92	9.36	<Null>	<Null>	<Null>	<Null>	<Null>	<Null>	<Null>	<Null>	5.97	21.81	20.61	25.79	25.79	2.9
SI-OTPP-1052	24.35	16.46	15.53	<Null>	13.65	8.51	15.58	8.51	<Null>	<Null>	<Null>	4.30	<Null>	<Null>	14.29	14.29	2.0
SI-OTPP-1053	11.26	14.68	11.84	<Null>	8.40	3.94	14.75	6.08	3.20	1.83	<Null>	5.22	<Null>	<Null>	11.26	6.08	0.7
SI-OTPP-1054	24.43	15.21	5.08	<Null>	4.64	4.84	14.17	3.00	<Null>	<Null>	<Null>	3.65	<Null>	<Null>	9.30	9.30	0.9
SI-OTPP-1055	10.43	6.77	<Null>	<Null>	<Null>	<Null>	<Null>	<Null>	<Null>	<Null>	<Null>	2.04	<Null>	<Null>	0.00	0.00	0.2
SI-OTPP-1056	14.34	12.31	<Null>	<Null>	6.96	<Null>	11.05	<Null>	<Null>	<Null>	<Null>	3.12	<Null>	<Null>	9.23	3.22	0.6
SI-OTPP-1057	8.29	11.61	<Null>	<Null>	<Null>	<Null>	<Null>	<Null>	<Null>	<Null>	<Null>	2.86	<Null>	<Null>	8.29	8.29	0.3
SI-OTPP-1058	9.98	14.28	14.28	<Null>	9.54	9.98	<Null>	<Null>	<Null>	<Null>	<Null>	4.34	<Null>	<Null>	9.98	0.00	0.6
SI-OTPP-1059	20.01	16.53	<Null>	<Null>	7.70	<Null>	16.35	<Null>	<Null>	<Null>	<Null>	4.68	<Null>	<Null>	8.97	8.97	1.7
SI-OTPP-1060	12.15	18.56	<Null>	<Null>	<Null>	<Null>	<Null>	<Null>	<Null>	<Null>	<Null>	3.37	<Null>	<Null>	0.00	0.00	0.6
SI-OTPP-1061	16.28	14.64	9.03	<Null>	7.49	2.95	14.45	4.58	2.57	2.66	<Null>	3.01	<Null>	<Null>	7.02	4.58	0.8
SI-OTPP-1062	13.62	11.14	<Null>	<Null>	<Null>	<Null>	11.30	<Null>	<Null>	<Null>	<Null>	2.03	<Null>	<Null>	3.56	0.00	0.3
SI-OTPP-1063	10.58	12.92	<Null>	<Null>	<Null>	<Null>	<Null>	<Null>	<Null>	<Null>	<Null>	2.46	<Null>	<Null>	4.15	0.00	0.4
SI-OTPP-1064	19.51	8.33	<Null>	<Null>	<Null>	2.84	<Null>	3.93	2.08	<Null>	<Null>	3.99	<Null>	<Null>	4.66	3.93	0.6
SI-OTPP-1065	11.58	14.12	<Null>	<Null>	<Null>	<Null>	<Null>	<Null>	<Null>	<Null>	<Null>	2.97	<Null>	<Null>	4.03	1.76	0.4
SI-OTPP-1066	16.96	21.20	<Null>	<Null>	16.15	<Null>	21.05	<Null>	2.65	1.18	<Null>	4.26	<Null>	<Null>	8.88	8.74	1.7
SI-OTPP-1067	6.83	18.67	18.67	0.61	<Null>	<Null>	<Null>	<Null>	<Null>	<Null>	<Null>	3.37	<Null>	<Null>	3.75	0.00	0.5
SI-OTPP-1068	9.03	16.31	16.31	<Null>	11.19	9.03	<Null>	<Null>	<Null>	<Null>	<Null>	3.08	<Null>	<Null>	9.03	0.00	0.5
SI-OTPP-1069	7.99	17.16	17.16	<Null>	<Null>	<Null>	<Null>	<Null>	<Null>	<Null>	<Null>	2.71	<Null>	<Null>	7.99	0.00	0.5
SI-OTPP-1070	18.49	15.74	<Null>	<Null>	<Null>	<Null>	<Null>	<Null>	<Null>	<Null>	<Null>	3.77	<Null>	<Null>	3.44	0.00	0.8
SI-OTPP-1071	10.00	15.22	15.22	2.33	<Null>	<Null>	<Null>	<Null>	2.33	<Null>	<Null>	2.95	<Null>	<Null>	3.57	2.33	0.4
SI-OTPP-1072	12.17	16.37	<Null>	<Null>	8.20	<Null>	16.37	<Null>	<Null>	<Null>	<Null>	4.18	<Null>	<Null>	3.94	1.15	0.8
SI-OTPP-1073	7.15	12.83	12.83	<Null>	6.78	5.33	<Null>	7.15	2.29	<Null>	<Null>	2.08	<Null>	<Null>	7.15	0.00	0.2

Catalog	MxLe	MxWd	BaWd	BaCo	NckWd	NckLe	ShlWd	ShlLe	NchDL	NchDR	NchDBs	MxTk	LGrn	RGrn	MxTB	MxWB	Mass (g)
SI-OTPP-1074	14.99	15.88	<Null>	<Null>	<Null>	<Null>	<Null>	8.83	<Null>	<Null>	<Null>	4.02	<Null>	<Null>	14.99	8.83	0.8
SI-OTPP-1075	14.27	10.54	<Null>	<Null>	<Null>	<Null>	<Null>	<Null>	<Null>	<Null>	<Null>	2.78	<Null>	<Null>	0.00	0.00	0.4
SI-OTPP-1076	9.30	8.91	<Null>	<Null>	<Null>	<Null>	<Null>	<Null>	<Null>	<Null>	<Null>	2.28	<Null>	<Null>	0.00	0.00	0.2
SI-OTPP-1077	14.66	15.51	<Null>	<Null>	4.86	<Null>	<Null>	<Null>	<Null>	<Null>	<Null>	3.08	<Null>	<Null>	6.31	0.00	0.7
SI-OTPP-1078	22.06	12.59	5.01	<Null>	4.26	6.64	10.46	4.01	<Null>	<Null>	<Null>	3.13	<Null>	<Null>	8.85	8.85	0.6
SI-OTPP-1079	15.61	10.84	7.67	<Null>	5.24	7.32	10.42	7.32	<Null>	<Null>	<Null>	2.81	<Null>	<Null>	12.01	7.32	0.4
SI-OTPP-1080	7.81	12.96	11.41	2.89	<Null>	<Null>	<Null>	<Null>	<Null>	<Null>	<Null>	3.85	5.66	7.81	7.81	7.81	0.5
SI-OTPP-1081	9.95	18.17	<Null>	<Null>	<Null>	<Null>	<Null>	<Null>	<Null>	<Null>	<Null>	2.98	<Null>	<Null>	5.95	5.95	0.4
SI-OTPP-1082	6.74	16.51	16.51	<Null>	<Null>	<Null>	<Null>	<Null>	<Null>	<Null>	<Null>	3.48	<Null>	<Null>	6.74	0.00	0.5
SI-OTPP-1083	5.38	15.84	15.84	<Null>	<Null>	<Null>	<Null>	<Null>	<Null>	<Null>	<Null>	3.22	<Null>	<Null>	5.38	0.00	0.3
SI-OTPP-1084	19.10	13.21	<Null>	<Null>	7.25	<Null>	13.05	<Null>	<Null>	<Null>	<Null>	3.83	<Null>	<Null>	19.10	1.22	0.9
SI-OTPP-1085	19.71	11.65	6.10	<Null>	5.29	4.45	9.88	4.45	<Null>	<Null>	<Null>	3.31	<Null>	<Null>	6.85	4.45	0.5
SI-OTPP-1086	14.01	9.71	<Null>	<Null>	<Null>	<Null>	<Null>	<Null>	<Null>	<Null>	<Null>	3.01	<Null>	<Null>	0.00	0.00	0.6
SI-OTPP-1087	11.80	12.58	<Null>	<Null>	<Null>	<Null>	<Null>	<Null>	<Null>	<Null>	<Null>	3.22	<Null>	<Null>	0.00	0.00	0.5
SI-OTPP-1088	12.12	9.13	<Null>	<Null>	5.61	3.88	<Null>	5.18	4.24	<Null>	<Null>	1.77	<Null>	<Null>	5.18	5.18	0.2
SI-OTPP-1089	11.44	12.47	<Null>	<Null>	6.28	<Null>	<Null>	<Null>	<Null>	<Null>	<Null>	3.72	<Null>	<Null>	4.17	4.17	0.5
SI-OTPP-1090	12.89	10.75	<Null>	1.33	<Null>	12.89	<Null>	12.89	1.97	<Null>	<Null>	4.56	7.02	<Null>	12.89	6.83	0.7
SI-OTPP-1091	18.55	12.52	11.56	0.77	<Null>	<Null>	<Null>	<Null>	<Null>	<Null>	<Null>	2.71	3.61	<Null>	6.56	6.56	0.7
SI-OTPP-1092	16.90	10.44	<Null>	<Null>	<Null>	<Null>	<Null>	<Null>	<Null>	<Null>	<Null>	4.81	<Null>	<Null>	9.45	9.45	1.2
SI-OTPP-1093	11.91	14.78	<Null>	<Null>	<Null>	<Null>	<Null>	<Null>	<Null>	<Null>	<Null>	3.11	<Null>	<Null>	0.00	0.00	0.6
SI-OTPP-1094	21.18	13.12	<Null>	<Null>	<Null>	<Null>	<Null>	<Null>	<Null>	<Null>	<Null>	4.60	<Null>	<Null>	0.00	0.00	1.6
SI-OTPP-1095	9.88	12.35	<Null>	1.27	<Null>	<Null>	<Null>	<Null>	<Null>	<Null>	<Null>	5.79	<Null>	<Null>	9.88	0.00	0.8
SI-OTPP-1096	16.80	11.57	<Null>	<Null>	<Null>	<Null>	<Null>	<Null>	<Null>	<Null>	<Null>	3.86	<Null>	<Null>	5.05	0.00	0.7
SI-OTPP-1097	15.61	12.38	<Null>	<Null>	<Null>	<Null>	<Null>	<Null>	<Null>	<Null>	<Null>	4.31	<Null>	<Null>	4.03	4.03	0.9
SI-OTPP-1098	7.13	11.48	<Null>	5.29	<Null>	<Null>	<Null>	<Null>	<Null>	<Null>	<Null>	3.64	<Null>	<Null>	7.13	7.13	0.2
SI-OTPP-1099	17.59	15.48	<Null>	<Null>	<Null>	<Null>	<Null>	<Null>	<Null>	<Null>	<Null>	4.63	<Null>	<Null>	0.00	0.00	1.4
SI-OTPP-1100	19.75	10.59	8.51	<Null>	<Null>	<Null>	<Null>	<Null>	<Null>	<Null>	<Null>	2.72	<Null>	<Null>	4.12	3.83	0.5
SI-OTPP-1101	23.55	14.13	<Null>	<Null>	13.60	9.07	14.13	9.07	<Null>	<Null>	<Null>	5.18	9.01	<Null>	14.18	9.07	1.6
SI-OTPP-1102	14.54	9.76	<Null>	<Null>	<Null>	<Null>	<Null>	<Null>	<Null>	<Null>	<Null>	1.77	<Null>	<Null>	3.63	3.63	0.2
SI-OTPP-1103	20.65	18.33	15.93	2.18	<Null>	20.65	<Null>	<Null>	<Null>	<Null>	<Null>	7.23	10.79	<Null>	18.11	18.11	3.5

Catalog	MxLe	MxWd	BaWd	BaCo	NckWd	NckLe	ShlWd	ShlLe	NchDL	NchDR	NchDBs	MxTk	LGrn	RGrn	MxTB	MxWB	Mass (g)
SI-OTPP-1104	12.26	12.50	11.23	<Null>	9.87	8.37	10.72	9.37	<Null>	<Null>	<Null>	3.41	<Null>	<Null>	12.26	12.26	0.6
SI-OTPP-1105	21.46	16.16	13.92	2.02	14.75	6.22	16.16	7.71	<Null>	<Null>	<Null>	4.67	5.65	4.93	11.61	7.71	1.6
SI-OTPP-1106	16.25	18.75	<Null>	<Null>	<Null>	<Null>	<Null>	<Null>	<Null>	<Null>	<Null>	3.53	<Null>	<Null>	2.62	2.62	1.1
SI-OTPP-1107	24.10	15.14	10.01	<Null>	8.91	6.01	12.83	6.89	<Null>	<Null>	<Null>	5.45	<Null>	<Null>	13.41	13.41	1.7
SI-OTPP-1108	29.11	14.90	10.48	1.62	10.39	8.71	14.90	8.71	<Null>	<Null>	<Null>	5.72	<Null>	<Null>	12.84	8.71	2.2
SI-OTPP-1109	19.23	19.75	15.16	<Null>	<Null>	<Null>	<Null>	<Null>	<Null>	<Null>	<Null>	5.17	<Null>	17.36	19.23	19.75	2.7
SI-OTPP-1110	23.62	20.18	20.18	2.94	<Null>	<Null>	<Null>	<Null>	<Null>	<Null>	<Null>	6.03	8.07	<Null>	17.91	0.00	3.0
SI-OTPP-1111	20.59	17.88	15.79	<Null>	17.88	20.59	<Null>	20.59	<Null>	<Null>	<Null>	6.78	17.23	17.01	20.08	20.59	3.1
SI-OTPP-1112	19.11	14.34	<Null>	<Null>	<Null>	<Null>	<Null>	<Null>	<Null>	<Null>	<Null>	3.66	18.59	<Null>	8.41	8.41	1.1
SI-OTPP-1113	8.20	9.37	9.30	<Null>	<Null>	<Null>	<Null>	<Null>	<Null>	<Null>	<Null>	3.08	<Null>	<Null>	6.86	6.86	0.3
SI-OTPP-1114	18.47	13.41	<Null>	<Null>	4.70	<Null>	<Null>	<Null>	<Null>	<Null>	<Null>	2.59	<Null>	<Null>	8.50	5.60	0.5
SI-OTPP-1115	11.01	13.93	<Null>	<Null>	<Null>	<Null>	<Null>	<Null>	<Null>	<Null>	<Null>	3.74	10.90	<Null>	6.62	0.00	0.4
SI-OTPP-1116	7.25	12.80	11.40	<Null>	12.59	6.70	<Null>	7.25	<Null>	<Null>	<Null>	3.10	<Null>	<Null>	7.25	7.25	0.3
SI-OTPP-1117	15.03	11.85	<Null>	<Null>	5.65	<Null>	11.01	<Null>	<Null>	<Null>	<Null>	2.76	<Null>	<Null>	0.00	1.30	0.4
SI-OTPP-1118	9.79	21.22	17.64	4.18	<Null>	<Null>	<Null>	<Null>	<Null>	<Null>	<Null>	5.76	7.20	4.76	9.79	2.63	1.0
SI-OTPP-1119	6.71	12.48	12.48	<Null>	<Null>	<Null>	<Null>	<Null>	<Null>	<Null>	<Null>	2.39	<Null>	<Null>	6.71	0.00	0.3
SI-OTPP-1120	16.09	20.36	16.97	<Null>	15.86	7.84	20.10	12.08	2.93	2.81	<Null>	4.28	<Null>	<Null>	12.15	4.78	1.6
SI-OTPP-1121	7.55	15.84	15.84	<Null>	<Null>	<Null>	<Null>	<Null>	<Null>	<Null>	<Null>	3.08	<Null>	<Null>	7.55	0.00	0.4
SI-OTPP-1122	8.73	17.29	17.29	<Null>	<Null>	7.30	<Null>	<Null>	5.04	<Null>	<Null>	4.09	<Null>	<Null>	8.73	0.00	0.5
SI-OTPP-1123	6.59	19.84	19.84	<Null>	<Null>	<Null>	<Null>	<Null>	<Null>	<Null>	<Null>	2.97	<Null>	<Null>	6.59	0.00	0.4
SI-OTPP-1124	12.83	13.70	<Null>	<Null>	<Null>	<Null>	<Null>	<Null>	<Null>	<Null>	<Null>	3.13	<Null>	<Null>	0.00	0.00	0.5
SI-OTPP-1125	6.55	15.36	15.36	<Null>	<Null>	<Null>	<Null>	<Null>	<Null>	<Null>	<Null>	3.43	<Null>	<Null>	0.00	0.00	0.4
SI-OTPP-1126	16.24	12.57	<Null>	<Null>	<Null>	<Null>	<Null>	<Null>	2.16	<Null>	<Null>	4.78	<Null>	<Null>	0.00	0.00	1.1
SI-OTPP-1127	7.69	9.50	<Null>	<Null>	<Null>	<Null>	<Null>	<Null>	<Null>	<Null>	<Null>	1.91	<Null>	<Null>	0.00	0.00	0.1
SI-OTPP-1128	17.69	11.66	11.66	1.30	10.07	6.51	11.15	6.51	<Null>	<Null>	<Null>	3.87	<Null>	<Null>	9.34	0.00	0.8
SI-OTPP-1129	22.05	16.55	9.96	<Null>	8.70	3.71	16.55	5.21	2.54	2.68	<Null>	3.40	<Null>	<Null>	13.33	16.55	1.0
SI-OTPP-1130	14.57	13.88	<Null>	<Null>	<Null>	<Null>	<Null>	<Null>	<Null>	<Null>	<Null>	3.23	<Null>	<Null>	0.00	0.00	0.6
SI-OTPP-1131	11.77	12.97	<Null>	<Null>	<Null>	<Null>	<Null>	<Null>	<Null>	<Null>	<Null>	3.19	<Null>	<Null>	0.00	0.00	0.5
SI-OTPP-1132	10.63	11.90	<Null>	<Null>	<Null>	<Null>	<Null>	<Null>	<Null>	<Null>	<Null>	2.28	<Null>	<Null>	0.00	0.00	0.3
SI-OTPP-1133	7.10	14.29	<Null>	<Null>	<Null>	<Null>	<Null>	<Null>	<Null>	<Null>	<Null>	3.53	<Null>	<Null>	7.10	0.00	0.5

Catalog	MxLe	MxWd	BaWd	BaCo	NckWd	NckLe	ShlWd	ShlLe	NchDL	NchDR	NchDBs	MxTk	LGrn	RGrn	MxTB	MxWB	Mass (g)
SI-OTPP-1134	12.51	15.61	<Null>	<Null>	<Null>	<Null>	<Null>	<Null>	<Null>	<Null>	<Null>	3.41	<Null>	<Null>	0.00	0.00	0.6
SI-OTPP-1135	8.47	15.02	<Null>	<Null>	<Null>	<Null>	<Null>	<Null>	<Null>	<Null>	<Null>	2.91	<Null>	<Null>	0.00	0.00	0.4
SI-OTPP-1136	7.77	10.74	<Null>	2.39	<Null>	<Null>	<Null>	<Null>	<Null>	<Null>	<Null>	4.48	<Null>	<Null>	7.77	7.77	0.3
SI-OTPP-1137	7.27	14.73	14.73	<Null>	<Null>	<Null>	<Null>	<Null>	<Null>	<Null>	<Null>	4.33	<Null>	<Null>	7.27	0.00	0.5
SI-OTPP-1138	8.05	10.62	8.82	<Null>	9.18	8.05	<Null>	8.05	<Null>	<Null>	1.50	3.06	<Null>	<Null>	8.05	2.68	0.3
SI-OTPP-1139	12.11	20.12	12.91	<Null>	15.70	7.31	<Null>	7.31	<Null>	<Null>	<Null>	4.81	7.31	7.20	12.11	8.69	1.1
SI-OTPP-1140	6.85	8.35	<Null>	<Null>	<Null>	<Null>	<Null>	<Null>	<Null>	<Null>	<Null>	3.12	<Null>	<Null>	0.00	0.00	0.2
SI-OTPP-1141	11.62	13.90	13.90	<Null>	10.76	8.07	<Null>	<Null>	2.99	1.90	<Null>	3.80	<Null>	<Null>	11.62	0.00	0.7
SI-OTPP-1142	11.97	14.72	14.72	<Null>	<Null>	8.78	<Null>	8.78	<Null>	<Null>	<Null>	4.95	<Null>	<Null>	9.10	9.10	0.7
SI-OTPP-1143	11.00	11.09	<Null>	<Null>	<Null>	<Null>	<Null>	<Null>	<Null>	<Null>	<Null>	2.18	<Null>	<Null>	0.00	0.00	0.3
SI-OTPP-1144	13.61	10.06	<Null>	2.48	<Null>	<Null>	<Null>	<Null>	<Null>	<Null>	<Null>	3.48	<Null>	<Null>	0.00	0.00	0.4
SI-OTPP-1145	12.84	15.12	<Null>	<Null>	6.51	<Null>	13.80	<Null>	<Null>	<Null>	<Null>	3.26	<Null>	<Null>	12.84	2.29	0.7
SI-OTPP-1146	12.20	9.49	<Null>	3.29	<Null>	<Null>	<Null>	<Null>	<Null>	<Null>	<Null>	2.90	<Null>	<Null>	12.20	12.20	0.3
SI-OTPP-1147	7.34	11.18	11.18	<Null>	<Null>	<Null>	<Null>	<Null>	<Null>	<Null>	<Null>	3.86	<Null>	<Null>	7.34	0.00	0.4
SI-OTPP-1148	14.42	17.70	12.36	<Null>	13.81	4.68	<Null>	5.63	2.83	<Null>	<Null>	3.87	<Null>	<Null>	6.96	6.96	1.3
SI-OTPP-1149	9.19	14.26	14.26	<Null>	<Null>	<Null>	<Null>	<Null>	<Null>	<Null>	<Null>	2.82	<Null>	<Null>	0.00	0.00	0.4
SI-OTPP-1150	9.01	22.67	22.67	<Null>	<Null>	<Null>	<Null>	<Null>	<Null>	<Null>	<Null>	5.11	<Null>	<Null>	9.01	0.00	1.1
SI-OTPP-1151	10.42	19.40	19.40	1.46	<Null>	<Null>	<Null>	<Null>	<Null>	<Null>	<Null>	5.85	<Null>	<Null>	10.42	0.00	1.1
SI-OTPP-1152	5.67	12.97	<Null>	<Null>	12.01	3.36	<Null>	5.67	1.37	<Null>	<Null>	2.60	<Null>	<Null>	5.67	0.00	0.3
SI-OTPP-1153	19.02	10.74	<Null>	<Null>	<Null>	<Null>	<Null>	<Null>	<Null>	<Null>	<Null>	3.41	<Null>	<Null>	0.00	0.00	0.6
SI-OTPP-1154	10.19	13.94	13.94	<Null>	6.89	5.79	13.40	7.48	3.33	3.35	<Null>	2.49	<Null>	<Null>	10.19	0.00	0.4
SI-OTPP-1155	8.37	14.46	14.46	<Null>	<Null>	<Null>	<Null>	<Null>	<Null>	<Null>	<Null>	3.50	<Null>	<Null>	0.00	0.00	0.5
SI-OTPP-1156	6.47	12.23	12.23	1.06	<Null>	<Null>	<Null>	<Null>	<Null>	<Null>	<Null>	2.72	<Null>	<Null>	0.00	0.00	0.2
SI-OTPP-1157	8.05	19.84	19.84	<Null>	<Null>	<Null>	<Null>	<Null>	<Null>	<Null>	<Null>	3.62	<Null>	<Null>	8.05	0.00	0.6
SI-OTPP-1158	6.52	16.10	16.10	<Null>	<Null>	<Null>	<Null>	<Null>	<Null>	<Null>	<Null>	3.61	<Null>	<Null>	6.52	0.00	0.4
SI-OTPP-1159	6.11	10.13	10.13	<Null>	<Null>	<Null>	<Null>	<Null>	<Null>	<Null>	<Null>	1.89	<Null>	<Null>	6.11	0.00	0.1
SI-OTPP-1160	8.65	5.05	<Null>	<Null>	<Null>	<Null>	<Null>	<Null>	<Null>	<Null>	<Null>	2.41	<Null>	<Null>	0.00	0.00	0.1

E1. Biface descriptive and metric data.

Catalog	Portion	GENMAT	SPECMAT	Nodule	Burning	MxLe	MxWd	MxTk	LGrn	RGrn	Mass(g)
CMPA-BF-1001	LT	CCS	TRT	TRT-08	NO	15.91	10.40	4.78	<Null>	<Null>	0.5
CMPA-BF-1002	LT	CCS	TRT	TRT-08	NO	12.59	10.36	5.81	<Null>	<Null>	0.9
CMPA-BF-1003	LT	CCS	TRT	TRT-16	NO	15.34	4.19	2.08	<Null>	<Null>	0.1
CMPA-BF-1004	LT	CCS	TRT	TRT-10	NO	7.21	25.15	8.97	<Null>	<Null>	1.7
CMPA-BF-1005	END	QZT	DAK	DAK-05	NO	23.61	23.69	4.73	<Null>	<Null>	2.4
CMPA-BF-1006	LT	CCS	UNK	UNK-07	NO	11.03	4.63	2.91	<Null>	<Null>	0.2
CMPA-BF-1007	LT	CCS	MOSC	MOSC-04	NO	35.85	23.86	8.54	<Null>	<Null>	6.6
CMPA-BF-1008	END	CCS	PED	PED-07	NO	18.87	25.96	8.51	<Null>	<Null>	4.3
CMPA-BF-1009	END	CCS	PED	PED-07	NO	37.53	29.19	10.19	<Null>	<Null>	11.9
CMPA-BF-1010	END	QZT	DAK	DAK-01	NO	21.07	16.60	3.46	<Null>	<Null>	1.3
CMPA-BF-1011	END	CCS	TRT	TRT-20	NO	10.25	11.57	3.69	<Null>	<Null>	0.6
CMPA-BF-1012	LT	CCS	TRT	TRT-02	NO	14.69	4.95	2.55	<Null>	<Null>	0.2
CMPA-BF-1013	LT	CCS	CUMB	CUMB-01	NO	19.54	13.96	4.34	<Null>	<Null>	1.7
CMPA-BF-1014	END	CCS	TRT	TRT-20	NO	12.57	7.94	2.28	<Null>	<Null>	0.3
CMPA-BF-1015	END	CCS	UNK	UNK-09	NO	17.39	16.66	4.18	<Null>	<Null>	1.0
CMPA-BF-1016	LT	CCS	TRT	TRT-05	POT	13.20	13.49	3.81	<Null>	<Null>	0.4
CMPA-BF-1017	END	VOL	DAC	DAC-01	NO	12.92	14.07	4.01	<Null>	<Null>	0.8
CMPA-BF-1018	END	VOL	OBS	OBS-03	NO	6.81	9.02	3.73	<Null>	<Null>	0.2
CMPA-BF-1019	END	VOL	OBS	OBS-02	NO	8.59	6.84	3.48	<Null>	<Null>	0.2
CMPA-BF-1020	MS	CCS	TRT	TRT-07	POT	9.15	18.51	3.96	<Null>	<Null>	0.7
CMPA-BF-1021	END	CCS	FLAT	FLAT-01	NO	19.12	17.66	3.41	<Null>	<Null>	1.0
CMPA-BF-1022	NC	CCS	UNK	UNK-11	NO	37.40	39.22	9.93	<Null>	<Null>	20.7
CMPA-BF-1023	END	QZT	DAK	DAK-04	NO	24.95	18.64	4.15	<Null>	<Null>	2.9
CMPA-BF-1024	END	CCS	PED	PED-03	NO	11.90	14.30	5.20	<Null>	<Null>	0.7
CMPA-BF-1025	LT	VOL	OBS	OBS-03	NO	25.41	14.04	4.39	<Null>	<Null>	1.9
CMPA-BF-1026	END	VOL	OBS	OBS-02	NO	10.55	13.23	3.19	<Null>	<Null>	0.4
CMPA-BF-1027	END	CCS	CUMB	CUMB-03	NO	17.93	14.51	5.12	<Null>	<Null>	1.5

Catalog	Portion	GENMAT	SPECMAT	Nodule	Burning	MxLe	MxWd	MxTk	LGrn	RGrn	Mass(g)
CMPA-BF-1028	END	SWD	SWD	SWD-07	NO	13.00	28.61	7.49	<Null>	<Null>	3.0
CMPA-BF-1029	LT	VOL	OBS	OBS-04	NO	36.15	19.20	4.33	<Null>	<Null>	3.2
CMPA-BF-1030	LT	CCS	CUMB	CUMB-03	NO	14.15	10.87	4.24	<Null>	<Null>	0.6
CMPA-BF-1031	MS	VOL	DAC	DAC-01	NO	19.87	18.31	3.63	<Null>	<Null>	1.3
CMPA-BF-1032	END	CCS	TRT	TRT-13	NO	16.51	13.33	2.53	<Null>	<Null>	0.5
CMPA-BF-1033	END	QZT	DAK	DAK-05	NO	13.72	23.80	7.12	<Null>	<Null>	1.6
CMPA-BF-1034	END	CCS	TRT	TRT-02	NO	25.05	34.39	9.49	<Null>	<Null>	8.9
CMPA-BF-1035	LT	VOL	OBS	OBS-02	NO	10.63	8.55	3.42	<Null>	<Null>	0.2
SI-BF-1001	MS	QZT	DAK	DAK-01	NO	16.33	22.10	4.21	<Null>	<Null>	2.2
SI-BF-1002	LT	QZT	MOR	MOR-02	NO	13.73	13.63	3.02	<Null>	<Null>	0.6
SI-BF-1003	LT	CCS	UNK	UNK-07	NO	14.19	12.51	4.55	<Null>	<Null>	0.8
SI-BF-1004	LT	CCS	TRT	TRT-10	NO	8.67	24.88	5.58	<Null>	<Null>	0.9
SI-BF-1005	END	SWD	SWD	SWD-07	NO	11.57	17.56	7.70	<Null>	<Null>	1.2
SI-BF-1006	END	CCS	TRT	TRT-05	NO	12.50	24.32	6.93	<Null>	<Null>	2.2
SI-BF-1007	END	CCS	TRT	TRT-08	POT	16.61	21.85	6.79	<Null>	<Null>	2.5
SI-BF-1008	LT	CCS	TRT	TRT-10	POT	33.02	23.11	8.11	<Null>	<Null>	6.3
SI-BF-1009	LT	QZT	MOR	MOR-02	NO	23.86	19.48	3.99	<Null>	<Null>	2.1
SI-BF-1010	LT	QZT	MOR	MOR-02	NO	19.84	25.73	4.01	<Null>	<Null>	3.0
SI-BF-1011	END	QZT	MOR	MOR-02	NO	14.77	26.65	4.45	<Null>	<Null>	1.8
SI-BF-1012	LT	CCS	UNK	UNK-07	NO	27.48	18.72	6.21	<Null>	<Null>	3.6
SI-BF-1013	LT	CCS	TRT	TRT-02	PTCZ	15.06	14.29	3.33	<Null>	<Null>	0.9
SI-BF-1014	LT	SWD	SWD	SWD-07	NO	29.25	14.24	6.03	<Null>	<Null>	2.8
SI-BF-1015	LT	CCS	MOSC	MOSC-03	NO	13.24	11.16	4.08	<Null>	<Null>	0.6
SI-BF-1016	LT	CCS	TRT	TRT-08	NO	17.13	7.62	4.02	<Null>	<Null>	0.6
SI-BF-1017	LT	CCS	TRT	TRT-19	NO	29.13	16.79	7.92	<Null>	<Null>	2.9
SI-BF-1018	LT	SWD	SWD	SWD-07	NO	14.16	16.96	5.32	<Null>	<Null>	1.1
SI-BF-1019	LT	CCS	TRT	TRT-02	NO	18.59	13.47	3.54	<Null>	<Null>	1.0
SI-BF-1020	END	CCS	TRT	TRT-02	NO	13.10	9.75	4.44	<Null>	<Null>	0.4
SI-BF-1021	LT	SWD	SWD	SWD-05	NO	14.61	7.08	4.67	<Null>	<Null>	0.6
SI-BF-1022	LT	CCS	TRT	TRT-06	NO	15.13	27.63	7.54	<Null>	<Null>	4.0

Catalog	Portion	GENMAT	SPECMAT	Nodule	Burning	MxLe	MxWd	MxTk	LGrn	RGrn	Mass(g)
SI-BF-1023	LT	CCS	TRT	TRT-17	NO	13.75	24.39	5.13	<Null>	<Null>	1.7
SI-BF-1024	LT	CCS	TRT	TRT-10	NO	12.05	24.24	5.42	<Null>	<Null>	1.5
SI-BF-1025	LT	CCS	PED	PED-07	NO	17.02	24.22	6.35	<Null>	<Null>	3.4
SI-BF-1026	LT	CCS	UNK	UNK-05	NO	11.59	11.11	4.33	<Null>	<Null>	0.7
SI-BF-1027	MS	CCS	PED	PED-06	NO	20.07	39.13	9.33	<Null>	<Null>	7.3
SI-BF-1028	LT	CCS	TRT	TRT-02	NO	40.37	31.60	11.44	<Null>	<Null>	14.3
SI-BF-1029	LT	CCS	TRT	TRT-10	POT	33.63	12.34	8.12	<Null>	<Null>	2.6
SI-BF-1030	END	SWD	SWD	SWD-04	NO	21.11	23.50	6.31	<Null>	<Null>	3.1
SI-BF-1031	END	CCS	PED	PED-08	NO	19.26	28.50	6.57	<Null>	<Null>	4.1
SI-BF-1032	LT	CCS	FLAT	FLAT-02	NO	19.54	21.87	6.89	<Null>	<Null>	3.5
SI-BF-1033	END	SWD	SWD	SWD-01	POT	12.54	18.81	5.35	<Null>	<Null>	0.9
SI-BF-1034	LT	CCS	TRT	TRT-15	POT	9.09	13.71	4.89	<Null>	<Null>	0.5
SI-BF-1035	LT	CCS	TRT	TRT-02	NO	11.55	7.69	3.20	10.05	<Null>	0.3
SI-BF-1036	END	CCS	TRT	TRT-16	PTCZ	8.15	16.90	3.56	<Null>	<Null>	0.6
SI-BF-1037	LT	CCS	PED	PED-02	NO	13.98	16.36	7.06	<Null>	<Null>	1.6
SI-BF-1038	LT	CCS	TRT	TRT-02	NO	9.46	6.17	2.18	<Null>	<Null>	0.2
SI-BF-1039	END	QZT	MOR	MOR-02	NO	21.44	19.66	5.24	<Null>	<Null>	2.6
SI-BF-1040	END	CCS	TRT	TRT-05	NO	10.49	12.36	2.67	<Null>	<Null>	0.3
SI-BF-1041	END	QZT	MOR	MOR-02	NO	9.72	13.67	2.33	<Null>	<Null>	0.3
SI-BF-1042	END	CCS	PED	PED-06	NO	10.89	21.59	3.34	<Null>	<Null>	0.9
SI-BF-1043	CO	CCS	TRT	TRT-02	NO	52.47	31.26	18.17	<Null>	<Null>	28.5
SI-BF-1044	END	QZT	DAK	DAK-05	NO	38.75	27.51	13.46	<Null>	<Null>	13.0
SI-BF-1045	MS	CCS	TRT	TRT-17	POT	16.69	19.70	7.81	<Null>	<Null>	2.8
SI-BF-1046	END	QZT	DAK	DAK-05	NO	12.18	9.33	5.46	<Null>	<Null>	0.6
SI-BF-1047	LT	CCS	TRT	TRT-07	NO	9.03	27.18	6.74	<Null>	<Null>	1.9
SI-BF-1048	LT	CCS	TRT	TRT-20	NO	14.91	15.04	3.18	<Null>	<Null>	0.7
SI-BF-1049	LT	CCS	PED	PED-07	POT	13.85	18.12	4.22	<Null>	<Null>	1.1
SI-BF-1050	LT	CCS	TRT	TRT-07	POT	13.33	5.94	2.90	<Null>	<Null>	0.3
SI-BF-1051	LT	CCS	PED	PED-05	NO	5.43	4.58	1.62	<Null>	<Null>	0.1
SI-BF-1052	LT	CCS	TRT	TRT-02	NO	10.36	6.18	4.30	<Null>	<Null>	0.3

Catalog	Portion	GENMAT	SPECMAT	Nodule	Burning	MxLe	MxWd	MxTk	LGrn	RGrn	Mass(g)
SI-BF-1053	LT	CCS	MOSC	MOSC-03	NO	7.07	6.98	3.01	<Null>	<Null>	0.2
SI-BF-1054	LT	CCS	TRT	TRT-12	NO	8.38	9.34	3.82	<Null>	<Null>	0.3
SI-BF-1055	LT	CCS	TRT	TRT-16	NO	6.72	9.44	6.12	<Null>	<Null>	0.4
SI-BF-1056	END	CCS	TRT	TRT-10	NO	7.62	12.69	3.39	<Null>	<Null>	0.4
SI-BF-1057	LT	QZT	DAK	DAK-04	NO	18.56	10.02	3.50	<Null>	<Null>	0.7
SI-BF-1058	END	CCS	UNK	UNK-02	NO	11.29	5.61	4.12	<Null>	<Null>	0.3
SI-BF-1059	END	CCS	UNK	UNK-11	NO	31.53	26.72	11.07	<Null>	<Null>	11.3
SI-BF-1060	LT	CCS	PED	PED-08	NO	19.35	6.11	2.89	<Null>	<Null>	0.4
SI-BF-1061	CO	CCS	PED	PED-07	NO	32.42	6.29	6.53	<Null>	<Null>	1.2
SI-BF-1062	END	CCS	PED	PED-07	NO	12.42	22.27	5.44	<Null>	<Null>	1.3
SI-BF-1063	END	QZT	DAK	DAK-03	NO	39.87	41.54	5.85	<Null>	<Null>	10.4
SI-BF-1064	LT	QZT	MOR	MOR-03	NO	16.25	16.03	4.40	<Null>	<Null>	0.9
SI-BF-1065	LT	CCS	CUMB	CUMB-02	NO	16.01	9.84	5.03	<Null>	<Null>	1.0
SI-BF-1066	LT	CCS	TRT	TRT-02	NO	13.50	23.02	4.78	<Null>	<Null>	1.9
SI-BF-1067	END	VOL	OBS	OBS-01	NO	8.07	16.77	3.80	<Null>	<Null>	0.6
SI-BF-1068	END	VOL	OBS	OBS-04	NO	24.55	22.20	5.59	<Null>	<Null>	3.6
SI-BF-1069	END	VOL	OBS	OBS-02	NO	15.59	19.63	3.47	<Null>	<Null>	1.4
SI-BF-1070	LT	CCS	TRT	TRT-18	POT	17.78	12.45	4.74	<Null>	<Null>	1.7
SI-BF-1071	LT	CCS	TRT	TRT-02	POT	8.69	9.01	4.48	<Null>	<Null>	0.4
SI-BF-1072	END	VOL	OBS	OBS-02	NO	28.35	20.04	6.05	<Null>	<Null>	3.2
SI-BF-1073	END	SWD	SWD	SWD-07	NO	12.67	28.09	5.33	<Null>	<Null>	2.1
SI-BF-1074	END	CCS	FLAT	FLAT-02	POT	8.54	11.56	2.85	<Null>	<Null>	0.3
SI-BF-1075	LT	SWD	SWD	SWD-04	NO	15.42	12.23	3.18	<Null>	<Null>	0.7
SI-BF-1076	END	QZT	DAK	DAK-03	NO	26.98	19.32	4.68	<Null>	<Null>	2.6
SI-BF-1077	END	VOL	OBS	OBS-04	NO	8.80	24.43	4.58	<Null>	<Null>	0.9
SI-BF-1078	LT	VOL	OBS	OBS-04	NO	12.73	15.73	3.71	<Null>	<Null>	0.7
SI-BF-1079	END	VOL	DAC	DAC-02	NO	22.26	15.40	3.69	<Null>	<Null>	1.4
SI-BF-1080	MS	VOL	DAC	DAC-01	NO	26.60	16.96	6.80	<Null>	<Null>	3.7
SI-BF-1081	END	VOL	OBS	OBS-04	NO	7.79	18.44	3.55	7.79	<Null>	0.6
SI-BF-1082	MS	VOL	OBS	OBS-02	NO	9.32	17.14	2.26	<Null>	<Null>	0.4

Catalog	Portion	GENMAT	SPECMAT	Nodule	Burning	MxLe	MxWd	MxTk	LGrn	RGrn	Mass(g)
SI-BF-1083	MS	QZT	DAK	DAK-05	NO	11.96	26.25	5.51	<Null>	<Null>	2.3
SI-BF-1084	LT	CCS	PED	PED-07	NO	11.92	17.83	3.31	<Null>	<Null>	0.5
SI-BF-1085	END	CCS	PED	PED-11	NO	27.09	25.77	3.68	<Null>	<Null>	1.9
SI-BF-1086	END	QZT	DAK	DAK-05	NO	28.97	23.02	4.19	<Null>	<Null>	2.9
SI-BF-1087	END	VOL	DAC	DAC-02	NO	13.83	11.60	3.10	<Null>	<Null>	0.5
SI-BF-1088	END	CCS	TRT	TRT-06	NO	16.46	13.22	4.13	<Null>	<Null>	0.9
SI-BF-1089	END	CCS	TRT	TRT-02	PTCZ	14.61	12.23	2.92	<Null>	<Null>	0.6
SI-BF-1090	LT	VOL	RHY	RHY-01	NO	15.59	13.80	4.29	<Null>	<Null>	1.3
SI-BF-1091	END	QZT	DAK	DAK-04	NO	10.14	20.52	4.77	9.46	<Null>	1.2
SI-BF-1092	END	CCS	PED	PED-11	NO	9.40	17.77	4.93	<Null>	<Null>	1.1
SI-BF-1093	LT	CCS	TRT	TRT-02	NO	18.54	8.16	4.71	<Null>	<Null>	0.5
SI-BF-1094	END	CCS	TRT	TRT-02	NO	11.78	11.63	3.14	<Null>	<Null>	0.5
SI-BF-1095	MS	QZT	DAK	DAK-05	NO	19.69	15.74	5.93	<Null>	<Null>	2.1
SI-BF-1096	END	QZT	DAK	DAK-02	NO	15.32	13.27	2.83	<Null>	<Null>	0.9
SI-BF-1097	END	VOL	OBS	OBS-02	NO	9.44	15.84	3.42	<Null>	<Null>	0.5
SI-BF-1098	END	CCS	MOSC	MOSC-01	NO	14.04	14.13	3.44	<Null>	<Null>	1.2
SI-BF-1099	END	CCS	TRT	TRT-06	NO	17.40	11.92	2.98	<Null>	<Null>	0.6
SI-BF-1100	MS	CCS	TRT	TRT-10	NO	14.72	14.01	3.20	<Null>	<Null>	1.0
SI-BF-1101	END	VOL	DAC	DAC-01	NO	20.10	18.27	5.38	<Null>	<Null>	2.2
SI-BF-1102	LT	QZT	DAK	DAK-01	NO	16.81	8.80	4.42	<Null>	<Null>	0.7
SI-BF-1103	LT	CCS	TRT	TRT-02	NO	11.07	8.80	2.11	<Null>	<Null>	0.1
SI-BF-1104	LT	QZT	DAK	DAK-05	NO	24.19	21.21	5.38	<Null>	<Null>	2.5
SI-BF-1105	LT	CCS	UNK	UNK-04	NO	7.59	14.68	6.12	<Null>	<Null>	0.8
SI-BF-1106	END	QZT	DAK	DAK-05	NO	26.15	26.63	7.20	<Null>	<Null>	5.3
SI-BF-1107	LT	VOL	OBS	OBS-01	NO	13.98	11.75	4.67	<Null>	<Null>	0.6
SI-BF-1108	MS	CCS	TRT	TRT-08	NO	10.63	19.25	4.48	<Null>	<Null>	1.4
SI-BF-1109	LT	SWD	SWD	SWD-07	NO	19.31	11.43	2.69	<Null>	<Null>	0.9
SI-BF-1110	LT	QZT	DAK	DAK-05	NO	16.67	18.87	3.74	<Null>	<Null>	1.9
SI-BF-1111	END	VOL	DAC	DAC-01	NO	24.12	27.72	5.11	<Null>	<Null>	2.4
SI-BF-1112	MS	VOL	OBS	OBS-02	NO	14.35	22.01	4.86	<Null>	<Null>	1.5

Catalog	Portion	GENMAT	SPECMAT	Nodule	Burning	MxLe	MxWd	MxTk	LGrn	RGrn	Mass(g)
SI-BF-1113	MS	VOL	OBS	OBS-02	NO	17.16	22.81	4.77	<Null>	<Null>	2.4
SI-BF-1114	END	SWD	SWD	SWD-07	NO	21.65	23.61	5.64	<Null>	<Null>	2.7
SI-BF-1115	END	SWD	SWD	SWD-07	NO	20.78	18.59	4.54	<Null>	<Null>	1.4
SI-BF-1116	LT	SWD	SWD	SWD-04	NO	14.86	6.78	4.96	<Null>	<Null>	0.4
SI-BF-1117	END	CCS	TRT	TRT-05	NO	20.82	21.31	3.55	<Null>	<Null>	1.8
SI-BF-1118	END	SWD	SWD	SWD-07	NO	17.43	21.44	6.68	<Null>	<Null>	2.9
SI-BF-1119	LT	VOL	OBS	OBS-02	NO	21.29	19.12	3.66	<Null>	<Null>	1.5
SI-BF-1120	LT	VOL	OBS	OBS-02	NO	17.77	4.83	3.56	<Null>	<Null>	0.4
SI-BF-1121	LT	QZT	DAK	DAK-01	NO	15.03	12.55	4.55	<Null>	<Null>	0.9
SI-BF-1122	LT	CCS	TRT	TRT-11	PTCZ	12.89	13.71	3.13	<Null>	<Null>	0.4
SI-BF-1123	END	VOL	DAC	DAC-01	NO	16.46	28.29	8.52	<Null>	<Null>	4.3
SI-BF-1124	LT	CCS	MOSC	MOSC-05	PTCZ	12.28	14.44	3.70	<Null>	<Null>	0.9
SI-BF-1125	END	SWD	SWD	SWD-05	NO	14.43	18.34	4.06	<Null>	<Null>	1.5
SI-BF-1126	MS	CCS	PED	PED-03	NO	9.37	14.12	3.65	<Null>	<Null>	0.6
SI-BF-1127	LT	VOL	OBS	OBS-01	NO	13.09	11.65	3.24	<Null>	<Null>	0.6
SI-BF-1128	LT	CCS	UNK	UNK-07	NO	5.57	11.97	2.62	<Null>	<Null>	0.2
SI-BF-1129	END	CCS	MOSC	MOSC-05	NO	8.91	19.55	4.76	<Null>	<Null>	0.7
SI-BF-1130	LT	QZT	DAK	DAK-09	NO	14.91	7.02	3.62	<Null>	<Null>	0.4
SI-BF-1131	MS	CCS	CUMB	CUMB-01	NO	19.22	25.91	5.23	<Null>	<Null>	3.1
SI-BF-1132	LT	VOL	OBS	OBS-03	NO	12.39	13.56	3.93	<Null>	<Null>	0.6
SI-BF-1133	LT	CCS	TRT	TRT-06	POT	12.90	14.11	3.54	<Null>	<Null>	0.6
SI-BF-1134	LT	VOL	OBS	OBS-01	NO	12.06	11.20	3.37	<Null>	<Null>	0.5
SI-BF-1135	END	CCS	TRT	TRT-07	NO	7.56	11.71	2.13	<Null>	<Null>	0.2
SI-BF-1136	LT	CCS	PED	PED-10	NO	9.47	8.04	2.99	<Null>	<Null>	0.3
SI-BF-1137	END	CCS	UNK	UNK-07	NO	20.34	13.89	3.22	<Null>	<Null>	1.0
SI-BF-1138	LT	CCS	PED	PED-01	NO	13.91	6.97	3.23	<Null>	<Null>	0.4
SI-BF-1139	END	CCS	PED	PED-08	NO	7.76	9.94	3.84	<Null>	<Null>	0.2
SI-BF-1140	END	VOL	OBS	OBS-03	NO	8.87	22.57	3.68	<Null>	<Null>	1.1
SI-BF-1141	END	VOL	OBS	OBS-02	NO	15.72	10.48	2.11	<Null>	<Null>	0.6
SI-BF-1142	LT	CCS	TRT	TRT-15	NO	17.77	9.26	2.23	<Null>	<Null>	0.3

Catalog	Portion	GENMAT	SPECMAT	Nodule	Burning	MxLe	MxWd	MxTk	LGrn	RGrn	Mass(g)
SI-BF-1143	END	CCS	TRT	TRT-05	NO	6.53	11.69	2.82	<Null>	<Null>	0.2
SI-BF-1144	LT	VOL	OBS	OBS-02	NO	13.44	9.48	2.80	<Null>	<Null>	0.4
SI-BF-1145	END	VOL	OBS	OBS-04	NO	11.90	15.93	2.73	<Null>	<Null>	0.8
SI-BF-1146	END	QZT	DAK	DAK-07	NO	9.39	10.35	3.77	<Null>	<Null>	0.2
SI-BF-1147	END	CCS	TRT	TRT-10	NO	8.15	18.13	5.75	<Null>	<Null>	0.6
SI-BF-1148	END	VOL	OBS	OBS-02	NO	14.67	14.58	2.57	<Null>	<Null>	0.5
SI-BF-1149	END	CCS	TRT	TRT-21	NO	10.02	24.01	3.85	<Null>	<Null>	1.0
SI-BF-1150	LT	CCS	PED	PED-10	NO	15.09	12.41	3.51	<Null>	<Null>	0.8
SI-BF-1151	LT	VOL	OBS	OBS-01	NO	19.38	19.68	2.97	<Null>	<Null>	1.5
SI-BF-1152	END	SWD	SWD	SWD-07	NO	17.34	19.38	4.48	<Null>	<Null>	1.6
SI-BF-1153	END	CCS	TRT	TRT-08	NO	16.42	16.82	2.57	<Null>	<Null>	1.1
SI-BF-1154	MS	QZT	MOR	MOR-03	NO	10.13	14.33	3.41	<Null>	<Null>	0.5
SI-BF-1155	END	VOL	OBS	OBS-01	NO	14.71	18.45	5.41	<Null>	<Null>	1.9
SI-BF-1156	LT	CCS	TRT	TRT-10	NO	19.61	12.24	4.14	<Null>	<Null>	1.1
SI-BF-1157	MS	CCS	UNK	UNK-12	NO	11.46	18.06	2.82	<Null>	<Null>	1.0
SI-BF-1158	LT	SWD	SWD	SWD-11	NO	19.56	13.18	6.08	<Null>	<Null>	1.9
SI-BF-1159	END	QZT	DAK	DAK-07	NO	26.56	13.85	6.01	<Null>	<Null>	2.4
SI-BF-1160	MS	VOL	OBS	OBS-02	NO	12.25	19.64	4.91	<Null>	<Null>	1.3
SI-BF-1161	END	SWD	SWD	SWD-07	NO	9.06	6.90	3.07	<Null>	<Null>	0.2
SI-BF-1162	END	CCS	TRT	TRT-03	PTCZ	22.30	22.40	6.64	<Null>	<Null>	2.6
SI-BF-1163	END	QZT	DAK	DAK-01	NO	22.31	27.36	10.37	<Null>	<Null>	6.1
SI-BF-1164	LT	CCS	MOSC	MOSC-02	NO	12.98	3.65	2.68	<Null>	<Null>	0.1
SI-BF-1165	END	CCS	CUMB	CUMB-04	NO	9.74	21.20	6.93	<Null>	<Null>	1.4
SI-BF-1166	LT	QZT	DAK	DAK-05	NO	53.60	26.47	8.89	<Null>	<Null>	15.9
SI-BF-1167	END	CCS	PED	PED-07	NO	8.61	9.94	2.43	<Null>	<Null>	0.2
SI-BF-1168	MS	VOL	DAC	DAC-01	NO	8.65	10.12	3.16	<Null>	<Null>	0.3
SI-BF-1169	MS	CCS	TRT	TRT-21	NO	8.03	9.24	2.13	<Null>	<Null>	0.2
SI-BF-1170	LT	CCS	TRT	TRT-21	POT	12.67	18.30	6.28	<Null>	<Null>	1.6
SI-BF-1171	MS	CCS	CUMB	CUMB-05	POT	19.39	15.31	5.07	<Null>	<Null>	1.7
SI-BF-1172	LT	CCS	PED	PED-11	NO	12.66	10.06	2.49	<Null>	<Null>	0.4

Catalog	Portion	GENMAT	SPECMAT	Nodule	Burning	MxLe	MxWd	MxTk	LGrn	RGrn	Mass(g)
SI-BF-1173	END	CCS	NARB	NARB-02	NO	7.08	10.95	3.85	<Null>	<Null>	0.3
SI-BF-1174	END	CCS	TRT	TRT-02	NO	11.96	18.68	3.75	<Null>	<Null>	1.0
SI-BF-1175	LT	CCS	TRT	TRT-07	NO	12.61	12.09	2.96	<Null>	<Null>	0.4
SI-BF-1176	END	CCS	CUMB	CUMB-05	NO	15.52	31.43	8.13	<Null>	<Null>	4.0
SI-BF-1177	LT	CCS	TRT	TRT-06	NO	12.80	8.67	3.85	<Null>	<Null>	0.5
SI-BF-1178	LT	CCS	TRT	TRT-10	POT	13.26	12.94	4.34	9.11	<Null>	0.7
SI-BF-1179	END	CCS	PED	PED-07	NO	21.98	26.52	5.63	<Null>	<Null>	3.4

E2. Retouched flakes descriptive and metric data.

Catalog	Portion	GENMAT	SPECMAT	Nodule	Burning	MxLe	MxWd	MxTk	RetOL	RetOR	RetODS	RetRL	RetRR	RetRDS	LGrn	RGrn	Mass (g)
CMPA-RFT-1001	DS	CCS	NARB	NARB-01	NO	9.14	18.35	4.39	<Null>	6.02	12.70	<Null>	<Null>	<Null>	<Null>	<Null>	0.8
CMPA-RFT-1002	PR	CCS	TRT	TRT-05	NO	11.46	17.06	5.10	5.51	<Null>	11.96	<Null>	<Null>	<Null>	<Null>	<Null>	1.0
CMPA-RFT-1003	CO	CCS	TRT	TRT-08	NO	17.85	18.27	2.78	9.65	11.47	10.96	<Null>	<Null>	<Null>	<Null>	<Null>	1.2
CMPA-RFT-1004	PR	CCS	TRT	TRT-05	NO	15.02	16.12	3.39	7.04	3.97	<Null>	<Null>	<Null>	<Null>	<Null>	<Null>	1.0
CMPA-RFT-1005	DS	CCS	TRT	TRT-10	NO	7.03	19.02	3.63	<Null>	<Null>	14.52	<Null>	<Null>	<Null>	<Null>	<Null>	0.7
CMPA-RFT-1006	LT	CCS	TRT	TRT-10	POT	16.23	10.78	7.46	16.17	<Null>	<Null>	<Null>	<Null>	<Null>	<Null>	<Null>	1.2
CMPA-RFT-1007	LT	CCS	EDW	EDW-01	NO	28.92	5.16	5.88	28.92	<Null>	<Null>	<Null>	<Null>	<Null>	<Null>	<Null>	0.8
CMPA-RFT-1008	LT	CCS	TRT	TRT-08	NO	16.47	12.7	2.61	<Null>	12.43	<Null>	<Null>	<Null>	<Null>	<Null>	<Null>	0.5
CMPA-RFT-1009	PR	SWD	SWD	SWD-01	NO	14.07	11.22	1.71	13.90	13.88	<Null>	5.29	10.04	<Null>	<Null>	<Null>	0.3
CMPA-RFT-1010	PR	QZT	MOR	MOR-02	NO	27.23	20.54	10.51	27.74	20.50	<Null>	<Null>	<Null>	<Null>	<Null>	<Null>	7.6
CMPA-RFT-1011	DS	CCS	TRT	TRT-02	NO	16.16	25.91	3.35	<Null>	11.88	19.77	<Null>	<Null>	<Null>	<Null>	<Null>	1.5
CMPA-RFT-1012	MS	CCS	MOSC	MOSC-06	NO	15.31	17.24	5.26	14.32	12.30	<Null>	<Null>	<Null>	<Null>	<Null>	7.40	1.8
CMPA-RFT-1013	LT	CCS	TRT	TRT-03	POT	11.32	14.52	3.32	<Null>	9.36	<Null>	<Null>	<Null>	<Null>	<Null>	<Null>	0.6
CMPA-RFT-1014	DS	CCS	TRT	TRT-10	NO	10.42	10.48	3.21	<Null>	<Null>	10.27	<Null>	<Null>	<Null>	<Null>	<Null>	0.4
CMPA-RFT-1015	MS	SWD	SWD	SWD-06	NO	17.21	14.93	3.83	<Null>	16.69	<Null>	<Null>	6.45	<Null>	<Null>	<Null>	1.3
CMPA-RFT-1016	LT	CCS	TRT	TRT-02	NO	24.99	17.01	3.82	18.47	<Null>	<Null>	<Null>	<Null>	<Null>	<Null>	<Null>	1.5
CMPA-RFT-1017	MS	SWD	SWD	SWD-06	NO	36.7	18.5	6.44	13.13	32.99	<Null>	<Null>	<Null>	<Null>	<Null>	<Null>	4.3
CMPA-RFT-1018	LT	CCS	TRT	TRT-02	NO	6.86	22.1	4.52	6.50	<Null>	<Null>	<Null>	<Null>	<Null>	<Null>	<Null>	0.7
CMPA-RFT-1019	LT	VOL	OBS	OBS-04	NO	12.12	10.12	3.47	12.12	<Null>	<Null>	<Null>	12.12	<Null>	<Null>	<Null>	0.3
CMPA-RFT-1020	LT	CCS	TRT	TRT-03	PTCZ	34.93	18.48	12.71	26.89	<Null>	<Null>	<Null>	21.55	<Null>	<Null>	<Null>	9.9
SI-RFT-1001	LT	CCS	PED	PED-05	NO	11.84	16.45	4.53	9.51	<Null>	<Null>	<Null>	8.90	<Null>	<Null>	<Null>	1.0

Catalog	Portion	GENMAT	SPECMAT	Nodule	Burning	MxLe	MxWd	MxTk	RetOL	RetOR	RetODS	RetRL	RetRR	RetRDS	LGrn	RGrn	Mass (g)
SI-RFT-1002	LT	CCS	TRT	TRT-03	NO	13.53	19.37	3.54	18.79	<Null>	<Null>	<Null>	<Null>	<Null>	<Null>	<Null>	1.2
SI-RFT-1003	PR	CCS	EDW	EDW-02	NO	30.39	14.01	5.78	28.59	27.37	<Null>	<Null>	<Null>	<Null>	<Null>	<Null>	3.0
SI-RFT-1004	LT	CCS	TRT	TRT-14	NO	14.51	31.05	4.98	11.45	<Null>	<Null>	<Null>	<Null>	<Null>	<Null>	<Null>	2.9
SI-RFT-1005	LT	SWD	SWD	SWD-07	NO	18.57	12.9	2.34	21.83	<Null>	<Null>	<Null>	<Null>	<Null>	<Null>	<Null>	0.8
SI-RFT-1006	MS	CCS	UNK	UNK-05	NO	14.43	30.57	6.53	19.91	<Null>	<Null>	<Null>	<Null>	<Null>	<Null>	<Null>	2.5
SI-RFT-1007	LT	CCS	PED	PED-05	NO	22.69	10.4	4.51	<Null>	13.49	<Null>	<Null>	9.01	<Null>	<Null>	<Null>	0.9
SI-RFT-1008	PR	CCS	TRT	TRT-01	NO	39.1	22.23	7.77	<Null>	29.72	<Null>	<Null>	<Null>	<Null>	<Null>	<Null>	7.8
SI-RFT-1009	DS	SWD	SWD	SWD-04	NO	15.85	34.78	4.56	14.35	34.22	<Null>	<Null>	<Null>	<Null>	<Null>	<Null>	3.8
SI-RFT-1010	PR	CCS	TRT	TRT-02	NO	47.44	41.81	7.14	<Null>	32.50	<Null>	<Null>	<Null>	<Null>	<Null>	<Null>	14.0
SI-RFT-1011	MS	CCS	TRT	TRT-06	NO	40.27	19.84	7.19	10.56	21.42	<Null>	<Null>	<Null>	<Null>	<Null>	<Null>	4.8
SI-RFT-1012	LT	SWD	SWD	SWD-04	NO	25.4	9.68	5.91	<Null>	25.40	<Null>	6.32	<Null>	<Null>	<Null>	<Null>	1.3
SI-RFT-1013	PR	CCS	TRT	TRT-06	NO	16.69	14.16	4.07	15.36	14.55	<Null>	<Null>	8.24	<Null>	<Null>	<Null>	1.2
SI-RFT-1014	LT	CCS	TRT	TRT-01	NO	24.05	14.02	9.98	<Null>	22.36	<Null>	<Null>	<Null>	<Null>	<Null>	<Null>	3.4
SI-RFT-1015	LT	CCS	MOSC	MOSC-03	NO	19.79	19.12	5.05	14.97	<Null>	<Null>	<Null>	5.45	<Null>	<Null>	<Null>	1.9
SI-RFT-1016	PR	CCS	TRT	TRT-19	NO	25.21	15.95	2.98	17.01	24.25	<Null>	<Null>	<Null>	<Null>	<Null>	<Null>	1.5
SI-RFT-1017	LT	CCS	TRT	TRT-18	POT	27.18	21.39	6.22	<Null>	14.99	<Null>	<Null>	<Null>	<Null>	<Null>	<Null>	4.2
SI-RFT-1018	CO	QZT	MOR	MOR-02	NO	30.65	27.21	7.34	<Null>	22.17	<Null>	<Null>	23.95	<Null>	<Null>	<Null>	6.7
SI-RFT-1019	PR	SWD	SWD	SWD-08	NO	46.71	35.93	13.39	28.95	27.79	<Null>	26.53	28.49	<Null>	<Null>	<Null>	27.3
SI-RFT-1020	PR	CCS	TRT	TRT-08	NO	31.1	22.9	9.84	14.83	<Null>	<Null>	<Null>	<Null>	<Null>	<Null>	<Null>	5.9
SI-RFT-1021	LT	CCS	TRT	TRT-02	NO	19.48	10.96	5.10	18.68	<Null>	<Null>	<Null>	<Null>	<Null>	<Null>	<Null>	1.2
SI-RFT-1022	DS	CCS	TRT	TRT-06	NO	20.74	21.66	3.06	<Null>	<Null>	21.42	<Null>	<Null>	<Null>	<Null>	<Null>	1.7
SI-RFT-1023	DS	CCS	MOSC	MOSC-03	NO	19.72	25.43	7.63	10.70	16.85	15.27	<Null>	<Null>	<Null>	<Null>	<Null>	3.7
SI-RFT-1024	DS	CCS	TRT	TRT-10	NO	15.29	8.92	4.22	16.58	15.13	1.31	<Null>	<Null>	<Null>	<Null>	<Null>	0.6
SI-RFT-1025	DS	CCS	TRT	TRT-02	NO	12.67	7.14	2.30	10.88	12.59	2.28	<Null>	<Null>	<Null>	<Null>	<Null>	0.3
SI-RFT-1026	PR	QZT	DAK	DAK-01	NO	21.23	26.96	3.65	21.88	20.79	<Null>	21.17	22.09	<Null>	<Null>	<Null>	2.1
SI-RFT-1027	DS	CCS	TRT	TRT-02	NO	19.03	19.83	3.49	17.80	4.76	12.91	4.11	6.45	9.73	<Null>	<Null>	1.5
SI-RFT-1028	DS	VOL	OBS	OBS-02	NO	24.47	22.1	3.82	24.24	<Null>	18.21	<Null>	24.24	18.21	<Null>	<Null>	2.0
SI-RFT-1029	MS	CCS	TRT	TRT-02	NO	25.54	16.46	5.09	18.81	14.43	<Null>	<Null>	<Null>	<Null>	<Null>	<Null>	2.3
SI-RFT-1030	PR	CCS	EDW	EDW-02	NO	19.68	11.73	3.37	17.75	<Null>	<Null>	<Null>	15.84	<Null>	<Null>	<Null>	1.0
SI-RFT-1031	DS	CCS	PED	PED-03	NO	20.22	15.64	2.47	10.58	9.52	<Null>	<Null>	10.58	<Null>	<Null>	<Null>	0.6

Catalog	Portion	GENMAT	SPECMAT	Nodule	Burning	MxLe	MxWd	MxTk	RetOL	RetOR	RetODS	RetRL	RetRR	RetRDS	LGrn	RGrn	Mass (g)
SI-RFT-1032	LT	CCS	TRT	TRT-10	NO	22.72	11.03	6.54	22.72	<Null>	<Null>	<Null>	<Null>	<Null>	<Null>	<Null>	1.4
SI-RFT-1033	CO	CCS	PED	PED-03	NO	32.86	16.35	5.74	26.99	28.34	<Null>	6.81	15.16	<Null>	<Null>	<Null>	2.1
SI-RFT-1034	CO	CCS	PED	PED-07	NO	59.35	50.57	13.44	27.57	15.87	28.24	<Null>	<Null>	<Null>	<Null>	<Null>	35.9
SI-RFT-1035	MS	QZT	DAK	DKA-03	POT	19.35	18.46	3.70	13.73	19.13	<Null>	17.67	11.42	<Null>	<Null>	<Null>	1.8
SI-RFT-1036	PR	CCS	NARB	NARB-01	POT	24.29	18.39	6.66	22.84	<Null>	<Null>	<Null>	22.84	<Null>	<Null>	<Null>	2.8
SI-RFT-1037	LT	CCS	PED	PED-07	NO	19.22	19.83	7.14	<Null>	19.22	<Null>	<Null>	<Null>	<Null>	<Null>	<Null>	3.5
SI-RFT-1038	PR	QZT	DAK	DAK-02	NO	15.6	19.94	5.30	<Null>	17.45	<Null>	<Null>	<Null>	<Null>	<Null>	<Null>	1.4
SI-RFT-1039	CO	CCS	TRT	TRT-08	NO	17.38	15.69	8.96	<Null>	<Null>	8.18	<Null>	<Null>	<Null>	<Null>	<Null>	2.5
SI-RFT-1040	LT	CCS	EDW	EDW-01	NO	9.95	16.67	4.25	7.08	<Null>	13.19	<Null>	7.08	<Null>	7.08	<Null>	0.7
SI-RFT-1041	LT	QZT	DAK	DAK-05	NO	20.5	20.8	5.32	20.50	<Null>	<Null>	<Null>	<Null>	<Null>	<Null>	<Null>	2.4
SI-RFT-1042	LT	CCS	TRT	TRT-08	NO	16.05	13.63	6.01	<Null>	16.05	<Null>	<Null>	<Null>	<Null>	<Null>	<Null>	1.3
SI-RFT-1043	LT	CCS	EDW	EDW-02	NO	14.71	13.66	2.77	9.55	<Null>	<Null>	<Null>	<Null>	<Null>	9.55	<Null>	0.8
SI-RFT-1044	MS	SWD	SWD	SWD-04	NO	11.26	15.89	1.60	11.26	<Null>	<Null>	<Null>	<Null>	<Null>	<Null>	<Null>	0.4
SI-RFT-1045	PR	CCS	TRT	TRT-14	NO	8.25	7.34	5.33	7.14	6.64	<Null>	<Null>	<Null>	<Null>	<Null>	<Null>	0.4
SI-RFT-1046	DS	CCS	TRT	TRT-02	NO	4.27	12.81	2.57	<Null>	<Null>	12.81	<Null>	<Null>	<Null>	<Null>	<Null>	0.2
SI-RFT-1047	DS	CCS	EDW	EDW-02	NO	11.37	17.33	4.80	<Null>	<Null>	10.85	<Null>	<Null>	<Null>	<Null>	<Null>	0.8
SI-RFT-1048	LT	CCS	TRT	TRT-17	NO	12.83	8.51	1.84	<Null>	8.46	<Null>	10.19	<Null>	<Null>	<Null>	<Null>	0.3
SI-RFT-1049	LT	CCS	TRT	TRT-15	NO	14.07	15.3	3.22	7.48	<Null>	<Null>	<Null>	<Null>	<Null>	<Null>	<Null>	0.9
SI-RFT-1050	PR	CCS	PED	PED-05	NO	29.83	21.07	7.50	15.90	6.87	<Null>	15.87	9.34	<Null>	<Null>	<Null>	5.3
SI-RFT-1051	LT	CCS	PED	PED-03	NO	28.06	13.25	7.26	20.04	<Null>	<Null>	<Null>	<Null>	<Null>	<Null>	<Null>	2.1
SI-RFT-1052	LT	CCS	TRT	TRT-02	NO	12.7	6.88	2.45	8.21	<Null>	<Null>	<Null>	<Null>	<Null>	<Null>	<Null>	0.3
SI-RFT-1053	LT	CCS	TRT	TRT-06	NO	21.87	11.92	4.33	23.01	<Null>	<Null>	<Null>	<Null>	<Null>	<Null>	<Null>	1.1
SI-RFT-1054	DS	CCS	TRT	TRT-02	NO	6.51	16.47	1.78	<Null>	<Null>	15.56	<Null>	<Null>	<Null>	<Null>	<Null>	0.3
SI-RFT-1055	DS	CCS	TRT	TRT-07	PTCZ	13.01	16.42	3.26	<Null>	<Null>	16.42	<Null>	<Null>	<Null>	<Null>	<Null>	0.8
SI-RFT-1056	DS	CCS	PED	PED-01	NO	14.25	25.02	4.79	<Null>	9.89	16.60	<Null>	12.18	16.60	<Null>	<Null>	1.6
SI-RFT-1057	LT	SWD	SWD	SWD-07	NO	14.91	10.58	3.12	13.59	<Null>	<Null>	<Null>	<Null>	<Null>	<Null>	<Null>	0.5
SI-RFT-1058	DS	CCS	TRT	TRT-08	NO	8.07	23.5	3.73	<Null>	<Null>	23.50	<Null>	<Null>	<Null>	<Null>	<Null>	0.9
SI-RFT-1059	LT	CCS	MOSC	MOSC-03	POT	23.3	9.55	4.35	<Null>	16.18	<Null>	<Null>	<Null>	<Null>	<Null>	<Null>	1.0
SI-RFT-1060	LT	SWD	SWD	SWD-07	NO	12.47	8.27	3.93	12.71	<Null>	<Null>	<Null>	<Null>	<Null>	<Null>	<Null>	0.3
SI-RFT-1061	DS	CCS	PED	PED-01	NO	7.35	18.68	2.71	14.78	9.75	2.61	<Null>	<Null>	<Null>	<Null>	<Null>	0.5

Catalog	Portion	GENMAT	SPECMAT	Nodule	Burning	MxLe	MxWd	MxTk	RetOL	RetOR	RetODS	RetRL	RetRR	RetRDS	LGrn	RGrn	Mass (g)
SI-RFT-1062	LT	CCS	UNK	UNK-03	NO	22.14	6.1	2.36	<Null>	22.14	<Null>	<Null>	<Null>	<Null>	<Null>	<Null>	0.4
SI-RFT-1063	LT	CCS	PED	PED-01	POT	13.61	10.85	3.98	10.71	<Null>	<Null>	<Null>	<Null>	<Null>	<Null>	<Null>	0.7
SI-RFT-1064	PR	CCS	PED	PED-08	NO	12.39	23.05	3.92	12.18	<Null>	<Null>	<Null>	<Null>	<Null>	<Null>	<Null>	1.3
SI-RFT-1065	LT	CCS	TRT	TRT-14	NO	13.57	16.34	2.62	10.25	<Null>	<Null>	<Null>	<Null>	<Null>	<Null>	<Null>	0.9
SI-RFT-1066	LT	CCS	TRT	TRT-05	NO	23.75	18.79	4.88	15.08	<Null>	<Null>	<Null>	<Null>	<Null>	<Null>	<Null>	1.4
SI-RFT-1067	LT	SWD	SWD	SWD-05	NO	19.92	18.6	3.44	13.50	<Null>	<Null>	<Null>	<Null>	<Null>	<Null>	<Null>	1.2
SI-RFT-1068	LT	CCS	UNK	UNK-02	NO	12.82	18.26	3.56	12.13	<Null>	<Null>	<Null>	<Null>	<Null>	<Null>	<Null>	0.8
SI-RFT-1069	LT	CCS	TRT	TRT-02	NO	18.54	13.4	3.03	17.95	<Null>	<Null>	<Null>	<Null>	<Null>	<Null>	<Null>	1.0
SI-RFT-1070	DS	CCS	TRT	TRT-08	NO	11.8	15.73	2.50	9.33	9.39	8.71	9.17	<Null>	<Null>	<Null>	<Null>	0.6
SI-RFT-1071	PR	QZT	MOR	MOR-02	NO	18.83	18.68	4.12	<Null>	19.67	<Null>	<Null>	<Null>	<Null>	<Null>	<Null>	1.8
SI-RFT-1072	DS	SWD	SWD	SWD-07	NO	18.09	18.71	5.06	14.10	14.96	<Null>	<Null>	<Null>	<Null>	<Null>	<Null>	2.1
SI-RFT-1073	LT	CCS	PED	PED-01	NO	15.35	12.83	4.06	<Null>	16.98	<Null>	<Null>	<Null>	<Null>	<Null>	<Null>	1.1
SI-RFT-1074	DS	SWD	SWD	SWD-04	NO	14.91	13.84	3.78	5.22	<Null>	7.16	<Null>	<Null>	<Null>	<Null>	<Null>	0.9
SI-RFT-1075	LT	CCS	TRT	TRT-17	NO	12.24	11.25	4.25	11.01	<Null>	<Null>	<Null>	<Null>	<Null>	<Null>	<Null>	0.7
SI-RFT-1076	DS	VOL	OBS	OBS-02	NO	20.33	12.27	2.94	<Null>	<Null>	10.51	<Null>	<Null>	<Null>	<Null>	<Null>	0.7
SI-RFT-1077	DS	VOL	OBS	OBS-02	NO	14.18	14.64	2.40	11.51	<Null>	8.05	<Null>	7.21	5.12	<Null>	<Null>	0.5
SI-RFT-1078	LT	VOL	OBS	OBS-02	NO	17.68	12.28	3.01	17.39	<Null>	<Null>	<Null>	16.61	<Null>	<Null>	<Null>	0.8
SI-RFT-1079	MS	VOL	OBS	OBS-01	NO	14.16	19.77	4.75	14.37	12.24	<Null>	8.62	9.41	<Null>	<Null>	<Null>	1.9
SI-RFT-1080	LT	VOL	OBS	OBS-04	NO	13.66	17.02	2.68	<Null>	15.09	12.59	15.98	<Null>	14.01	<Null>	<Null>	0.8
SI-RFT-1081	DS	VOL	OBS	OBS-03	NO	18.16	14.41	3.22	5.86	11.02	2.74	<Null>	<Null>	<Null>	<Null>	<Null>	0.5
SI-RFT-1082	PR	SWD	SWD	SWD-04	NO	17.83	23.49	2.25	12.36	<Null>	<Null>	<Null>	<Null>	<Null>	<Null>	<Null>	1.4
SI-RFT-1083	LT	SWD	SWD	SWD-05	NO	12.69	21.12	3.63	11.58	<Null>	<Null>	<Null>	<Null>	<Null>	<Null>	<Null>	1.4
SI-RFT-1084	CO	CCS	QTC	QTC-01	NO	23.07	14.97	3.64	9.54	<Null>	<Null>	<Null>	<Null>	<Null>	<Null>	<Null>	1.4
SI-RFT-1085	LT	CCS	TRT	TRT-06	NO	23.25	14.3	5.28	<Null>	<Null>	14.53	<Null>	<Null>	<Null>	<Null>	<Null>	1.5
SI-RFT-1086	LT	CCS	PED	PED-06	NO	19.37	20.22	5.52	<Null>	<Null>	17.16	<Null>	<Null>	<Null>	<Null>	<Null>	2.3
SI-RFT-1087	DS	CCS	TRT	TRT-18	NO	14.89	13.34	2.78	<Null>	<Null>	8.94	<Null>	<Null>	<Null>	<Null>	<Null>	0.7
SI-RFT-1088	LT	CCS	CUMB	CUMB-05	NO	26.83	16.08	3.58	<Null>	25.45	<Null>	<Null>	<Null>	<Null>	<Null>	<Null>	1.8
SI-RFT-1089	MS	CCS	TRT	TRT-03	NO	12.46	25.42	3.86	9.82	8.58	<Null>	<Null>	<Null>	<Null>	<Null>	<Null>	1.4
SI-RFT-1090	LT	QZT	MOR	MOR-02	NO	15.63	20.02	5.59	14.25	<Null>	<Null>	<Null>	<Null>	<Null>	<Null>	<Null>	2.9
SI-RFT-1091	MS	CCS	TRT	TRT-16	POT	14.86	20.06	5.57	13.51	<Null>	<Null>	<Null>	<Null>	<Null>	<Null>	<Null>	2.2

Catalog	Portion	GENMAT	SPECMAT	Nodule	Burning	MxLe	MxWd	MxTk	RetOL	RetOR	RetODS	RetRL	RetRR	RetRDS	LGrn	RGrn	Mass (g)
SI-RFT-1092	LT	CCS	PED	PED-10	NO	15.06	14.14	2.80	<Null>	12.67	7.33	<Null>	<Null>	<Null>	<Null>	<Null>	0.8
SI-RFT-1093	DS	CCS	UNK	UNK-05	NO	9.24	19.67	2.95	<Null>	<Null>	14.50	<Null>	<Null>	<Null>	<Null>	<Null>	1.0
SI-RFT-1094	PR	CCS	EDW	EDW-01	NO	23.26	10.01	2.89	17.29	<Null>	<Null>	<Null>	<Null>	<Null>	<Null>	<Null>	0.9
SI-RFT-1095	LT	CCS	TRT	TRT-02	NO	15.9	17.11	5.37	14.01	<Null>	<Null>	<Null>	<Null>	<Null>	<Null>	<Null>	1.1
SI-RFT-1096	LT	CCS	PED	PED-02	NO	19.69	13.52	4.21	<Null>	12.62	13.27	<Null>	<Null>	<Null>	<Null>	<Null>	1.4

E3. End scraper descriptive and metric data.

Catalog	Portion	GENMAT	SPECMAT	Nodule	Burning	SPUR	MxLe	MxWd	MxTk	RetOL	RetOR	RetODS	RetRL	RetRR	RetRDS	LGrn	RGrn	MxTDS	Mass (g)
CMPA-ES-1001	LT	CCS	PED	PED-05	NO	NO	17.18	11.00	15.91	<Null>	12.04	7.88	<Null>	<Null>	<Null>	<Null>	<Null>	5.36	0.8
CMPA-ES-1002	CO	CCS	TRT	TRT-08	NO	NO	28.34	24.89	9.04	<Null>	<Null>	24.89	<Null>	<Null>	<Null>	<Null>	<Null>	14.30	5.2
CMPA-ES-1003	DS	CCS	TRT	TRT-08	NO	NO	22.48	26.77	6.90	15.05	10.98	24.66	<Null>	6.77	9.53	<Null>	10.98	3.06	5.3
CMPA-ES-1004	DS	SWD	SWD	SWD-07	PTCZ	NO	9.54	19.53	5.12	<Null>	<Null>	19.53	<Null>	<Null>	<Null>	<Null>	<Null>	3.94	1.0
CMPA-ES-1005	DS	CCS	TRT	TRT-17	NO	NO	8.18	15.53	3.28	<Null>	<Null>	12.95	<Null>	<Null>	<Null>	<Null>	<Null>	3.64	0.5
CMPA-ES-1006	LT	CCS	TRT	TRT-02	NO	NO	12.40	12.64	3.99	<Null>	6.13	12.61	<Null>	<Null>	<Null>	<Null>	<Null>	2.44	0.7
CMPA-ES-1007	DS	CCS	TRT	TRT-03	PTCZ	YES	24.57	16.95	5.82	<Null>	<Null>	16.47	<Null>	9.01	<Null>	<Null>	<Null>	12.25	2.3
CMPA-ES-1008	DS	CCS	FLAT	FLAT-02	NO	NO	6.24	12.01	4.17	<Null>	<Null>	12.01	<Null>	<Null>	<Null>	<Null>	<Null>	2.89	0.3
CMPA-ES-1009	LT	CCS	TRT	TRT-02	NO	NO	22.28	19.09	4.91	16.30	<Null>	<Null>	<Null>	<Null>	<Null>	<Null>	<Null>	9.48	2.4
CMPA-ES-1010	DS	CCS	TRT	TRT-02	NO	NO	16.83	17.55	6.40	9.54	<Null>	16.81	<Null>	<Null>	<Null>	<Null>	<Null>	4.94	3.0
CMPA-ES-1011	LT	CCS	TRT	TRT-20	POT	NO	22.57	23.70	10.13	10.67	<Null>	21.89	<Null>	<Null>	<Null>	<Null>	<Null>	3.96	6.3
CMPA-ES-1012	CO	CCS	TRT	TRT-10	NO	NO	31.99	33.50	8.30	8.82	<Null>	28.70	16.53	9.63	<Null>	<Null>	<Null>	17.62	9.1
CMPA-ES-1013	LT	CCS	CUMB	CUMB-03	NO	NO	28.54	15.25	11.56	<Null>	8.32	19.11	<Null>	<Null>	<Null>	<Null>	<Null>	5.45	5.1
CMPA-ES-1014	LT	VOL	RHY	RHY-01	NO	NO	21.40	14.91	7.17	7.54	<Null>	14.54	<Null>	<Null>	<Null>	<Null>	<Null>	3.19	2.4
CMPA-ES-1015	LT	CCS	TRT	TRT-05	NO	NO	24.84	14.54	7.86	10.31	<Null>	18.15	<Null>	<Null>	<Null>	<Null>	<Null>	5.67	2.8
CMPA-ES-1016	DS	CCS	PED	PED-10	NO	NO	15.30	22.59	9.54	<Null>	<Null>	23.84	<Null>	<Null>	<Null>	<Null>	<Null>	14.93	2.9
CMPA-ES-1017	DS	CCS	TRT	TRT-08	NO	NO	11.48	28.46	6.84	<Null>	<Null>	28.46	<Null>	<Null>	<Null>	<Null>	<Null>	5.17	2.8
CMPA-ES-1018	LT	CCS	TRT	TRT-03	NO	NO	21.43	14.31	6.33	4.88	<Null>	14.31	<Null>	<Null>	<Null>	15.58	<Null>	2.33	2.0
CMPA-ES-1019	LT	CCS	TRT	TRT-01	NO	NO	19.28	19.77	5.24	<Null>	5.28	19.77	<Null>	<Null>	<Null>	<Null>	<Null>	13.16	2.5
CMPA-ES-1020	DS	CCS	TRT	TRT-10	NO	NO	22.01	16.35	9.39	<Null>	<Null>	16.35	<Null>	<Null>	<Null>	<Null>	<Null>	6.86	2.9
CMPA-ES-1021	CO	CCS	CUMB	CUMB-04	NO	YES	30.22	22.87	8.58	<Null>	<Null>	22.87	<Null>	<Null>	<Null>	17.50	9.86	2.91	5.1
SI-ES-1001	CO	CCS	UNK	UNK-03	NO	YES	23.77	25.28	5.69	8.29	20.62	20.99	<Null>	<Null>	<Null>	<Null>	<Null>	13.06	3.5
SI-ES-1002	CO	CCS	TRT	TRT-03	NO	NO	26.77	27.25	13.15	<Null>	26.60	26.93	<Null>	<Null>	<Null>	<Null>	<Null>	9.89	8.2

Catalog	Portion	GENMAT	SPECMAT	Nodule	Burning	SPUR	MxLe	MxWd	MxTk	RetOL	RetOR	RetODS	RetRL	RetRR	RetRDS	LGrn	RGrn	MxTDS	Mass (g)
SI-ES-1003	DS	CCS	TRT	TRT-04	NO	YES	16.45	24.95	7.58	<Null>	9.90	24.74	<Null>	<Null>	<Null>	<Null>	<Null>	16.04	2.2
SI-ES-1004	CO	CCS	TRT	TRT-10	NO	NO	34.36	27.79	10.93	<Null>	26.55	25.85	<Null>	32.04	<Null>	<Null>	<Null>	7.96	9.6
SI-ES-1005	LT	CCS	TRT	TRT-02	NO	NO	23.64	28.20	10.57	<Null>	<Null>	15.63	<Null>	<Null>	<Null>	<Null>	<Null>	6.73	7.6
SI-ES-1006	DS	CCS	TRT	TRT-08	NO	NO	10.27	22.79	6.05	9.11	<Null>	19.24	<Null>	<Null>	<Null>	<Null>	<Null>	3.90	1.4
SI-ES-1007	CO	CCS	UNK	UNK-10	NO	NO	26.67	25.76	5.72	10.47	11.93	24.30	<Null>	<Null>	<Null>	<Null>	<Null>	15.26	4.9
SI-ES-1008	DS	CCS	TRT	TRT-02	NO	NO	19.49	32.13	11.77	13.33	9.77	30.05	<Null>	<Null>	<Null>	<Null>	<Null>	2.24	9.0
SI-ES-1009	DS	CCS	TRT	TRT-01	NO	NO	19.24	28.32	7.12	<Null>	<Null>	28.19	<Null>	<Null>	<Null>	<Null>	<Null>	16.46	4.0
SI-ES-1010	PR	CCS	TRT	TRT-02	NO	NO	19.55	24.29	7.59	19.52	19.33	<Null>	<Null>	<Null>	<Null>	11.21	7.62	<Null>	3.7
SI-ES-1011	DS	CCS	TRT	TRT-05	NO	NO	7.43	18.12	3.85	<Null>	<Null>	16.04	<Null>	<Null>	<Null>	<Null>	<Null>	2.79	0.7
SI-ES-1012	CO	CCS	TRT	TRT-01	NO	NO	19.91	16.51	6.20	<Null>	<Null>	16.02	<Null>	4.48	5.57	<Null>	<Null>	14.47	2.6
SI-ES-1013	DS	CCS	NARB	NARB-01	NO	NO	13.18	22.98	4.79	11.62	<Null>	22.24	<Null>	<Null>	<Null>	<Null>	<Null>	3.85	1.3
SI-ES-1014	DS	CCS	TRT	TRT-02	NO	NO	11.29	27.04	7.29	<Null>	13.09	21.97	<Null>	<Null>	<Null>	<Null>	<Null>	2.59	2.3
SI-ES-1015	DS	CCS	PED	PED-03	NO	NO	15.42	24.41	6.43	<Null>	<Null>	24.95	<Null>	<Null>	<Null>	<Null>	<Null>	9.77	2.0
SI-ES-1016	DS	CCS	TRT	TRT-17	PTCZ	NO	11.87	24.36	4.93	<Null>	<Null>	25.64	<Null>	<Null>	<Null>	<Null>	<Null>	6.19	1.5
SI-ES-1017	DS	CCS	TRT	TRT-16	POT	NO	14.92	27.07	4.94	8.23	9.76	21.30	7.32	<Null>	<Null>	<Null>	6.56	5.81	2.7
SI-ES-1018	CO	SWD	SWD	SWD-02	NO	YES	21.29	25.01	5.01	12.42	22.94	23.21	<Null>	<Null>	<Null>	<Null>	<Null>	2.34	3.1
SI-ES-1019	CO	CCS	TRT	TRT-01	NO	NO	26.56	26.67	12.52	8.13	6.17	23.10	<Null>	<Null>	<Null>	8.13	<Null>	3.20	7.9
SI-ES-1020	DS	CCS	TRT	TRT-02	NO	YES	18.43	26.52	5.62	4.44	<Null>	26.66	<Null>	3.74	<Null>	<Null>	<Null>	1.99	3.8
SI-ES-1021	CO	CCS	UNK	UNK-07	POT	NO	33.21	22.84	8.68	13.57	<Null>	20.17	<Null>	<Null>	<Null>	<Null>	<Null>	21.84	6.3
SI-ES-1022	CO	SWD	SWD	SWD-03	NO	NO	18.83	25.25	6.95	17.55	20.62	24.69	<Null>	11.95	<Null>	<Null>	15.02	2.43	3.7
SI-ES-1023	CO	CCS	TRT	TRT-02	NO	YES	24.44	29.64	6.24	21.83	<Null>	29.64	<Null>	8.55	<Null>	<Null>	<Null>	2.52	5.2
SI-ES-1024	DS	CCS	MOSC	MOSC-03	NO	NO	33.50	34.38	8.75	28.58	25.83	34.38	<Null>	<Null>	<Null>	11.26	<Null>	4.63	13.3
SI-ES-1025	LT	CCS	TRT	TRT-02	NO	NO	20.51	28.64	6.60	10.79	<Null>	28.64	<Null>	<Null>	<Null>	<Null>	<Null>	3.03	4.1
SI-ES-1026	CO	CCS	TRT	TRT-02	NO	NO	29.35	22.07	9.99	28.36	20.42	18.93	<Null>	<Null>	<Null>	13.75	11.25	3.63	5.3
SI-ES-1027	DS	CCS	TRT	TRT-17	NO	NO	15.44	11.82	3.56	13.07	<Null>	12.28	<Null>	<Null>	<Null>	<Null>	<Null>	4.02	0.8
SI-ES-1028	CO	CCS	TRT	TRT-05	NO	NO	23.66	22.58	6.74	13.19	16.63	22.58	<Null>	<Null>	<Null>	13.19	9.91	12.38	3.5
SI-ES-1029	LT	CCS	TRT	TRT-02	POT	NO	28.02	32.72	8.17	<Null>	14.04	30.05	<Null>	<Null>	<Null>	<Null>	<Null>	2.01	6.5
SI-ES-1030	CO	CCS	UNK	UNK-11	NO	YES	29.26	22.25	9.45	23.94	19.22	21.17	<Null>	<Null>	<Null>	<Null>	<Null>	6.41	6.3
SI-ES-1031	CO	CCS	TRT	TRT-02	NO	NO	26.96	31.89	10.97	<Null>	8.54	31.89	<Null>	<Null>	<Null>	<Null>	<Null>	13.50	9.8
SI-ES-1032	LT	CCS	TRT	TRT-18	POT	YES	19.59	21.73	5.99	15.36	<Null>	17.89	<Null>	<Null>	<Null>	<Null>	<Null>	2.70	2.7

Catalog	Portion	GENMAT	SPECMAT	Nodule	Burning	SPUR	MxLe	MxWd	MxTk	RetOL	RetOR	RetODS	RetRL	RetRR	RetRDS	LGrn	RGrn	MxTDS	Mass (g)
SI-ES-1033	LT	CCS	TRT	TRT-16	PTCZ	NO	33.41	28.20	9.07	13.04	<Null>	24.61	<Null>	<Null>	<Null>	<Null>	<Null>	5.64	6.7
SI-ES-1034	DS	CCS	TRT	TRT-02	PTCZ	NO	6.85	18.58	6.02	<Null>	<Null>	18.58	<Null>	<Null>	<Null>	<Null>	<Null>	2.39	0.9
SI-ES-1035	DS	QZT	DAK	DAK-01	NO	NO	9.17	24.41	10.56	<Null>	<Null>	24.41	<Null>	<Null>	<Null>	<Null>	<Null>	5.76	1.8
SI-ES-1036	DS	CCS	TRT	TRT-05	NO	NO	7.88	12.57	3.52	<Null>	<Null>	11.24	<Null>	<Null>	<Null>	<Null>	<Null>	4.74	0.4
SI-ES-1037	DS	CCS	PED	PED-01	NO	NO	16.05	20.30	5.38	<Null>	<Null>	20.30	<Null>	<Null>	<Null>	<Null>	<Null>	3.98	1.7
SI-ES-1038	LT	CCS	TRT	TRT-15	POT	NO	13.92	10.57	4.39	10.82	<Null>	10.22	<Null>	<Null>	<Null>	<Null>	<Null>	2.88	0.8
SI-ES-1039	DS	CCS	TRT	TRT-08	POT	NO	10.38	19.14	6.50	<Null>	<Null>	17.61	<Null>	<Null>	<Null>	<Null>	<Null>	3.91	1.3
SI-ES-1040	DS	CCS	TRT	TRT-08	NO	NO	10.67	12.92	3.91	<Null>	<Null>	12.92	<Null>	<Null>	<Null>	<Null>	<Null>	2.04	0.4
SI-ES-1041	LT	CCS	TRT	TRT-10	NO	NO	16.64	16.07	8.87	3.03	<Null>	9.47	<Null>	<Null>	<Null>	<Null>	<Null>	13.93	2.4
SI-ES-1042	CO	CCS	TRT	TRT-06	NO	YES	29.11	21.05	5.73	<Null>	<Null>	21.05	<Null>	<Null>	<Null>	10.72	<Null>	2.16	3.8
SI-ES-1043	LT	CCS	TRT	TRT-09	NO	NO	28.66	17.17	5.76	<Null>	19.43	15.38	<Null>	<Null>	<Null>	<Null>	10.81	4.64	3.6
SI-ES-1044	DS	CCS	TRT	TRT-16	POT	NO	5.60	28.95	6.85	<Null>	<Null>	28.95	<Null>	<Null>	<Null>	<Null>	<Null>	5.60	1.6
SI-ES-1045	DS	QZT	MOR	MOR-02	NO	NO	15.80	23.73	7.59	7.38	6.50	19.63	<Null>	<Null>	<Null>	<Null>	<Null>	3.55	4.4

E4. Graver descriptive and metric data.

Catalog	Portion	BfUf	MULTI	GENMAT	SPECMAT	Nodule	BURN	MxLe	MxWd	MxTk	GrLL	GrWdL	GrTkL	GrLR	GrWdR	GrTkR	Mass (g)
CMPA-GR-1001	DS	UF	NO	CCS	TRT	TRT-02	NO	14.94	13.74	4.01	2.60	1.81	0.88	<Null>	<Null>	<Null>	0.7
CMPA-GR-1002	DS	UF	NO	VOL	OBS	OBS-02	NO	5.87	11.52	2.45	1.14	1.26	0.58	<Null>	<Null>	<Null>	0.1
SI-GR-1001	CO	UF	NO	CCS	TRT	TRT-14	NO	14.43	8.83	1.33	1.08	0.87	0.90	<Null>	<Null>	<Null>	0.1
SI-GR-1002	DS	UF	NO	CCS	TRT	TRT-14	NO	11.96	14.55	1.96	1.03	1.29	1.07	<Null>	<Null>	<Null>	0.4
SI-GR-1003	DS	UF	NO	CCS	NARB	NARB-01	NO	9.92	18.98	3.40	0.98	1.66	1.04	<Null>	<Null>	<Null>	0.5
SI-GR-1004	DS	UF	NO	SWD	SWD	SWD-07	NO	17.03	11.51	3.13	2.57	2.79	1.16	<Null>	<Null>	<Null>	0.7
SI-GR-1005	CO	BF	YES	CCS	PED	PED-06	NO	14.82	8.67	2.14	1.77	1.76	0.96	1.77	1.58	0.72	0.3
SI-GR-1006	LT	UF	NO	CCS	FLAT	FLAT-02	NO	15.66	9.45	2.14	1.82	1.65	1.24	<Null>	<Null>	<Null>	0.4
SI-GR-1007	CO	UF	YES	CCS	PED	PED-05	NO	27.42	29.39	4.63	1.09	1.03	1.10	1.04	1.01	0.98	3.7
SI-GR-1008	DS	UF	YES	CCS	FLAT	FLAT-02	NO	16.25	24.09	7.55	1.80	2.10	2.35	2.64	3.88	1.69	2.3
SI-GR-1009	CO	BF	YES	CCS	UNK	UNK-05	NO	19.74	16.59	3.01	2.21	2.26	1.95	2.12	1.36	1.09	0.8
SI-GR-1010	LT	UF	NO	CCS	EDW	EDW-01	NO	29.56	14.78	2.53	1.53	1.45	1.19	<Null>	<Null>	<Null>	1.2
SI-GR-1011	CO	UF	NO	SWD	SWD	SWD-07	NO	18.20	18.71	3.22	2.07	2.22	1.21	<Null>	<Null>	<Null>	1.2
SI-GR-1012	DS	UF	NO	QZT	MOR	MOR-03	NO	19.01	19.99	3.70	2.45	1.88	1.48	<Null>	<Null>	<Null>	1.4

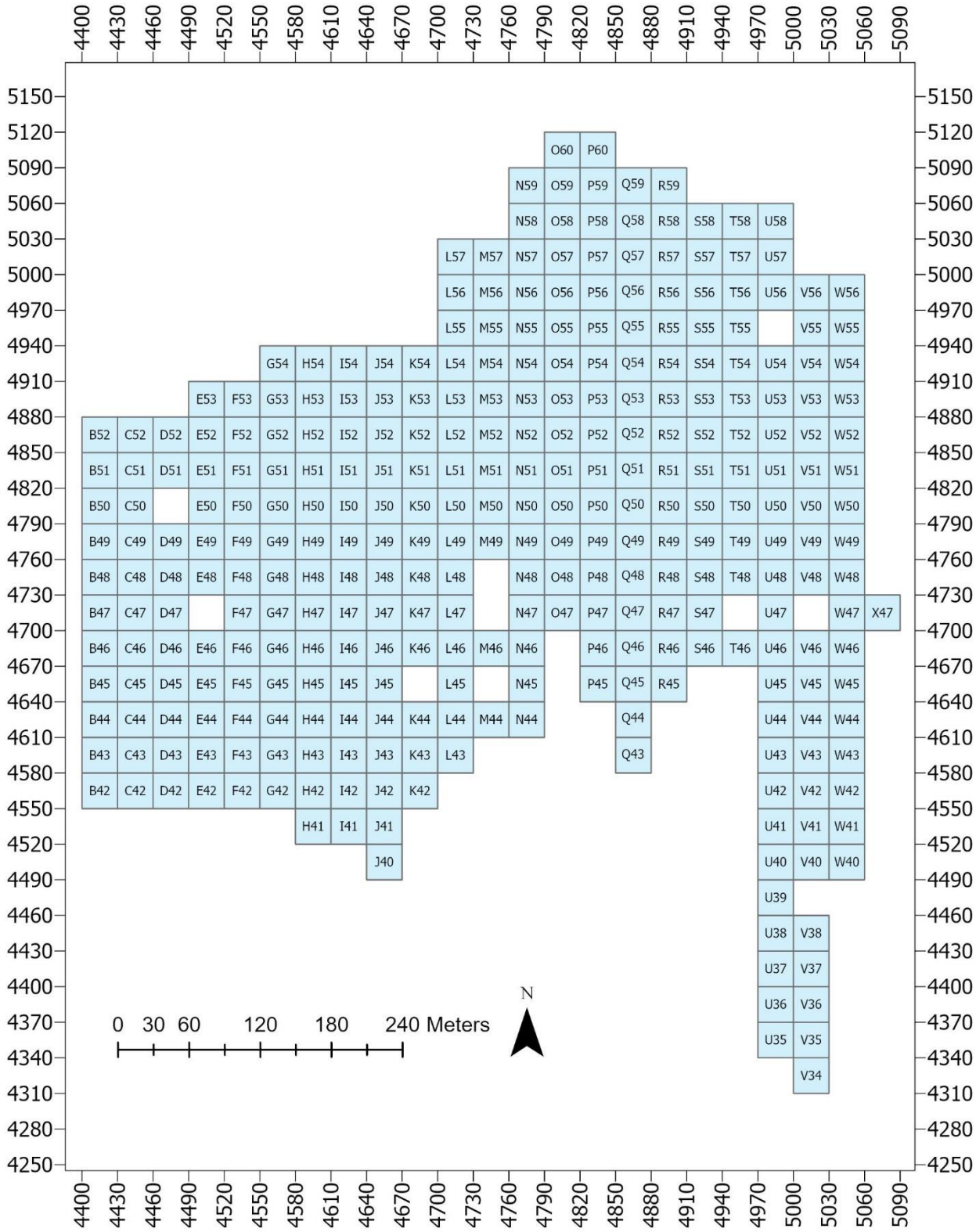
Catalog	Portion	BfUf	MULTI	GENMAT	SPECMAT	Nodule	BURN	MxLe	MxWd	MxTk	GrLL	GrWdL	GrTkL	GrLR	GrWdR	GrTkR	Mass (g)
SI-GR-1013	DS	BF	NO	SWD	SWD	SWD-06	NO	13.62	21.11	4.26	1.75	1.83	1.56	<Null>	<Null>	<Null>	1.3
SI-GR-1014	DS	BF	NO	SWD	SWD	SWD-05	NO	17.13	16.54	2.91	5.96	5.92	1.77	<Null>	<Null>	<Null>	0.9
SI-GR-1015	CO	UF	NO	CCS	MOSC	MOSC-07	NO	23.95	13.34	4.78	2.99	1.99	1.05	<Null>	<Null>	<Null>	1.7
SI-GR-1016	DS	UF	YES	CCS	NARB	NARB-02	NO	15.78	11.45	3.18	1.79	1.03	1.66	1.84	2.28	2.06	0.9
SI-GR-1017	LT	BF	NO	CCS	PED	PED-06	NO	22.28	11.43	3.06	2.18	2.01	1.36	<Null>	<Null>	<Null>	0.9
SI-GR-1018	DS	UF	NO	CCS	PED	PED-03	NO	16.39	13.73	4.56	2.99	3.36	2.54	<Null>	<Null>	<Null>	0.9
SI-GR-1019	LT	UF	NO	CCS	TRT	TRT-01	NO	16.95	13.70	2.64	2.18	1.10	1.31	<Null>	<Null>	<Null>	0.6
SI-GR-1020	MS	BF	YES	CCS	TRT	TRT-10	NO	11.76	16.23	2.02	1.51	1.82	1.05	1.79	1.19	0.98	0.4
SI-GR-1021	DS	UF	NO	CCS	TRT	TRT-07	NO	10.05	9.54	2.13	2.07	2.15	0.74	<Null>	<Null>	<Null>	0.2
SI-GR-1022	DS	UF	NO	CCS	UNK	UNK-05	NO	13.10	12.37	3.41	1.95	2.15	1.34	<Null>	<Null>	<Null>	0.5
SI-GR-1023	DS	UF	YES	SWD	SWD	SWD-06	NO	13.80	18.33	2.27	2.26	1.41	0.87	1.72	1.27	1.38	0.6
SI-GR-1024	LT	UF	NO	CCS	TRT	TRT-10	NO	12.18	8.49	2.11	3.36	2.73	1.81	<Null>	<Null>	<Null>	0.2
SI-GR-1025	LT	UF	NO	CCS	TRT	TRT-10	NO	10.14	8.91	2.31	2.48	1.01	1.58	<Null>	<Null>	<Null>	0.3
SI-GR-1026	LT	UF	NO	CCS	EDW	EDW-01	NO	14.83	18.13	2.73	4.54	4.18	2.22	<Null>	<Null>	<Null>	0.9
SI-GR-1027	LT	UF	YES	CCS	UNK	UNK-07	NO	17.94	8.93	2.38	1.66	2.21	1.27	2.18	1.70	1.50	0.4
SI-GR-1028	LT	UF	NO	CCS	TRT	TRT-01	NO	15.43	10.73	3.40	1.21	1.20	1.03	<Null>	<Null>	<Null>	0.6
SI-GR-1029	LT	BF	NO	VOL	DAC	DAC-02	NO	36.62	24.75	7.74	3.13	2.31	1.15	<Null>	<Null>	<Null>	4.9
SI-GR-1030	LT	UF	NO	SWD	SWD	SWD-06	NO	9.01	19.69	6.13	2.26	1.86	1.36	<Null>	<Null>	<Null>	1.1
SI-GR-1031	LT	UF	NO	VOL	OBS	OBS-02	NO	10.19	14.16	3.57	1.08	1.29	0.77	<Null>	<Null>	<Null>	0.6
SI-GR-1032	MS	UF	NO	SWD	SWD	SWD-07	NO	13.19	11.60	4.38	9.52	7.32	3.60	<Null>	<Null>	<Null>	0.6

E5. Utilized flake descriptive and metric data.

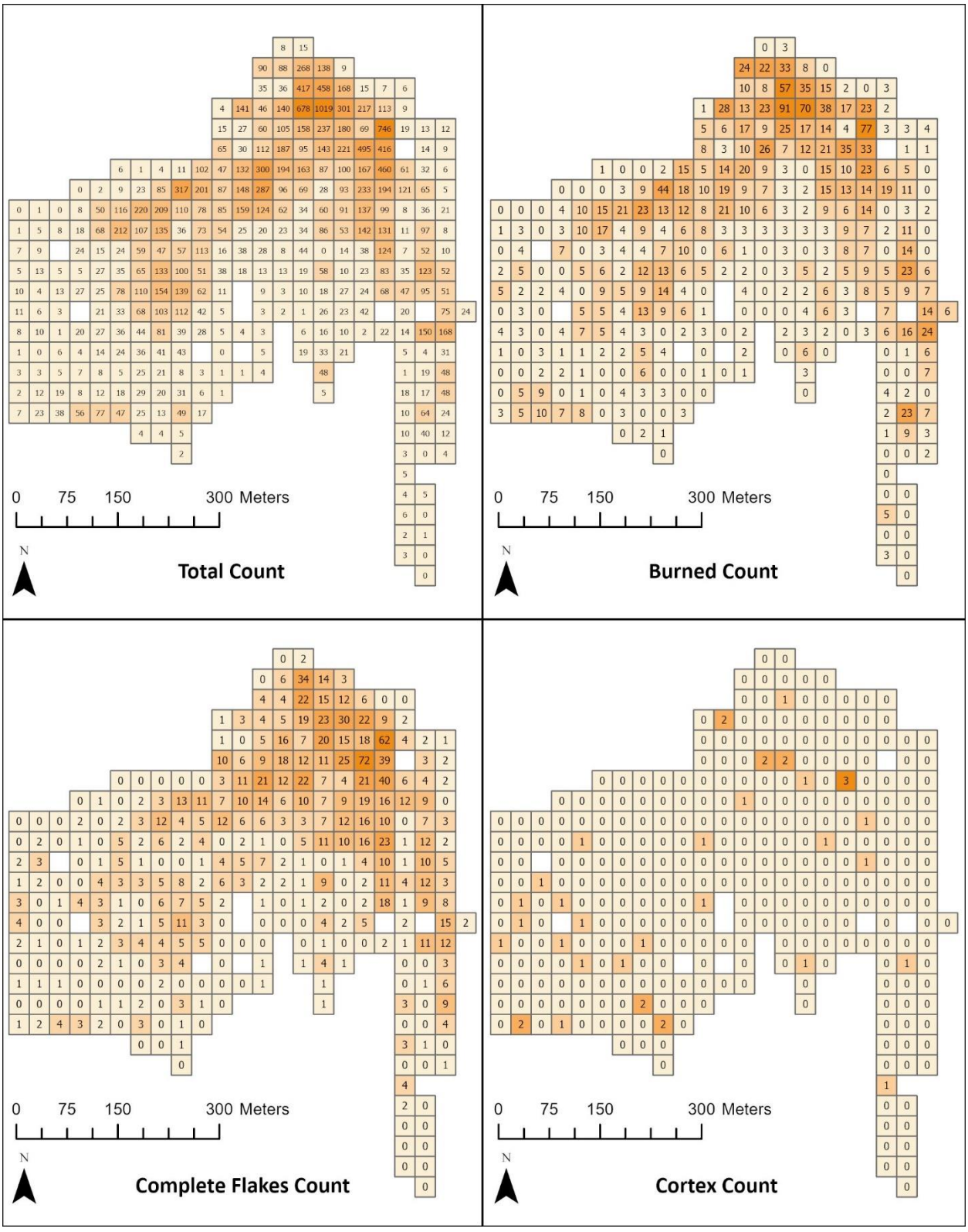
Catalog	Portion	GENMAT	SPECMAT	Nodule	Burning	MxLe	MxWd	MxTk	UtlOL	UtlOR	UtlODS	UtlRL	UtlRR	UtlRDS	Mass (g)
CMPA-UFT-1001	PR	CCS	TRT	TRT-13	NO	14.93	14.15	4.79	8.84	9.88	<Null>	<Null>	3.54	<Null>	1.3
CMPA-UFT-1002	LT	CCS	TRT	TRT-02	NO	9.87	13.36	4.95	9.40	<Null>	<Null>	<Null>	<Null>	<Null>	0.6
CMPA-UFT-1003	DS	CCS	TRT	TRT-01	NO	30.56	24.05	8.25	<Null>	<Null>	17.38	<Null>	<Null>	<Null>	5.7
CMPA-UFT-1004	DS	QZT	MOR	MOR-02	NO	37.59	20.69	7.68	13.77	24.89	4.19	<Null>	13.94	<Null>	5.4
SI-UFT-1001	PR	VOL	OBS	OBS-01	NO	13.19	14.76	3.70	<Null>	12.67	<Null>	<Null>	<Null>	<Null>	0.8
SI-UFT-1002	MS	CCS	TRT	TRT-03	NO	19.18	25.51	4.72	6.86	7.17	<Null>	<Null>	4.47	<Null>	2.1

Catalog	Portion	GENMAT	SPECMAT	Nodule	Burning	MxLe	MxWd	MxTk	UtlOL	UtlOR	UtlODS	UtlRL	UtlRR	UtlRDS	Mass (g)
SI-UFT-1003	MS	SWD	SWD	SWD-06	NO	20.80	22.83	5.16	7.07	7.05	<Null>	14.65	11.53	<Null>	1.9
SI-UFT-1004	MS	CCS	TRT	TRT-02	NO	10.94	19.55	3.40	6.53	6.50	<Null>	5.77	<Null>	<Null>	0.9
SI-UFT-1005	LT	CCS	TRT	TRT-06	NO	14.65	8.08	2.53	10.92	<Null>	<Null>	<Null>	<Null>	<Null>	0.3
SI-UFT-1006	MS	CCS	TRT	TRT-15	NO	28.60	21.92	7.01	4.59	4.07	<Null>	9.16	8.96	<Null>	4.3
SI-UFT-1007	LT	CCS	TRT	TRT-10	NO	16.46	20.96	7.08	9.87	<Null>	<Null>	<Null>	<Null>	<Null>	1.9
SI-UFT-1008	LT	CCS	PED	PED-06	NO	11.94	7.00	3.29	<Null>	10.07	<Null>	6.97	<Null>	<Null>	0.3
SI-UFT-1009	MS	CCS	TRT	TRT-02	NO	15.05	13.41	2.92	8.70	<Null>	<Null>	<Null>	<Null>	<Null>	0.6
SI-UFT-1010	DS	CCS	TRT	TRT-10	NO	11.11	13.01	2.65	<Null>	<Null>	11.05	<Null>	<Null>	<Null>	0.5
SI-UFT-1011	LT	CCS	UNK	UNK-06	NO	7.36	9.14	1.96	7.35	<Null>	<Null>	<Null>	<Null>	<Null>	0.2
SI-UFT-1012	LT	CCS	TRT	TRT-15	NO	11.67	6.81	3.24	<Null>	6.11	<Null>	<Null>	<Null>	<Null>	0.3
SI-UFT-1013	PR	CCS	TRT	TRT-10	NO	11.13	11.00	2.12	11.07	<Null>	<Null>	9.91	<Null>	<Null>	0.3
SI-UFT-1014	CO	CCS	UNK	UNK-11	NO	24.05	31.78	8.42	<Null>	10.11	10.88	<Null>	<Null>	<Null>	4.6
SI-UFT-1015	CO	CCS	CUMB	CUMB-02	NO	25.35	21.28	6.50	15.29	12.71	15.90	<Null>	<Null>	<Null>	3.7
SI-UFT-1016	PR	SWD	MOSC	MOSC-03	NO	20.15	23.70	6.68	10.51	9.18	<Null>	<Null>	<Null>	<Null>	3.2
SI-UFT-1017	CO	CCS	FLAT	FLAT-02	NO	27.13	11.37	4.99	10.15	12.20	3.29	<Null>	12.49	<Null>	1.8
SI-UFT-1018	PR	CCS	PED	PED-06	NO	15.52	29.46	9.06	6.92	11.47	<Null>	11.48	<Null>	<Null>	3.3
SI-UFT-1019	CO	QZT	DAK	DAK-05	NO	24.17	10.18	4.92	16.27	<Null>	<Null>	<Null>	<Null>	<Null>	1.4
SI-UFT-1020	CO	CCS	FLAT	FLAT-02	NO	26.69	22.88	8.74	<Null>	<Null>	16.33	<Null>	<Null>	<Null>	4.8
SI-UFT-1021	PR	CCS	TRT	TRT-02	NO	18.66	17.98	3.67	<Null>	5.41	<Null>	5.26	7.02	<Null>	1.1
SI-UFT-1022	LT	SWD	SWD	SWD-04	NO	16.43	11.52	4.23	11.18	<Null>	<Null>	<Null>	<Null>	<Null>	1.2
SI-UFT-1023	PR	CCS	TRT	TRT-10	NO	13.40	16.17	1.82	<Null>	<Null>	<Null>	11.14	<Null>	<Null>	0.5
SI-UFT-1024	MS	CCS	TRT	TRT-05	NO	11.64	14.55	2.31	9.11	11.24	<Null>	<Null>	<Null>	<Null>	0.5
SI-UFT-1025	DS	CCS	TRT	TRT-16	POT	6.63	17.31	2.56	<Null>	<Null>	14.49	<Null>	<Null>	<Null>	0.3
SI-UFT-1026	LT	SWD	SWD	SWD-04	NO	13.35	23.95	2.82	9.30	<Null>	<Null>	<Null>	<Null>	<Null>	1.3
SI-UFT-1027	LT	CCS	TRT	TRT-08	NO	11.90	16.97	2.08	<Null>	11.15	<Null>	<Null>	<Null>	<Null>	0.6
SI-UFT-1028	LT	CCS	TRT	TRT-15	NO	17.69	11.78	3.02	17.07	<Null>	<Null>	<Null>	<Null>	<Null>	0.8
SI-UFT-1029	DS	CCS	TRT	TRT-02	NO	14.57	17.03	2.90	14.51	16.75	3.97	<Null>	<Null>	<Null>	0.6
SI-UFT-1030	LT	SWD	MOSC	MOSC-03	NO	9.50	14.63	3.09	<Null>	<Null>	<Null>	<Null>	7.57	<Null>	0.3
SI-UFT-1031	LT	CCS	UNK	UNK-03	NO	10.66	9.57	1.66	9.99	<Null>	<Null>	<Null>	<Null>	<Null>	0.2
SI-UFT-1032	LT	CCS	TRT	TRT-12	NO	14.57	9.46	2.65	14.09	<Null>	<Null>	<Null>	<Null>	<Null>	0.4

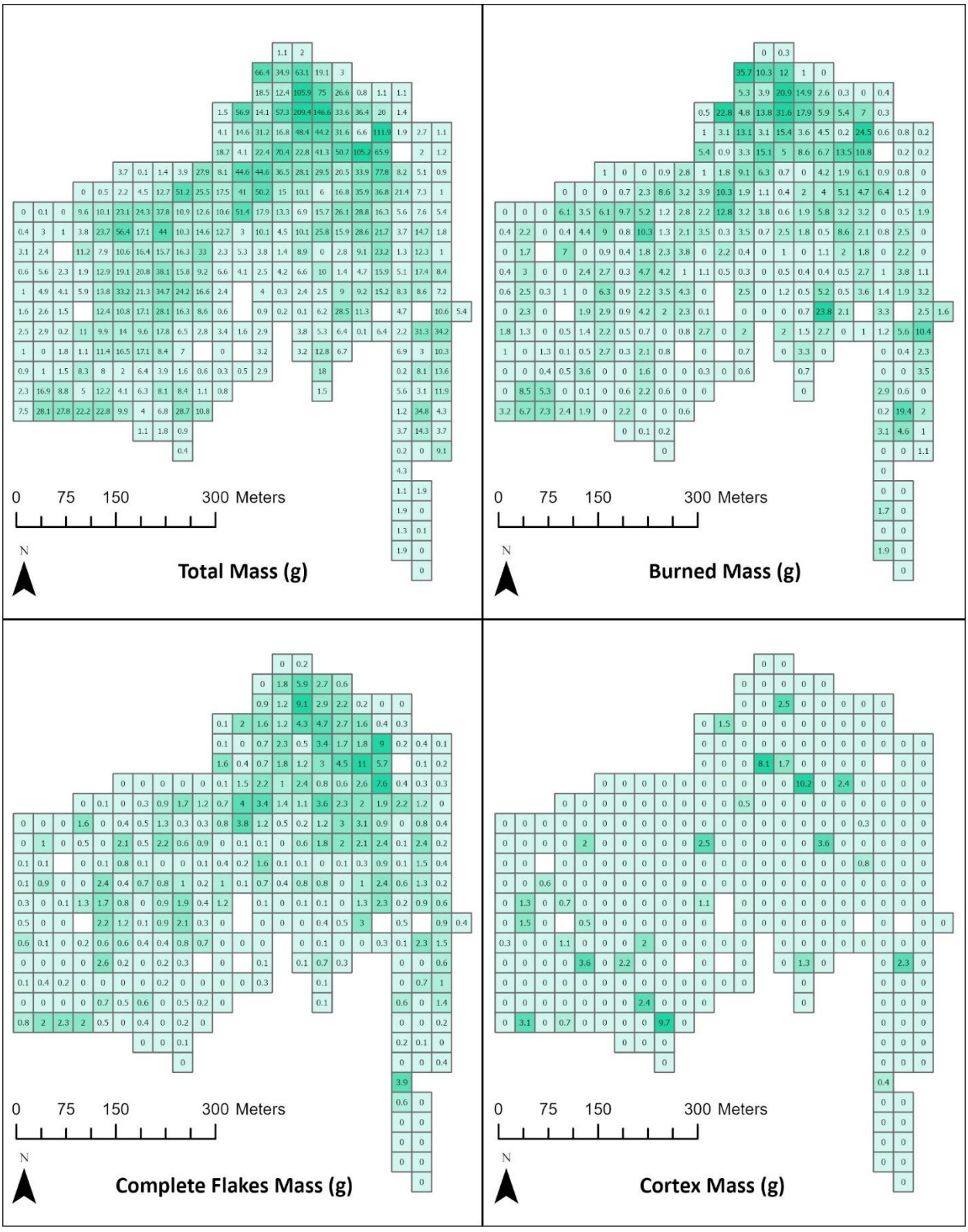
Catalog	Portion	GENMAT	SPECMAT	Nodule	Burning	MxLe	MxWd	MxTk	UtlOL	UtlOR	UtlODS	UtlRL	UtlRR	UtlRDS	Mass (g)
SI-UFT-1033	DS	CCS	PED	PED-01	NO	16.29	14.56	2.47	<Null>	<Null>	11.32	<Null>	<Null>	<Null>	0.7
SI-UFT-1034	LT	CCS	FLAT	FLAT-01	NO	19.84	14.66	4.50	<Null>	13.27	<Null>	<Null>	<Null>	<Null>	1.6
SI-UFT-1035	LT	CCS	UNK	UNK-05	NO	20.20	15.87	3.37	18.64	<Null>	<Null>	<Null>	<Null>	<Null>	1.2
SI-UFT-1036	MS	QZT	MOR	MOR-02	NO	21.10	15.13	3.59	17.52	8.43	<Null>	<Null>	<Null>	<Null>	1.5
SI-UFT-1037	MS	SWD	SWD	SWD-03	NO	32.12	10.53	5.06	<Null>	12.87	<Null>	<Null>	10.45	<Null>	1.6
SI-UFT-1038	DS	VOL	OBS	OBS-02	NO	22.96	16.29	3.39	12.93	10.51	2.96	18.32	<Null>	<Null>	0.9
SI-UFT-1039	DS	VOL	OBS	OBS-03	NO	16.78	12.77	4.95	<Null>	14.87	9.61	<Null>	<Null>	<Null>	1.3
SI-UFT-1040	PR	VOL	OBS	OBS-01	NO	17.56	13.05	6.69	<Null>	11.06	<Null>	<Null>	<Null>	<Null>	1.5
SI-UFT-1041	DS	VOL	OBS	OBS-04	NO	15.39	25.03	4.62	6.32	12.99	14.26	9.77	<Null>	<Null>	2.0



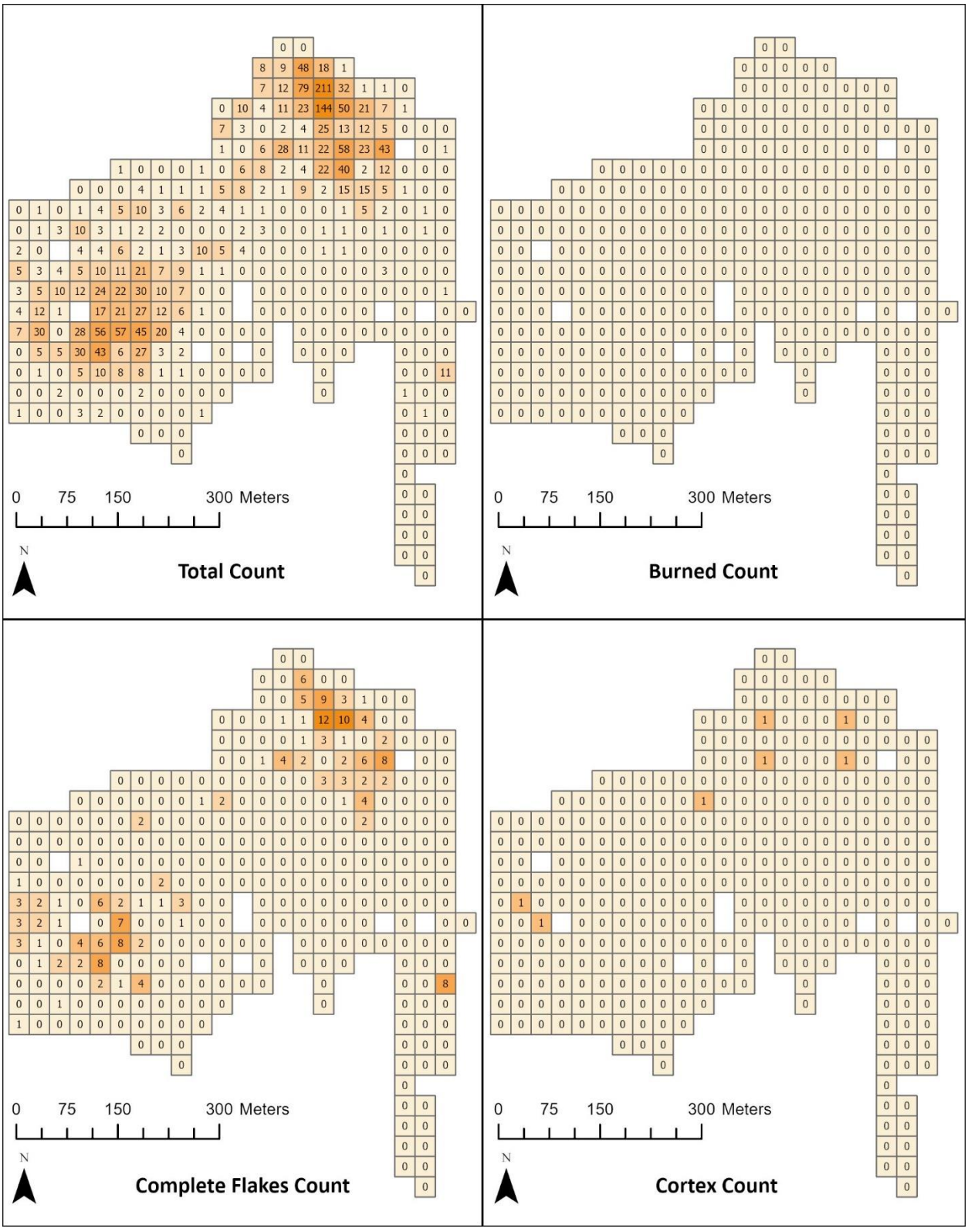
F1. Smithsonian survey grid with positive debitage collections (CSU adjusted datum and names).



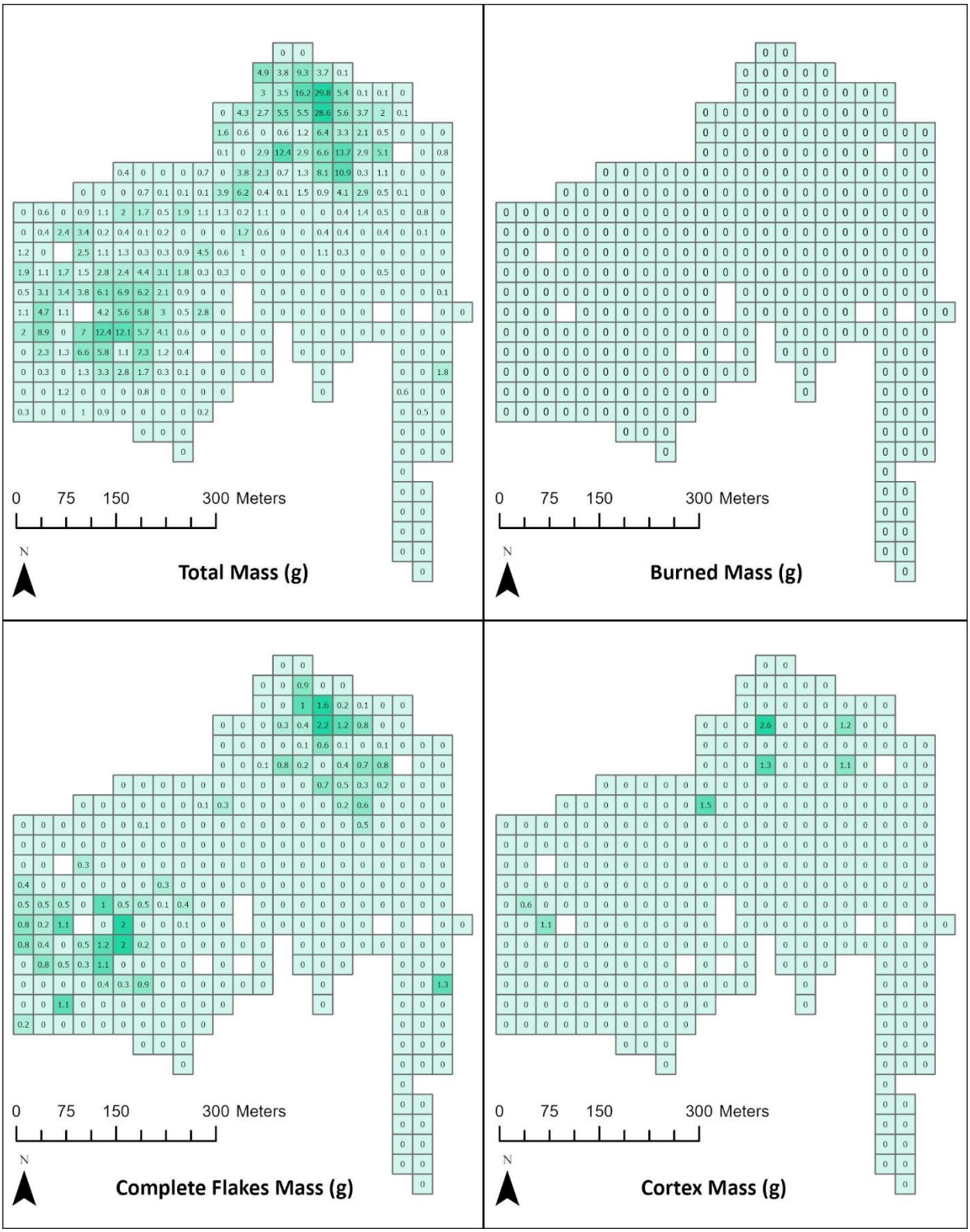
F2. Counts and attributes for Trout Creek jasper debitage.



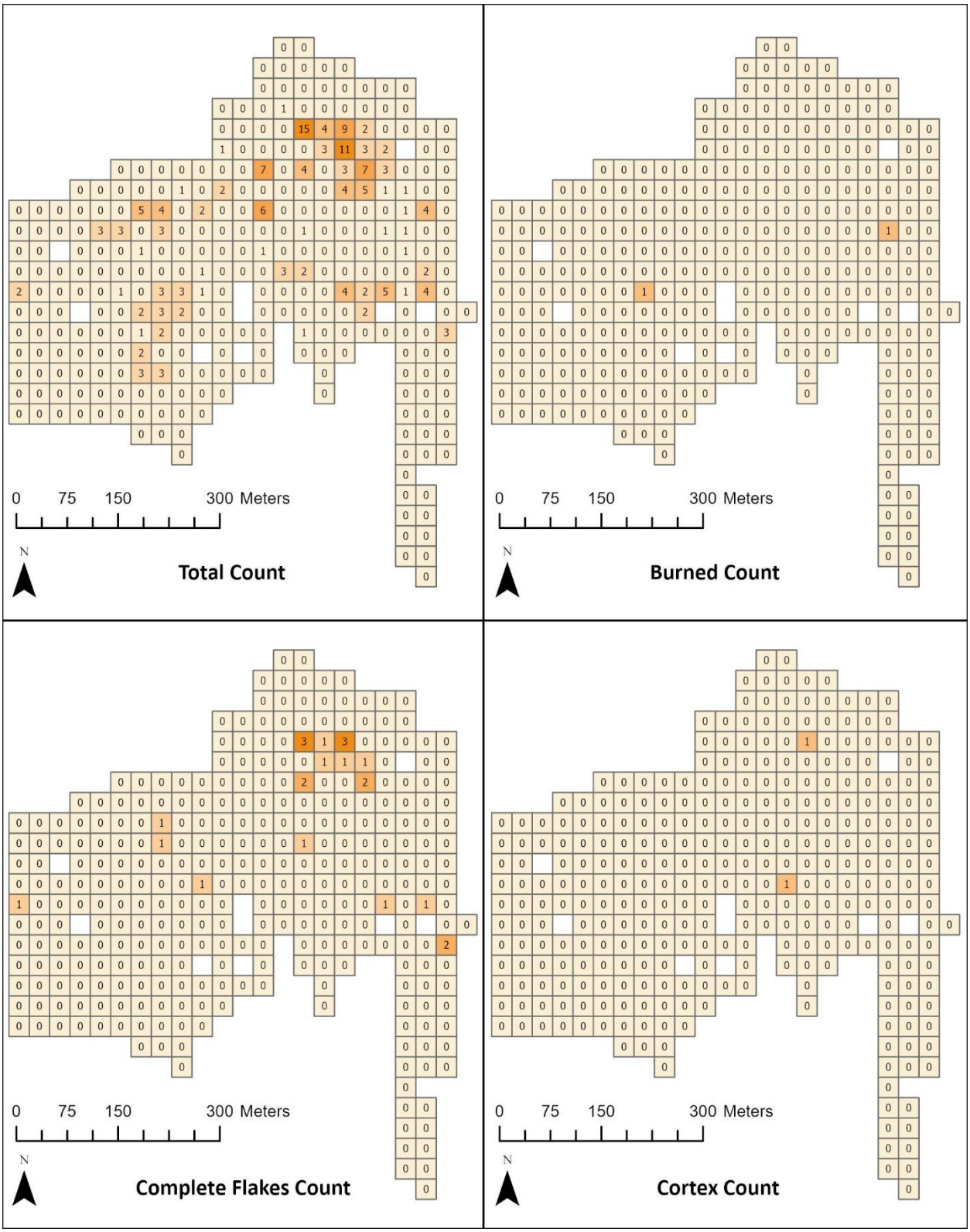
F3. Mass (g) and attributes for Trout Creek jasper debitage.



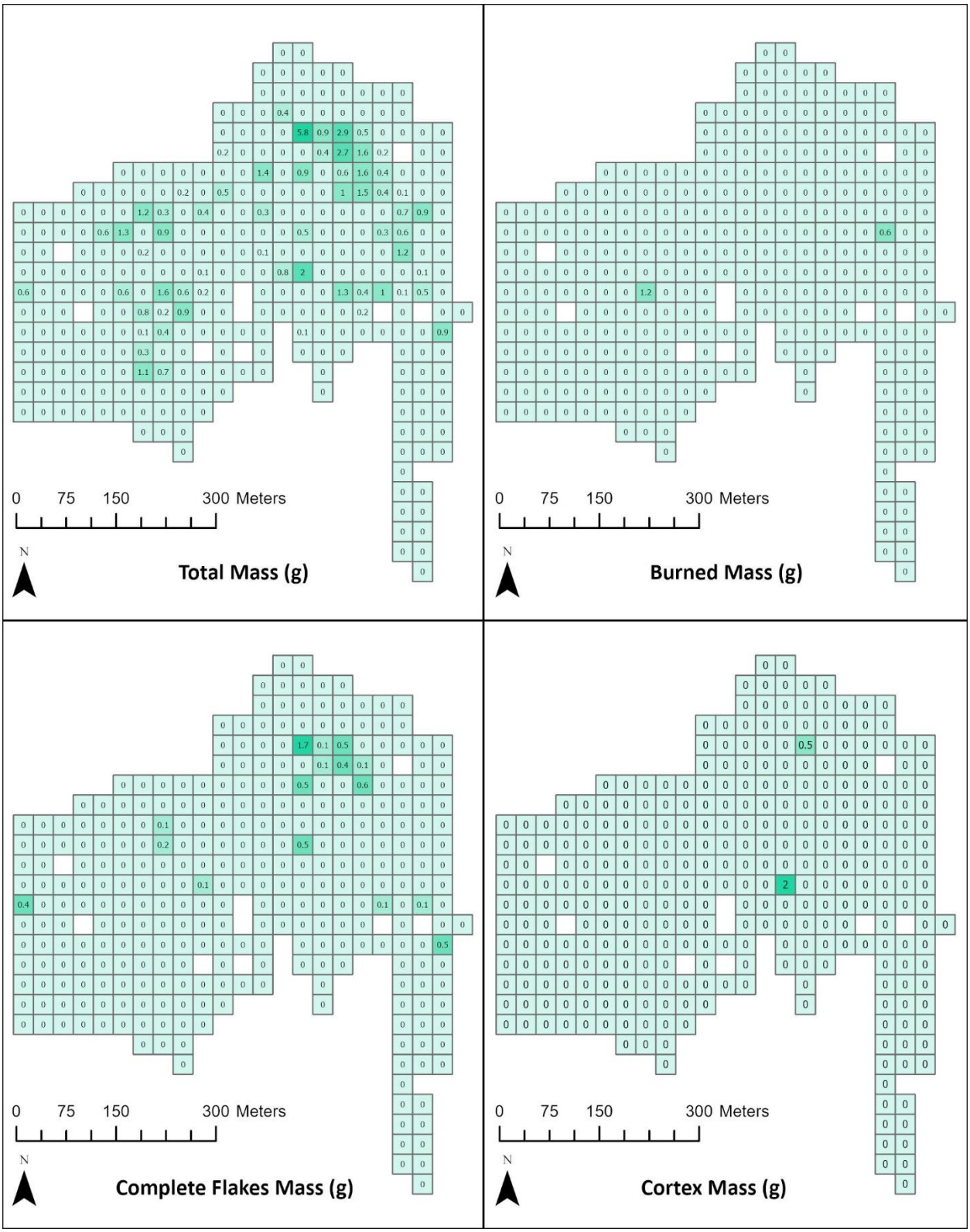
F4. Counts and attributes for obsidian debitage.



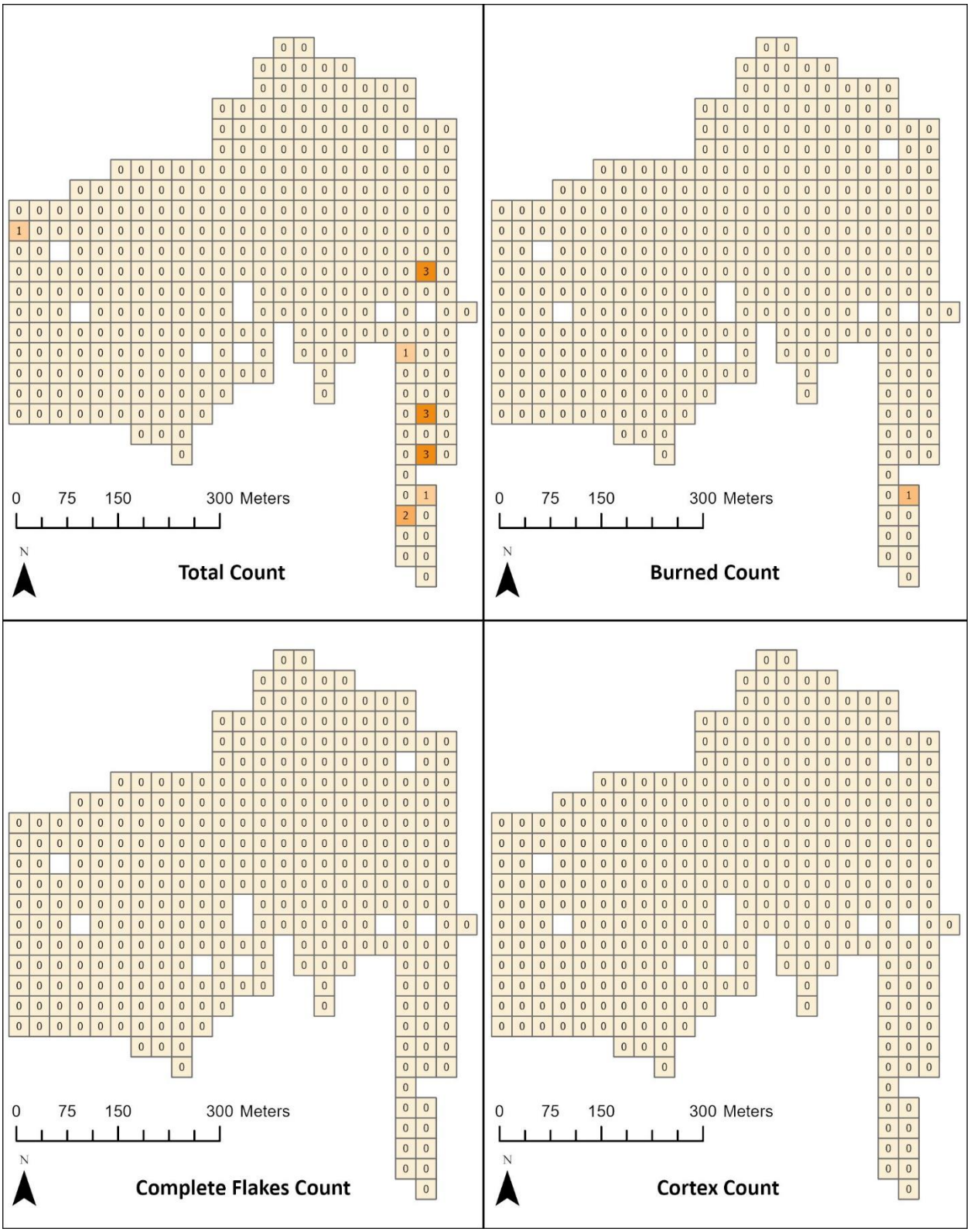
F5. Mass (g) and attributes for obsidian debitage.



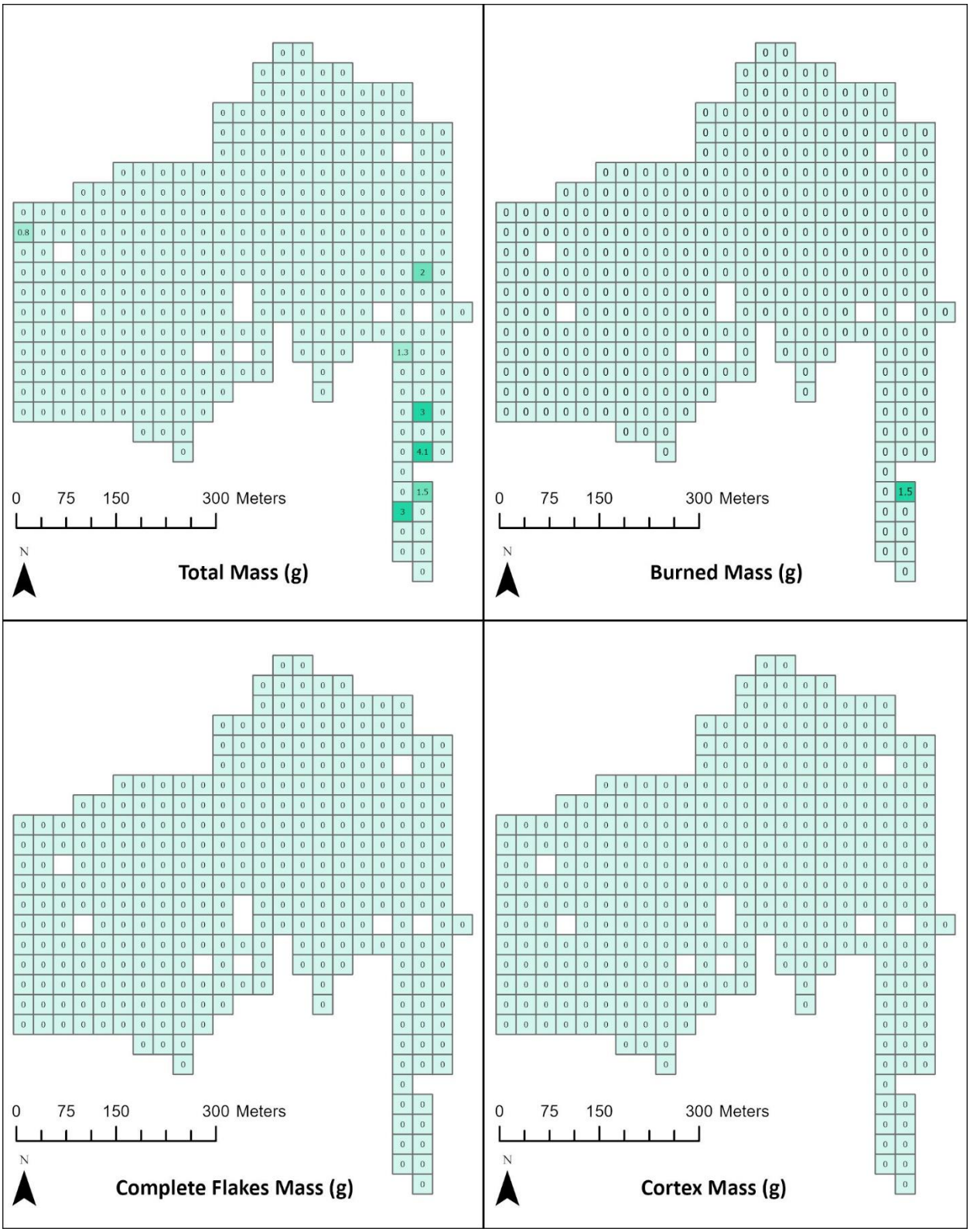
F6. Counts and attributes for Edwards chert debitage.



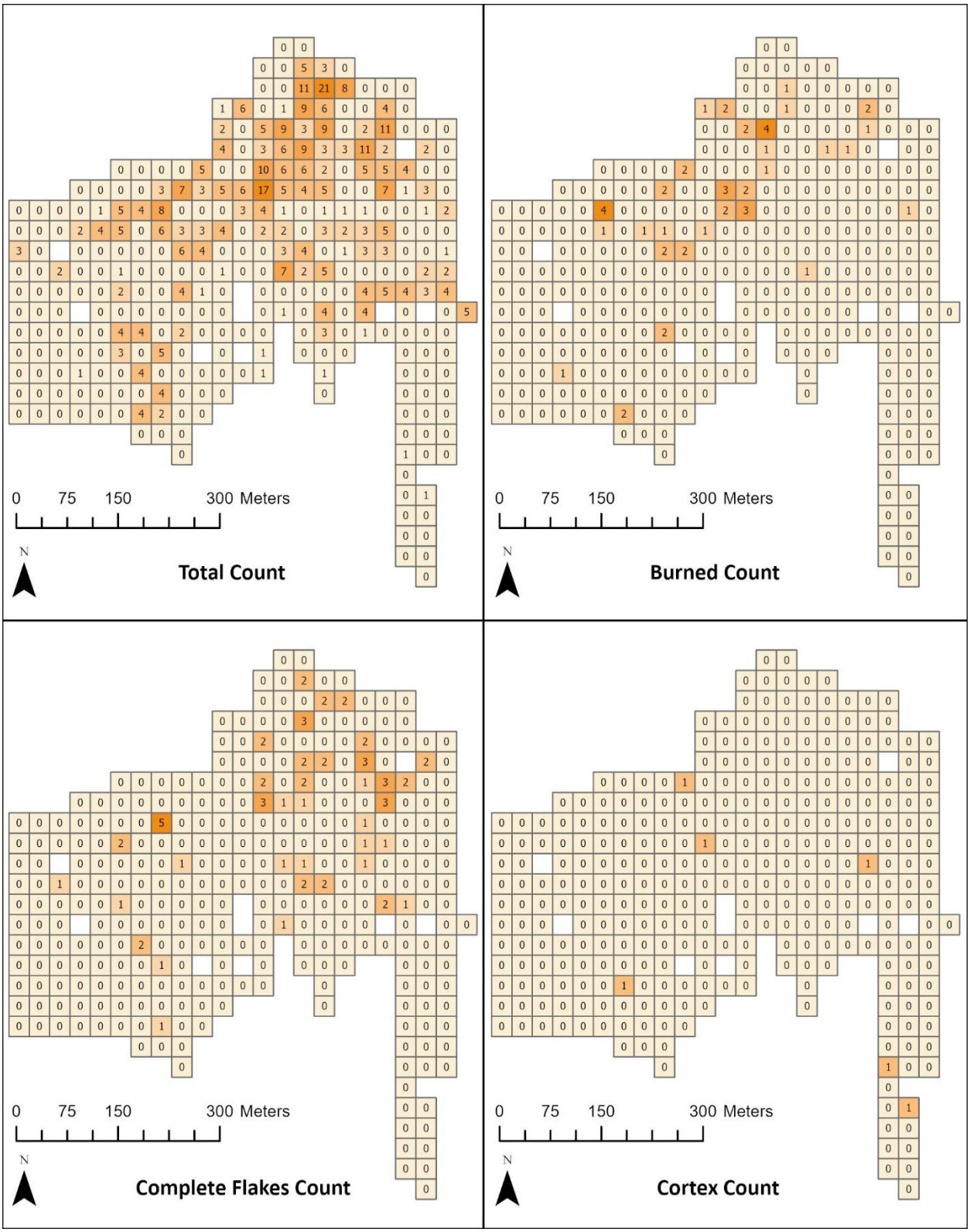
F7. Mass (g) and attributes for Edwards chert debitage.



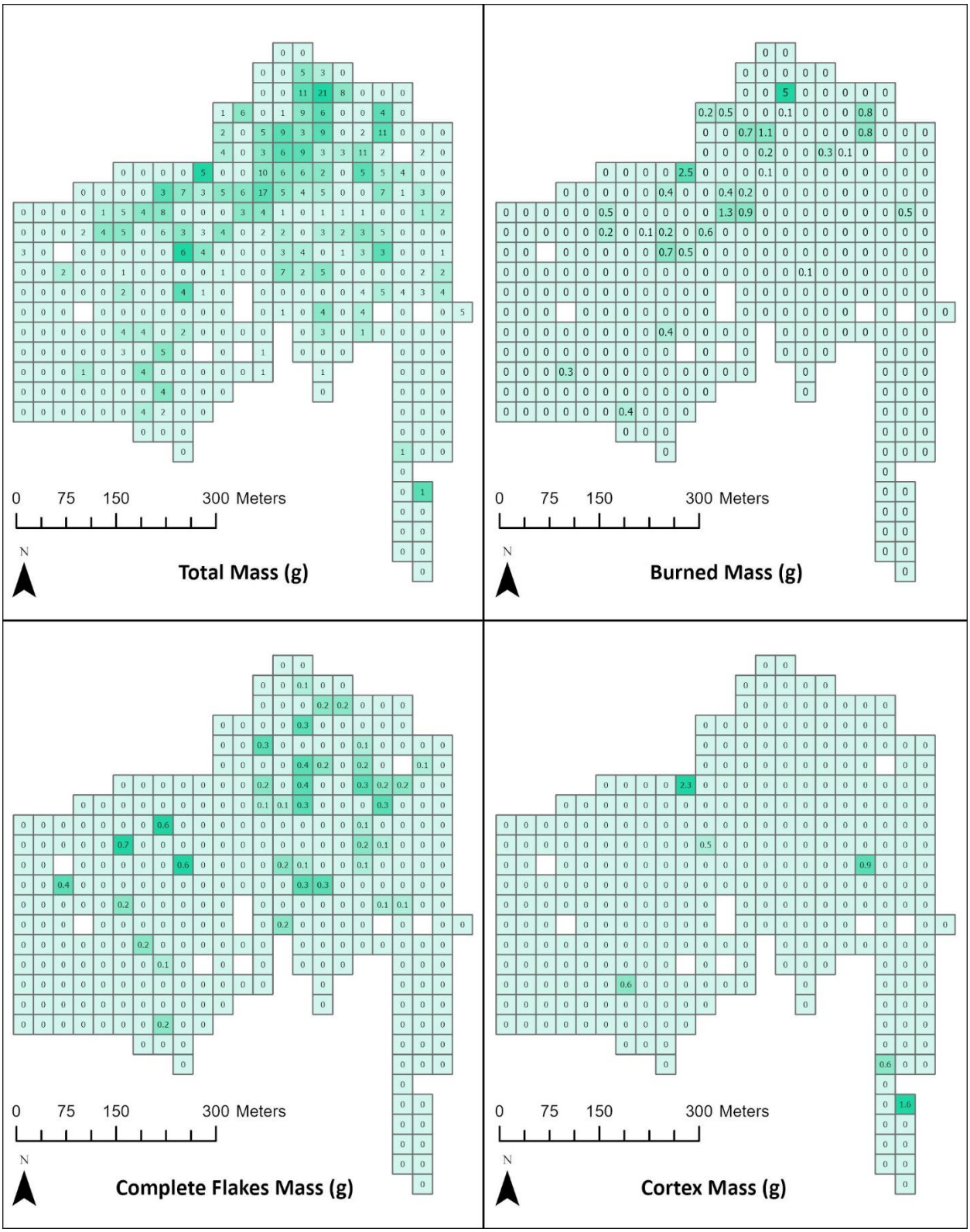
F8. Counts and attributes for Flattop chalcedony debitage.



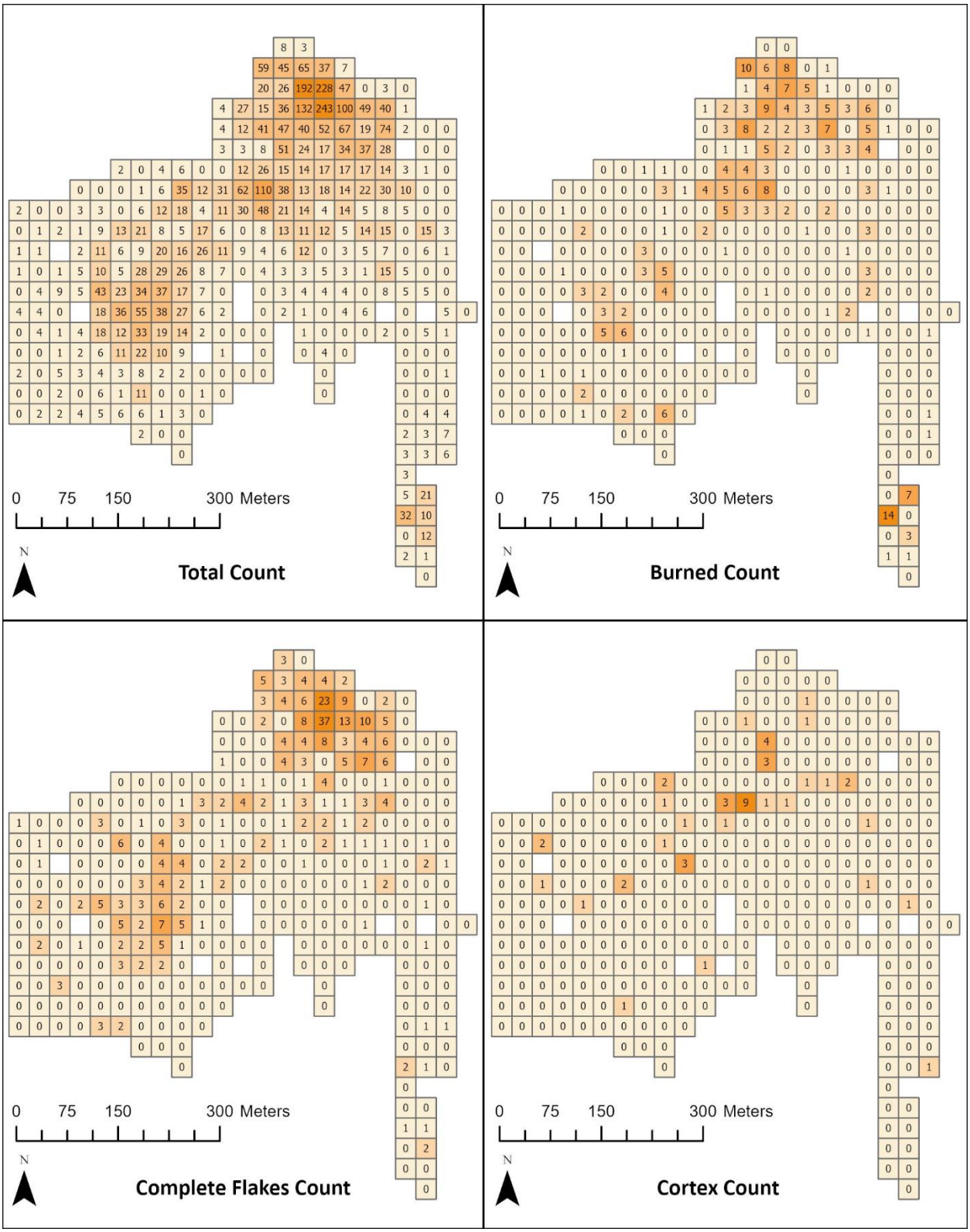
F9. Mass (g) and attributes for Flattop chalcedony debitage.



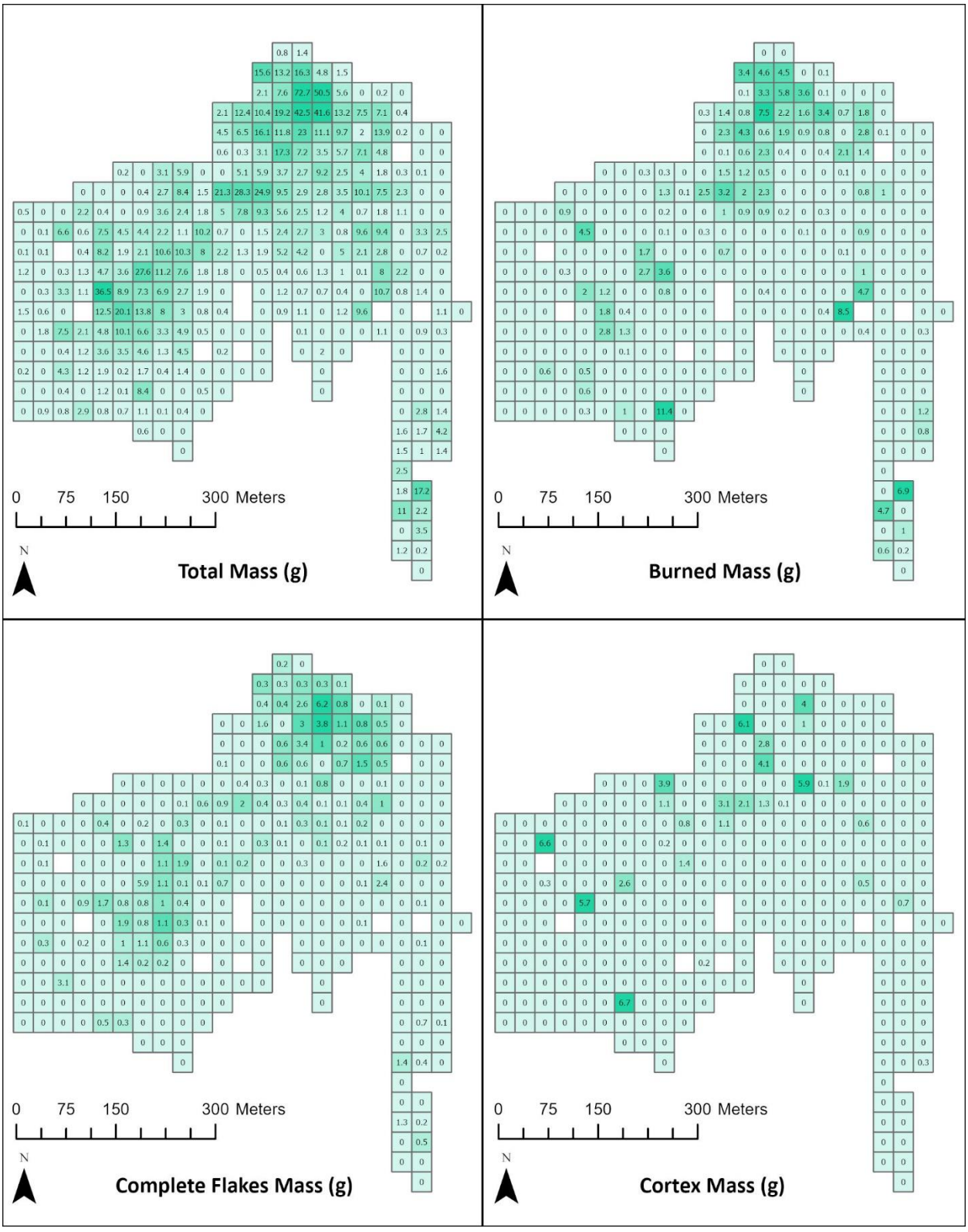
F10. Counts and attributes for Narbona (Chuska) chalcedony debitage.



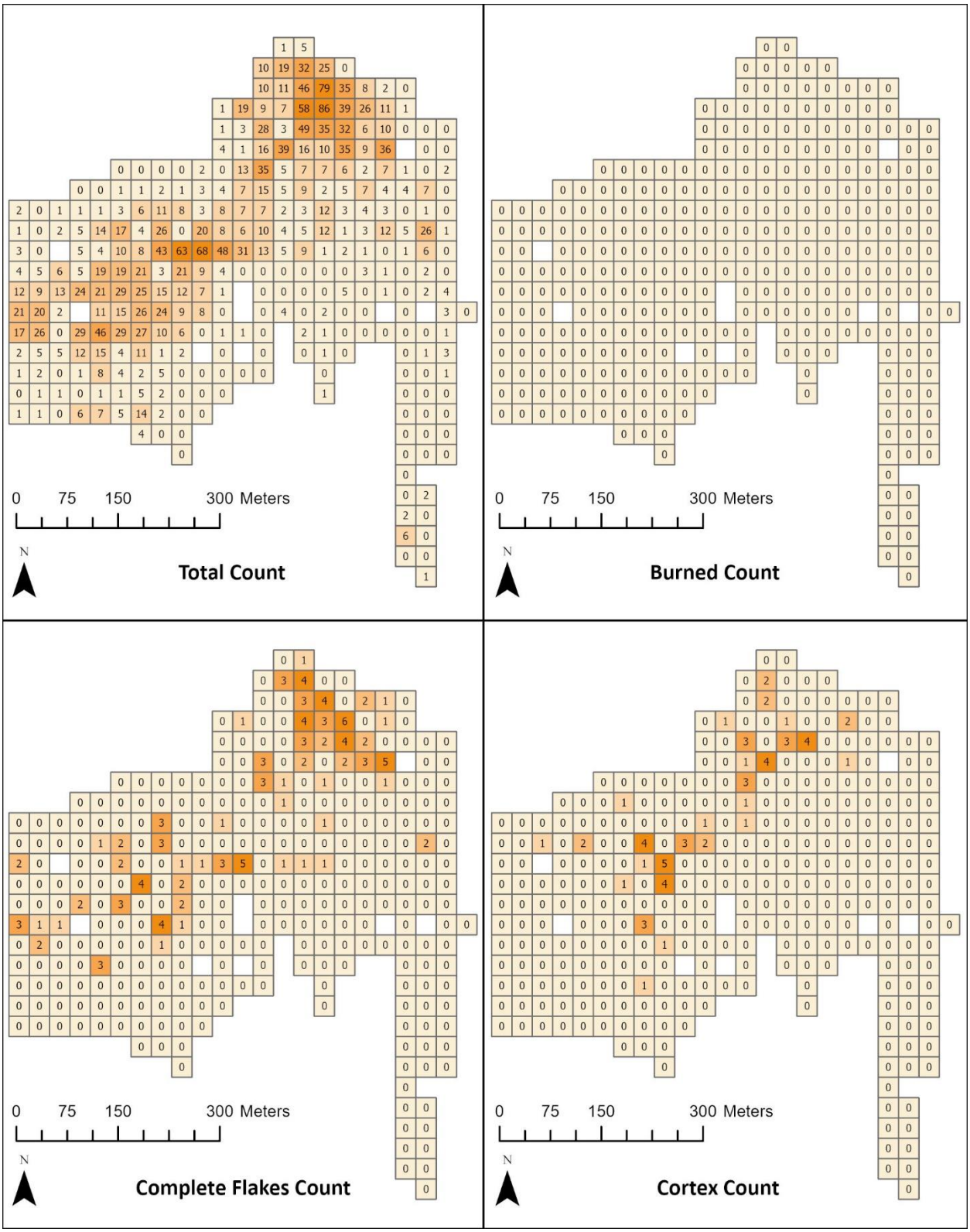
F11. Mass (g) and attributes for Narbona (Chuska) chalcedony debitage.



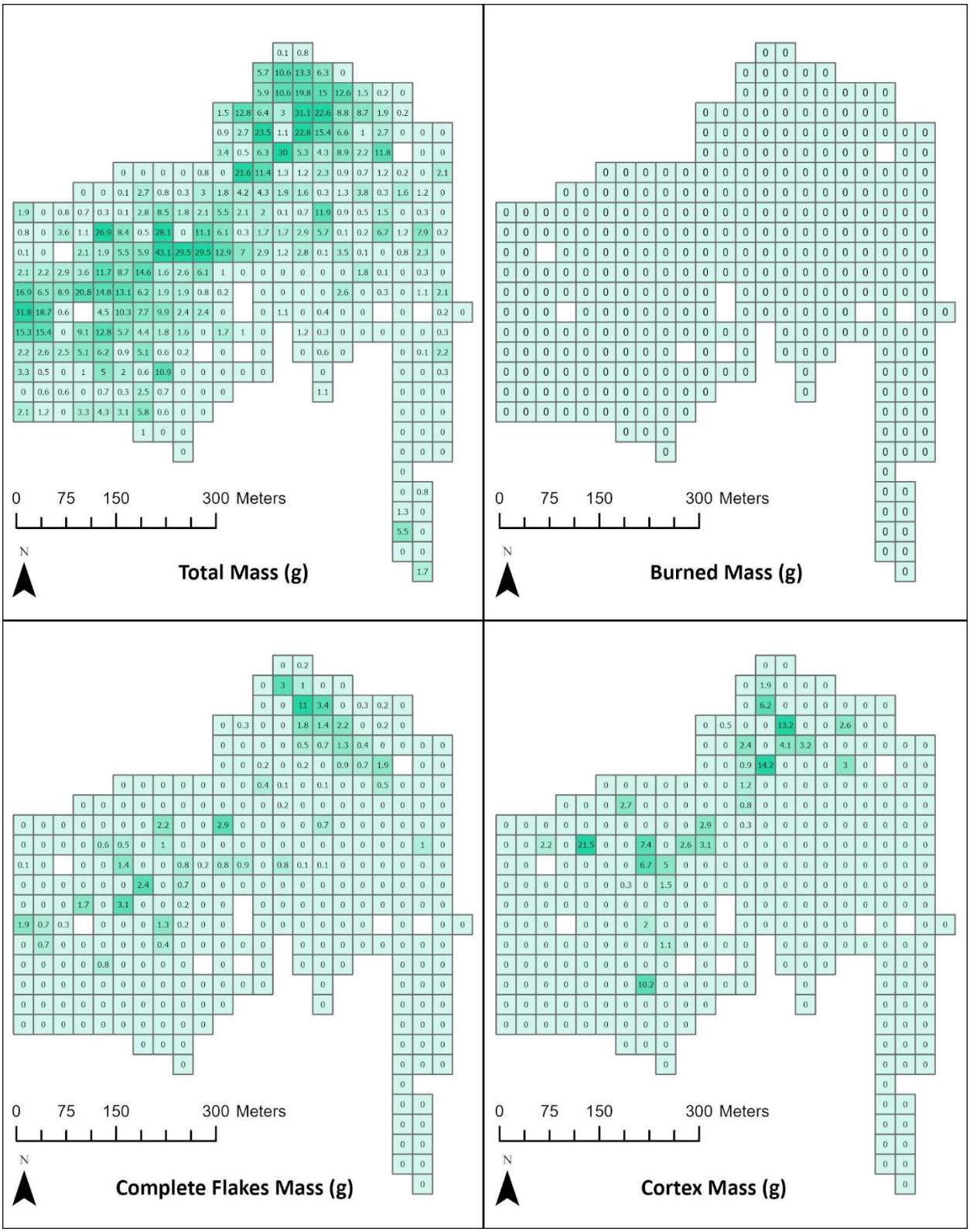
F12. Counts and attributes for Pedernal chert debitage.



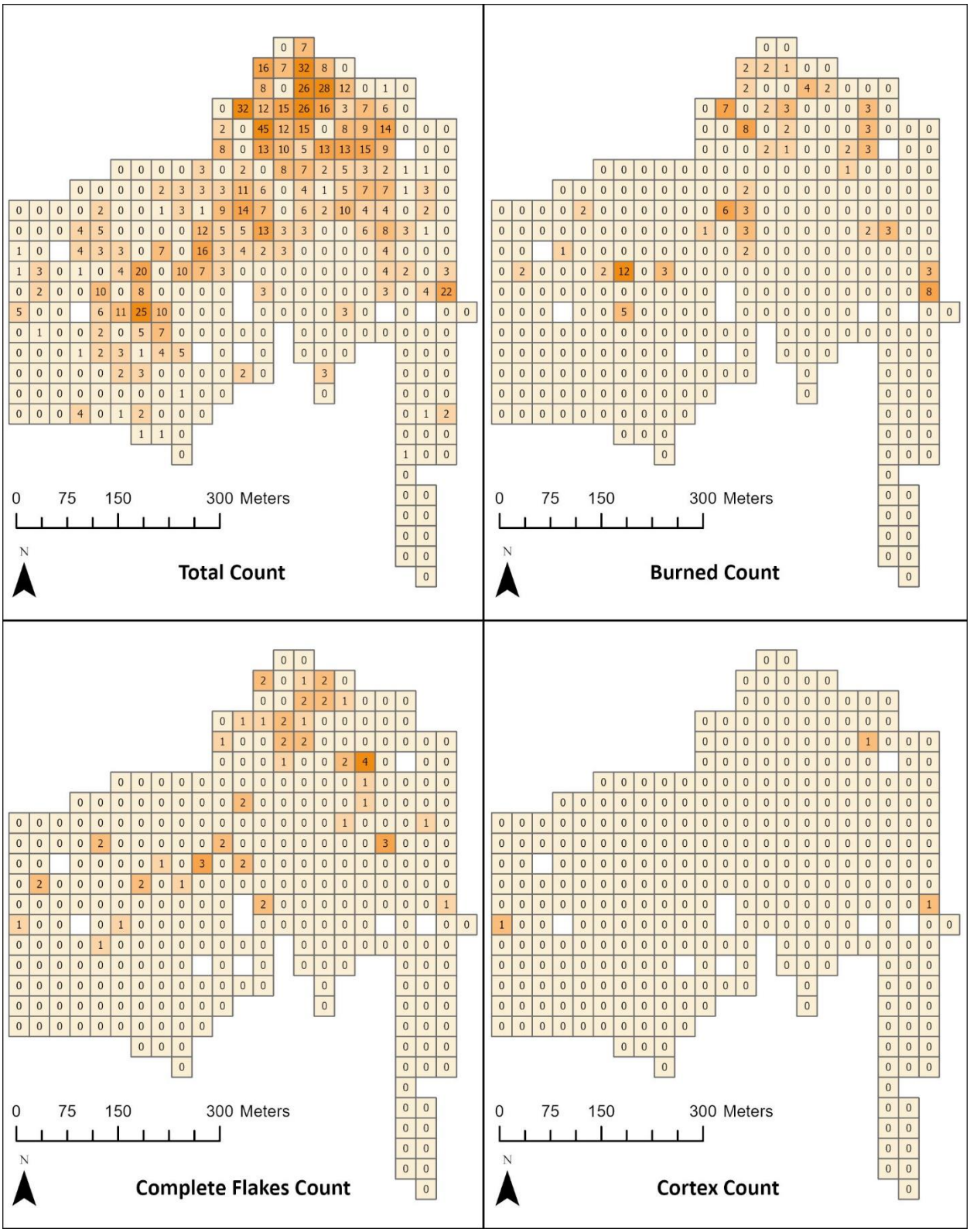
F13. Mass (g) and attributes for Pedernal chert debitage.



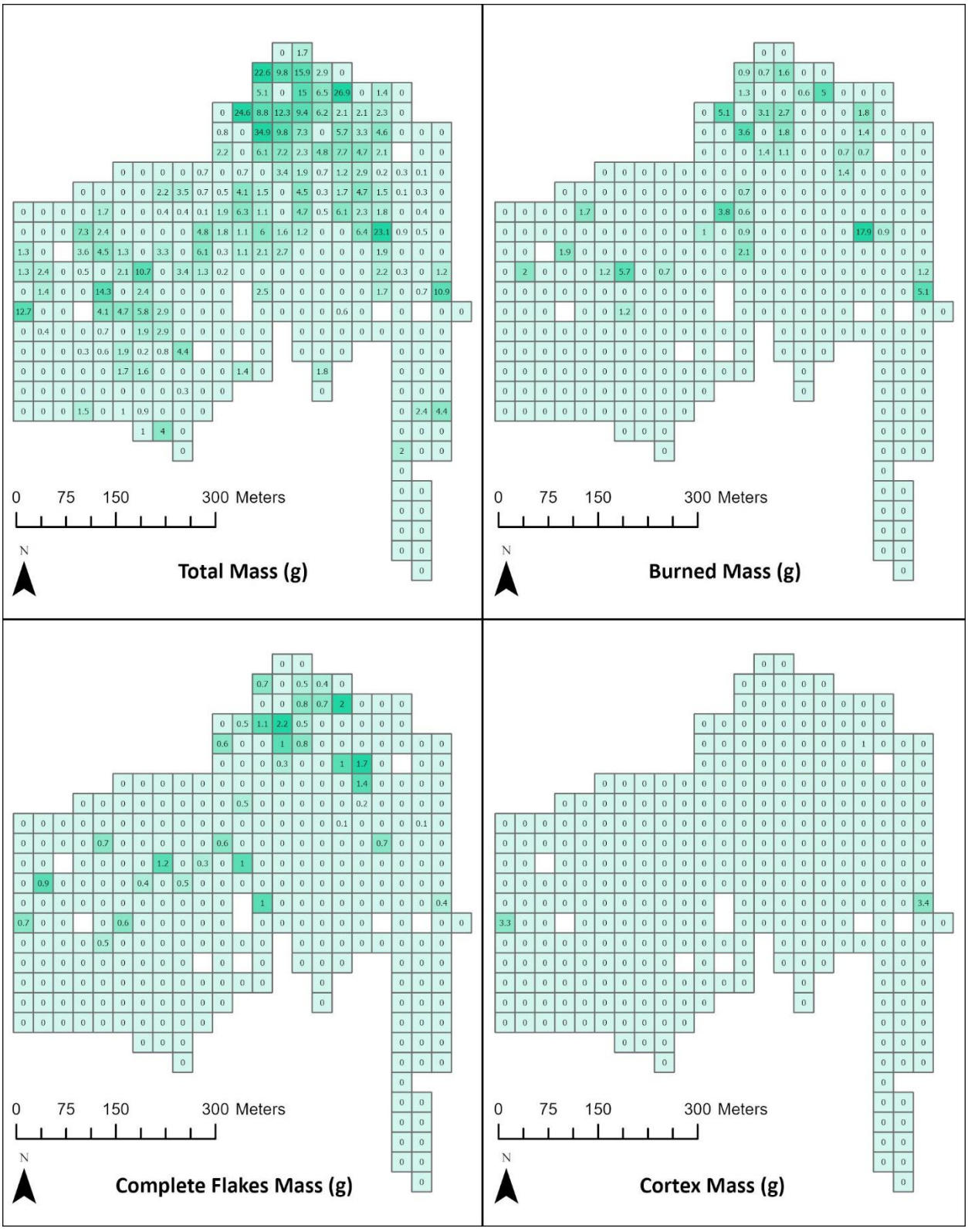
F14. Counts and attributes for dacite (or fine-grained volcanic) debitage.



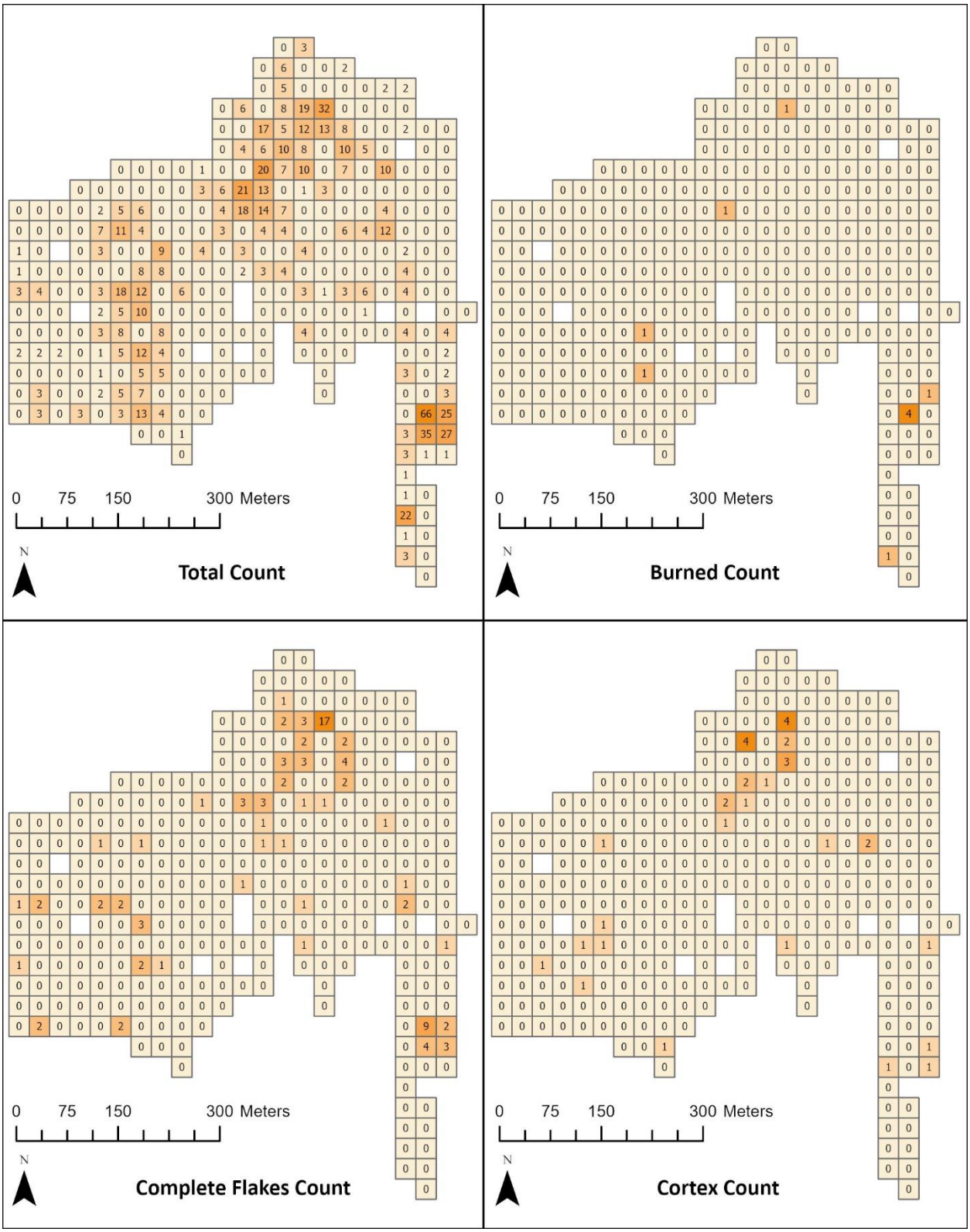
F15. Mass (g) and attributes for dacite (or fine-grained volcanic) debitage.



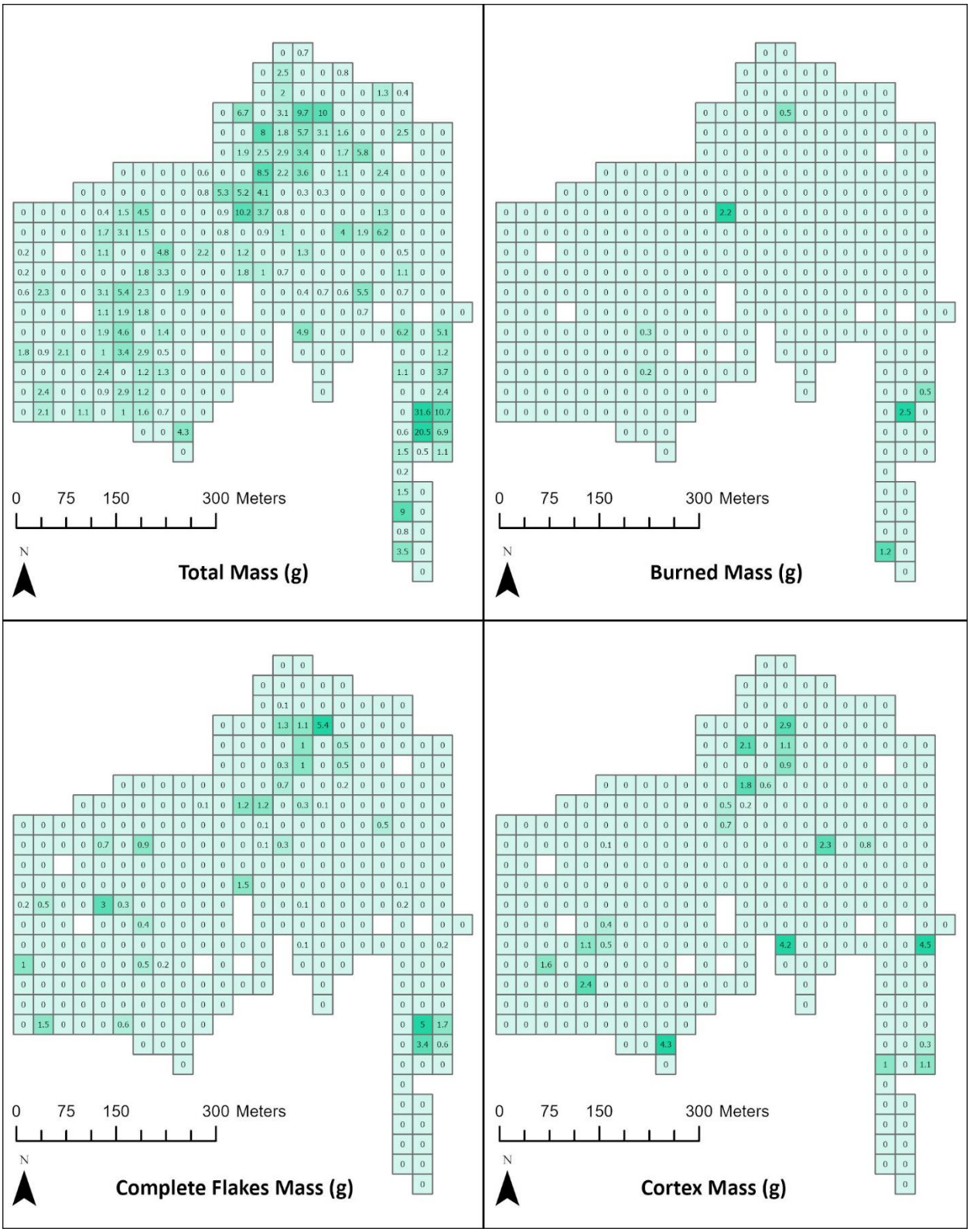
F16. Counts and attributes for Cumbres chert debitage.



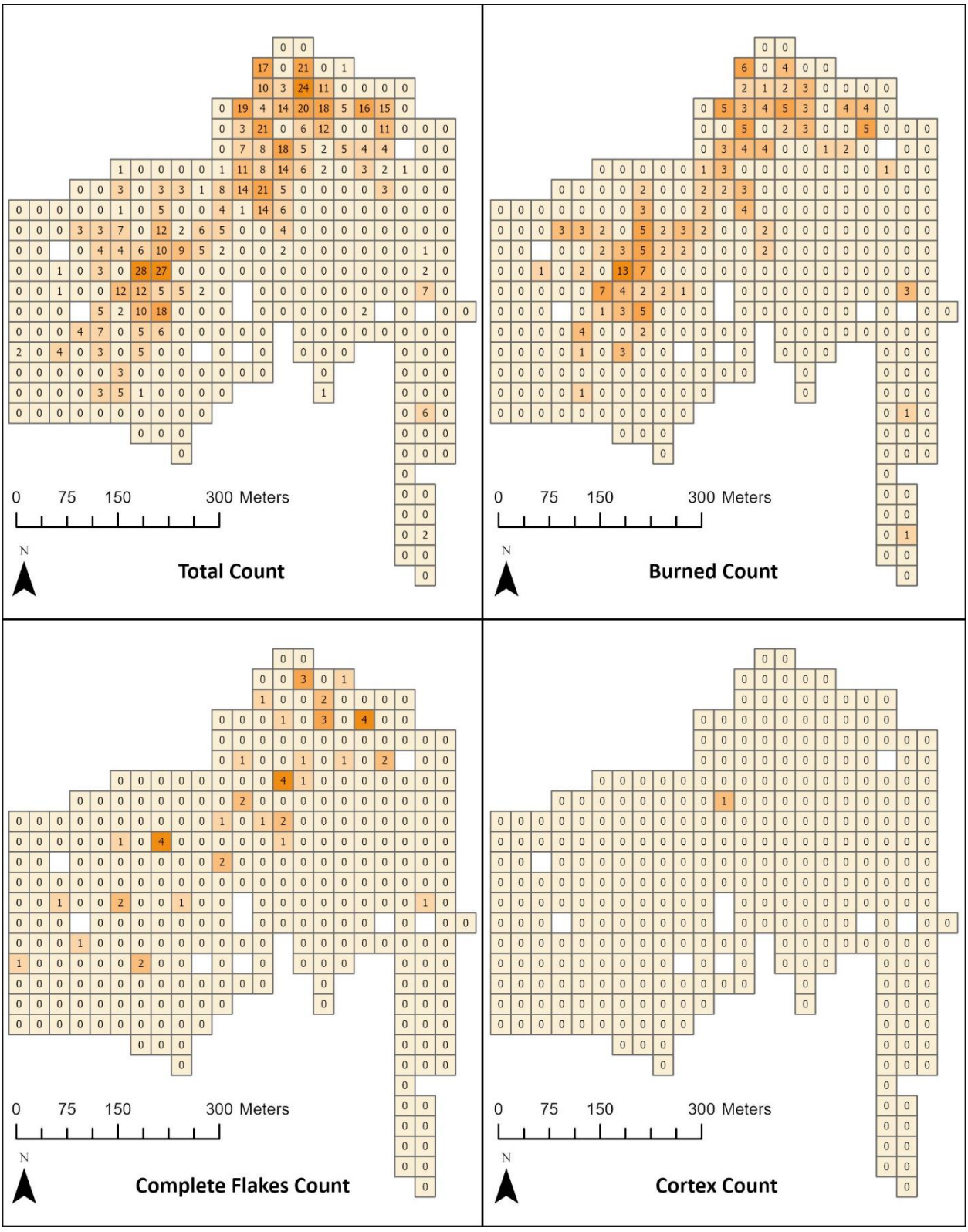
F17. Mass (g) and attributes for Cumbres chert debitage.



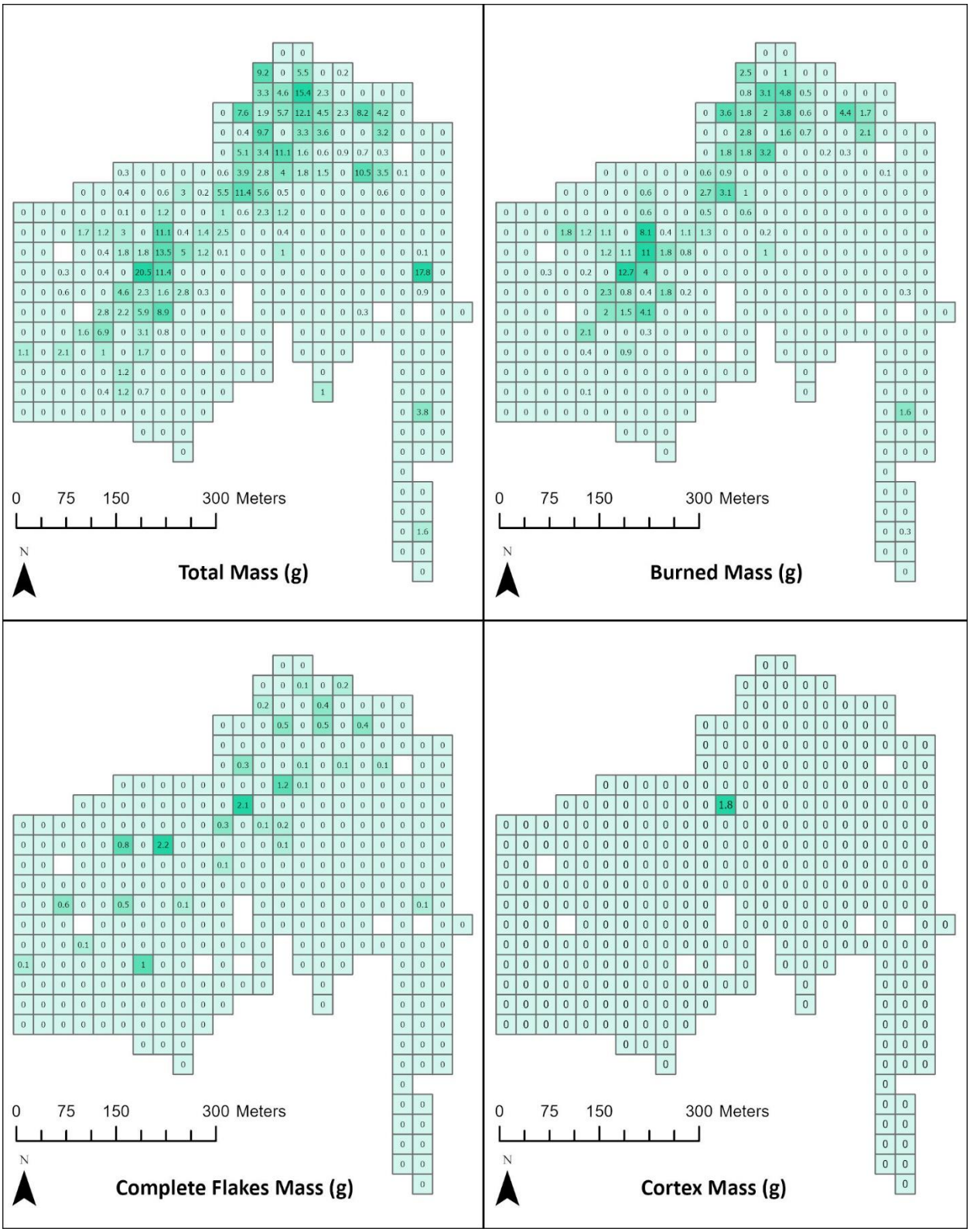
F18. Counts and attributes for silicified wood debitage.



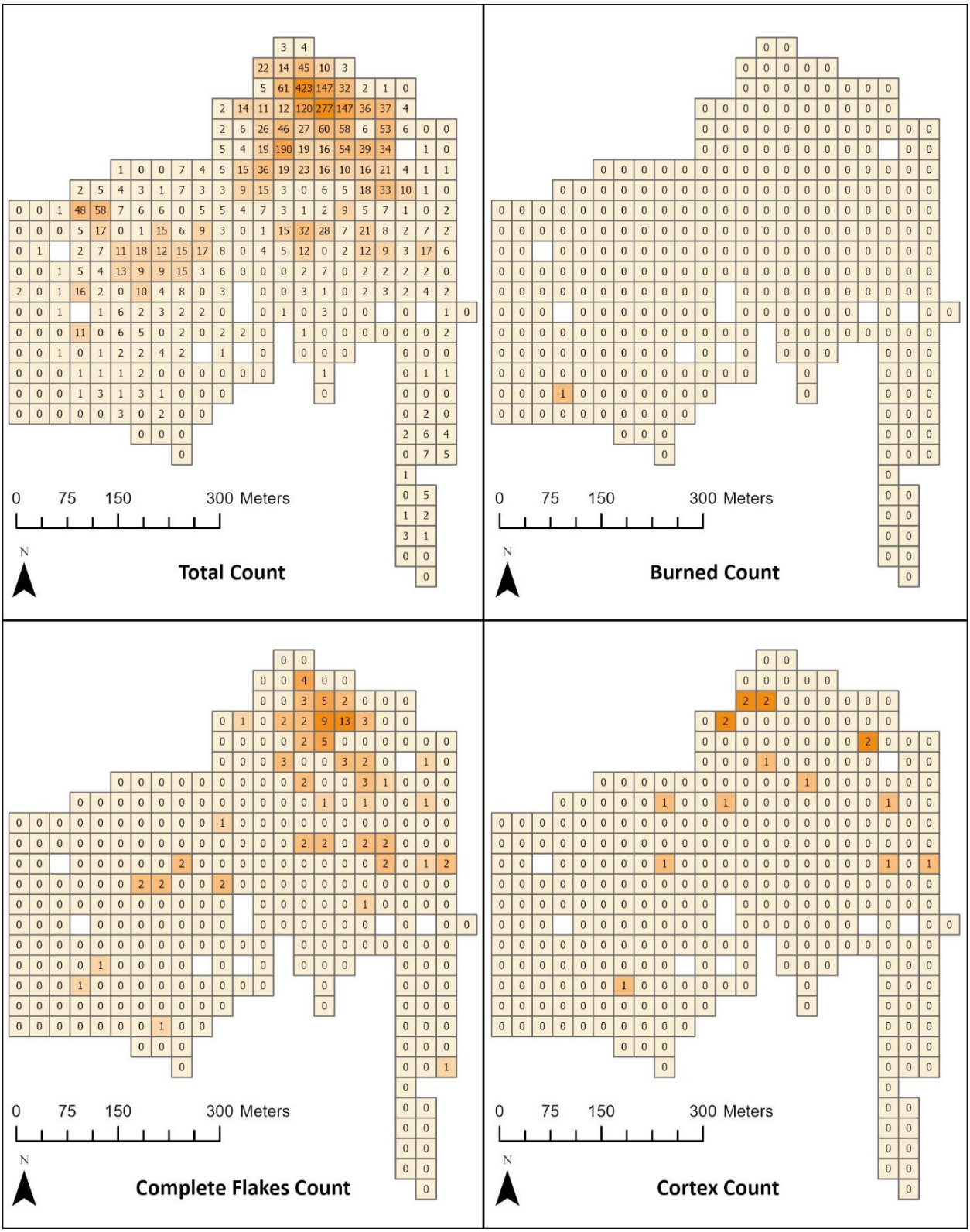
F19. Mass (g) and attributes for silicified wood debitage.



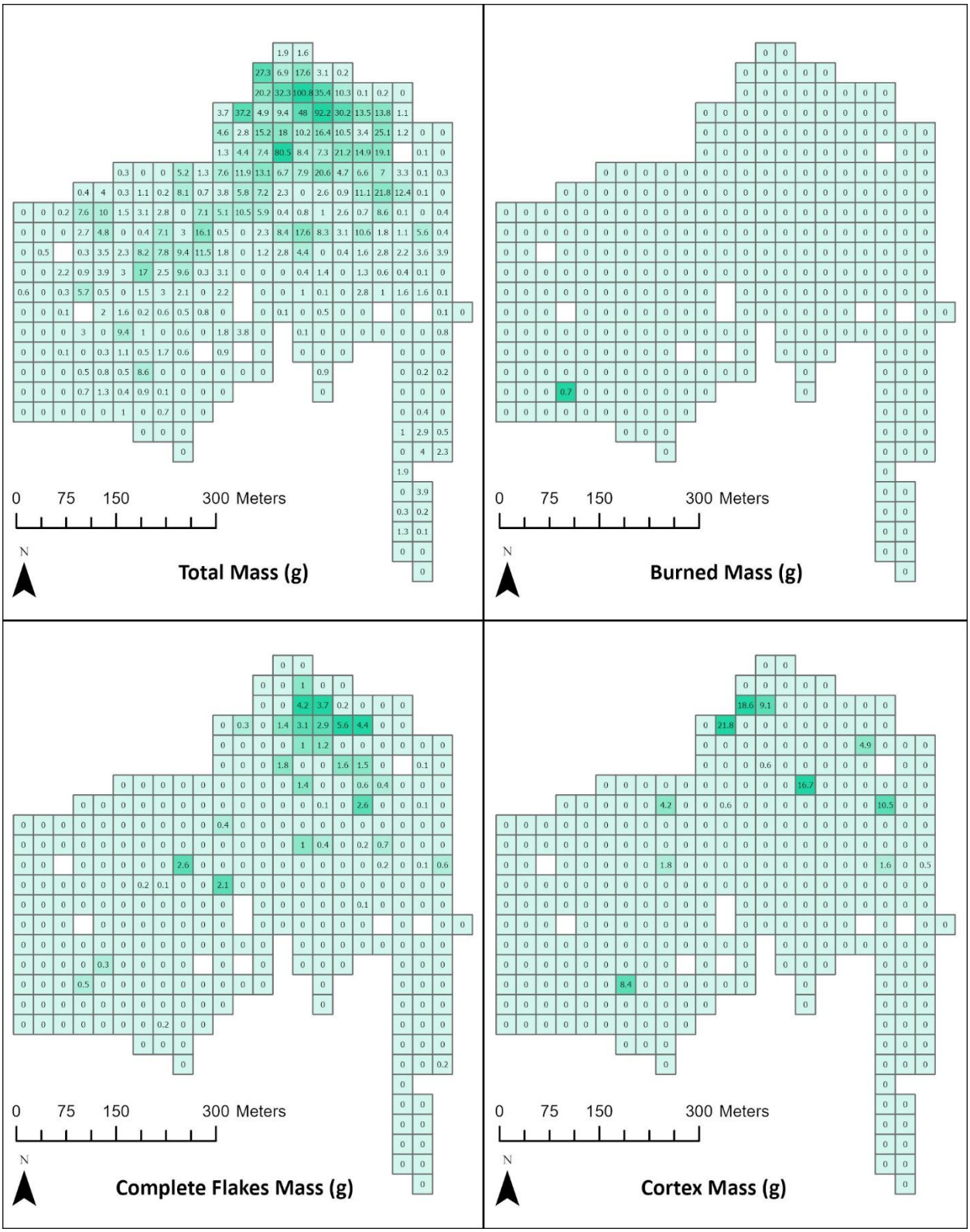
F20. Counts and attributes for Mosca chert debitage.



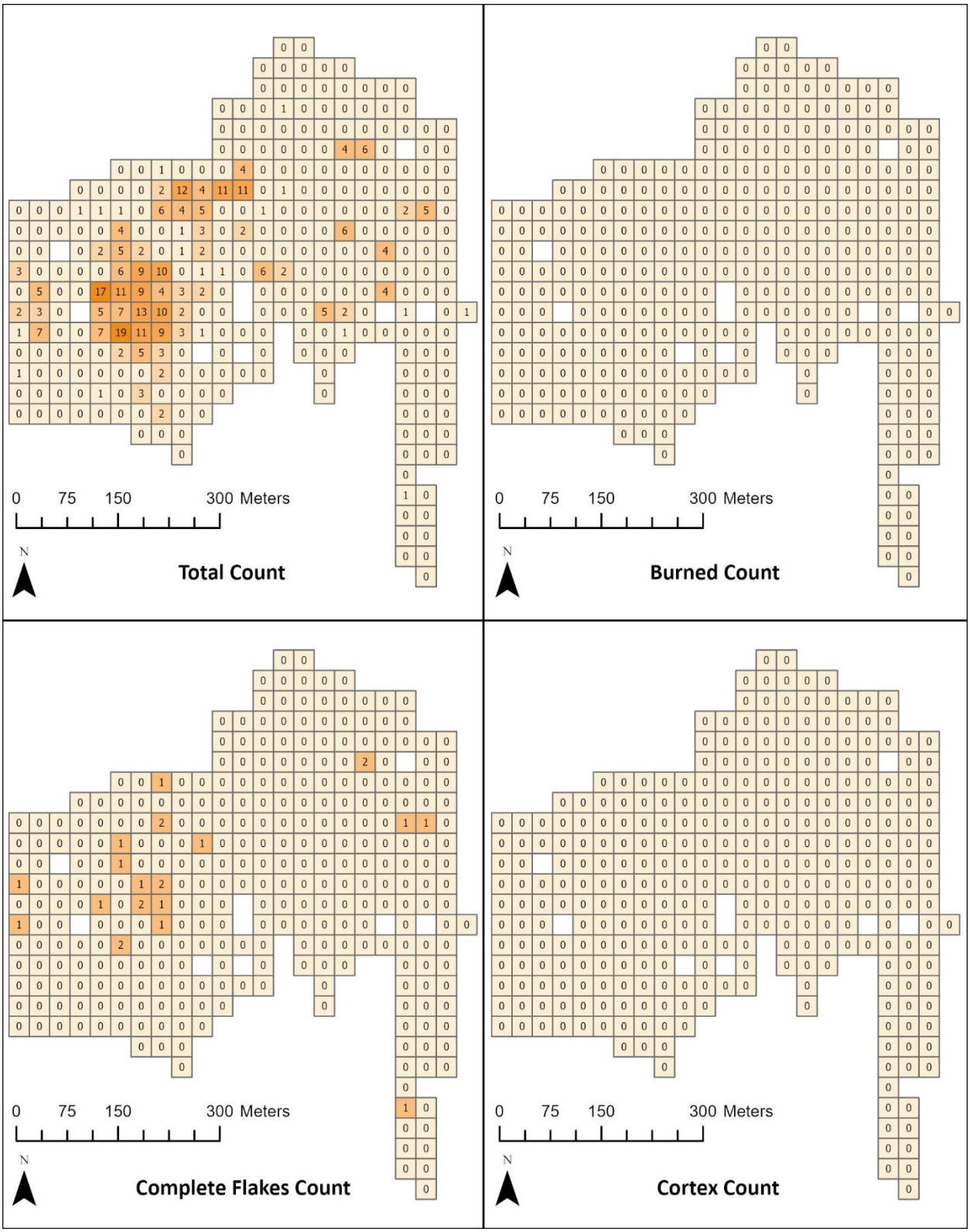
F21. Mass (g) and attributes for Mosca chert debitage.



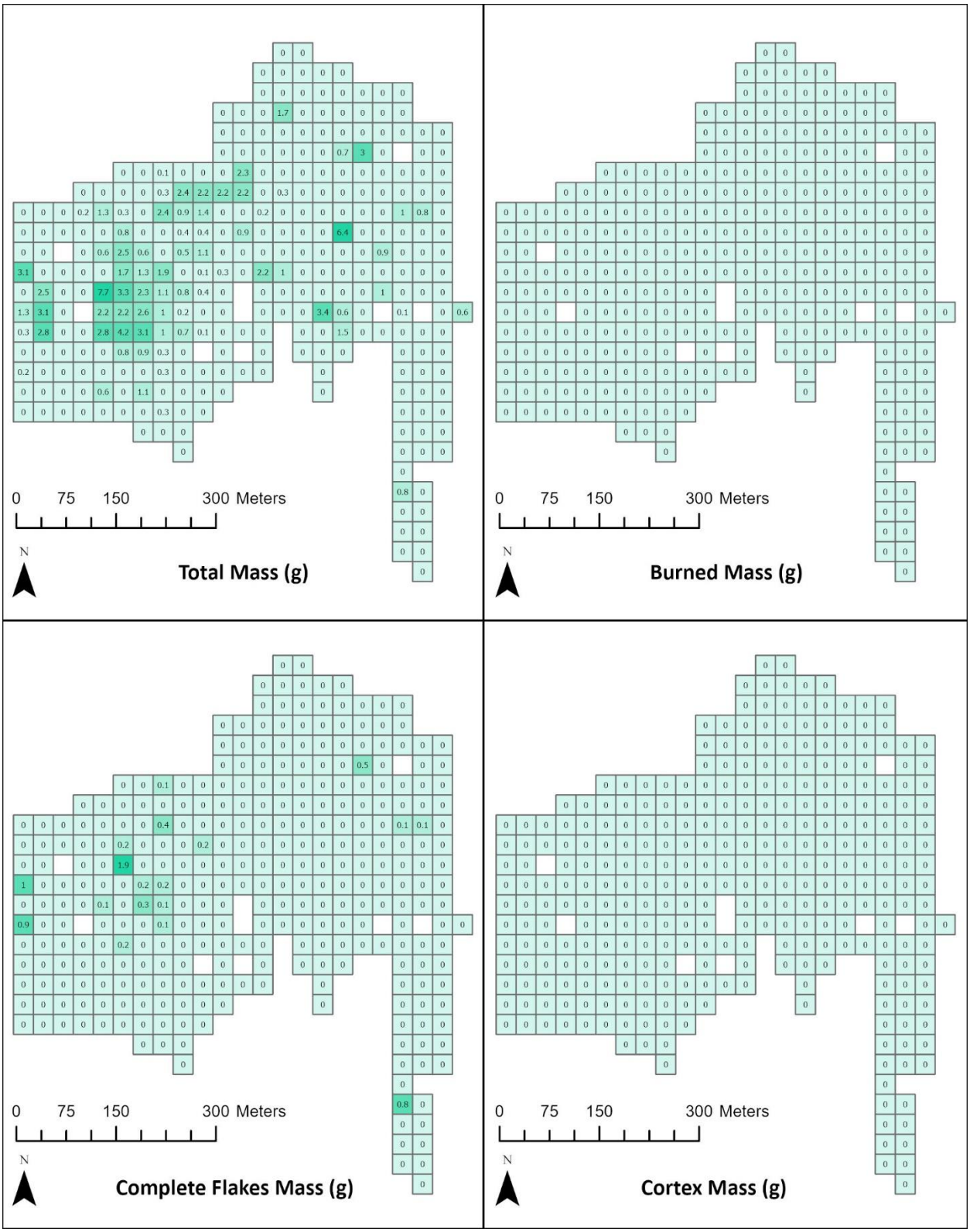
F22. Counts and attributes for Dakota Formation quartzite debitage (Trickle Mountain).



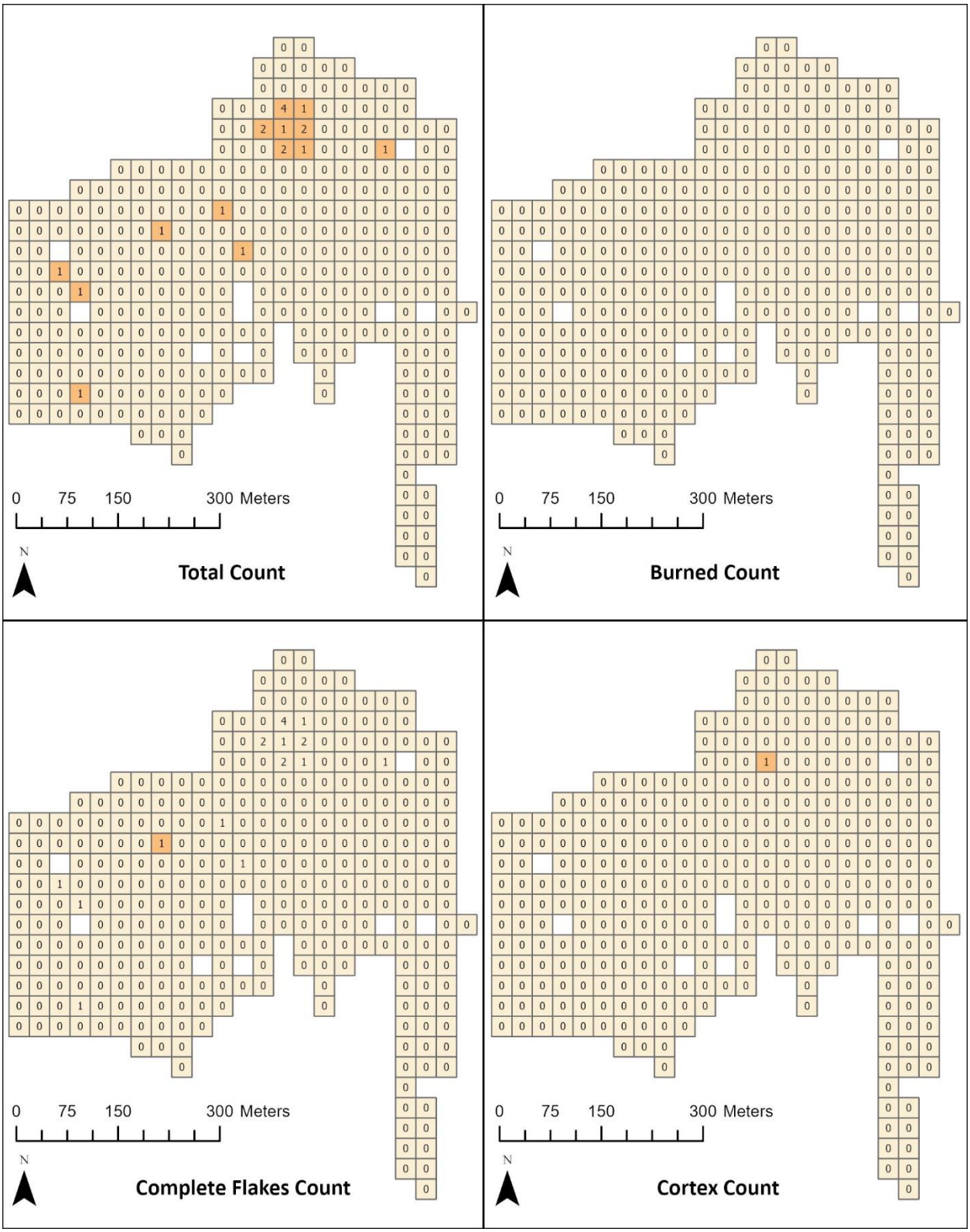
F23. Mass (g) and attributes for Dakota Formation quartzite debitage (Trickle Mountain).



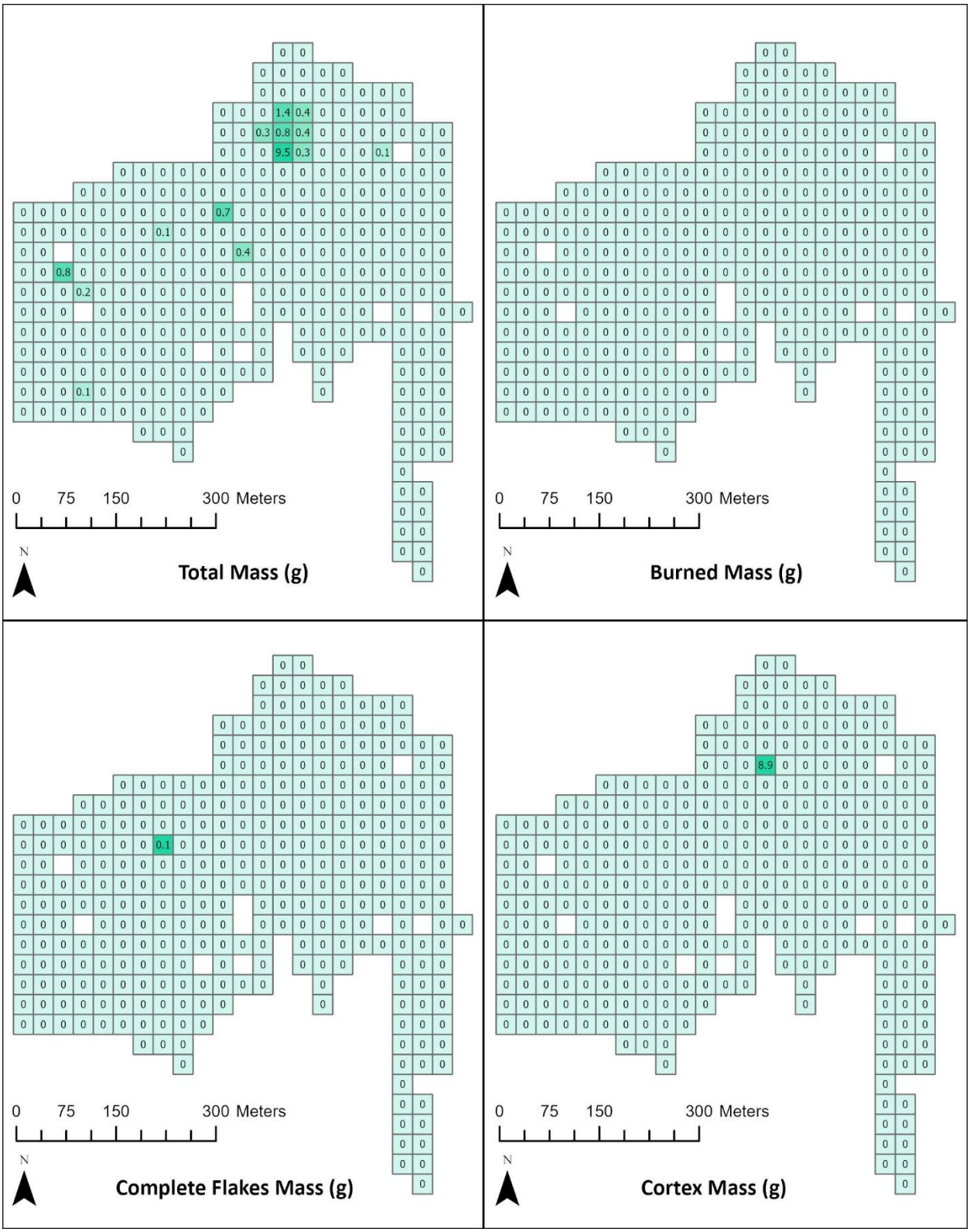
F24. Counts and attributes for Morrison Formation quartzite debitage.



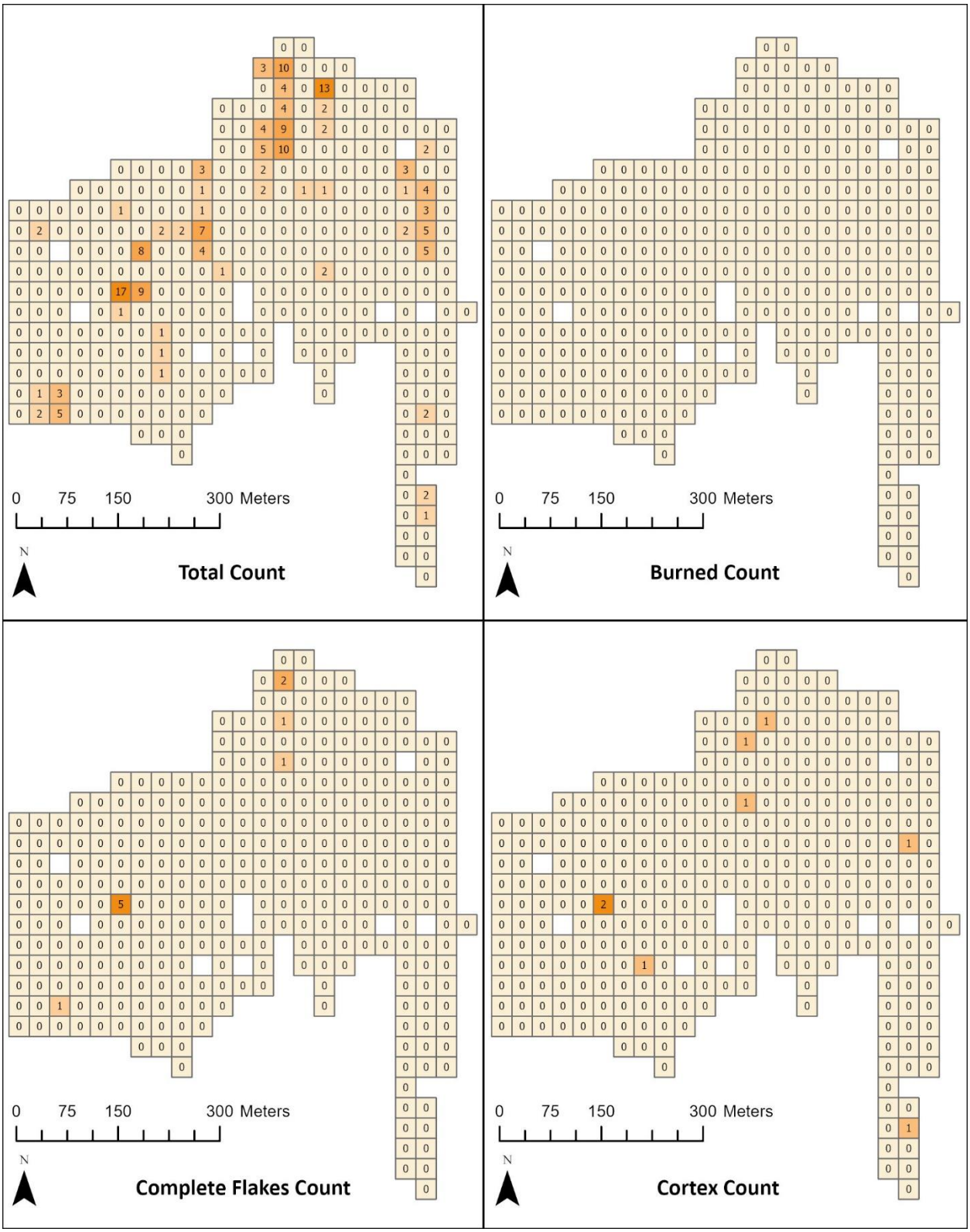
F25. Mass (g) and attributes for Morrison Formation quartzite debitage.



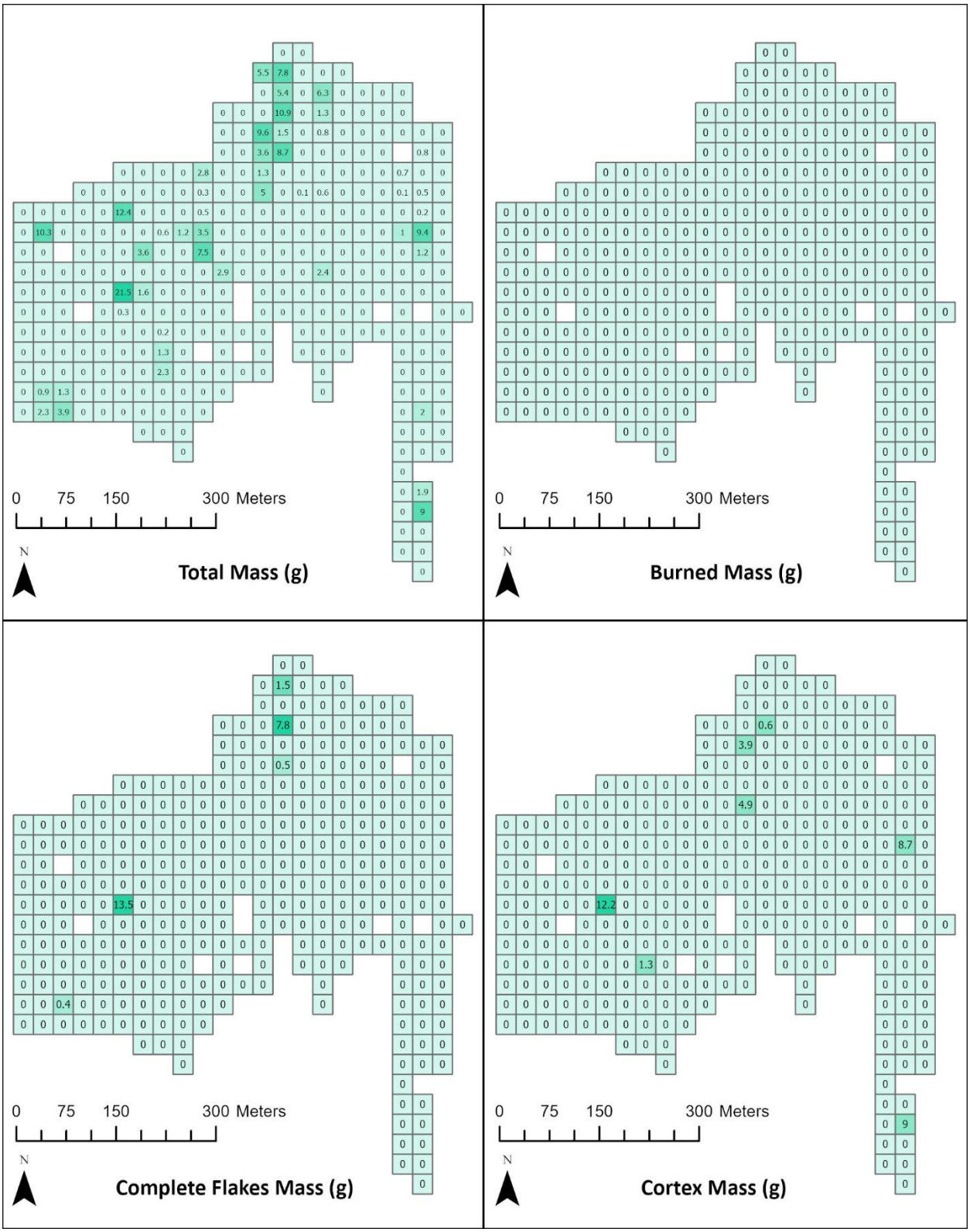
F26. Counts and attributes for quartz crystal debitage.



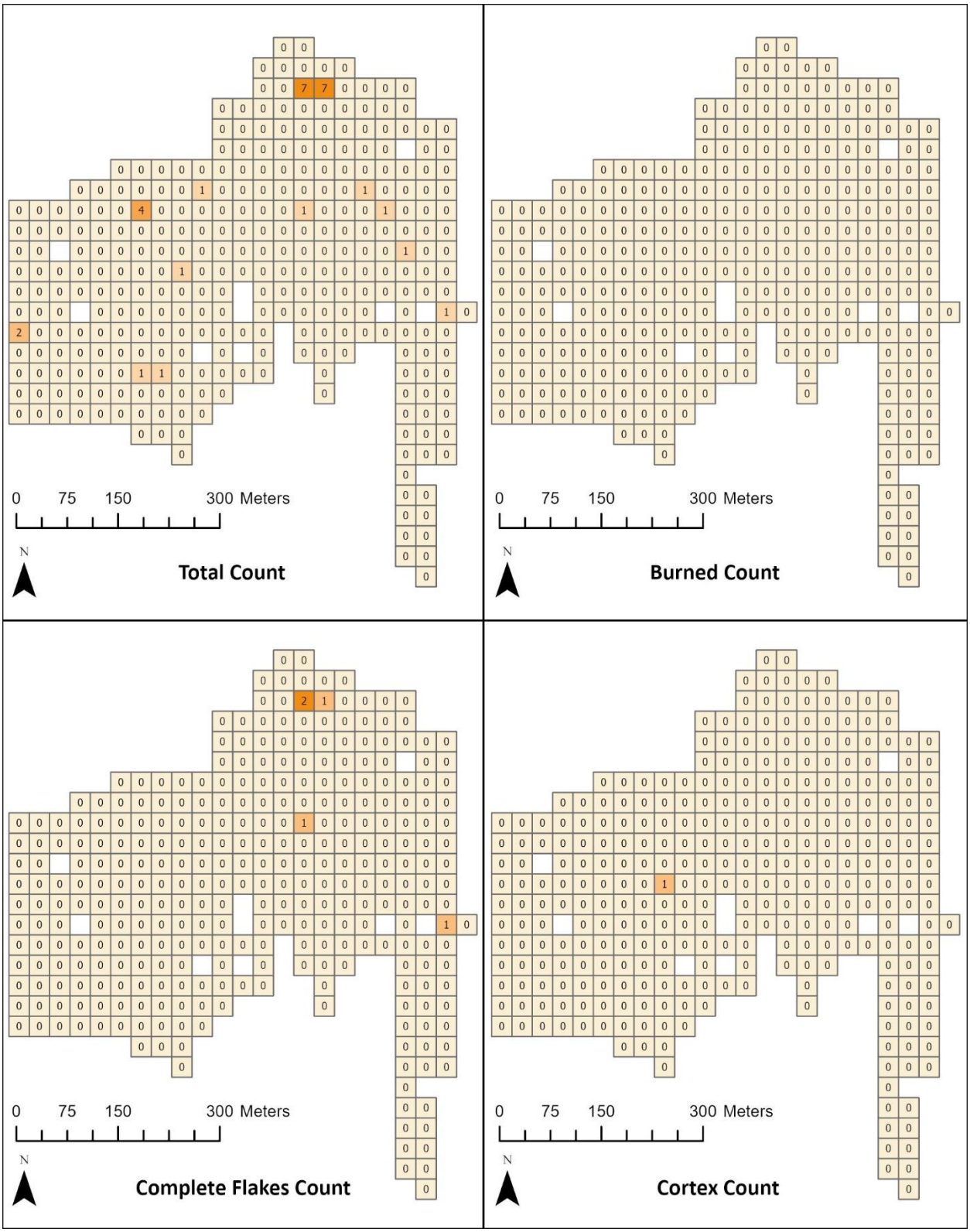
F27. Mass (g) and attributes for quartz crystal debitage.



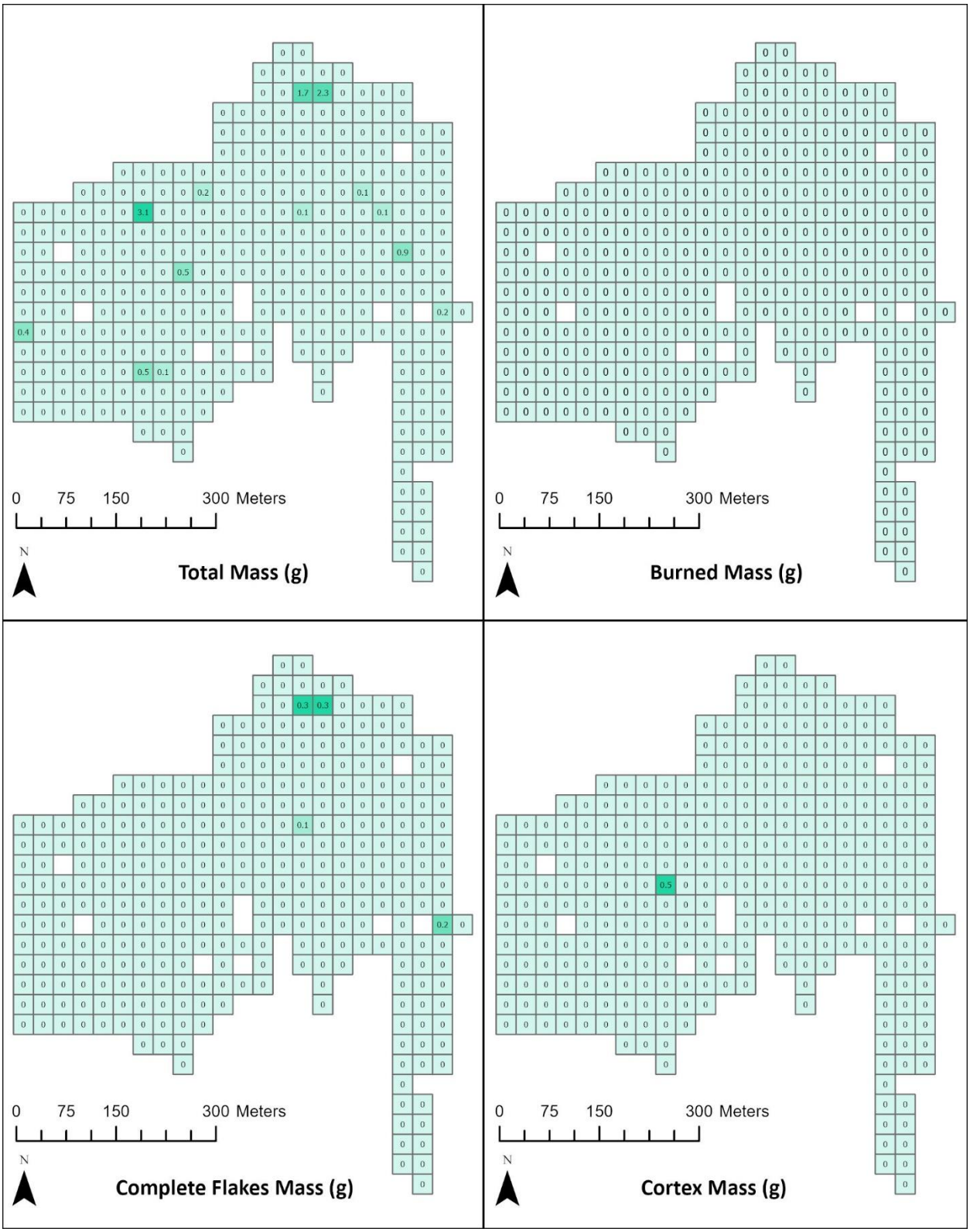
F28. Counts and attributes for rhyolite debitage.



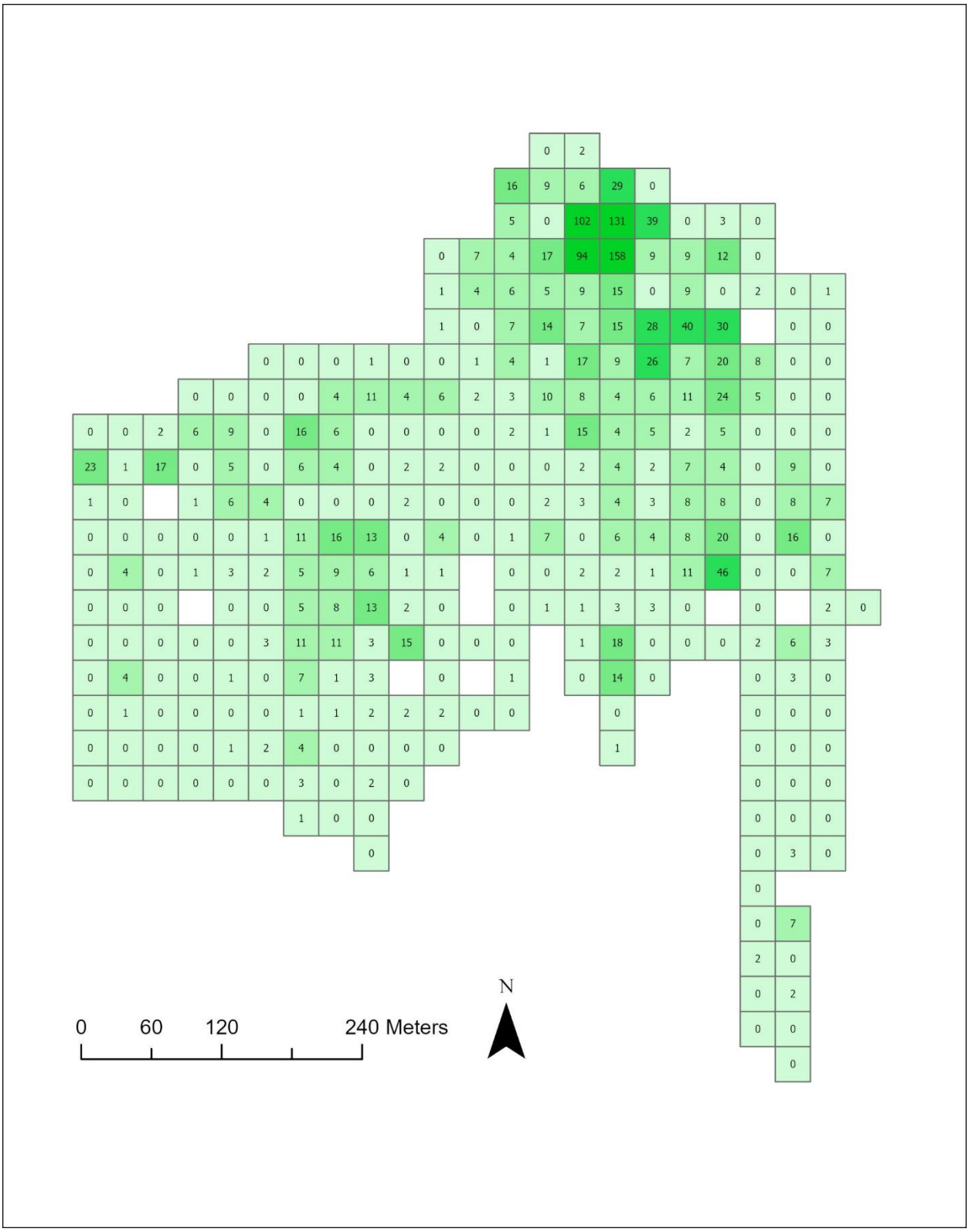
F29. Mass (g) and attributes for rhyolite debitage.



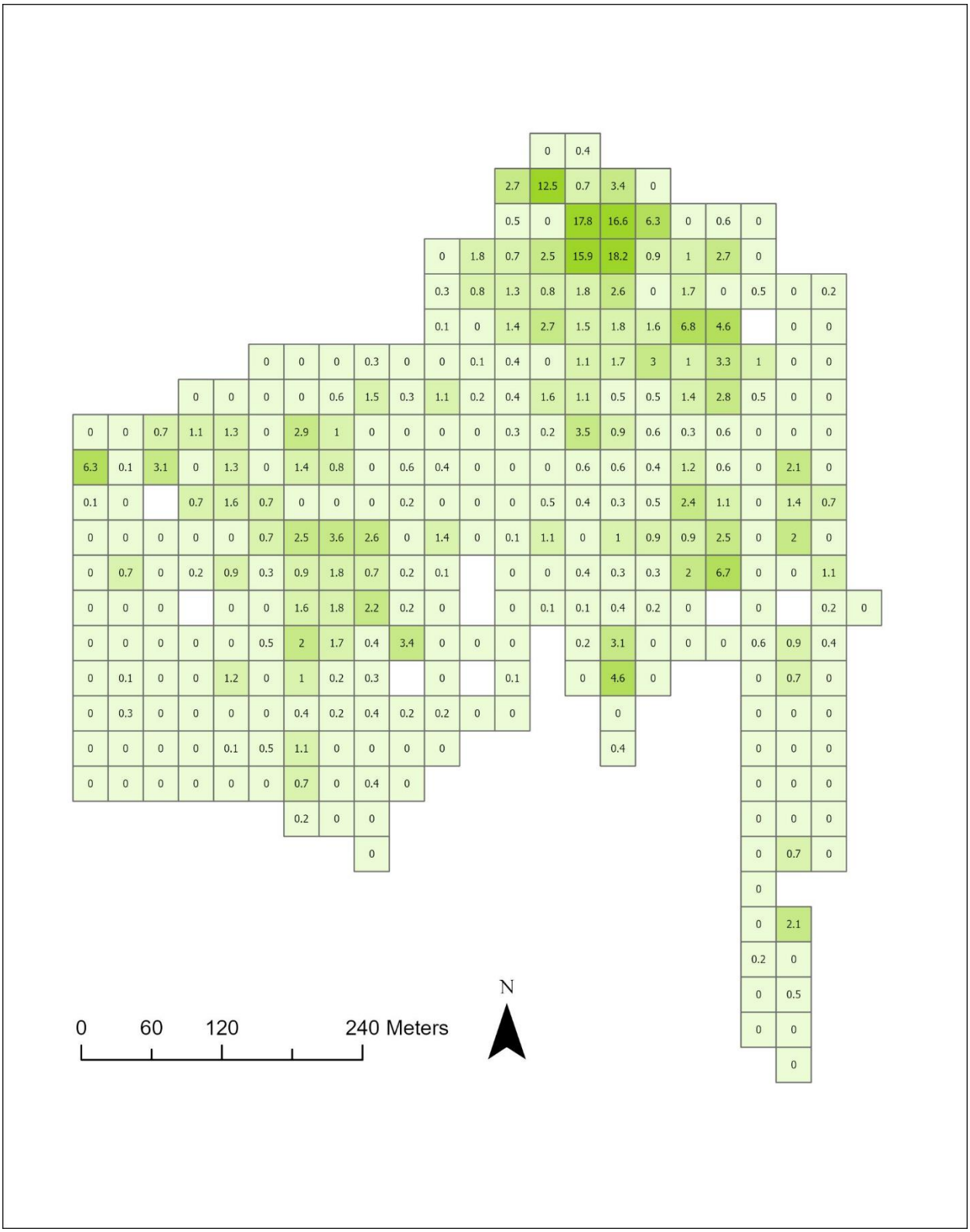
F30. Counts and Attributes for unknown chert debitage (includes one oolitic chert).



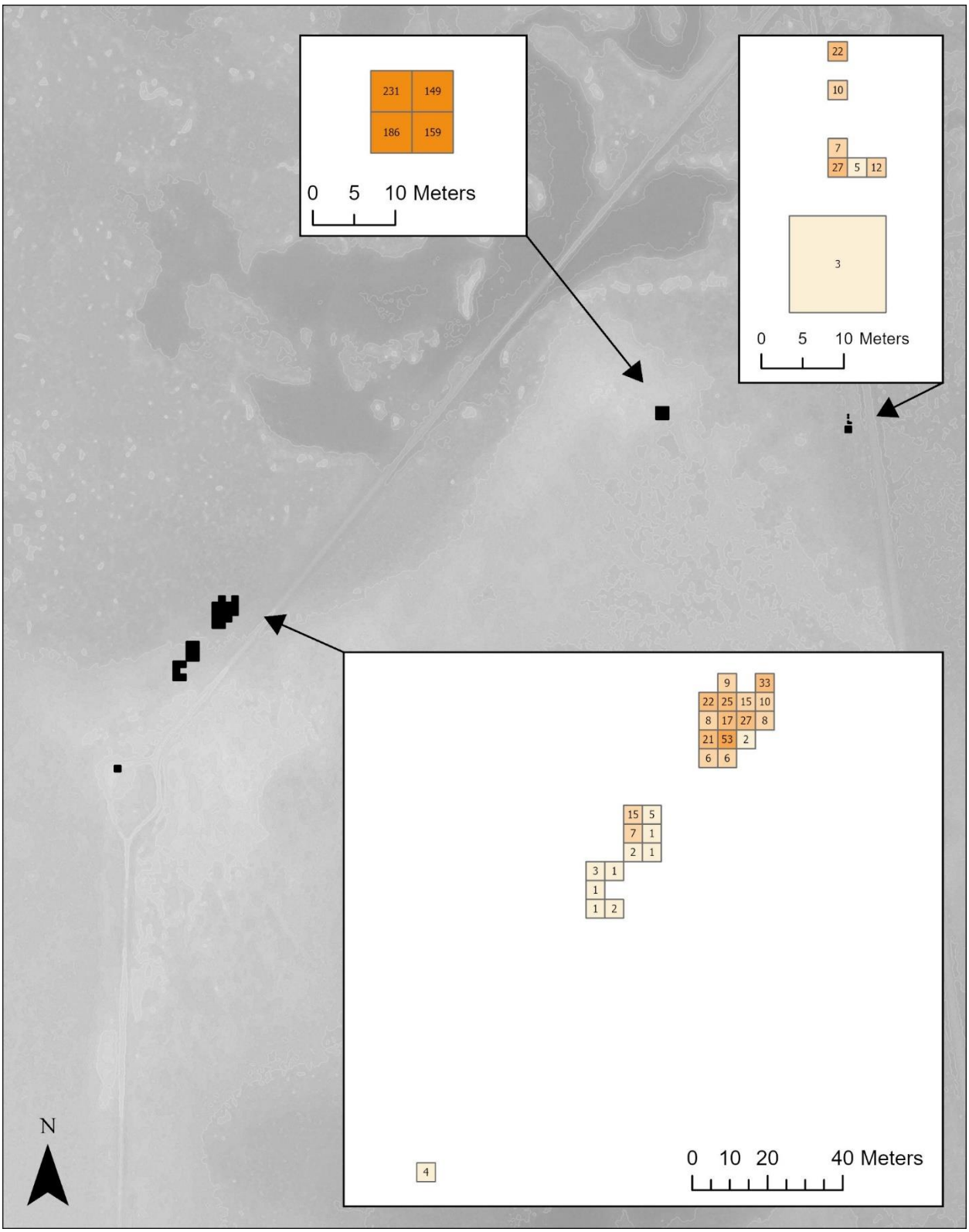
F31. Mass (g) and attributes for unknown chert debitage (includes one oolitic chert).



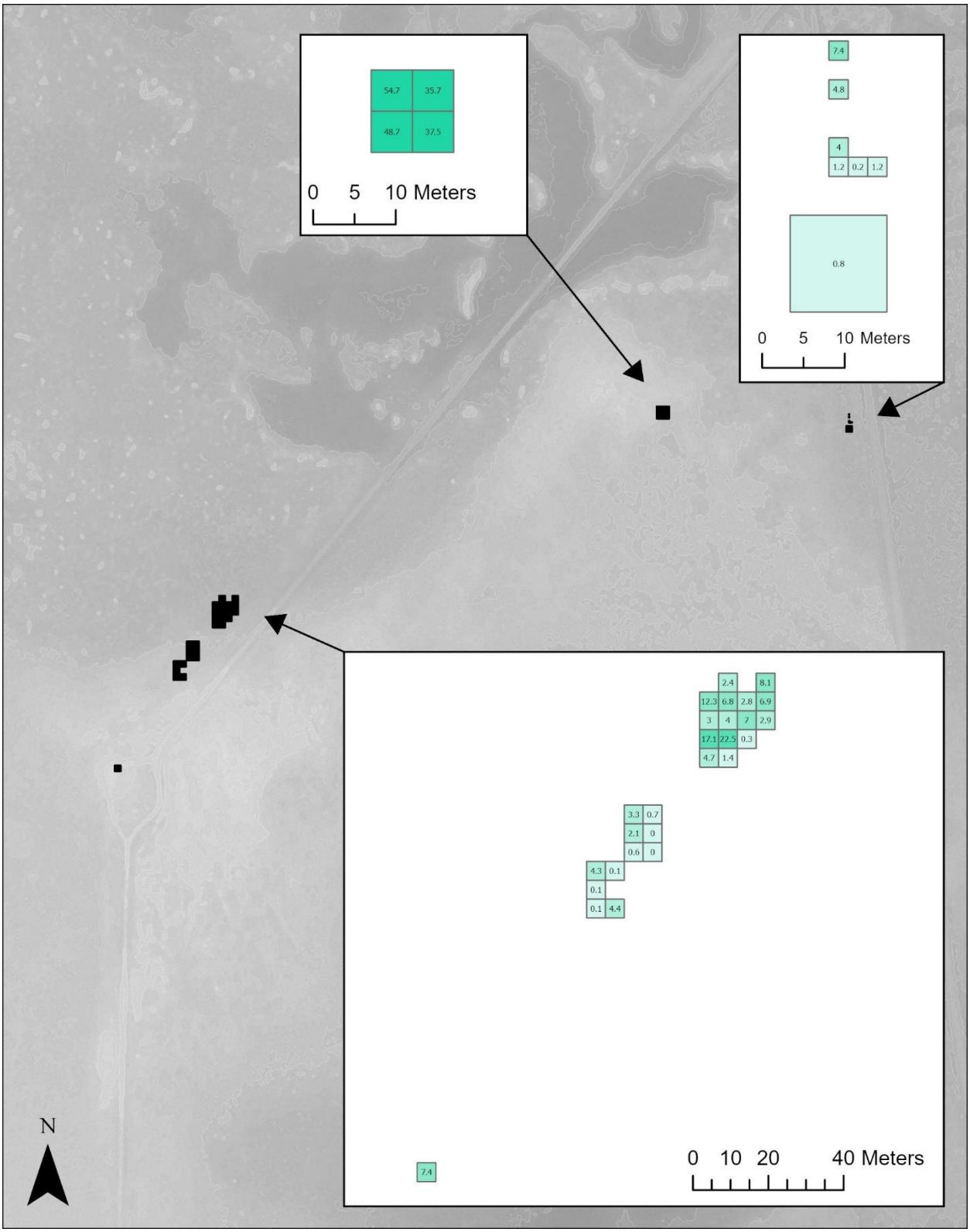
G1. Counts of unidentified tooth enamel fragments.



G2. Mass (g) of unidentified tooth enamel fragments.



H1. Counts of debitage in Smithsonian 1983 excavation units (unsorted).



H2. Mass (g) of debitage in Smithsonian 1983 excavation units (unsorted).

I1. Trace element values for a sample of Folsom artifacts made from obsidian and/or volcanic rock, based on EDXRF analysis prepared by Shackley (2022). Measurements in parts per million (ppm). USGS RGM-1 rhyolite standard and USGS recommended values.

Catalog	Ti	Mn	Fe	Zn	Rb	Sr	Y	Zr	Nb	Ba	Ce	Pb	Th	Source
SI-PP-1133	6368	2198	40196	198	123	364	46	227	35	923	149	54	26	andesite (unk)
SI-PP-1134	948	391	10260	93	162	15	42	166	55	44	66	27	22	Cerro del Medio
SI-PP-1135	8316	280	6469	66	1	213	7	36	5	174	20	14	10	Sedillo Hill
SI-PP-1136	890	475	10317	158	203	11	60	171	92	14	19	33	24	Cerro Toledo
SI-PP-1138	3974	386	7588	59	155	9	24	77	46	0	35	23	20	El Rechuelos
SI-PRE-1080	857	407	7855	41	155	17	25	82	50	24	23	27	14	El Rechuelos
SI-PRE-1081	897	502	10419	135	200	9	63	176	92	8	52	38	23	Cerro Toledo
SI-PRE-1082	973	417	10532	68	167	13	51	181	61	55	88	29	23	Cerro del Medio
SI-CF-1230	4372	1021	43201	202	157	249	34	210	20	694	33	40	21	trachy-andesite
SI-CF-1231	4297	550	41907	239	153	246	31	195	12	716	43	35	17	trachy-andesite
RGM1-S4	1643	281	13106	41	147	109	26	218	10	821	20	21	17	standard
RGM1-S4	1549	279	13258	41	148	112	26	222	10	799	43	21	12	standard
RGM-1	1619	280	12998	32	150	110	25	220	9	810	47	24	15	recommended

I2. Major and minor oxides for non-obsidian Folsom artifacts made from volcanic rock, based on Shackley (2022). USGS RGM-1 rhyolite and AGV-1 andesite standard and recommended values. Measurements in weight percentages (%).

Catalog	Na2O	MgO	Al2O3	SiO2	K2O	CaO	TiO2	V2O5	MnO	Fe2O3	∑
SI-PP-1133	2.25	4.24	16.48	61.18	4.01	1.95	1.42	0.11	0.52	7.05	99.21
SI-PP-1135	3.77	0.82	0.11	85.73	0.92	3.77	3.18	0.08	0.10	0.89	99.37
SI-CF-1230	2.39	1.00	8.94	56.59	6.84	6.06	1.66	0.09	0.34	15.20	99.11
SI-CF-1231	2.71	0.89	8.99	57.74	6.45	6.29	1.46	0.11	0.17	14.04	98.85
RGM1-S4 std.	3.90	0.00	13.31	73.71	4.90	1.41	0.27	0.00	0.04	2.21	99.75
RGM-1 rec.	4.07	0.28	13.70	73.40	4.30	1.15	0.27	no report	0.04	1.86	
AGV-1 std.	3.94	1.21	17.15	61.17	2.98	5.21	1.07	0.05	0.1	6.83	99.71
AGV-1 rec.	4.26	1.53	17.15	58.84	2.92	4.94	1.05	no report	no report	6.77	